NUREG/CR-6143
SAND93-2440
Vol. 6, Part 2

Evaluation of Potential Severe Accidents During Low Power and Shutdown Operations at Grand Gulf, Unit 1

Evaluation of Severe Accident Risks for Plant Operational State 5 During a Refueling Outage

Supporting MELCOR Calculations

Manuscript Completed: December 1994
Date Published: March 1995

Prepared by
L. N. Kmetyk, T. D. Brown

Sandia National Laboratories
Albuquerque, NM 87185

Prepared for
Division of Systems Technology
Office of Nuclear Regulatory Research
U.S. Nuclear Regulatory Commission
Washington, DC 20555-0001
NRC Job Code L1679

This page is intentionally left blank.

Abstract

To gain a better understanding of the risk significance of low power and shutdown modes of operation, the Office of Nuclear Regulatory Research at the NRC established programs to investigate the likelihood and severity of postulated accidents that could occur during low power and shutdown (LP&S) modes of operation at commercial nuclear power plants. To investigate the likelihood of severe core damage accidents during off power conditions, probabilistic risk assessments (PRAs) were performed for two nuclear plants: Unit 1 of the Grand Gulf Nuclear Station, which is a BWR-6 Mark III boiling water reactor (BWR), and Unit 1 of the Surry Power Station, which is a three-loop, subatmospheric, pressurized water reactor (PWR). The analysis of the BWR was conducted at Sandia National Laboratories while the analysis of the PWR was performed at Brookhaven National Laboratory.

This multi-volume report presents and discusses the results of the BWR analysis. The subject of this part presents the deterministic code calculations, performed with the MELCOR code, that were used to support the development and quantification of the PRA models. The background for the work documented in this report is summarized, including how deterministic codes are used in PRAs, why the MELCOR code is used, what the capabilities and features of MELCOR are, and how the code has been used by others in the past. Brief descriptions of the Grand Gulf plant and its configuration during LP&S operation and of the MELCOR input model developed for the Grand Gulf plant in its LP&S configuration are given. The results of MELCOR analyses of various accident sequences for the plant operating state (POS) 5 configuration during refueling (approximately Cold Shutdown as defined by Grand Gulf Technical Specifications) are presented for accidents initiated at several different times after scram and shutdown, including shortened thermal/hydraulic and core damage calculations done in support of the Level 1 analysis and full plant analyses, including containment response and source terms, supporting the Level 2 analysis. MELCOR calculations of various accident scenarios for POS 6 (i.e., a selected regime of refueling mode of operation) also are given; these include a reference calculation and sensitivity studies on assumed plant configurations and code input options used.

This page is intentionally left blank.

Contents

Contents (continued)

List of Figures

List of Figures (continued)

List of Figures (continued)

List of Figures (continued)

List of Figures (continued)

List of Figures (continued)

List of Figures (continued)

List of Figures (continued)

List of Figures (continued)

List of Figures (continued)

List of Figures (continued)

List of Tables

List of Tables (continued)

List of Tables (continued)

Acronyms

ADHR	Auxiliary Decay Heat Removal
ADS	Automatic Depressurization System
APB	Accident Progression Bin
APET	Accident Progression Event Tree
BNL	Brookhaven National Laboratory
BWR	Boiling Water Reactor
CCI	Core-Concrete Interaction
CD	Core Damage
CDS	Condensate
CNMT	Containment
CRD	Control Rod Drive
CS	Containment Spray
CVS	Containment Venting System
DCH	Direct Containment Heating
ECCS	Emergency Core Cooling Systems
EOC	End-of-Cycle
EOP	Emergency Operating Procedures
EPS	Emergency Power System
ES	End State
ESF	Engineered Safety Feature
FCI	Fuel-Coolant Interaction
FSAR	Final Safety Analysis Report
HEP	Human Error Probability
HIS	Hydrogen Igniter System
HPCS	High Pressure Core Spray
HRA	Human Reliability Analysis
LHS	Latin Hypercube Sampling
LBLOCA	Large Break Loss of Coolant Accident
LOCA	Loss of Coolant Accident
LPCI	Low Pressure Coolant Injection
LPCS	Low Pressure Core Spray
LP&S	Low Power and Shutdown
MSIV	Main Steam Isolation Valve
NRC	Nuclear Regulatory Commission
OC	Operating Condition
PDS	Plant Damage State
POS	Plant Operating State
PRA	Probabilistic Risk Assessment
PWR	Pressurized Water Reactor
RCIC	Reactor Core Isolation Cooling
RFO	Refueling Outage
RHR	Residual Heat removal
RPV	Reactor Pressure Vessel
SBO	Station Blackout
SDC	Shutdown Cooling System(s)
SGTS	Standby Gas Treatment System
SP	Suppression Pool
SPC	Suppression Pool Cooling
SPMU	Suppression Pool Makeup
SRV	Safety Relief Valve
SSW	Standby Service Water Crosstie

Acronyms (continued)

STG	Source Term Group
TAF	Top-of-Active-Fuel
UFSAR	Updated Final Safety Analysis Report
USDOE	U.S. Department of Energy
VB	Vessel Breach

Foreword

(NUREG/CR-6143 and 6144)
Low Power and Shutdown Probabilistic Risk Assessment Program

Traditionally, probabilistic risk assessments (PRA) of severe accidents in nuclear power plants have considered initiating events potentially occurring only during full power operation. Some previous screening analyses that were performed for other modes of operation suggested that risks during those modes were small relative to full power operation. However, more recent studies and operational experience have implied that accidents during low power and shutdown could be significant contributors to risk.

During 1989, the Nuclear Regulatory Commission (NRC) initiated an extensive program to carefully examine the potential risks during low power and shutdown operations. The program includes two parallel projects performed by Brookhaven National Laboratory (BNL) and Sandia National Laboratories (SNL), with the seismic analysis performed by Future Resources Associates. Two plants, Surry (pressurized water reactor) and Grand Gulf (boiling water reactor), were selected as the plants to be studied.

The objectives of the program are to assess the risks of severe accidents due to internal events, internal fires, internal floods, and seismic events initiated during plant operational states other than full power operation and to compare the estimated core damage frequencies, important accident sequences and other qualitative and quantitative results with those accidents initiated during full power operation as assessed in NUREG-1150. The scope of the program includes that of a level-3 PRA.

The results of the program are documented in two reports, NUREG/CR-6143 and 6144. The reports are organized as follows:

For Grand Gulf:

NUREG/CR-6143 - Evaluation of Potential Severe Accidents During Low Power and Shutdown Operations at Grand Gulf, Unit 1

- Volume 1: Summary of Results
- Volume 2: Analysis of Core Damage Frequency from Internal Events for Plant Operational State 5 During a Refueling Outage
  - Part 1: Main Report
  - Part 2: Internal Events Appendices A to H
  - Part 3: Internal Events Appendices I and J
  - Part 4: Internal Events Appendices K to M
- Volume 3: Analysis of Core Damage Frequency from Internal Fire Events for Plant Operational State 5 During a Refueling Outage
- Volume 4: Analysis of Core Damage Frequency from Internal Flooding Events for Plant Operational State 5 During a Refueling Outage
- Volume 5: Analysis of Core Damage Frequency from Seismic Events for Plant Operational State 5 During a Refueling Outage
- Volume 6: Evaluation of Severe Accident Risks for Plant Operational State 5 During a Refueling Outage
  - Part 1: Main Report
  - Part 2: Supporting MELCOR Calculations

For Surry:

NUREG/CR-6144 - Evaluation of Potential Severe Accidents During Low Power and Shutdown Operations at Surry Unit-1

Volume 1: Summary of Results
Volume 2: Analysis of Core Damage Frequency from Internal Events During Mid-loop Operations
Part 1: Main Report
Part 2: Internal Events Appendices A to D
Part 3: Internal Events Appendix E
Part 4: Internal Events Appendices F to H
Part 5: Internal Events Appendix I
Volume 3: Analysis of Core Damage Frequency from Internal Fires During Mid-loop Operations
Volume 4: Analysis of Core Damage Frequency from Internal Floods During Mid-loop Operations
Volume 5: Analysis of Core Damage Frequency from Seismic Events During Mid-loop Operations
Volume 6: Evaluation of Severe Accident Risks During Mid-loop Operations
Part 1: Main Report
Part 2: Appendices

Acknowledgments

The authors wish to thank the NRC project manager, Chris Ryder, for his support, interest, and thoughtful management of the project. We would also like to thank the MELCOR development team at Sandia for making the modifications to the code that enable us to analyze accidents at conditions other than full power.

This page is intentionally left blank.

1 Introduction

1.1 Background

The safety of commercial nuclear plants during power operation has been previously assessed in many probabilistic safety assessment studies. The U.S. Nuclear Regulatory Commission (NRC) has been an active participant in these studies including the landmark Reactor Safety Study [Nuclear Regulatory Commission, 1975], the five plant studies performed as part of the NUREG-1150 study [Nuclear Regulatory Commission, 1989] and the LaSalle plant analysis performed under RMIEP/PRUEP programs [Payne, 1992; Shaffer et al., 1992]. Furthermore, all licensees are required to perform an individual plant examination (IPE) that assesses the safety of the plant during full power operation.

Recent events at several nuclear power generating stations, recent safety studies, and operational experience, however, have all highlighted the need to assess the safety of plants during low power and shutdown modes of operation. In contrast to full power operation, there is very little information on the safety of plants during low power and shutdown modes of operation. In the past, the assumption has been that power operation is the risk-dominant mode of operation because the decay energy is greatest at the time of shutdown and then decays as a function of time. Thus, the rationale was that during shutdown modes of operation the decay heat would be sufficiently low that there would be plenty of time to respond to any abnormal event that may threaten the core cooling function. Furthermore, given the unlikely event that a release did occur, radioactive decay would lessen the radiological potential of the release. This argument's Achilles' heel is that the technical specifications allow for more equipment to be inoperable in off-power conditions. Thus, while there may be more time to respond to an accident during shutdown, many of the systems that are relied on to mitigate an accident during power operation may not be available during shutdown.

To gain a better understanding of the risk significance of low power and shutdown modes of operation, the Office of Nuclear Regulatory Research at the NRC established programs to investigate the likelihood and severity of postulated accidents that could occur during low power and shutdown (LP&S) modes of operation at commercial nuclear power plants. To investigate the likelihood of severe core damage accidents during off power conditions, probabilistic risk assessments (PRAs) were performed for two nuclear plants: Unit 1 of the Grand Gulf Nuclear Station which is a BWR-6 Mark III boiling water reactor (BWR) and Unit 1 of the Surry Power Station which is a three-loop, subatmospheric, pressurized water reactor (PWR). These studies are Level 3 PRAs and, as such, consist of the following five analysis components: accident frequency analysis, accident progression analysis, analysis of the release and transport of radioactive material (i.e., source term analysis), consequence analysis, and a risk integration analysis. A principal product of a Level 3 PRA is an expression for risk.

The analysis of the BWR was conducted at Sandia National Laboratories while the analysis of the PWR was performed at Brookhaven National Laboratory. The LP&S PWR analysis is reported in NUREG/CR-6144 [NUREG/CR-6144] and will not be discussed any further in this report. This multi-volume report presents and discusses the results of the BWR analysis. Volumes 2-5 present the accident frequency analysis (i.e., Level 1). Volume 6 presents the Level 2/3 analysis performed under FIN L1679[1]. Part 1 of Volume 6 presents the accident progression, radionuclide release and transport, consequence and risk analyses. The subject of this part, i.e., Part 2 of Volume 6, presents the deterministic code calculations, performed with the MELCOR code [Summers et al., 1991], that were used to support the development and quantification of the PRA models.

1.2 Use of Deterministic Codes in Level 3 PRA

Deterministic calculations are vital analyses that are used to support the development and quantification of the PRA models used in the Level 1 and 2 analyses. Deterministic calculations are used to define success criteria and timing characteristics for the Level 1 analysis. For example, these calculations are used to: (1) define the regimes under which certain injection system can be used to cool the core, (2) determine the amount of time the operators have to respond to an initiating event and perform appropriate actions to terminate or mitigate the accident,

1. The Level 1 analysis consists of the accident frequency analysis; the Level 2 analysis consists of the accident progression and radionuclide release and transport analyses; and the Level 3 analysis consists of the consequence analysis). A Level 3 PRA combines the results from each of the constituent analyses and develops an expression for risk.

and (3) determine when the onset of core damage occurs. In the Level 2 analysis, deterministic calculations are used to estimate the timing of key events in the accident (e.g., the onset of core damage, the time at which the vessel fails, and the time when the containment fails), characteristics of the core degradation process, the conditions in the containment as a function of time (e.g., temperature, pressure, composition of the atmosphere), the occurrence and impact of certain phenomena (e.g., hydrogen combustion), and the release and transport of radioactive material in the containment. Wherever possible, a consistent set of calculations is used to support both the Level 1 and Level 2 analyses to ensure that a consistent set of assumptions is being used and to maintain continuity in the timing of events.

The results from deterministic analyses are incorporated in the Level 2 analysis in the following manner:

- Calculations are performed for the important accident sequences (i.e., typically Plant Damage States) that lead to core damage; sensitivity calculations are performed to investigate important facets of the accident.

- Following a general understanding of the possible accident progressions from the deterministic calculations and other source of information (e.g., results from experiments), major events that can affect the progression of the accident and the release and transport of radioactive material are identified. These events form some of the top events of the Level 2 Accident Progression Event Tree.

- Results from these calculations supplemented by other information serve as the basis for quantifying the PRA models. Since uncertainty is unavoidable in these calculations (e.g., in the initial conditions, phenomenological models, and the model of the plant), judgement techniques are often used to translate results from deterministic analyses into a form suitable for probabilistic analysis. For example, a deterministic calculation may indicate that based on the prescribed initial and boundary conditions, a combustible mixture of hydrogen will form in the containment and combustion of this mixture will result in a peak pressure. However, the initial and boundary conditions are uncertain and there are many uncertainties associated with the phenomena involved in this process, for example, the amount of hydrogen produced, the likelihood that the mixture will ignite, and once ignited, the rate of combustion. Thus, the results from the calculations are assessed in light of the uncertainties involved in the process to yield expressions for the likelihood that the burn occurs and the likelihood that various pressures are realized.

In this PRA, the MELCOR code was used to perform the deterministic calculations because:

- It addresses all major aspects of a severe core damage accident,

- Its input structure allows the user to modify the plant model such that the many possible plant configurations during shutdown can be modelled,

- It runs quickly enough that integral calculations (i.e., from accident initiation to the release of radioactive material from the plant into the environment) and supporting sensitivity calculations can be performed for the dominant accident scenarios, and

- It allows parametric studies to be performed on parameters that may be important to the progression of the accident and the release of radioactive material.

1.3 Description of MELCOR

MELCOR [Summers et al., 1991] is an integrated, relatively fast-running, engineering-level computer code that models the progression of severe accidents in light water reactor nuclear power plants, being developed at Sandia National Laboratories for the NRC and the U. S. Department of Energy (USDOE). A spectrum of severe accident phenomena from before core degradation to the release of fission products to the environment is modelled in MELCOR in a unified framework for both boiling water reactors and pressurized water reactors. Characteristics of severe accident progression that can be treated with MELCOR include the thermal/hydraulic response in the reactor coolant system, reactor cavity, containment, and confinement buildings; core heatup, degradation and relocation; fission product release and transport; hydrogen production, transport and combustion; core-concrete attack; heat structure response; and the impact of engineered safety features on thermal/hydraulic and radionuclide behavior.

MELCOR is composed of a number of different packages, each of which models a different portion of the accident phenomenology or program control. For example, the Control Volume Hydrodynamics (CVH) package calculates the thermal/hydraulics of control volumes, and the Core (COR) package evaluates the core behavior. Each of the packages presently in MELCOR is listed:

BH Bottom Head: Models the bottom head in BWR systems. (This model was developed by Oak Ridge National Laboratory.)

BUR Combustion of Gases: Compares conditions within control volumes against criteria for deflagrations and detonations. Initiates and propagates deflagrations involving hydrogen and carbon monoxide. Calculates burn completeness and flame speed.

CAV Core-concrete Interactions: CORCON-MOD2 with enhanced sensitivity analysis and multi-cavity capabilities.

CF Control Functions: Evaluates user-specified "control functions" and applies them to define or control various aspects of the computation such as opening and closing of valves; controlling plot, edit, and restart frequencies; defining new plot variables, etc.

COR Core Behavior: Evaluates the behavior of the fuel and other core and lower plenum structures including heatup, candling, flow blockages, debris formation and relocation, bottom head failure, and release of core material to containment.

CVH Control Volume Hydrodynamics: In conjunction with the FL package, evaluates mass and energy flows between control volumes.

CVT Control Volume Thermodynamics: Evaluates the thermodynamic state within each control volume for the CVH package.

DCH Decay Heat: Used by other packages to evaluate decay heat power associated with radionuclide decay.

EDF External Data Files: Controls the reading and writing of large external data files, in close interface to the Control Function and Transfer Process packages.

EOS Equation of State: The CVT, H2O, and NCG packages are stored as one block of code under this name.

ESF Engineered Safety Features: Models the thermal/hydraulics of fan coolers, storage tanks, injection and recirculation pumps and heat exchangers, and ice condensers. Currently, only the fan cooler model is included. The containment sprays are a separate package.

EXEC Executive Package: Controls execution of MELGEN and MELCOR.

FDI Fuel Dispersal Interactions: Models ex-vessel debris relocation, heat transfer, and oxidation due to fuel-coolant interactions and direct heating.

FL Flow Paths: Models, in conjunction with the CVH package, the flow rates of gases and liquid water through the flow paths that connect control volumes.

H2O Water Properties: Evaluates the water properties based on the Keenan and Keyes equation of state extended to high temperatures using the JANAF data.

HS Heat Structures: Models the thermal response of heat structures and mass and heat transfer between heat structures and control volume pools and atmospheres. Treats conduction, condensation, convection, and radiation, as well as degassing of unlined concrete.

MP Material Properties: Evaluates the physical properties of materials for other packages except for common steam and non-condensible gas properties (see H2O and NCG).

NCG Non-Condensable Gas Equation of State: Evaluates the properties of noncondensable gas mixtures using an equation of state based on the JANAF data.

PROG Part of MELGEN/MELCOR executive package separated for computer library and link purposes.

RN Radionuclide Behavior: Models radionuclide releases, aerosol and fission product vapor behavior, transport through flow paths, and removal due to ESFs. Allows for simplified chemistry.

SPR Containment Sprays: Models the mass and heat transfer rates between containment spray droplets and control volumes.

TF Tabular Functions: Evaluates user-selected "tabular functions" to define or control various aspects of the computation such as mass and energy sources; integral decay heat; plot, edit, and restart frequencies, etc.

TP Transfer Process: Controls the transfer of core debris between various packages and the associated transfer of radionuclides within the RN package.

UTIL Utility Package: Contains various utilities employed by the rest of the code.

Only a brief summary of the phenomenological modelling in the major packages can be included here; for more detailed information, see [Summers et al., 1991].

Thermal/hydraulic processes are modelled in MELCOR by the CVH/FL packages, while the thermodynamic calculations are performed within the CVT package. The CVH package is concerned with control volumes and their contents, and the FL package represents the connections which allow transfer of these contents between control volumes.

No formal distinction is made between the reactor coolant system and containment; the same models and solution algorithms are used for both and the resulting equations solved simultaneously. Within the basic control volume formulation, the treatment is quite general; unlike the MAAP code [Fauske and Associates, 1990], no specific nodalization is built in, and there are no predefined models for reactor components such as steam generators. All systems and components are built up from general control volumes, flow paths, and other elements (such as heat structures and control functions). In some cases, the control volumes may correspond to physical tanks, with the flow paths representing pipes connecting them; in other cases, the volumes may be geometrical regions such as portions of larger physical rooms, with the flow paths representing the geometrical surfaces separating them.

Hydrodynamic materials in control volumes (i.e., coolant and noncondensables) are assumed to separate under gravity within a control volume to form a pool beneath an atmosphere. The separation need not be complete; the pool may contain vapor bubbles and the atmosphere may contain liquid droplets. The shape of the volume is defined though a user-input volume/altitude table to allow the elevation of the pool surface to be determined. The mass exchange models include both an optional thermal and mechanical equilibrium model which assumes the same pressure and temperature for both pool and atmosphere, and the default thermal nonequilibrium model which assumes the same pressure but different temperatures for pool and atmosphere.

The control volumes are connected by flow paths through which hydrodynamic materials move without residence time, driven by a momentum equation. Each control volume may be connected to an arbitrary number of others, and parallel flow paths (connecting the same pair of control volumes) are permitted; there are no restrictions on the connectivity of the network built up in this way. The flow path area can be modified by input to model valves, obstructions, etc. Appropriate hydrostatic head terms are included in the momentum equation for the flow paths, allowing calculation of natural circulation.

The HS package in MELCOR calculates one-dimensional heat conduction within an intact, solid structure and energy transfer across its boundary surfaces into control volumes. The modelling capabilities of heat structures are general and can include pressure vessel internals and walls, fuel rods with nuclear or electrical heating, steam generator tubes, piping walls, etc.

Convective heat transfer is calculated using an extensive set of heat transfer coefficient correlations for natural or forced convection to both the pool and atmosphere; pool boiling heat transfer utilizes correlations for nucleate boiling, critical heat flux, film boiling and transition

boiling. Radiation heat transfer can be specified between a heat structure surface and the boundary volume atmosphere, with two options (an equivalent band model and a gray gas model) available.

Mass transfer models for heat structure surfaces include condensation and evaporation in the presence of noncondensables with an appropriate limit for pure steam, and flashing in any environment. Liquid films on heat structure surfaces are also modelled. A user-input degassing model is provided for the release of gases from materials which are contained in heat structures, for example, to represent the release of water vapor or carbon dioxide from concrete as its temperature increases.

The MELCOR COR package calculates the thermal response of the core and lower plenum structures, including the portion of the lower head directly beneath the core, and models the relocation of core materials during melting, slumping and debris formation. The core and lower plenum are divided into a number of user-specified axial levels and concentric radial rings. A number of component types and materials are modelled. Fuel pellets, cladding, grid spacers, canister walls (for BWRs), other structure (e.g., support plates, control rods, guide tubes) and particulate debris are modelled separately within individual COR cells. Either PWR or BWR systems may be modelled.

A number of heat transfer processes are modelled in each COR cell. Thermal radiation within a cell and between cells in both the axial and radial directions is calculated, as well as radiation to boundary heat structures (e.g., the core shroud or upper plenum) from the outer and upper cells; radiation to a liquid pool (or the lower head if no pool is present) and to steam is also included. Conduction radially across the fuel-clad gap and axially between cells, and optionally between the core and radial boundary heat structures, is modelled; an analytical model for axial conduction is applied within structures that are partially covered with a liquid pool. Convection to the control volume fluids is modelled for a wide variety of fluid conditions and structure surface temperatures, including nucleate and film boiling.

Oxidation of zircaloy and steel is modelled for both the limiting cases of solid-state diffusion of oxygen through the oxide layer and gaseous diffusion of steam or oxygen through the mixture. The core degradation model treats eutectic liquefaction and dissolution reactions, candling of molten core materials (i.e., downward flow and refreezing), and the formation of liquid and particulate debris. Geometric variables (e.g., cell surface areas and volumes) are updated for changing core geometry. A lower head penetration failure model is also included.

The interaction of the core debris released from the vessel with the concrete basemat in the cavity is modelled by the CAV package in MELCOR using the CORCON-Mod2 code [Cole et al., 1984]. The molten debris may contain large amounts of unoxidized metals such as zirconium and chromium as well as oxidic species such as ZrO_2 and UO_2. These materials are assumed to stratify in the cavity because they have different densities. CORCON calculates the rate of erosion in the concrete basemat; the temperature and composition of the molten layers; and the temperature, flow rate and composition of gases (such as CO_2, CO, H_2 and water vapor) evolving from the concrete. Heat generation in the molten pool is due both to decay heat and to the heat of reactions.

The molten core debris in the cavity is assumed to be stratified as a dense bottom layer and a lighter top layer. Initially, the oxide layer is calculated to be less dense than the metallic layer, but after the molten concrete slag dilutes the heavy oxide layer, the oxide layer becomes less dense than the metallic layer and rises to the top. Each layer is assumed to be isothermal. Heat is exchanged between the melt and the concrete, between the layers in the melt, and from the top surface of the melt to the atmosphere and structures above it. The melt-concrete heat transfer is modelled by a gas film model which assumes the occurrence of Taylor-instability bubbling on the pool bottom and a flowing gas film vertically along the melt pool. Inter-layer heat transfer in the presence of gas bubbling is modelled. If a coolant layer is present over the melt pool, boiling heat transfer to the overlying coolant layer is also modelled.

The RN package models the behavior of fission product aerosols and vapors and other trace species, including release from fuel and debris, aerosol dynamics with vapor condensation and revaporization, deposition on structure surfaces, transport through flow paths and removal by engineered safety features. The package also allows for simplified chemistry controlled by the user.

Rather than tracking all fission product isotopes, the masses of all the isotopes of an element are modelled as a sum; furthermore, elements are combined into classes, groups of elements with similar chemical characteristics. Fifteen material classes are used by default: twelve containing fission products, plus boron, water and concrete oxides. User-specified combination of classes to form new classes upon release (e.g., Cs + I to CsI) is permitted.

The release of fission products from the fuel within the vessel is modelled using either the CORSOR, CORSOR-M or CORSOR-Booth representations of radiological release data for irradiated fuel. The CORSOR model is a simple correlational relationship based on data from early experiments [Nuclear Regulatory Commission, 1981]. Release of volatiles is assumed to be limited by diffusion, and all volatiles share the same release parameters, obtained by averaging experimental results; release of nonvolatiles is assumed to be limited by vaporization, and vapor pressures are scaled for consistency with experimental observations. The fractional release coefficients in CORSOR are simple exponentials, with constants selected for each species in specific temperature ranges based upon fitting experimental data; the fractional release coefficients used in CORSOR-M utilize an Arrhenius-type equation with constants representing empirical fits to experimental data. Other parameters possibly affecting release rates (such as pressure, atmospheric composition, fuel characteristics, chemistry, radiation environment, flow rates and the extent of fuel degradation) are not considered explicitly in either the CORSOR or CORSOR-M correlations. Time-dependent Cs release data from the expanded experiment data base currently available were used to fit parameters describing an effective diffusion coefficient in the new diffusion- and mass-transfer-based CORSOR-Booth model [Ramamurthi and Kuhlman, 1990]; release rates of other species are then scaled to the Cs release rate. This model includes high- and low-burnup expressions, and also is a function of fuel grain size.

Releases of radionuclides occurring during core-concrete interactions in the reactor cavity are calculated using the VANESA [Powers et al., 1986] release model, which is designed to accept melt temperatures and gas generation rates from CORCON.

Aerosol dynamic processes and the condensation and evaporation of fission product vapors after release from fuel are considered by codes included within the RN package. The aerosol dynamics models are based upon MAEROS [Gelbard, 1982], a multisection, multicomponent aerosol dynamics code, but without calculation of condensation. Aerosols can deposit directly onto surfaces such as heat structures and water pools, or can agglomerate and eventually settle out. The condensation and evaporation of radionuclide vapors at aerosol surfaces, pool surfaces and heat structure surfaces are evaluated by rate equations from the TRAP-MELT2 code [Kuhlman et al., 1986], which are based on the surface area, mass transfer coefficients, and the differences between the present surface concentration and the saturation surface concentration.

Models are available for the removal of radionuclides by pool scrubbing, filter trapping and containment spray scrubbing. The pool scrubbing model is based on the SPARC code [Owczarski et al., 1985], and treats both spherical and elliptical bubbles; the model includes condensation at the pool entrance, Brownian diffusion, gravitational settling, inertial impaction and evaporative forces for the rising bubble. The filter model can remove aerosols and fission products vapors with a specified maximum mass loading. The containment spray model is based on the model in HECTR 1.5 [Dingman, 1986] and removes both vapors and aerosols from the atmosphere.

1.4 Related MELCOR Applications

The MELCOR computer code has been developed to the point that it is now being successfully applied in both experiment analyses, intended for code validation, and in plant analyses, in support of PRAs and accident management studies. A review of MELCOR verification, validation and assessment to date reveals that most of the severe accident phenomena modelled by MELCOR have received or are receiving some evaluation [Kmetyk, 1994c].

MELCOR has been assessed against experimental test data for primary system thermal/hydraulics, in-vessel core damage and fission product release and transport, and ex-vessel and containment phenomenology, as summarized in the survey of MELCOR assessment maintained by Sandia [Kmetyk, 1994c]. Note that only analyses that are completed or already underway are included in that survey; analyses scheduled but not yet begun are not included.

Reactor coolant system thermal/hydraulic response, core heatup and degradation, and fission product and aerosol release and transport in a PWR geometry all were studied at full plant scale in the TMI-2 accident analysis, and are important in LOFT LP-FP-2. However, there is no experiment (not even the TMI accident) which represents all features of a severe accident (i.e., primary system thermal/hydraulics; in-vessel core damage; fission product and aerosol release, transport and deposition; ex-vessel core-concrete interaction; and containment thermal/hydraulics, and hydrogen transport and combustion), and only the TMI accident is at full, plant scale. It is therefore necessary for severe accident codes to supplement standard assessment against experiment (and

against simple problems with analytic or otherwise obvious solutions) with plant calculations that cannot be fully verified, but that can be judged against expert opinion for reasonableness and internal self-consistency (particularly using sensitivity studies) and also can be compared to other code calculations for consistency. Table 1 lists some of the plant analyses done with MELCOR to date, many with sensitivity studies and/or code-to-code comparisons. Only analyses that are completed are included; analyses in progress or scheduled but not yet begun are not included.

In the NUREG-1150 study reassessing risk at five plants, MELCOR was used to perform containment response calculations. In the phenomenology and risk uncertainty evaluation program (PRUEP), MELCOR calculations were performed as part of an integrated risk assessment for the LaSalle plant. MELCOR calculations have been done updating the source term for three accident sequences (AG, S2D and S3D) in the Surry plant. A TMLB' station blackout analysis for Surry, comparing results from MELCOR 1.8.2 with results from MELCOR 1.8.1 for the same transient, was done as a task in the Sandia MELCOR development project. SCDAP/RELAP5 calculations of natural circulation in the Surry TMLB' accident scenario were independently reviewed and assessed by Sandia; a number of identified uncertainties were examined by building a corresponding MELCOR model of the Surry plant and performing sensitivity studies with MELCOR on several modelling parameters. MELCOR calculations have been done to study the effects of air ingression on the consequences of various severe accident scenarios; one set of calculations analyzed a station blackout with surge line failure prior to vessel breach, starting from nominal operating conditions, while the other set of calculations analyzed a station blackout occurring during shutdown (refueling) conditions, both for the Surry plant. MELCOR calculations have been done at Sandia recently for severe accident sequences in the ABWR and the results compared with MAAP calculations for the same sequences.

The BNL MELCOR assessment effort includes plant analyses for the Peach Bottom BWR; Zion, a 4-loop Westinghouse PWR, as part of a MAAP/MELCOR comparison exercise; Oconee, a B&W PWR plant; and Calvert Cliffs, a CE PWR plant, including comparison to other code calculations. ORNL has completed a MELCOR analysis characterizing the severe accident source term for a low-pressure, short-term station blackout sequence, with flooded and dry cavities, and a LBLOCA, in the Peach Bottom BWR-4. MELCOR has been used as a severe accident analysis tool for several of the Oak Ridge test reactor programs. MELCOR has been validated by ORNL as part of the High Flux Isotope Reactor (HFIR) Safety Analysis Report (SAR) quality assurance program, before using MELCOR as the primary analysis tool for their Chapter-15 design-basis accident analyses. As part of a severe accident study for the Advanced Neutron Source (ANS) Conceptual Safety Analysis Report (CSAR), MELCOR has been used at Oak Ridge to predict the transport of fission product nuclides and their release from containment. A MAAP/MELCOR comparison study for the Point Beach plant was done as a master's thesis at the University of Wisconsin.

AEA Technology at Winfrith Technology Centre has examined the performance of the code in plant calculations, in particular for the TMLB' sequence in Surry with and without surge line failure. Three accident sequences (AB, V, and SGTR) for the Ascó II plant, and two station blackout sequences in the Garoña plant, have been done by the Catedra de Tecnologia Nuclear, Universidad Politecnica de Madrid. MELCOR has been used by the Netherlands Energy Research Foundation, Energieonderzoek Centrum Nederland (ECN) mainly to analyze severe accidents for the General Electric ABWR and SBWR designs.

MELCOR calculations have been done for two plant scenarios, a station blackout and a main steam line break, in the Teollisuuden Voima Oy (TVO Power Company) nuclear power plant, including a MAAP/MELCOR comparison study with the MAAP runs done by TVO and the MELCOR runs done by Valtion Teknillinen Tutkimuskeskus (VTT), the Technical Research Centre of Finland. More recently, an initial station blackout with a 10% break in the main steam line with recovery of power and reflooding of the overheated reactor core with auxiliary feedwater has been analyzed for the TVO plant using the MAAP, MELCOR and SCDAP/RELAP5/MOD3 computer codes.

There is substantial MELCOR use and experience at HSK (Hauptabteilung für die Sicherheit der Kernanlagen, the Swiss Federal Nuclear Safety Inspectorate). The extensive set of plant analyses done for four plants includes a number of accident sequences, sensitivity studies and a MELCOR/MAAP comparison.

MELCOR is being used in the Nuclear Power Engineering Center of the Japan Institute of Nuclear Safety (NUPEC/JINS) as a second generation code for once-through analysis of light water reactor severe accidents, to improve the accuracy of containment event

Table 1. MELCOR Plant Calculations

Plant	Plant Type
TMI-2	B&W PWR
LaSalle	BWR/5, Mark II Containment
Surry	3-loop PWR
Peach Bottom	BWR/4, Mark I Containment
Oconee	B&W PWR
Calvert Cliffs	CE 3-loop PWR
Zion	4-loop PWR
Point Beach	2-loop PWR
Browns Ferry	BWR/4, Mark I Containment
TVO	ABB, BWR
Loviisa	VVER-440
Mühleberg	BWR/4, Mark I Containment
Beznau	2-loop PWR
Gösgen	3-loop PWR
Leibstadt	BWR/6, Mark III Containment
Ascó II	3-loop PWR
Garoña	BWR/3, Mark I Containment

tree analysis and source term analysis in level 2 PSAs for Japanese light water reactors. Preliminary calculations performed using MELCOR 1.8.0 included calculations of two Peach Bottom BWR plant severe accident sequences. More recent calculations done with MELCOR 1.8.1 include PWR and BWR plant sequence analyses in support of PSA studies. The Japanese Atomic Energy Research Institute (JAERI) has done a comparative study of source terms in a BWR severe accident as predicted by THALES-2, the Source Term Code Package (STCP), and MELCOR.

MELCOR is being used by a number of groups to model VVER nuclear power plants, even though the code models are not all readily applicable to the VVER design and even though there has been no development of MELCOR for VVER phenomenology. MELCOR is being used in Hungary and in Russia to model a VVER-440/213 reactor and plant.

There have been other innovative applications of MELCOR, beyond its original planned uses. A Level 3 PRA was done for N Reactor, a USDOE production reactor, with phenomenological supporting calculations performed with HECTR and MELCOR. MELCOR was used to perform independent safety calculations for two proposed SP-100 space reactors designs; it proved possible to model and analyze simple pressure and temperature excursions for lithium coolant with the existing code. (This successful application to space reactors helps demonstrate the code's worth as a flexible analysis tool.)

1.5 Report Outline

Section 1 summarizes the background for the work documented in this report, including how deterministic codes are used in PRAs, why the MELCOR code is used, what the capabilities and features of MELCOR are, and how the code has been used by others in the past. Section 2 provides a brief description of the Grand Gulf plant and its configuration during LP&S operation. The MELCOR input model developed for the Grand Gulf plant in its LP&S configuration is described in Section 3. Section 4 presents the results of MELCOR analyses of various accident sequences for the POS 5 plant configuration, initiated at several different times after shutdown, including shortened thermal/hydraulic and core damage calculations done in support of the Level 1 analysis and full plant analyses, including containment response and source terms, supporting the Level 2 analysis. MELCOR calculations of various accident scenarios for POS 6 are given in Section 5; these include a reference calculation and sensitivity studies on assumed plant configurations and code input options used.

This page is intentionally left blank.

2 Plant Description

2.1 General Description

The Grand Gulf Nuclear Station, Unit 1 utilizes a Mark III containment design to house a BWR/6 boiling water reactor (BWR). The Grand Gulf Nuclear Station is operated by Entergy Operations Inc. Unit 1 was constructed by Bechtel Corporation and began commercial operation in July 1985. The plant is located on the east bank of the Mississippi River in southwestern Mississippi, about 10 km (6 mi) northwest of Port Gibson, Mississippi. The nearest large city is Jackson, Mississippi approximately 89 km (55 mi) to the northeast of the plant.

Because of their importance to the progression of an accident following the onset of core damage, the subsections that follow will discuss in greater detail the following features of the plant:

- primary system,
- the containment structure,
- the drywell structure and suppression pool,
- the reactor pedestal cavity,
- the hydrogen ignition system,
- the shutdown cooling system,
- the containment heat removal systems,
- the coolant injection systems, and
- secondary containment.

Much of the discussion provided in the following subsections has been extracted from the Grand Gulf Updated Final Safety Analysis Report (UFSAR) [Grand Gulf UFSAR].

2.1.1 Primary System

The nuclear reactor of Grand Gulf Unit 1 is a 3833 MWt BWR-6 single-cycle forced circulation boiling water reactor (BWR) designed and supplied by General Electric Company. In the Mark III design the reactor pressure vessel (RPV) is founded on the reactor pedestal located in the drywell. The RPV contains the core, the jet pumps, the steam separators, and the steam dryers. The vessel has an internal diameter of 6.4 m (21 ft) and an internal height of 22.3 m (73 ft). It is fabricated of low alloy steel and is clad internally with stainless steel (except for the top head, nozzles, and nozzle weld zones which are unclad). The reactor vessel has a design pressure and temperature of 8.7 MPa (1250 psig) and 575 K (575°F), respectively. The nominal pressure and temperature in the steam dome are 7.2 MPa (1040 psia) and 560 K (549°F), respectively. The reactor is cooled by water that enters the lower portion of the core and boils as it flows upward around the fuel rods. The steam leaving the core is dried by the steam separators and dryers located in the upper portion of the reactor vessel. The steam is then directed to the turbine through four main steam lines. Each steam line is provided with two isolation valves in series (i.e., main steam line isolation valves, MSIVs); one on each side of the containment barrier. Following closure of the MSIVs, 20 safety relief valves (SRVs) and associated piping are available to direct the steam in the vessel to the suppression pool and thereby provide pressure relief for the vessel. Eight of the SRVs are connected to the automatic depressurization system (ADS) which is designed to rapidly depressurize the primary system to a pressure at which the low pressure injection systems can provide coolant to the core.

The BWR-6 reactor utilizes a recirculation system to circulate the required coolant through the reactor core. The system consists of two loops external to the reactor vessel, each containing a pump, associated piping and valves, and a series of internal jet jumps (i.e., jet pumps located within the reactor vessel). The inlets to the jet pumps are located approximately 1/3 of the core height from the top of the core. The location of the jet pump inlet relative to the core is important because it will determine the amount of the core that is covered by water following a large break LOCA in the recirculation system. If injection is not restored to the vessel following a break in the recirculation system, which is the assumed location for all of the large break LOCA accidents analyzed in this study, the core coolant will drain such that only the lower 2/3 of the core is covered with water.

The reactor core is arranged as an upright circular cylinder composed of essentially two components: fuel assemblies and control rods. The core contains 800 fuel assemblies. The fuel assembly consists of a zircaloy-4 fuel channel and the fuel rods (the number of fuel rods and water rods can vary depending on the fuel design). The fuel channel provides a fixed flow path for the boiling coolant, serves as a guiding surface for the control rods, and protects the fuel during handling operations. A fuel rod consists of slightly enriched UO_2 pellets sealed in a zircaloy-2 cladding tube. The reactivity of the core is controlled by cruciform control rods dispersed throughout the lattice of fuel assemblies. The control rods, which consist of B_4C in stainless steel tubes surrounded by a stainless steel sheath, enter the core from the bottom and are positioned by individual control rod drives. The core

has an equivalent diameter of approximately 4.9 m (16 ft) and an active fuel height of 3.8 m (12.5 ft).

The RPV includes a two inch vent line. One end of the vent line is attached to the top of the vessel head; the other end of the line discharges into the sump located in the reactor cavity directly below the vessel. While this line is closed and is not used during normal operation, it is opened during cold shutdown.

2.1.2 Containment Structure

The Grand Gulf plant has a Mark III containment. The general arrangement of the containment is displayed in Figure 2-1. The containment is a cylindrical reinforced concrete structure with a steel liner and a hemispherical dome. The containment encloses both the drywell and the suppression pool. During normal operation, the drywell and containment communicate through passive vents in the suppression pool. In addition to the passive vents, there are vacuum breakers in between the containment and the drywell that allow the containment atmosphere to be vented into the drywell if the drywell pressure should drop below the containment pressure. An important feature of the Mark III containment is its large free volume 39,600 m^3 ($1.4x10^6$ ft^3) which allows it to have a low design pressure 205 kPa (15 psig). The internal design temperature is 358 K (185°F). The assessed mean failure pressure of the containment is 480 kPa (55 psig) [Harper, 1994]. Because of its large volume, the Grand Gulf containment is not inerted. Hydrogen control is accomplished via the hydrogen ignition system (HIS). The HIS is designed to deliberately burn the hydrogen at low concentrations so the accompanying containment pressurization is negligible. The ultimate heat sink is comprised of mechanical draft cooling tower structures.

Personnel can enter the containment through 3 penetrations: the equipment hatch, the upper personnel lock and the lower personnel lock. The equipment hatch is a 5.8 m (19 ft) diameter, steel pressure seating hatch. The center line of the equipment hatch penetration is located at an elevation of 52.5 m (172.25 ft). The hatch is attached from inside the containment via 20 bolts. Each personnel airlock consists of a cylindrical steel shell with steel bulkheads at each end and two steel doors in the bulkheads which open toward the reactor. Sealing of each door is accomplished by two, continuous inflatable seals which surround the door edge. The normal operating pressure of the airlock inflatable seals is 515 kPa (60 psig). The airlock doors are 2 m (6.6 ft) high by 1.1 m (3.6 ft) wide. The center line of the upper lock is 64.8 m (212.6 ft). The center line elevation of the lower lock is 38 m (124.67 ft) which is approximately 4 m (13 ft) above the nominal suppression pool level.

In the event that the containment pressure cannot be maintained below the primary containment pressure limit, the containment vent system (CVS) can be used to reduce the containment pressure. The vent path is a 0.51-m (20-in) diameter purge exhaust line which is part of the containment ventilation and filtration system. This line includes four air-operated dampers which are normally closed. The CVS discharges to the roof of the auxiliary building. The emergency operating procedures require containment venting when the containment pressure exceeds 239 kPa (20 psig).

2.1.3 Drywell Structure and Suppression Pool

In the Mark III design, the drywell and suppression pool are completely surrounded by the containment structure. The drywell structure is a cylindrical reinforced concrete structure with a flat roof and a steel drywell head. The drywell contains the reactor vessel, the SRV valves, the control rod drive (CRD) housings and the recirculation pumps. The drywell has a free volume of 7650 m^3 ($2.7x10^5$ ft^3), a design pressure of 207 kPa differential (30 psid) and an internal design temperature of 439 K (330°F). The assessed mean failure pressure of the drywell structure is 586 kPa differential (85 psid) [Harper, 1994].

The drywell volume communicates with the containment volume through the vapor suppression pool. The suppression pool serves as a heat sink during accident conditions. Passive horizontal vents in the drywell wall allow steam and noncondensibles released in the drywell to pass into the suppression pool where the steam is condensed and the noncondensibles are released into the containment atmosphere. The suppression pool has two regions. The first region is located in the containment (i.e., wetwell) and is bounded on one side by the containment wall and on the other side by the drywell wall. The second region is in the drywell and is bounded on the one side by the drywell wall and on the other side by the weir wall. The passive horizontal vents in the drywell wall connect the two regions of the pool. There are a total of 135 vents (three rows of vents and each row has 45 vents); each vent has a nominal diameter of 0.71 m (2.33 ft). The suppression pool has a nominal volume of 368 m^3 (136,000 ft^3).

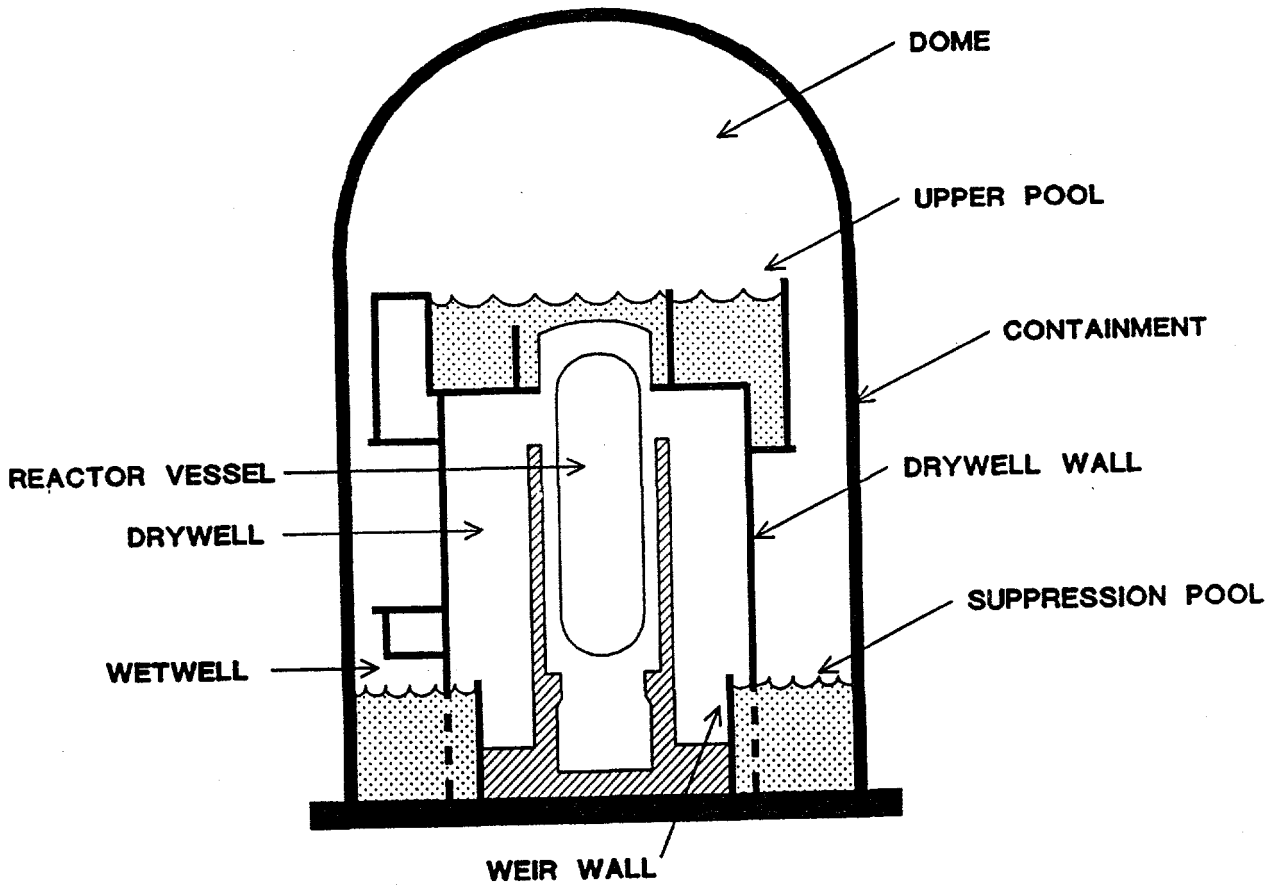

Figure 2.1. Schematic of Grand Gulf Containment

In the event that the drywell pressure drops below the containment pressure, there are vacuum breakers in the drywell wall that will open and allow the pressure in the two volumes to equilibrate. These vacuum breakers are powered by emergency ac power.

Personnel can access the drywell through two penetrations: the drywell equipment hatch and the drywell personnel lock. The drywell equipment hatch is approximately 3 m (10 ft) in diameter and its center line is located at an elevation of 37.3 m (122.4 ft). The drywell personnel lock is similar in design to the containment personnel locks. The center line of the drywell personnel lock is located at an elevation of 36.6 m (120 ft).

2.1.4 Reactor Pedestal Cavity

The reactor pedestal cavity is located directly below the RPV. The upper section of the cavity is formed by the 1.8 m (5.75 ft) thick pedestal wall and the lower section of the cavity is recessed into the drywell floor. The pedestal cavity is essentially a right cylinder with a diameter of 6.5 m (21.17 ft) and a depth of approximately 8.5 m (28 ft). The upper section of the cavity contains CRD housings. The major pedestal penetrations are the CRD piping penetrations at the top of the pedestal and the CRD removal opening which is a 0.9 m (3 ft) by 2.1 m (7 ft) doorway located 2.9 m (9.5 ft) above the cavity floor.

When the drywell is flooded to the top of the weir wall, a water depth of 6.9 m (22.8 ft) can be established in the cavity. Water can enter the cavity from either the vessel following failure of the bottom head of the RPV or from the drywell. Water can enter the drywell during a LOCA or from overflow from the suppression pool. There are two paths by which water in the drywell can enter the reactor cavity. The first pathway is through the drywell floor drains. There are four 0.1-m (4-in) drains in the drywell floor that connect to the equipment drain sump in the pedestal. The second pathway is through a door in the pedestal located 1.0 m (3.33 ft) above the drywell floor.

2.1.5 Hydrogen Ignition System

The Grand Gulf containment utilizes a hydrogen ignition system (HIS) to control the accumulation of hydrogen during accident conditions. In the core region there is an abundant supply of zirconium (i.e., fuel cladding, channel boxes) which, at the elevated temperatures typical of core damage accidents, readily reacts with steam to produce hydrogen. The function of the HIS is to prevent the buildup of large quantities of hydrogen inside the containment during accident conditions. This is accomplished by igniting, via a spark, small amounts of hydrogen before large amounts accumulate. The HIS consists of 90 General Motors ac powered glow plugs (Model 7G). The HIS is manually actuated. Igniters are located throughout the containment and drywell volumes. The Grand Gulf Emergency Procedures indicate that the HIS is not to be used after hydrogen levels exceed 9%.

2.1.6 Shutdown Cooling System

The shutdown cooling system (SDC) is used to remove decay heat generated in the core following shutdown. The SDC system is but one mode of the residual heat removal (RHR) system and, as such, shares components with the other modes (i.e., containment spray and suppression pool cooling) The SDC system is a two train system consisting of motor-operated valves and motor driven pumps. Both trains have two heat-exchangers in series down stream of the pump. The SDC system takes reactor coolant from one of the recirculation pumps suction lines, passes it through the SDC system pump, cools it in the heat exchanger, and then injects it back into the vessel.

The valves that isolate the low pressure piping components of the SDC system from the primary system require ac power to change position. Therefore, if the SDC system is being used to cool the core and there is a loss of both offsite and onsite power, these valves will remain open. In the event that the primary system pressurizes significantly above the design pressure of the SDC system, it estimated that the low pressure components of the SDC system will fail resulting in a large break LOCA outside the containment. Since the break is effectively in the recirculation system, the core coolant will drain to approximately 2/3 core height if coolant makeup is not provided to the core.

2.1.7 Containment Heat Removal Systems

Suppression pool cooling (SPC) and the containment spray system (CSS) are two modes of the RHR system. The RHR system is a two train system with motor-operated valves and pumps. Both trains have two heat exchangers in series downstream from the pump. The function of SPC is to remove decay heat from the suppression pool during accident conditions. The SPC system takes suction from the suppression pool, cools the

water by passing the water through heat exchangers (with service water on the shell side), and returns the water to the suppression pool. The SPC system is manually initiated and controlled. The function of the CS system is to suppress the pressure in the containment during accidents. This is accomplished by taking suppression pool water, passing it through a heat exchanger and distributing the water as fine droplets into the containment atmosphere via a series of spray headers in the containment dome. There are no spray headers in the drywell. Both the SPC and the CS modes of RHR require ac power.

2.1.8 Coolant Injection Systems

In a BWR there are many systems that can be used to supply coolant to the core. Systems that can be used when the reactor pressure is high include the high pressure core spray system (HPCS) and the reactor core isolation cooling system (RCIC). The control rod drive system (CRD) can be used as a backup source of high pressure injection. Systems that are used when reactor pressure is low include the low pressure core spray system (LPCS) and the low pressure coolant injection system (LPCI). Additional systems that can be aligned and used as alternate sources of low pressure injection include the service water cross-tie system (SSW cross-tie), the condensate system, and the firewater system.

In some of the accident sequences the operators attempt to flood the containment prior to core damage in an effort to prevent fuel failure. In these sequences, the operators use the SSW cross-tie system to take water from the cooling tower basin and inject it into the reactor vessel via the LPCI system train B injection lines. Once the vessel is full, the water passes into the suppression pool via the SRV tailpipes. By this mode of injection, the containment can be flooded by flooding the suppression pool.

In most of the accident scenarios analyzed with MELCOR, coolant injection was not available after the onset of core damage. In the few scenarios in which injection was recoverable, the only system that could be used was the firewater system.

The firewater system can be used as a backup source of low pressure injection. The firewater system is a three train system consisting of one motor-driven pump and two diesel-driven pumps. The pumps feed into a common header that supplies water to the fire hoses. The pumps take suction from two 1136 m^3 (300,000 gallon) water storage tanks. The fire hoses are connected, via an adapter, to various test connections in the auxiliary building. These connections feed into various injection systems and water can then be injected through the systems' injection valve. The firewater system can supply approximately 20.2 l/s (320 GPM) at a vessel pressure of 101 kPa (0 psig); the shut off head is approximately 736 kPa (92 psig). The operator is required to align the system and to start the pumps.

2.1.9 Secondary Containment

The Grand Gulf plant utilizes a secondary containment that completely encloses the primary containment. The performance objective of the secondary containment is to provide a volume completely surrounding the primary containment which can be used to hold up and dilute fission products that might otherwise leak to the environment following a design basis accident. Two buildings form the secondary containment.

The auxiliary building is a reinforced concrete structure which completely surrounds the lower portion of the containment. This building, which contains safety systems, fuel storage and shipping equipment and necessary auxiliary support systems, consists of four floors with each floor consisting of many rooms that can be isolated from the rest of the floor by doors. The free volume of the auxiliary building is approximately 85,000 m^3 ($3x10^6$ ft^3).

The enclosure building is a metal-siding structure that completely encloses the upper portion of the containment above the auxiliary building roof. The free volume of the enclosure building is approximately 17,000 m^3 (600,000 ft^3).

Following a design basis accident during normal operation, the standby gas treatment system (SGTS) functions to provide a mixing of these volumes (i.e., auxiliary building and enclosure building), and maintains the volumes at a slightly negative pressure. The exhaust air required to maintain the negative pressure is discharged through the SGTS charcoal filter trains. During the modes of shutdown investigated in this study, however, the SGTS is not required to be available and, therefore, it is assumed not to be available in this analysis. Furthermore, without the SGTS to providing mixing of the building atmosphere, the volume available to hold up radioactive releases can vary depending on which rooms are isolated and which are open.

This page is intentionally left blank.

3 MELCOR Computer Model

The base case MELCOR input model used for these Grand Gulf shutdown analyses is shown in Figure 3.1. There are a total of 19 control volumes, 36 flow paths, and 57 heat structures in this base case model; a few control volumes, flow paths and/or heat structures were added to or removed from this model for various analyses, as required. All control volumes were specified to use nonequilibrium thermodynamics and were specified to be vertical volumes; all heat structures used the steady-state temperature-gradient self-initialization option. Detailed volume-altitude tables and junction flow segments were used to correctly represent subcomponents in and between the major components modelled.

The primary system (i.e., the reactor pressure vessel) was represented by six control volumes: one each for the downcomer, lower plenum, upper plenum, steam separators, steam dome, and the core and bypass channels. The vessel model [Shaffer, memo, 1991] is depicted in more detail in Figure 3.2, with flow paths and heat structures shown. (The core model is discussed separately later in this section.) The recirculation loop piping was not modelled for these calculations, because it was assumed that circulation within the recirculation piping would not significantly affect the boiloff results.

Previous Grand Gulf calculations [Dingman et al., 1991] used a modified LaSalle core and reactor cooling system. These models, particularly the core model, have been improved since then to better represent Grand Gulf [Shaffer et al., 1992]; these models still contain LaSalle-specific data but the parameters of importance have been converted to or verified as Grand Gulf data to the extent possible given the limited available plant data. For instance, the core model has the proper fuel assembly and control rod masses, and the primary system volumes are in reasonable agreement with the volumes stated in the FSAR (Grand Gulf Nuclear Station), but certain flow loss coefficients were not known specifically for Grand Gulf.

For the POS 5 analyses discussed in Section 4, a flow path was added representing the RPV head vent, a piping line extending from the upper head to the pedestal cavity; depending on the sequence being simulated, the RPV head vent flow path was open or closed, and the SRV flow path was locked open, locked closed, or cycled in the relief mode, as required. Flow paths were added for the open MSIV line and for the SDC break as needed for individual POS 5 scenarios. For the POS 6 analyses discussed in Section 5, a flow path was added representing the vessel upper head open to the drywell and the flow path representing the SRVs was set to a zero area. In all cases, a flow path representing the vessel breach provided the thermal/hydraulic outflow when penetrations in the lower head failed, because the COR package only handles ejection of core debris.

Figure 3.3 highlights the MELCOR input model for the containment, taken directly from the MELCOR model used for the NUREG-1150 supporting analyses [Dingman et al., 1991]. The outer containment was represented by five control volumes (dome, equipment hatch, upper annulus and lower annulus, and wetwell) and the inner containment by three (upper drywell, pedestal cavity and weirwall). Flow paths representing the drywell personnel lock and the containment personnel locks and the containment equipment hatch were added. In the POS 5 analyses described in Section 4, the flow path modelling the drywell personnel lock was always fully open, while the flow paths for the containment upper and lower personnel locks and equipment hatch were open or closed as required in particular accident sequences; in the POS 6 analyses described in Section 5, the drywell head was modelled as open, the flow path modelling the containment equipment hatch was always open, while the flow paths for the upper and lower containment personnel locks were sometimes open, and closed in other calculations. Several of the flow paths between volumes in the containment were divided into higher-elevation and lower-elevation flow-path pairs to allow better representation of gas and liquid flows. In some calculations the containment was assumed open to the auxiliary building or directly to the environment; in others, a 489.5 kPa (71 psia) containment failure pressure was used.

The cavity was specified to be a flat-bottomed cylinder with an internal depth and radius of 3.921 m and 3.226 m, respectively; the concrete is 1.752 m thick on the sides and 2.0 m thick below the cavity. The cavity consists of limestone/common sand concrete with 0.135 kg/kg rebar; the ablation temperature is set to 1503 K.

A model for the auxiliary building, depicted in Figure 3.4, was developed specifically for these analyses, primarily from the limited information in the FSAR (Grand Gulf Nuclear Station). Two variations were considered; in both, the auxiliary building model consists of four control volumes (one for each floor), a number of flow paths (three between floors, one from the stairwell to the environment and various inflow paths from containment)

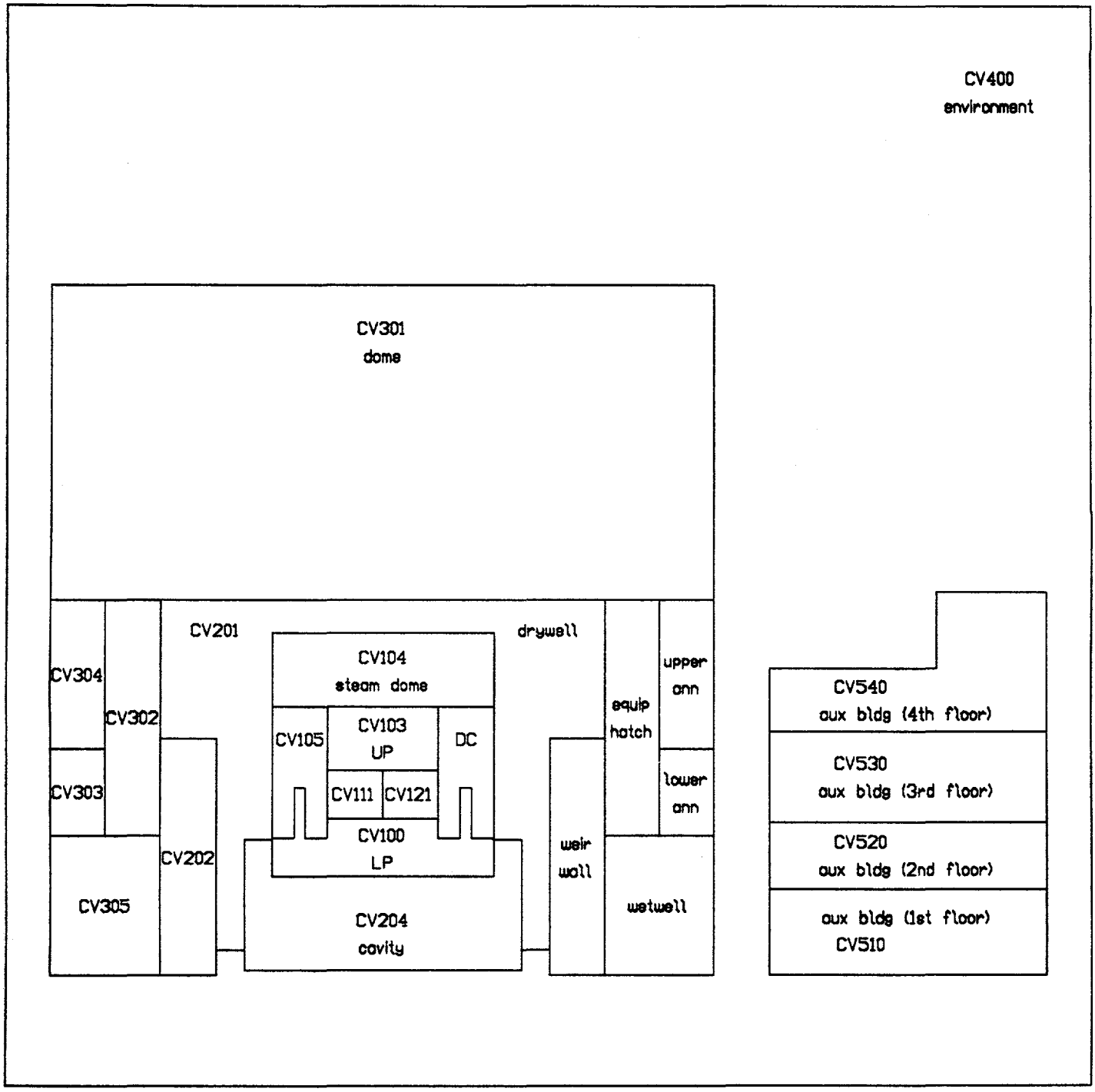

Figure 3.1. Base Case MELCOR Model for Grand Gulf Analyses

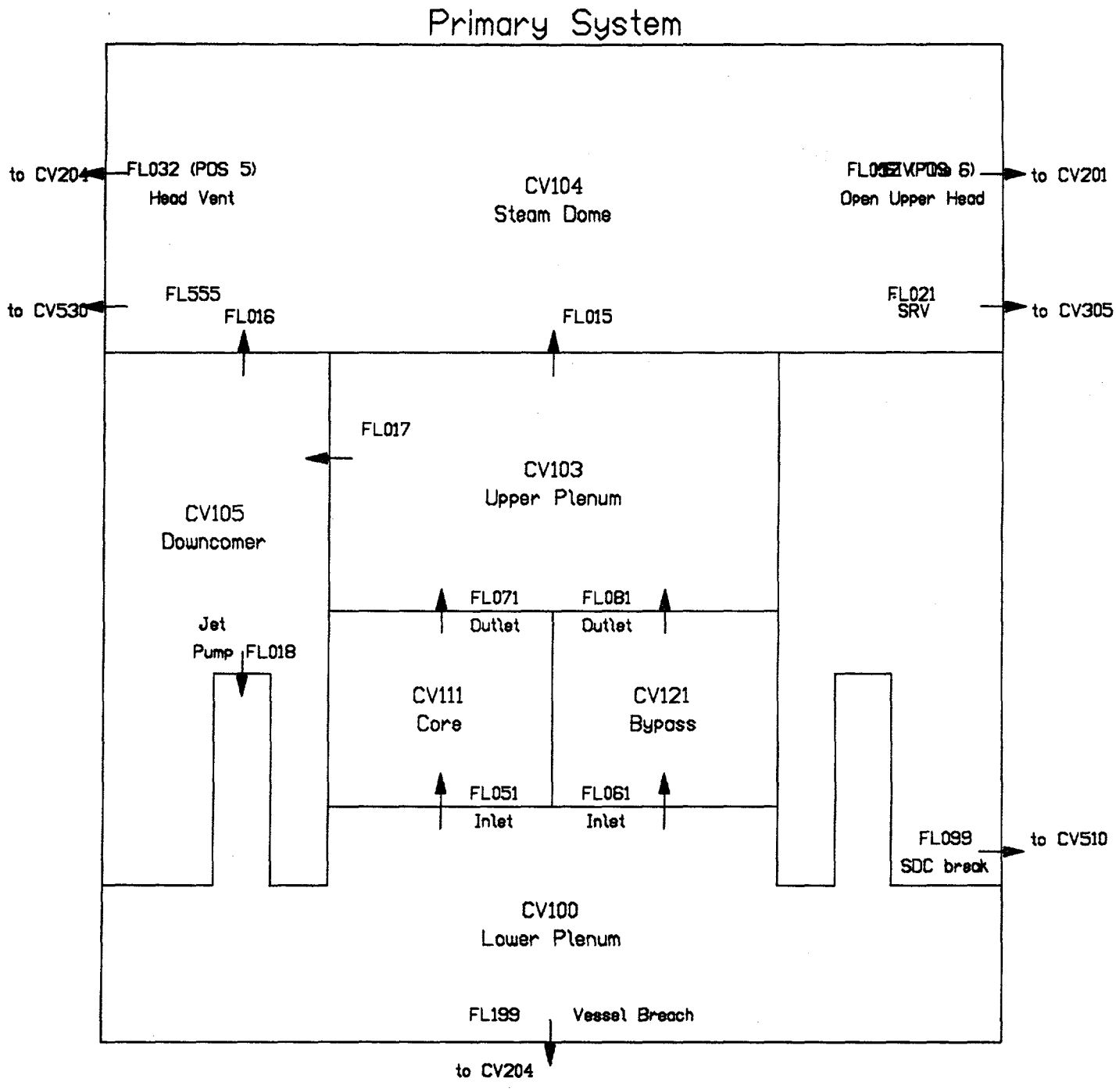

Figure 3.2. MELCOR Model for Grand Gulf Primary System

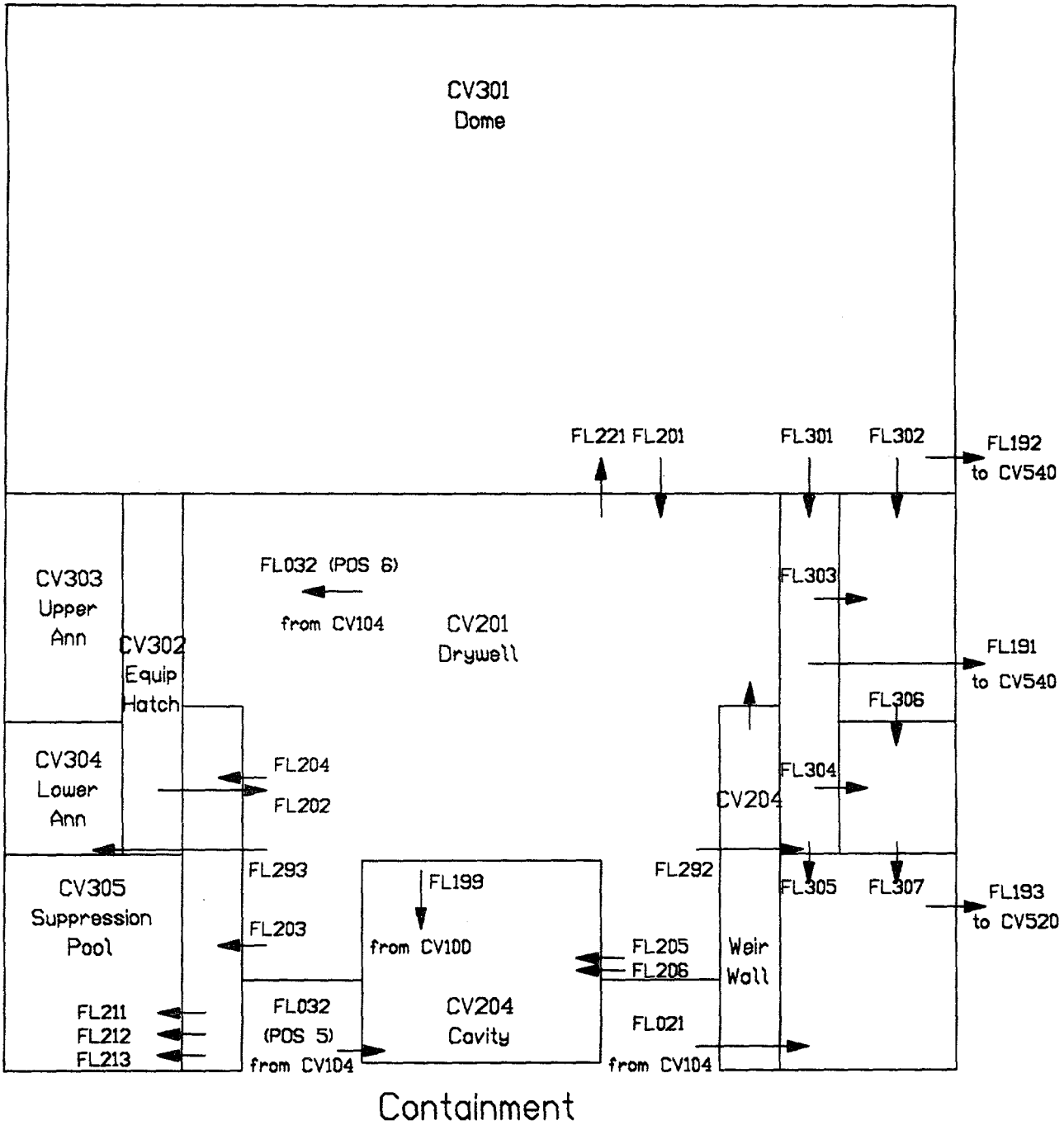

Figure 3.3 MELCOR Model for Grand Gulf Containment

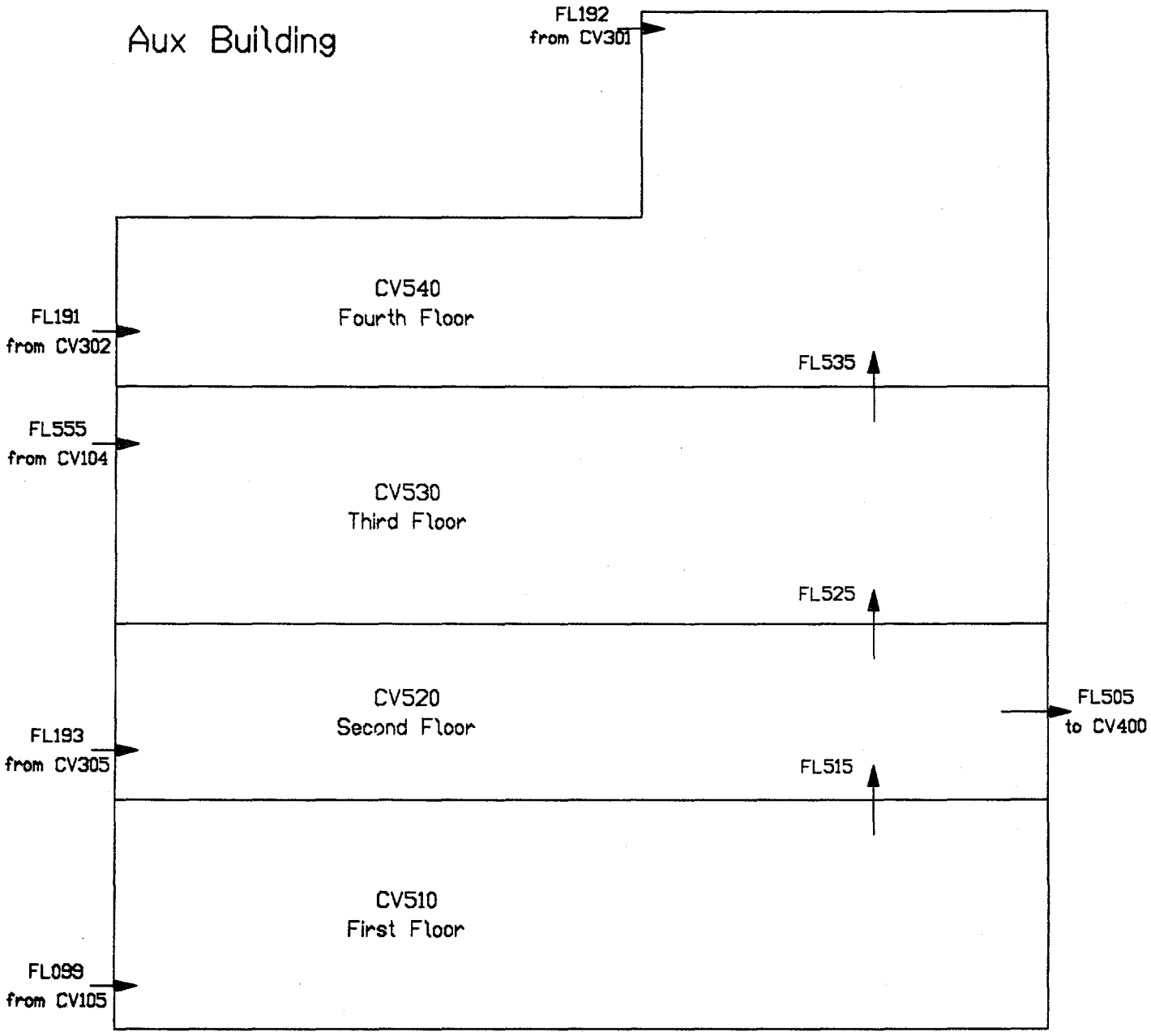

Figure 3.4. MELCOR Model for Grand Gulf Auxiliary Building

and heat structures (five for floors and/or ceilings, four for external walls and four for internal walls), but the volumes and surface areas are changed. The open auxiliary building model represented open interior doors, resulting in larger open volumes and heat structure surface areas for flow-through and potential retention and/or deposition of aerosols before the stairwell door to the environment is blown open at 135.85 kPa (5 psig overpressure). The closed auxiliary building model represented the interior doors remaining closed while the stairwell door to the environment is blown open.

The containment equipment hatch and upper personnel lock open to the fourth floor in the auxiliary building, while the containment lower personnel lock opens to the second floor. For one POS 5 sequence the flow path representing the MSIV line was open, and goes from the upper vessel to the third floor of the auxiliary building. For several other POS 5 scenarios a break in the SDC line is represented, which goes from the vessel downcomer to the first floor of the auxiliary building. The auxiliary building can vent to the environment through a stairway door, taken as coming from the second floor of the auxiliary building.

The base case core model [Shaffer, memo, 1991] consists of six radial rings and 13 axial levels, for a total of 78 core cells, as illustrated in Figure 3.5. Axially, five levels are used in the lower plenum, one of which corresponds to the core support plate, and eight levels are used in the core itself. The active fuel region of the core was subdivided into six axial levels of equal height (25 in); the lowest and highest levels in the core region contain only support structures, not fuel.

The 800-assembly Grand Gulf core contains a total of 179,760 lbm of Zr, 98.7 lbm in each assembly canister and 126 lbm in the fuel rods. In addition, the FSAR gives the total fuel mass as 458 lbm/assembly for a total UO_2 mass of 366,400 lbm. The total fuel assembly and control masses are given as 699 and 218 lbm, respectively; there are 193 control rods in the core. The Grand Gulf fuel rods appear to be identical to the LaSalle rods and both have an 8 x 8 matrix. Grand Gulf, however, has a thicker canister than LaSalle, in addition to 36 more fuel assemblies and 8 more control rods than LaSalle.

LaSalle data was used for the top guide, core plate, fuel supports, control rod tubes and housings masses. These were subdivided into radial and axial cells corresponding to the cells for the power distribution. The subdivided masses are reasonably accurate for the active fueled core region and the correct total masses are maintained. The mass distribution outside of the fueled region (i.e., the handles, the lower tie plate, the fuel support pieces, control rod velocity limiters, etc.) were estimated from the available data and drawings.

Other core model input quantities were computed in a similar manner as the masses; these include the component surface areas, the flow areas, cross-sectional areas, and equivalent diameters. Inputs for the vessel lower head and penetrations still reflect the LaSalle data.

The core decay power distribution was developed from FSAR end-of-cycle (EOC) data. Since the radial power distribution dips at the core center, the inner portion of the core was subdivided to focus on the region with the highest power density (the second ring). The time-dependent decay power was calculated using the normalized time-dependent power distribution developed for the LaSalle plant (which is the same power curve used in previous Grand Gulf calculations). The operating power level was 3833 MW when the reactor was tripped.

The default classes in the MELCOR RN and DCH packages were used. The default classes and initial inventories are presented in Table 3.1; as shown in this table, a small fraction of these inventories was specified to be in the gap rather than in the fuel. Most of our calculations were done using the MELCOR default fission product release model (i.e., CORSOR-M); Section 5.4.1 presents the results of using a POS 6 analysis using the alternative CORSOR release model option. These Grand Gulf shutdown analyses also were done specifying two MAEROS components and five aerosol distribution size bins (the MELCOR default), with the minimum diameter reduced by an order of magnitude from the default value, to 0.1μm.

MELCOR gives radionuclide inventories in terms of both "total" mass and "radioactive" mass. Only the radioactive masses are given in this report. The total and radioactive values can be different for the Cs, Ba, Te, Ru, Mo, Ce, U and Sn classes. For several of these, the difference is due only to the use of a different compound molecular weight for the total than the elemental weight used for the radioactive mass, i.e., CsOH vs Cs, TeO vs Te, and UO_2 vs U. There is no difference in the default elemental and compound molecular weights for the other classes with unequal total and radioactive masses; instead, the differences between total and radioactive masses are due to the inclusion of aerosolized core structural materials and clad. The platinoids class (Class 6,

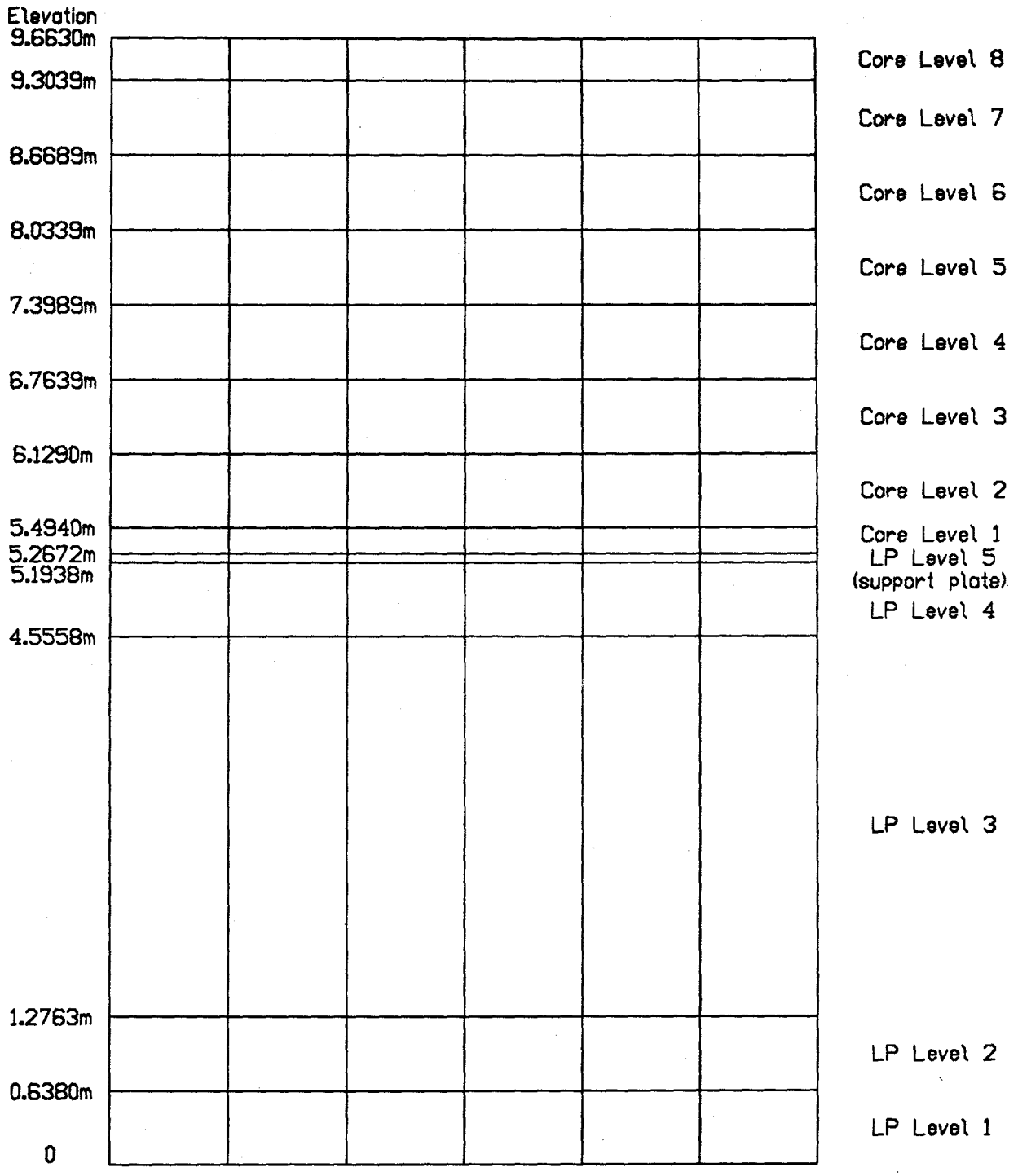

Figure 3.5. Base Case MELCOR COR Model for Grand Gulf

Table 3.1. Initial Radionuclide Class Inventories

Class	Initial Mass (kg)	Initial Gap Inventory (%)
1 (Xe)	463.71	3.0
2 (Cs)	268.35	5.0
3 (Ba)	207.52	0.0001
4 (I)	20.931	1.7
5 (Te)	40.789	0.01
6 (Ru)	306.99	0.0
7 (Mo)	350.64	0.0
8 (Ce)	593.95	0.0
9 (La)	571.05	0.0
10 (U)	132,386	0.0
11 (Cd)	1.4065	0.0
12 (Sn)	8.5872	0.0

represented by ruthenium) includes nickel, found in stainless steel; the other major components of stainless steel, iron and chromium, are included in the Mo class. The tetravalent class (Class 8, represented by cerium) includes zirconium, a major clad component; the Sn class includes the tin found normally in zircaloy and released as the clad melts.

Also note that, while there are 15 default RN classes in MELCOR and those default classes were used for the POS 6 analyses (with CsI added as Class 16 in most of the POS 5 analyses), no values are given in this report for Class 13 (boron), Class 14 (water) or Class 15 (nonradioactive aerosols generated during core-concrete interaction), all of which have identically zero radioactive masses.

A large number of control functions were used to track the total and radioactive masses of each class released from the intact fuel and/or debris in the vessel (either in the core, the bypass or in the lower plenum); released from the debris in the cavity; remaining in the primary system (i.e., the reactor vessel); in the inner containment (in the drywell and cavity, and the weirwall atmosphere and walls); in the outer containment (in the dome, annulus, equipment hatch, and suppression pool atmosphere and walls); in the water in the suppression pool and weirwall; in the auxiliary building; and in the environment. Those control functions provided time-dependent source term release and distribution data for subsequent postprocessing. Control functions were used also to force edit and restart dumps when specified events occurred (e.g., when the clad first failed, when specified amounts of hydrogen had been generated, when each lower head penetration failed, when the containment and/or auxiliary building failed).

Most of the MELCOR calculations done for the POS 5 Level 1 study described in Section 4.1 were run with MELCOR 1.8.2 (version 1.8OC) on an IBM/RISC-6000 Model 550 workstation; most of the MELCOR calculations done for the POS 5 Level 2/3 study described in Section 4.2 were run with MELCOR 1.8.2 (version 1.8OM) on a HP/9000 Model 755 workstation. All MELCOR calculations for the POS 6 study were run with MELCOR 1.8.1 (version 1.8IV) on the IBM/RISC-6000 Model 550 workstation.

4 POS 5 Calculations

4.1 Description of POS 5

POS 5 is rigorously defined as: "Cold Shutdown (Operating Condition 4) and Refueling (Operating Condition 5) only to the point where the vessel head is off." POS 5 can be entered coming down from power or in going back up to power. During a refueling outage the plant can be in POS 5 for an extended period of time; the event that initiates the accident can occur anytime during this time period. Since the decay heat load from the core decreases with time, the amount of time that is available to the operators to respond to an accident will depend on when the event that initiates the accident occurs during POS 5. Because of this dependency on time, the time the plant is in POS 5 is divided into segments or "time windows"; a unique decay heat level is then assigned to each window. To keep the calculations manageable, only three time windows were defined for POS 5. The selection of the time windows was based on the availability of systems used to mitigate the accident and the time required to perform actions necessary to restore systems designed to mitigate the accident. In POS 5, there are two natural time segments, the time the plant is in POS 5 before refueling (i.e., coming down from power) and the time the plant is in POS 5 following refueling (i.e., going back up to power). The decay heats for these two segments will be significantly different. The first segment was further subdivided to account for the availability of an alternate source of decay heat removal. The Alternate Decay Heat Removal System (ADHRS) can be used to remove decay heat from the core once the reactor has been shut down for at least 24 hours. Thus, the first segment was divided to distinguish the time in POS 5 prior to 24 hours after shutdown from the time in POS 5 after 24 hours after shutdown.

Based on reviews of the refueling outage (RFO) critiques for RFOs 2, 3, and 4, on average, the plant enters POS 5 14 hours after shutdown and remains in POS 5 for 80 hours before entering POS 6. On the way back up to power, the plant again enters POS 5 40 days after shutdown and remains in POS 5 for 10.4 days. Based on this information, the three time windows were defined as:

Time Window 1: Starts 14 hours after shutdown and has a duration of 10 hours.

Time Window 2: Starts 24 hours after shutdown and has a duration of 70 hours.

Time Window 3: Starts 40 days after shutdown and has a duration of 10.4 days.

Although the plant can enter POS 5 during a refueling outage (RFO) as fast as 7 hours after shutdown, 7 hours was not used as the start time for Window 1 because review of the refueling outage critiques indicated that 14 hours was a more typical value. However, to account for the fact that the plant could enter POS 5 as soon as 7 hours after shutdown, the decay heat load used to represent Window 1 was the decay heat load 7 hours after shutdown. The decay heat used to represent Window 2 is the decay heat load 24 hours after shutdown. Similarly, the decay heat used to represent Window 3 is the decay heat load 40 days after shutdown.

The configuration of the plant during POS 5, as modelled in the Level 2/3 analysis, was determined from requirements imposed by the technical specifications [Nuclear Regulatory Commission, 1984] and from plant procedures and practices during a refueling outage (i.e., information was received in the form of critiques of refueling outages and interviews with plant personnel). The technical specifications were used to define the minimum set of requirements. If a system was not required by the technical specifications to be operable, then the plant procedures and practices were reviewed to obtain the status of the system. In actual practice, the configuration of the plant continues to change during POS 5. For example, the containment equipment hatch is removed during this POS. Thus, when the POS is initially entered, the hatch is attached and then it is subsequently removed during the POS changing the configuration of the plant in the process. To keep the analysis manageable, it was often necessary to make simplifying assumptions with regard to the configuration of the plant when the accident was initiated. The configuration of the plant at the start of the accident, as modelled in the Level 2/3 analysis, is defined below:

Containment: The technical specifications do not require the primary or the secondary containments during POS 5. Review of the Grand Gulf refueling critiques indicated that the containment equipment hatch is typically removed shortly after entering POS 5. In this analysis, it was assumed that the equipment hatch and both personnel locks are open when the accident is initiated. Given that the necessary support systems are available, it was assumed that the containment could be vented in the event

that the containment was closed prior to the onset of core damage.

Drywell Integrity: The technical specifications do not require that the drywell integrity be maintained during POS 5. Review of the Grand Gulf refueling critiques indicated that the drywell personnel lock is open and equipment hatch is typically removed early in POS 5. Furthermore, during POS 5 a portion of the upper reactor pool is drained and the drywell head is removed. It was assumed that either the drywell equipment hatch or the drywell personnel locks were open and remained open throughout the accident.

Reactor Pressure Vessel: In cold shutdown the reactor pressure vessel head is on. While the technical specifications do not require any SRVs to be available, Grand Gulf administrative procedures require at least two SRVs to be available. Therefore, in this analysis it was assumed that two SRVs were available. The temperature of the vessel water is required by the technical specifications to be less than 200°F. The water level can either be at the normal level or the natural circulation level. For the purposes of this analysis, it was assumed that at the start of the accident the reactor water was at the normal level and its temperature was 200°F. The RPV head vent was assumed to be open at the start of the accident. The status of the MSIVs (i.e., open or closed) is accident-specific.

Suppression Pool: The suppression pool inventory is accident specific. Three levels were considered: (1) low water level 5.6 m (18.375 ft), (2) drained level 3.86 m (12.67 ft), and (3) empty with 170,000 gal available to HPCS from the condensate storage tank.

Hydrogen Ignition System: The technical specifications do not require the HIS to be available during POS 5. However, since it is the practice at the plant to perform train-based maintenance during a refueling outage, and half of the igniters are on Train A and the other half are on Train B, it was assumed in this analysis that at least one train of HIS will always be available (note, however, the HIS will not operate without ac power).

4.2 Level 1 Thermal/Hydraulic Support Calculations

A series of MELCOR calculations was done to support the quantification of the Level 1 PRA models. For these calculations, the parameters of interest include the times to reach various pressure and/or levelsetpoints, the time to top-of-active-fuel (TAF) uncovery, the times to core heatup and clad failure (at 1173 K) and the time to vessel failure.

Several general scenarios when the plant is in POS 5 have been considered:

1. Open MSIVs: At the initiation of the accident, the MSIVs on all four steam lines are open. The initiating event then results in a loss of all core cooling and coolant makeup. The SRVs and the reactor pressure vessel head vent are closed at the beginning of the transient.

2. Low Pressure Boiloff: At the initiation of the accident, two SRVs are open. The initiating event then results in a loss of all core cooling and coolant makeup. The reactor pressure vessel head vent is closed at the beginning of the transient.

3. High Pressure Boiloff with Closed RPV Head Vent: At the initiation of the accident, the SRVs are closed. The SRVs remain closed during the accident and only open to relieve pressure at the safety setpoint. The initiating event then results in a loss of all core cooling and coolant makeup. The reactor pressure vessel head vent is closed at the beginning of the transient.

4. High Pressure Boiloff with Open RPV Head Vent: This scenario is identical to case 3, except that the reactor pressure vessel head vent is open.

5. Large Break LOCA: This accident is initiated by a large break LOCA in a 24 in-OD recirculation line. At the start of the accident, the SRVs are closed. The break drains the vessel to 2/3 core height. The initiating event then results in a loss of all core cooling and coolant makeup. The reactor pressure vessel head vent is closed at the beginning of the transient.

6. Station Blackout with Failure to Isolate SDC: The accident is initiated by a loss of offsite

power. Following the initiating event, onsite power is lost leading to a SBO and loss of all core cooling and coolant makeup. The operator fails to open the SRVs and steam the core at low pressure (i.e., the SRVs operate in the relief mode). Since the SRVs are closed, the RPV will pressurize. The SBO precludes the isolation of the low pressure piping in the SDC system. This low-pressure SDC system piping fails when the RPV pressure reaches 3.135 MPa (440 psig) resulting in an interfacing systems LOCA.

7. Station Blackout with Firewater Addition: The accident is initiated by a loss of offsite power. Following the initiating event, onsite power is lost leading to a SBO and loss of all core cooling and coolant makeup. The operator opens two SRVs at 2 hr and steams the core at low pressure while adding coolant from the firewater system to the core bypass region. Firewater addition can be maintained indefinitely.

8. Station Blackout with 10 hr Firewater Addition Followed by High Pressure Boiloff: The accident is initiated by a loss of offsite power. Following the initiating event, onsite power is lost leading to a SBO and loss of all core cooling and coolant makeup. The operator opens two SRVs at 2 hr and steams the core at low pressure while adding coolant from the firewater system to the core bypass region. The SRVs are shut at 12 hr after accident initiation, after which they operate in the relief mode. Since the SRVs are now closed, the RPV can pressurize.

9. Station Blackout with 10 hr Firewater Addition Followed by Failure to Isolate SDC: The accident is initiated by a loss of offsite power. Following the initiating event, onsite power is lost leading to a SBO and loss of all core cooling and coolant makeup. The operator opens two SRVs at 2 hr and steams the core at low pressure while adding coolant from the firewater system to the core bypass region. The SRVs are shut at 12 hr after accident initiation, after which they will operate in the relief mode. Since the SRVs are now closed, the RPV will pressurize. The SBO precludes the isolation of the low pressure piping in the SDC system. This low-pressure SDC system piping fails when the RPV pressure reaches 3.135 MPa (440 psig) resulting in an interfacing systems LOCA.

In all cases, at the initiation of the accident, the reactor vessel is depressurized, and the coolant is at the normal level (i.e., 554.7 inches actual level or 569.7 inches measured level). Also, in all these cases, the drywell personnel lock is open; the containment equipment hatch and both of the containment personnel locks are open (i.e., "open containment").

Calculations were performed for several different times from shutdown for each of these accident scenarios: 7 hr, 24 hr, 59 hr, 12 days, and 40 days. The first two times correspond to the times used to determine the decay heats for the first and second time windows; the third time corresponds to the midpoint of the second time window; the last time corresponds to the time corresponding to the decay heat level in the third time window. (Some calculations were done for 12 days after shutdown while the decay heat table in the MELCOR deck only extended to 1.0×10^6 s after shutdown; after the decay heat table was extended to ≥50 days, calculations were done starting 40 days after shutdown.)

Because the primary interest was in time to core damage, these Level 1 support calculations were run until any of the following occurred: vessel failure, code abort or 24 hr of transient. If any sequence produced no significant core damage within 24 hr for a given decay heat level, no further calculations were done with longer shutdown times (i.e., lower decay heat levels).

4.2.1 Open MSIVs

At the initiation of the accident, the reactor vessel is depressurized, the coolant is at the normal level and the MSIVs on all four steam lines are open. The vessel water inventory is at 366.5 K (200°F), which corresponds to the maximum temperature allowed by the Grand Gulf technical specifications for operation in POS 5. The initiating event then results in a loss of all core cooling and coolant makeup. The SRVs and the reactor pressure vessel head vent are closed at the beginning of the transient. The drywell personnel lock is open; the containment equipment hatch and both of the containment personnel locks are open (i.e., "open containment").

Figure 4.2.1.1 gives the vessel pressures calculated starting this accident scenario at several different times after shutdown. In all cases, the system begins pressurizing as all core cooling is lost but only pressurizes to about 150 kPa before the steam flow out the open MSIVs is sufficient to remove all the decay heat. The steam flow out the MSIVs in turn pressurizes the

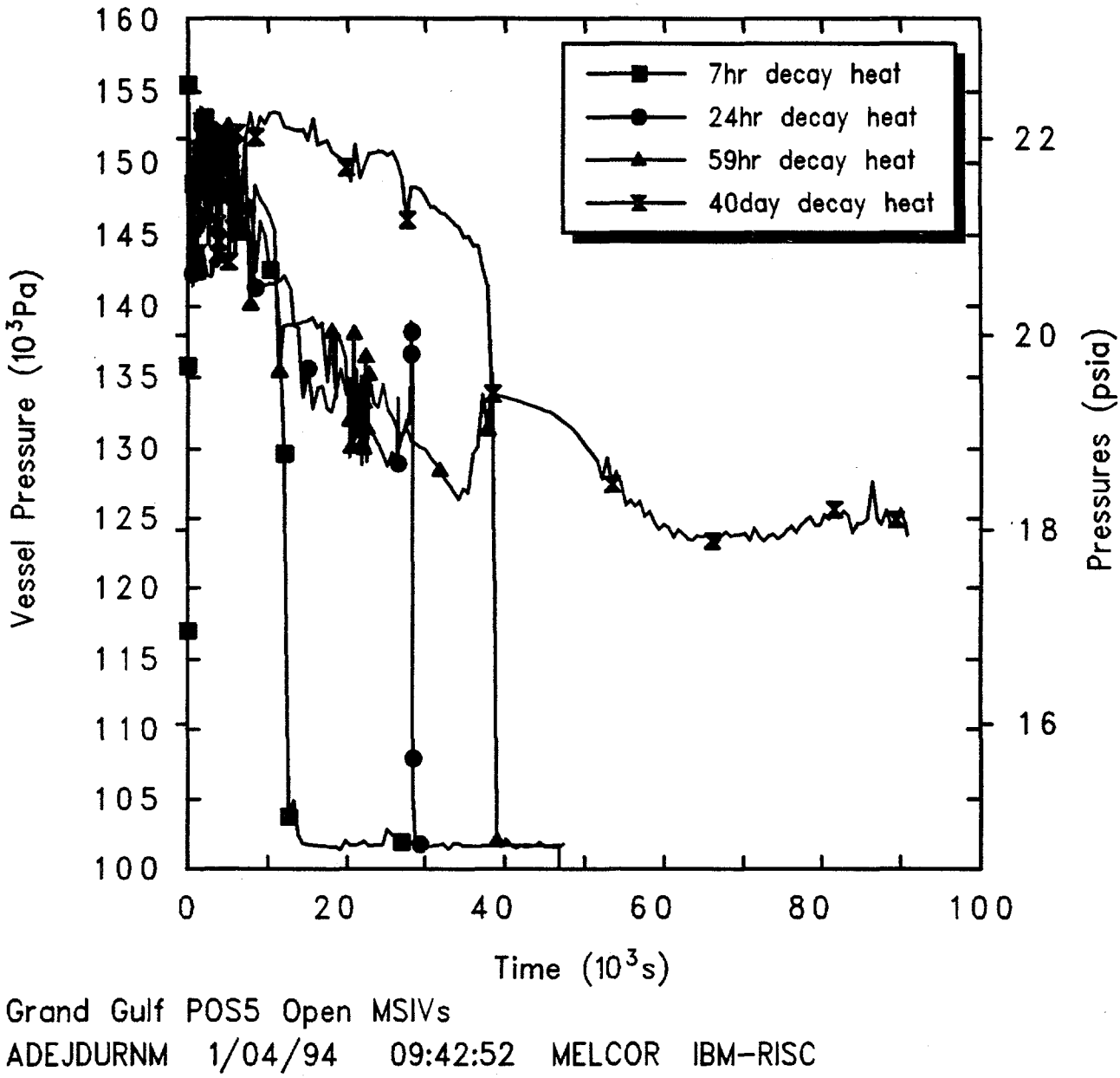

Figure 4.2.1.1. Reactor Vessel Pressures for Grand Gulf POS 5 -- Open MSIVs, Initiated at Various Times After Shutdown.

auxiliary building and, through the open equipment hatch and personnel locks, pressurizes the containment, as shown in Figure 4.2.1.2. The auxiliary building is assumed to fail on a 0.345 kPa (5 psig) overpressure. The longer after shutdown that this accident sequence begins, the lower the decay heat and the longer it takes to fail the auxiliary building.

The coolant inventory in the vessel drops as the decay heat boils water to steam which is lost out the open MSIVs, faster for higher decay heat levels than for lower decay heat levels, as presented in Figure 4.2.1.3. Figure 4.2.1.4 gives the predicted upper plenum liquid level drop due to this inventory loss, for different decay heat levels and highlighting when a Level 3 trip (544.4 in) would be generated; this is the autoisolation signal for SDC. Figure 4.2.1.5 gives the upper plenum and corresponding core liquid level drops due to this inventory loss, for different decay heat levels and highlighting when TAF uncovery is calculated to occur; horizontal lines indicate both the boundary between the upper plenum and the core at 9.6 m and the top-of-active-fuel elevation at 9.3 m. The core uncovery begins when the upper plenum still has substantial liquid left, with liquid downflow restricted by countercurrent flow of the steam being generated in the core, but the two-phase level in the core does not drop substantially below the top of the active fuel until after the upper plenum is mostly drained. We take TAF uncovery as the drop of the collapsed level in the core below the TAF elevation.

The early core heatup is illustrated in Figures 4.2.1.6 through 4.2.1.8 as calculated for accident sequences initiated by stuck-open MSIVs at 7 hr, 24 hr and 59 hr after shutdown. As with TAF uncovery, core uncovery begins sooner and proceeds more rapidly at higher decay heat levels. (The calculation begun 40 days after shutdown showed no core heatup by about 90,000 s, when stopped.)

Tables 4.2.1.1 and 4.2.1.2 summarize the timings of various key events predicted using MELCOR for this sequence assuming various times after shutdown and associated decay heat levels.

4.2.2 Low Pressure Boiloff

At the initiation of the accident, the reactor vessel is depressurized, the coolant is at the normal level and two SRVs are open. The vessel water inventory is at 366.5 K (200°F), which corresponds to the maximum temperature allowed by the Grand Gulf technical specifications for operation in POS 5. The initiating event then results in a loss of all core cooling and coolant makeup. The reactor pressure vessel head vent is closed at the beginning of the transient. The drywell personnel lock is open; the containment equipment hatch and both of the containment personnel locks are open (i.e., "open containment").

Figure 4.2.2.1 gives the vessel pressures calculated starting this accident scenario at several different times after shutdown. In all cases, the system begins pressurizing as all core cooling is lost but only pressurizes slightly before the steam flow out the two open SRVs is sufficient to remove all the decay heat; the higher the decay heat (i.e., the sooner after shutdown), the higher the early-time pressure peak before the flow out the open SRVs can fully remove the decay heat.

The steam flow out of the two open SRVs in turn pressurizes the containment and, through the open equipment hatch and personnel locks, pressurizes the auxiliary building, as shown in Figure 4.2.2.2. The longer after shutdown that this accident sequence begins, the lower the decay heat and the longer it takes to fail the auxiliary building.

The coolant inventory in the vessel drops as the decay heat boils water to steam which is lost out the open SRVs, faster for higher decay heat levels than for lower decay heat levels, as presented in Figure 4.2.2.3. Figure 4.2.2.4 gives the predicted upper plenum liquid level drop due to this inventory loss, for different decay heat levels and highlighting when a Level 3 trip (544.4 in) would be generated. Both collapsed and swollen (two-phase) liquid levels in the upper plenum are quite oscillatory, and we chose the first time the collapsed level crossed the 544.4 in level setpoint as the signal generation.

Figure 4.2.2.5 gives the corresponding core liquid level drop due to this inventory loss, for different decay heat levels and highlighting when TAF uncovery is calculated to occur; horizontal lines are included both at the top of the core (9.6 m) and at the TAF elevation (9.3 m). The collapsed liquid level in the upper core generally drops rapidly and smoothly; the swollen liquid level in the upper core in contrast oscillates substantially. The core uncovery begins when the upper plenum still has substantial liquid left, with liquid downflow restricted by countercurrent flow of the steam being generated in the core, but the two-phase level in the core does not drop substantially below the top of the active fuel until after the upper plenum is mostly drained. We take TAF

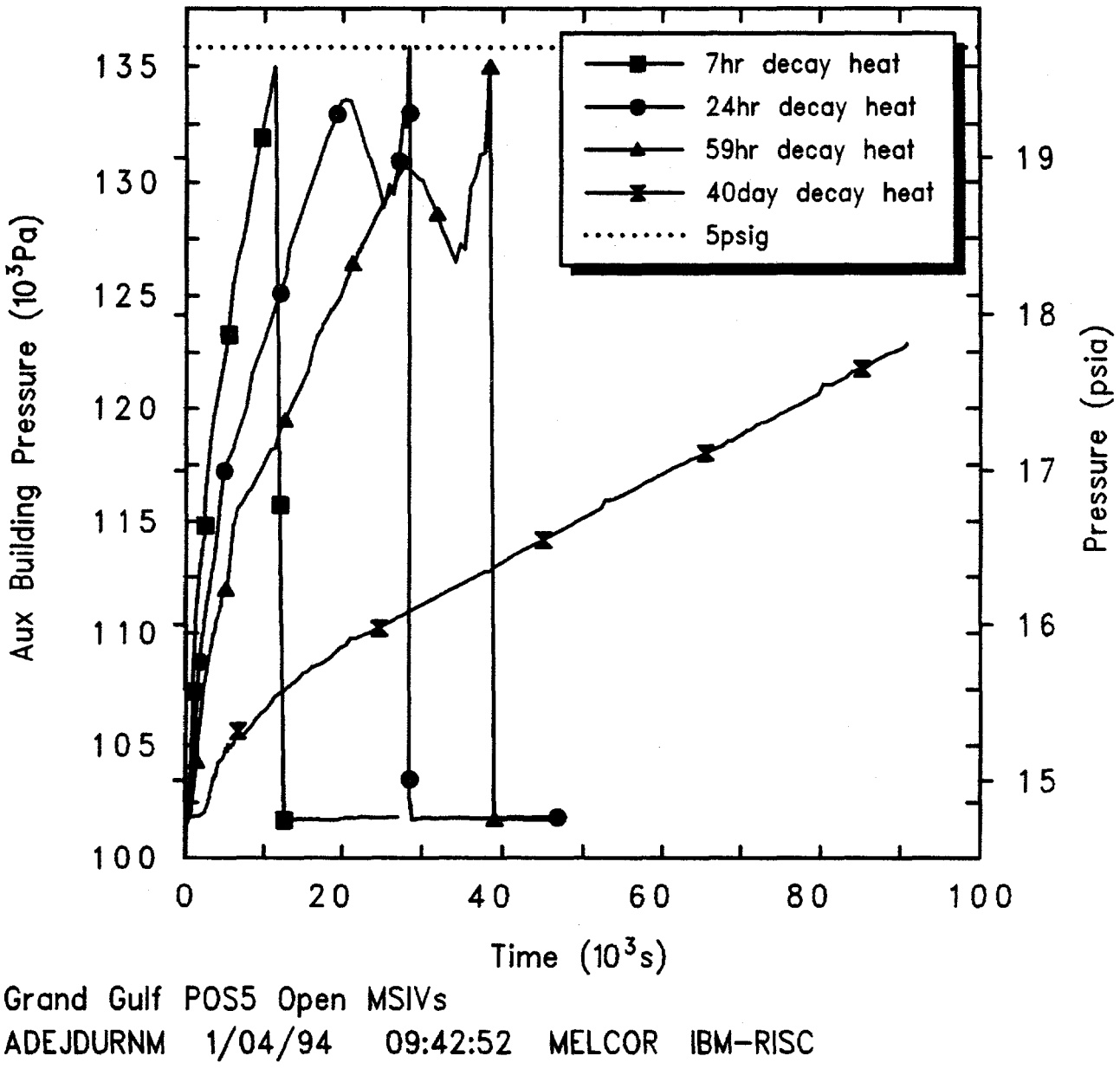

Figure 4.2.1.2. Auxiliary Building Pressures for Grand Gulf POS 5 -- Open MSIVs, Initiated at Various Times After Shutdown.

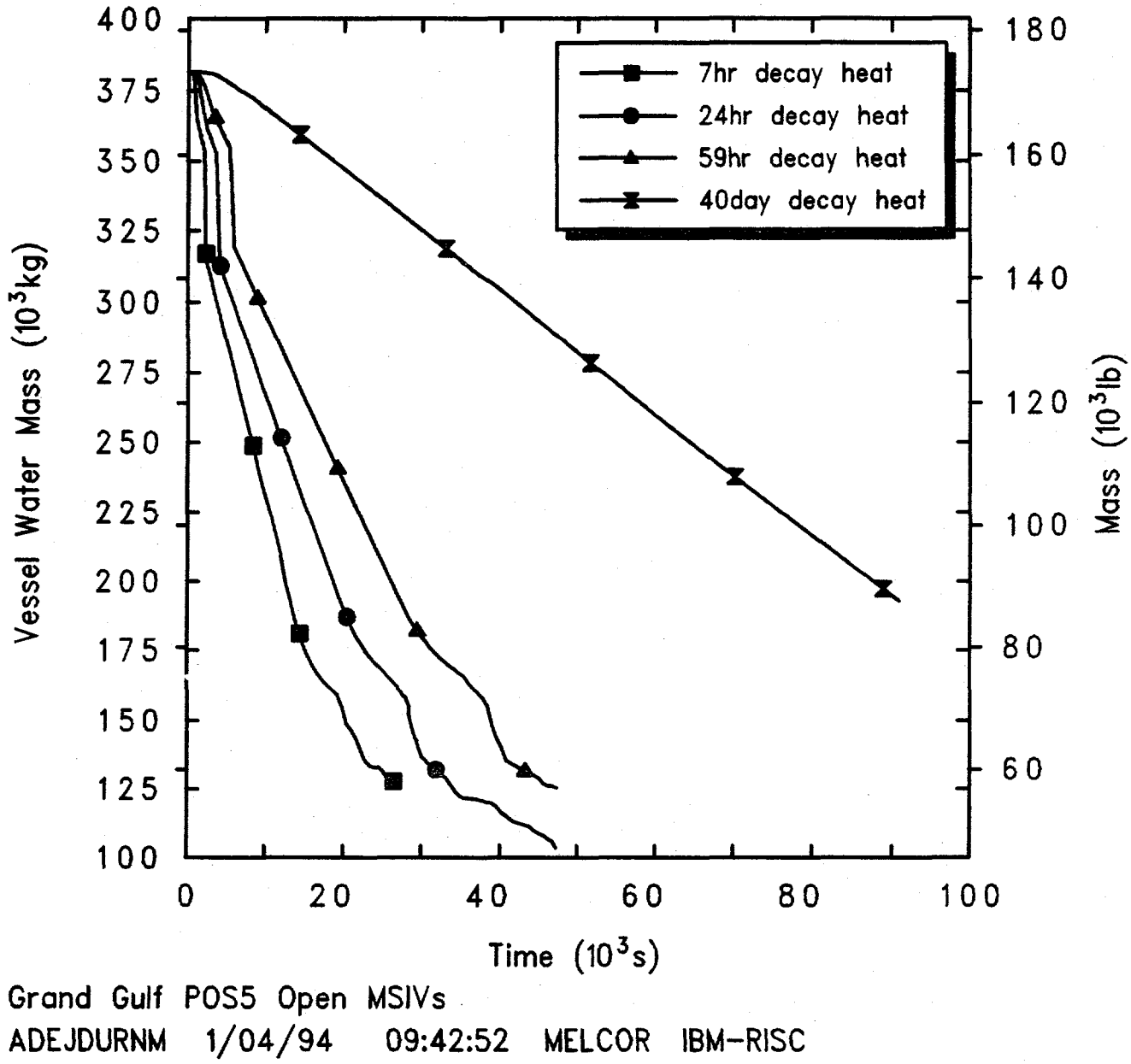

Figure 4.2.1.3. Reactor Vessel Water Masses for Grand Gulf POS 5 -- Open MSIVs, Initiated at Various Times After Shutdown.

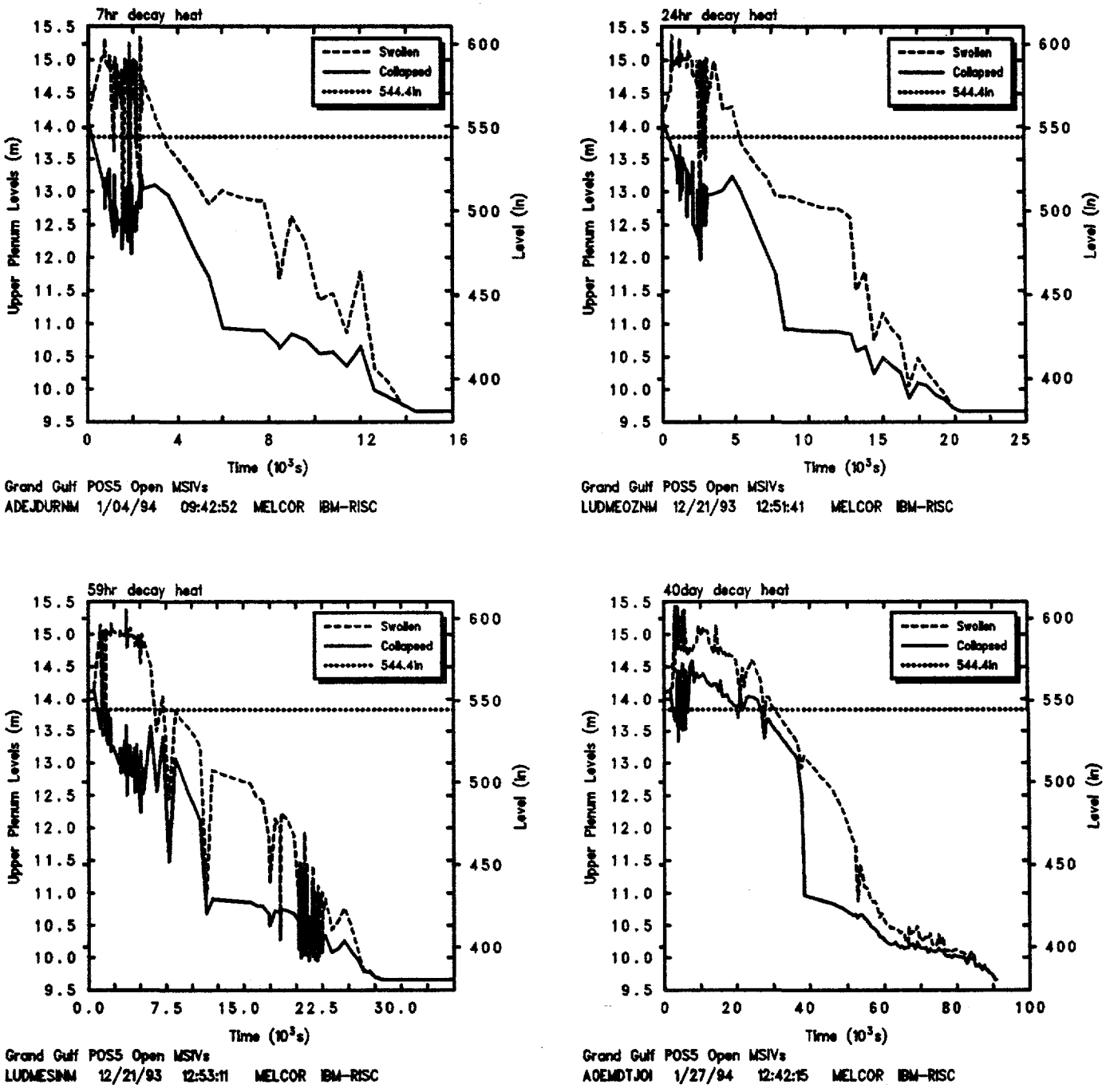

Figure 4.2.1.4. Upper Plenum Liquid Levels for Grand Gulf POS 5 -- Open MSIVs, Initiated 7 hr (upper left). 24 hr (upper right), 59 hr (lower left) and 40 days (lower right) After Shutdown.

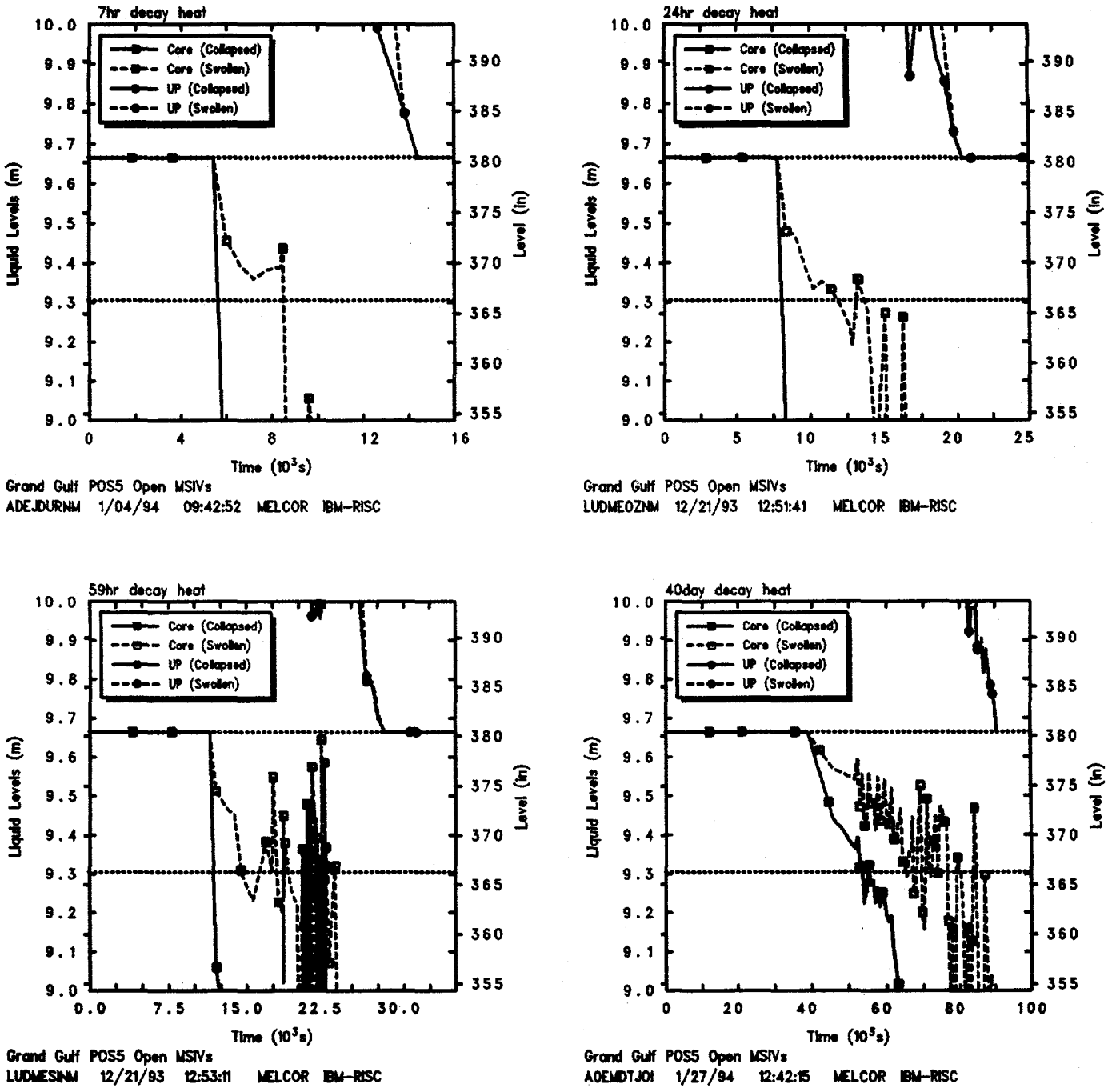

Figure 4.2.1.5. Core Liquid Levels for Grand Gulf POS 5 -- Open MSIVs, Initiated 7 hr (upper left), 24 hr (upper right), 59 hr (lower left) and 40 days (lower right) After Shutdown.

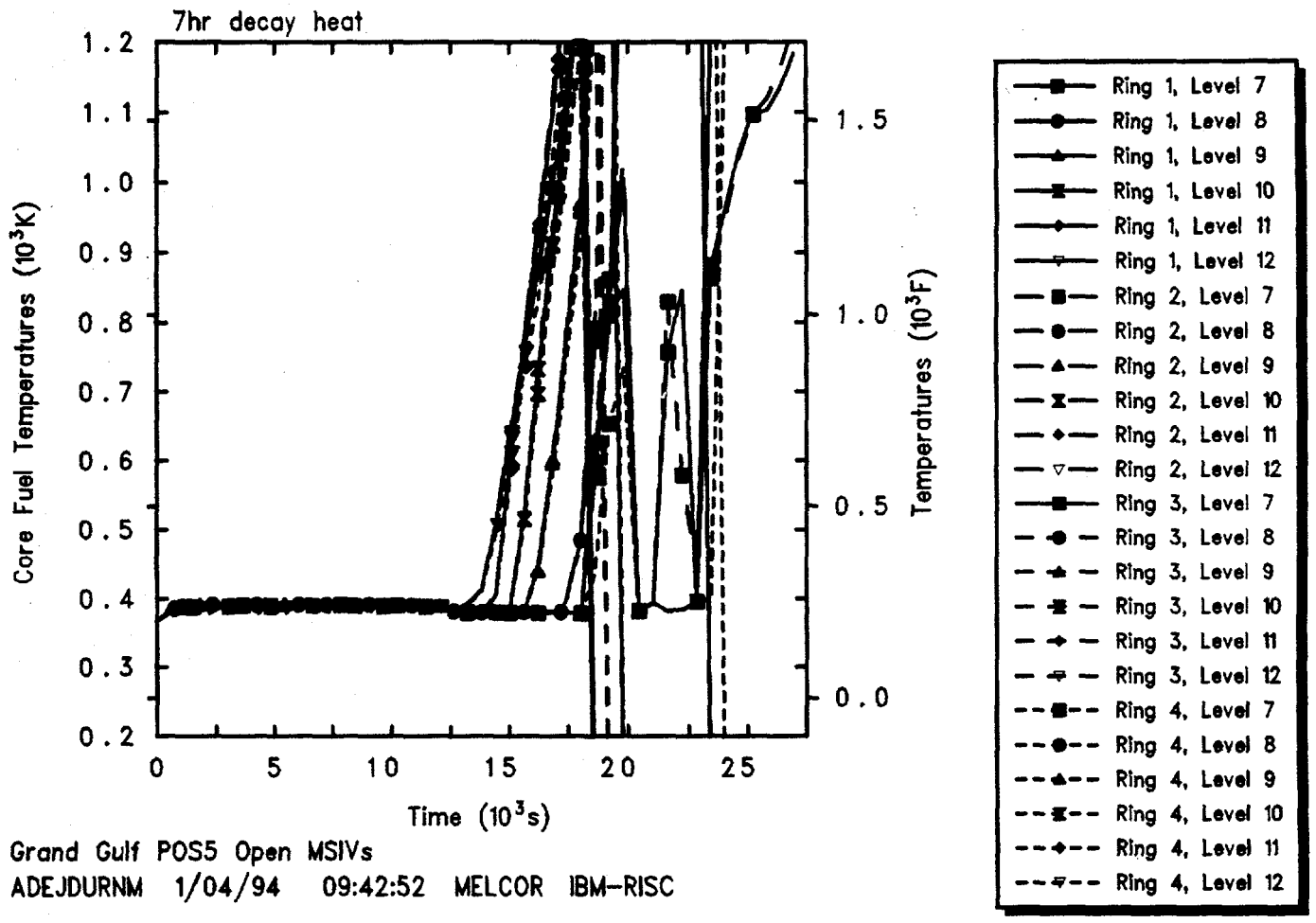

Figure 4.2.1.6. Core Fuel Temperatures for Grand Gulf POS 5 -- Open MSIVs, Initiated 7 hr After Shutdown.

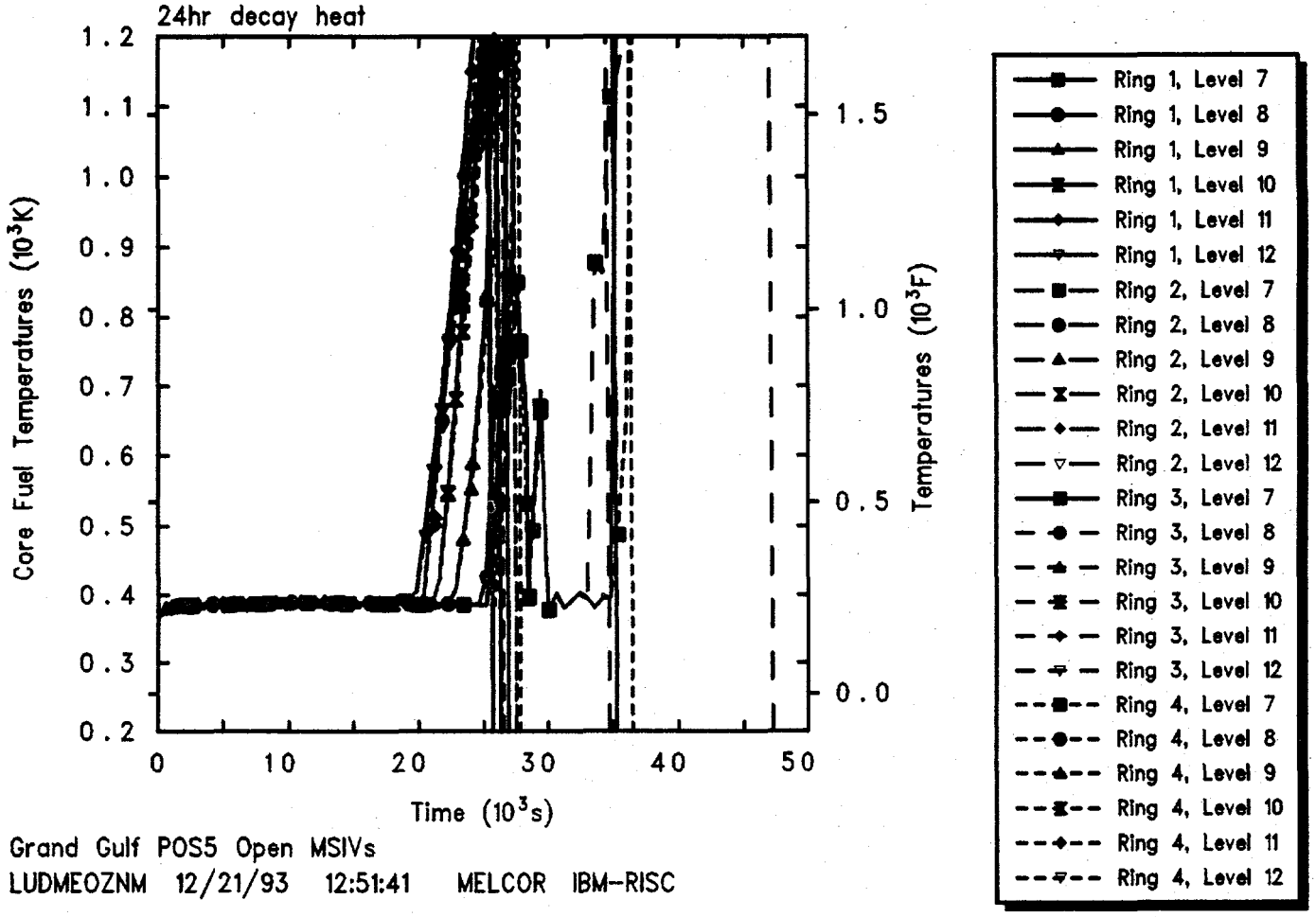

Figure 4.2.1.7. Core Fuel Temperatures for Grand Gulf POS 5 -- Open MSIVs, Initiated 24 hr After Shutdown.

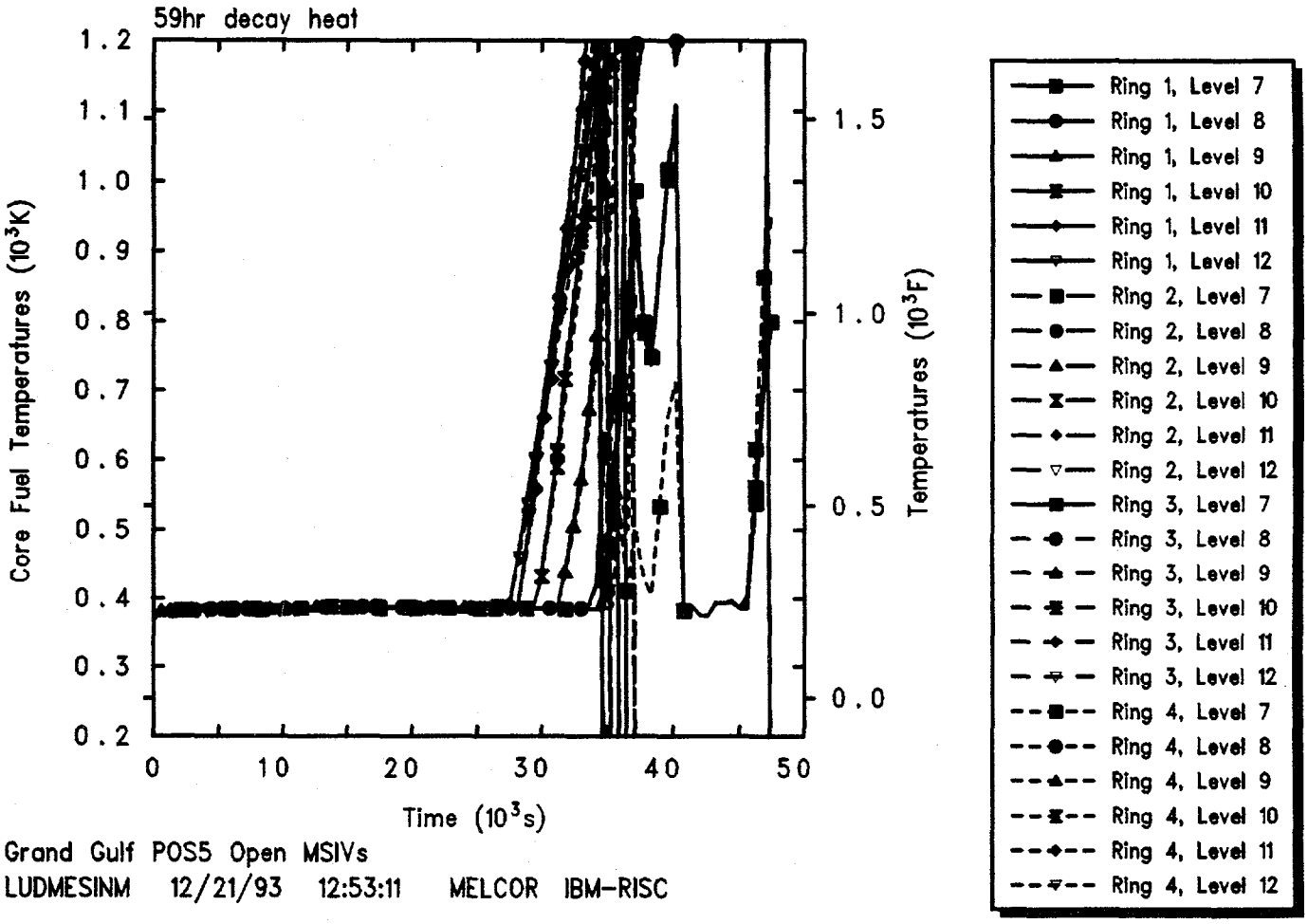

Figure 4.2.1.8. Core Fuel Temperatures for Grand Gulf POS 5 -- Open MSIVs, Initiated 59 hr After Shutdown.

Table 4.2.1.1. Key Event Times for Grand Gulf POS 5 -- Open MSIVs, Initiated at Various Times After Shutdown

Initiation Time After Shutdown	Time to (s) TAF Uncovery*	Core Heatup	First Gap Release	Vessel Failure
7 hr	5,500	13,000	17,000	--**
24 hr	8,000	20,000	24,100	--**
59 hr	10,500	27,000	33,200	--**
40 days	54,000	90,000	--**	--**

* Collapsed liquid level.
** Calculation stopped before event occurred.

Table 4.2.1.2 Key Signal Times for Grand Gulf POS 5 -- Open MSIVs, Initiated at Various Times After Shutdown

Initiation Time After Shutdown	Time to (s) Collapsed Level <544.4 in	Swollen Level <544.4 in
7 hr	200	3,500
24 hr	500	5,250
59 hr	1000	6,500
40 days	3600	30,500

uncovery as the drop of the collapsed level in the core below the TAF elevation.

The early core heatup is illustrated in Figures 4.2.2.6 through 4.2.2.8 as calculated for low-pressure boiloffs starting at 7 hr, 24 hr and 59 hr after shutdown. As with TAF uncovery, core uncovery begins sooner and proceeds more rapidly at higher decay heat levels. The calculation begun 12 days after shutdown showed core heatup just beginning by about 63,000 s, when stopped; the calculation begun 40 days after shutdown showed no core heatup by 90,000 s, when stopped. (Recall that the period of interest for all these Level 1 analyses is either from accident initiation to core heatup, or 1 day after accident start.)

Tables 4.2.2.1 and 4.2.2.2 summarize the timings of various key events predicted using MELCOR for this sequence assuming various times after shutdown and associated decay heat levels.

4.2.3 High Pressure Boiloff with Closed RPV Head Vent

At the initiation of the accident, the reactor vessel is depressurized, the coolant is at the normal level and the SRVs are closed. The SRVs remain closed during the accident and only open to relieve pressure at the safety setpoint. The vessel water inventory is at 366.5 K

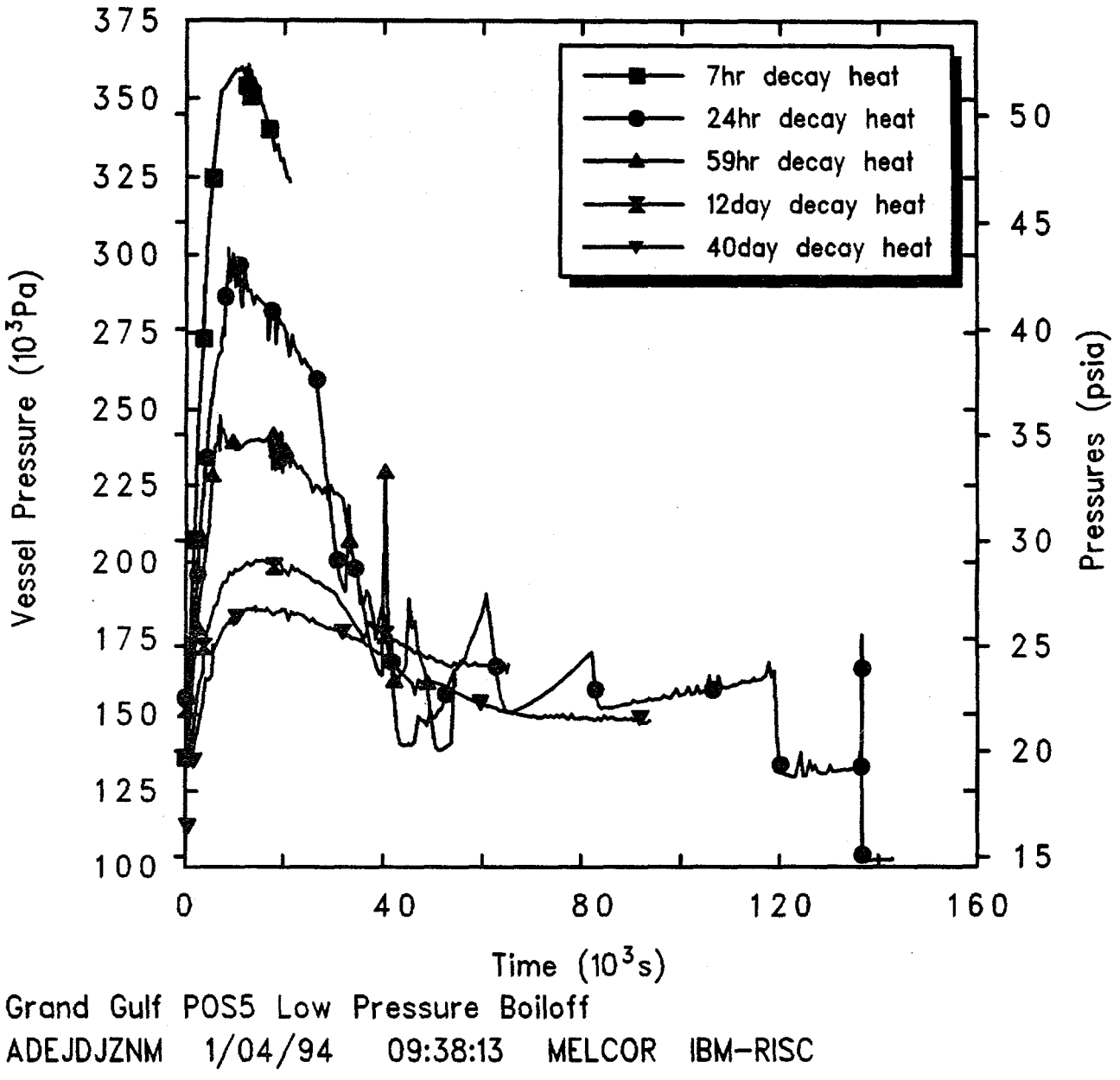

Figure 4.2.2.1. Reactor Vessel Pressures for Grand Gulf POS 5 -- Low Pressure Boiloff, Initiated at Various Times After Shutdown.

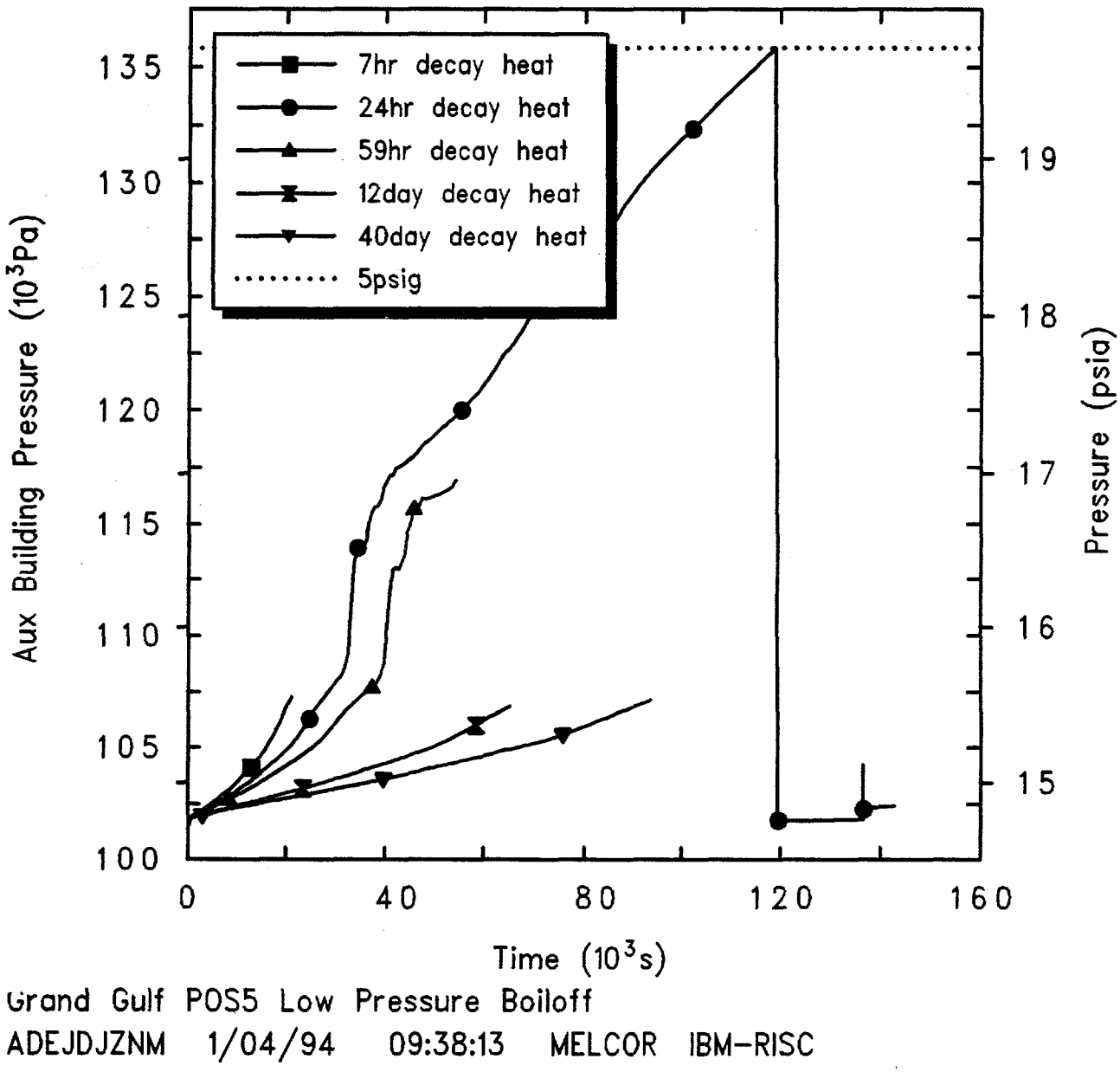

Figure 4.2.2.2. Auxiliary Building Pressures for Grand Gulf POS 5 -- Low Pressure Boiloff, Initiated at Various Times After Shutdown.

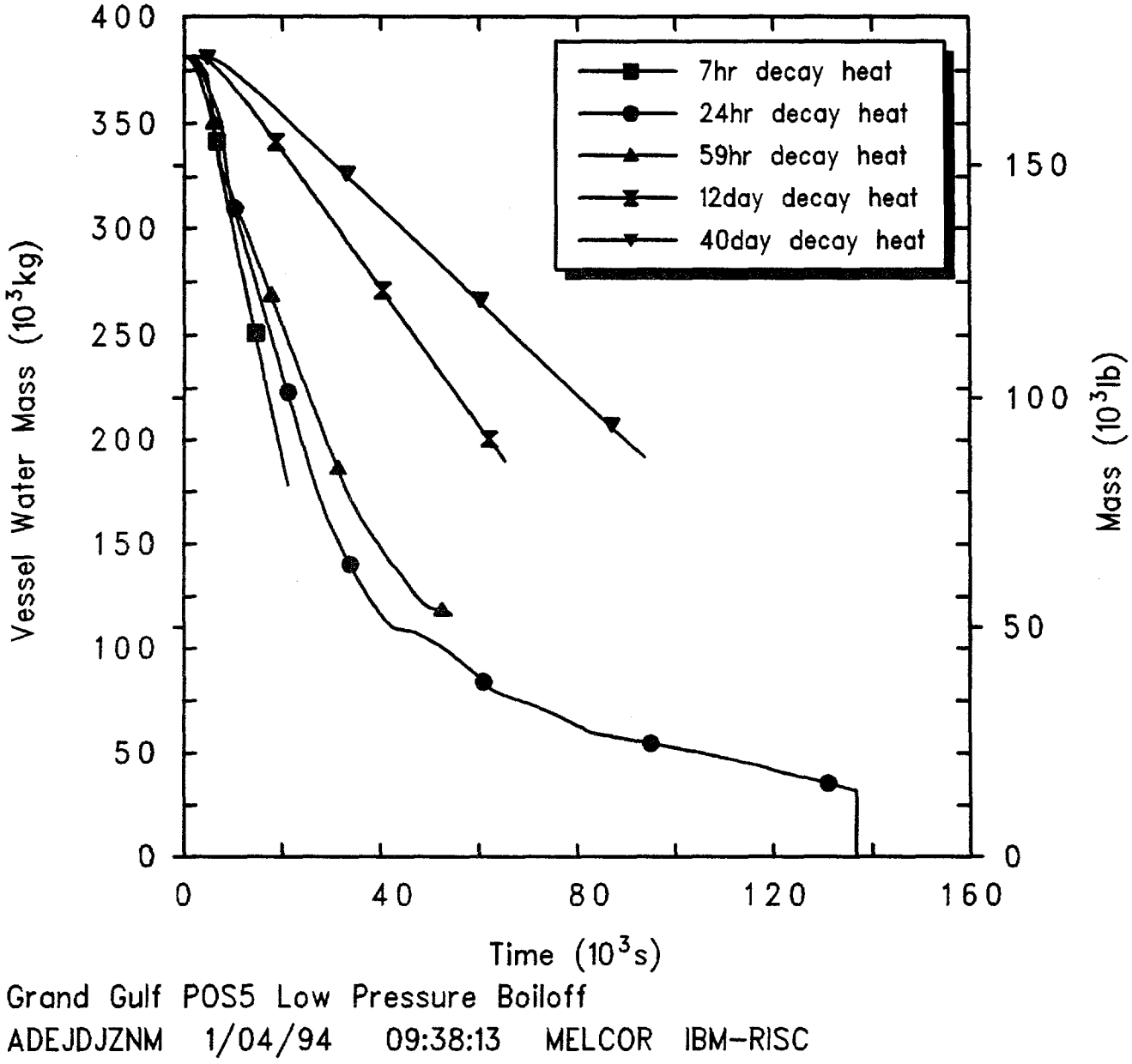

Figure 4.2.2.3. Reactor Vessel Water Masses for Grand Gulf POS 5 -- Low Pressure Boiloff, Initiated at Various Times After Shutdown.

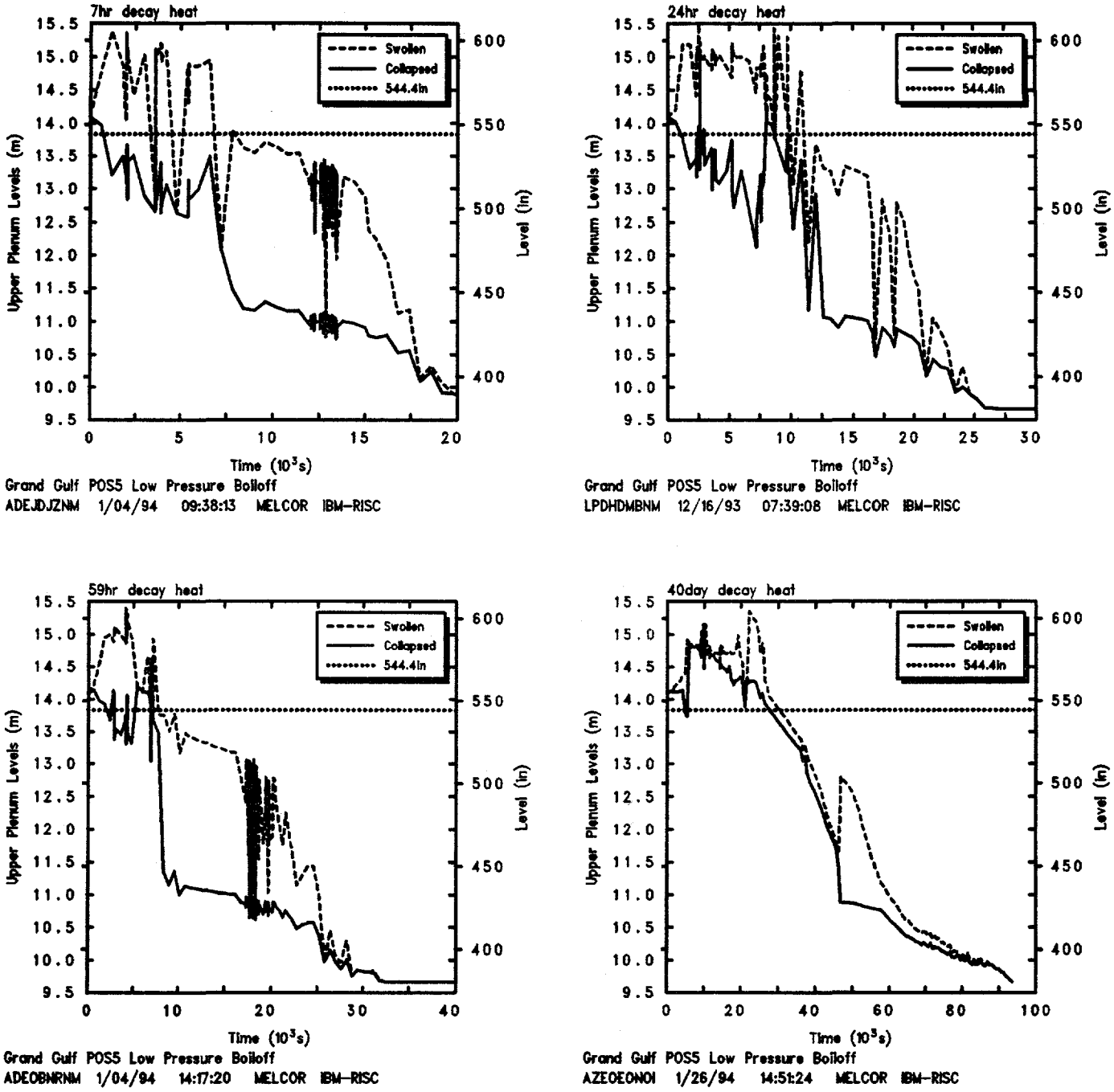

Figure 4.2.2.4. Upper Plenum Liquid Levels for Grand Gulf POS 5 -- Low Pressure Boiloff, Initiated 7 hr (upper left), 24 hr (upper right), 59 hr (lower left) and 40 days (lower right) After Shutdown.

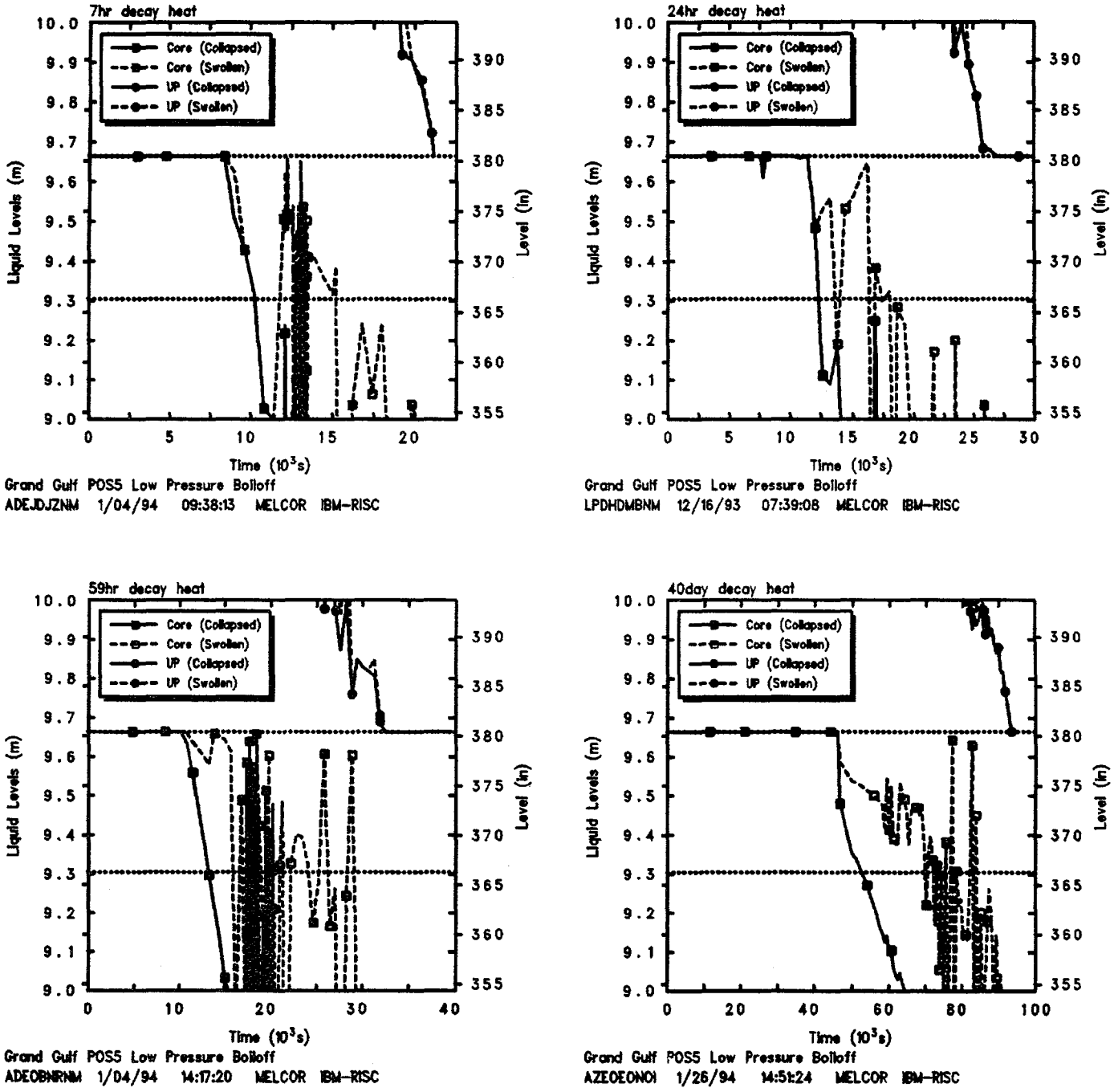

Figure 4.2.2.5. Core Liquid Levels for Grand Gulf POS 5 -- Low Pressure Boiloff, Initiated 7 hr (upper left), 24 hr (upper right), 59 hr (lower left) and 40 days (lower right) After Shutdown.

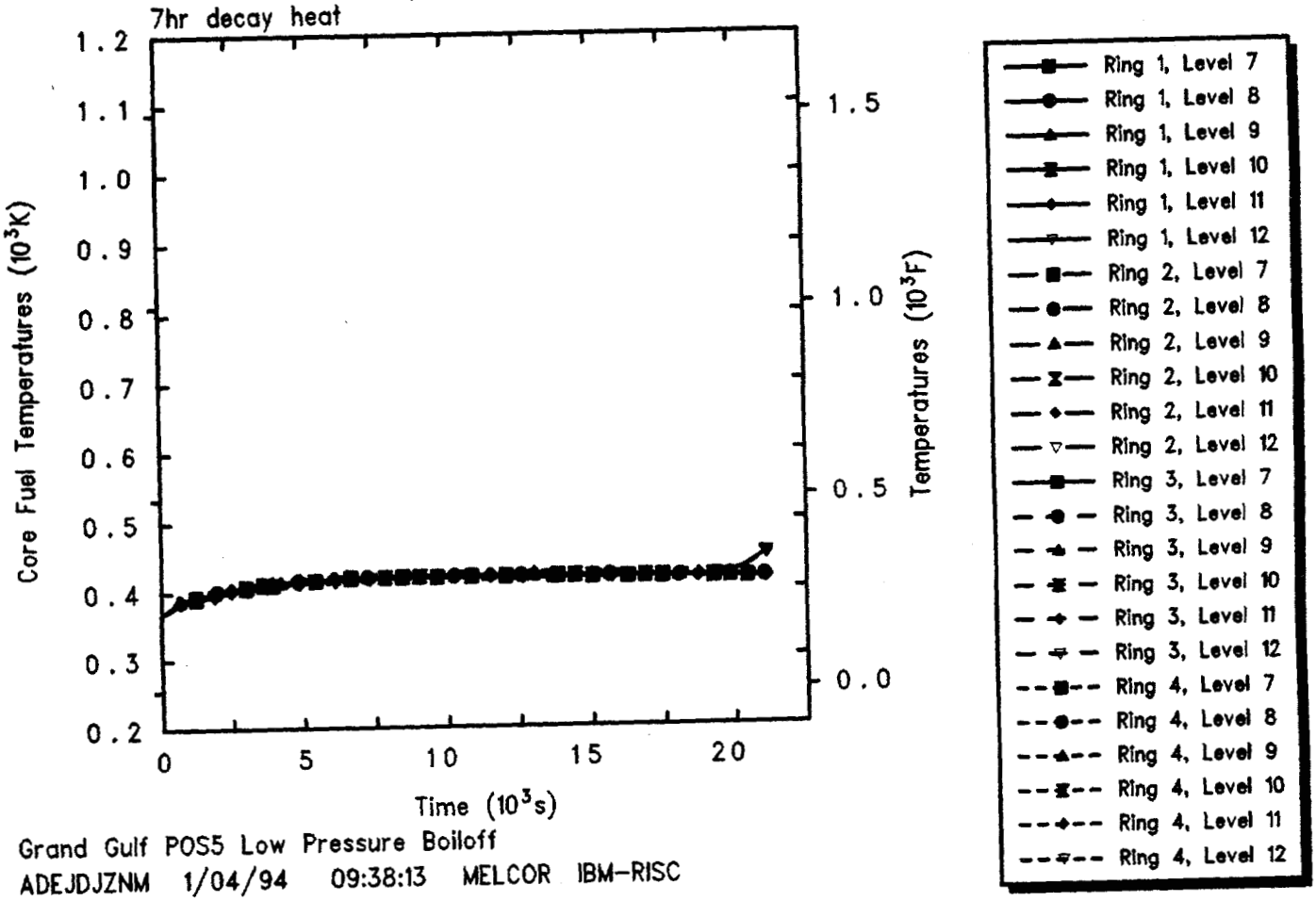

Figure 4.2.2.6. Core Fuel Temperatures for Grand Gulf POS 5 -- Low Pressure Boiloff, Initiated 7 hr After Shutdown.

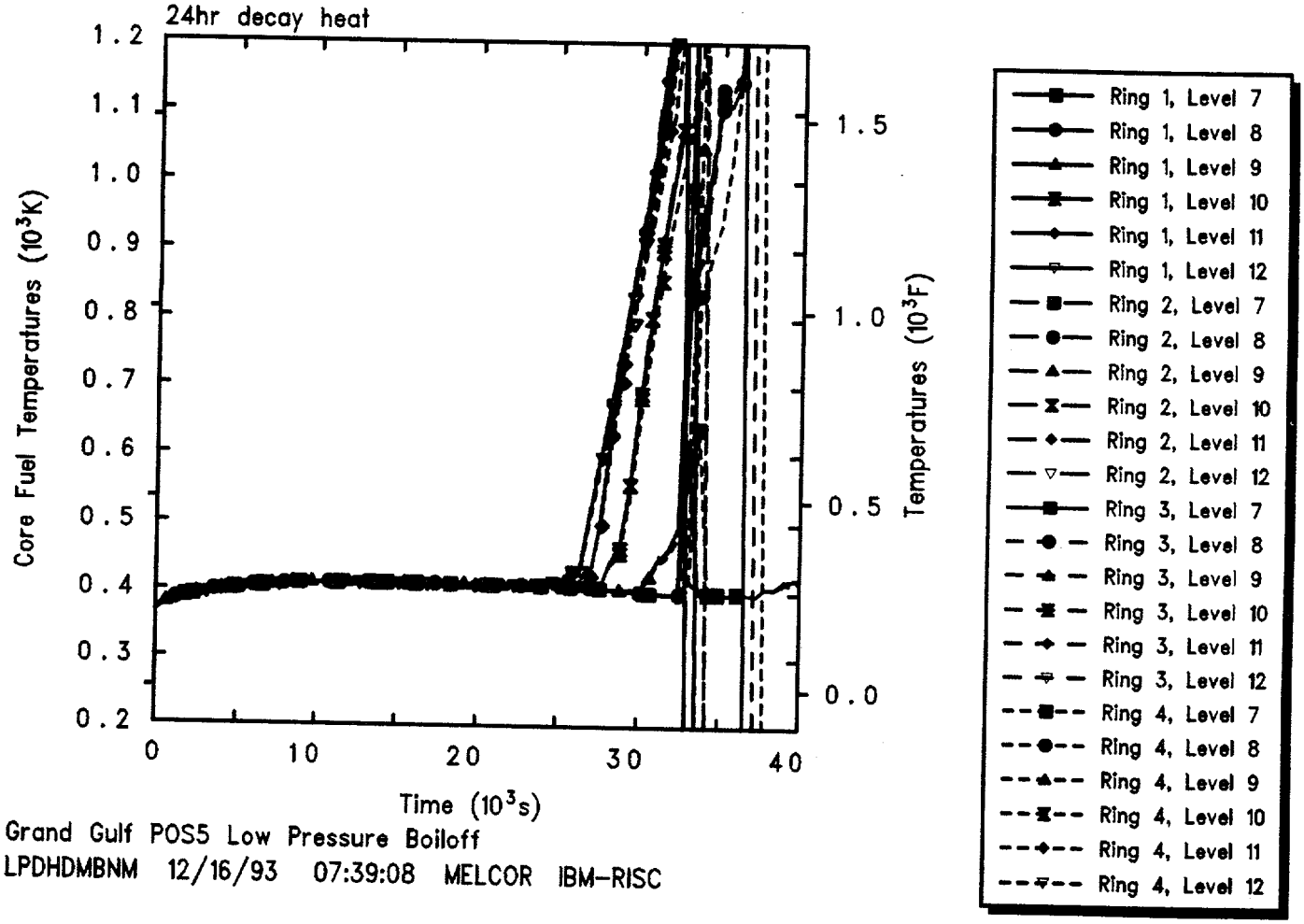

Figure 4.2.2.7. Core Fuel Temperatures for Grand Gulf POS 5 -- Low Pressure Boiloff, Initiated 24 hr After Shutdown.

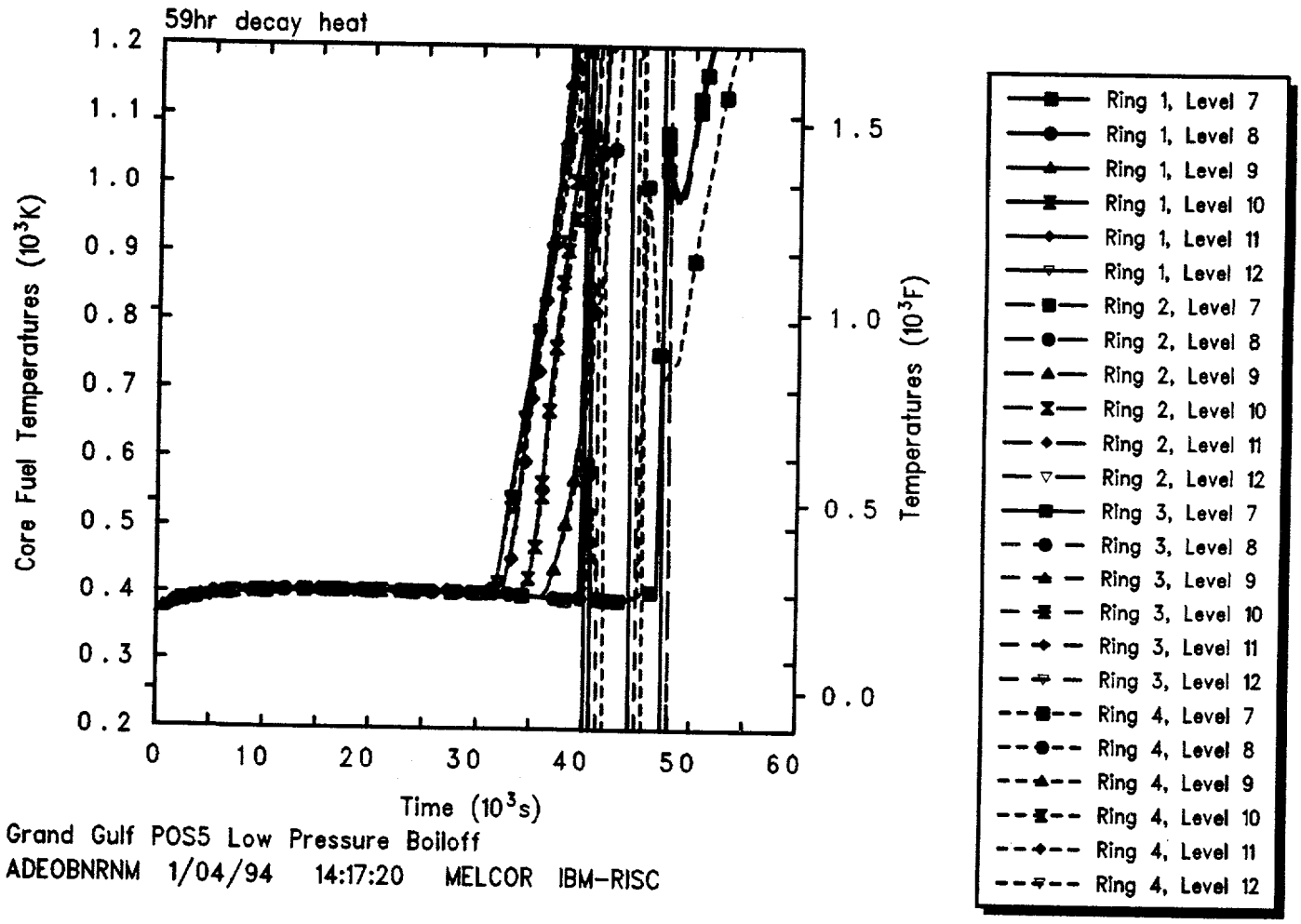

Figure 4.2.2.8. Core Fuel Temperatures for Grand Gulf POS 5 -- Low Pressure Boiloff, Initiated 59 hr After Shutdown.

Table 4.2.2.1. Key Event Times for Grand Gulf POS 5 -- Low Pressure Boiloff, Initiated at Various Times After Shutdown

Initiation Time After Shutdown	Time to (s) TAF Uncovery *	Core Heatup	First Gap Release	Vessel Failure
7 hr	10,250	20,000	-- **	-- **
24 hr	12,250	25,400	31,600	136,386
59 hr	13,200	31,600	32,500	-- **
12 days	30,400	63,000	-- **	-- **
40 days	52,000	>90,000	-- **	-- **

* Collapsed liquid level.
** Calculation stopped before event occurred.

Table 4.2.2.2. Signal Times for Grand Gulf POS 5 -- Low Pressure Boiloff, Initiated at Various Times After Shutdown

Initiation Time After Shutdown	Time to (s) Collapsed Level <544.4 in	Swollen Level <544.4 in
7 hr	750	7,800
24 hr	1,000	14,250
59 hr	2,000	7,800
12 days	3,600	25,200
40 days	5,000	30,000

(200°F), which corresponds to the maximum temperature allowed by the Grand Gulf technical specifications for operation in POS 5. The initiating event then results in a loss of all core cooling and coolant makeup. The reactor pressure vessel head vent is closed at the beginning of the transient. The drywell personnel lock is open; the containment equipment hatch and both of the containment personnel locks are open.

(A calculation beginning 40 days after shutdown was not done for this sequence because the results of the analysis beginning 12 days after shutdown showed no significant core uncovery or damage within the 1 day maximum time window of interest.)

Figure 4.2.3.1 gives the vessel pressures calculated starting this accident scenario at several different times after shutdown. In all cases, the system begins pressurizing as all core cooling is lost and continues pressurizing, with no relief, until reaching the SRV setpoint. The SRVs then cycle around the valve setpoints, intermittently opening and allowing the steam flow out the SRVs to remove the decay heat. The higher the decay heat (i.e., the sooner after shutdown), the faster the initial pressurization and associated inventory loss, and the earlier the vessel fails.

The steam flow out of the SRVs in turn pressurizes the containment and, through the open equipment hatch and

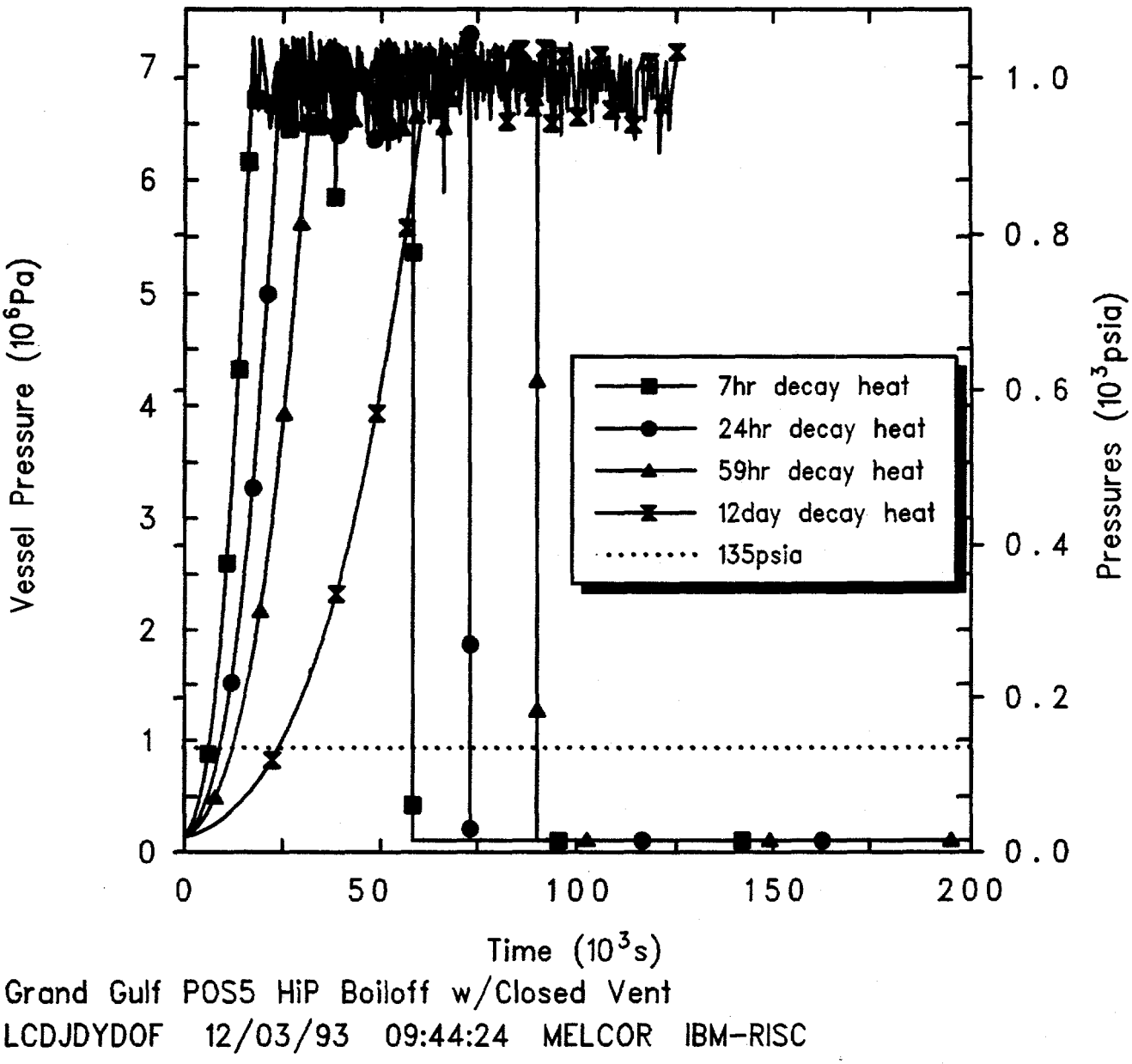

Figure 4.2.3.1. Reactor Vessel Pressures for Grand Gulf POS 5 -- High Pressure Boiloff with Closed RPV Vent, Initiated at Various Times After Shutdown.

personnel locks, pressurizes the auxiliary building, as shown in Figure 4.2.3.2. The longer after shutdown that this accident sequence begins, the lower the decay heat and the slower the auxiliary building pressurizes. In all these cases, the auxiliary building does not reach its 5 psig overpressure failure setpoint before vessel failure; the auxiliary building fails on a sudden pressure spike corresponding to vessel failure and debris ejection.

Initially, the vessel water mass remains constant while the system pressurizes due to the loss of core cooling. After the SRV setpoint is reached, the coolant inventory in the vessel drops as the decay heat boils water to steam which is lost out the open SRVs, faster for higher decay heat levels, as presented in Figure 4.2.3.3.

Figure 4.2.3.4 gives the predicted upper plenum liquid level drop due to this inventory loss, for different decay heat levels and highlighting when a Level 3 trip (544.4 in) would be generated. The level initially rises as the vessel pressurizes, faster for higher decay heat levels, until the SRV begins cycling. The level then appears to remain constant for a brief time, and then drops as inventory continues to be lost out the SRV. The plateau in liquid level is an artifact of the MELCOR nodalization, in which the upper plenum volume extends up to just over 15.43 m; during the apparent level plateau, the liquid level in the vessel rises into the dryer/steam-dome control volume just above the upper-plenum/steam-separators control volume.

Figure 4.2.3.5 gives the corresponding upper core liquid level drop due to this inventory loss, for different decay heat levels and highlighting when TAF uncovery is calculated to occur; horizontal lines are included both at the top of the core (9.6 m) and at the TAF elevation (9.3 m). The swollen and collapsed liquid levels in the upper plenum generally drop rapidly and smoothly; the swollen and collapsed liquid levels in the upper core in contrast oscillate substantially. The core uncovery begins when the upper plenum still has substantial liquid left, with liquid downflow restricted by countercurrent flow limiting by upflow of the steam being generated in the core, but the two-phase level in the core does not drop substantially below the top of the active fuel until after the upper plenum is mostly drained. We take TAF uncovery as the final, substantive drop of the collapsed level below the TAF elevation, rather than as any of the earlier, intermittent oscillations.

The core heatup is illustrated in Figures 4.2.3.6 through 4.2.3.8 as calculated for this high-pressure boiloff with closed RPV vent starting at 7 hr, 24 hr and 59 hr after shutdown. As with TAF uncovery, core uncovery begins sooner and proceeds more rapidly at higher decay heat levels. The calculation begun 12 days after shutdown showed core heatup beginning after about 90,000 s, and is not shown because the period of interest for all these Level 1 analyses is the shorter of either accident initiation to core damage or 1 day after accident start.

Tables 4.2.3.1 and 4.2.3.2 summarize the timings of various key events predicted using MELCOR for this sequence assuming various times after shutdown and associated decay heat levels. A calculation beginning 40 days after shutdown was not done for this sequence because the results of the analysis beginning 12 days after shutdown showed no significant core uncovery or damage within the 1 day maximum time window of interest.

4.2.4 High Pressure Boiloff with Open RPV Head Vent

At the initiation of the accident, the reactor vessel is depressurized, the coolant is at the normal level and the SRVs are closed. The SRVs remain closed during the accident and only open to relieve pressure at the safety setpoint. The vessel water inventory is at 366.5 K (200°F), which corresponds to the maximum temperature allowed by the Grand Gulf technical specifications for operation in POS 5. The drywell personnel lock is open; the containment equipment hatch and both of the containment personnel locks are open (i.e., "open containment"). This scenario is identical to case 3, except that the reactor pressure vessel head vent is open.

(As for the high pressure boiloff with closed RPV head vent in the previous section, a calculation beginning 40 days after shutdown was not done for this sequence because the results of the analysis beginning 12 days after shutdown showed no significant core uncovery or damage within the 1 day time window of interest.)

Figure 4.2.4.1 gives the vessel pressures calculated starting this accident scenario at several different times after shutdown. In all cases, the system begins pressurizing as all core cooling is lost and continues pressurizing until reaching the SRV setpoint. As in the sequence with a closed RPV vent, the SRVs then cycle around the valve setpoints, intermittently opening. However, with the RPV vent line open, there is continual, limited relief out the vent line throughout the entire period. This increases inventory loss. The system does not remain at the SRV cycling setpoints until vessel

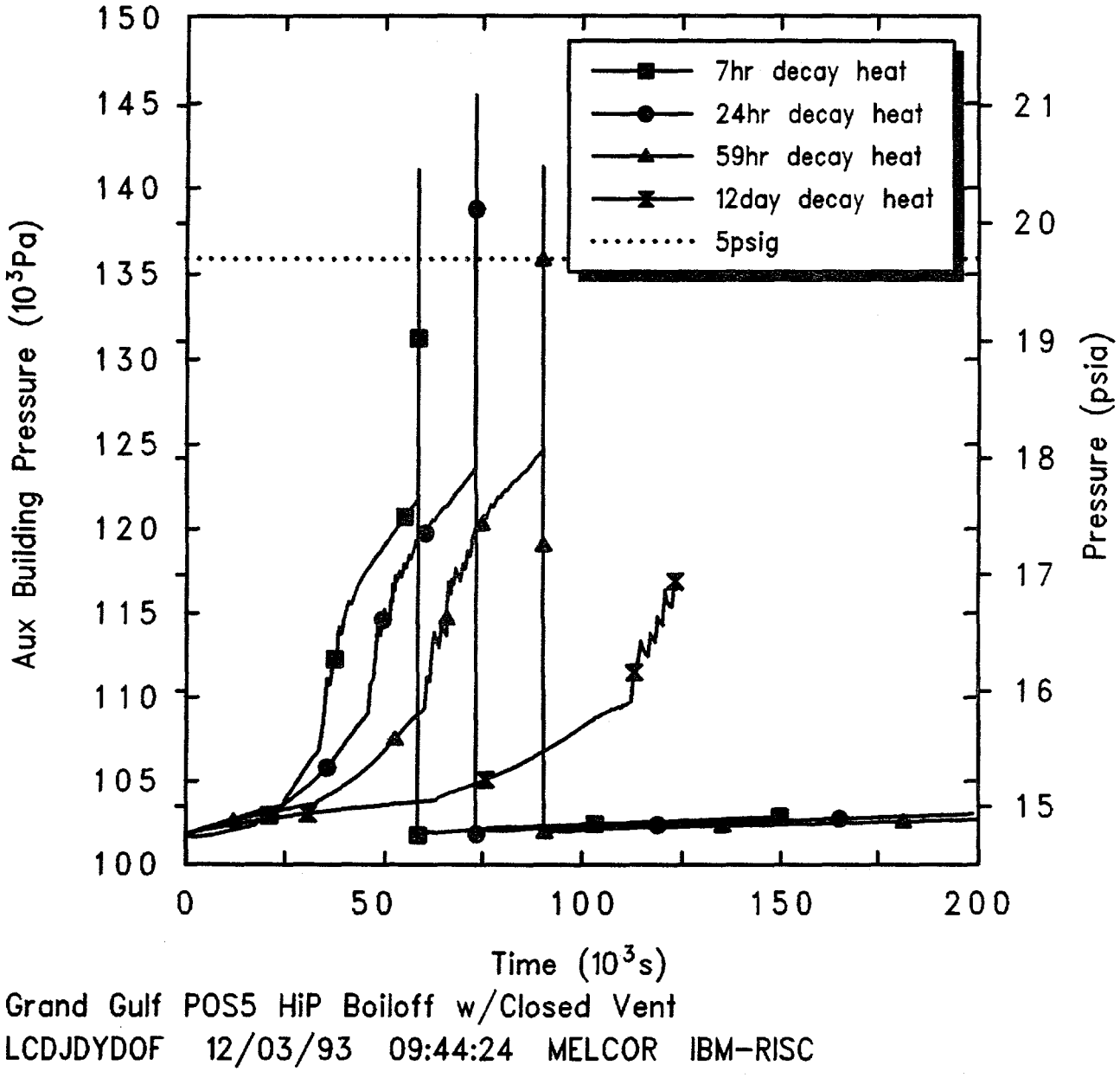

Figure 4.2.3.2. Auxiliary Building Pressures for Grand Gulf POS 5 -- High Pressure Boiloff with Closed RPV Vent, Initiated at Various Times After Shutdown.

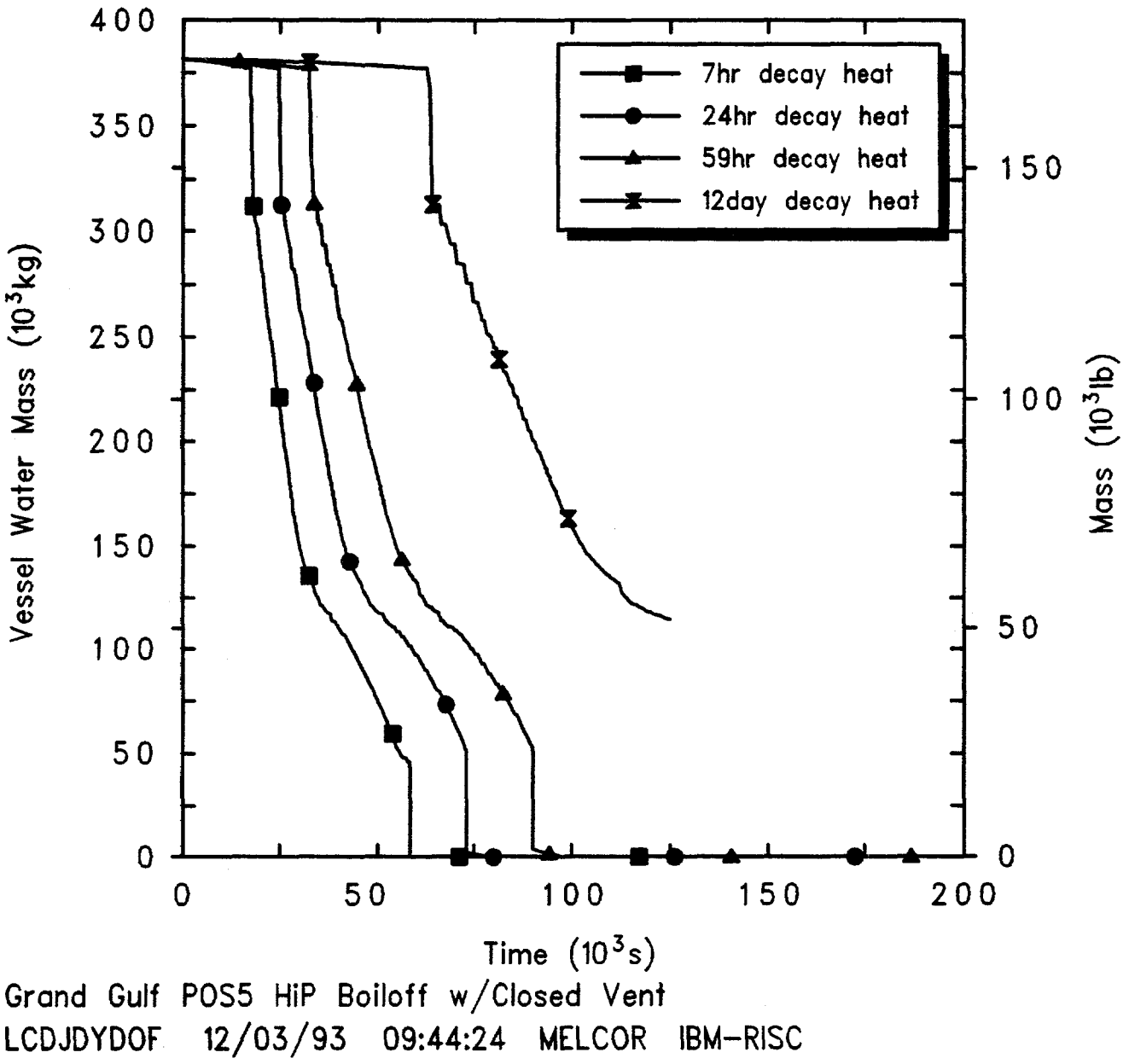

Figure 4.2.3.3. Reactor Vessel Water Masses for Grand Gulf POS 5 -- High Pressure Boiloff with Closed RPV Vent, Initiated at Various Times After Shutdown.

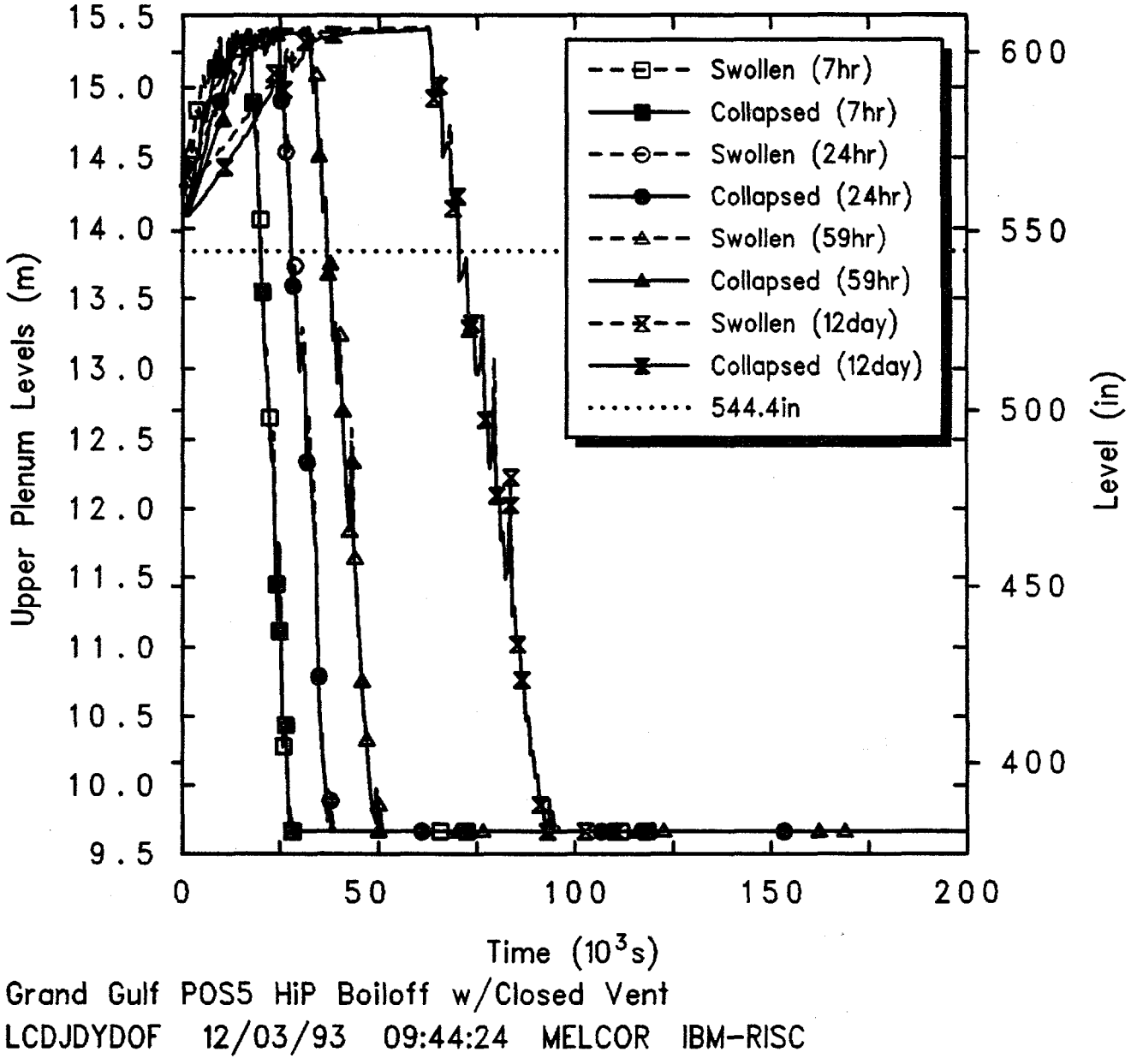

Figure 4.2.3.4. Upper Plenum Liquid Levels for Grand Gulf POS 5 -- High Pressure Boiloff with Closed RPV Vent, Initiated at Various Times After Shutdown.

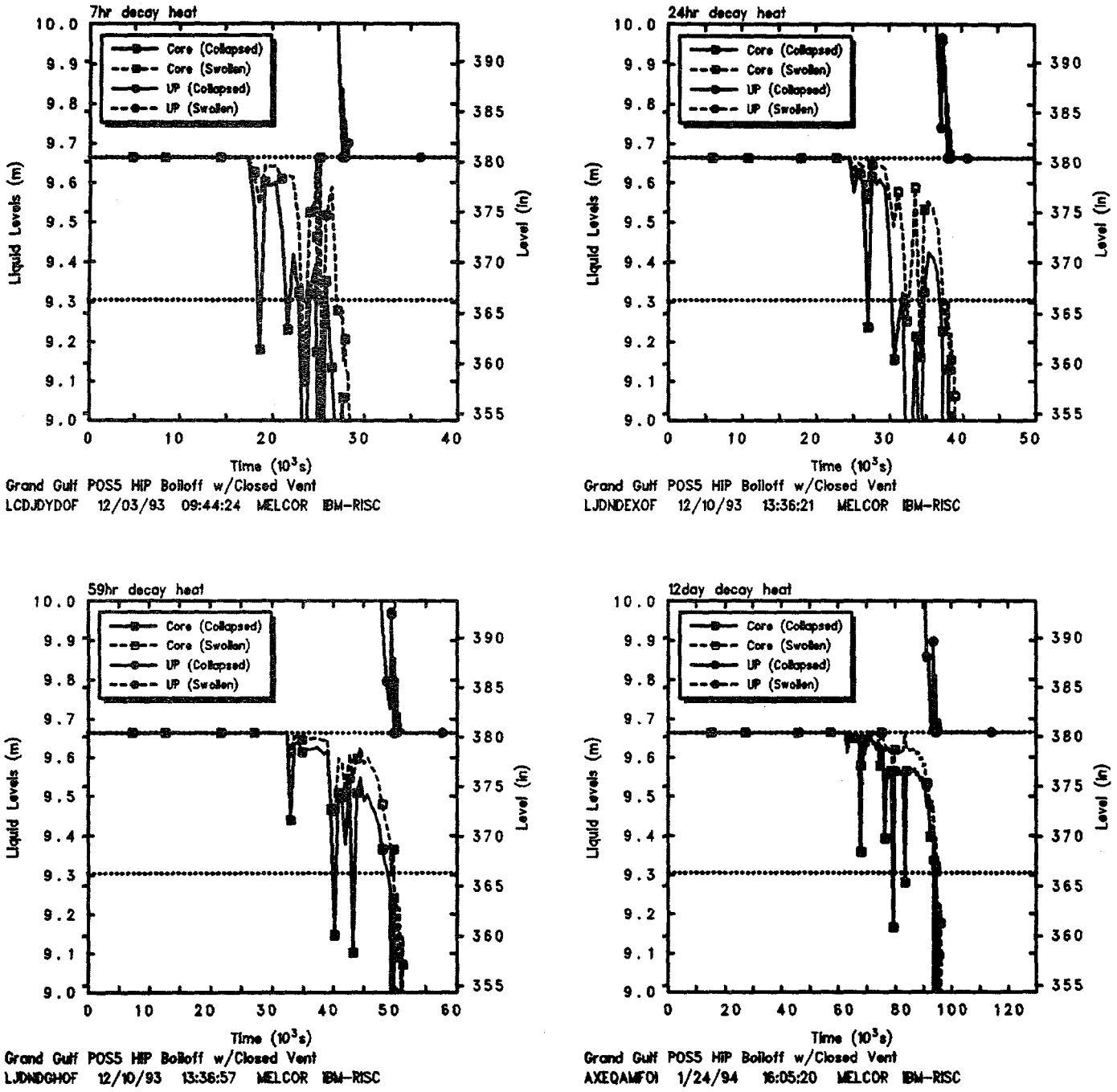

Figure 4.2.3.5. Core Liquid Levels for Grand Gulf POS 5 -- High Pressure Boiloff with closed RPV Vent, Initiated 7 hr (upper left), 24 hr (upper right), 59 hr (lower left) and 12 days (lower right) After Shutdown.

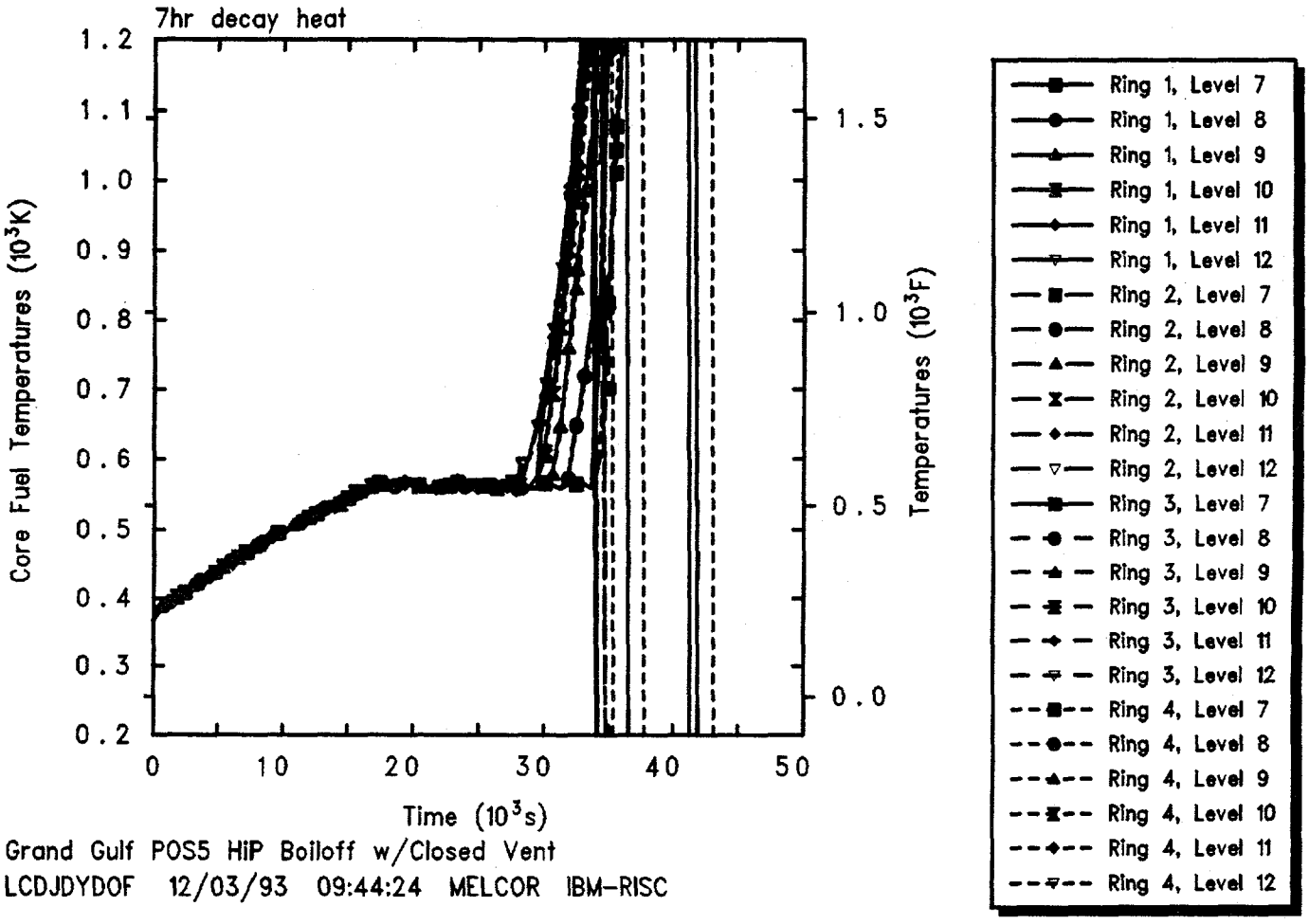

Figure 4.2.3.6. Core Fuel Temperatures for Grand Gulf POS 5 -- High Pressure Boiloff with Closed RPV Vent, Initiated 7 hr After Shutdown.

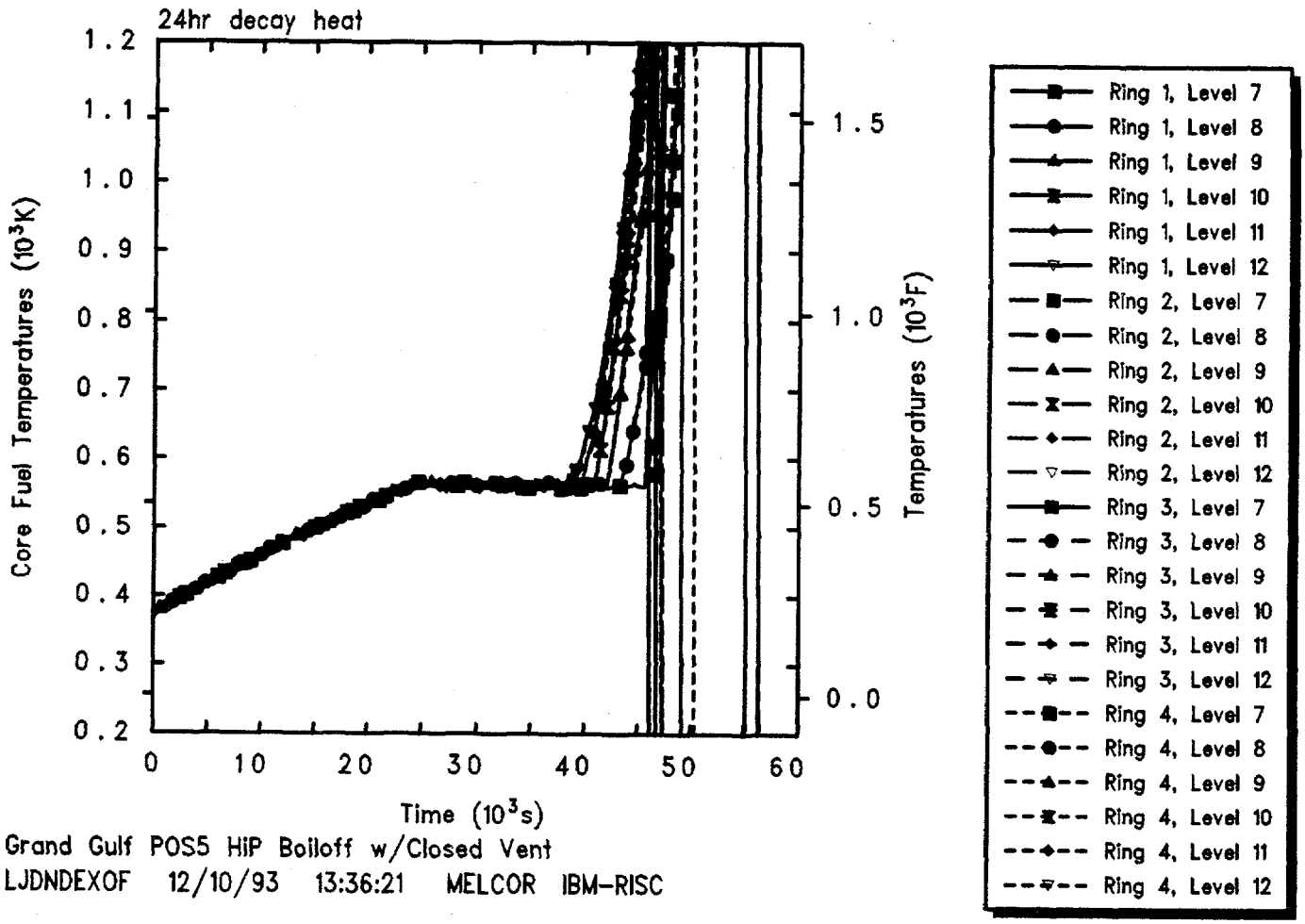

Figure 4.2.3.7. Core Fuel Temperatures for Grand Gulf POS 5 -- High Pressure Boiloff with Closed RPV Vent, Initiated 24 hr After Shutdown.

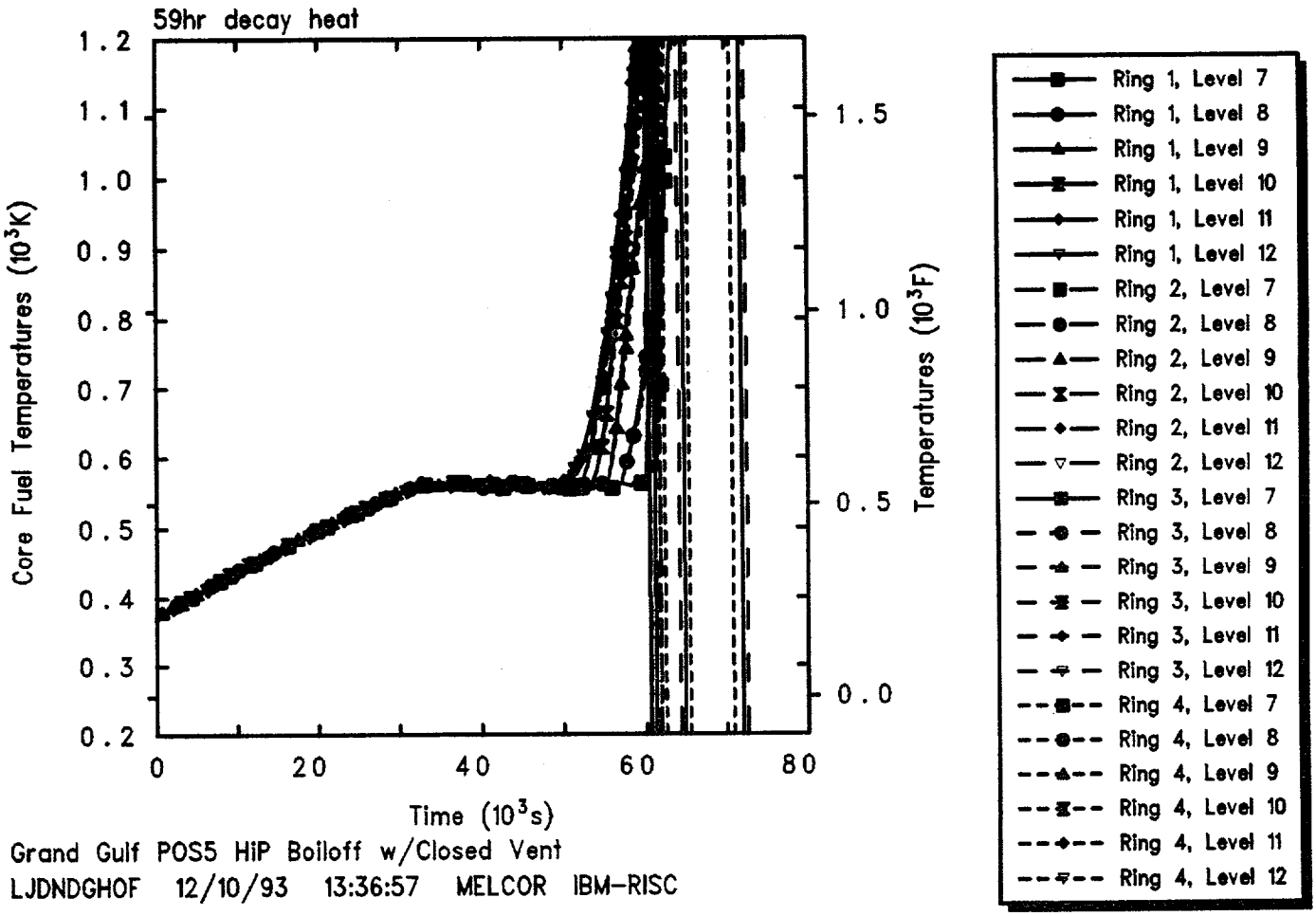

Figure 4.2.3.8. Core Fuel Temperatures for Grand Gulf POS 5 -- High Pressure Boiloff with Closed RPV Vent, Initiated 59 hr After Shutdown.

Table 4.2.3.1. Key Event Times for Grand Gulf POS 5 -- High Pressure Boiloff with Closed RPV Head Vent, Initiated at Various Times After Shutdown

Initiation Time After Shutdown	Time to (s) TAF Uncovery *	Core Heatup	First Gap Release	Vessel Failure
7 hr	26,000	28,400	32,638	58,043
24 hr	36,650	37,800	44,451	72,784
59 hr	48,800	50,400	58,624	89,888
12 days	93,000	96,200	110,500	--**

* Collapsed liquid level.
** Calculation stopped before event occurred.

Table 4.2.3.2. Key Signal Times for Grand Gulf POS 5 -- High Pressure Boiloff with Closed RPV Head Vent, Initiated at Various Times After Shutdown

Initiation Time After Shutdown	Time to (s) Collapsed Level <544.4 in	Swollen Level <544.4 in	Pressure >135 psia
7 hr	20,000	20,000	6,200
24 hr	25,500	25,500	9,000
59 hr	37,200	37,200	12,200
12 days	70,000	70,000	23,500

failure, but instead remains at the SRV cycling setpoints for only a few valve cycles before dropping due to continual inventory loss out the open RPV vent line. However, whether the RPV vent is open or closed, the higher the decay heat (i.e., the sooner after shutdown), the faster the initial pressurization and associated inventory loss, and the earlier the vessel fails.

The steam flow out both the SRVs and the RPV vent pressurizes the containment and the auxiliary building, as shown in Figure 4.2.4.2. The longer after shutdown that this accident sequence begins, the lower the decay heat and the slower the auxiliary building pressurizes. Unlike the results with the RPV vent closed, the auxiliary building reaches its 5 psig overpressure failure setpoint before vessel failure, due to the continued inventory loss through the open RPV vent for the higher decay heat level cases (i.e., 7 hr, 24 hr and 59 hr after shutdown). Only for lower decay heat levels (i.e., 12 days after shutdown) is the behavior the same with the RPV vent open or closed: the auxiliary building does not reach its 5 psig overpressure failure setpoint before vessel failure, but instead fails on a containment pressure spike caused by vessel failure and debris ejection.

Figure 4.2.4.3 illustrates that the vessel water mass drops more continuously with the RPV vent open than for the same accident scenario but with the RPV vent closed (Figure 4.2.3.3), in both cases dropping faster for higher decay heat levels.

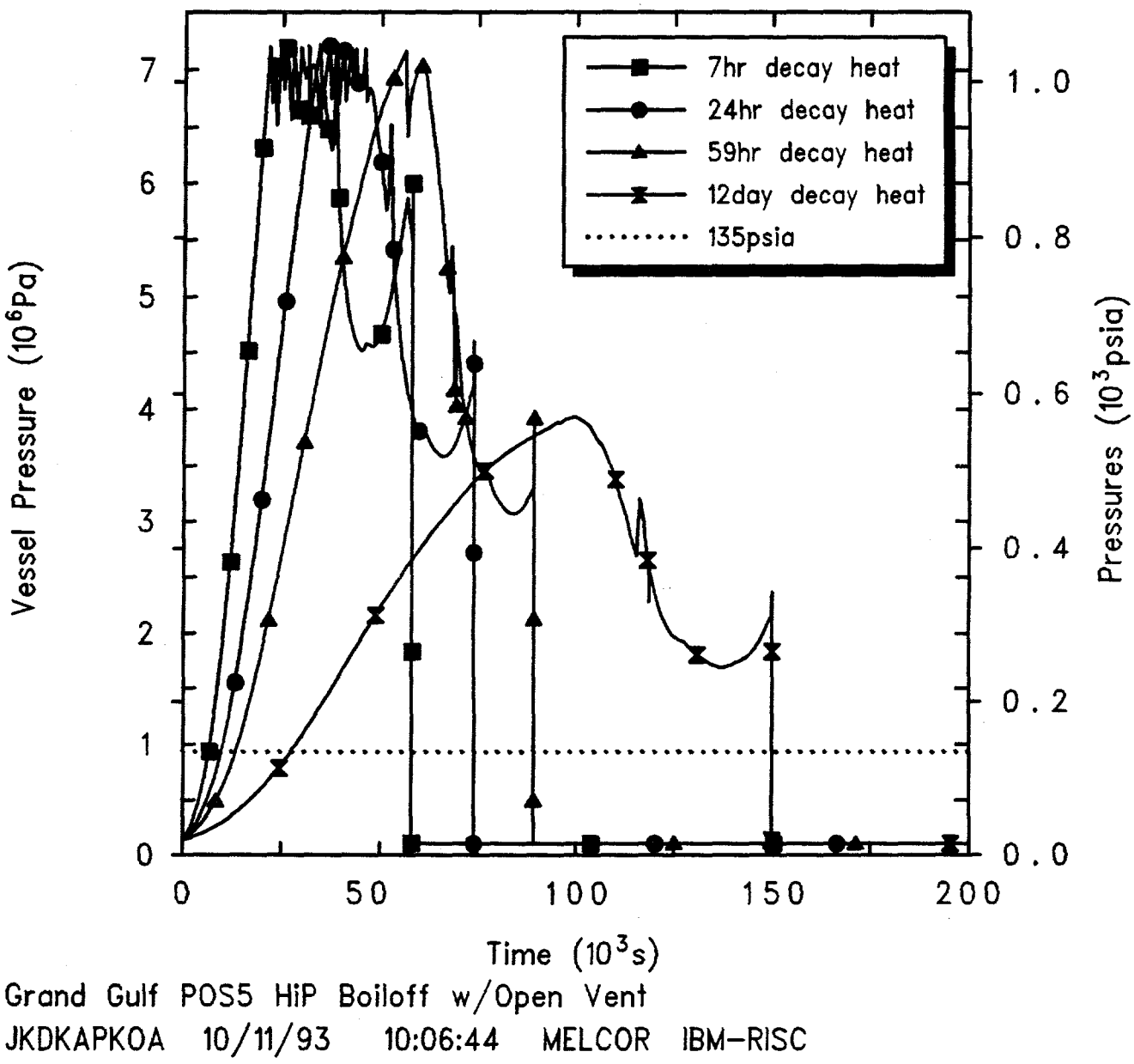

Figure 4.2.4.1. Reactor Vessel Pressures for Grand Gulf POS 5 -- High Pressure Boiloff with Open RPV Vent, Initiated at Various Times After Shutdown.

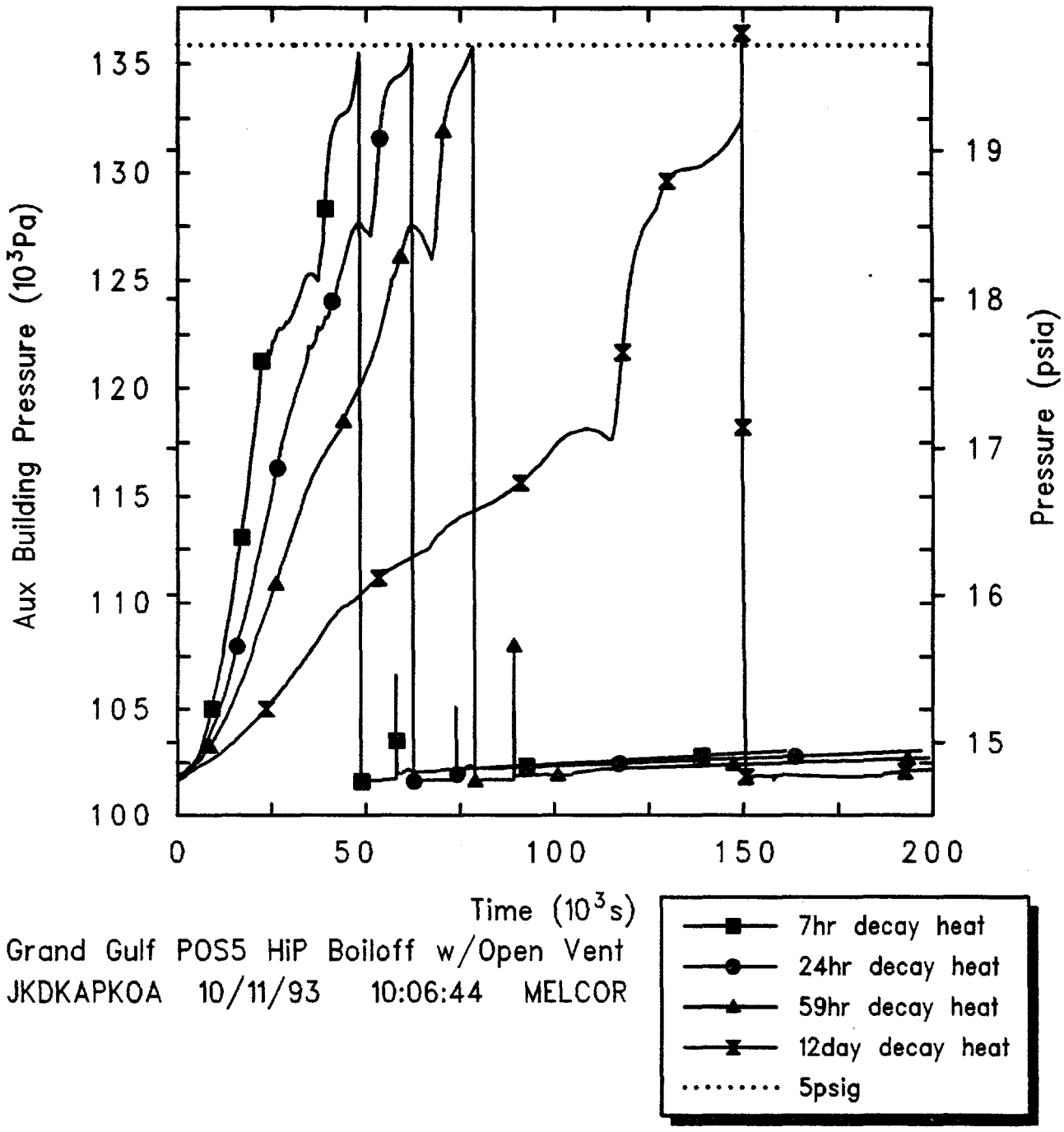

Figure 4.2.4.2. Auxiliary Building Pressures for Grand Gulf POS 5 -- High Pressure Boiloff with Open RPV Vent. Initiated at Various Times After Shutdown.

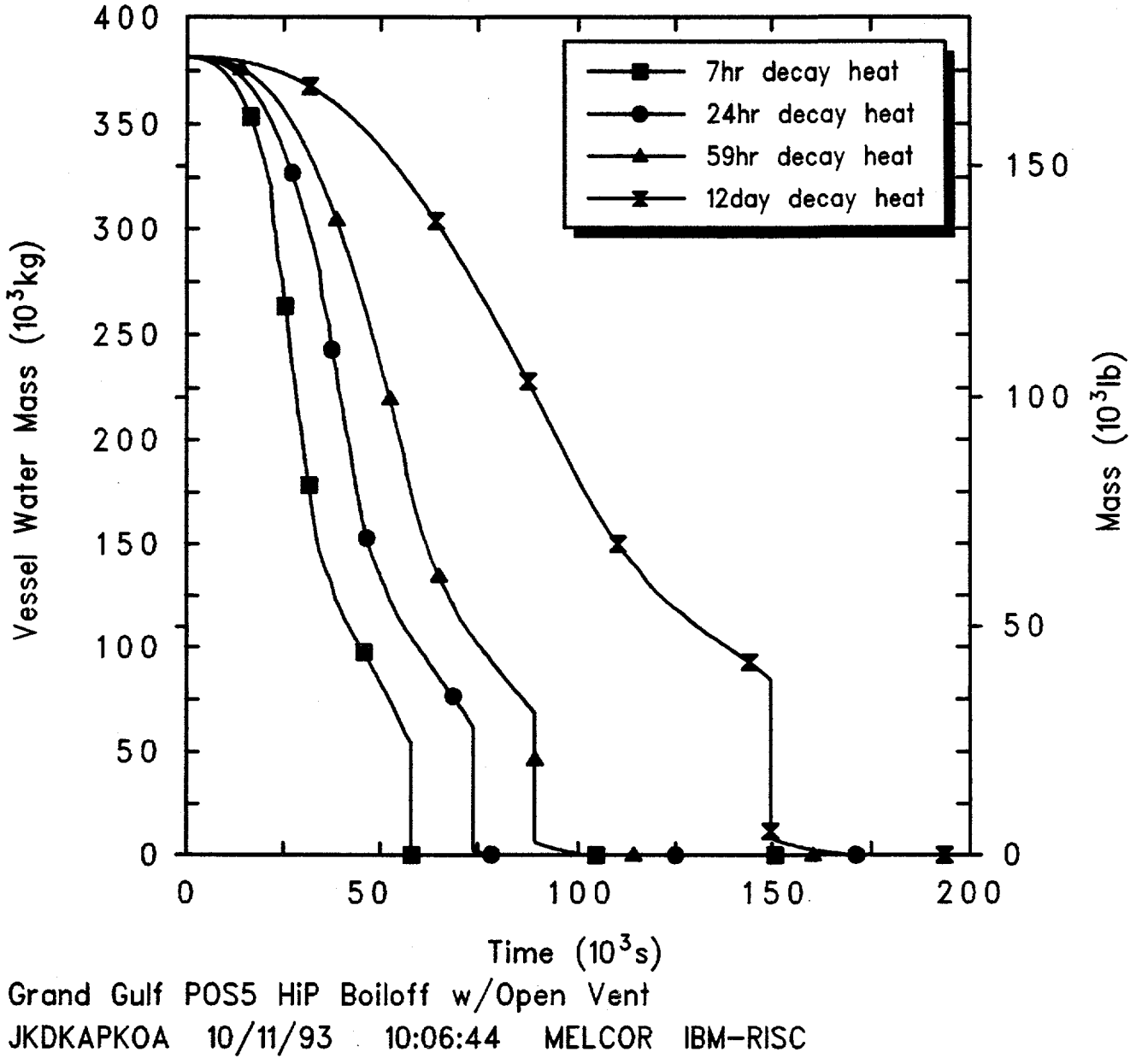

Figure 4.2.4.3. Reactor Vessel Water Masses for Grand Gulf POS 5 -- High Pressure Boiloff with Open RPV Vent, Initiated at Various Times After Shutdown.

Figure 4.2.4.4 gives the predicted upper plenum swollen and collapsed liquid levels for different decay heat levels and highlighting when a Level 3 trip (544.4 in) would be generated. The level initially rises as the vessel pressurizes, faster for higher decay heat levels, and then drops as inventory continues to be lost out the RPV vent and the SRV. The levels rise more slowly and later drop more slowly with the RPV vent open than with it closed (Figure 4.2.3.4), reflecting the difference between a more gradual, continual loss of inventory out the RPV vent in addition to flow out the cycling SRVs in the case with the RPV head vent open, compared to an inventory loss out the SRVs beginning later but progressing more rapidly as the system remains at pressure at the SRV setpoint longer with the RPV vent closed.

Figure 4.2.4.5 gives the corresponding upper core liquid level drop due to this inventory loss, for different decay heat levels and highlighting when TAF uncovery is calculated to occur; horizontal lines are included both at the top of the core (9.6 m) and at the TAF elevation (9.3 m). With the RPV vent open, the swollen and collapsed liquid levels in the upper core generally drop more smoothly than corresponding analyses with the RPV vent closed (Figure 4.2.3.5).

The core heatup is illustrated in Figures 4.2.4.6 through 4.2.4.8 as calculated for this high-pressure boiloff with the RPV vent open starting at 7 hr, 24 hr and 59 hr after shutdown. The results with the RPV vent open and closed are generally quite similar. As with TAF uncovery, core uncovery begins sooner and proceeds more rapidly at higher decay heat levels. As with the RPV vent closed, the calculation with the RPV vent open and initial decay heat corresponding to 12 days after shutdown showed core heatup beginning only after about 90,000 s, and is not shown because the period of interest for all these Level 1 analyses is the first 24 hr after accident initiation.

Tables 4.2.4.1 and 4.2.4.2 summarize the timings of various key events predicted using MELCOR for this sequence assuming various times after shutdown and associated decay heat levels. (A calculation beginning 40 days after shutdown was not done for this sequence because the results of the analysis beginning 12 days after shutdown showed no significant core uncovery or damage within the 1 day time window of interest.)

4.2.5 Large Break LOCA

This accident is initiated by a large break LOCA in the recirculation line. At the start of the accident, the reactor vessel is depressurized, the coolant is at the normal level and the SRVs are closed. The vessel water inventory is at 366.5 K (200°F), which corresponds to the maximum temperature allowed by the Grand Gulf technical specifications for operation in POS 5. The break drains the vessel to 2/3 core height. The initiating event then results in a loss of all core cooling and coolant makeup. The reactor pressure vessel head vent is closed at the beginning of the transient. The drywell personnel lock is open; the containment equipment hatch and both of the containment personnel locks are open (i.e., "open containment").

Figure 4.2.5.1 gives the vessel pressures calculated for this accident scenario initiated at several different times after shutdown. In all cases, the primary system remains near atmospheric as the large break maintains pressure near-equilibrium between the primary and the containment, while the open personnel locks and equipment hatch vent the containment to the auxiliary building. For any given decay heat level, the smaller pressure spikes seen in Figure 4.2.5.1 generally correspond to core heatup and damage, while the largest pressure spikes seen in Figure 4.2.5.1 correspond to vessel failure.

The water and steam coolant flowing out through the break pressurizes the containment and, through the open equipment hatch and personnel locks, pressurizes the auxiliary building, as shown in Figure 4.2.5.2. The longer after shutdown that this accident sequence begins, the lower the decay heat and the longer it takes to fail the auxiliary building. The auxiliary building pressure rises somewhat more slowly during the early stages of core uncovery, heatup and damage, then spikes up to the failure point at vessel failure.

The coolant inventory in the vessel drops due to coolant and steam loss out the break, with a very rapid loss of about 60-70% of the inventory as liquid followed by a more gradual loss of the remaining inventory due to boiling and steam outflow, as presented in Figure 4.2.5.3.

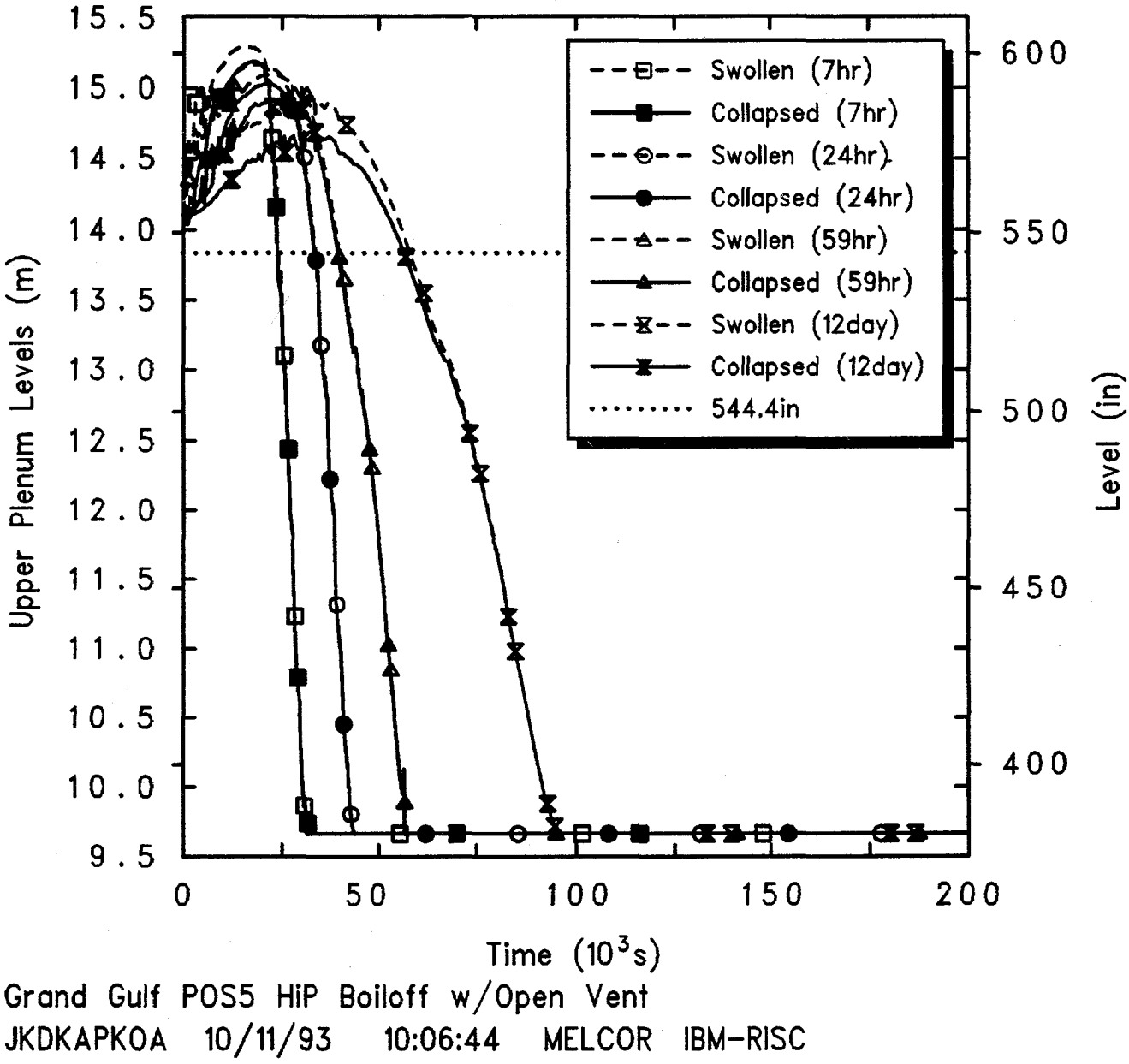

Figure 4.2.4.4. Upper Plenum Liquid Levels for Grand Gulf POS 5 -- High Pressure Boiloff with Open RPV Vent, Initiated at Various Times After Shutdown.

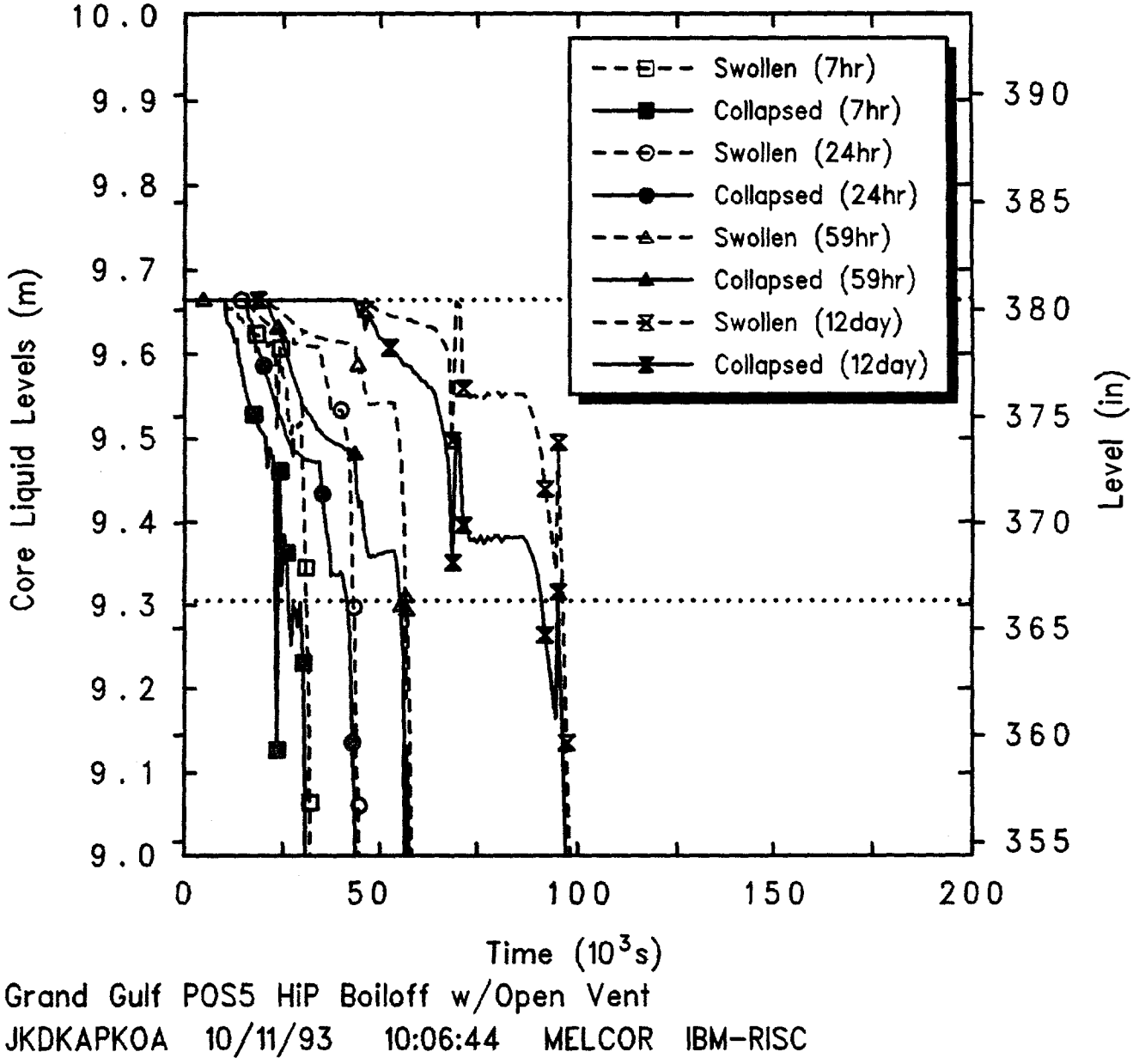

Figure 4.2.4.5. Core Liquid Levels for Grand Gulf POS 5 -- High Pressure Boiloff with Open RPV Vent, Initiated at Various Times After Shutdown.

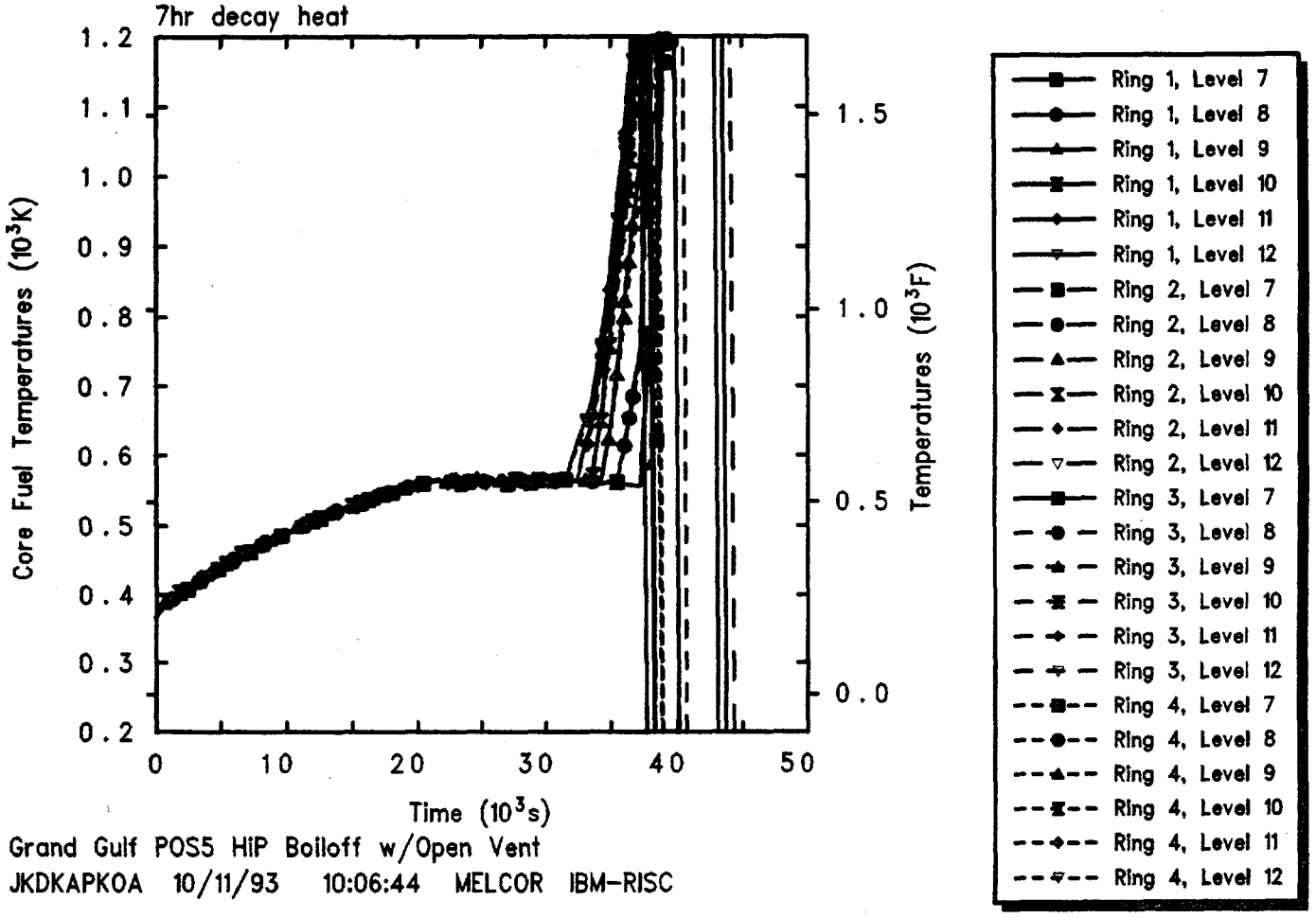

Figure 4.2.4.6. Core Fuel Temperatures for Grand Gulf POS 5 -- High Pressure Boiloff with Open RPV Vent, Initiated 7 hr After Shutdown.

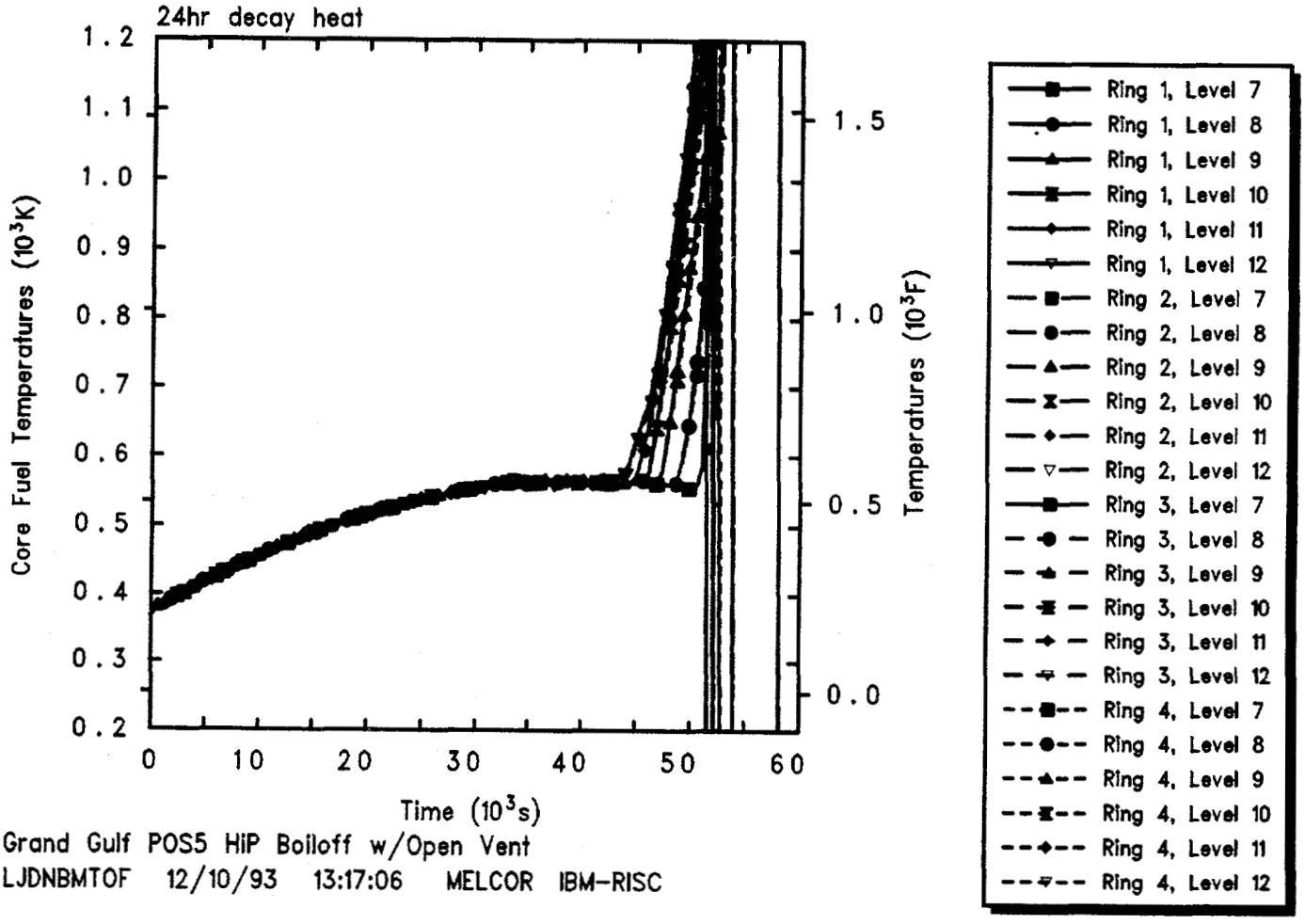

Figure 4.2.4.7. Core Fuel Temperatures for Grand Gulf POS 5 -- High Pressure Boiloff with Open RPV Vent, Initiated 24 hr After Shutdown.

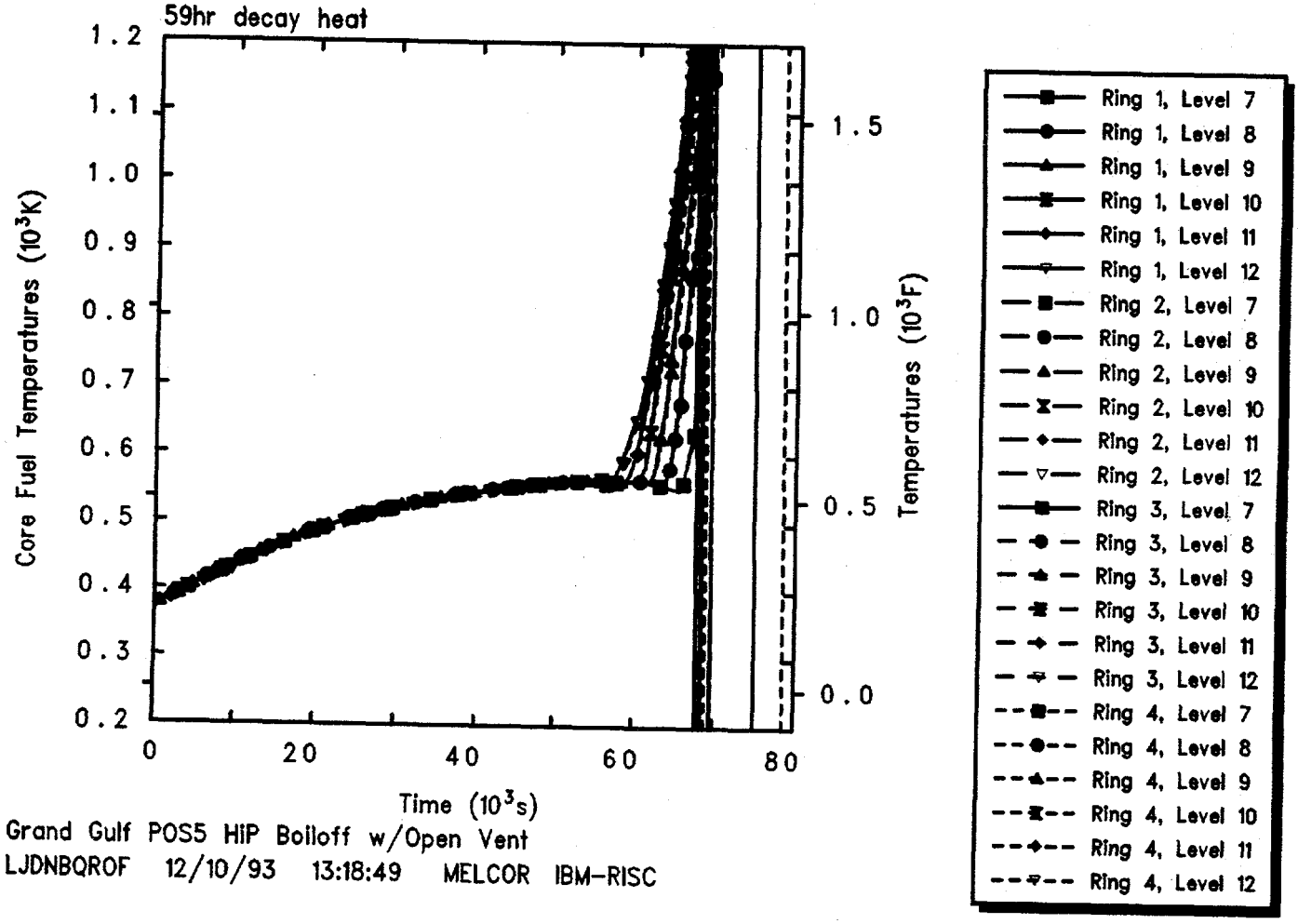

Figure 4.2.4.8. Core Fuel Temperatures for Grand Gulf POS 5 -- High Pressure Boiloff with Open RPV Vent, Initiated 59 hr After Shutdown.

Table 4.2.4.1. Key Event Times for Grand Gulf POS 5 -- High Pressure Boiloff with Open RPV Head Vent, Initiated at Various Times After Shutdown

Initiation Time After Shutdown	Time to (s) TAF Uncovery *	Core Heatup	First Gap Release	Vessel Failure
7 hr	30,000	31,600	36,470	57,780
24 hr	40,850	43,800	49,930	73,550
59 hr	55,200	58,400	65,890	88,970
12 days	91,000	97,500	113,000	--**

* Collapsed liquid level.
** Calculation stopped before event occurred.

Table 4.2.4.2. Key Signal Times for Grand Gulf POS 5 -- High Pressure Boiloff with Open RPV Head Vent, Initiated at Various Times After Shutdown

Initiation Time After Shutdown	Time to (s) Collapsed Level <544.4 in	Swollen Level <544.4 in	Pressure >135 psia
7 hr	24,000	24,000	6,700
24 hr	33,500	33,500	9,900
59 hr	39,600	39,750	13,200
12 days	56,000	57,500	27,300

The amount of liquid inventory lost in the initial liquid blowdown is determined by the elevation of the break and is therefore about the same regardless of the decay heat level; later, as would be expected, the gradual inventory loss due to continued steaming is faster for higher decay heat levels.

The upper plenum and core liquid levels drop very quickly as the break drains the vessel to 2/3 core height, within seconds or minutes, and are not shown for this accident scenario.

The early core heatup is illustrated in Figures 4.2.5.4 through 4.2.5.7 as calculated for LBLOCA accidents initiated at 7 hr, 24 hr, 59 hr and 40 days after shutdown. Core uncovery and heatup begins sooner and proceeds more rapidly at higher decay heat levels.

Table 4.2.5.1 summarizes the timings of various key events predicted using MELCOR for this sequence assuming various times after shutdown and associated decay heat levels.

4.2.6 Station Blackout with Failure to Isolate SDC

The accident is initiated by a loss of offsite power with the reactor vessel depressurized and the coolant at the normal level. The vessel water inventory is at 366.5 K (200°F), which corresponds to the maximum temperature allowed by the Grand Gulf technical specifications for operation in POS 5. Following the initiating event, onsite power is lost leading to a SBO and loss of all core

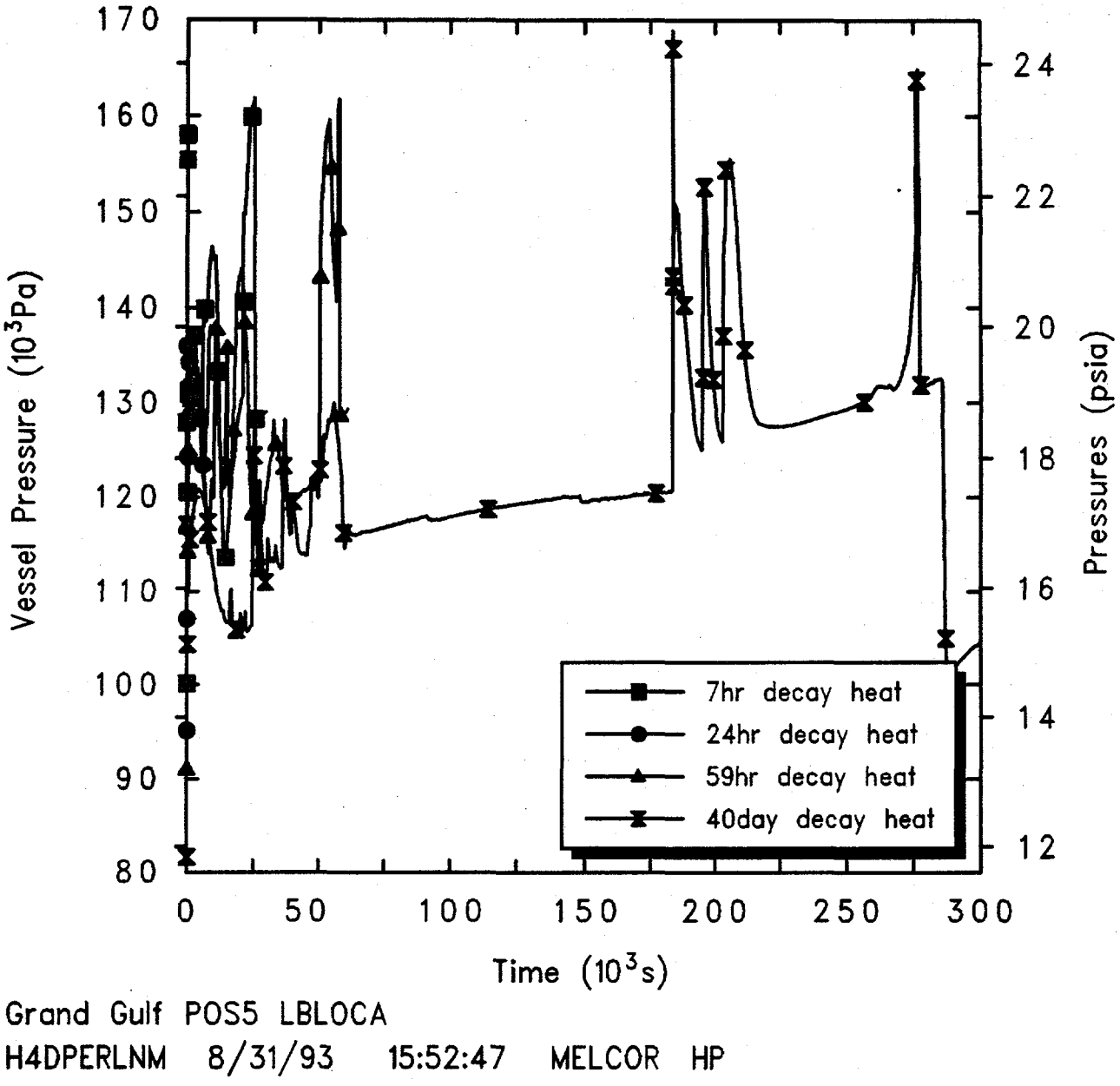

Figure 4.2.5.1. Reactor Vessel Pressures for Grand Gulf POS 5 -- Large Break LOCA, Initiated at Various Times After Shutdown.

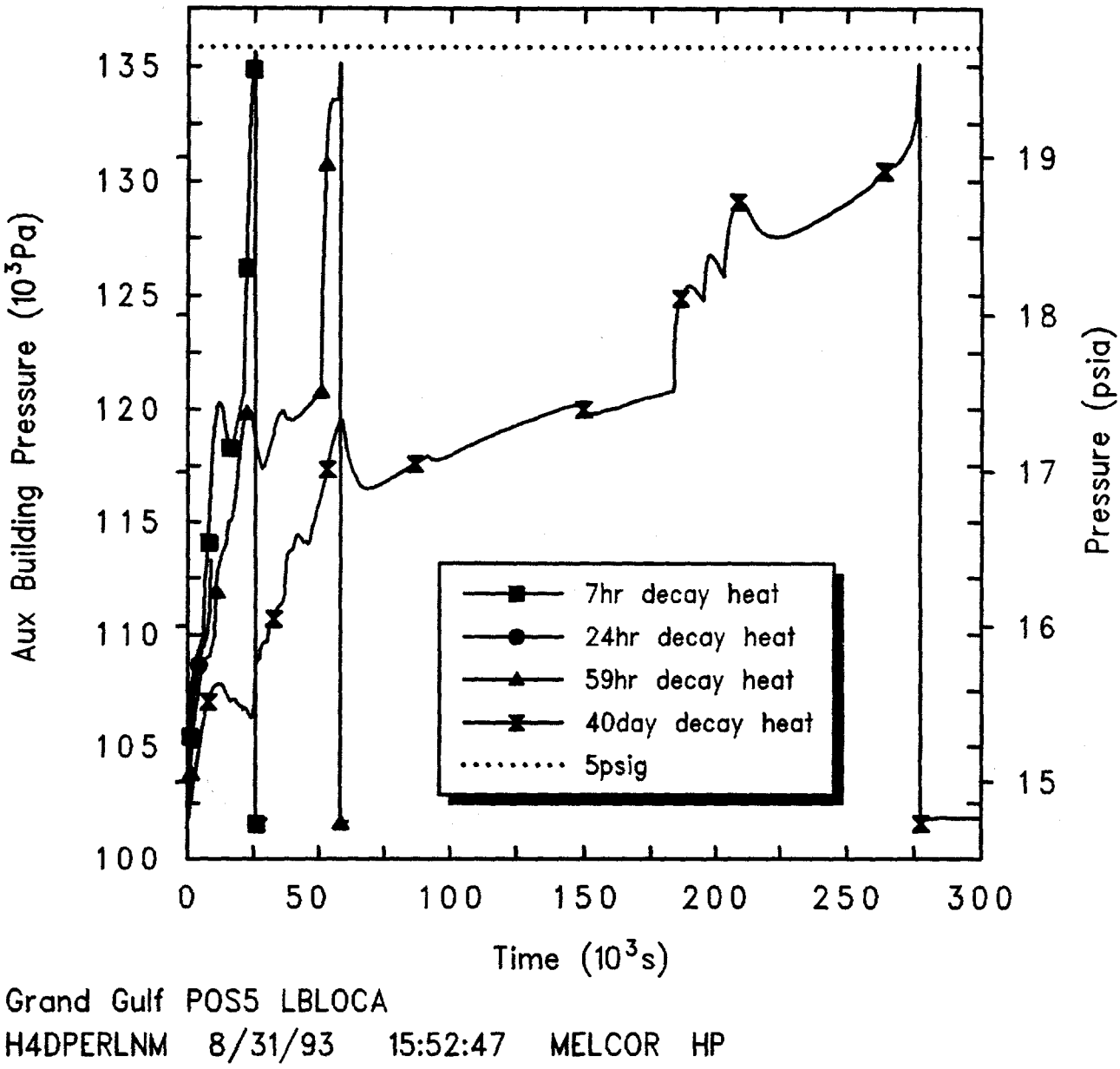

Figure 4.2.5.2. Auxiliary Building Pressures for Grand Gulf POS 5 -- Large Break LOCA, Initiated at Various Times After Shutdown.

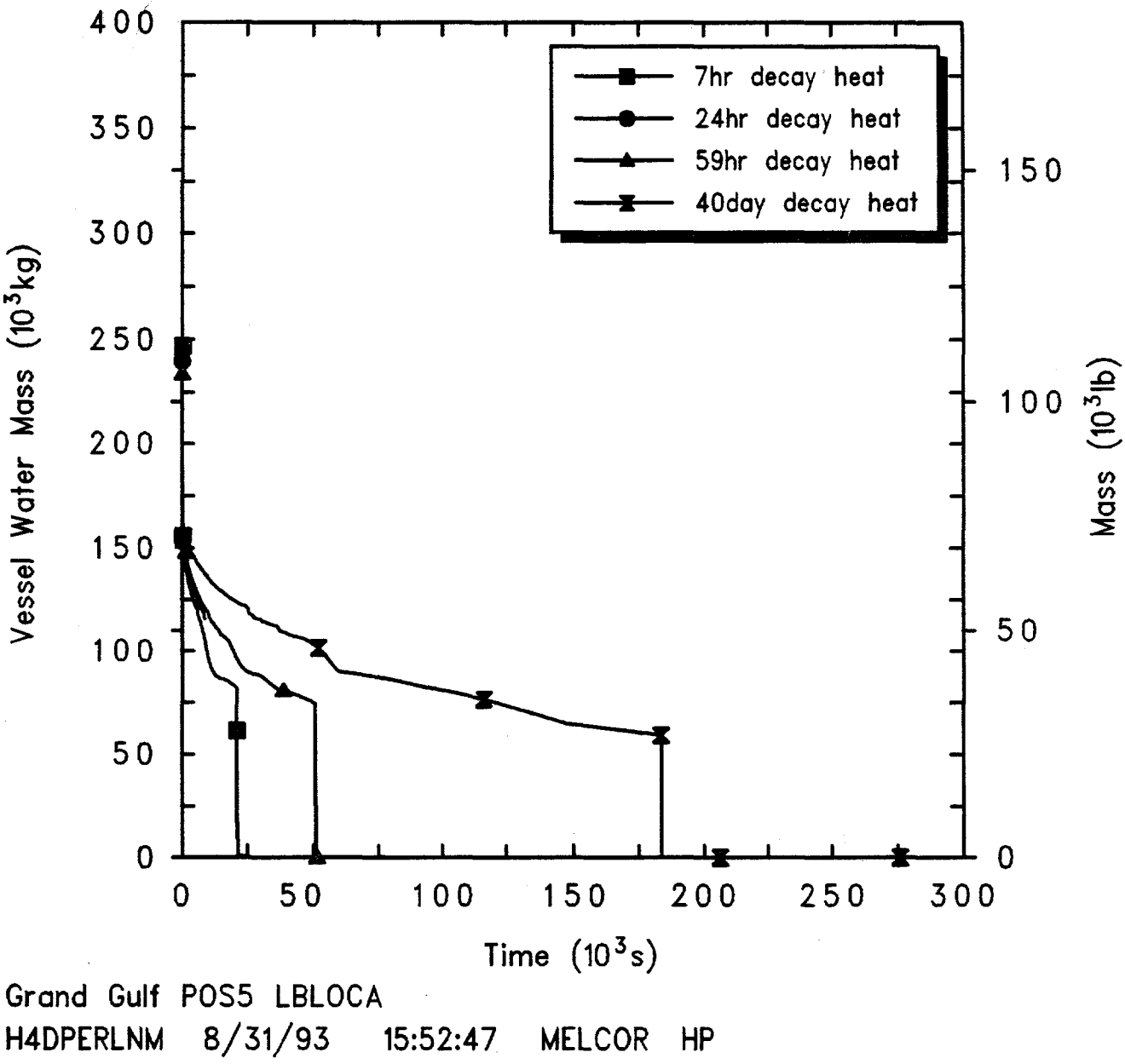

Figure 4.2.5.3. Reactor Vessel Water Masses for Grand Gulf POS 5 -- Large Break LOCA, Initiated at Various Times After Shutdown.

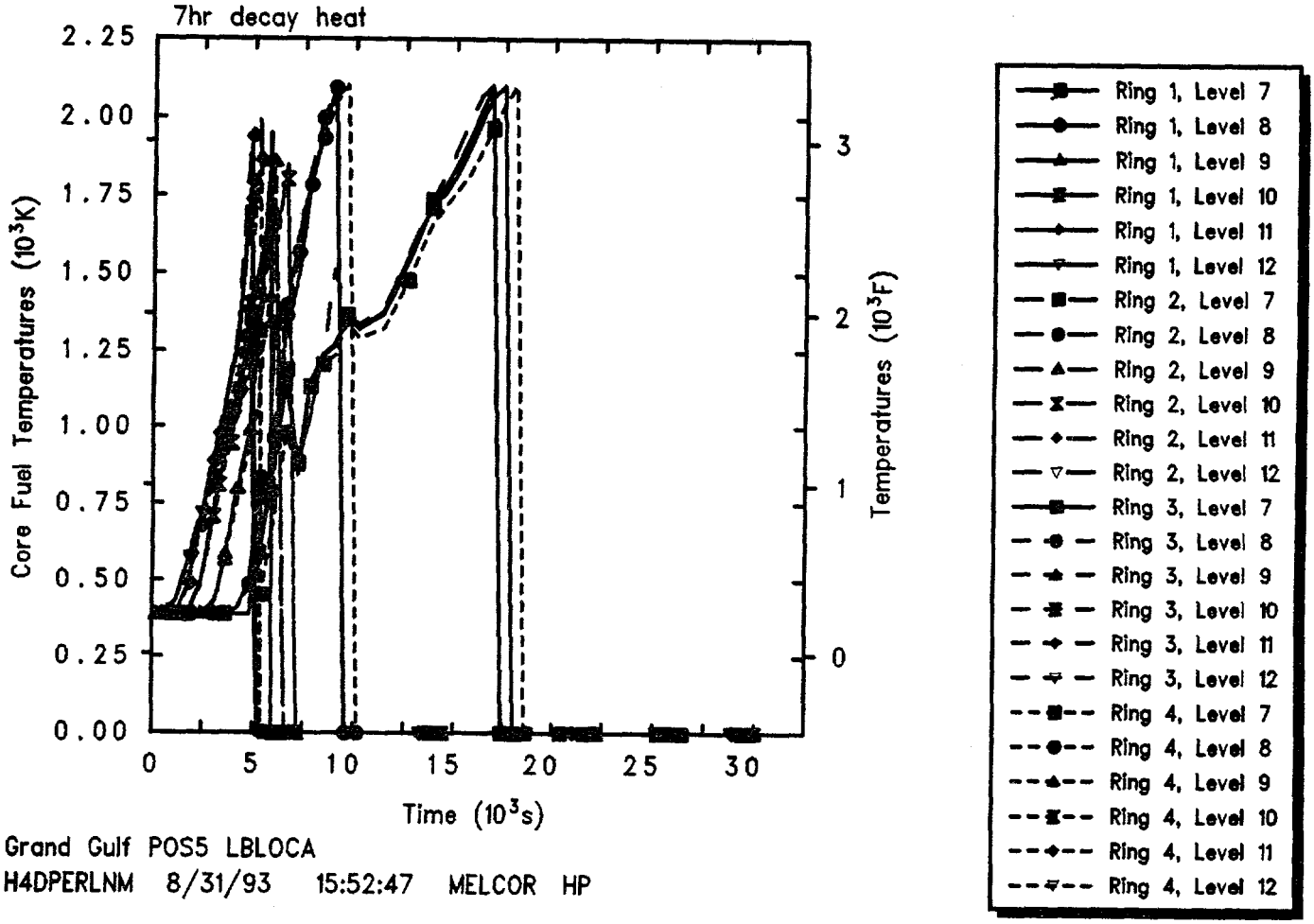

Figure 4.2.5.4. Core Fuel Temperatures for Grand Gulf POS 5 -- Large Break LOCA, Initiated 7 hr After Shutdown.

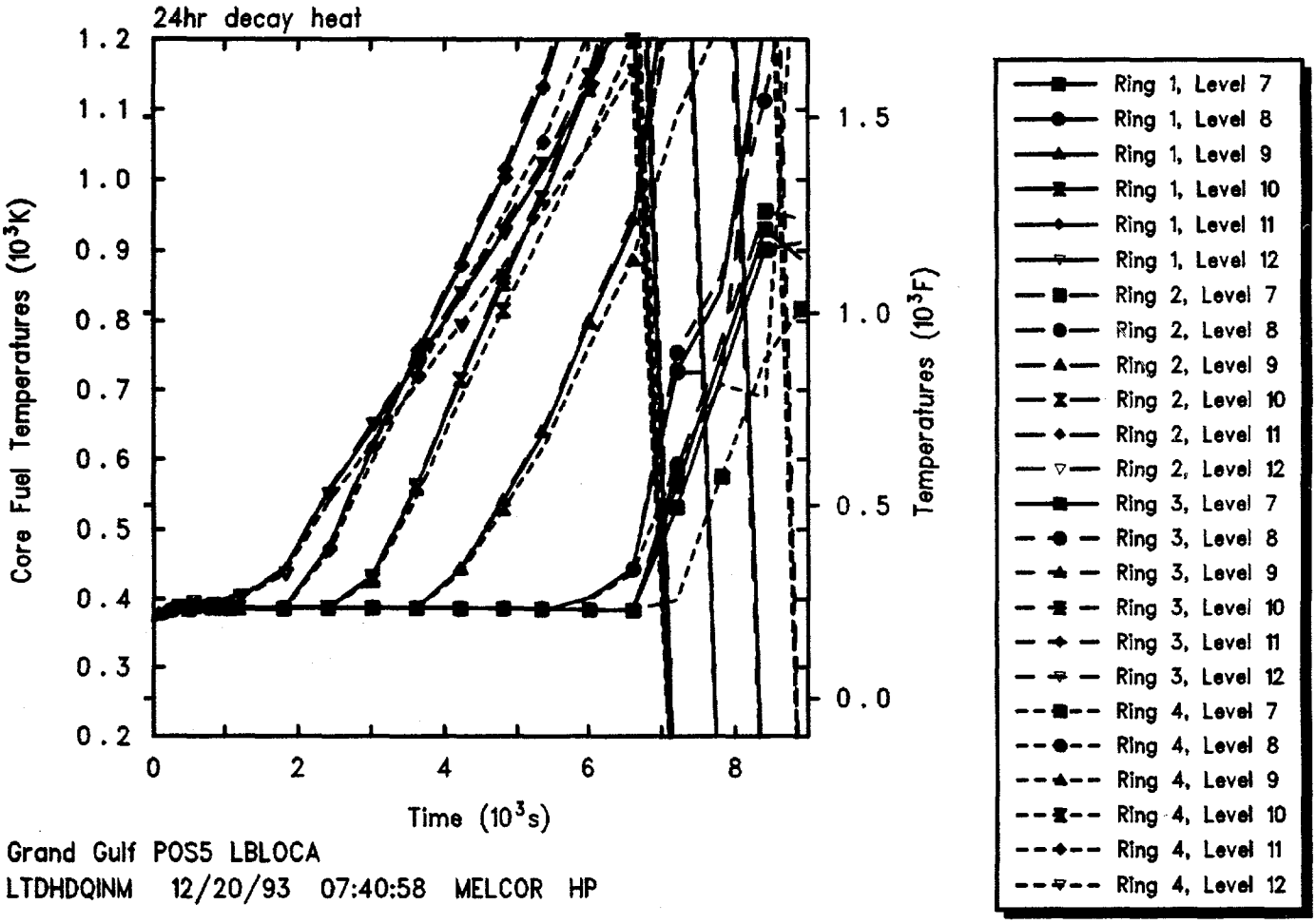

Figure 4.2.5.5. Core Fuel Temperatures for Grand Gulf POS 5 -- Large Break LOCA, Initiated 24 hr After Shutdown.

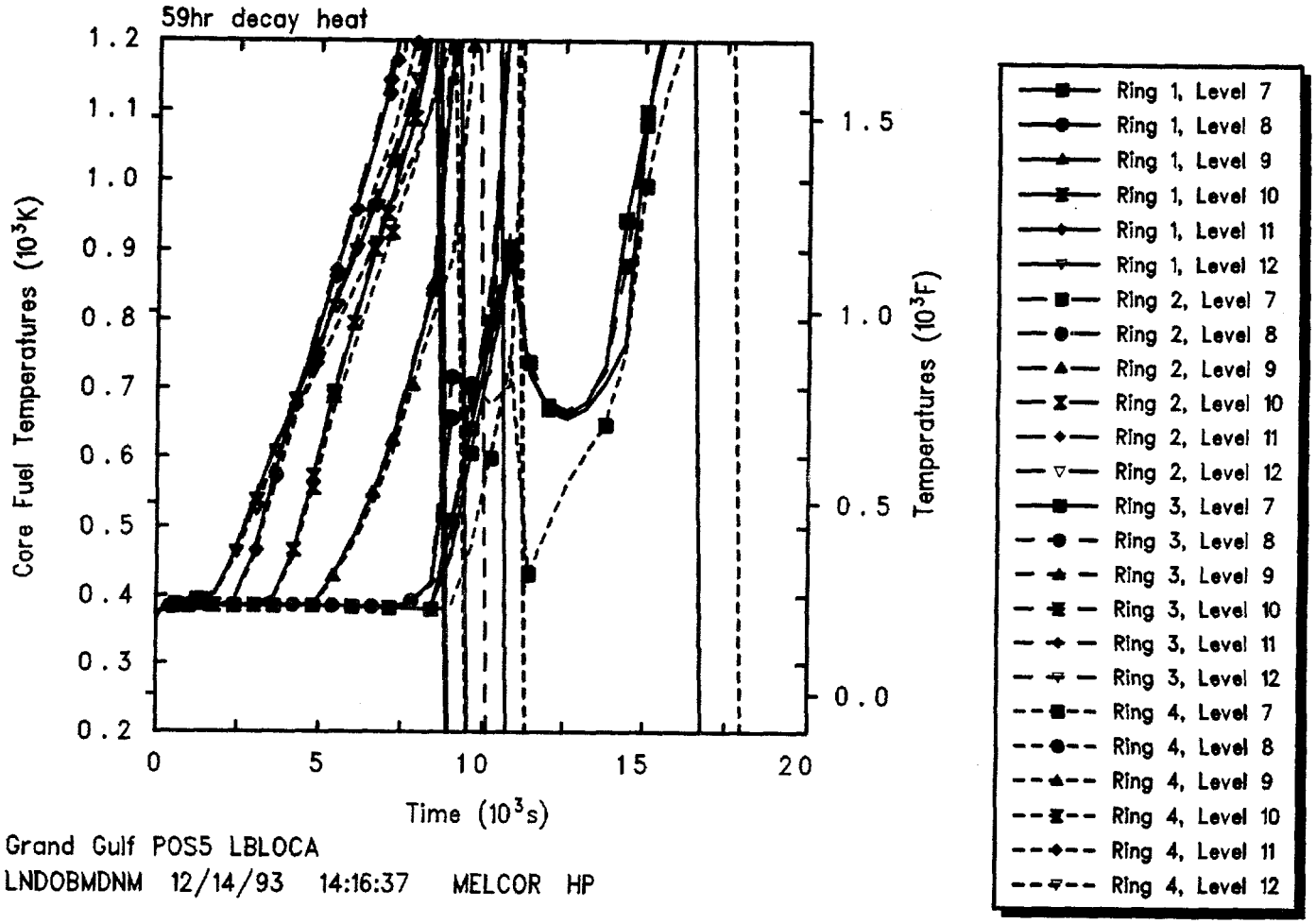

Figure 4.2.5.6. Core Fuel Temperatures for Grand Gulf POS 5 -- Large Break LOCA, Initiated 59 hr After Shutdown.

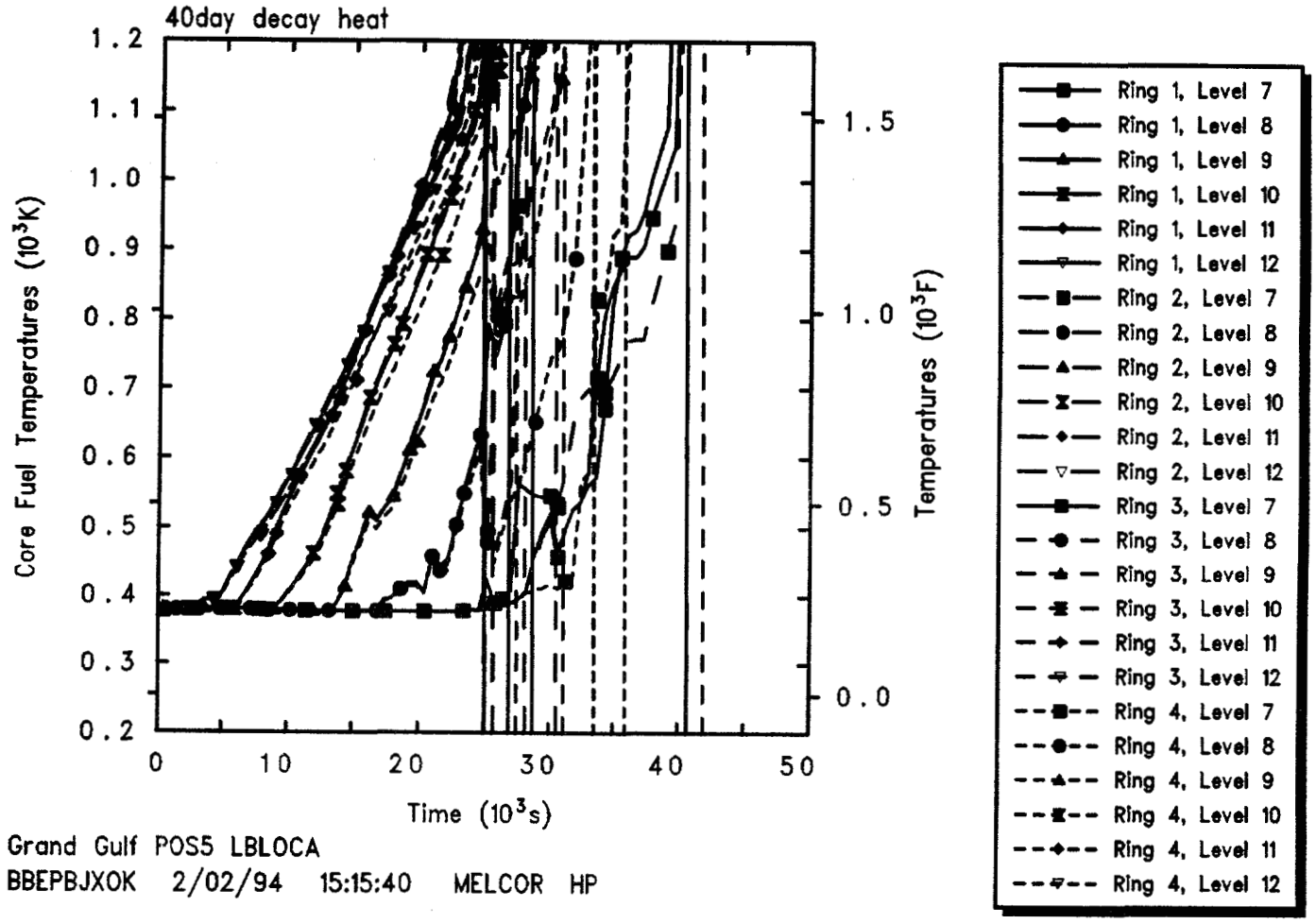

Figure 4.2.5.7. Core Fuel Temperatures for Grand Gulf POS 5 -- Large Break LOCA, Initiated 40 days After Shutdown.

Table 4.2.5.1. Key Event Times for Grand Gulf POS 5 -- Large Break LOCA, Initiated at Various Times After Shutdown

Initiation Time After Shutdown	TAF Uncovery *	Time to (s) Core Heatup	First Gap Release	Vessel Failure
7 hr	61	500	3,875	21,030
24 hr	62	1,000	5,445	33,850
59 hr	65	1,500	7,125	50,475
40 days	71	4,500	22,200	183,500

* Collapsed liquid level.

cooling and coolant makeup. The operator fails to open the SRVs and steam the core at low pressure (i.e., the SRVs operate in the relief mode). Since the SRVs are closed, the RPV will pressurize. The SBO precludes the isolation of the low pressure piping in the SDC system. This low-pressure SDC system piping fails when the RPV pressure reaches 3.135 MPa (440 psig) resulting in an interfacing systems LOCA with outflow from the vessel downcomer to the first floor of the auxiliary building. The drywell personnel lock is open; the containment equipment hatch and both of the containment personnel locks are open (i.e., "open containment").

Figure 4.2.6.1 presents the vessel pressures calculated starting this accident scenario at several different times after shutdown; Figure 4.2.6.1 also includes horizontal lines at 440 psig, the postulated SDC break setpoint, and at 160 psig, a pressure signal of interest because it is the failure pressure for any shutdown cooling provided by the ADHRS. In all cases, the system begins pressurizing as all core cooling is lost. For most decay heat levels the primary system pressurizes to 3.135 MPa (440 psig), which actuates the postulated SDC break; however, for a decay heat level corresponding to 40 days after shutdown, relief through the open RPV vent line is sufficient to cause the primary system pressure to begin dropping before reaching the SDC break setpoint. The flow out the SDC line break goes directly to the auxiliary building first floor and pressurizes the auxiliary building, as indicated in Figure 4.2.6.2. Even with the SDC break remaining closed for the sequence initiated 40 days after shutdown, the flow out the open RPV vent line pressurizes the containment and, through the open equipment hatch and personnel locks, pressurizes the auxiliary building. As expected, the lower the decay heat the slower the auxiliary building pressurizes and the longer it takes to fail the auxiliary building.

The coolant inventory in the vessel drops as the decay heat boils water to steam which is lost out the SDC break and the open RPV vent, faster for higher decay heat levels, as presented in Figure 4.2.6.3. The opening of the SDC break is reflected in the extremely rapid loss of about 75% of the vessel inventory seen at various times; that inventory loss then slows down when the break uncovers, until subsequent vessel failure.

Figure 4.2.6.4 gives the predicted upper plenum liquid level drop due to this inventory loss, for different decay heat levels and highlighting when a Level 3 trip (544.4 in) would be generated. In all cases, the upper plenum level initially rises as the primary system pressurizes and then falls rapidly when the SDC break is opened. For lower decay heat levels (i.e., longer after shutdown), the upper plenum level peaks and begins dropping steadily before the SDC break opens, due to flow out the open RPV vent.

Figure 4.2.6.5 gives the corresponding core liquid level drop due to this inventory loss, for different decay heat levels and highlighting when TAF uncovery is calculated to occur; horizontal lines indicate both the boundary between the upper plenum and the core at 9.6 m and the top-of-active-fuel elevation at 9.3 m. Note that, for decay heat levels such that the primary system pressurizes sufficiently to open the postulated SDC break, the core

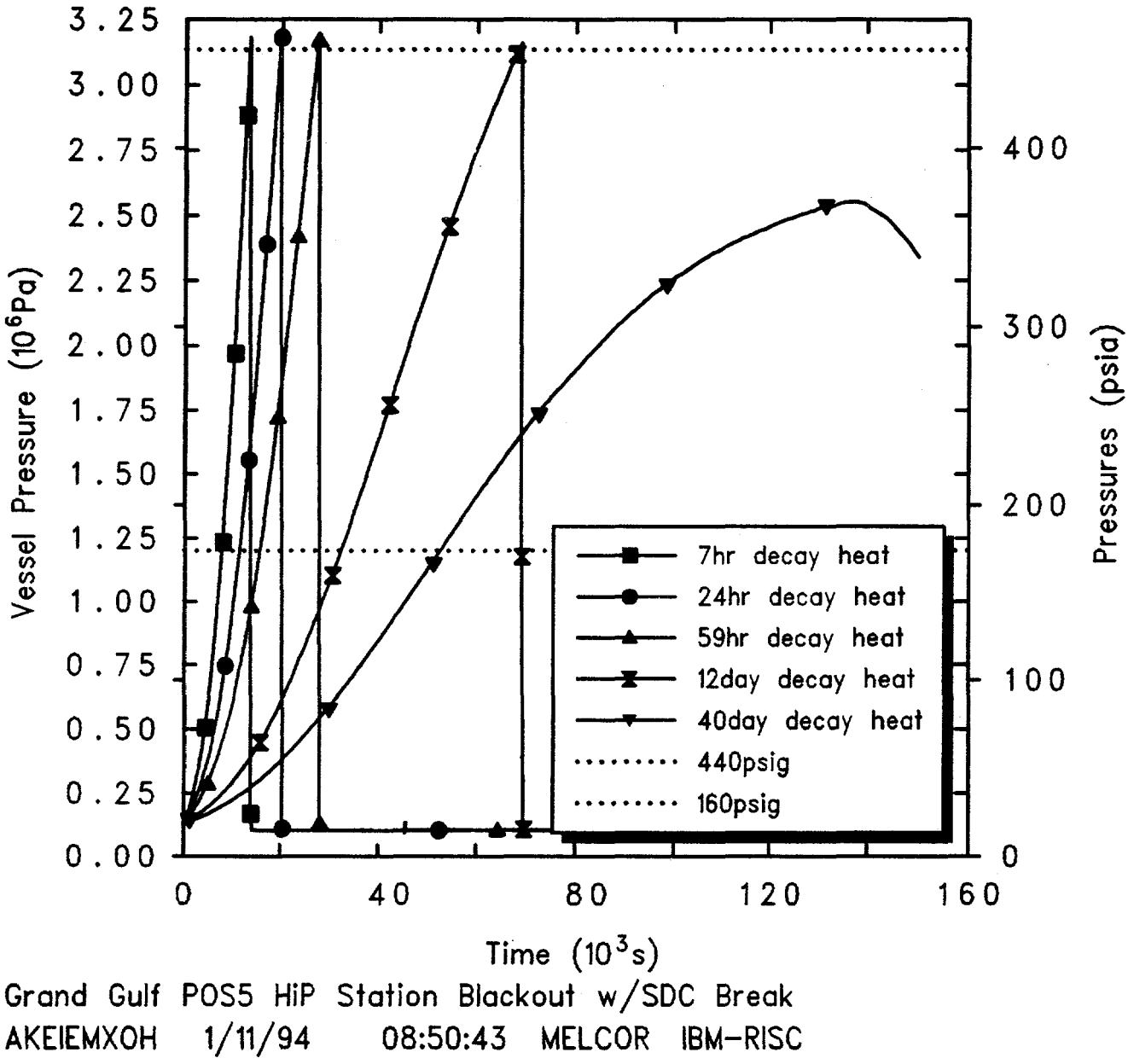

Figure 4.2.6.1. Reactor Vessel Pressures for Grand Gulf POS 5 -- Station Blackout with SDC Break, Initiated at Various Times After Shutdown.

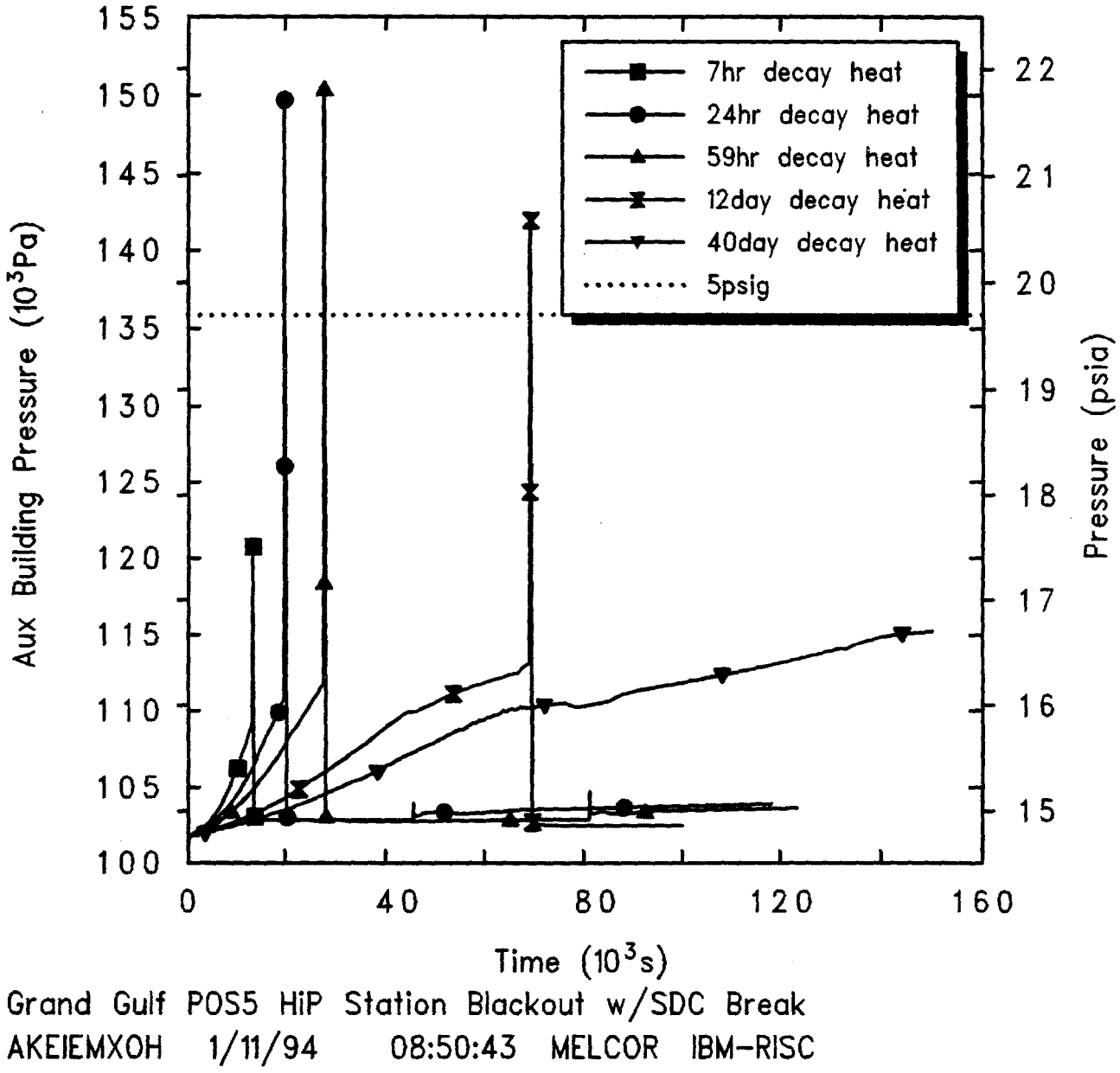

Figure 4.2.6.2. Auxiliary Building Pressures for Grand Gulf POS 5 -- Station Blackout with SDC Break, Initiated at Various Times After Shutdown.

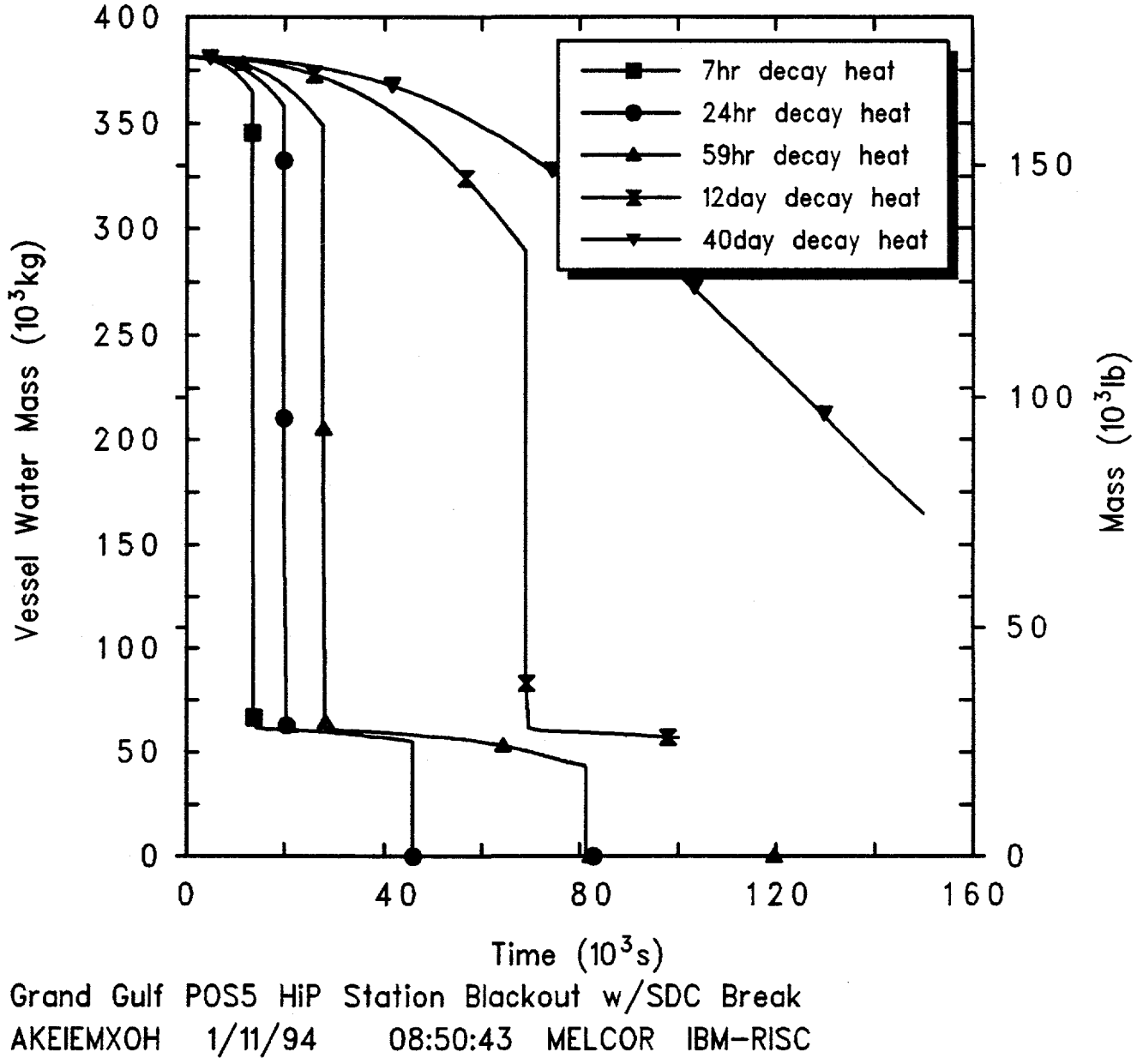

Figure 4.2.6.3. Reactor Vessel Water Masses for Grand Gulf POS 5 -- Station Blackout with SDC Break, Initiated at Various Times After Shutdown.

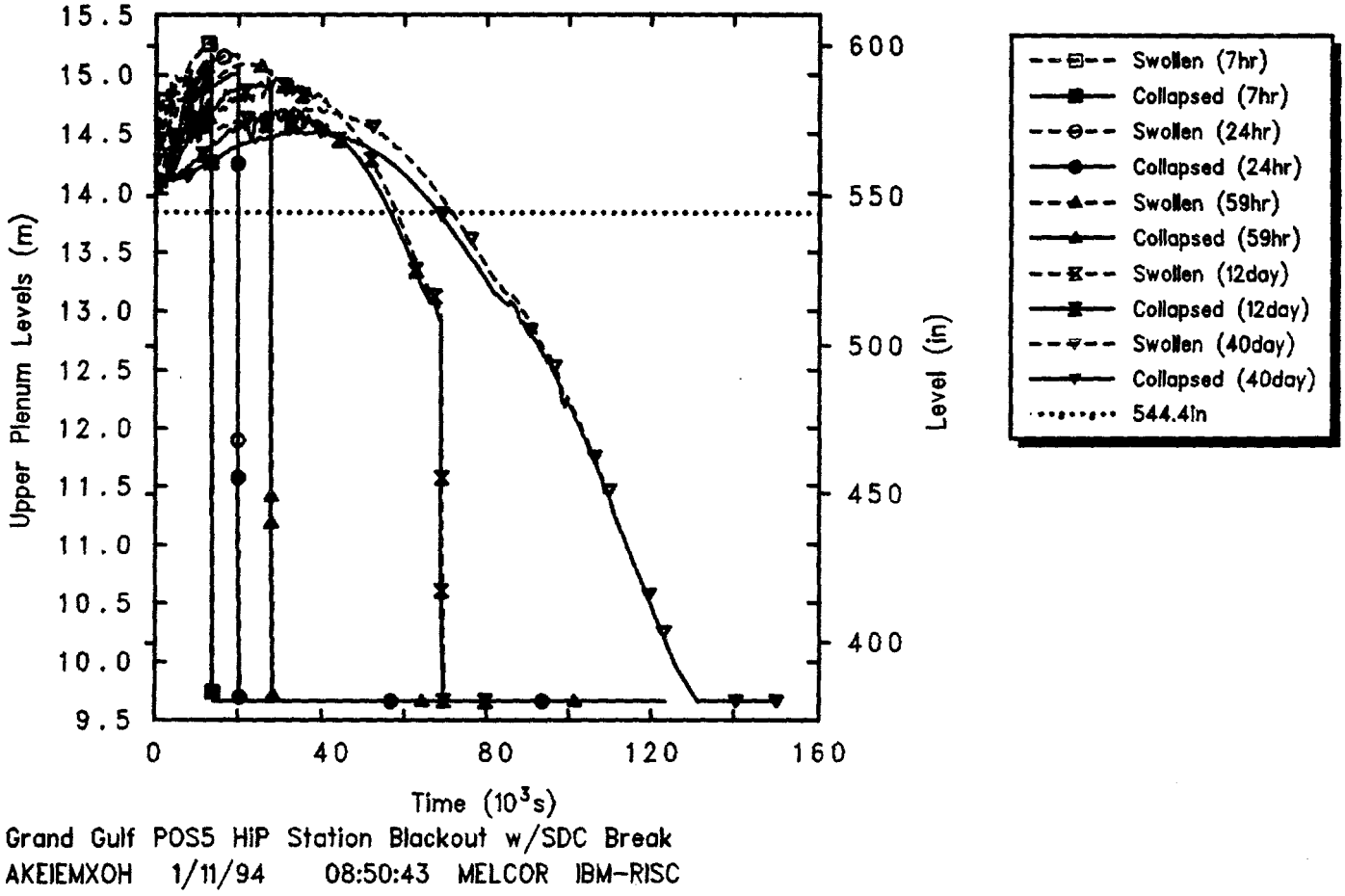

Figure 4.2.6.4. Upper Plenum Liquid Levels for Grand Gulf POS 5 -- Station Blackout with SDC Break, Initiated at Various Times After Shutdown.

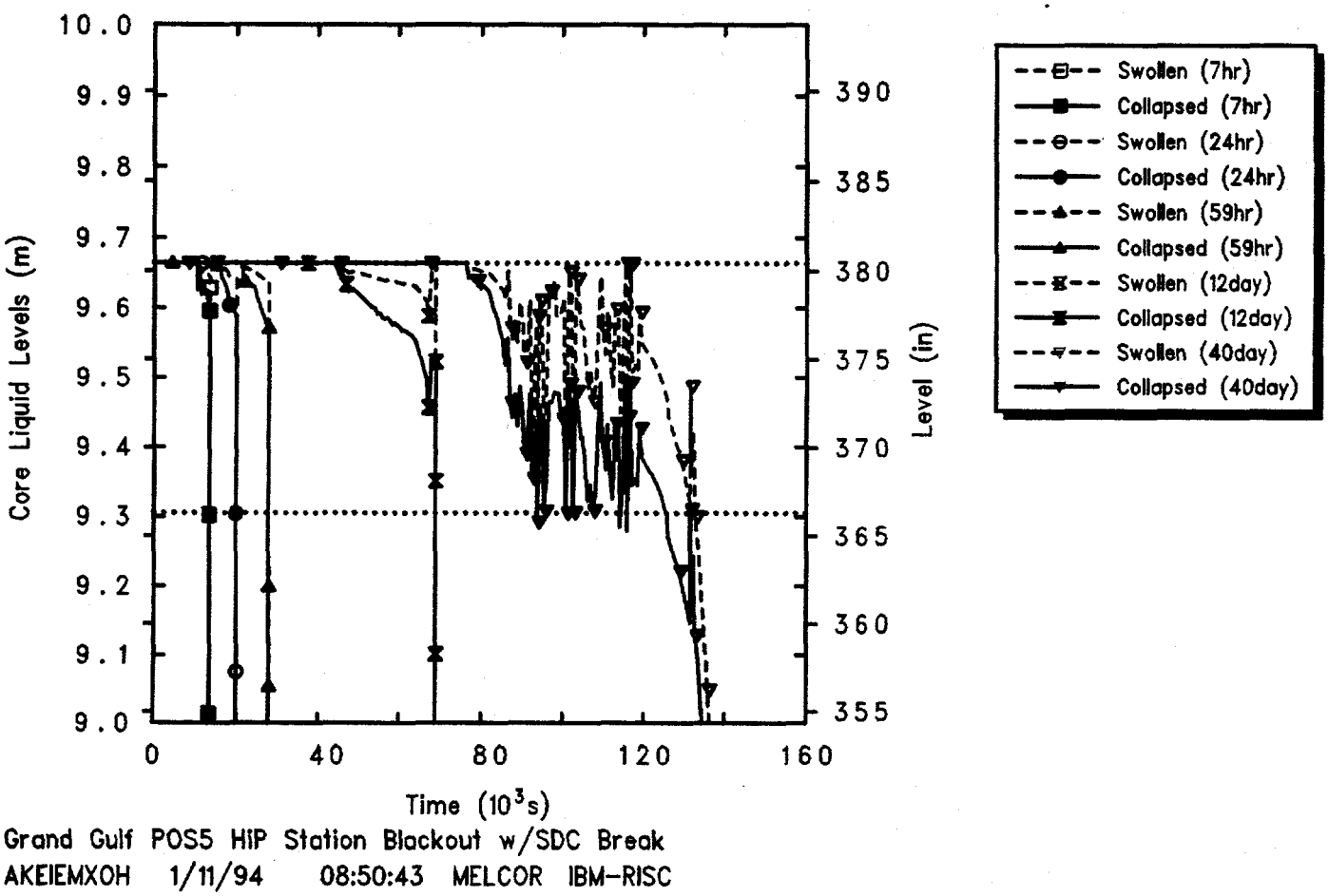

Figure 4.2.6.5. Core Liquid Levels for Grand Gulf POS 5 -- Station Blackout with SDC Break, Initiated at Various Times After Shutdown.

liquid levels drop precipitously when the SDC break opens, as did the upper plenum liquid levels also. The behavior is qualitatively different for a decay heat level low enough that relief through the open RPV vent line is sufficient to cause the primary system pressure to begin dropping before reaching the SDC break setpoint. While the upper plenum levels are dropping gradually, as illustrated in Figure 4.2.6.4 the uppermost core is being uncovered slowly and intermittently; after the upper plenum has uncovered completely the core then begins sustained uncovery.

The early core heatup is illustrated in Figures 4.2.6.6 through 4.2.6.10 as calculated for accident sequences initiated by station blackouts at 7 hr, 24 hr and 59 hr, and 12 days and 40 days, after shutdown. As with TAF uncovery, core uncovery begins sooner and proceeds more rapidly at higher decay heat levels. The calculation begun 40 days after shutdown showed core heatup only beginning when the calculation was stopped at ~150,000 s; the calculation was stopped because this was long after the 1 day (86,400 s) maximum time period of interest for these Level 1 analyses.

Tables 4.2.6.1 and 4.2.6.2 summarize the timings of various key events predicted using MELCOR for this sequence assuming various times after shutdown and associated decay heat levels.

4.2.7 Station Blackout with Firewater Addition

The accident is initiated by a loss of offsite power with the reactor vessel depressurized and the coolant at the normal level. The vessel water inventory is at 366.5 K (200°F), which corresponds to the maximum temperature allowed by the Grand Gulf technical specifications for operation in POS 5. Following the initiating event, onsite power is lost leading to a SBO and loss of all core cooling and coolant makeup. The operator opens two SRVs at 2 hr and steams the core at low pressure while adding coolant from the firewater system. The drywell personnel lock is open; the containment equipment hatch and both of the containment personnel locks are open (i.e., "open containment").

Figure 4.2.7.1 presents the vessel pressures calculated starting this accident scenario at two different times after shutdown. Initially, the system begins pressurizing as all core cooling is lost, more quickly for higher decay heat; the pressure then begins dropping after two SRVs are opened 2 hr after the start of the accident. The flow out the open RPV vent line and later out the SRVs also pressurizes the containment and the auxiliary building, as indicated in Figure 4.2.7.2 more rapidly for higher decay heat.

Although the operator aligns the firewater system to inject coolant into the vessel starting at 2 hr after accident initiation, injection does not begin until the vessel has depressurized sufficiently (as determined by the pump characteristics). Figure 4.2.7.3 shows that firewater can be injected as soon as desired if the accident is assumed to start 24 hr after shutdown, but firewater injection can not begin until the vessel is depressurized for about 4 hr if the accident is assumed to start 7 hr after shutdown (a higher decay heat level). At the lower decay heat the firewater injection quickly rises to its maximum level after beginning, while at higher decay heat levels the firewater injection rises to its maximum level more slowly as the vessel continues to depressurize through the open SRVs.

Coolant addition from firewater is partially countered by increased steaming in the core and steam flow out the open SRVs. Figure 4.2.7.4 indicates that, at lower decay heats the firewater injection causes a net increase in vessel inventory, while at higher decay heat levels firewater injection does not equal and reverse inventory loss for about 5 hr.

Figure 4.2.7.5 gives the predicted upper plenum liquid level drop due to this inventory loss, for different decay heat levels and highlighting when a Level 3 trip (544.4 in) would be generated. The upper plenum liquid levels reflect the overall vessel coolant inventory response presented in Figure 4.2.7.4 -- at lower decay heats the upper plenum levels remain nearly constant, while at higher decay heat levels the upper plenum levels drop for about 5 hr after the SRVs are opened before the firewater addition is sufficient to begin raising the liquid levels back up.

The same general response is found in the core also, as illustrated in Figure 4.2.7.6. (Horizontal lines are included in the figure to indicate both the boundary between the upper plenum and the core at 9.6 m and the top-of-active-fuel elevation at 9.3 m.) The collapsed level in the core drops below the core midplane before stabilizing and rising again for the case initiated at 7 hr after shutdown, but the swollen level drops only about a foot into the active fuel region before the firewater

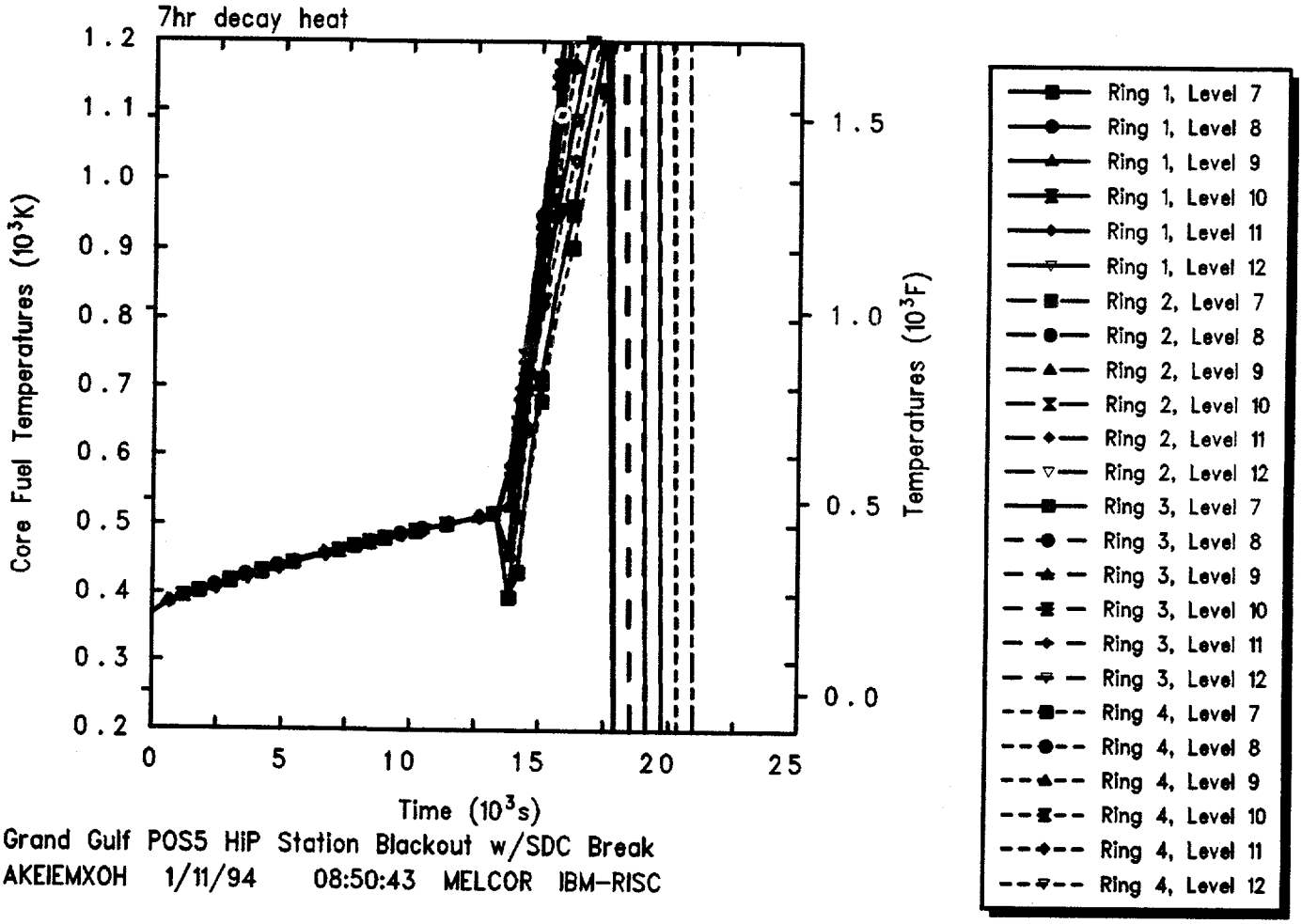

Figure 4.2.6.6. Core Fuel Temperatures for Grand Gulf POS 5 -- Station Blackout with SDC Break, Initiated 7 hr After Shutdown.

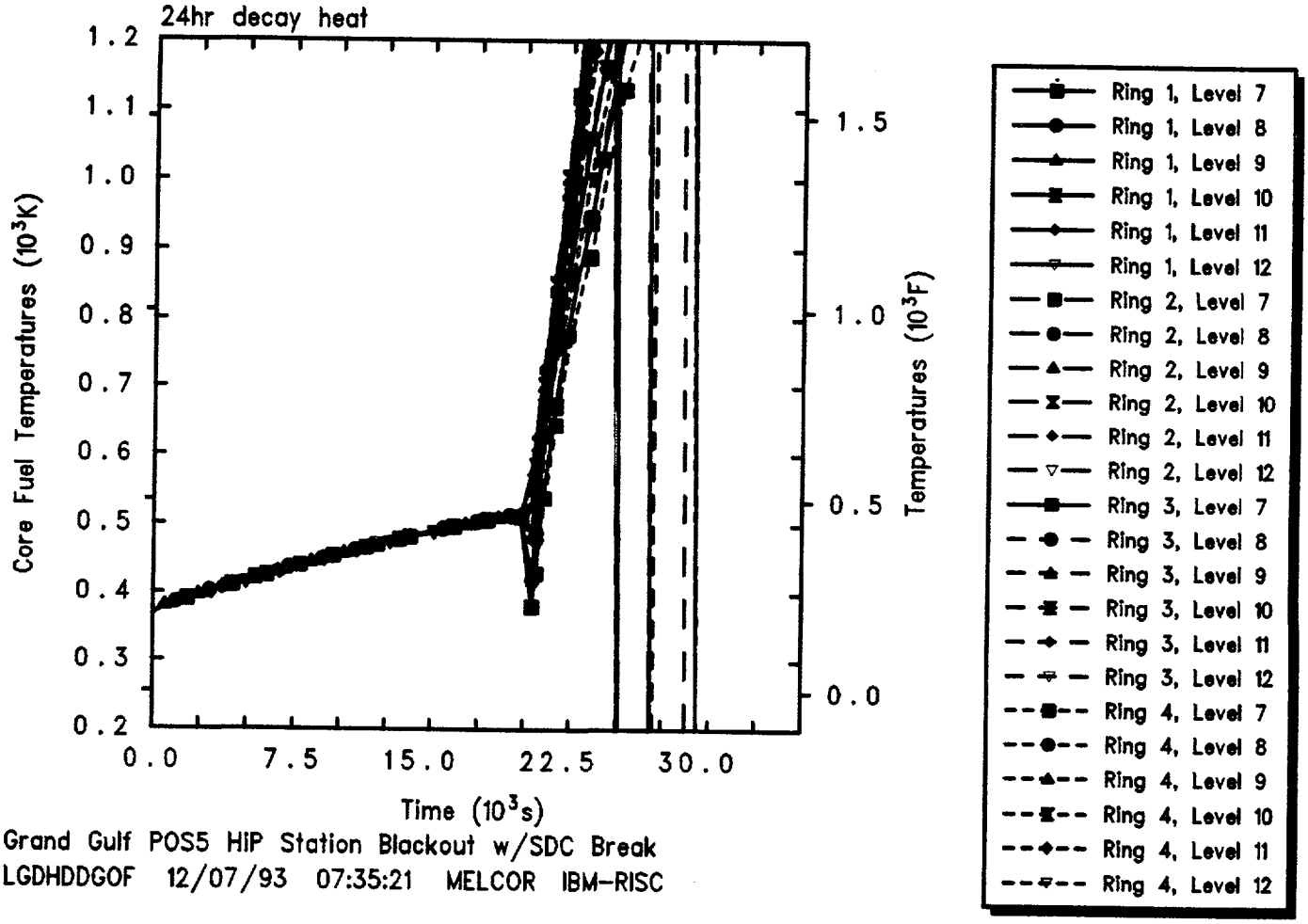

Figure 4.2.6.7. Core Fuel Temperatures for Grand Gulf POS 5 -- Station Blackout with SDC Break, Initiated 24 hr After Shutdown.

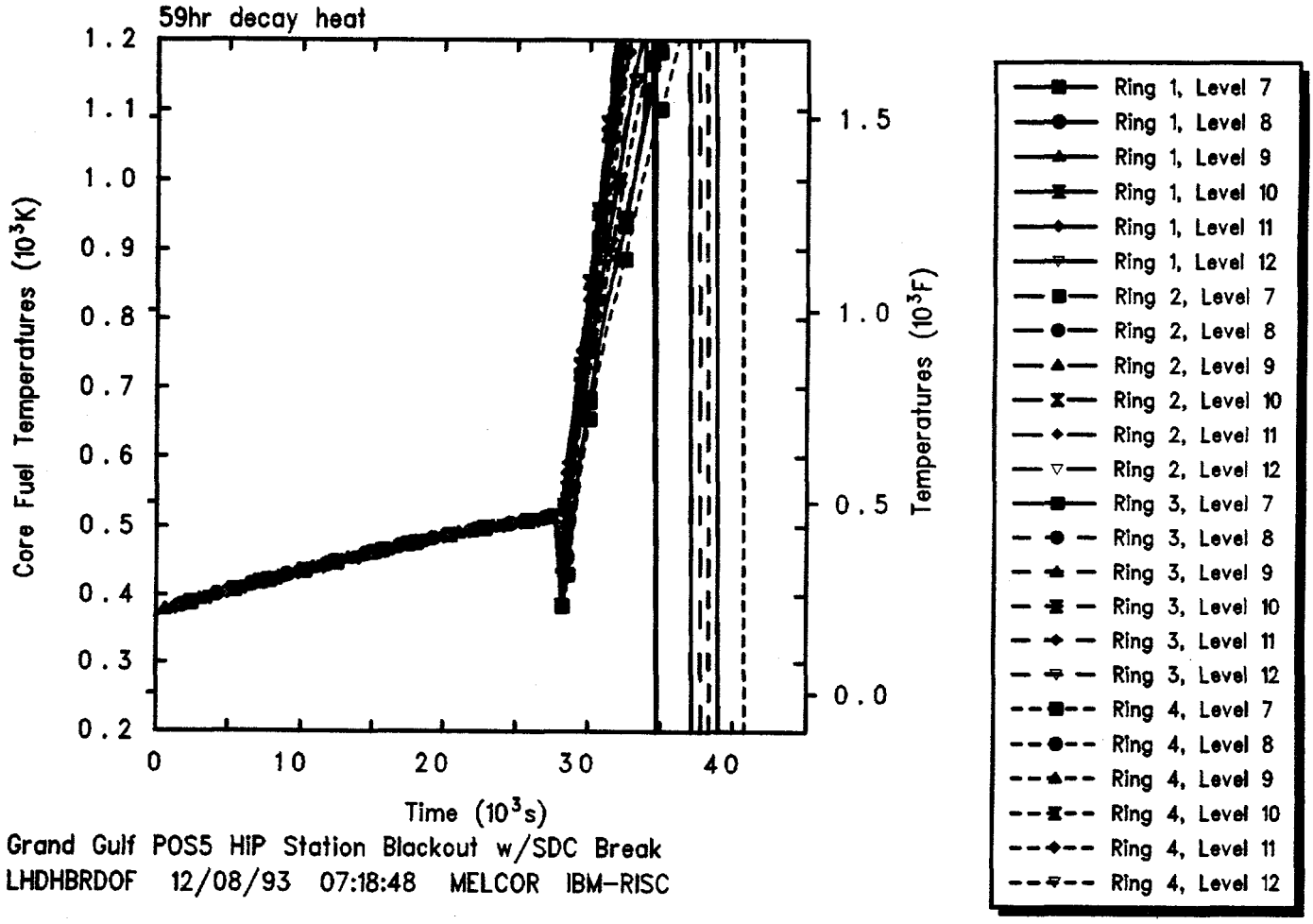

Figure 4.2.6.8. Core Fuel Temperatures for Grand Gulf POS 5 -- Station Blackout with SDC Break, Initiated 59 hr After Shutdown.

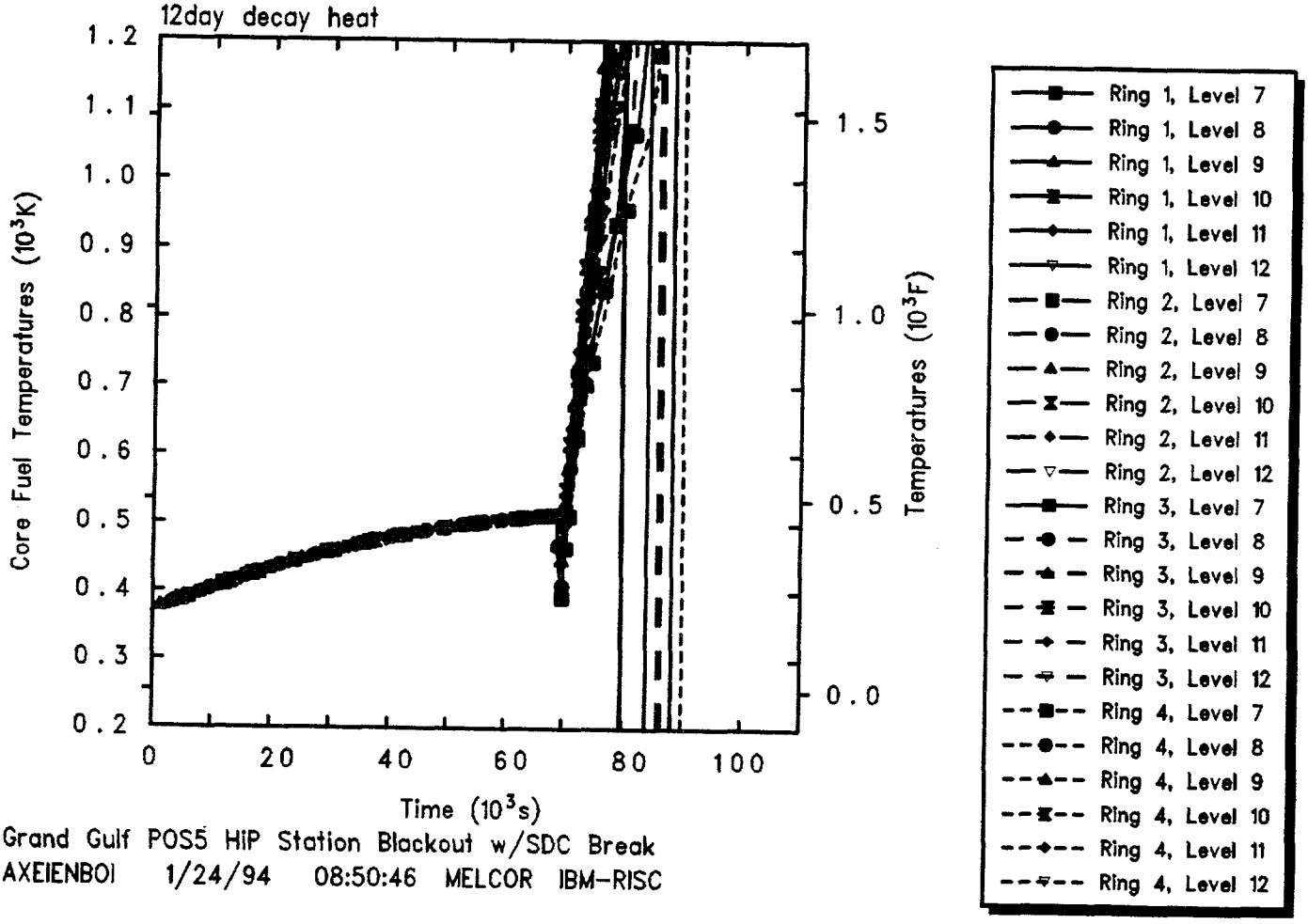

Figure 4.2.6.9. Core Fuel Temperatures for Grand Gulf POS 5 -- Station Blackout with SDC Break, Initiated 12 days After Shutdown.

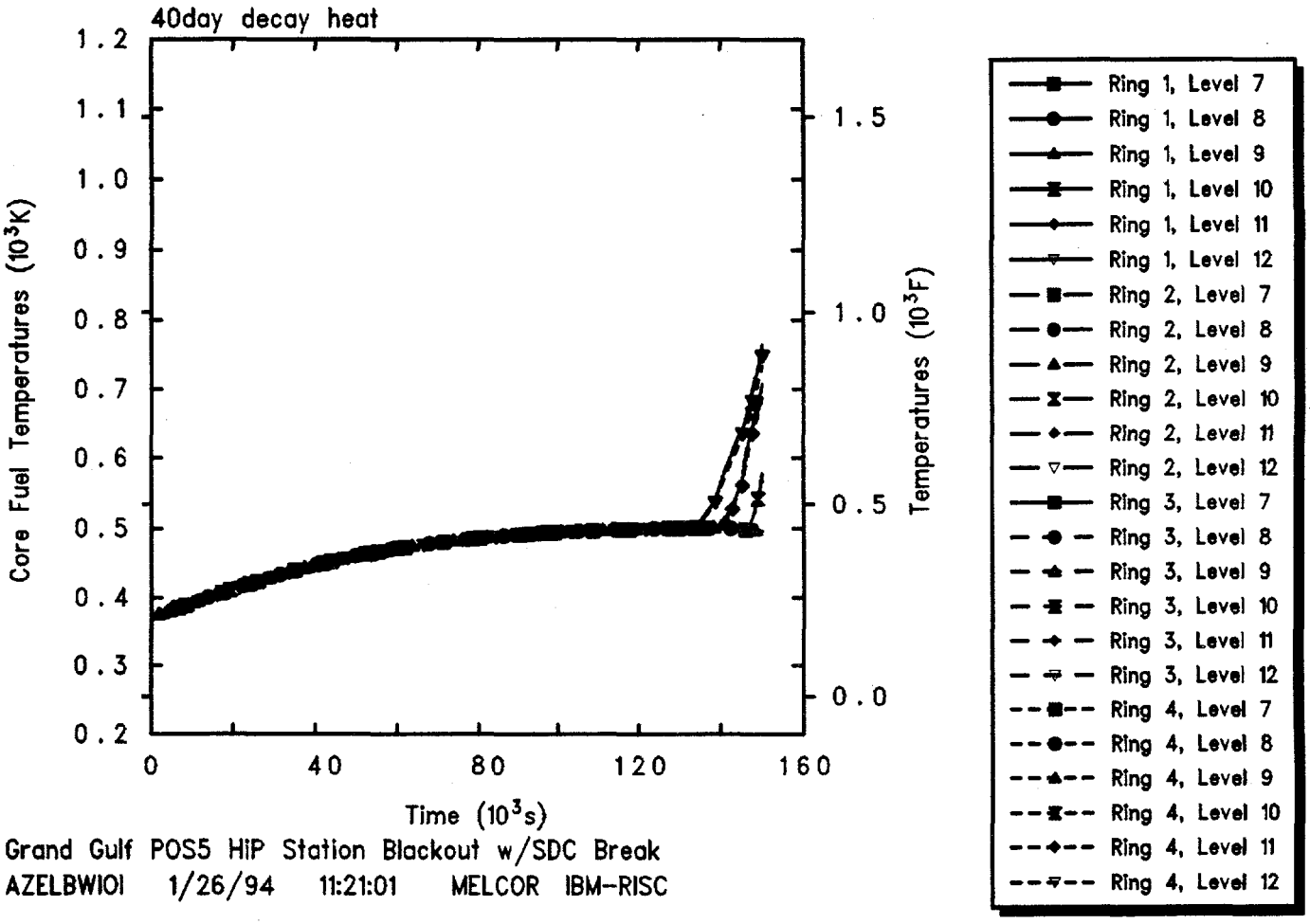

Figure 4.2.6.10. Core Fuel Temperatures for Grand Gulf POS 5 -- Station Blackout with SDC Break, Initiated 40 days After Shutdown.

Table 4.2.6.1 Key Event Times for Grand Gulf POS 5 -- Station Blackout with SDC Break, Initiated at Various Times After Shutdown

Initiation Time After Shutdown	Time to (s) TAF Uncovery *	Core Heatup	First Gap Release	Vessel Failure
7 hr	13,300	31,600	15,685	51,770
24 hr	19,750	43,800	22,840	45,390
59 hr	26,200	58,400	31,570	81,135
12 days	75,600	75,600	82,800	**
40 days	124,800	132,800	**	**

* Collapsed liquid level.
** Calculation stopped before event occurred.

Table 4.2.6.2. Key Signal Times for Grand Gulf POS 5 -- Station Blackout with SDC Break, Initiated at Various Times After Shutdown

Initiation Time After Shutdown	Time to (s) Collapsed Level <544.4 in	Swollen Level <544.4 in	Pressure >160 psig
7 hr	13,440	13,450	7,600
24 hr	19,200	19,200	11,400
59 hr	28,000	28,000	15,600
12 days	56,800	58,400	32,000
40 days	68,000	70,400	52,200

addition is sufficient to begin raising the vessel inventory and liquid levels back up. At lower decay heat levels, there is no core uncovery at all.

The small core uncovery at the higher decay heat level does not result in significant core heatup before the firewater addition is sufficient to begin raising the vessel inventory and liquid levels back up, as demonstrated in Figure 4.2.7.7. At lower decay heat levels (i.e., for 24 hr after shutdown), there is no core heatup at all because there is no uncovery at all (while firewater injection continues). Because firewater injection was sufficient to prevent core uncovery and heatup at decay heats 1 day after shutdown, calculations were not done for lower decay heat levels.

4.2.8 Station Blackout with 10 hr Firewater Addition Followed by High Pressure Boiloff

The accident is initiated by a loss of offsite power. The vessel water inventory is at 366.5 K (200°F), which corresponds to the maximum temperature allowed by the Grand Gulf technical specifications for operation in POS 5. Following the initiating event, onsite power is lost leading to a SBO and loss of all core cooling and coolant makeup. The operator opens two SRVs at 2 hr and steams the core at low pressure while adding coolant from the firewater system to the core bypass region. The depletion of the station batteries 12 hr after the start of the accident cause the SRVs to close (i.e., the SRVs require DC power to remain open), after which they

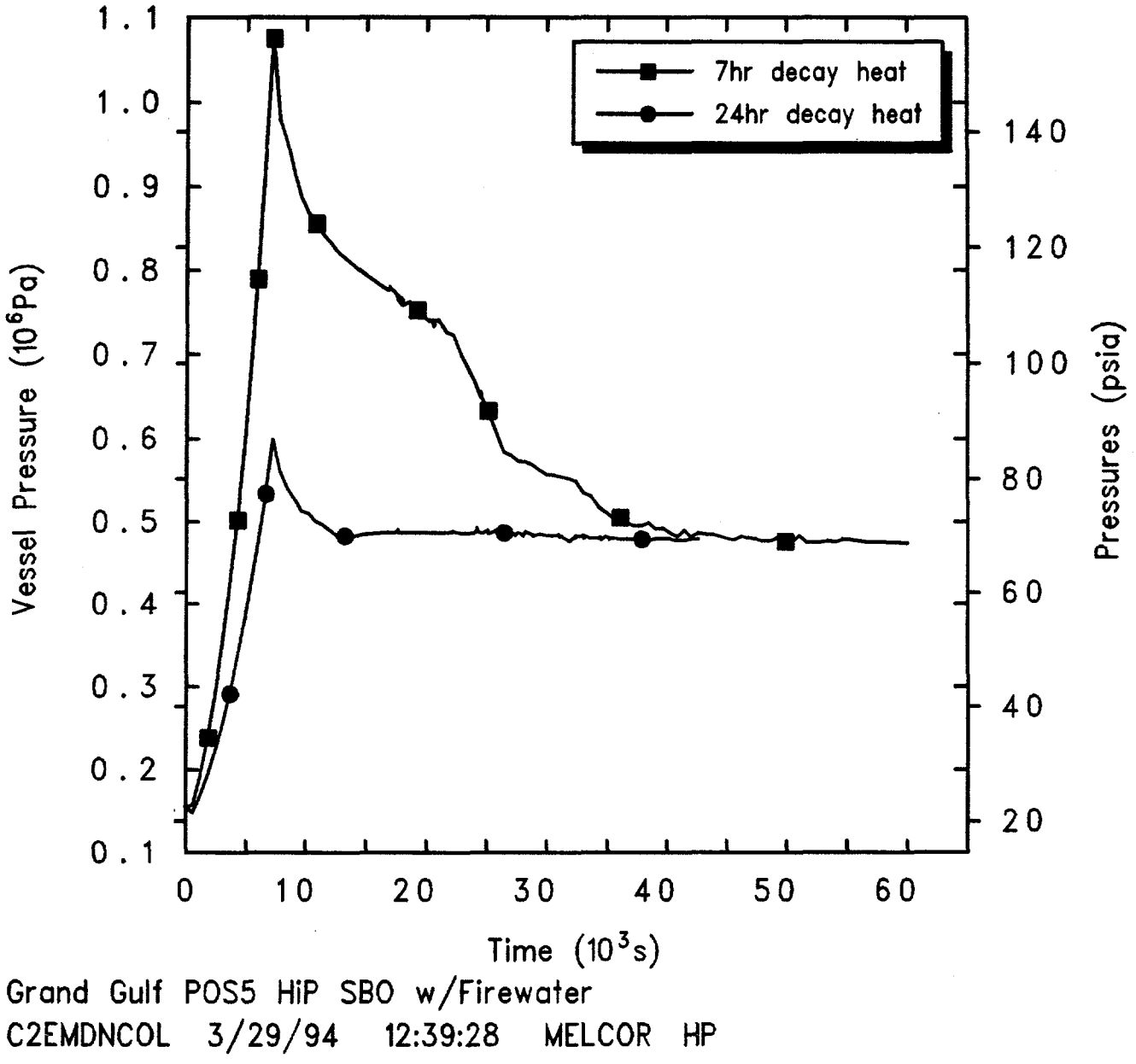

Figure 4.2.7.1. Reactor Vessel Pressures for Grand Gulf POS 5 -- Station Blackout with Firewater, Initiated at Various Times After Shutdown.

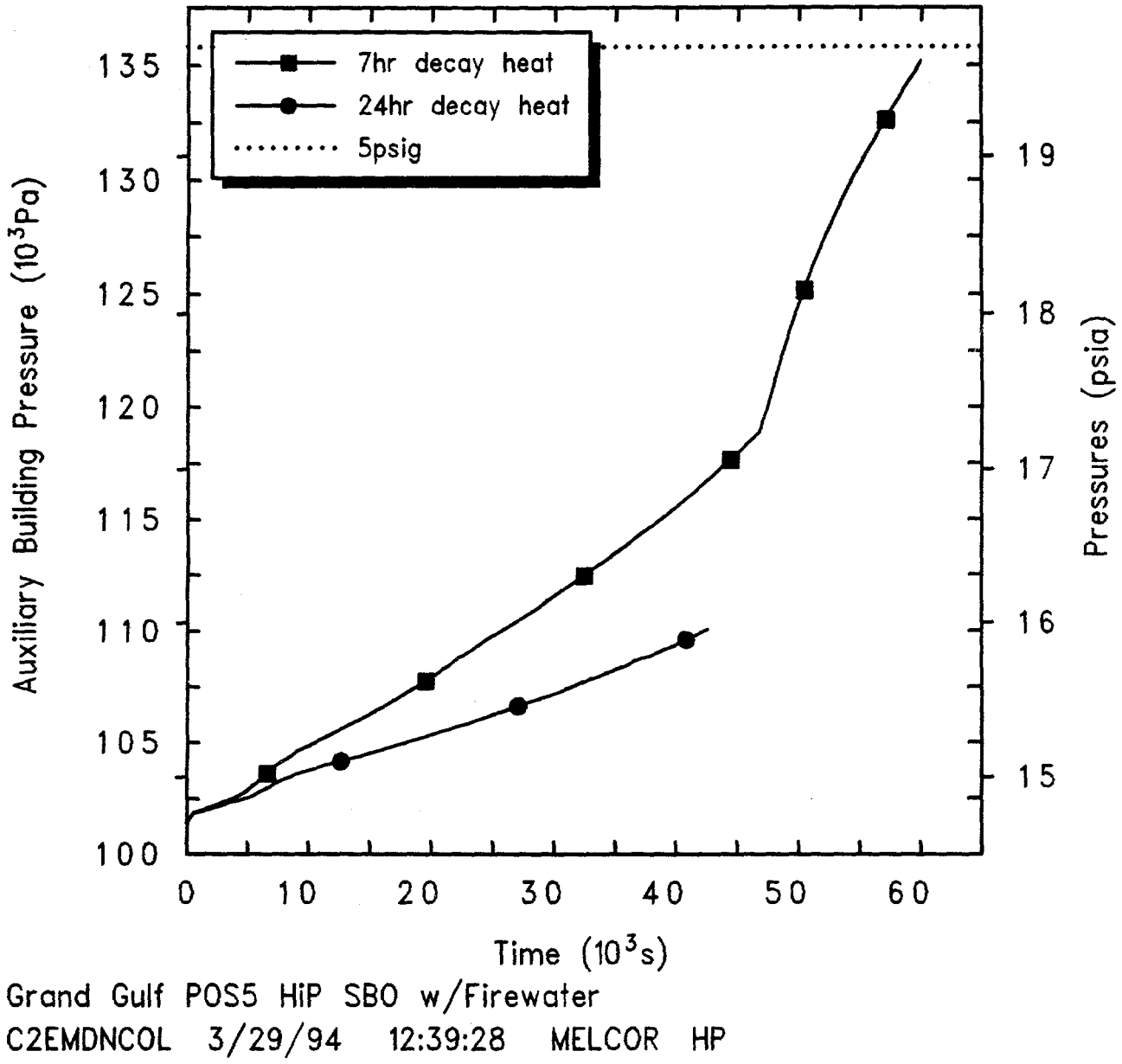

Figure 4.2.7.2. Auxiliary Building Pressures for Grand Gulf POS 5 -- Station Blackout with Firewater, Initiated at Various Times After Shutdown.

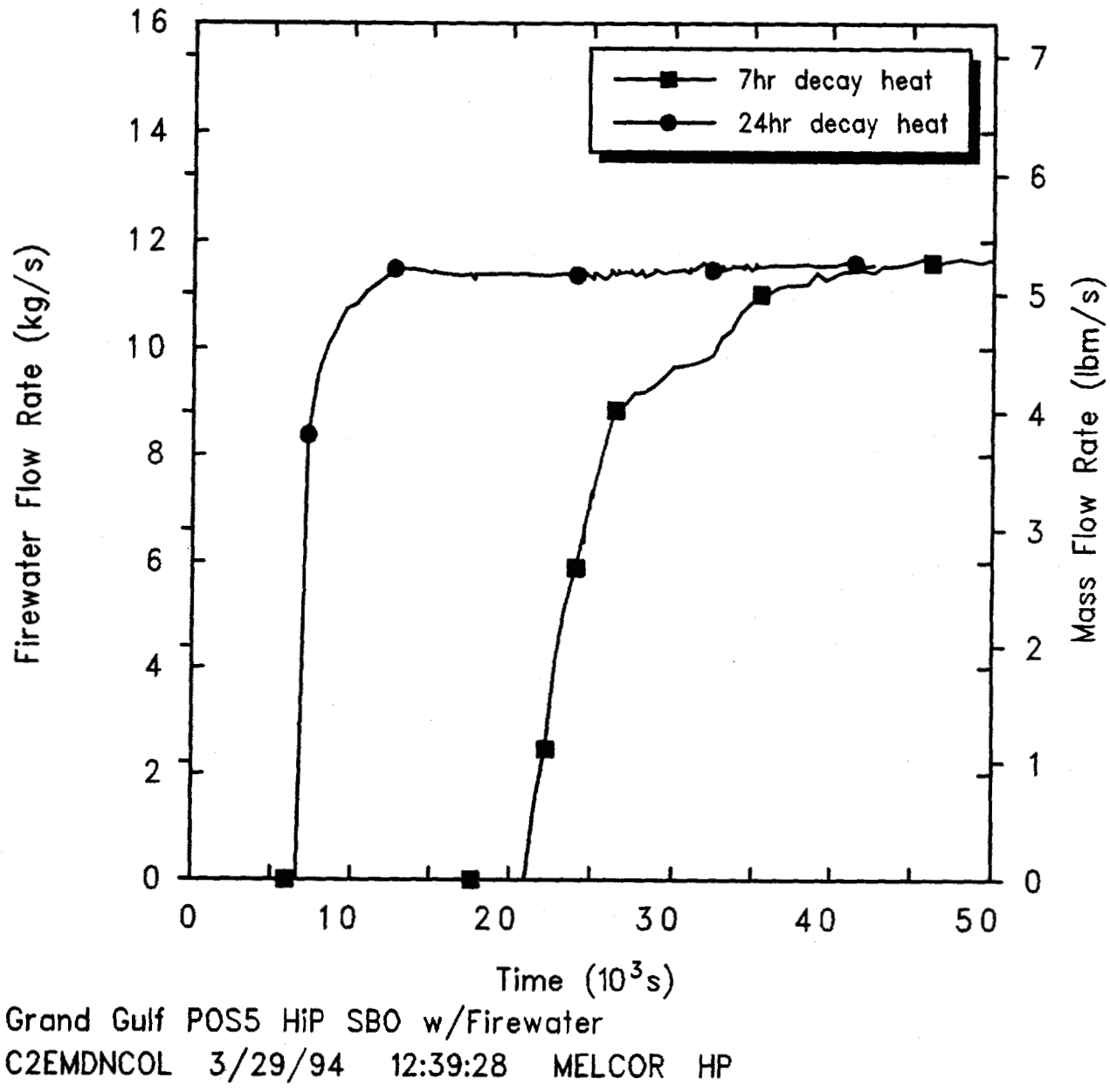

Figure 4.2.7.3. Firewater Injection Flow Rates for Grand Gulf POS 5 -- Station Blackout with Firewater, Initiated at Various Times After Shutdown.

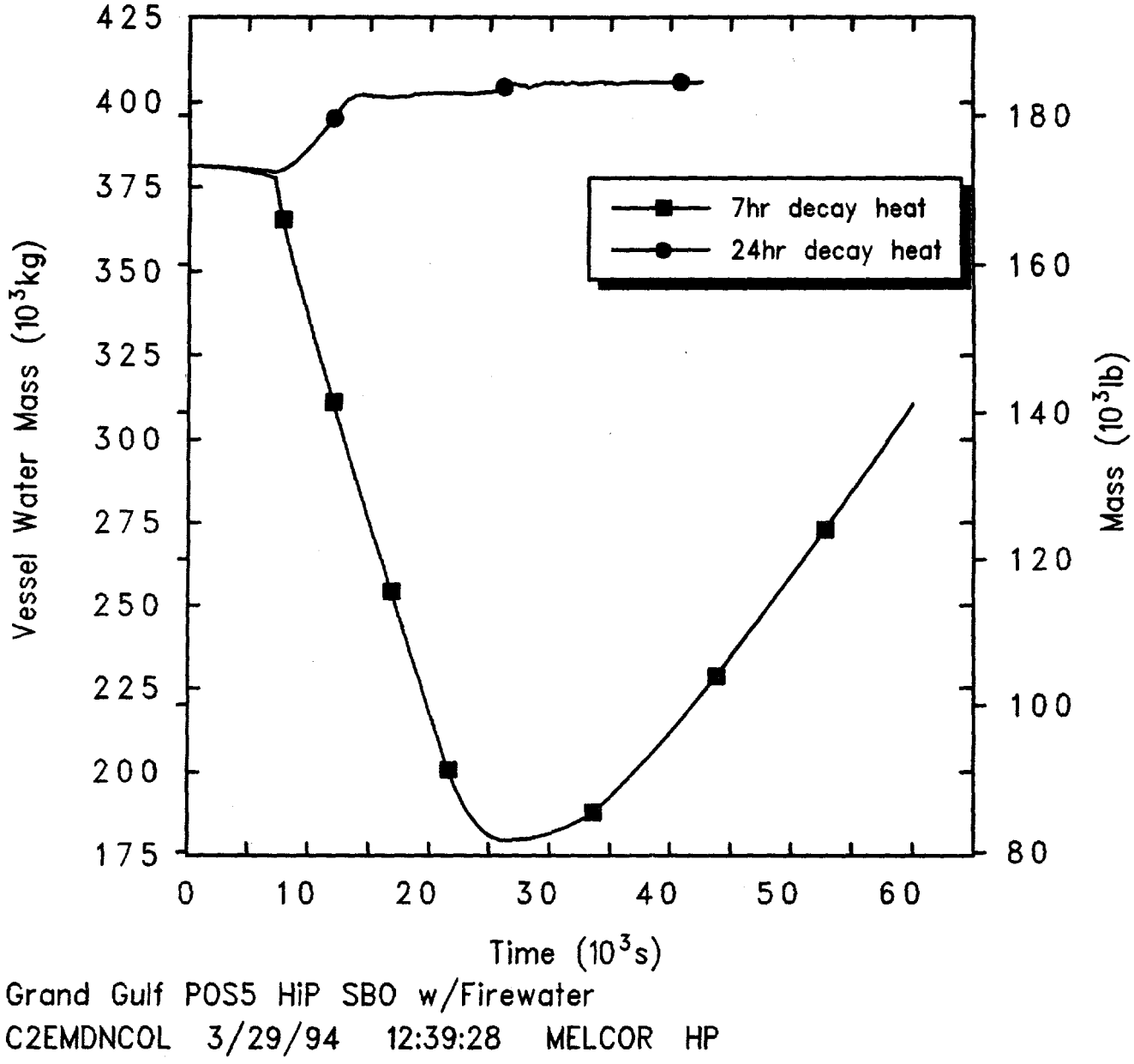

Figure 4.2.7.4. Reactor Vessel Water Masses for Grand Gulf POS 5 -- Station Blackout with Firewater, Initiated at Various Times After Shutdown.

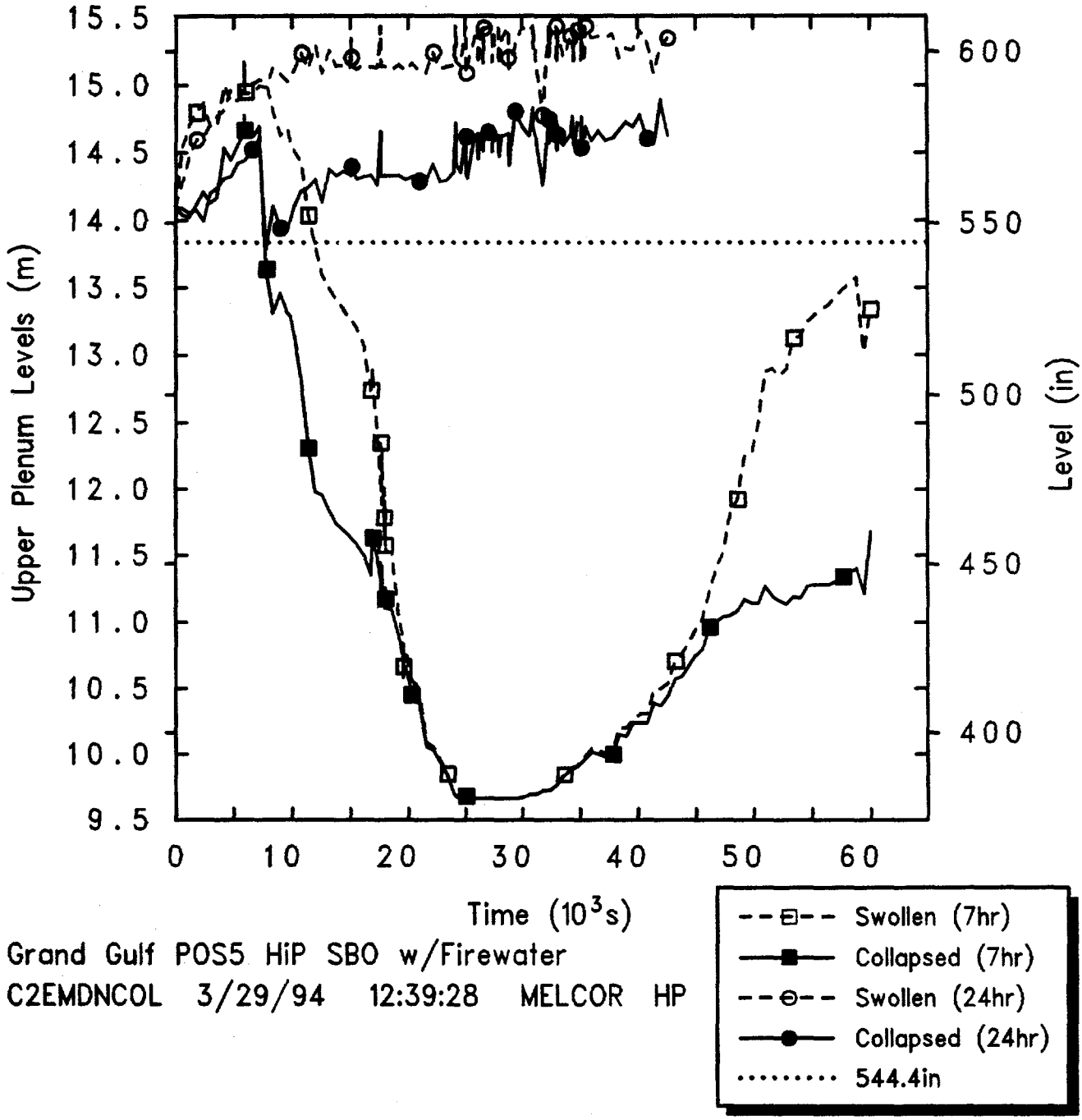

Figure 4.2.7.5. Upper Plenum Liquid Levels for Grand Gulf POS 5 -- Station Blackout with Firewater, Initiated at Various Times After Shutdown.

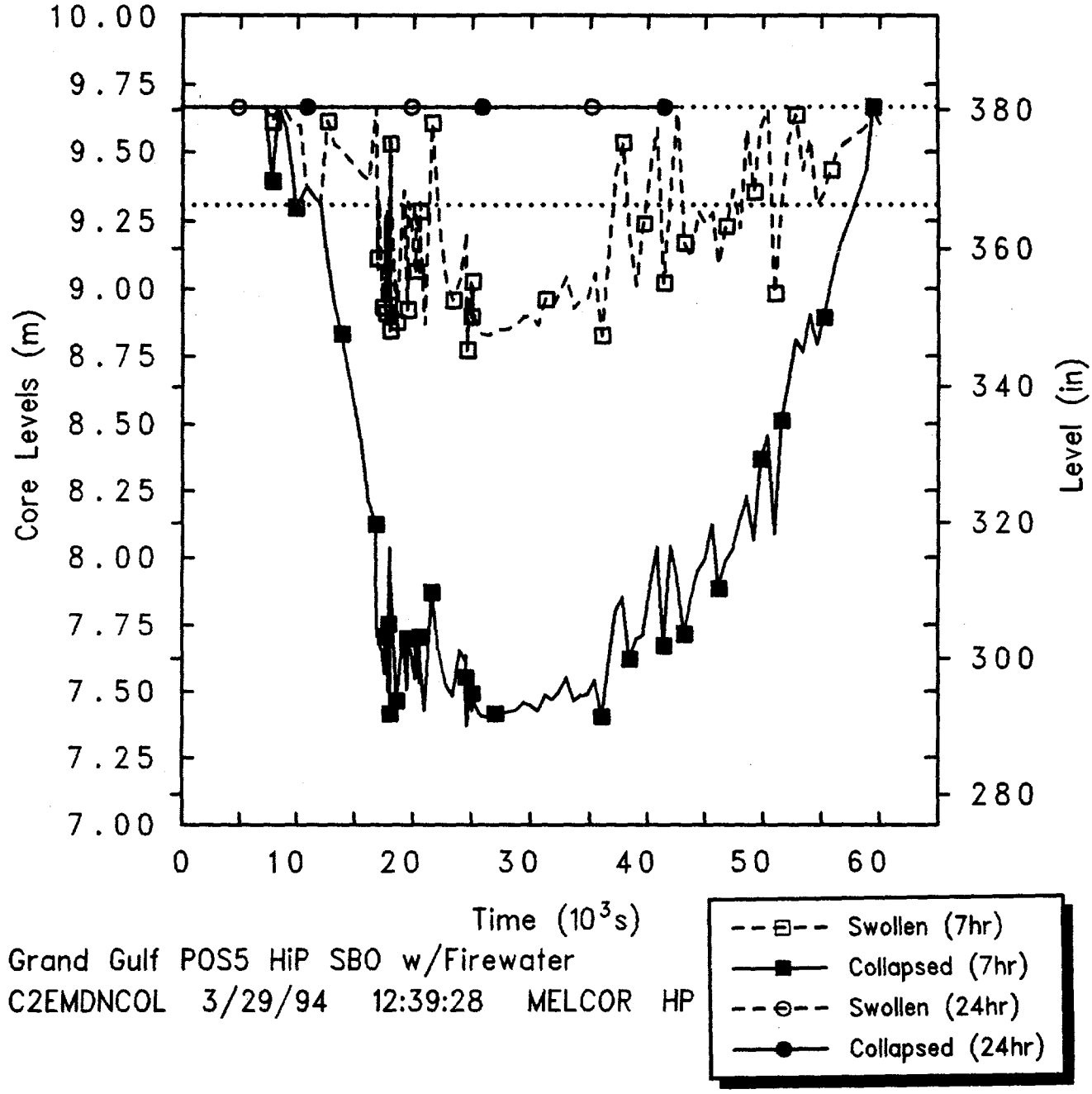

Figure 4.2.7.6. Core Liquid Levels for Grand Gulf POS 5 -- Station Blackout with Firewater, Initiated at Various Times After Shutdown.

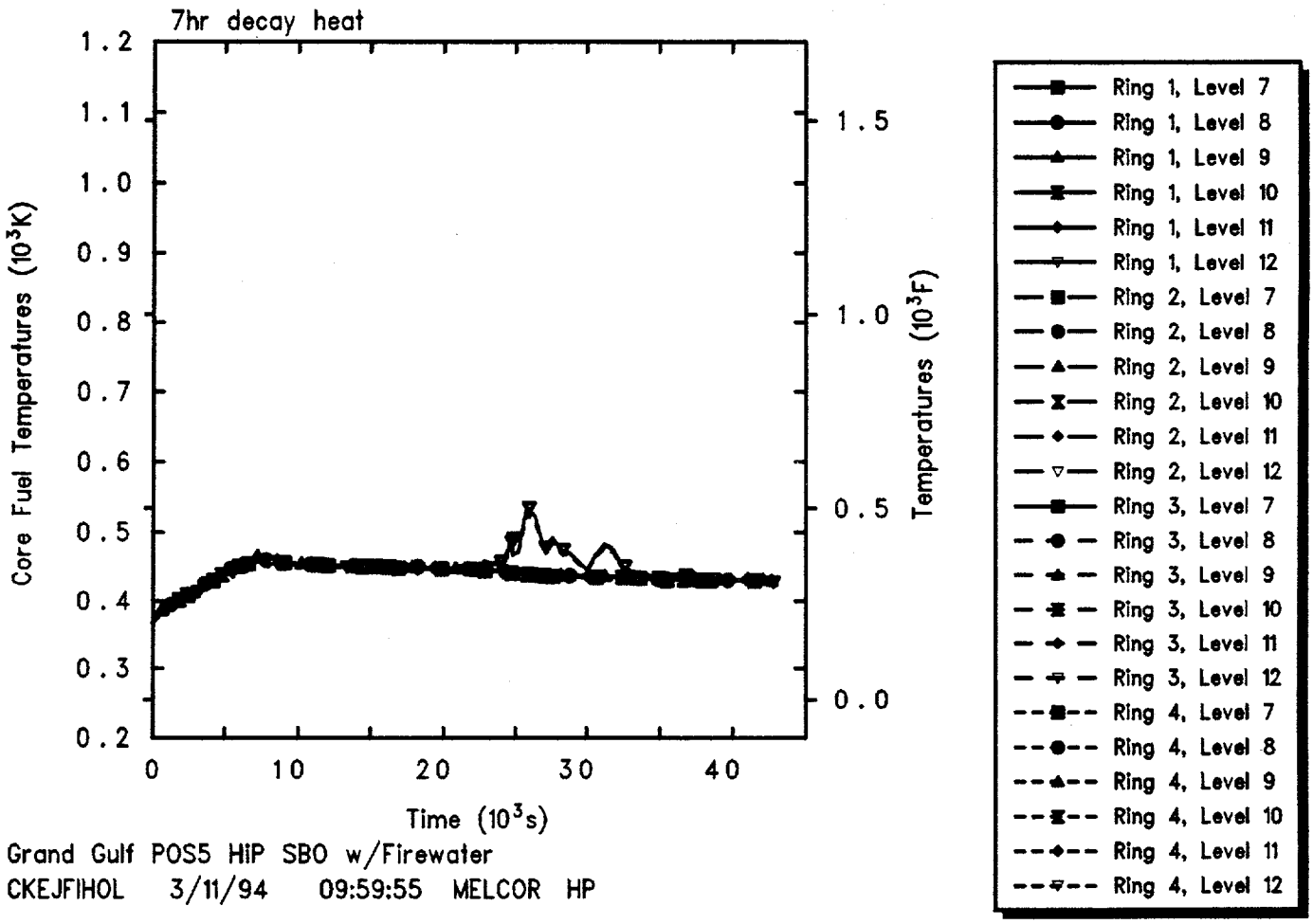

Figure 4.2.7.7. Core Fuel Temperatures for Grand Gulf POS 5 -- Station Blackout with Firewater, Initiated 7 hr After Shutdown.

operate in the relief mode. Since the SRVs are now closed, the RPV can pressurize. The reactor pressure vessel head vent is open. The drywell personnel lock is open, and the containment equipment hatch and both of the containment personnel locks are open (i.e., "open containment").

Although the operator aligns the firewater system to inject coolant into the vessel starting at 2 hr after accident initiation, injection does not begin until the vessel has depressurized sufficiently (as determined by the pump characteristics). Figure 4.2.8.1 shows that firewater can be injected as soon as desired if the accident is assumed to start 24 hr after shutdown, but firewater injection can not begin until the vessel is depressurized for about 4 hr if the accident is assumed to start 7 hr after shutdown (a higher decay heat level). At the lower decay heat the firewater injection quickly rises to its maximum level after beginning, while at higher decay heat levels the firewater injection rises to its maximum level more slowly as the vessel continues to depressurize through the open SRVs. Firewater injection stops soon after 12 hr because after the SRVs close the system quickly repressurizes.

Figure 4.2.8.2 presents the vessel pressures calculated starting this accident scenario at two different times after shutdown. Initially, the system begins pressurizing as all core cooling is lost, more quickly for higher decay heat; the pressure then begins dropping after two SRVs are opened 2 hr after the start of the accident. Firewater cooling and steaming out the SRVs keep the vessel pressure down until 12 hr, when depletion of the station batteries causes the SRVs to close. Since the SRVs are now closed, the RPV pressurizes until the SRVs begin operating in the relief mode. After some time, the continued inventory loss out the open RPV vent is sufficient to relieve the steaming in the core and the SRVs close. The pressure continues to drop until core heatup and damage begins; there is then a brief repressurization, followed very quickly by a final, sharp depressurization due to vessel failure.

The flow out the open RPV vent line and later out the SRVs also pressurizes the containment and the auxiliary building, as indicated in Figure 4.2.8.3 more rapidly for higher decay heat than for lower decay heats. At both decay heat levels, for this scenario the auxiliary building fails when the SRVs begin cycling at their safety setpoint. The auxiliary building pressure briefly spikes later when the vessel fails.

As in the results presented in the previous section for a station blackout with continual firewater injection, Figure 4.2.8.4 indicates that at lower decay heats the firewater injection causes a net increase in vessel inventory, while at higher decay heat levels firewater injection does not equal and reverse inventory loss for about 5 hr. After the SRVs close at 12 hr, the system pressurizes until the SRV setpoint is reached; coolant inventory is then lost as the SRVs cycle at the safety setpoint until vessel failure, when all the remaining coolant in the vessel drains to the cavity abruptly.

Figure 4.2.8.5 gives the predicted upper plenum liquid level drop due to this inventory loss, for different decay heat levels and highlighting when a Level 3 trip (544.4 in) would be generated. The upper plenum liquid levels reflect the overall vessel coolant inventory response presented in Figure 4.2.8.4 -- at lower decay heats the upper plenum levels remain nearly constant, while at higher decay heat levels the upper plenum levels drop for about 5hr after the SRVs are opened before the firewater addition is sufficient to raise the liquid levels back up briefly. The liquid level in the upper plenum resumes dropping soon after firewater injection is stopped after 12 hr for the accident initiated 7 hr after shutdown. For the same scenario initiated 24 hr after shutdown the liquid level in the upper plenum drops later, reflecting the higher vessel inventory when the SRVs are closed and firewater injection stops and the longer period to pressurize to the SRV setpoint at the lower decay heat level; the upper plenum levels in both cases drop when the SRVs begin cycling in the relief mode.

The same general response is found in the core also, as illustrated in Figure 4.2.8.6. (Horizontal lines are included in the figure to indicate both the boundary between the upper plenum and the core at 9.6 m and the top-of-active-fuel elevation at 9.3 m.) The collapsed level in the core drops below the core midplane before stabilizing and rising again for the case initiated at 7 hr after shutdown, but the swollen level drops only about a foot into the active fuel region before the firewater addition is sufficient to begin raising the vessel inventory and liquid levels back up. At lower decay heat levels, there is no core uncovery at all while firewater injection continues. The liquid level in the core resumes dropping soon after firewater injection is stopped after 12 hr for the accident initiated 7 hr after shutdown. For the same scenario initiated 24 hr after shutdown the liquid levels in the core also begin dropping when firewater injection stops. However, the liquid levels in the core do not drop

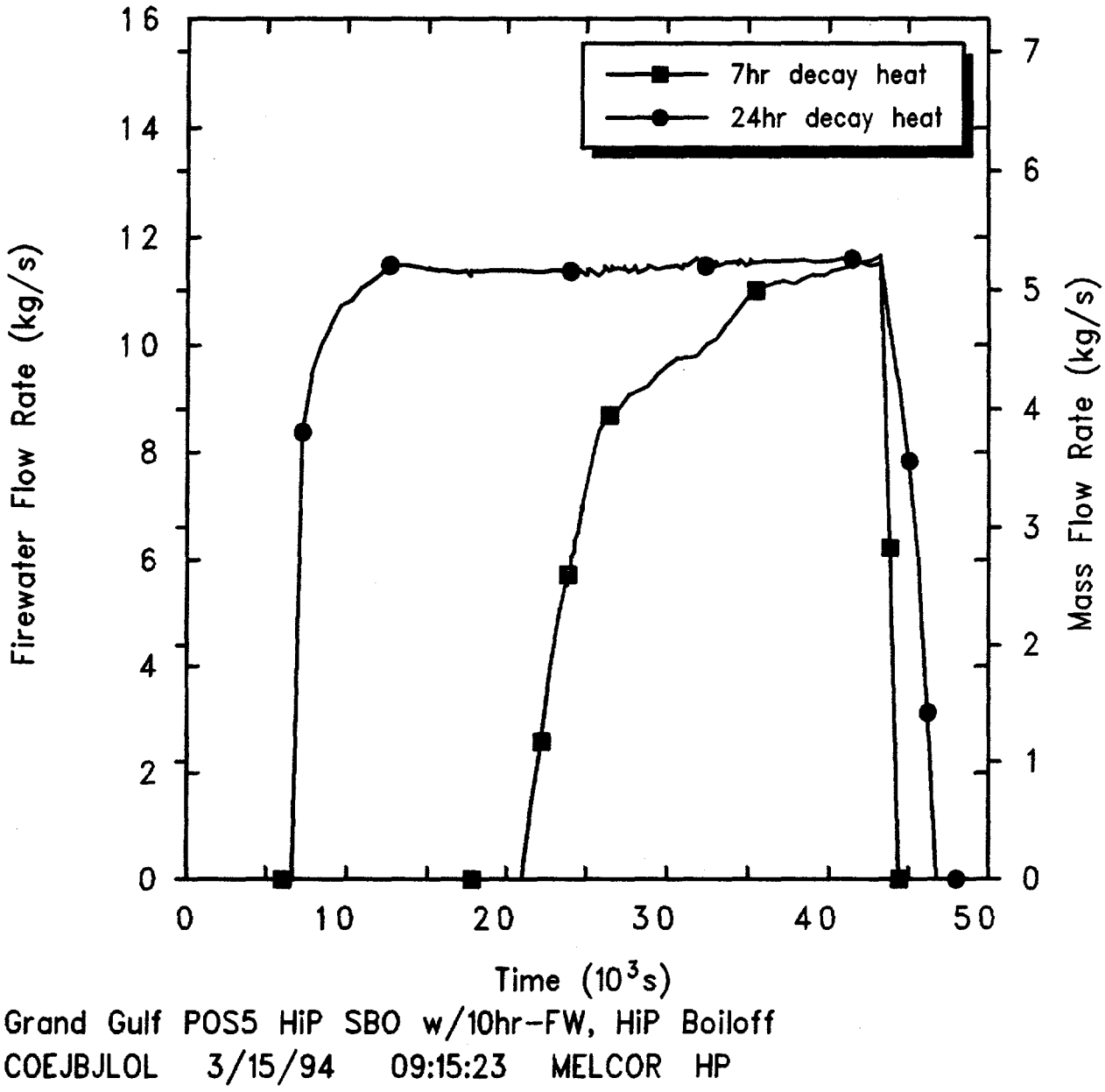

Figure 4.2.8.1. Firewater Injection Flow Rates for Grand Gulf POS 5 -- Station Blackout with 10 hr Firewater Addition Followed by High Pressure Boiloff, Initiated at Various Times After Shutdown.

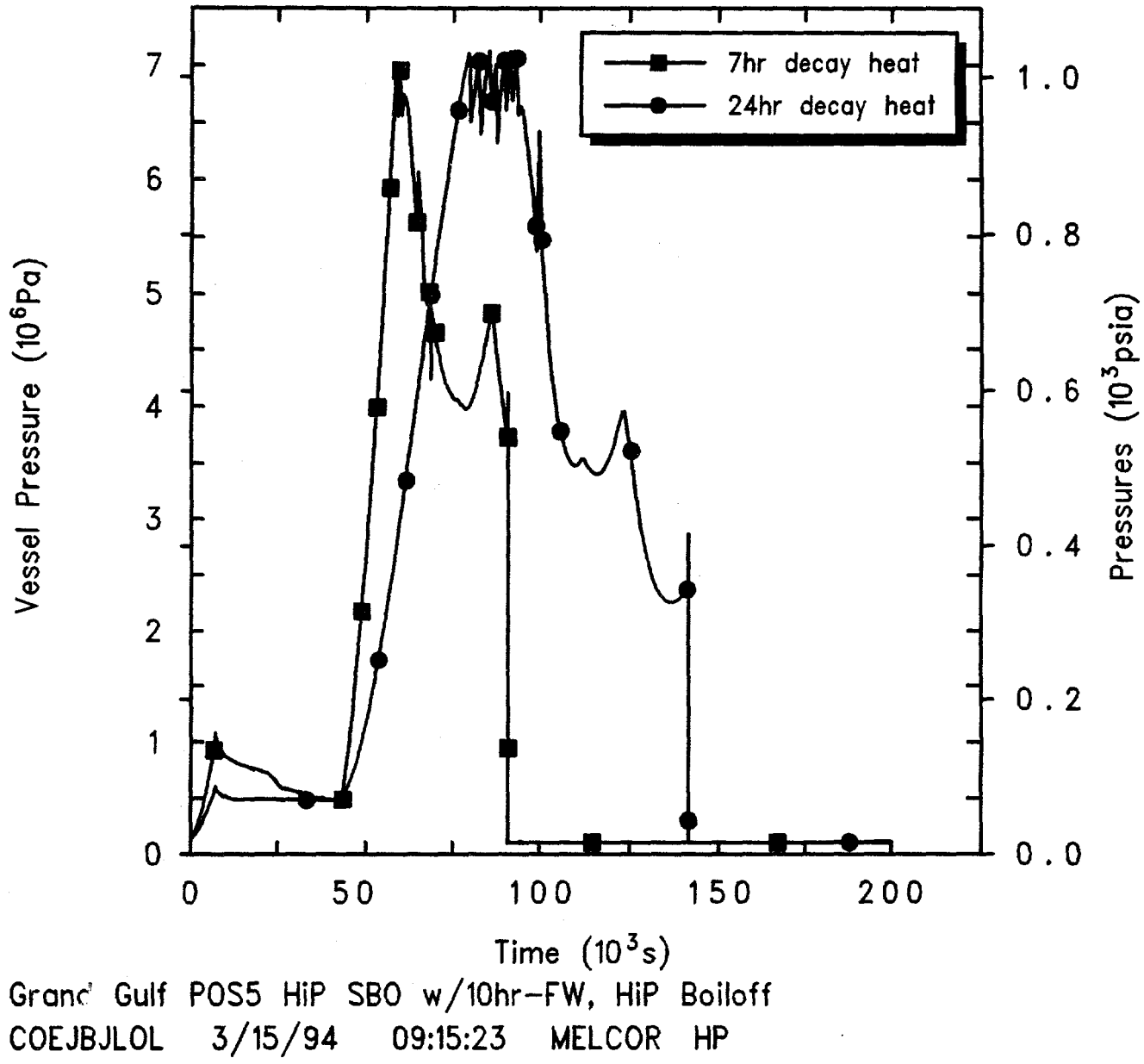

Figure 4.2.8.2. Reactor Vessel Pressures for Grand Gulf POS 5 -- Station Blackout with 10 hr Firewater Addition Followed by High Pressure Boiloff, Initiated at Various Times After Shutdown.

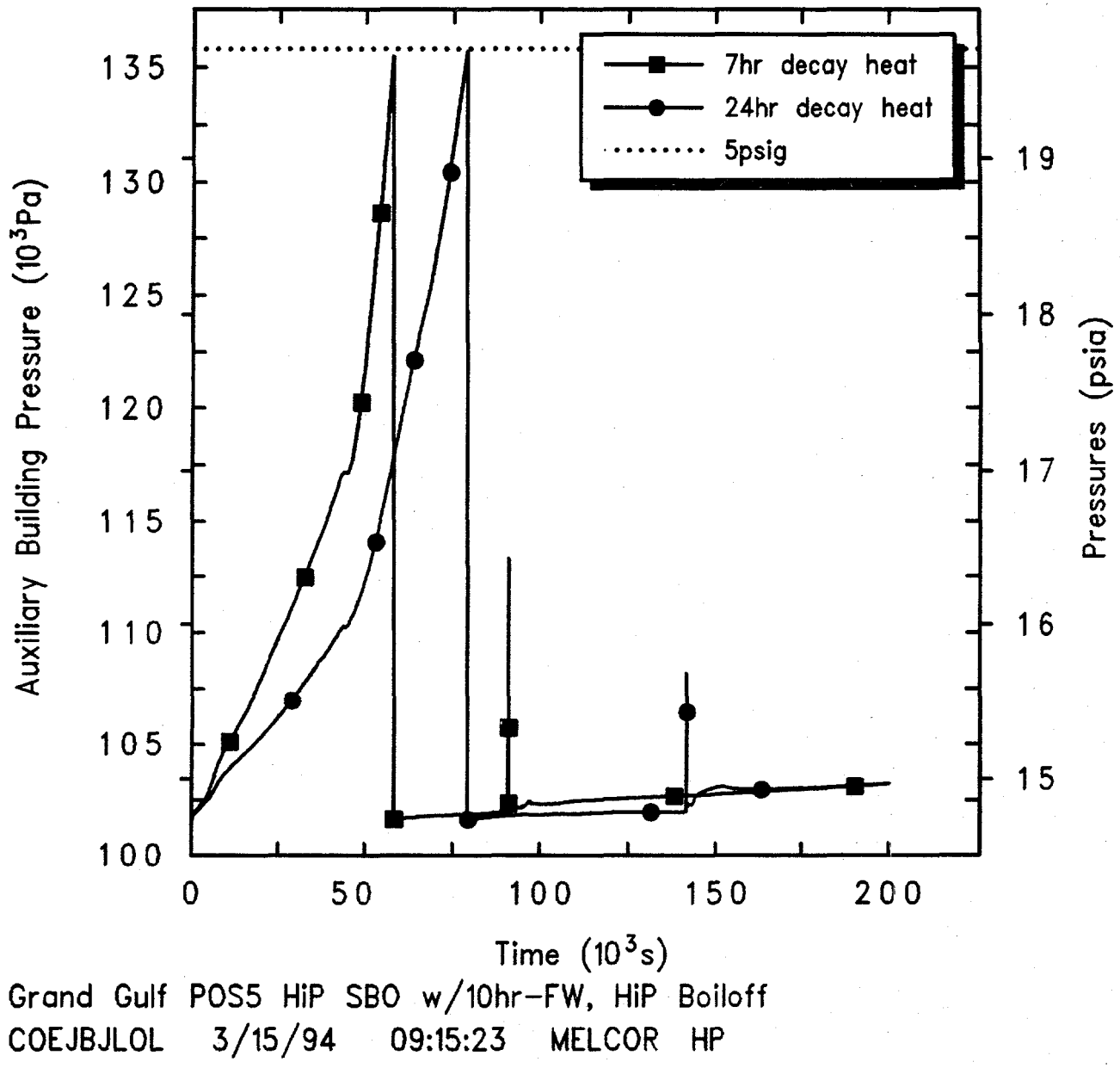

Figure 4.2.8.3. Auxiliary Building Pressures for Grand Gulf POS 5 -- Station Blackout with 10 hr Firewater Addition Followed by High Pressure Boiloff, Initiated at Various Times After Shutdown.

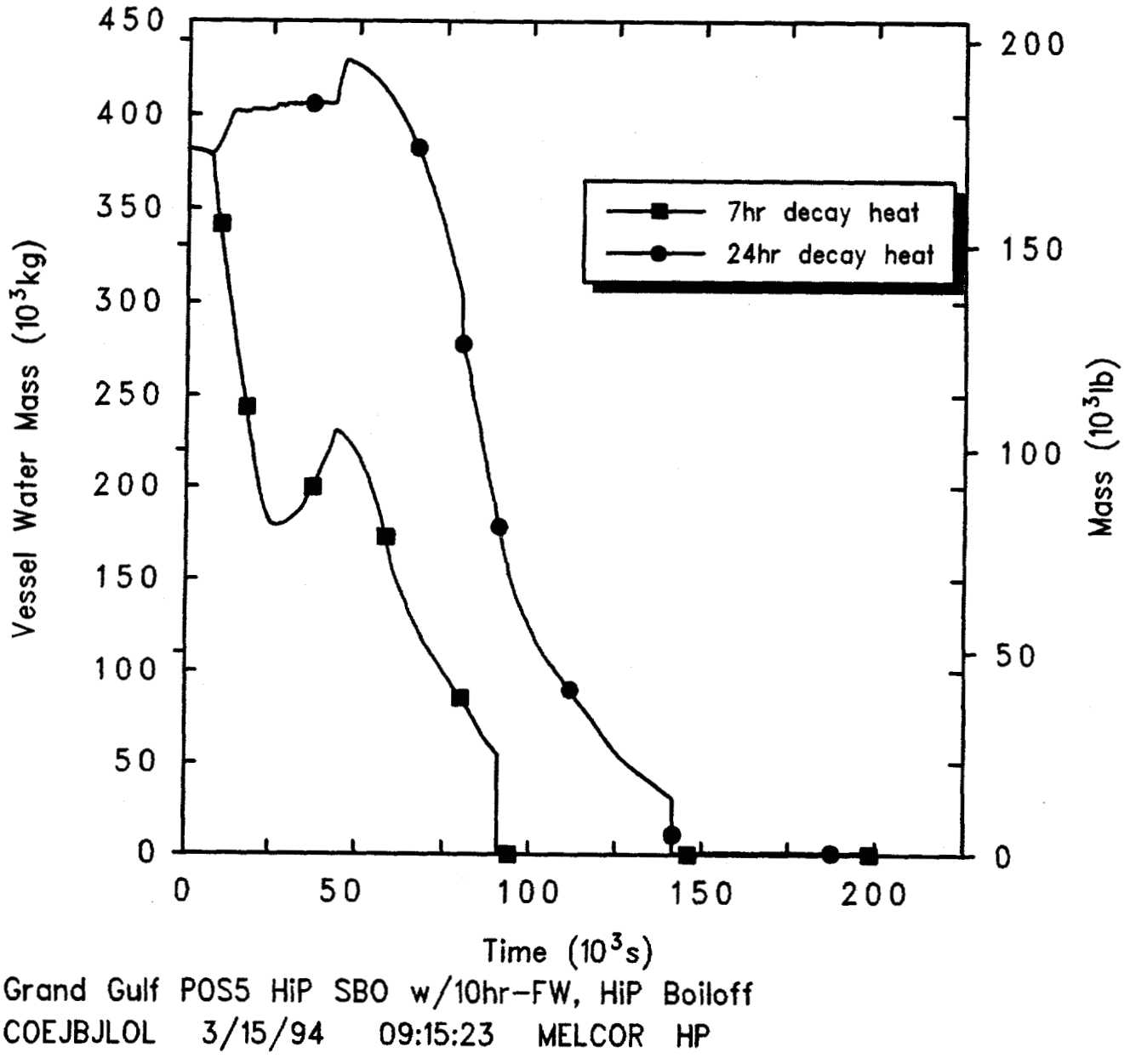

Figure 4.2.8.4. Reactor Vessel Water Masses for Grand Gulf POS 5 -- Station Blackout with 10 hr Firewater Addition Followed by High Pressure Boiloff, Initiated at Various Times After Shutdown.

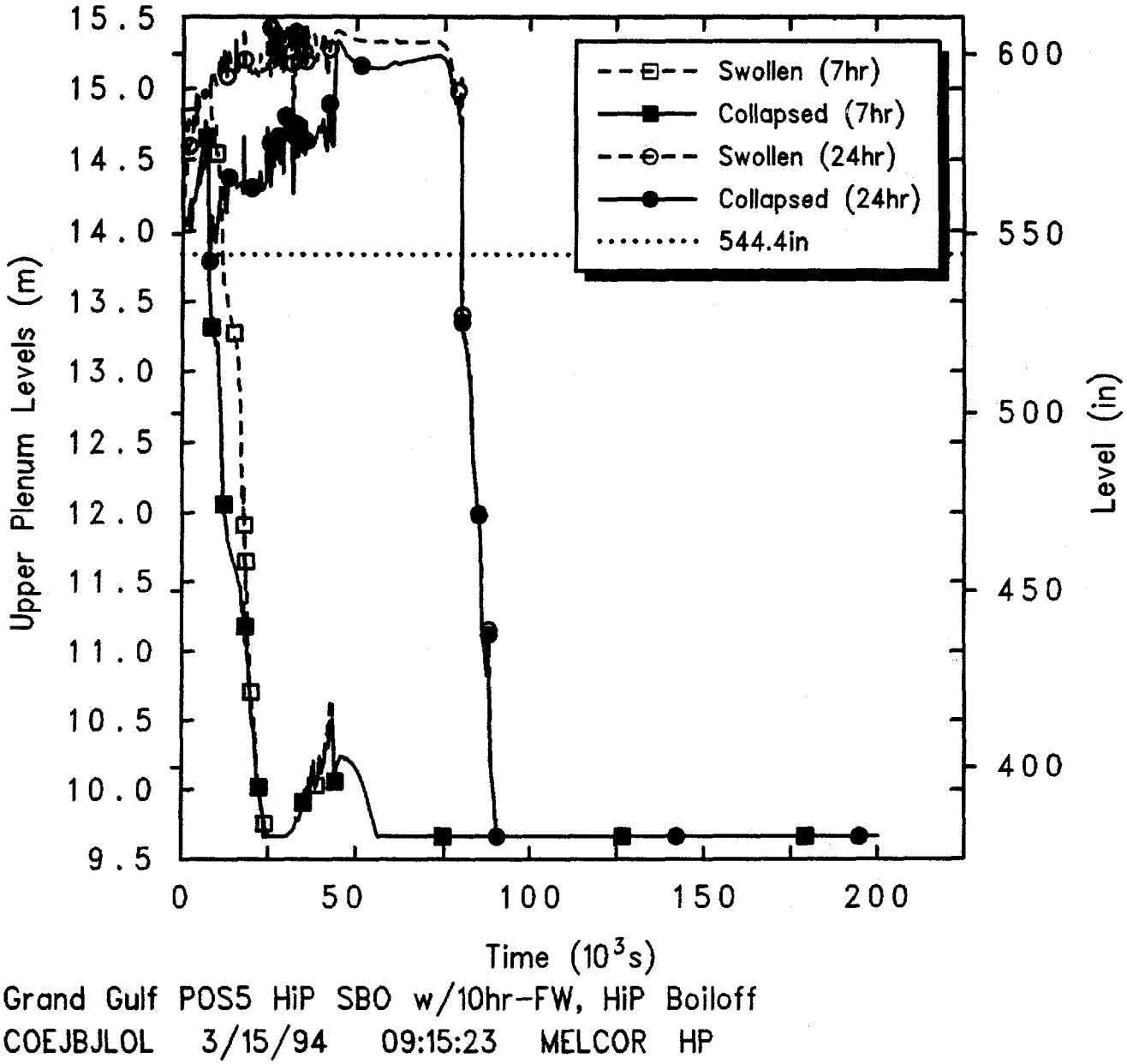

Figure 4.2.8.5. Upper Plenum Liquid Levels for Grand Gulf POS 5 -- Station Blackout with 10 hr Firewater Addition Followed by High Pressure Boiloff, Initiated at Various Times After Shutdown.

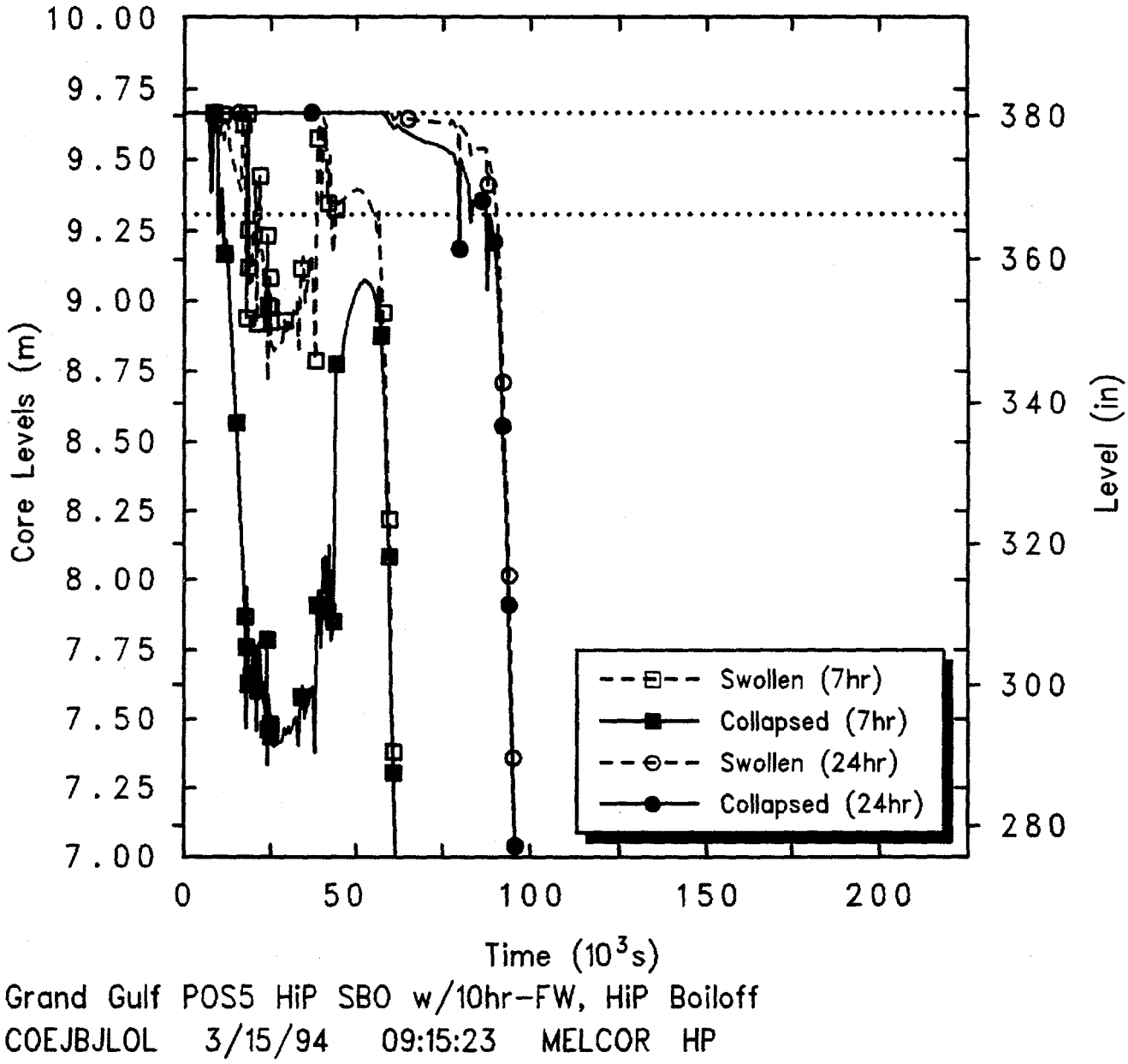

Figure 4.2.8.6. Core Liquid Levels for Grand Gulf POS 5 -- Station Blackout with 10 hr Firewater Addition Followed by High Pressure Boiloff, Initiated at Various Times After Shutdown.

below the TAF elevation until later, when the upper plenum is empty. The core levels in both cases drop sharply when the SRVs begin cycling in the relief mode.

The small core uncovery at the higher decay heat level does not result in significant core heatup before the firewater addition is sufficient to begin raising the vessel inventory and liquid levels back up, as demonstrated in Figure 4.2.8.7. At lower decay heat levels (i.e., for 24 hr after shutdown), there is no core heatup at all because there is no uncovery at all while firewater injection continues. In both cases, after firewater injection ends at 12 hr there is a slow temperature increase, reflecting the rise in saturation temperature as the system pressurizes to the SRV setpoint. Later, after TAF uncovery, core heatup and damage begins. Because core heatup and damage did not begin until more than 1 day after accident initiation for the case initiated 24 hr after shutdown, calculations were not done for lower decay heat levels.

Table 4.2.8.1 summarizes the timings of various key events predicted using MELCOR for this sequence assuming various times after shutdown and associated decay heat levels.

4.2.9 Station Blackout with 10 hr Firewater Addition Followed by Failure to Isolate SDC

The accident is initiated by a loss of offsite power. The vessel water inventory is at 366.5 K (200°F), which corresponds to the maximum temperature allowed by the Grand Gulf technical specifications for operation in POS 5. Following the initiating event, onsite power is lost leading to a SBO and loss of all core cooling and coolant makeup. The operator opens two SRVs at 2 hr and steams the core at low pressure while adding coolant from the firewater system to the core bypass region. The depletion of the station batteries 12 hr after the start of the accident causes the SRVs to close (i.e., the SRVs require DC power to remain open), after which they operate in the relief mode. Since the SRVs are now closed, the RPV will pressurize. The SBO precludes the isolation of the low pressure piping in the SDC system. This low-pressure SDC system piping fails when the RPV pressure reaches 3.135 MPa (440 psig) resulting in an interfacing systems LOCA. The break in the SDC line is opened when the vessel pressure reaches 3.135 MPa (440 psig). The SDC break runs from the vessel downcomer, 4.38 m above the bottom of the vessel to the first floor of the auxiliary building, 8.18 m below the bottom of the vessel. The reactor pressure vessel head vent is open. The drywell personnel lock is open; the containment equipment hatch and both of the containment personnel locks are open (i.e., "open containment").

The thermal/hydraulic and core damage behavior for this scenario are quite similar to those in the station blackout with 10 hr firewater addition followed by high pressure boiloff, described in the previous section; they are completely identical for the first ≥12 hr, until the system pressurization is interrupted by the failure to isolate SDC at 3.135 MPa (440 psig) in this case. Figure 4.2.9.1 presents the vessel pressures calculated starting this accident scenario at two different times after shutdown.

Figure 4.2.9.2 gives the predicted upper plenum and core liquid levels, highlighting when a Level 3 trip (544.4 in) would be generated and when TAF (at 9.3 m) is uncovered. There is a temporary core uncovery for this scenario initiated 7 hr after shutdown but no core uncovery while firewater injection continues for this scenario initiated at 24 hr decay heat, as noted in the previous two sections. The upper plenum and core liquid levels both drop very quickly after the SDC break opens.

Figures 4.2.9.3 and 4.2.9.4 present the core clad temperatures during the firewater addition period and the subsequent core heatup for this scenario initiated 7 hr and 24 hr after shutdown, respectively. There is a brief core heatup during the early, temporary core uncovery in this sequence initiated 7 hr after shutdown; At decay heat levels corresponding to accident initiation 24 hr after shutdown, there is no core heatup at all while firewater injection continues, because there is no uncovery at all. In both cases, after firewater injection ends at 12 hr there is a slow temperature increase, reflecting the rise in saturation temperature as the system pressurizes to the SRV setpoint. Later, after TAF uncovery, core heatup and damage begins.

Table 4.2.9.1 summarizes the timings of various key events predicted using MELCOR for this sequence initiated 24 hr after shutdown.

4.3 Level 2 Support Calculations

Based partly on the results of the MELCOR calculations done in support of the Level 1 analysis, a number of accident sequences were eliminated from consideration as not resulting in core damage within the first 24 hr from

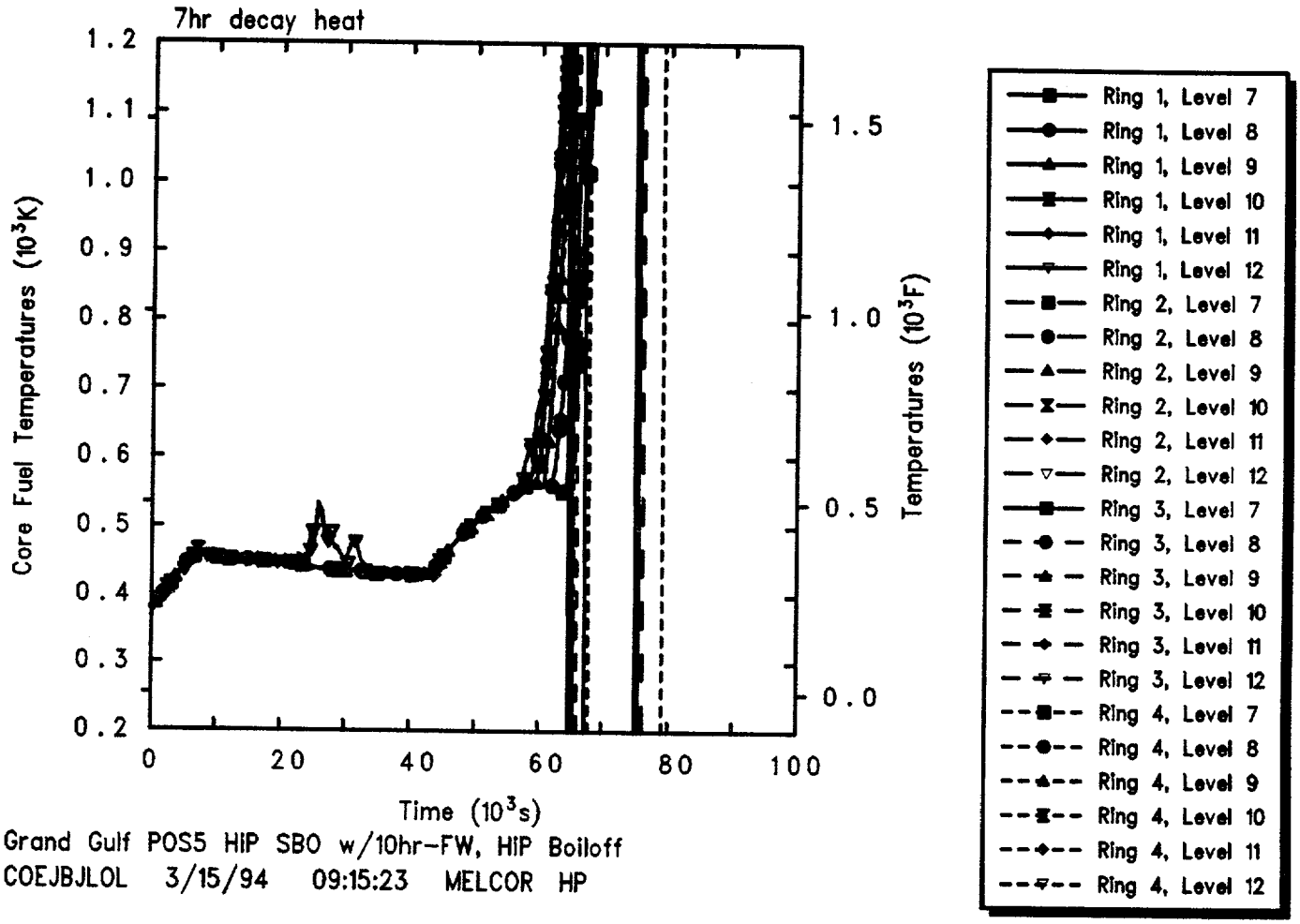

Figure 4.2.8.7. Core Fuel Temperatures for Grand Gulf POS 5 -- Station Blackout with 10 hr Firewater Addition Followed by High Pressure Boiloff, Initiated 7 hr After Shutdown.

Table 4.2.8.1. Key Event Times for Grand Gulf POS 5 -- Station Blackout with 10 hr Firewater Addition Followed by High Pressure Boiloff, Initiated at Various Times After Shutdown

Initiation Time After Shutdown	Time to (s) TAF Uncovery *	Core Heatup	First Gap Release	Vessel Failure
7 hr	9,780	56,500	63,038	90,582
24 hr	79,530	90,000	97,950	141,447

* Collapsed liquid level.

the start of the accident. The remaining sequences, those leading to core damage within 1 day and with a frequency greater than the Level 1 truncation frequency, were grouped into plant damage states or PDSs (see Section 7 of Volume 2). The plant damage states are ranked by their relative contribution to core damage frequency in Table 4.3.1. Complete MELCOR accident analyses have been done for these sequences in support of the Level 2 PRA, with results described in the following subsections. (The last two sequences in the table are identical to other sequences in the table with regard to MELCOR calculations, but with different recovery assumptions in the Level 2 PRA.)

4.3.1 Large Break LOCA with Flooded Containment, Initiated 7 hr, 24 hr and 40 days After Shutdown

This accident is initiated by a large break LOCA in the recirculation line. At the start of the accident, the reactor vessel is depressurized, the coolant is at the normal level and the SRVs are closed. The vessel water inventory is at 366.5 K (200°F), which corresponds to the maximum temperature allowed by the Grand Gulf technical specifications for operation in POS 5. The break drains the vessel to 2/3 core height. The initiating event then results in a loss of all core cooling and coolant makeup. The reactor pressure vessel head vent is open at the beginning of the transient. The containment has been flooded to the elevation of the lower personnel lock, 9.65 m or 31.67 ft above the suppression pool floor. The containment (suppression pool, pedestal cavity and drywell) water inventory is at 300.5 K (80°F); the containment is at 305.4 K (90°F). The drywell personnel lock is open; the containment equipment hatch and both of the containment personnel locks are open (i.e., "open containment").

This sequence is almost identical to the large break LOCA scenario discussed in Section 4.2.5 except that in those Level 1 analyses the containment was dry while in these Level 2 analyses the containment was assumed to be flooded.

The sequence of events predicted by MELCOR for this accident with different initiation times is given in Table 4.3.1.1.

Figure 4.3.1.1 gives the vessel pressures calculated for this same accident scenario initiated at three different times after shutdown. In all cases, the primary system remains near atmospheric as the large break maintains pressure near-equilibrium between the primary and the containment, while the open personnel locks and equipment hatch vent the containment to the auxiliary building. For any given decay heat level, the smaller pressure spikes seen in Figure 4.3.1.1 generally correspond to core heatup and damage, while the largest pressure spikes seen in Figure 4.3.1.1 correspond to vessel failure and to auxiliary building failure.

The water and steam coolant flowing out through the break pressurizes the containment and, through the open equipment hatch and personnel locks, pressurizes the auxiliary building, as shown in Figure 4.3.1.2. The longer after shutdown that this accident sequence begins, the lower the decay heat and the longer it takes to fail the

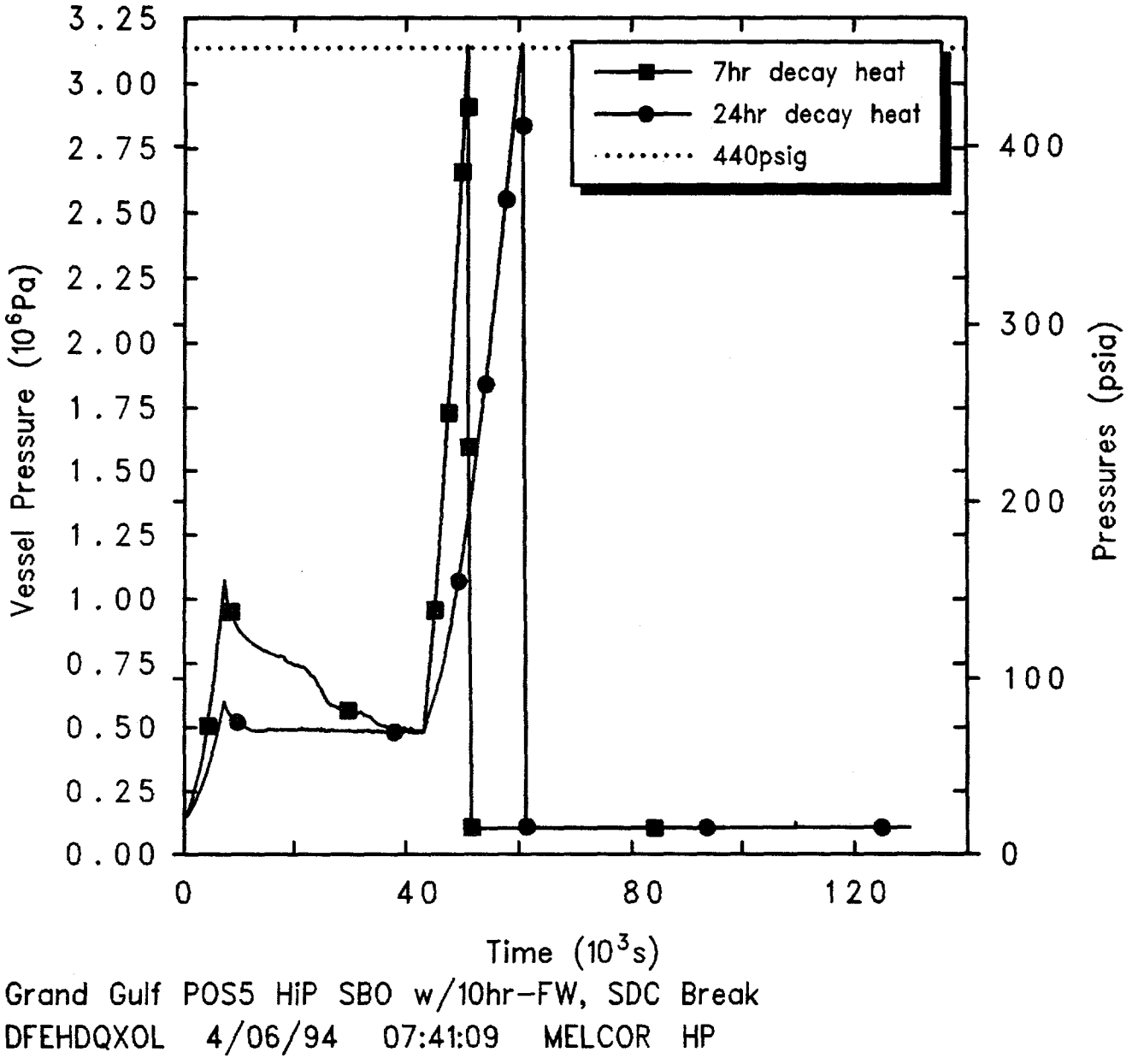

Figure 4.2.9.1. Reactor Vessel Pressures for Grand Gulf POS 5 -- Station Blackout with 10 hr Firewater Addition Followed by Failure to Isolate SDC, Initiated at Various Times After Shutdown.

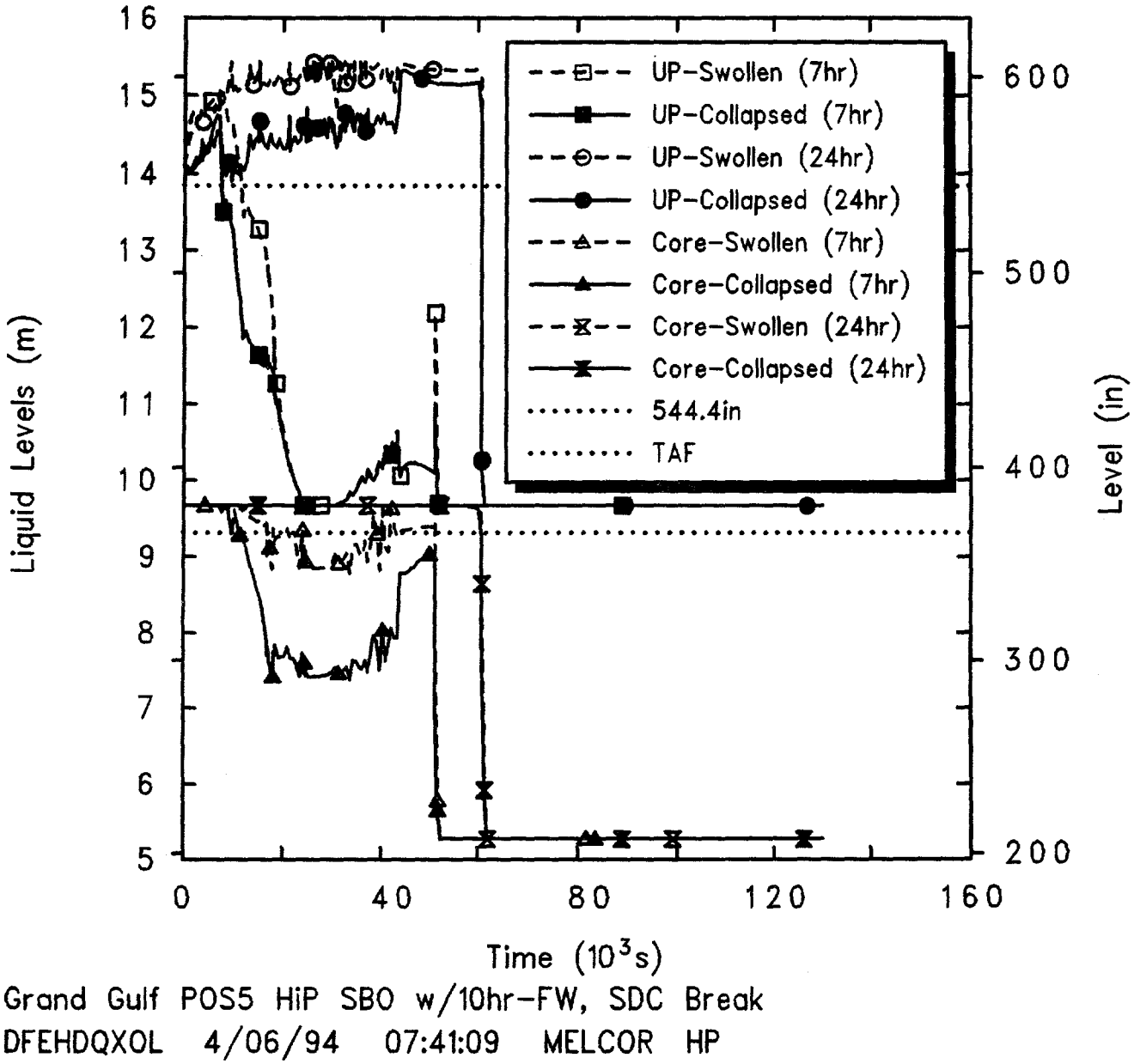

Figure 4.2.9.2. Upper Plenum and Core Liquid Levels for Grand Gulf POS 5 -- Station Blackout with 10 hr Firewater Addition Followed by Failure to Isolate SDC, Initiated at Various Times After Shutdown.

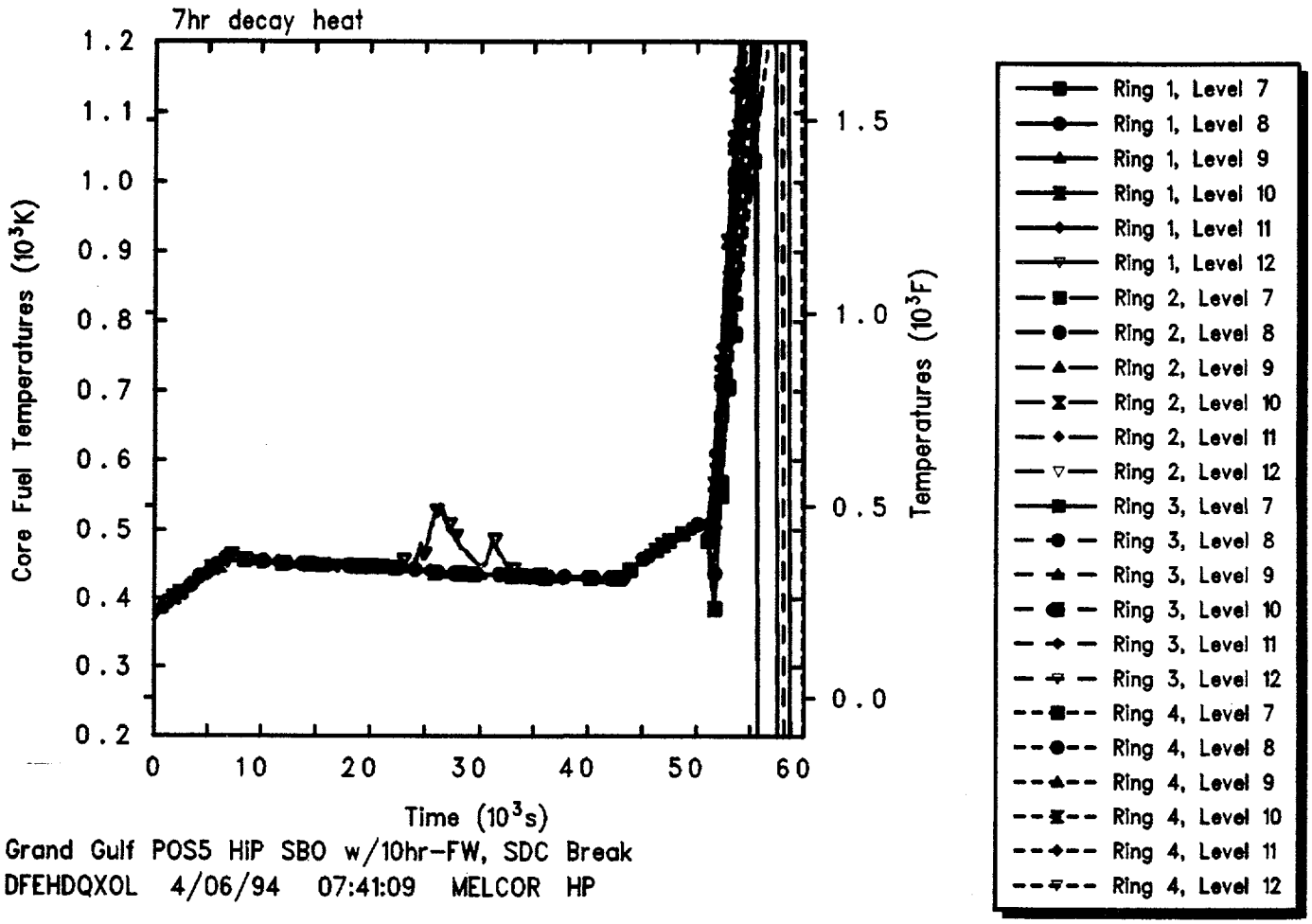

Figure 4.2.9.3. Core Fuel Temperatures for Grand Gulf POS 5 -- Station Blackout with 10 hr Firewater Addition Followed by Failure to Isolate SDC, Initiated 7 hr After Shutdown.

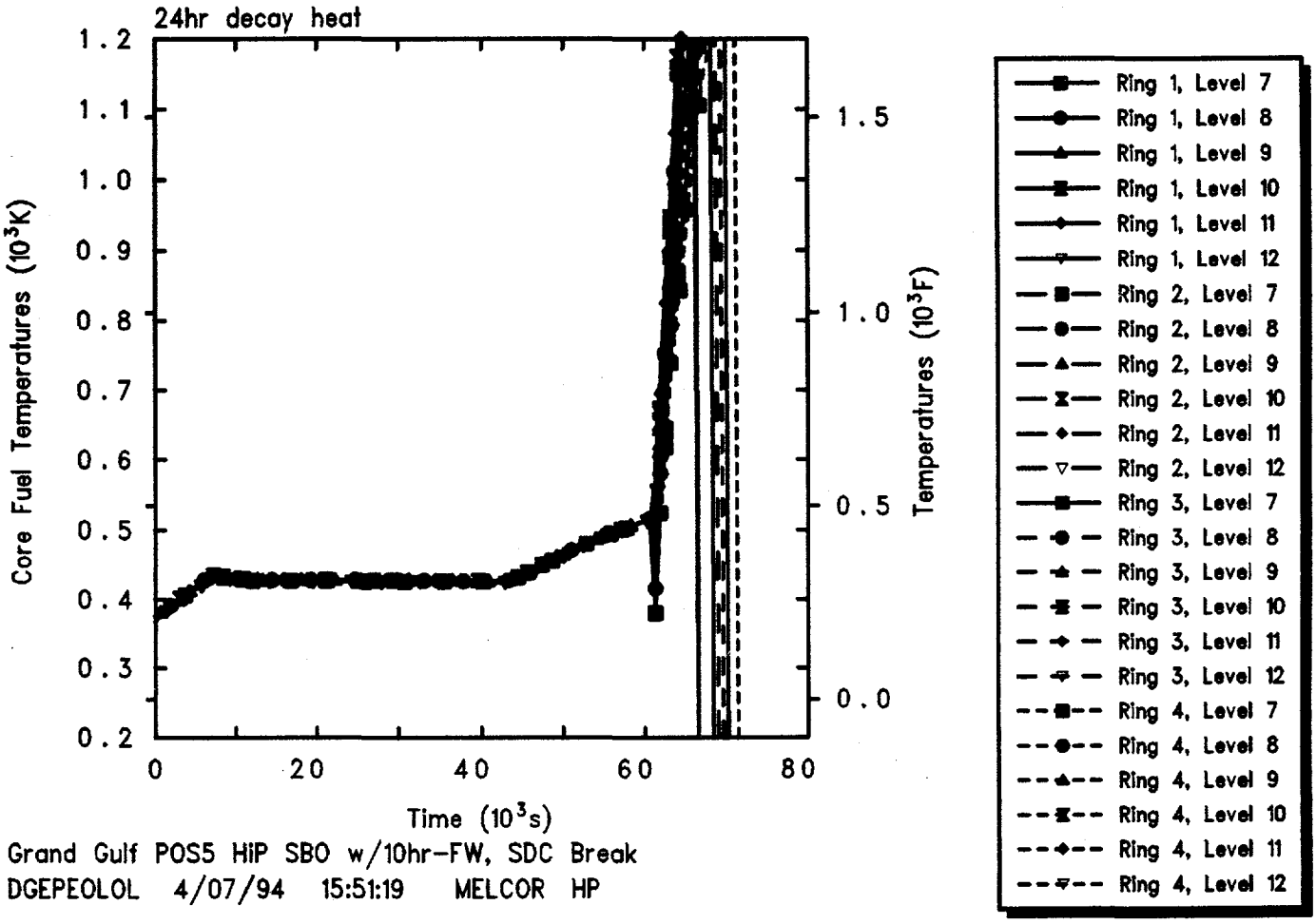

Figure 4.2.9.4. Core Fuel Temperatures for Grand Gulf POS 5 -- Station Blackout with 10 hr Firewater Addition Followed by Failure to Isolate SDC, Initiated 24 hr After Shutdown.

Table 4.2.9.1. Key Event Times for Grand Gulf POS 5 -- Station Blackout with 10 hr Firewater Addition Followed by Failure to Isolate SDC, Initiated 24 hr After Shutdown

Initiation Time After Shutdown	Time to (s) TAF Uncovery *	Core Heatup	First Gap Release	Vessel Failure
7 hr	9,924	53,000	53,720	93,800
24 hr	60,520	63,000	63,940	109,527

* Collapsed liquid level.

auxiliary building. The auxiliary building pressure rises somewhat more slowly during the early stages of core uncovery, heatup and damage, then spikes up to the failure point after vessel failure. Because of the rapid decrease in the exponentially dropping decay heat soon after shutdown and the much more gradual decline in decay heat much later after shutdown, the time to vessel and auxiliary building failure for this accident initiated 40 days after shutdown is not proportionally greater than the time to vessel and auxiliary building failure for this accident initiated 24 hr after shutdown.

The pressure histories in all the control volumes modelling the vessel are virtually identical to the results shown in Figure 4.3.1.1 for the core control volume; the pressure histories in the four control volumes modelling different floors in the auxiliary building are all virtually identical to the results shown in Figure 4.3.1.2 for the second floor. In each case, the pressure response in the drywell and cavity generally tracks the vessel pressure, while the pressure response in the outer containment (i.e., dome, equipment hatch, etc.) is very similar to that shown for the auxiliary building.

The coolant inventory in the vessel drops due to coolant and steam loss out the break, with a very rapid loss of about 60-70% of the inventory as liquid followed by a more gradual loss of the remaining inventory due to boiling and steam outflow, as presented in Figure 4.3.1.3. The amount of liquid inventory lost in the initial liquid blowdown is determined by the elevation of the break and is therefore about the same regardless of the decay heat level; later, as would be expected, the gradual inventory loss due to continued boiloff is faster for higher decay heat levels than for lower decay heat levels. The vessel inventory then drops to zero very quickly upon vessel failure.

Figures 4.3.1.4 and 4.3.1.5 give the core and lower plenum swollen and collapsed liquid levels for this accident sequence initiated at three different times after shutdown. (Note the change in time scale on the abcissa in these two figures.) The upper plenum liquid levels drop very quickly as the break drains the vessel to 2/3 core height, within seconds or minutes, and are not shown. As with the vessel total inventory comparison, the core levels initially drop rapidly to 2/3 core height as liquid inventory is lost out the break, followed by a more gradual loss of the remaining inventory due to boiling and steam outflow, as presented in Figure 4.3.1.4. The swollen (i.e., two-phase, frothy) liquid levels in the core remain substantially above the collapsed liquid levels during most of core uncovery. The level drop continues from the core region down into the lower plenum, shown in Figure 4.3.1.5 with the levels dropping more slowly once the core is uncovered and less swelling predicted in the lower plenum region than in the core. The lower plenum is still mostly full when vessel failure occurs and any remaining liquid inventory is lost out the vessel break to the cavity.

The heatup of the intact fuel and clad is illustrated in Figures 4.3.1.6 through 4.3.1.8 as calculated for scenarios initiated at 7 hr, 24 hr and 40 days after shutdown, respectively. Core uncovery and heatup begins sooner and proceeds more rapidly at higher decay heat levels than for the same accident initiated longer after shutdown. The fuel/clad component temperatures in MELCOR are set to zero in a cell when that component fails, so these

Table 4.3.1. MELCOR Level 2 Support Calculations -- Sequences and Relative Contribution of Plant Damage States to Core Damage Frequency

Plant Damage State	Time After Shutdown	Fraction Contributed	Sequence Description
PDS 3-1	40 day	0.338	LBLOCA with flooded containment
PDS 2-2	24 hr	0.242	SBO w/o firewater, break in SDC
PDS 2-1	24 hr	0.17	LBLOCA with flooded containment
PDS 2-4	24 hr	0.104	Low-P Boiloff with flooded containment
PDS 1-3	7 hr	0.032	SBO w/10 hr-firewater, High-P Boiloff
PDS 1-1	7 hr	0.019	LBLOCA with flooded containment
PDS 1-2	7 hr	0.015	SBO w/o firewater, break in SDC
PDS 1-5	7 hr	0.008	Low-P Boiloff with flooded containment
PDS 2-5	24 hr	0.007	High-P Boiloff with closed containment
PDS 2-6	24 hr	0.006	Open MSIVs with closed containment
PDS 2-3	24 hr	0.054	Same as PDS 2-2, but with potential to recover AC power
PDS 1-4	7 hr	0.005	Same as PDS 1-2, but with potential to recover AC power

figures show both the overall heatup rate and the time to failure.

Figures 4.3.1.9 through 4.3.1.11 present corresponding core debris temperatures in the active fuel region calculated for scenarios initiated at 7 hr, 24 hr and 40 days after shutdown, respectively; these are the temperatures of the debris bed formed by the failure of the intact fuel/clad component in MELCOR in a core cell, whose (intact) temperatures were given in Figures 4.3.1.6 through 4.3.1.8. The intact fuel/clad component temperatures reach a peak of over 2000 K (3140°F) since the component generally fails at the zircaloy clad melt temperature, taken as 2098 K (3317°F) in MELCOR. The debris bed in the active fuel region in contrast reaches peak temperatures over 3250 K (5390°F), just above the UO_2 melt temperature of 3113 K (5144°F). The debris bed temperatures reached in the active fuel region are slightly higher for accidents initiated at higher decay heat levels than for lower decay heat levels, as would be expected.

The temperatures of the active fuel region debris bed drop to zero when the core plate fails and the debris relocates to the lower plenum. This occurs much later than the collapse of the intact fuel and clad into a debris bed. The core support plate is assumed to fail at 1273 K (1832°F) and, with the new debris radial relocation model added in MELCOR 1.8.2, the core support plate needs to fail in only one ring before debris from cells in the active fuel region in all radial rings can potentially flow sideways and down, fall through the failed plate, and then spread sideways into cells in the lower plenum in all radial rings. (Thus a lower head penetration can now fail in a ring before the core plate in that ring fails.)

The predicted temperatures in the debris bed in the lower plenum and core plate are given in Figures 4.3.1.12

Table 4.3.1.1. Sequence of Events Predicted by MELCOR for Large Break LOCA with Flooded Containment, Initiated at Various Times After Shutdown

Event	Time After Shutdown 7 hr	24 hr	40 days
Accident initiation	0	0	0
Core uncovery (TAF) begins	69 s	70 s	70 s
Core heatup begins	2,000 s (0.56 hr)	3,000 s (0.83 hr)	4,500 s (1.25 hr)
Clad failure/Gap release			
(Ring 1)	9,393 s (2.61 hr)	14,766 s (4.10 hr)	22,264 s (6.18 hr)
(Ring 2)	9,296 s (2.58 hr)	14,590 s (4.05 hr)	22,102 s (6.14 hr)
(Ring 3)	9,409 s (2.61 hr)	14,832 s (4.12 hr)	22,465 s (6.24 hr)
(Ring 4)	10,007 s (2.78 hr)	15,754 s (4.38 hr)	23,773 s (6.60 hr)
(Ring 5)	12,563 s (3.49 hr)	19,612 s (5.45 hr)	28,391 s (7.89 hr)
(Ring 6)	16,461 s (4.57 hr)	25,602 s (7.11 hr)	34,570 s (9.60 hr)
Core plate failed			
(Ring 1)	98,755 s (27.43 hr)	146,396 s (40.67 hr)	218,961 s (60.82 hr)
(Ring 2)	95,954 s (26.65 hr)	145,749 s (40.49 hr)	218,100 s (60.58 hr)
(Ring 3)	98,940 s (27.48 hr)	141,858 s (39.41 hr)	218,090 s (60.58 hr)
(Ring 4)	101,503 s (28.20 hr)	141,478 s (39.30 hr)	217,619 s (60.45 hr)
(Ring 5)	94,884 s (26.36 hr)	140,514 s (39.03 hr)	216,292 s (60.08 hr)
(Ring 6)	92,455 s (25.68 hr)	139,997 s (38.89 hr)	213,691 s (59.36 hr)
Vessel LH penetration failed			
(Ring 1)	92,646 s (25.74 hr)	141,280 s (39.24 hr)	218,100 s (60.58 hr)
(Ring 2)	92,603 s (25.72 hr)	140,621 s (39.06 hr)	214,252 s (59.51 hr)
(Ring 3)	92,574 s (25.72 hr)	140,257 s (38.96 hr)	213,956 s (59.43 hr)
(Ring 4)	92,559 s (25.71 hr)	140,146 s (38.93 hr)	213,868 s (59.41 hr)
(Ring 5)	92,544 s (25.71 hr)	140,100 s (38.92 hr)	213,823 s (59.40 hr)
(Ring 6)	92,571 s (25.71 hr)	140,100 s (38.92 hr)	213,801 s (59.39 hr)
Commence debris ejection	92,544 s (25.71 hr)	140,100 s (28.92 hr)	213,823 s (59.40 hr)
Auxiliary building failed	117,500 s (32.6 hr)	205,000 s (57.0 hr)	315,000 s (87.5 hr)
Cavity rupture			
End of calculation	500,000 s (138.9 hr)	662,916 s (184.1 hr)	787,100 s (218.6 hr)

through 4.3.1.14 for scenarios initiated at 7 hr, 24 hr and 40 days after shutdown, respectively. In all cases, prior to core support plate failure there is some cold, refrozen debris both on the core support plate (level 5) and on the lower core structural material just above the core support plate (level 6); the cooling and refreezing of this debris is the cause of the continued gradual drop in lower plenum liquid level due to steaming seen in Figure 4.3.1.5. The debris temperature rises gradually to the core support plate failure temperature of 1273 K (1832°F). After core support plate failure, hot high-temperature debris begins appearing in the lower plenum as debris falls from the active fuel region into the lower plenum. The lower head penetrations begin failing almost immediately, and the

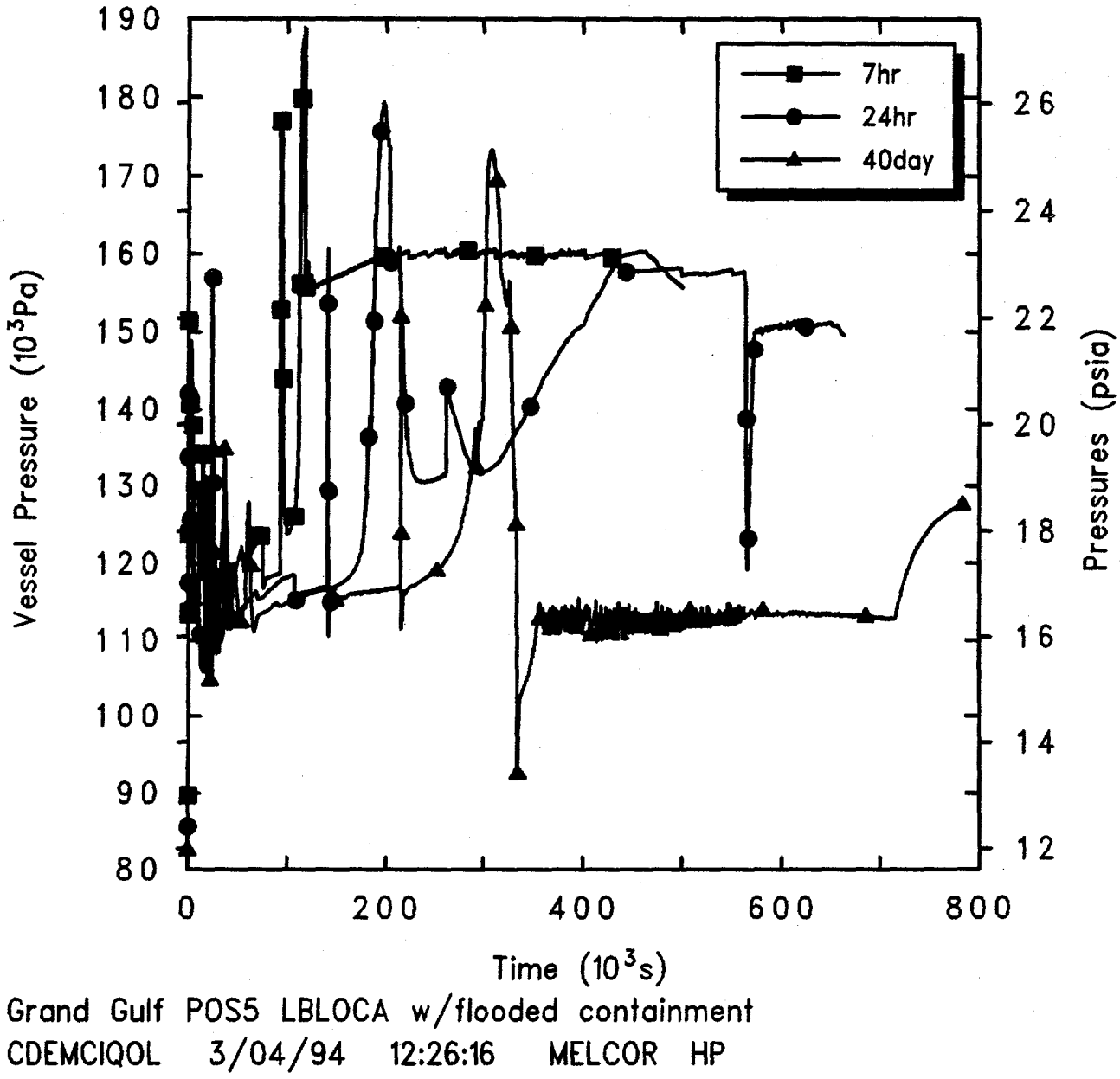

Figure 4.3.1.1. Reactor Vessel Pressures for Grand Gulf POS 5 -- Large Break LOCA with Flooded Containment, Initiated at Various Times After Shutdown.

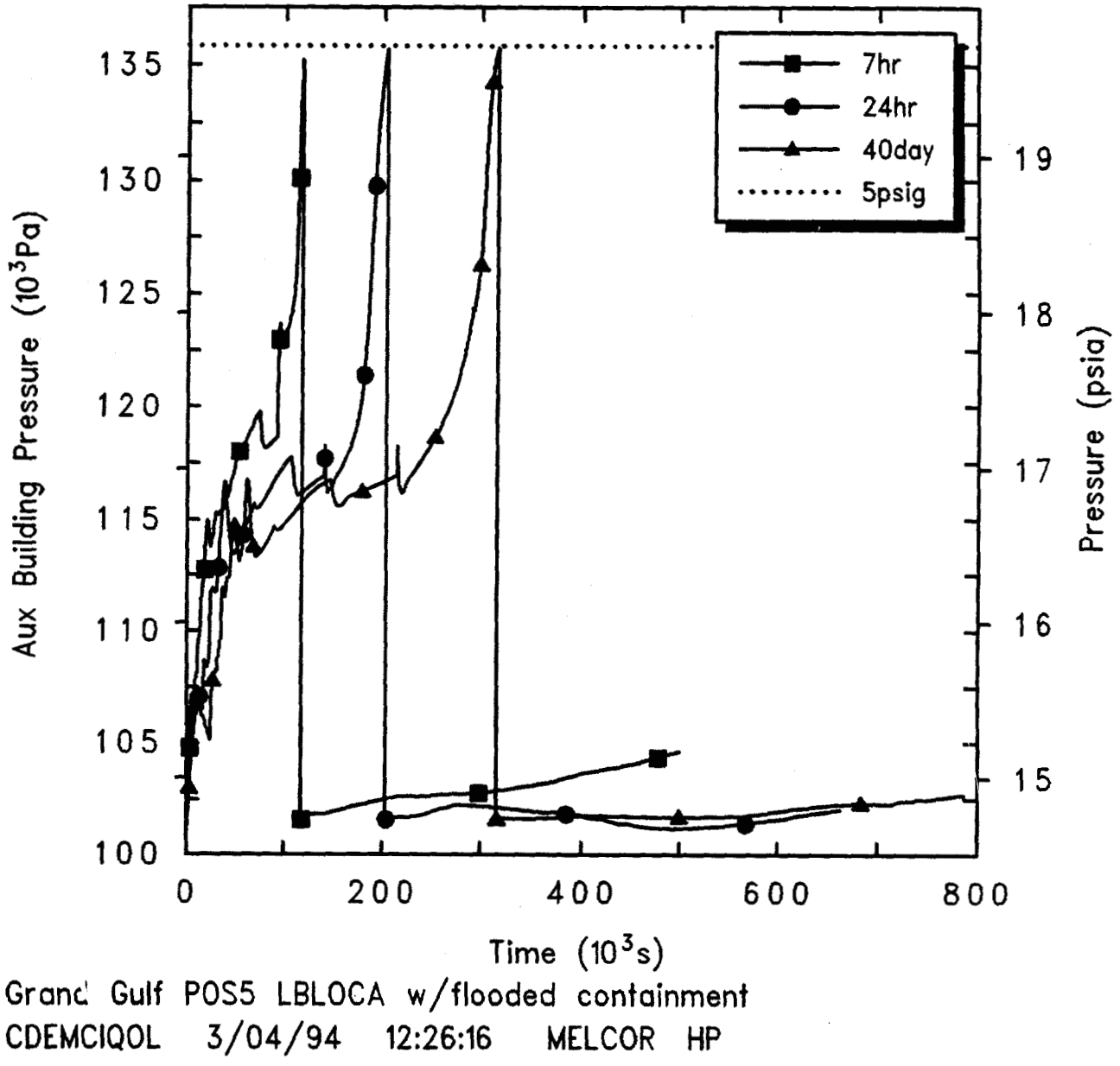

Figure 4.3.1.2. Auxiliary Building Pressures for Grand Gulf POS 5 -- Large Break LOCA with Flooded Containment, Initiated at Various Times After Shutdown.

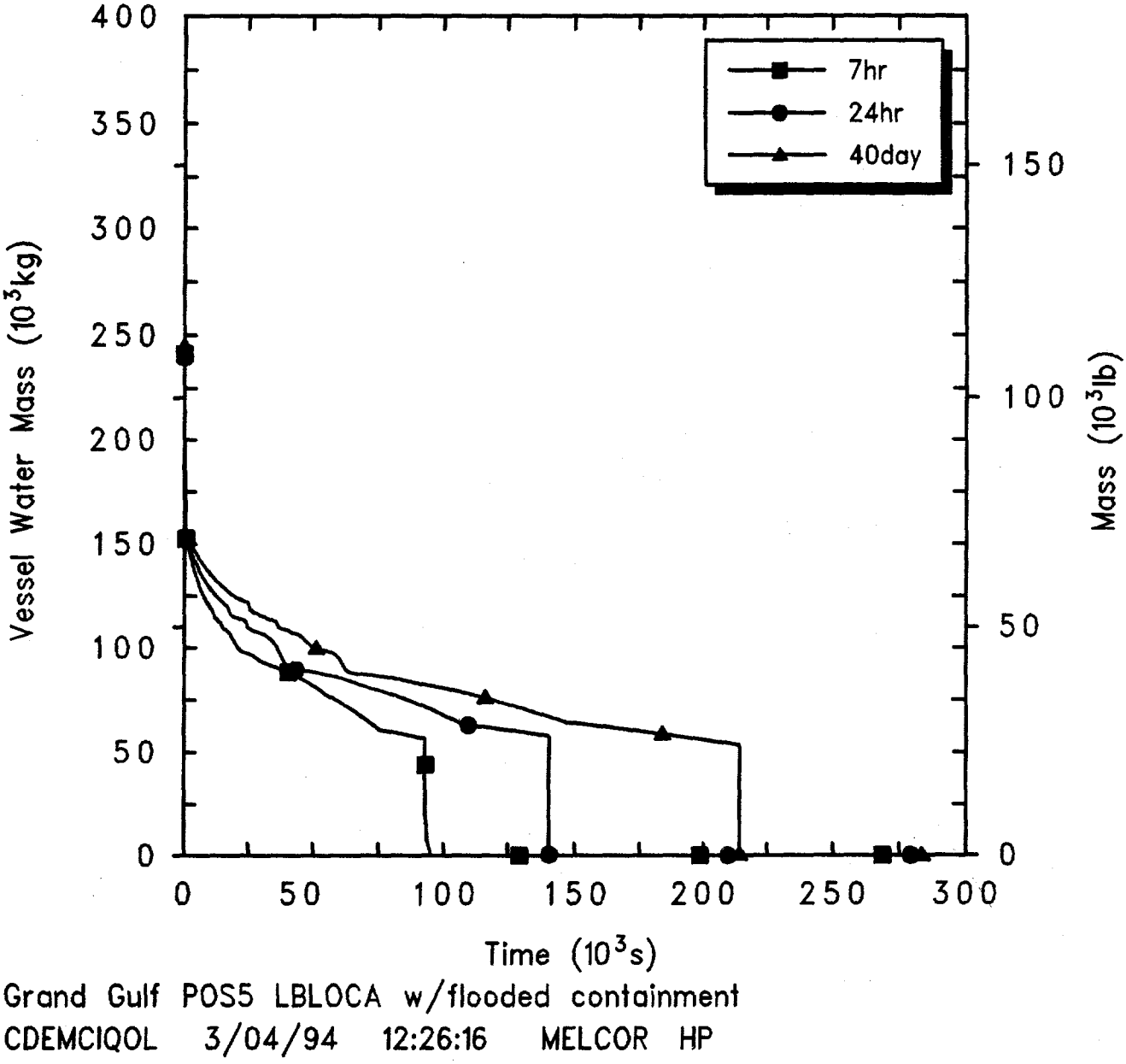

Figure 4.3.1.3 Reactor Vessel Water Masses for Grand Gulf 5 -- Large Break LOCA with Flooded Containment, Initiated at Various Times After Shutdown

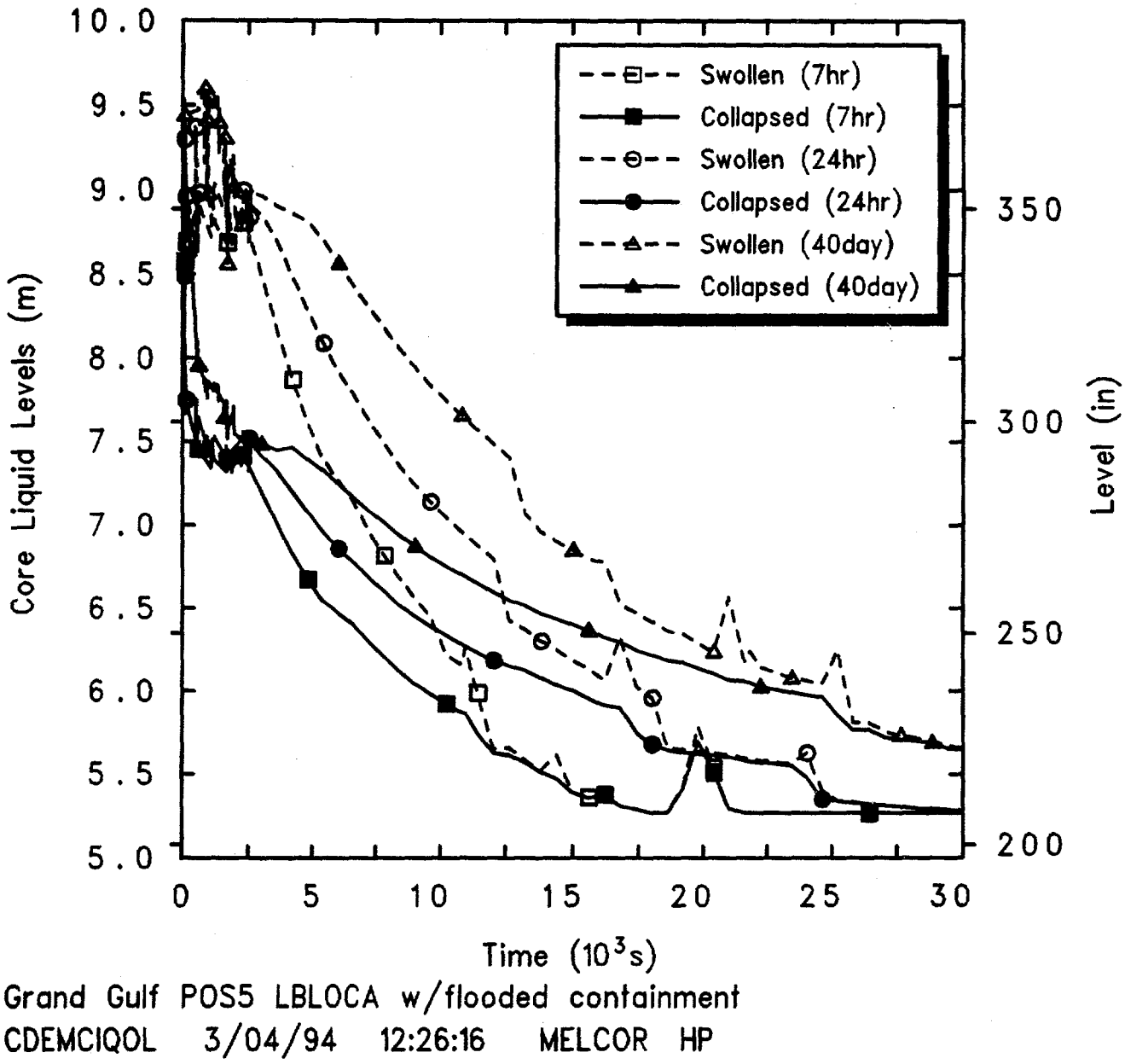

Figure 4.3.1.4. Core Liquid Levels for Grand Gulf POS 5 -- Large Break LOCA with Flooded Containment, Initiated at Various Times After Shutdown.

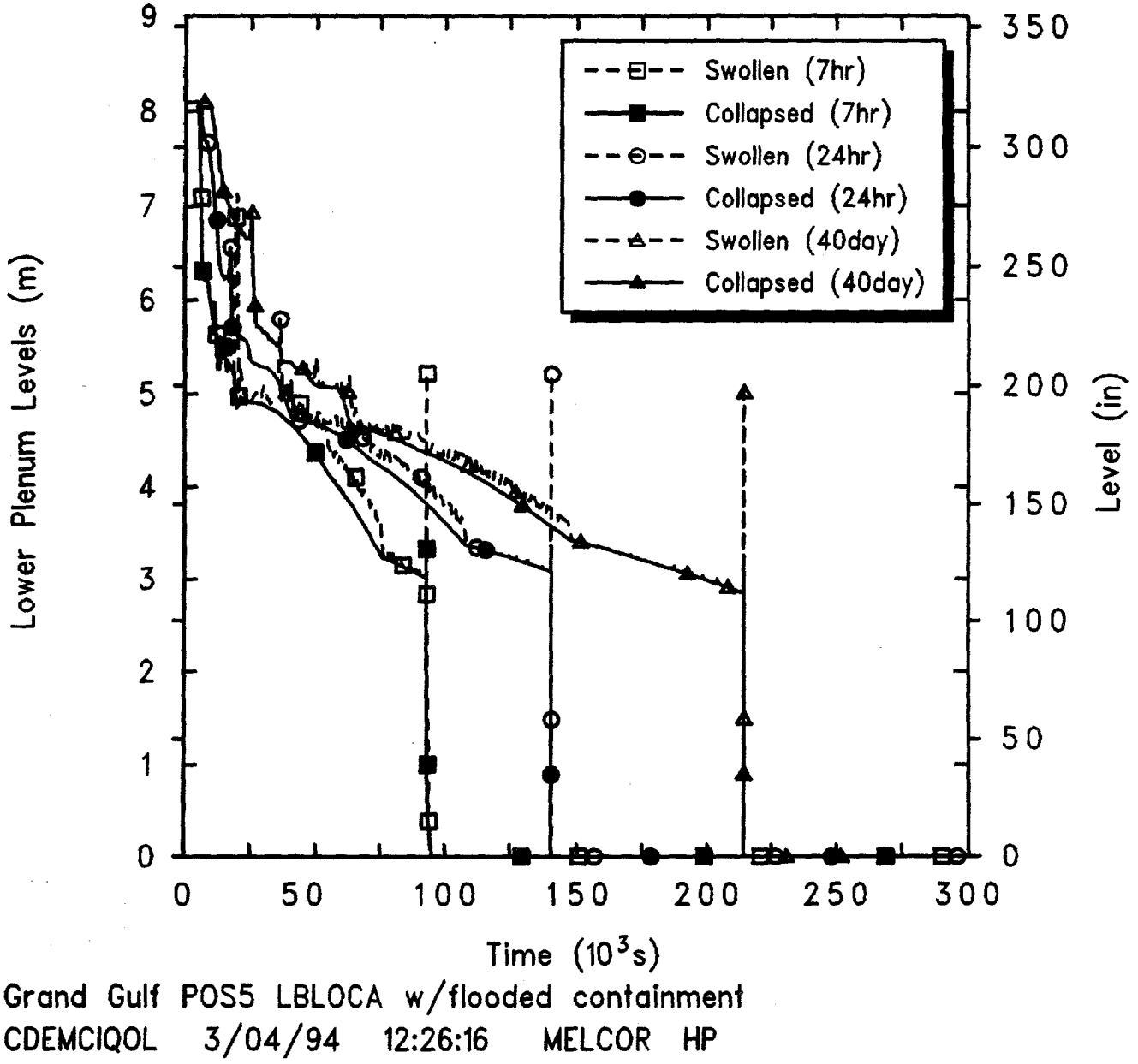

Figure 4.3.1.5. Lower Plenum Liquid Levels for Grand Gulf POS 5 -- Large Break LOCA with Flooded Containment, Initiated at Various Times After Shutdown.

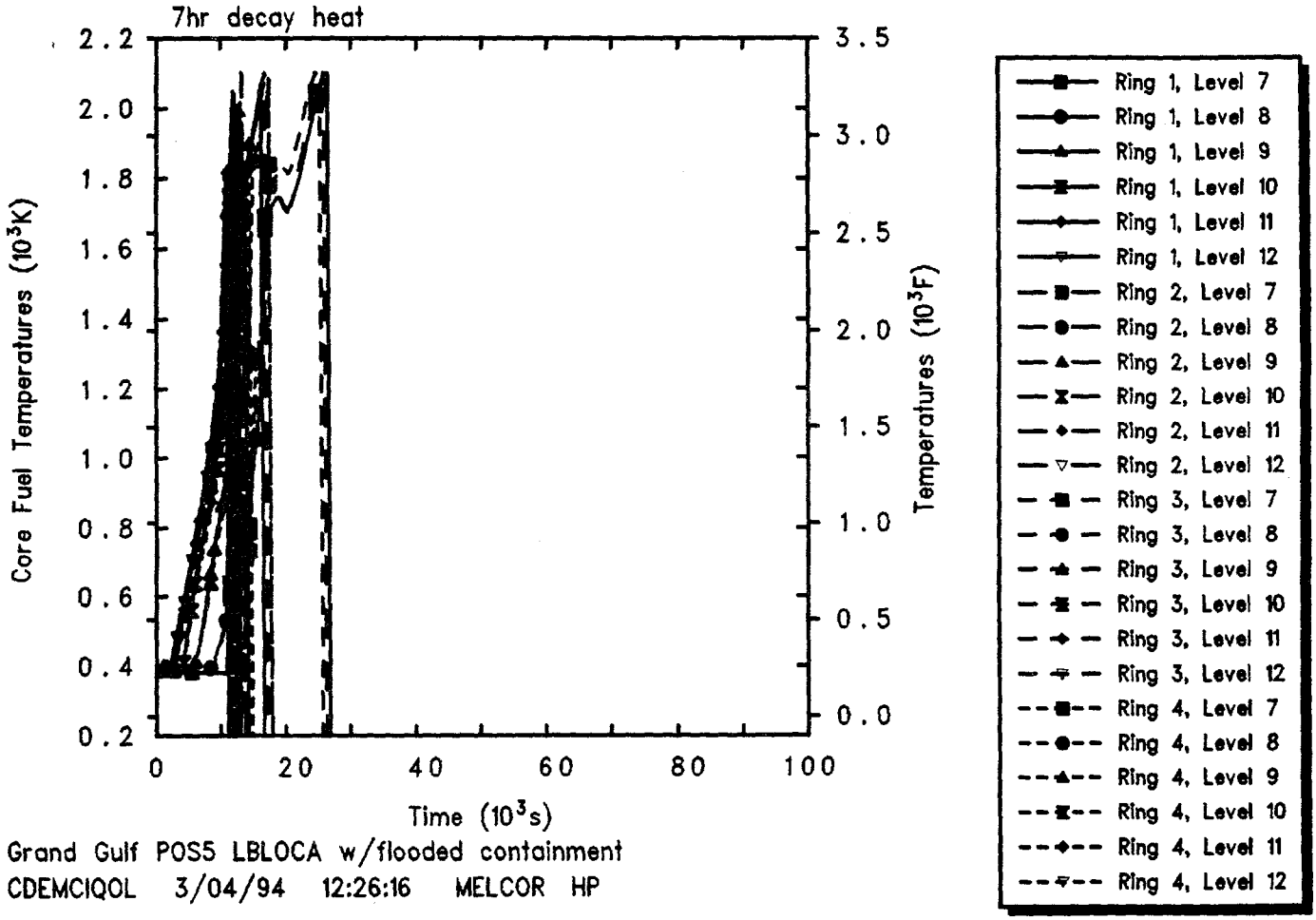

Figure 4.3.1.6. Core Intact Fuel/Clad Temperatures for Grand Gulf POS 5 -- Large Break LOCA with Flooded Containment, Initiated 7 hr After Shutdown.

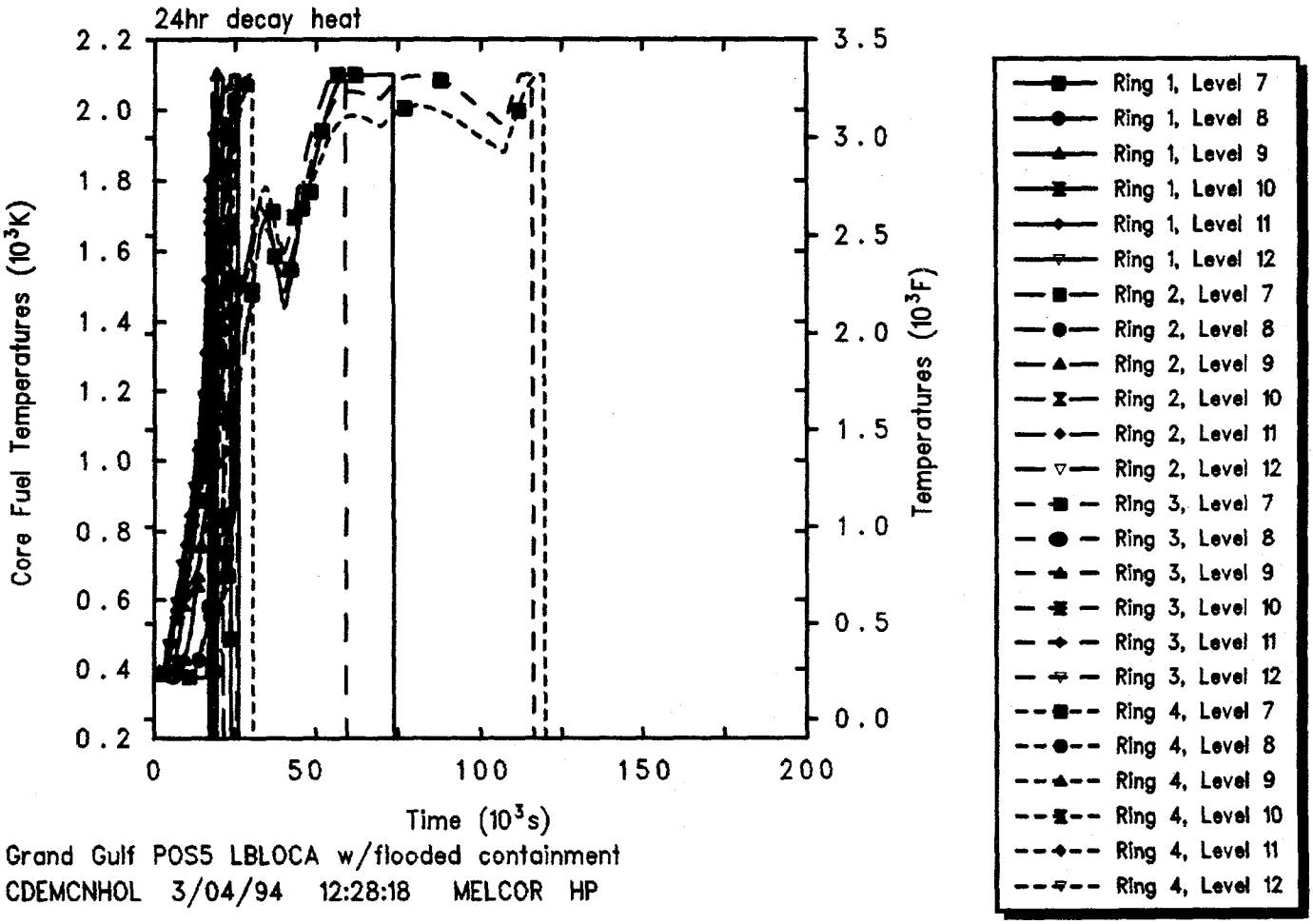

Figure 4.3.1.7. Core Intact Fuel/Clad Temperatures for Grand Gulf POS 5 -- Large Break LOCA with Flooded Containment, Initiated 24 hr After Shutdown.

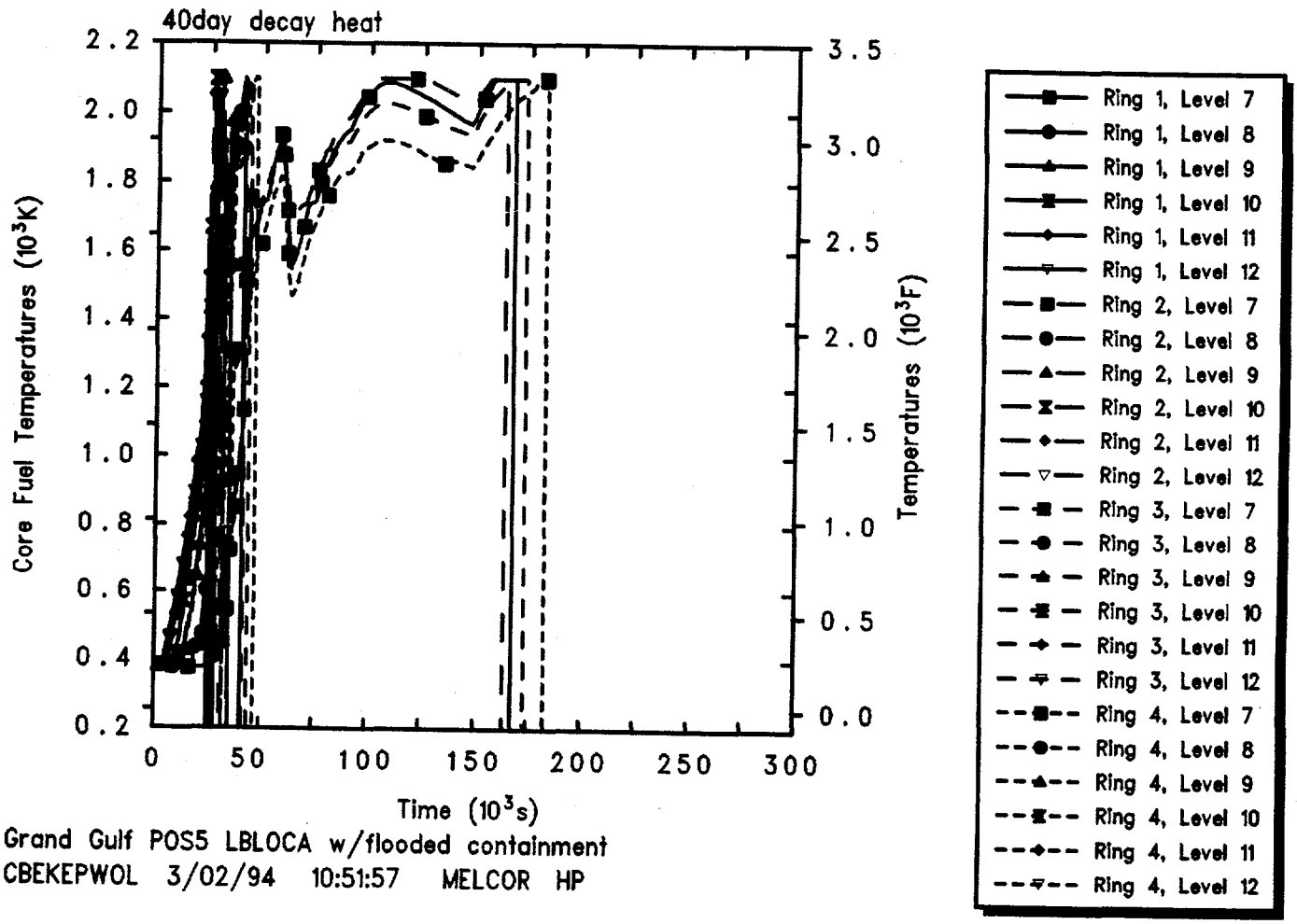

Figure 4.3.1.8. Core Intact Fuel/Clad Temperatures for Grand Gulf POS 5 -- Large Break LOCA with Flooded Containment, Initiated 40 days After Shutdown.

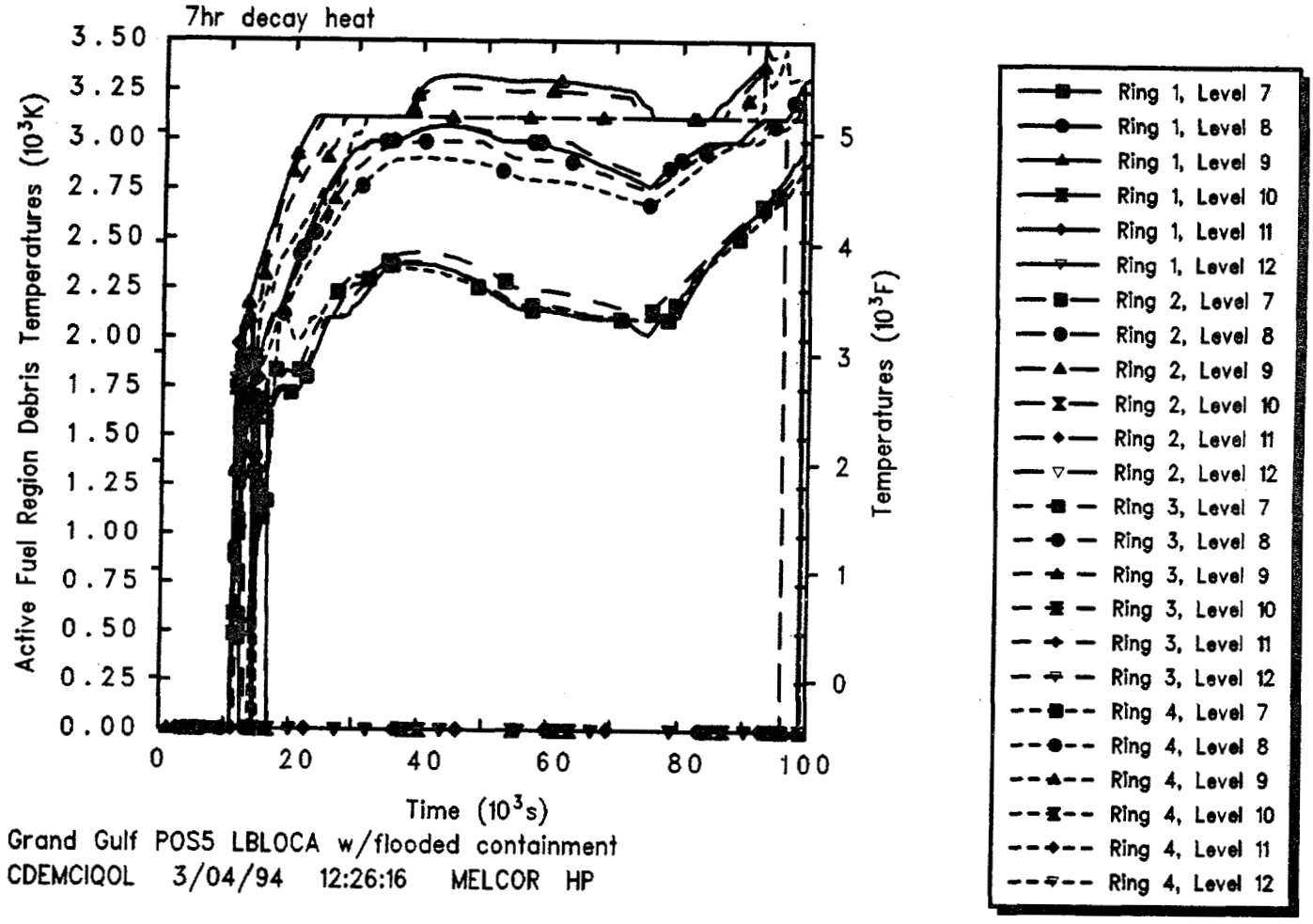

Figure 4.3.1.9. Core Active Fuel Region Debris Bed Temperatures for Grand Gulf POS 5 -- Large Break LOCA with Flooded Containment, Initiated 7 hr After Shutdown.

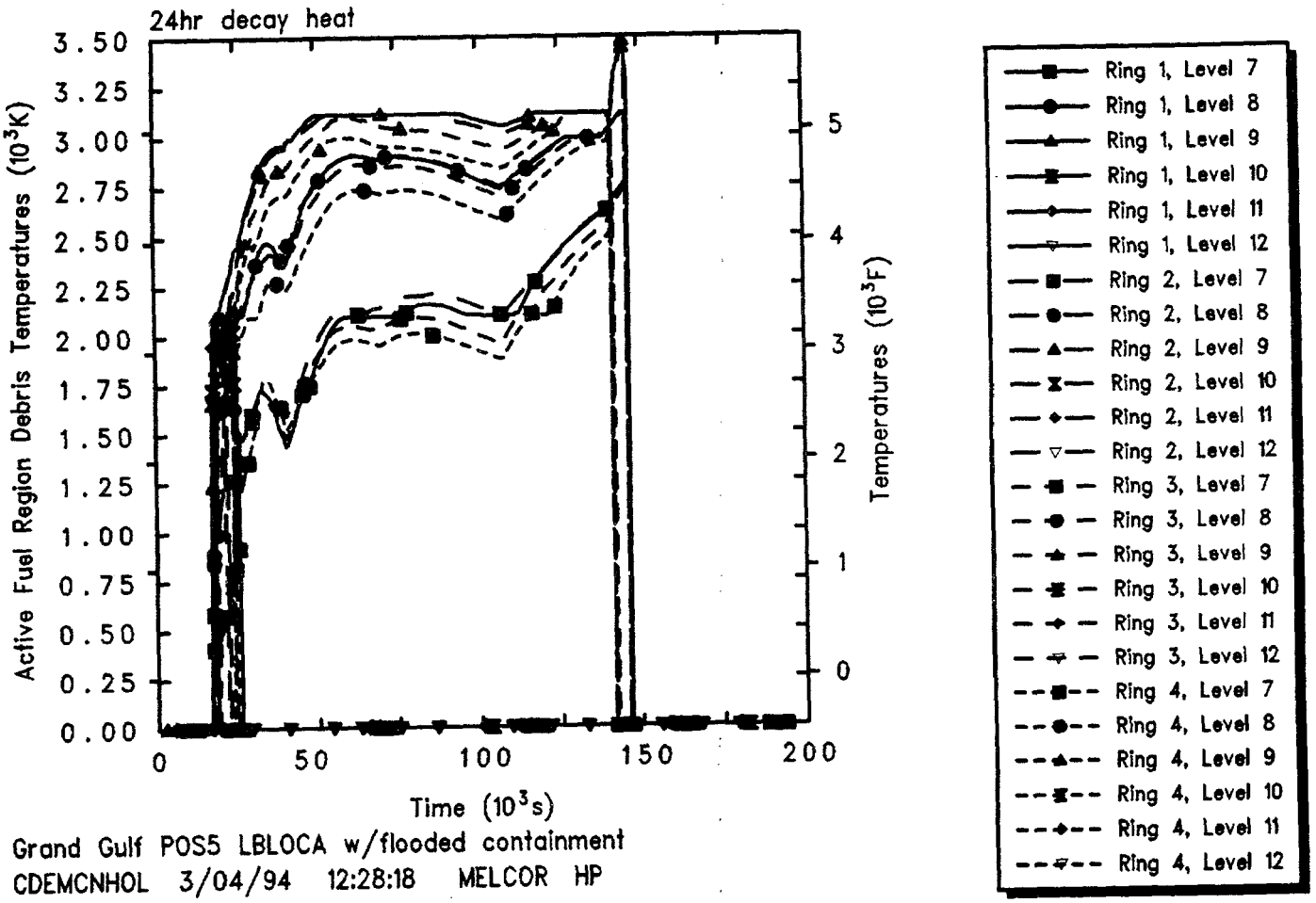

Figure 4.3.1.10. Core Active Fuel Region Debris Bed Temperatures for Grand Gulf POS 5 -- Large Break LOCA with Flooded Containment, Initiated 24 hr After Shutdown.

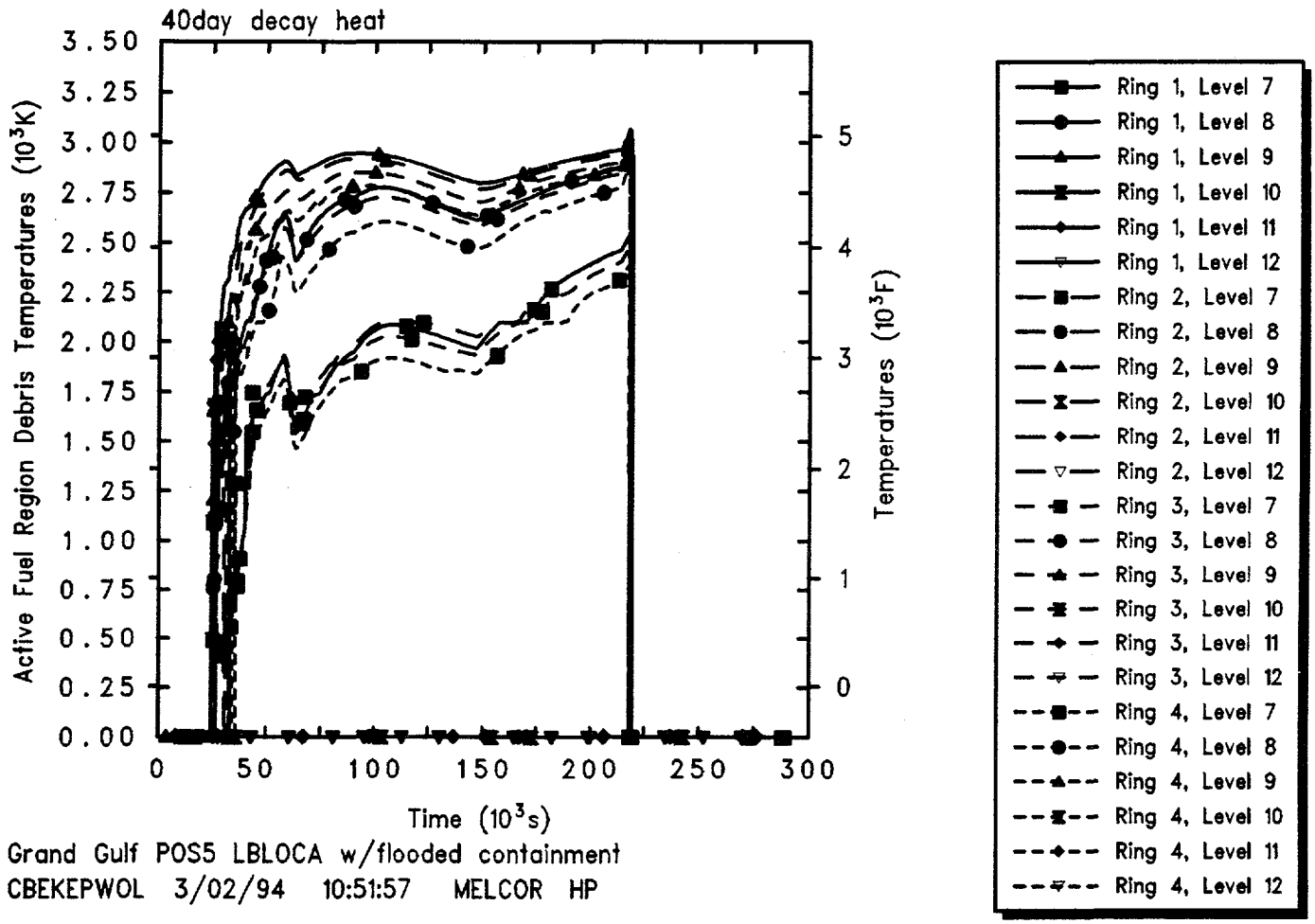

Figure 4.3.1.11. Core Active Fuel Region Debris Bed Temperatures for Grand Gulf POS 5 -- Large Break LOCA with Flooded Containment, Initiated 40 days After Shutdown.

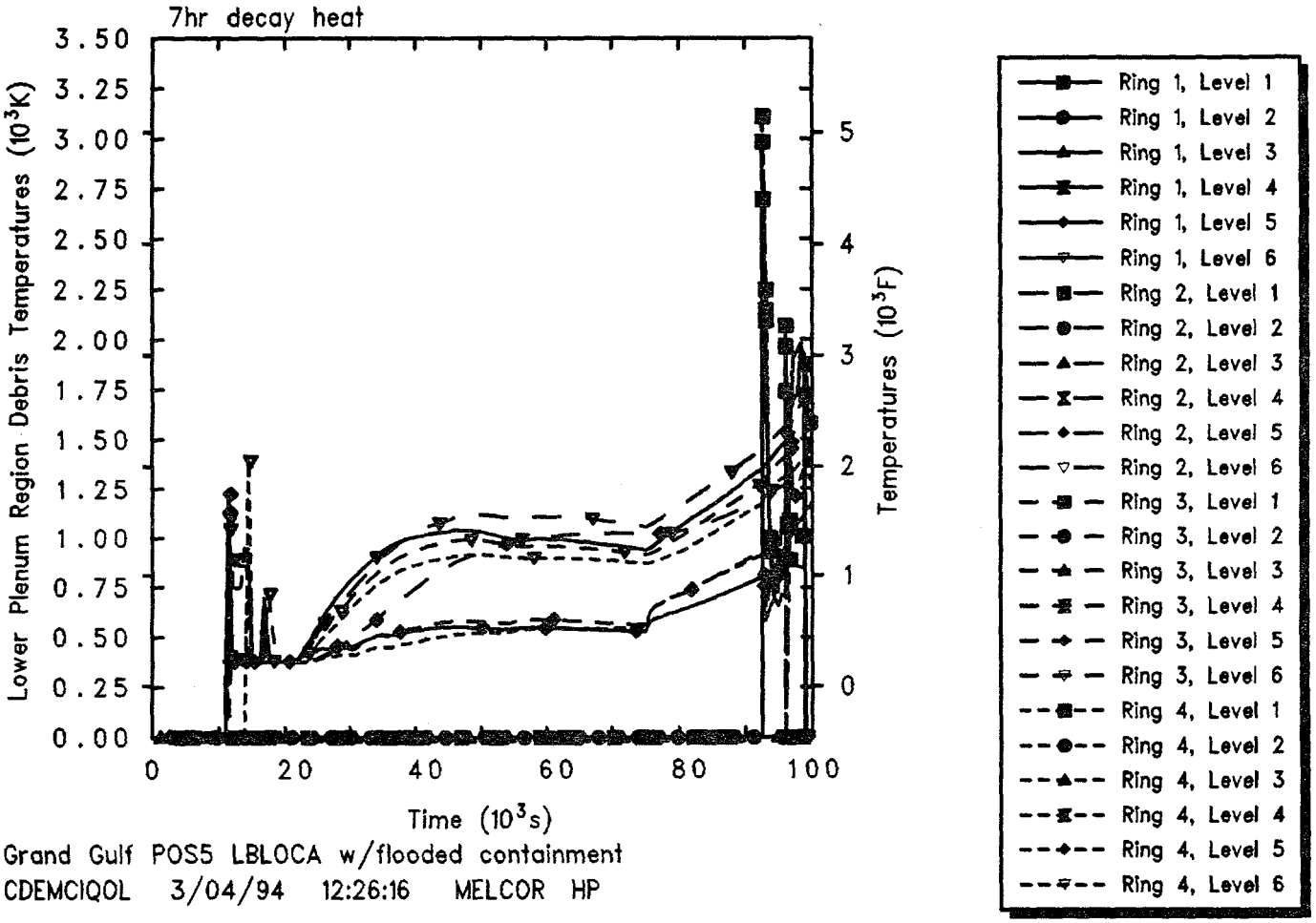

Figure 4.3.1.12. Core Lower Plenum and Core Support Plate Debris Bed Temperatures for Grand Gulf POS 5 -- Large Break LOCA with Flooded Containment, Initiated 7 hr After Shutdown.

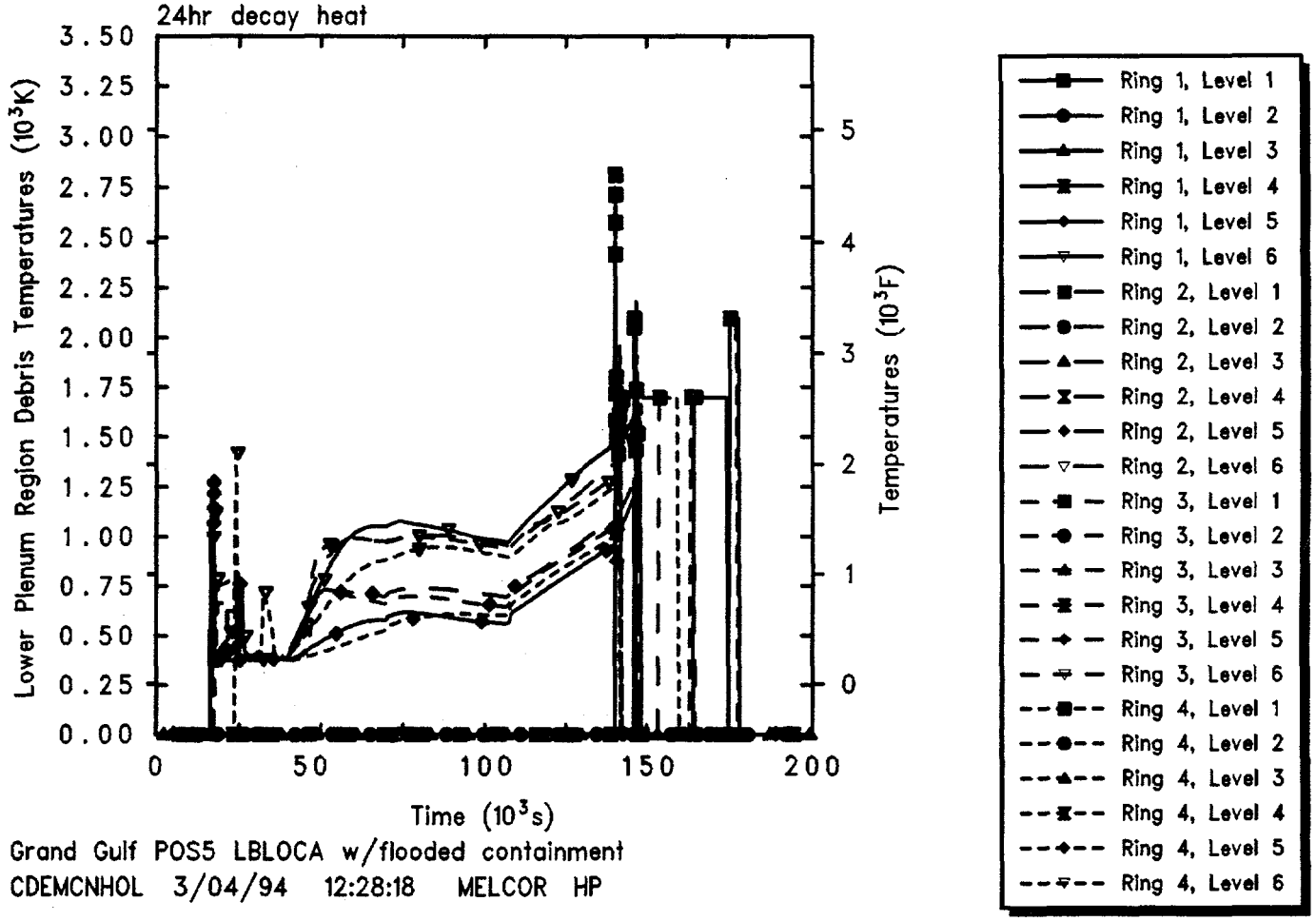

Figure 4.3.1.13. Core Lower Plenum and Core Support Plate Debris Bed Temperatures for Grand Gulf POS 5 -- Large Break LOCA with Flooded Containment, Initiated 24 hr After Shutdown.

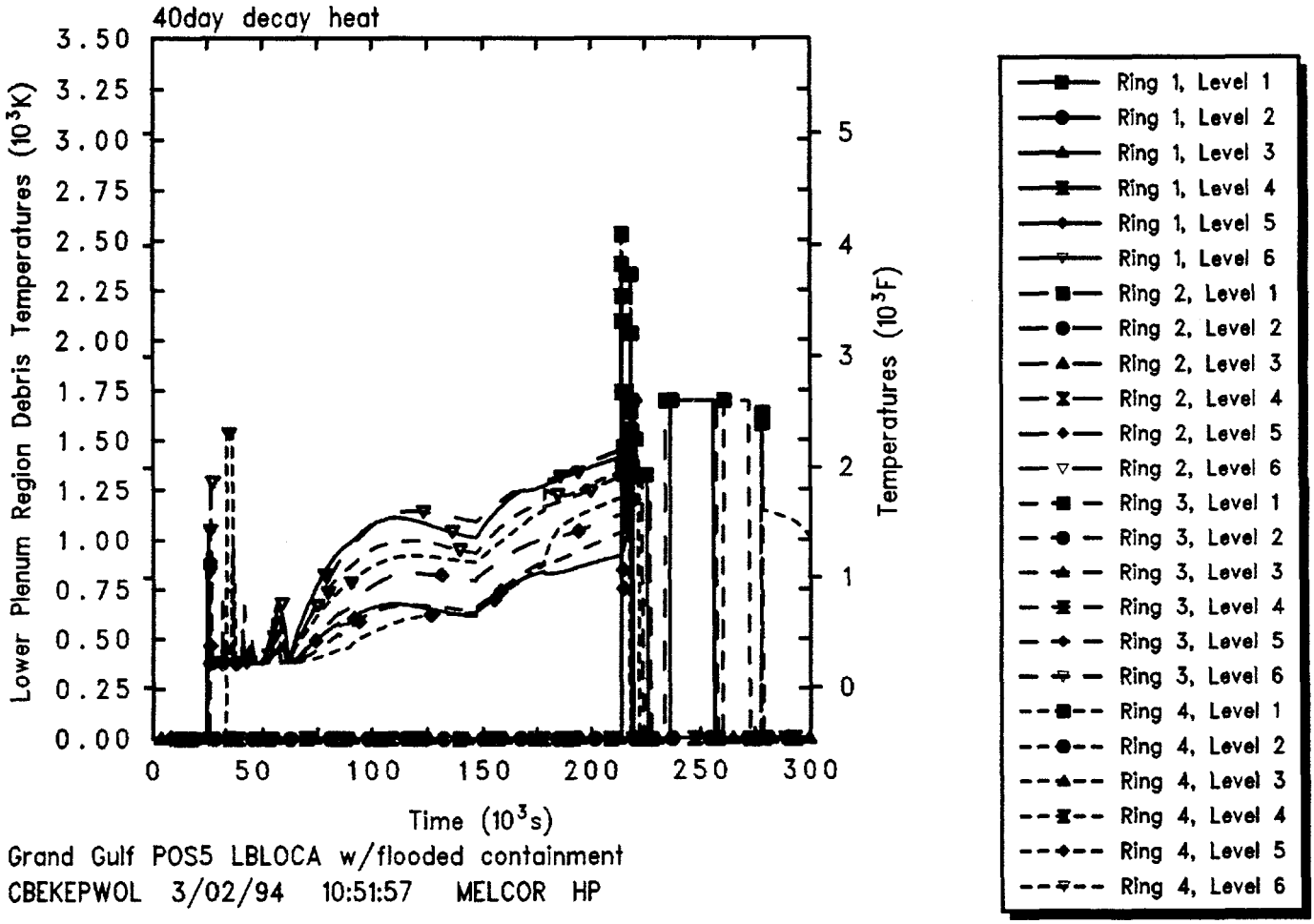

Figure 4.3.1.14. Core Lower Plenum and Core Support Plate Debris Bed Temperatures for Grand Gulf POS 5 -- Large Break LOCA with Flooded Containment, Initiated 40 days After Shutdown.

lower plenum debris temperatures begin dropping to zero as debris is ejected from the vessel to the cavity.

Figures 4.3.1.15 through 4.3.1.17 indicate what fraction of each material in the active fuel region has collapsed into a debris rubble bed held up by the core support plate, prior to core plate failure and subsequent lower head failure and debris ejection, for this large break LOCA scenario initiated at 7 hr, 24 hr and 40 days after shutdown, respectively. The debris bed forms relatively quickly, taking 10,000-20,000 s to reach its final configuration. The fraction of material in the debris bed then remains nearly constant for 50,000-100,000 s as the debris material continues to heat up.

Figure 4.3.1.18 shows the total masses of core materials (UO_2, zircaloy and ZrO_2, stainless steel and steel oxide, and control rod poison) remaining in the vessel. This includes both material in the active fuel region and in the lower plenum. Debris ejection began very soon after lower head failure. This figure illustrates that most of the core material was lost from the vessel to the cavity quickly, in step-like stages. In all cases, all of the UO_2 was transferred to the cavity within about 1 hr after initial lower head penetration failure, as was the unoxidized zircaloy, the associated zirconium oxide and the control rod poison. A small fraction (1-10%) of the structural steel in the lower plenum, and some associated steel oxide, was predicted to remain unmelted and in place throughout the entire transient period (most noticably for the sequence initiated 40 days after shutdown).

The debris material lost from the vessel is ejected to the reactor pedestal cavity. Since almost all the material in the core active fuel region and lower plenum is lost within a very short time period after vessel failure, the core debris mass in the cavity is about the same for this sequence initiated at three different times after shutdown. Figure 4.3.1.19 indicates that the amount of concrete ablated and the total cavity debris mass (i.e., core debris combined with concrete ablation products) is also similar for this sequence initiated at three different times after shutdown, except for a shift in timing (with debris ejection occurring and core-concrete interaction beginning later at lower decay heat levels than for higher decay heat levels). In all cases, concrete ablation is quite rapid soon after debris ejection (while the core debris is hot, >2000 K, and consists of a layer of metallic debris above a heavy oxide layer), and concrete ablation slows significantly after a short time (after enough concrete has been ablated for the debris bed configuration to invert to a light oxide layer above a layer of metallic debris, mixed to a lower average temperature of ~1500 K).
The calculated production of noncondensable gases (H_2, CO, CO_2 and H_2O) is summarized in Figure 4.3.1.20. The hydrogen production shown includes both in-vessel production (the initial step increase) and ex-vessel production in the cavity (the later-time increase). The in-vessel hydrogen generation corresponds to the oxidation of about 15-20% of the zircaloy and about 1-2% of the steel in the core and lower plenum, prior to vessel failure and debris ejection. As soon as the core debris enters the cavity, core-concrete interaction begins, resulting in the production of carbon dioxide and hydrogen; reduction of these gases by the molten metal in the core debris also gives rise to carbon monoxide and hydrogen.

This generation of noncondensables changes the composition of the atmosphere in the containment and in the auxiliary building. The mole fractions in the drywell, containment dome, containment equipment hatch and auxiliary building (second floor) are presented in Figures 4.3.1.21 through 4.3.1.23 for this sequence initiated at various times after shutdown, including a vertical dotted line at vessel failure for reference. The drywell control volume atmosphere consists mostly of steam both before and after vessel and auxiliary building failure. The atmosphere composition in the outer containment volumes and in most of the auxiliary building is generally similar, with little steam or hydrogen (about 5% each) present before vessel failure but a steadily increasing steam concentration and potentially flammable amounts of hydrogen and CO building up late in time. The behavior is qualitatively the same in all three cases, just stretched out in time more at the lower decay heat levels compared to higher decay heats.

Figures 4.3.1.24 through 4.3.1.26 illustrate the time-dependent release of radionuclides from the fuel debris both within the vessel and in the cavity, for cases initiated 7 hr, 24 hr and 40 days after shutdown, respectively. The vertical dotted lines within the plots mark the time of vessel failure, indicating that most of the in-vessel release occurs prior to vessel failure, from the hot debris bed in the active fuel region, while most of the ex-vessel release occurs within a short time period after vessel failure and debris ejection to the cavity, while the core debris is still hot, >2000 K, and consists of a layer of metallic debris above a heavy oxide layer, before enough concrete has been ablated for the debris bed configuration to invert to a light oxide layer above a layer of metallic debris, mixed to a lower average temperature of ~1500 K. Table 4.3.1.2 summarizes the in-vessel, ex-vessel and total

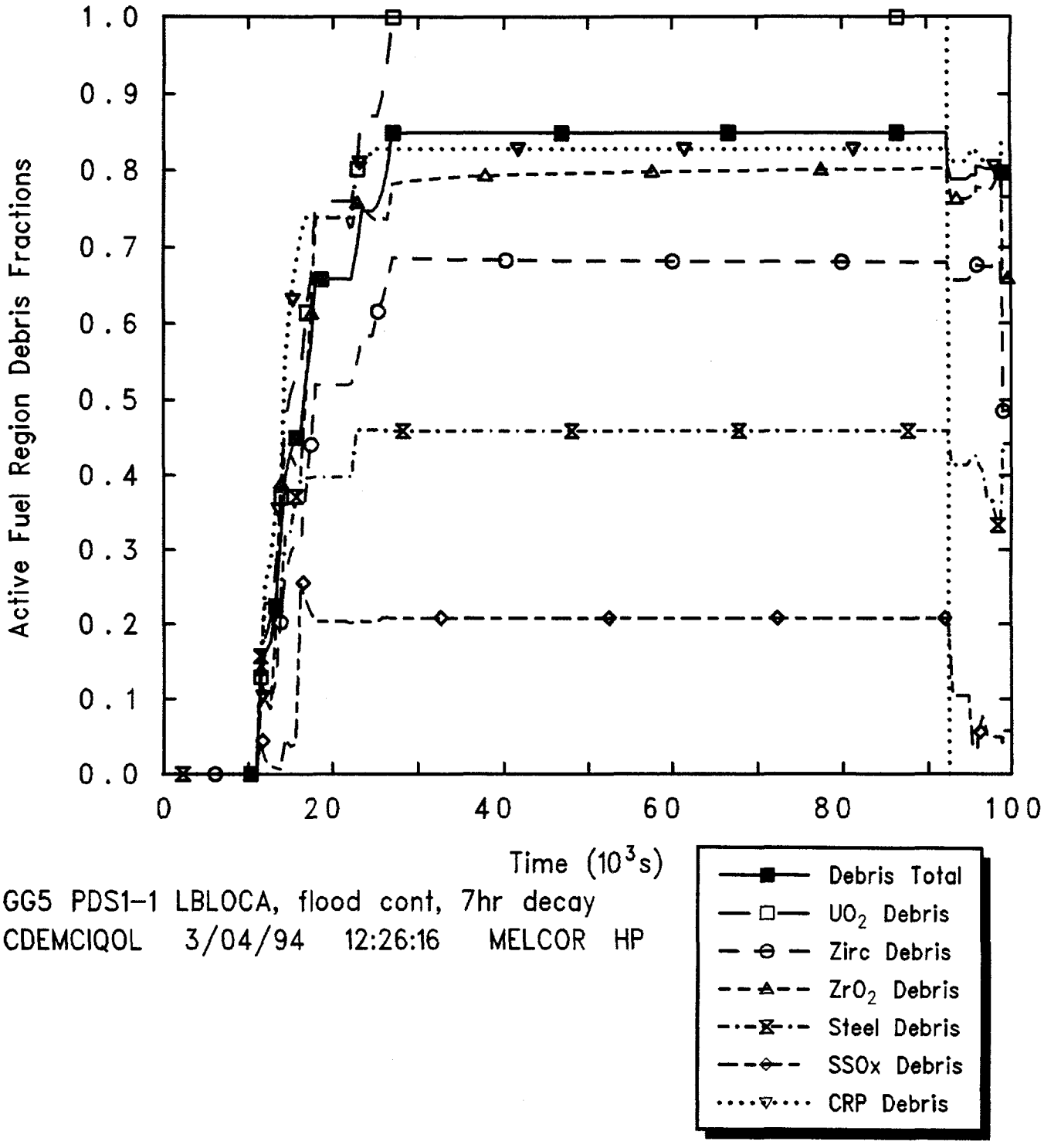

Figure 4.3.1.15. Core Active Fuel Region Degraded Material Fractions for Grand Gulf POS 5 -- Large Break LOCA with Flooded Containment, Initiated 7 hr After Shutdown.

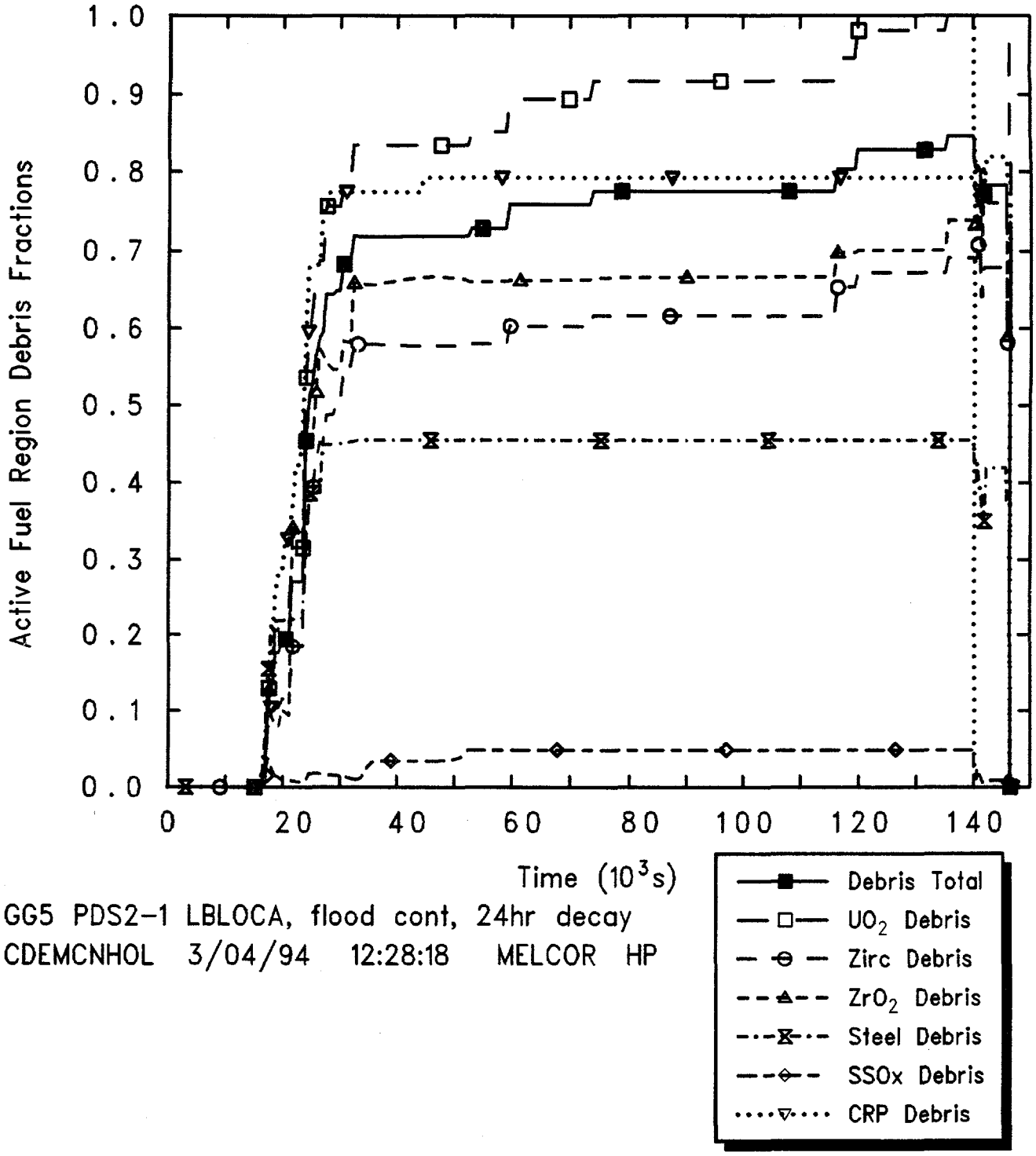

Figure 4.3.1.16. Core Active Fuel Region Degraded Material Fractions for Grand Gulf POS 5 -- Large Break LOCA with Flooded Containment, Initiated 24 hr After Shutdown.

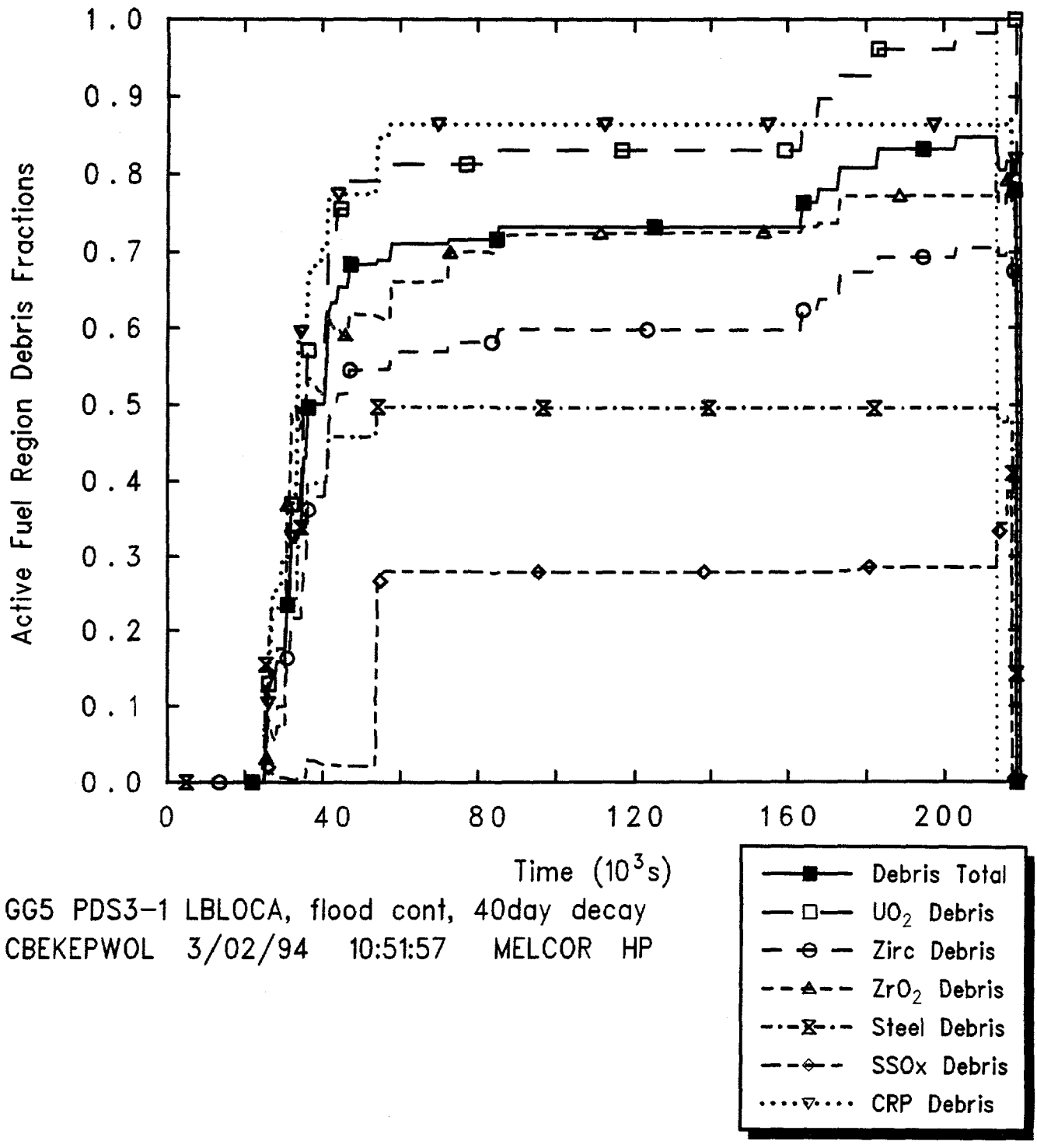

Figure 4.3.1.17. Core Active Fuel Region Degraded Material Fractions for Grand Gulf POS 5 -- Large Break LOCA with Flooded Containment, Initiated 40 days After Shutdown.

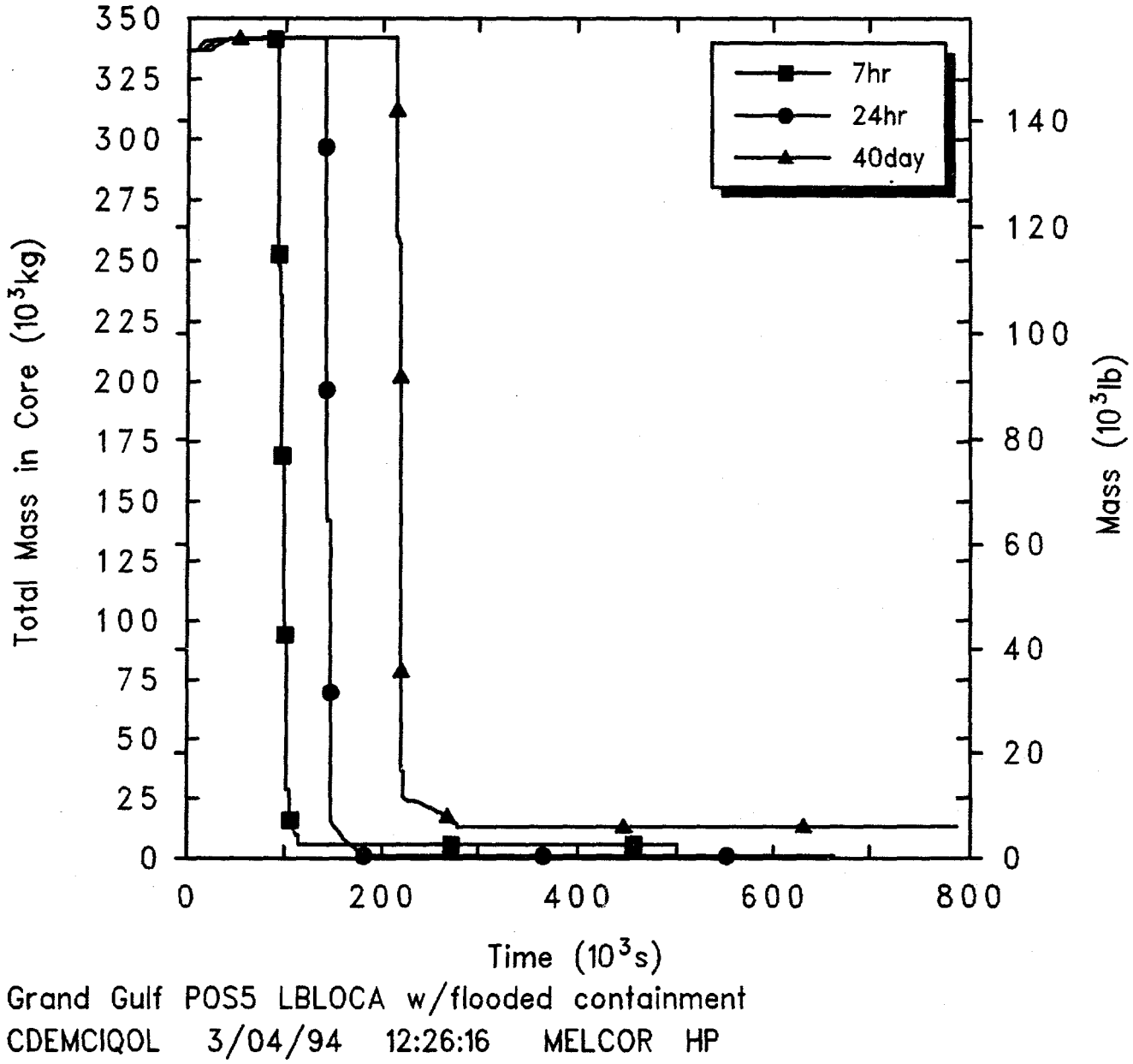

Figure 4.3.1.18. Total Core Material Masses for Grand Gulf POS 5 -- Large Break LOCA with Flooded Containment, Initiated at Various Times After Shutdown.

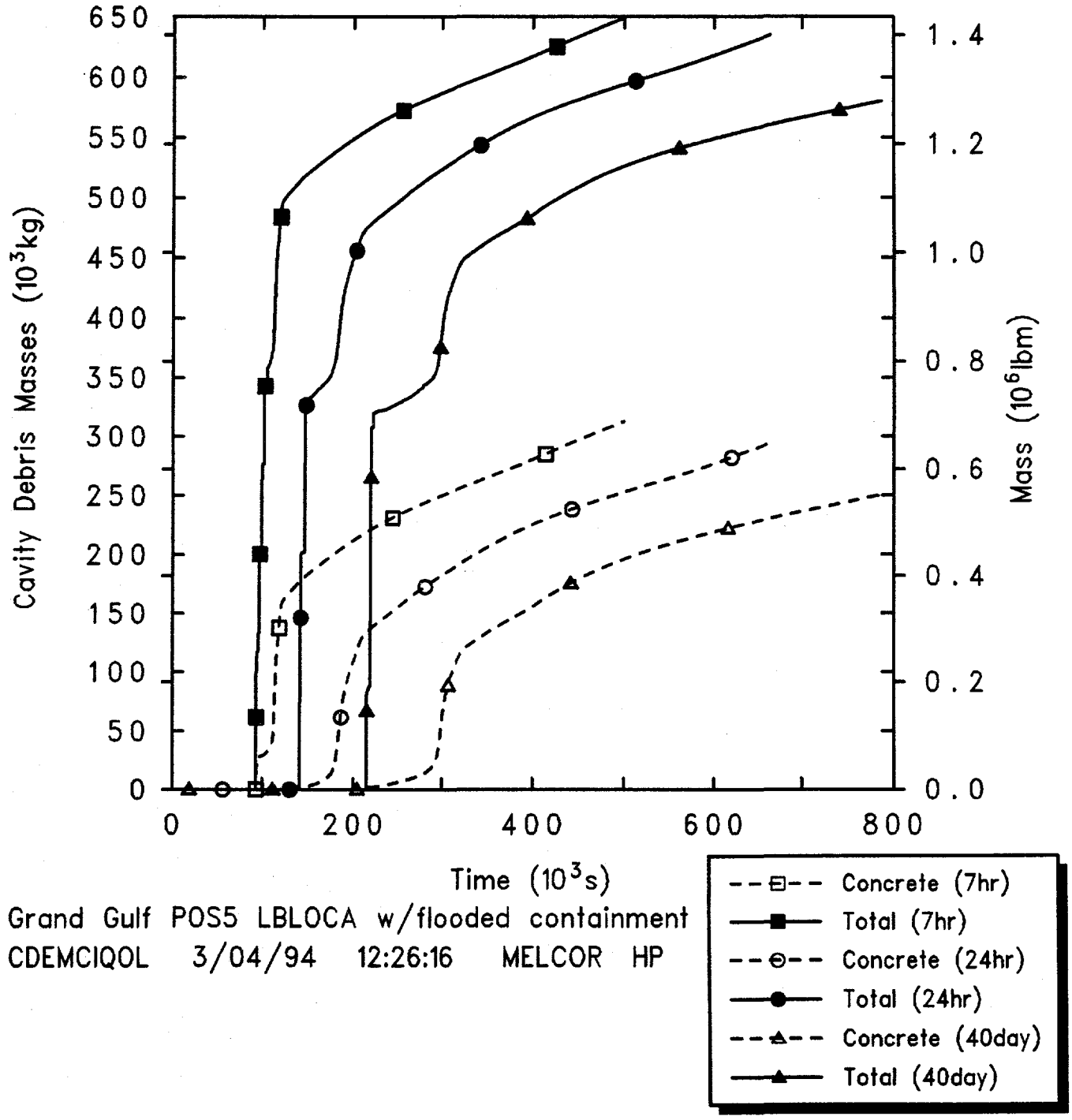

Figure 4.3.1.19. Cavity Total and Concrete Debris Masses for Grand Gulf POS 5 -- Large Break LOCA with Flooded Containment, Initiated at Various Times After Shutdown.

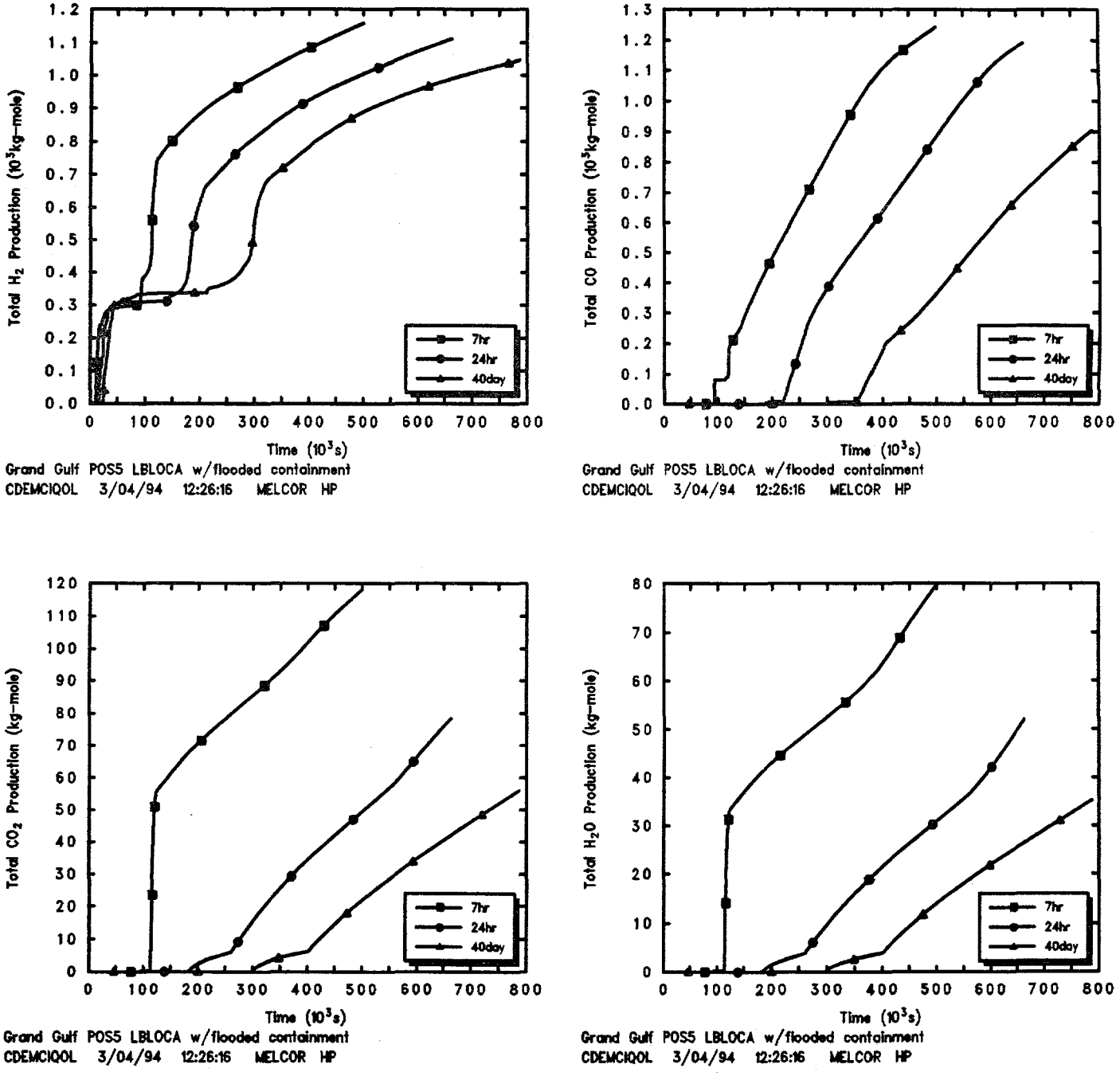

Figure 4.3.1.20. Hydrogen (upper left), Carbon Monoxide (upper right), Carbon Dioxide (lower left) and Steam (lower right) Generation for Grand Gulf POS 5 -- Large Break LOCA with Flooded Containment, Initiated at Various Times After Shutdown.

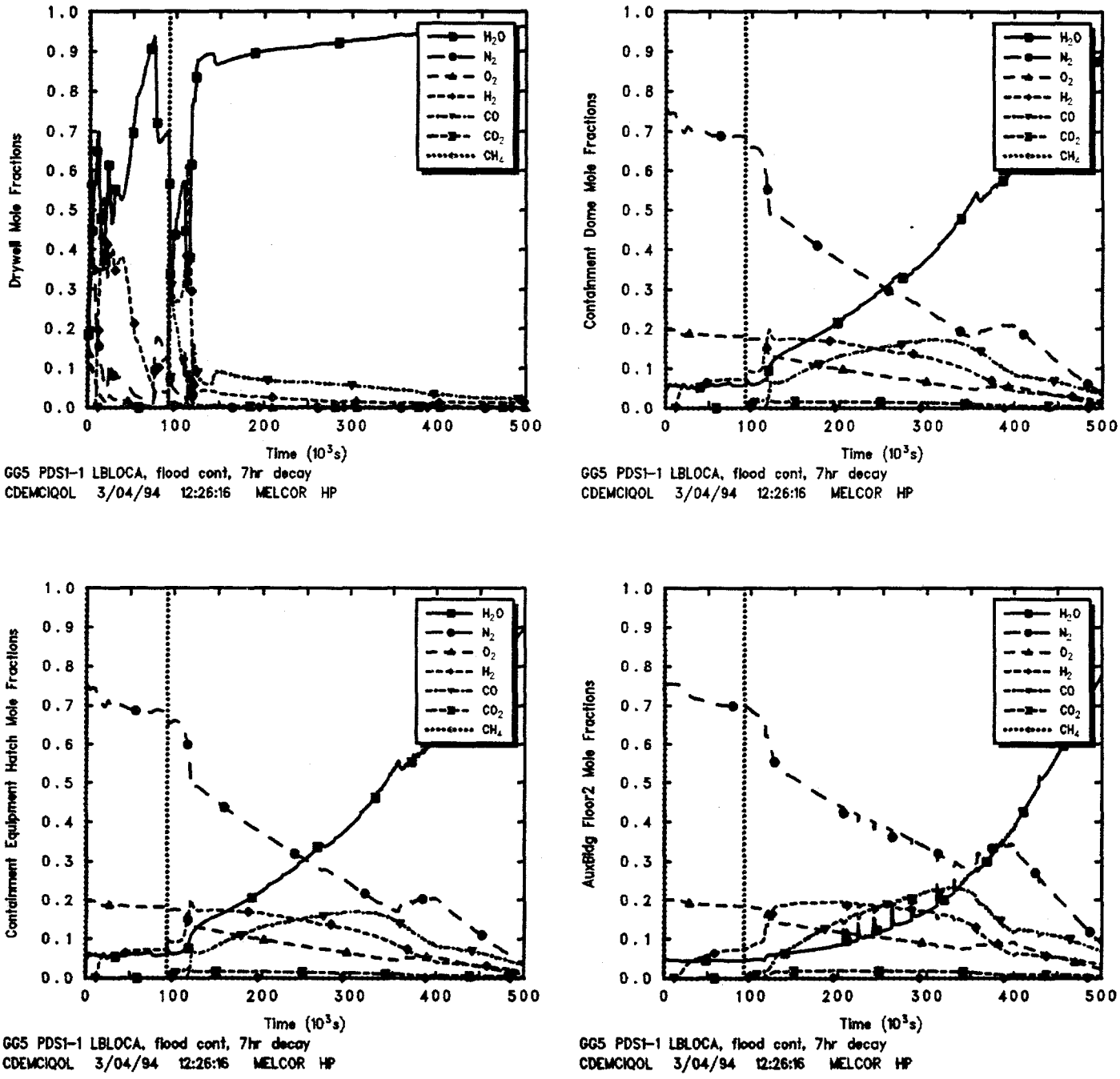

Figure 4.3.1.21. Mole Fractions in Drywell (upper left), Containment Dome (upper right), Containment Equipment Hatch (lower left) and Auxiliary Building (lower right) for Grand Gulf POS 5 -- Large Break LOCA with Flooded Containment, Initiated 7 hr After Shutdown.

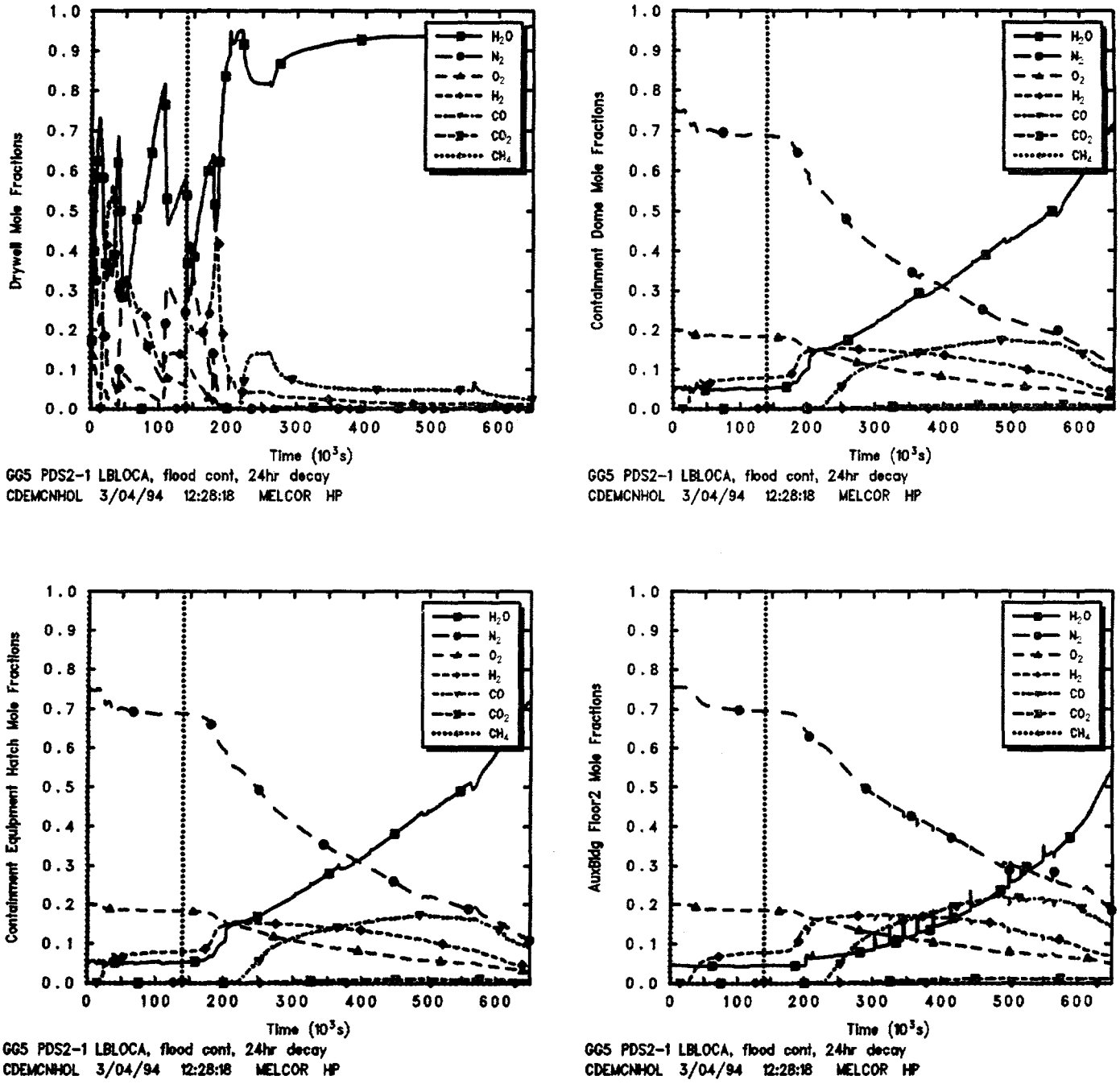

Figure 4.3.1.22. Mole Fractions in Drywell (upper left), Containment Dome (upper right), Containment Equipment Hatch (lower left) and Auxiliary Building (lower right) for Grand Gulf POS 5 -- Large Break LOCA with Flooded Containment, Initiated 24 hr After Shutdown.

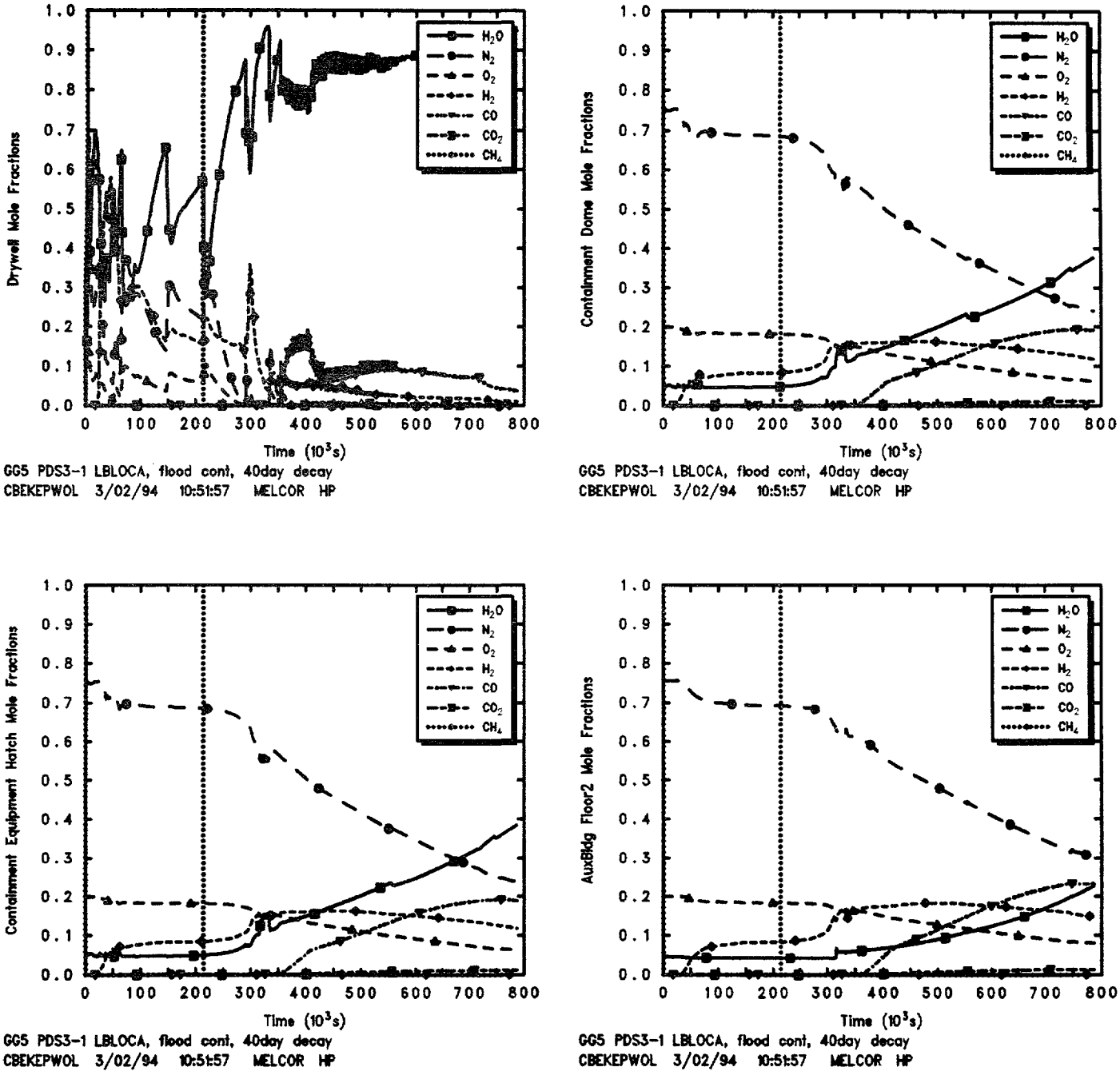

Figure 4.3.1.23. Mole Fractions in Drywell (upper left), Containment Dome (upper right), Containment Equipment Hatch (lower left) and Auxiliary Building (lower right) for Grand Gulf POS 5 -- Large Break LOCA with Flooded Containment, Initiated 40 days After Shutdown.

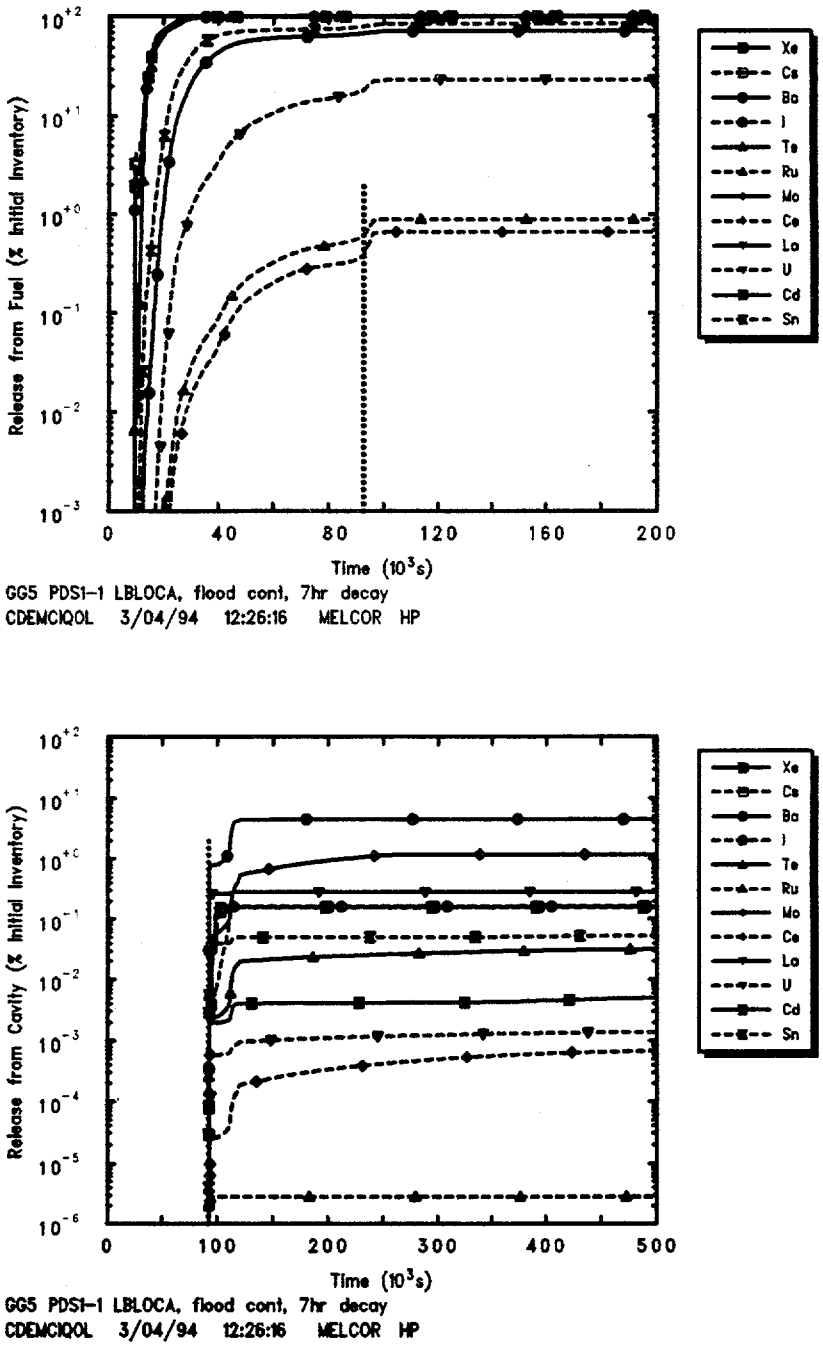

Figure 4.3.1.24. In-Vessel (top) and Ex-Vessel (bottom) Radionuclide Release Mass Fractions for Grand Gulf POS 5 -- Large Break LOCA with Flooded Containment, Initiated 7 hr After Shutdown.

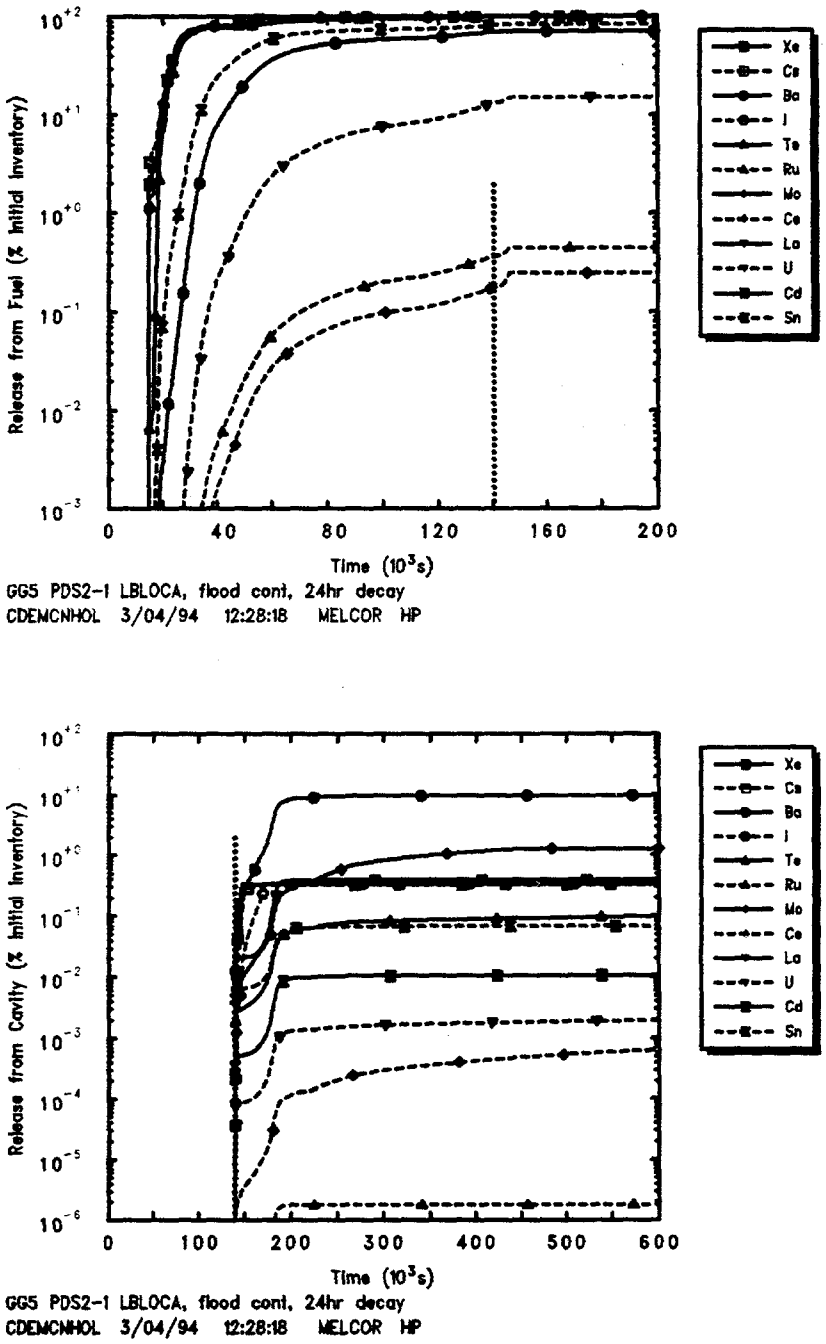

Figure 4.3.1.25. In-Vessel (top) and Ex-Vessel (bottom) Radionuclide Release Mass Fractions for Grand Gulf POS 5 -- Large Break LOCA with Flooded Containment, Initiated 24 hr After Shutdown.

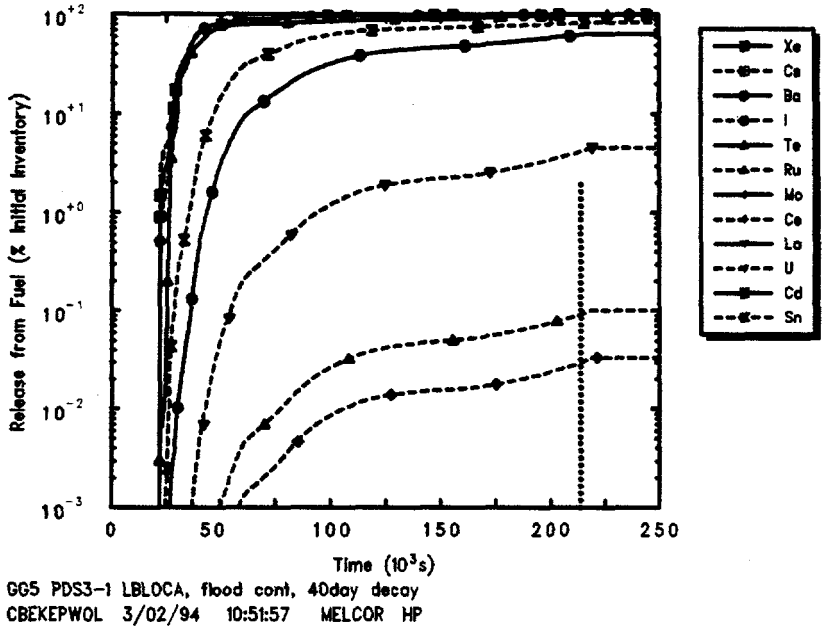

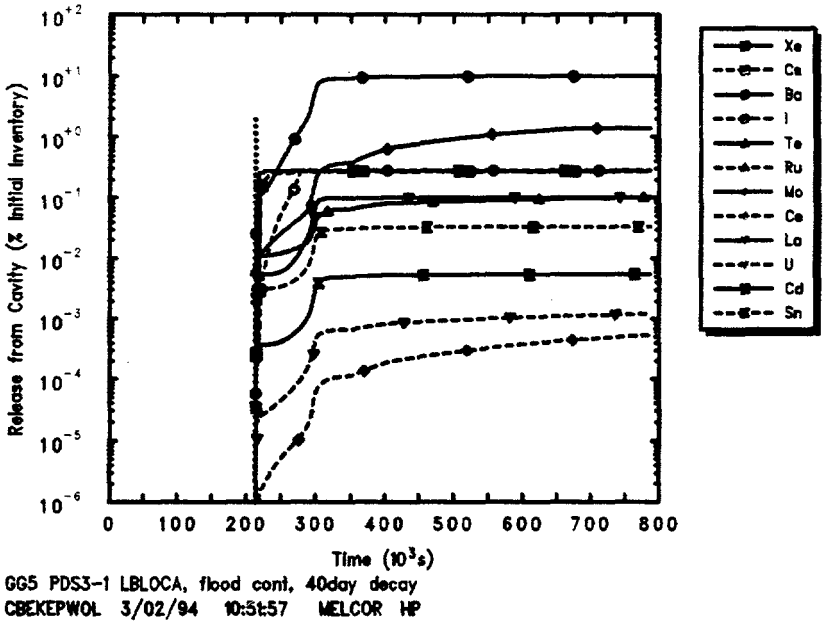

Figure 4.3.1.26. In-Vessel (top) and Ex-Vessel (bottom) Radionuclide Release Fractions for Grand Gulf POS 5 -- Large Break LOCA with Flooded Containment, Initiated 40 days After Shutdown.

Table 4.3.1.2. Final Radionuclide Release Fractions for Grand Gulf POS 5 -- Large Break LOCA with Flooded Containment, Initiated at Various Times After Shutdown

Class	Fission Products Released from Fuel (% Initial Inventory-Mass Fraction)								
	7 hr			24 hr			40 days		
	In-Vessel	Ex-Vessel	Total	In-Vessel	Ex-Vessel	Total	In-Vessel	Ex-Vessel	Total
Xe	99.81	0.16	99.96	99.61	0.33	99.94	99.7	0.28	99.97
Cs	99.75	0.15	99.91	99.6	0.32	99.92	99.74	0.26	100
Ba	71.54	4.47	76.02	70.51	9.59	80.1	63.66	9.74	73.4
I	99.77	0.16	99.93	99.59	0.34	99.93	99.71	0.28	99.99
Te	99.77	0.03	99.81	99.58	0.1	99.68	99.52	0.1	99.63
Ru	0.89	$3x10^{-6}$	0.89	0.44	$2x10^{-6}$	0.44	0.1	$3x10^{-7}$	0.1
Mo	0	1.15	1.15	0	1.23	1.23	0	1.35	1.35
Ce	0.67	0.0007	0.67	0.25	0.0007	0.25	0.03	0.0005	0.03
La	0	0.28	0.28	0	0.39	0.39	0	0.1	0.1
U	23.11	0.0014	23.11	14.92	0.0019	14.92	4.5	0.0012	4.51
Cd	0	0.005	0.005	0	0.011	0.011	0	0.006	0.006
Sn	84.7	0.05	84.75	83.05	0.068	83.12	82.81	3.29	86.1

amounts of each radionuclide class released, all normalized as mass fractions of the initial inventories of each class. (Note that these amounts generally consider only the release of radioactive forms of these classes, and not additional releases of nonradioactive aerosols from structural materials.)

The release behavior predicted by MELCOR can be grouped into several subdivisions. Almost all ~100% of the volatile Class 1 (noble gases), Class 2 (CsOH), Class 4 (I_2) and Class 5 (Te) radionuclide species are released, primarily in-vessel, as are most (~75-85%) of the Class 3 (Ba) and Class 12 (Sn) inventories. The next major release fraction, dropping rapidly with lower decay heat levels and cooler debris (as shown in Figures 4.3.1.9 through 4.3.1.11) is for uranium. Around 1% of the total inventories of Ru and Mo, Ce and La, are released. Finally, a total ≤0.01% of the initial inventory of Class 11 (Cd) is predicted to be released. Note that the CORSOR-M fission product release model option used in these analyses has identically zero release in-vessel of Class 7 (Mo), Class 9 (La) and Class 11 (Cd). These are higher release fractions of Ba, Te, Ru, Ce, La and Sn than seen in MELCOR analyses of severe accidents at full power operation in LWR plants [Kmetyk and Smith, 1994d; Kmetyk, 1994b; Carbajo, 1993], reflecting the higher debris temperatures calculated during in-vessel core degradation (shown in Figures 4.3.1.9 through 4.3.1.11).

Figure 4.3.1.27 gives the total radioactive release to the environment in these three cases. The releases are similar in magnitude for accidents begun at different times after shutdown, but shifted in time reflecting the slower accident progression at lower decay heat levels than at higher decay heat levels. These environmental releases do not correspond to immediate release of all radionuclides released from the fuel; there is considerable retention of most radionuclide species within the containment and auxiliary building (as discussed below). Only the noble gases and halogens (i.e., iodine) have substantial releases to the environment by the end of the transient periods simulated, because gaseous forms are not scrubbed, filtered, deposited or otherwise retained. There is a total of 484.63 kg of noble gases and halogens released from the fuel; the release to the environment is >90% of this by the end of the simulations begun at 7 hr and 24 hr after shutdown, and is about 75% of this when the calculation begun 40 days after shutdown was stopped. The temperatures are low enough in these shutdown sequences with flooded containment that the other volatile species released from the fuel (i.e., Cs and Te) are found mostly in aerosol form and are retained in the primary system, containment and auxiliary building.

Tables 4.3.1.3 through 4.3.1.5 summarize the mass fraction distribution of the initial radionuclide inventory at the end of the three calculations initiated at various times after shutdown; they provide an overview of how much of

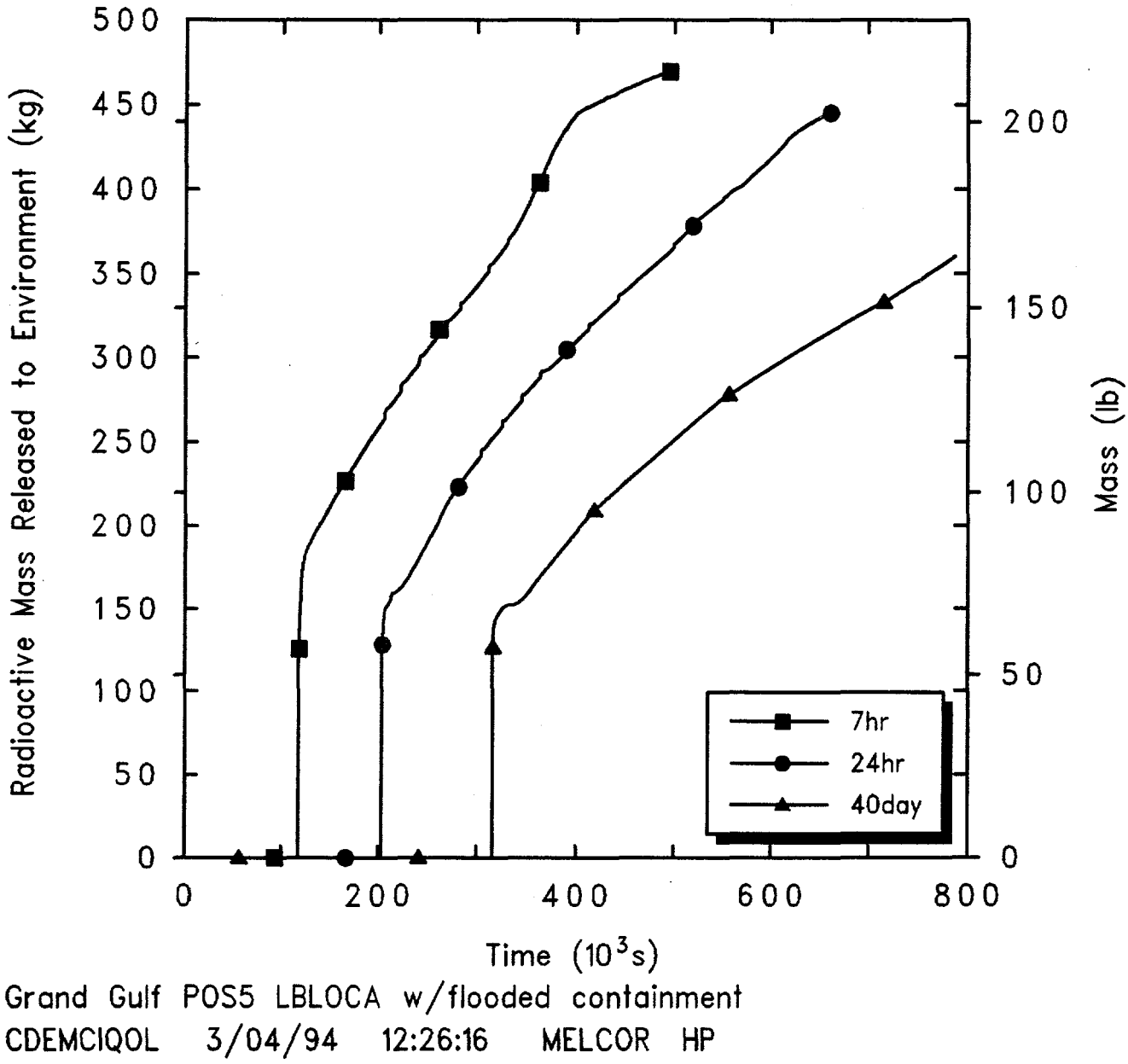

Figure 4.3.1.27. Total Environmental Radionuclide Releases for Grand Gulf POS 5 -- Large Break LOCA with Flooded Containment, Initiated at Various Times After Shutdown.

Table 4.3.1.3. Final Radionuclide Distribution for Grand Gulf POS 5 -- Large Break LOCA with Flooded Containment, Initiated 7 hr After Shutdown

Class	Fission Product Distribution (% Initial Inventory-Mass Fraction)				
	Fuel Debris	Primary System	Containment	Auxiliary Building	Environment
Xe	~0	~0	0.426	3.413	96.1
CsOH	~0	0.658	88.76	10.56	0.0044
Ba	24	39.1	35.22	1.6	0.0042
Te	0.137	0.657	89.07	10.25	0.0026
Ru	99.1	0.375	0.496	0.021	0.0002
Mo	98.9	0.001	1.063	0.077	0.006
Ce	99.3	0.242	0.406	0.016	0.0002
La	99.7	0.0008	0.272	0.007	0.00007
U	78.7	10.2	10.6	0.47	0.0033
Cd	~100	0.00002	0.004	0.0004	0.0001
Sn	15.3	39.3	43	2.43	0.004

Table 4.3.1.4. Final Radionuclide Distribution for Grand Gulf POS 5 -- Large Break LOCA with Flooded Containment, Initiated 24 hr After Shutdown

Class	Fission Product Distribution (% Initial Inventory - Mass Fraction)				
	Fuel Debris	Primary System	Containment	Auxiliary Building	Environment
Xe	~0	~0	1.8	6.46	91.7
CsOH	~0	1.17	85.36	13.2	0.14
Ba	19.9	45.4	31.68	3.06	0.0101
Te	0.292	1.07	85.31	13.18	0.19
Ru	99.6	0.237	0.191	0.016	0.00002
Mo	98.8	0.149	0.902	0.17	0.0103
Ce	99.8	0.119	0.117	0.01	0.00003
La	99.6	0.044	0.327	0.018	0.00009
U	86.3	7.79	5.59	0.383	0.00062
Cd	~100	0.0012	0.009	0.0007	0.00004
Sn	16.9	46.8	32.15	4.17	0.0015

the radionuclides remain bound up in fuel debris in either the core or the cavity, and of how much of the released radionuclides are retained in the primary system vs how much of the released radionuclides are released to, or released in, either the containment or the auxiliary building and the environment, all normalized to the initial inventories of each class. Table 4.3.1.6 presents a slightly different breakdown of the released radionuclide final distribution, giving the fractions of released inventory for each class in control volume atmospheres (including the environment), in pools, or deposited or settled onto heat structures at the end of the calculations. (As in Table

Table 4.3.1.5. Final Radionuclide Distribution for Grand Gulf POS 5 -- Large Break LOCA with Flooded Containment, Initiated 40 days After Shutdown

Class	Fission Product Distribution (% Initial Inventory-Mass Fraction)				
	Fuel Debris	Primary System	Containment	Auxiliary Building	Environment
Xe	~0	~0	9.29	16.41	74.3
CsOH	~0	0.881	92.76	6.4266	0.00065
Ba	26.6	38.6	34.06	0.75	0.0037
Te	0.358	0.745	92.9	6.03	0.0019
Ru	99.9	0.0584	0.0406	0.00073	3.5e-06
Mo	98.7	0.0003	1.34	0.008	0.00033
Ce	~100	0.018	0.014	0.00024	1.3e-06
La	99.9	0.00006	0.098	0.0005	0.00002
U	95.8	2.44	1.68	0.34	0.00014
Cd	~100	4.0e-07	0.0054	0.00005	1.8e-06
Sn	17.2	45.1	37.5	1.54	0.0006

4.3.1.2, these amounts consider only the release of radioactive forms of these classes, and not additional releases of nonradioactive aerosols from structural materials.)

These fission product distribution tables show that, of the radionuclides with significant (≥80% of initial inventory) release from fuel, most of the noble gases released are in the environment, in the atmosphere. While most of the volatile species (Cs and Te) releases occurred in-vessel, the largest part (about 90%) of those releases is retained in the containment, in water pools; most of the remaining volatiles release are retained in the auxiliary building, very small fractions of these volatiles are released to the environment for this large break LOCA scenario with flooded containment. (Only the low-pressure boiloff sequence discussed in Section 4.3.4 also with flooded containment, shows similarly high retention and small environmental releases of volatiles.) Two classes of radionuclides which are modelled as forming only aerosols (i.e., assumed to have zero vapor pressure) had substantial releases (also occurring mostly in-vessel); for those classes (Ba and Sn), about half the releases is retained in the vessel, primarily deposited on structures, while the other half of the releases is retained in the containment, mostly in water pools and a small fraction deposited on structure surfaces.

4.3.2 Station Blackout with Failure to Isolate SDC, Initiated 7 hr and 24 hr After Shutdown

At the initiation of the accident, the reactor vessel is depressurized and the coolant is at the normal level. The vessel water inventory is at 366.5 K (200°F), which corresponds to the maximum temperature allowed by the Grand Gulf technical specifications for operation in POS 5. The reactor pressure vessel head vent is open. At the start of the accident all core cooling and injection is lost and the SRVs are closed. Before the SRVs can cycle at their pressure relief setpoint, the break in the SDC line is opened when the vessel pressure reaches 3.135 MPa (440 psig). The SDC break runs from the vessel downcomer, 4.38 m above the bottom of the vessel to the first floor of the auxiliary building, 8.18 m below the bottom of the vessel. The suppression pool level is 3.86 m (12.67 ft) from the suppression pool floor. The containment is at 305.4 K (90°F) and the suppression pool is at 308.2 K (95°F). The drywell personnel lock is open; the containment equipment hatch and both of the containment personnel locks are open.

This sequence is identical to the Level 1 analysis of a station blackout with failure to isolate SDC discussed in Section 4.2.6 initiated at 7 hr and 24 hr after shutdown.

Table 4.3.1.6. Final Radionuclide State for Grand Gulf POS 5 -- Large Break LOCA with Flooded Containment, Initiated at Various Times After Shutdown

Class	Fission Products Released from Fuel (% Released Inventory-Mass Fraction)								
	7 hr			24 hr			40 days		
	Atmosphere	Pool	Deposited	Atmosphere	Pool	Deposited	Atmosphere	Pool	Deposited
Xe	~100	0	0	~100	0	0	~100	0	0
CsOH	0.004	84.6	15.3	0.15	74.65	25.23	0	79.48	20.52
Ba	0.006	40.9	59.1	0.013	29.24	70.74	0.005	39.03	60.97
I	~100	0	0	~100	0	0	~100	0	0
Te	0.003	84	16	0.005	74.67	25.75	0.086	78.73	21.27
Ru	0.02	49.14	50.86	0.005	31.69	68.33	0.00034	32.34	67.66
Mo	0.5	97.96	1.49	0.84	52	47.17	0.025	99.89	0.089
Ce	0.03	55.33	44.65	0.018	35.35	64.63	0.0001	34.78	65.26
La	0.03	97.3	2.64	0.025	56.13	43.87	0.0015	99.86	0.13
U	0.02	42.9	57.1	0.005	29.14	70.74	0.0034	31.77	68.1
Cd	3.6	93.98	2.42	1.1	55.28	43.65	0.033	99.75	0.21
Sn	0.005	45.48	54.52	0.002	31.9	68.09	0.00074	36.23	63.76

The sequence of events predicted by MELCOR for this accident with different initiation times is given in Table 4.3.2.1.

Figure 4.3.2.1 gives the vessel pressures calculated for this same accident scenario initiated at two different times after shutdown. In both cases, the primary system pressure rises to the SDC failure pressure at 3.135 MPa (440 psig), which actuates the postulated SDC break. The flow out the SDC line break goes directly to the auxiliary building first floor and pressurizes the auxiliary building, as indicated in Figure 4.3.2.2. As expected, the lower the decay heat the slower the auxiliary building pressurizes and the longer it takes to fail the auxiliary building. The open personnel locks and equipment hatch keep the containment equilibrated to the auxiliary building in this sequence.

The coolant inventory in the vessel drops as the decay heat boils water to steam which is lost out the SDC break and the open RPV vent, faster for higher decay heat levels, as presented in Figure 4.3.2.3. The opening of the SDC break is reflected in the extremely rapid loss of about 75% of the vessel inventory seen at various times; that inventory loss then slows down when the break uncovers, and is followed by a more gradual loss of the remaining inventory due to boiling and steam outflow until vessel failure. The amount of liquid inventory lost in the initial liquid blowdown is determined by the elevation of the break and is therefore about the same regardless of the decay heat level; later, as would be expected, the gradual inventory loss due to continued boiloff is faster for higher decay heat levels than for lower decay heat levels. The vessel inventory then drops to zero very quickly upon vessel failure.

Figure 4.3.2.4 presents the upper plenum, core and lower plenum swollen and collapsed liquid levels for this accident sequence initiated at two different times after shutdown. The upper plenum level initially rises as the primary system pressurizes and then falls rapidly when the SDC break is opened. The vessel liquid level drops smoothly through the upper plenum into the core and continues dropping smoothly partway into the lower plenum, followed by a more gradual loss of the remaining inventory due to boiling and steam outflow. The amount of liquid inventory lost in the blowdown out the SDC break is determined by the elevation of the break and is therefore about the same regardless of the decay heat level; later, as would be expected, the gradual core uncovery due to continued boiloff is faster for higher decay heat levels than for lower decay heat levels. There is very little pool frothing or swelling in any of the vessel volumes.

The heatup of the intact fuel and clad is illustrated in Figures 4.3.2.5 and 4.3.2.6 as calculated for scenarios initiated at 7 hr and 24 hr after shutdown, respectively. Core uncovery and heatup begins sooner and proceeds more rapidly at the higher decay heat level resulting from beginning this accident 7 hr after shutdown than for a lower decay heat in the same accident initiated 24 hr after shutdown. The fuel/clad component temperatures in MELCOR are set to zero in a cell when that component fails, so these figures show both the overall heatup rate and the time that the intact fuel/clad component fails through melting of the clad.

Figures 4.3.2.7 and 4.3.2.8 present corresponding core debris temperatures in the active fuel region calculated for scenarios initiated at 7 hr and 24 hr after shutdown, respectively; these are the temperatures of the debris bed formed by the failure of the intact fuel/clad component in MELCOR in a core cell, whose (intact) temperatures were given in Figures 4.3.2.5 and 4.3.2.6. The intact fuel/clad component temperatures reach a peak above 2000 K (3140°F) since the component generally fails at the zircaloy clad melt temperature, taken as 2098 K (3317°F) in MELCOR. The debris bed in the active fuel region in contrast reaches peak temperatures over 4250 K (7190°F), significantly above the UO_2 melt temperature of 3113 K (5144°F), except in the lowermost active fuel level where the debris bed temperature remains near the UO_2 melt temperature. The debris bed temperatures reached in the active fuel region are slightly higher for the accident initiated at a higher decay heat level than at the lower decay heat level, as would be expected. (Notice that the debris bed temperatures predicted in these station blackout sequences with failure to isolate SDC are substantially higher than those predicted in the large break LOCA analyses presented in the previous section.)

The temperatures of the active fuel region debris bed drop to zero when the core plate fails and the debris relocates to the lower plenum. This occurs much later than the collapse of the intact fuel and clad into a debris bed. An unexpected result in these station blackout sequences with failure to isolate SDC is the failure of the core plate (and subsequently the vessel) earlier in the case initiated 24 hr after shutdown than in the case initiated 7 hr after shutdown.

Figures 4.3.2.9 and 4.3.2.10 depict the structure temperatures for the core support plate ("level 5") and for

Table 4.3.2.1. Sequence of Events Predicted by MELCOR for Station Blackout with Failure to Isolate SDC, Initiated 7 hr and 24 hr After Shutdown

Event	Time After Shutdown 7 hr	24 hr
Accident initiation	0	0
Core uncovery (TAF) begins	13,375 s (3.72 hr)	19,717 s (5.48 hr)
Core heatup begins	13,500 s (3.75 hr)	20,000 s (5.56 hr)
SDC break at 440 psig	13,750 s (3.82 hr)	20,250 s (5.63 hr)
Auxiliary building failed	13,750 s (3.82 hr)	20,250 s (5.63 hr)
Clad failure/Gap release		
(Ring 1)	15,714 s (4.36 hr)	22,876 s (6.35 hr)
(Ring 2)	15,670 s (4.35 hr)	22,817 s (6.34 hr)
(Ring 3)	15,708 s (4.36 hr)	22,869 s (6.35 hr)
(Ring 4)	15,941 s (4.43 hr)	23,180 s (6.44 hr)
(Ring 5)	16,959 s (4.71 hr)	24,520 s (6.81 hr)
(Ring 6)	19,279 s (5.36 hr)	27,389 s (7.61 hr)
Core plate failed		
(Ring 1)	55,519 s (15.42 hr)	56,345 s (15.65 hr)
(Ring 2)	55,477 s (15.41 hr)	44,848 s (12.46 hr)
(Ring 3)	55,399 s (15.39 hr)	55,630 s (15.45 hr)
(Ring 4)	56,138 s (15.59 hr)	55,875 s (15.52 hr)
(Ring 5)	54,003 s (15.00 hr)	58,377 s (16.22 hr)
(Ring 6)	52,994 s (14.72 hr)	59,495 s (16.53 hr)
Vessel LH penetration failed		
(Ring 1)	53,123 s (14.76 hr)	44,930 s (12.48 hr)
(Ring 2)	53,105 s (14.75 hr)	44,941 s (12.48 hr)
(Ring 3)	53,079 s (14.74 hr)	44,931 s (12.48 hr)
(Ring 4)	53,074 s (14.74 hr)	44,934 s (12.48 hr)
(Ring 5)	53,074 s (14.74 hr)	44,938 s (12.48 hr)
(Ring 6)	53,139 s (14.76 hr)	44,939 s (12.48 hr)
Commence debris ejection	53,074 s (14.74 hr)	44,930 s (12.48 hr)
Cavity rupture	218,431 s (60.68 hr)	
End of calculation	218,431 s (60.68 hr)	200,000 s (55.56 hr)

the lower core support structure in the level just above the core support plate and below the first active fuel level ("level 6", with active fuel beginning in "level 7"). The core support plate is assumed to fail at 1273 K (1832°F), a criterion also shown in these figures. The support structure above the core plate reaches this temperature at about the time the debris bed forms in the active fuel region, but the temperature of the support structure above the core plate then remains nearly constant and increases only gradually as the temperature of the debris bed in the active fuel region reaches values of 3100-4200 K; this growing temperature gradient is probably due to the neglect of axial conduction in the particulate debris component in the MELCOR COR package. The core support plate itself remains substantially cooler than the support structure above the core plate, increasing only slowly. In the calculation initiated 7 hr after shutdown, the core support plate temperatures in all radial rings remain nearly equal as the core plate is heated, while in the calculation initiated 24 hr after shutdown, the lower

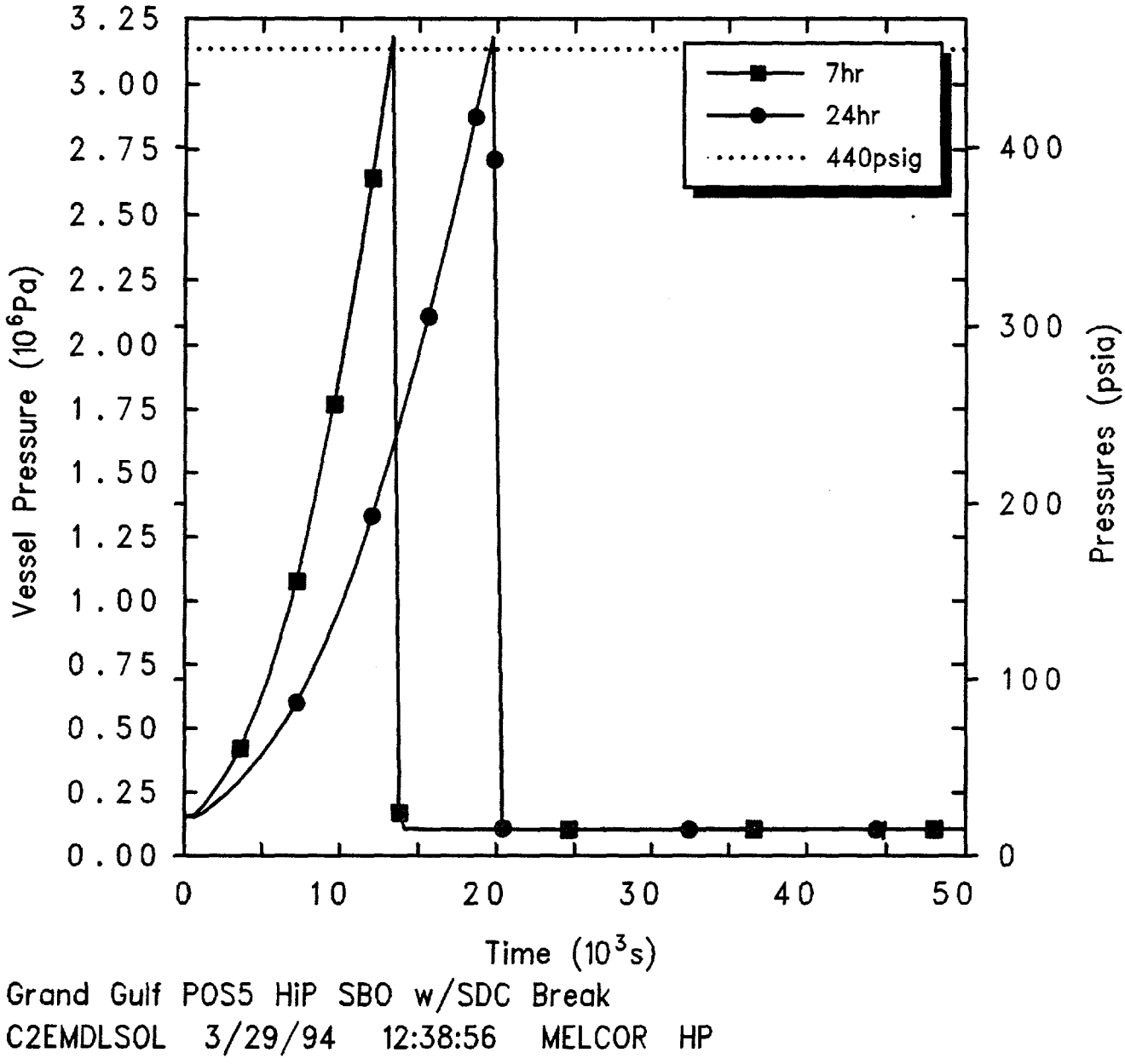

Figure 4.3.2.1. Reactor Vessel Pressures for Grand Gulf POS 5 -- Station Blackout with Failure to Isolate SDC, Initiated at Various Times After Shutdown.

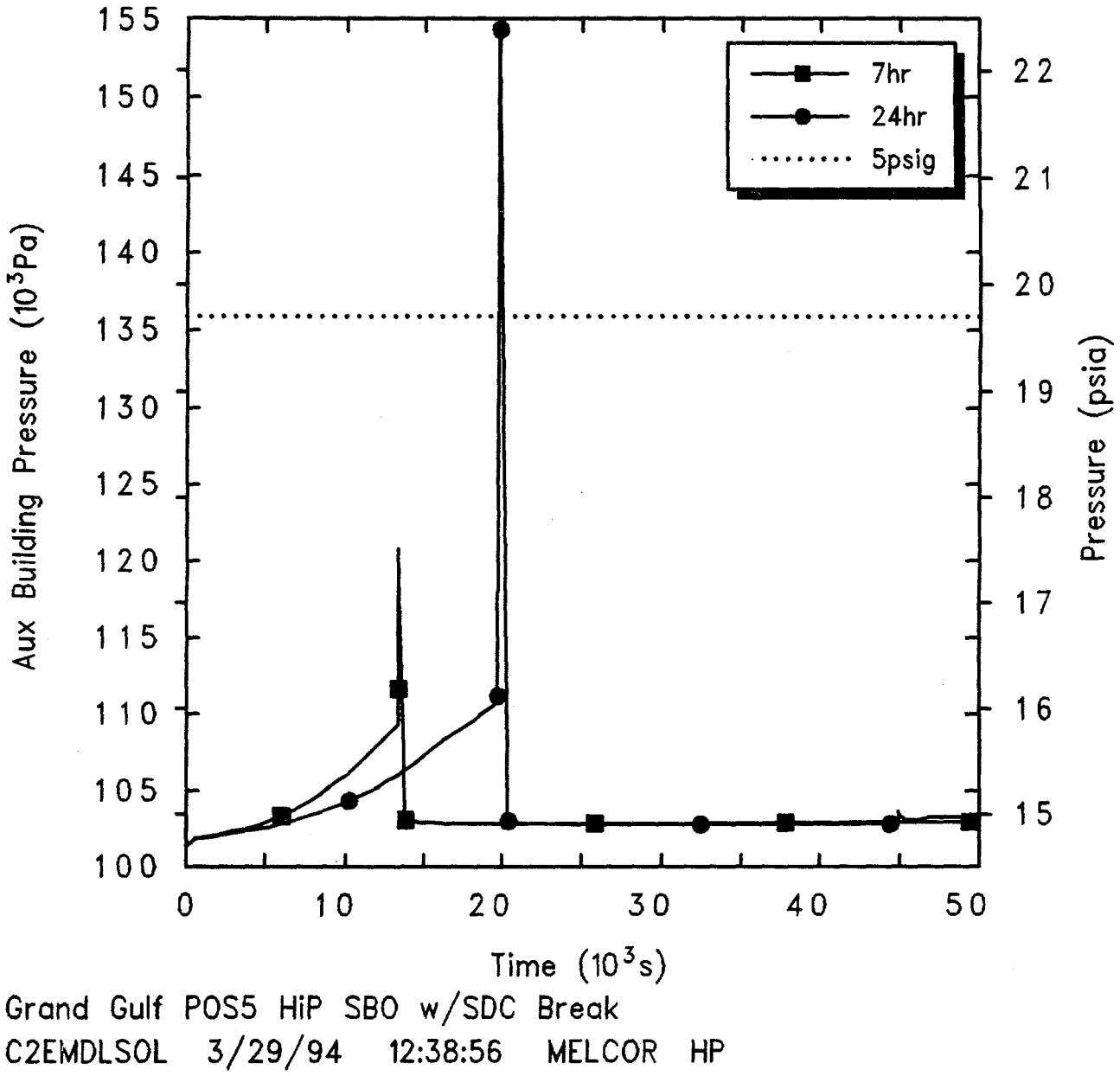

Figure 4.3.2.2. Auxiliary Building Pressures for Grand Gulf POS 5 -- Station Blackout with Failure to Isolate SDC, Initiated at Various Times After Shutdown.

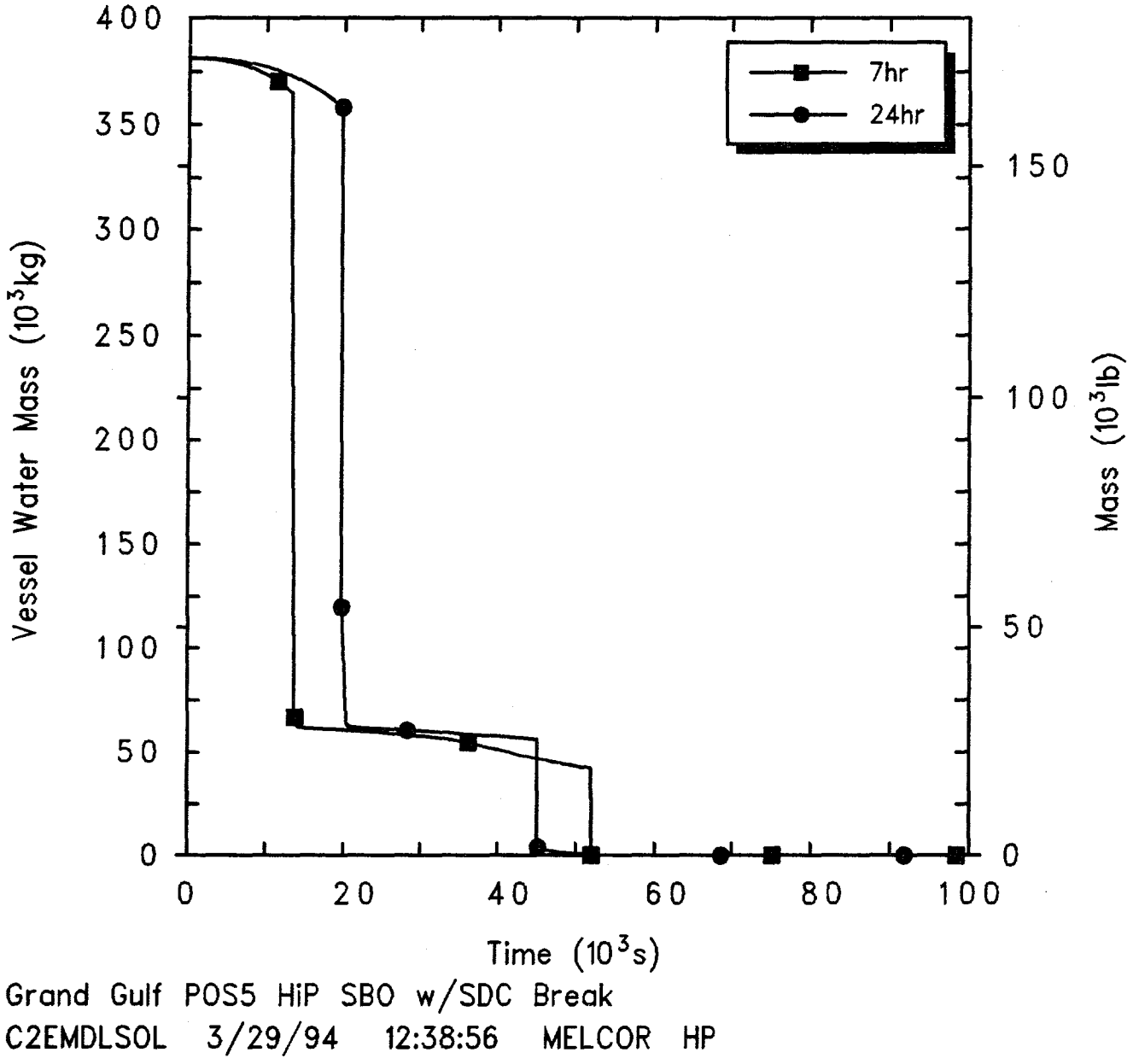

Figure 4.3.2.3. Reactor Vessel Water Masses for Grand Gulf POS 5 -- Station Blackout with Failure to Isolate SDC, Initiated at Various Times After Shutdown.

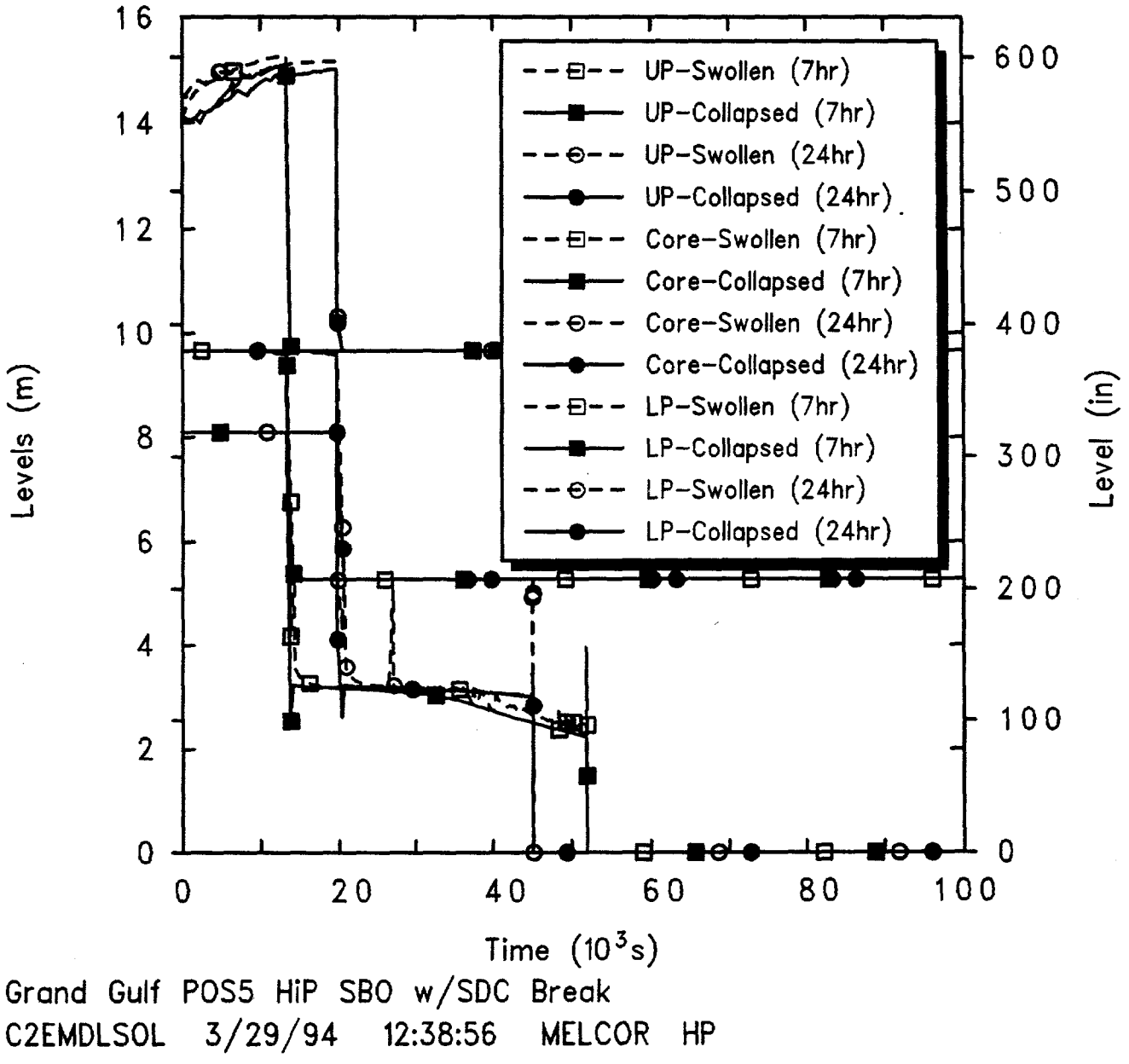

Figure 4.3.2.4. Upper Plenum, Core and Lower Plenum Liquid Levels for Grand Gulf POS 5 -- Station Blackout with Failure to Isolate SDC, Initiated at Various Times After Shutdown.

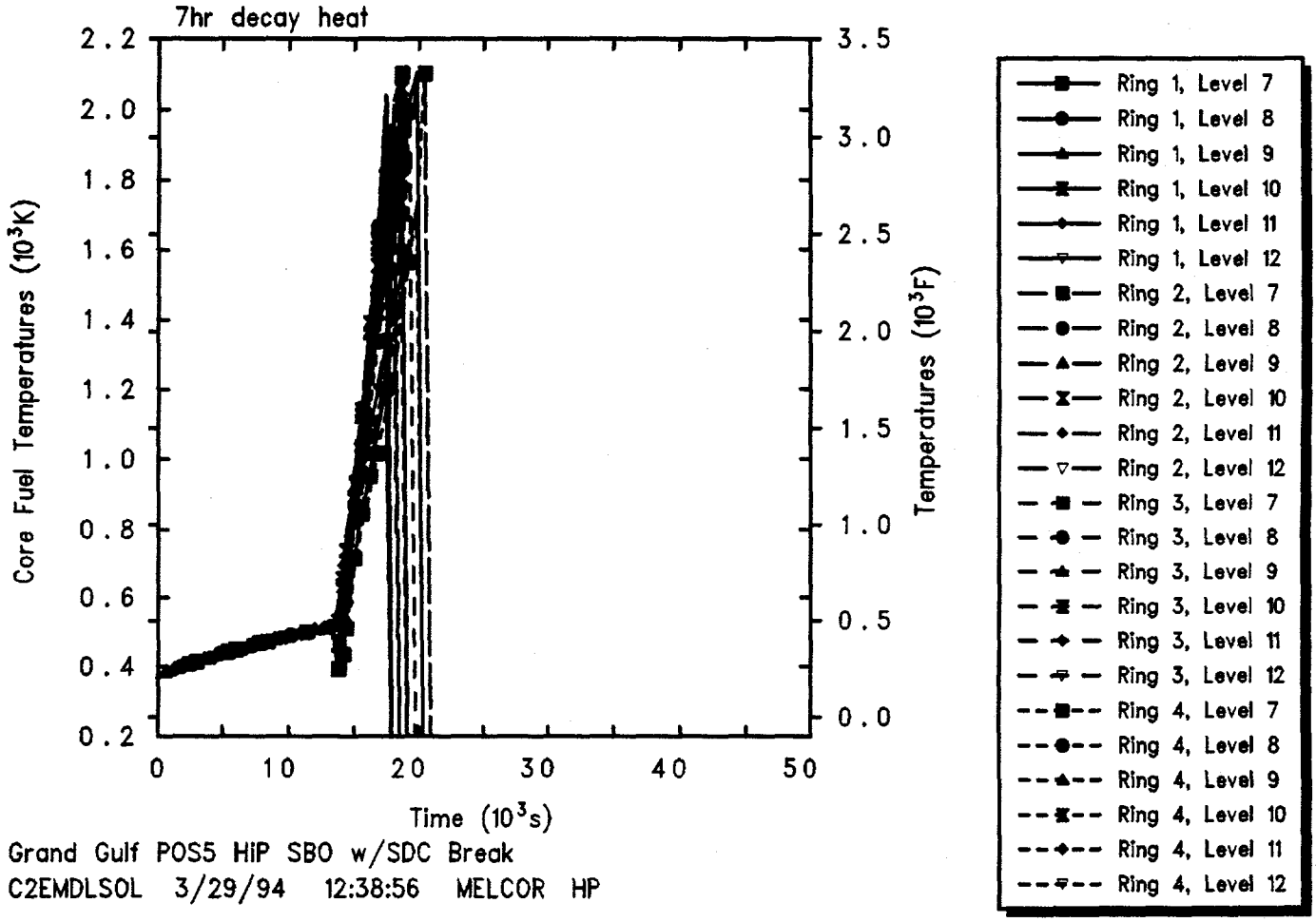

Figure 4.3.2.5. Core Intact Fuel/Clad Temperatures for Grand Gulf POS 5 -- Station Blackout with Failure to Isolate SDC, Initiated 7 hr After Shutdown.

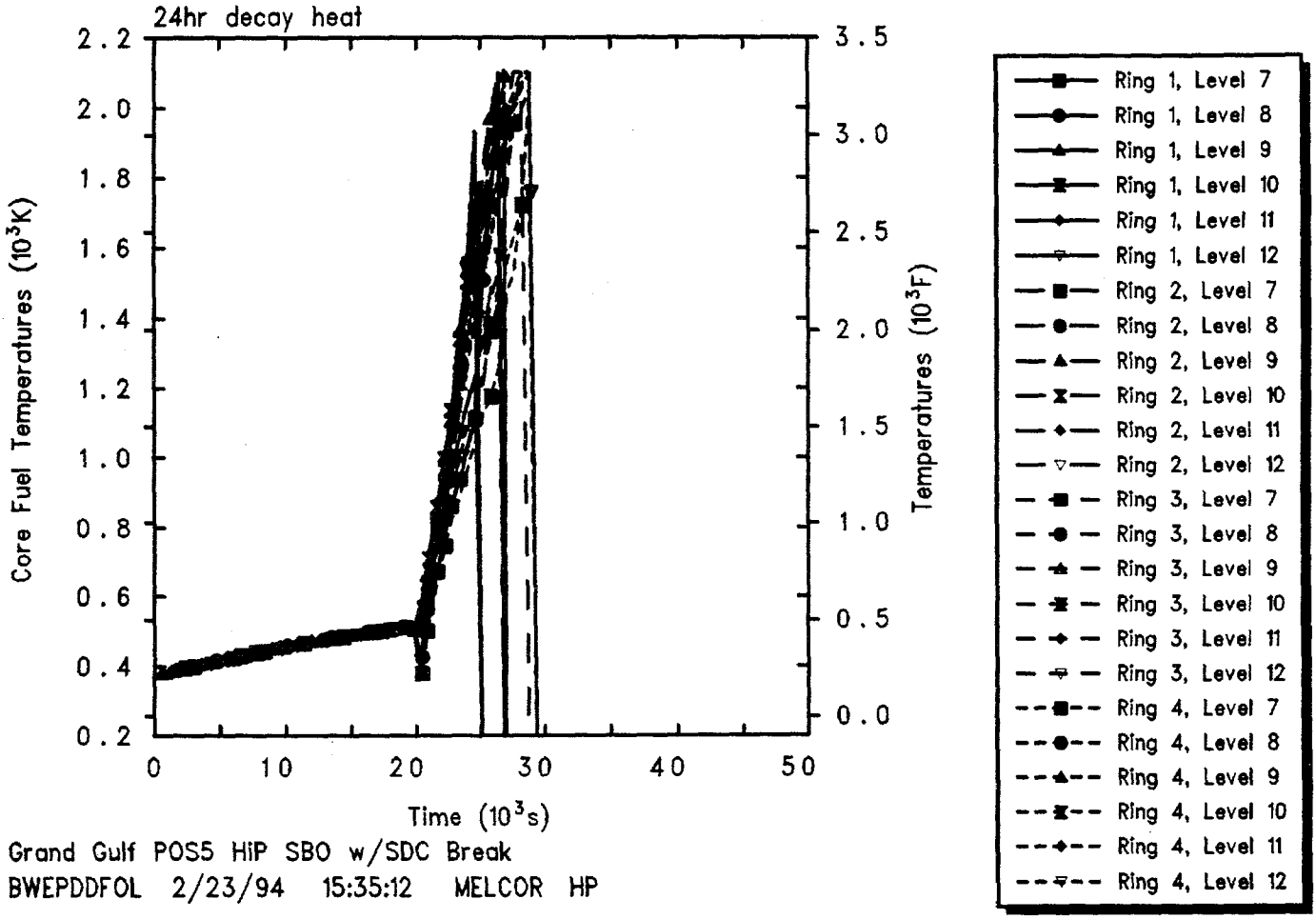

Figure 4.3.2.6. Core Intact Fuel/Clad Temperatures for Grand Gulf POS 5 -- Station Blackout with Failure to Isolate SDC, Initiated 24 hr After Shutdown.

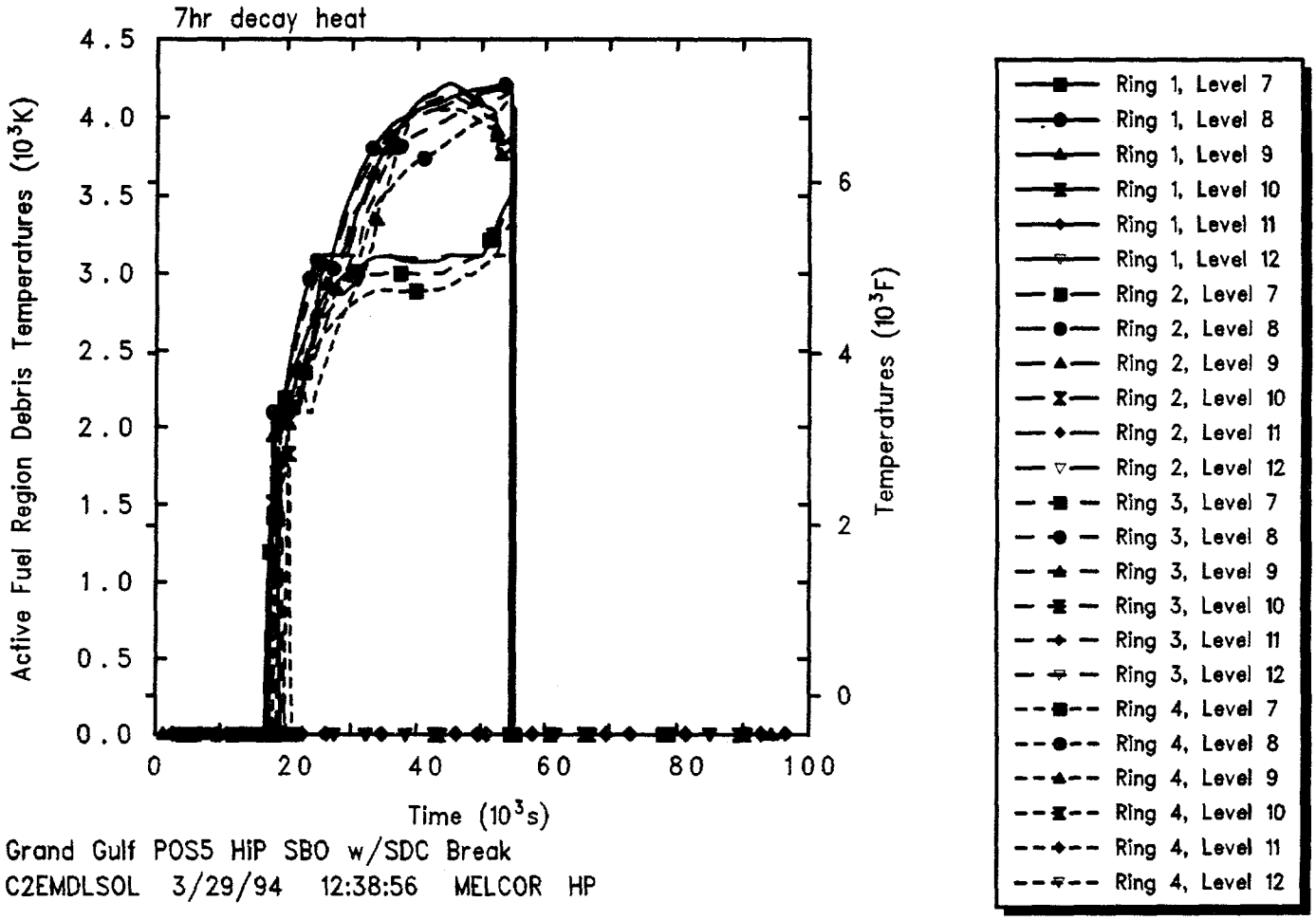

Figure 4.3.2.7. Core Active Fuel Region Debris Bed Temperatures for Grand Gulf POS 5 -- Station Blackout with Failure to Isolate SDC, Initiated 7 hr After Shutdown.

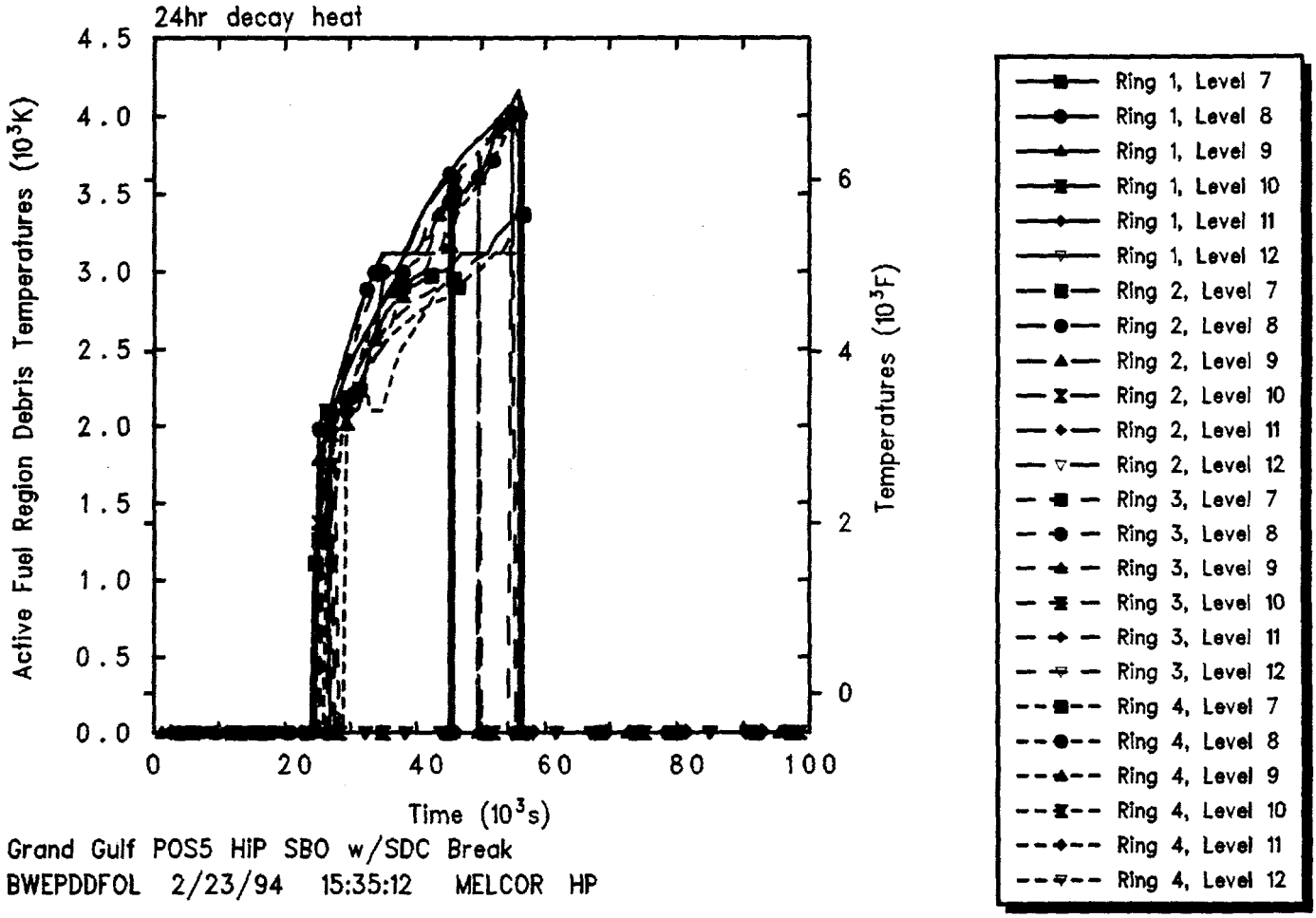

Figure 4.3.2.8. Core Active Fuel Region Debris Bed Temperatures for Grand Gulf POS 5 -- Station Blackout with Failure to Isolate SDC, Initiated 24 hr After Shutdown.

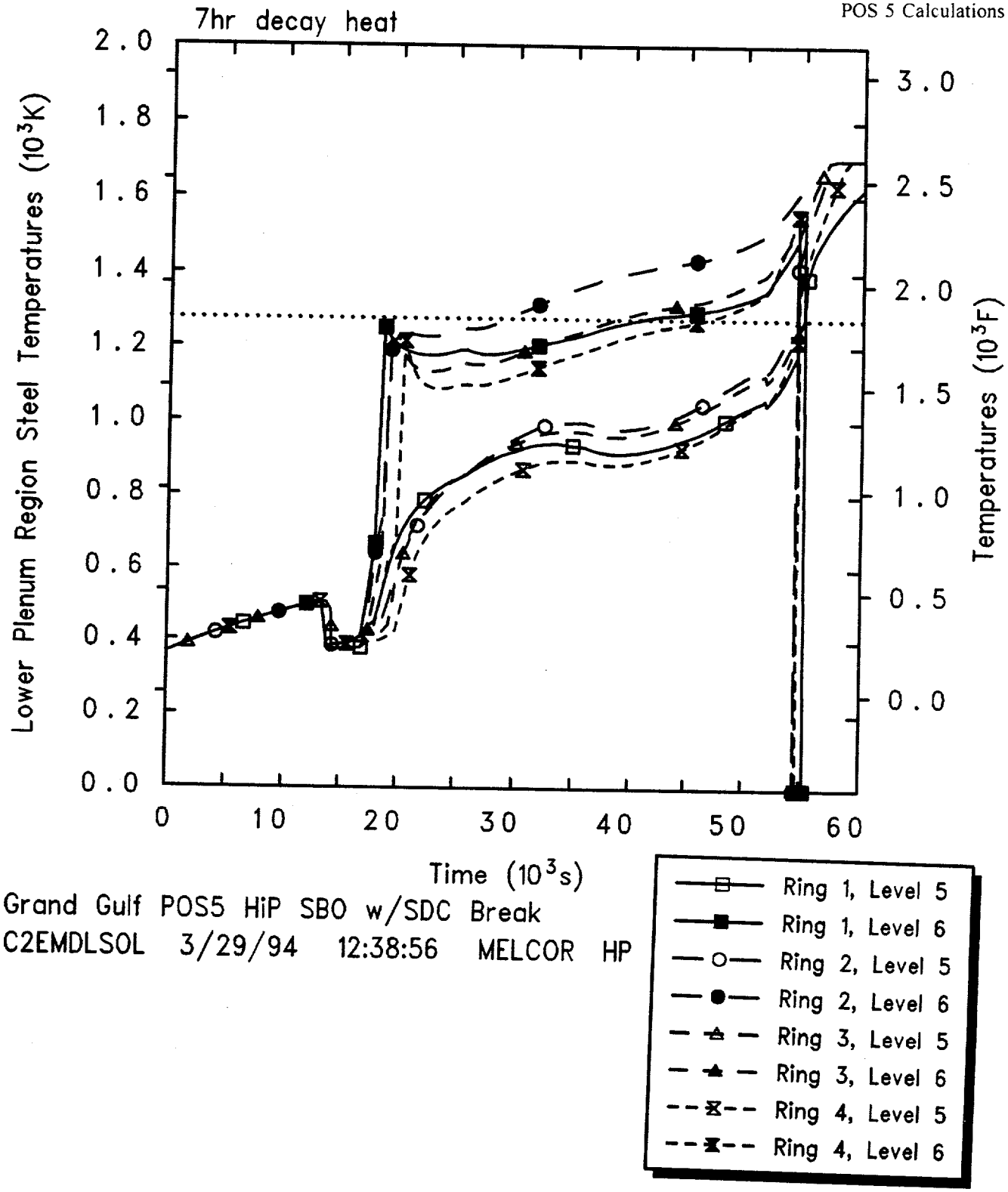

Figure 4.3.2.9. Core Support Plate and Lower Core Support Structure Temperatures for Grand Gulf POS 5 -- Station Blackout with Failure to Isolate SDC, Initiated 7 hr After Shutdown.

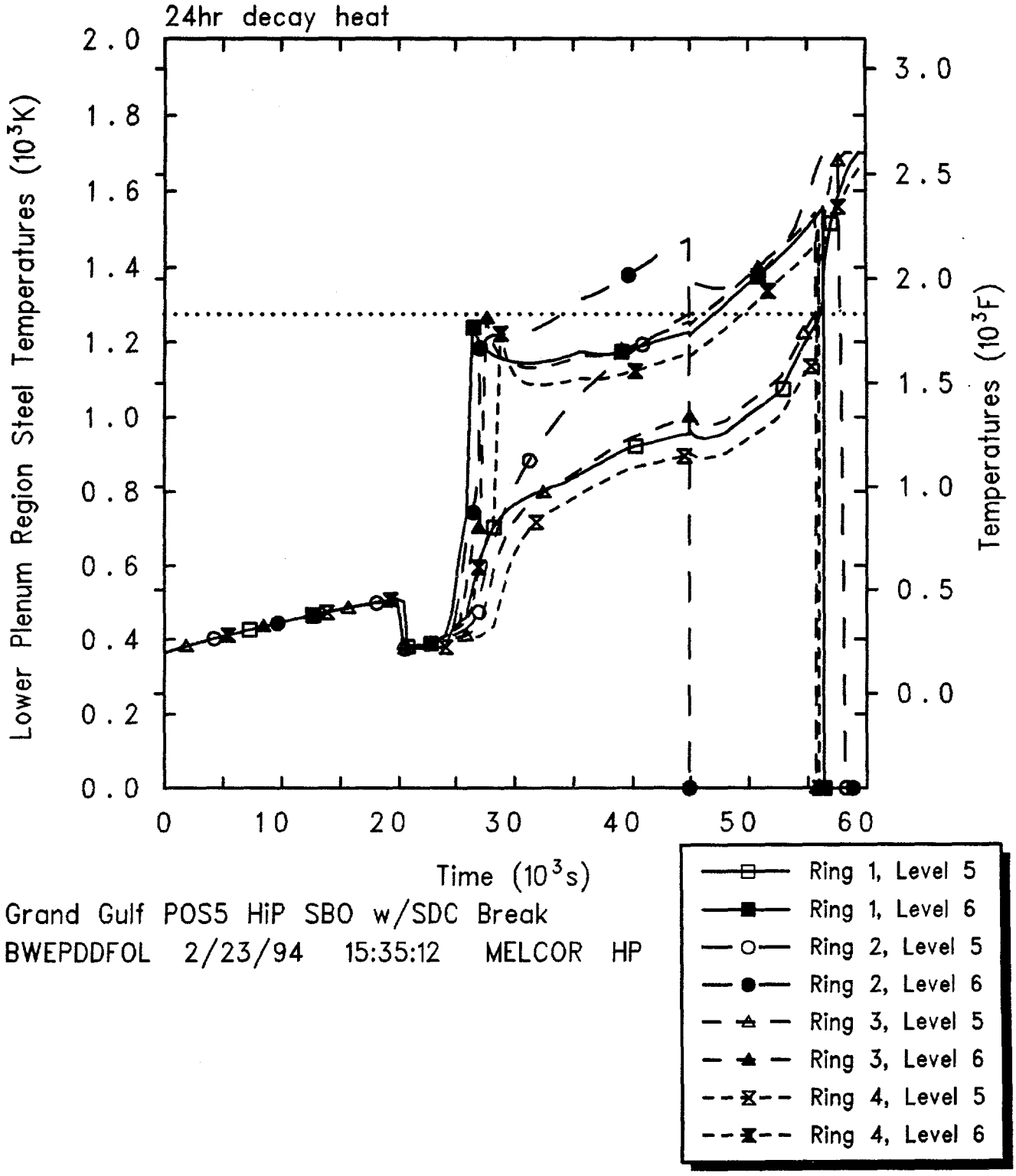

Figure 4.3.2.10. Core Support Plate and Lower Core Support Structure Temperatures for Grand Gulf POS 5 -- Station Blackout with Failure to Isolate SDC, Initiated 24 hr After Shutdown.

core support structure and the core support plate temperatures in the second ring increase much more quickly than for the other three rings. On physical grounds, given most of the active fuel material forming a relatively uniform debris bed, the core plate temperatures in the various radial rings should remain nearly equal; if this had happened in the calculation initiated at 24 hr after shutdown, Figure 4.3.2.10 indicates that the core plate should have failed at ~56,000 s, later than in the calculation initiated 7 hr after shutdown.

The predicted temperatures in the debris bed in the lower plenum and core plate are given in Figures 4.3.2.11 and 4.3.2.12 for scenarios initiated at 7 hr and 24 hr after shutdown, respectively. In both cases, prior to core plate failure there is some cold, refrozen debris both on the core support plate and on the lower core structural material just above the core support plate; the cooling and refreezing of this debris is the cause of the continued gradual drop in lower plenum liquid level due to steaming seen in Figure 4.3.2.4. The debris temperature rises gradually to the core support plate failure temperature of 1273 K (1832°F). After core plate failure hot, high-temperature debris begins appearing in the lower plenum as debris falls from the active fuel region into the lower plenum. With the new debris radial relocation model added in MELCOR 1.8.2, the core plate needs to fail in only one ring before debris from cells in the active fuel region in all radial rings can potentially flow sideways and down, fall through the failed plate, and then spread sideways into cells in the lower plenum in all radial rings. (Thus a lower head penetration can now fail in a ring before the core plate in that ring fails.) The lower head penetrations begin failing almost immediately, and the lower plenum debris temperatures begin dropping to zero as debris is ejected from the vessel to the cavity. (Notice that the calculation initiated 24 hr after shutdown shows some quenched debris fallen into the lower plenum in the second ring prior to core plate failure, not seen in the other rings or in any ring in the calculation initiated 7 hr after shutdown; this is probably related to the anomalous core plate heatup and failure behavior discussed above.)

Figures 4.3.2.13 and 4.3.2.14 indicate what fraction of each material in the active fuel region has collapsed into a debris rubble bed held up by the core support plate, prior to core plate failure, debris relocation, lower head failure and debris ejection, for this station blackout scenario with failure to isolate SDC initiated at 7 hr and 24 hr after shutdown, respectively. The fractions of each material and the overall fraction of total material in the active fuel region degraded into particulate debris and are similar in the two calculations. The majority of the debris bed is formed within about 8,000 s at the higher decay heat level and within about 9,000 s at the lower decay heat level.

Figure 4.3.2.15 shows the total masses of core materials (UO_2, zircaloy and ZrO_2, stainless steel and steel oxide, and control rod poison) remaining in the vessel. This includes both material in the active fuel region and in the lower plenum. Debris ejection began very soon after lower head failure. This figure illustrates that most of the core material was lost from the vessel to the cavity quickly, in step-like stages. In all cases, all of the UO_2 was transferred to the cavity within ~1 hr after vessel failure, as was the unoxidized zircaloy, the associated zirconium oxide and the control rod poison. A small fraction (1-5%) of the structural steel in the lower plenum, and some associated steel oxide, was predicted to remain unmelted and in place.

The debris material lost from the vessel is ejected to the drywell pedestal cavity. Since almost all the material in the core active fuel region and lower plenum is lost within a very short time period after vessel failure, the core debris mass in the cavity is about the same for these two calculations initiated at different times after shutdown. Figure 4.3.2.16 indicates that the amount of concrete ablated and the total cavity debris mass (i.e., core debris combined with concrete ablation products) are also very similar for this sequence initiated at different times after shutdown. In both cases, concrete ablation is quite rapid soon after debris ejection (while the core debris is hot, >2000 K, and consists of a layer of metallic debris above a heavy oxide layer), and concrete ablation slows significantly after a short time (after enough concrete has been ablated for the debris bed configuration to invert to a light oxide layer above a layer of metallic debris, mixed to a lower average temperature of ~1500 K).

The calculated production of steam and noncondensable gases (H_2, CO, CO_2 and H_2O) is summarized in Figure 4.3.2.17. The hydrogen production shown includes both in-vessel production (the initial step increase) and ex-vessel production in the cavity (the later-time increase). The in-vessel hydrogen generation corresponds to the oxidation of about 10-20% of the zircaloy and about 1% of the steel in the core and lower plenum, prior to vessel failure and debris ejection. As soon as the core debris enters the cavity, core-concrete interaction begins, resulting in the production of carbon dioxide and hydrogen; reduction of these gases by the molten metal in the core debris also gives rise to carbon monoxide and hydrogen. The production rate of noncondensables from

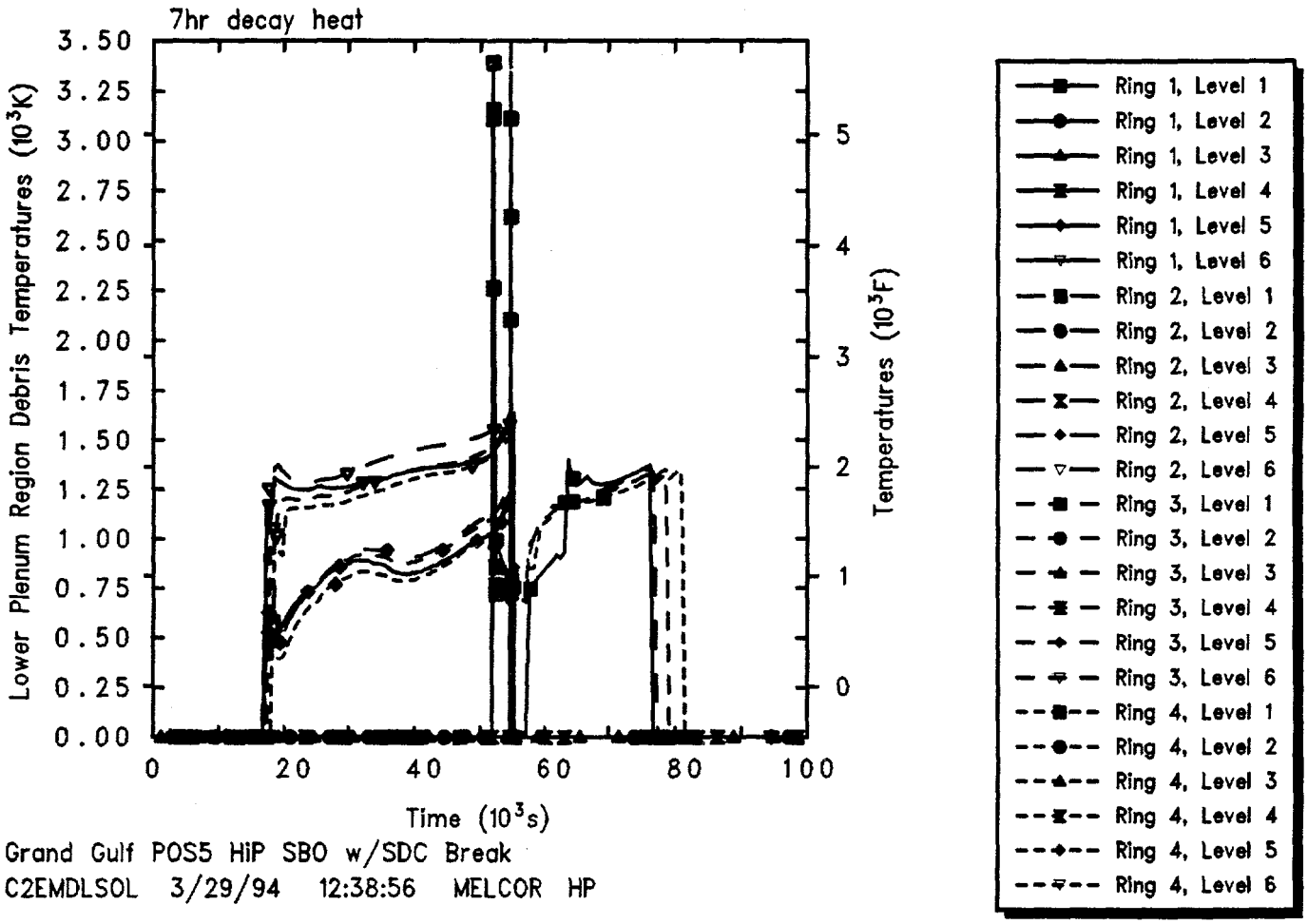

Figure 4.3.2.11. Core Lower Plenum and Core Support Plate Debris Bed Temperatures for Grand Gulf POS 5 -- Station Blackout with Failure to Isolate SDC, Initiated 7 hr After Shutdown.

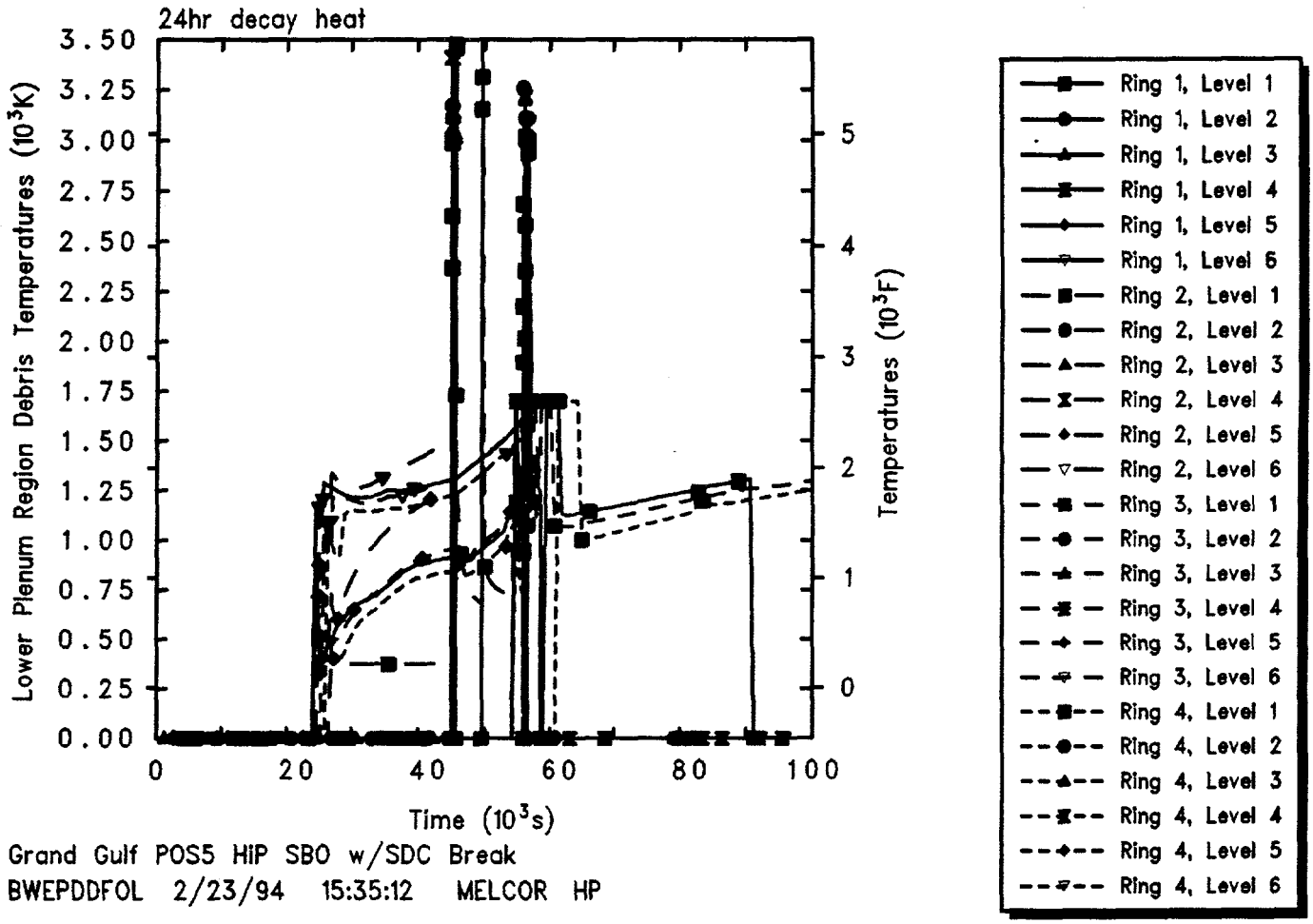

Figure 4.3.2.12. Core Lower Plenum and Core Support Plate Debris Bed Temperatures for Grand Gulf POS 5 -- Station Blackout with Failure to Isolate SDC, Initiated 24 hr After Shutdown.

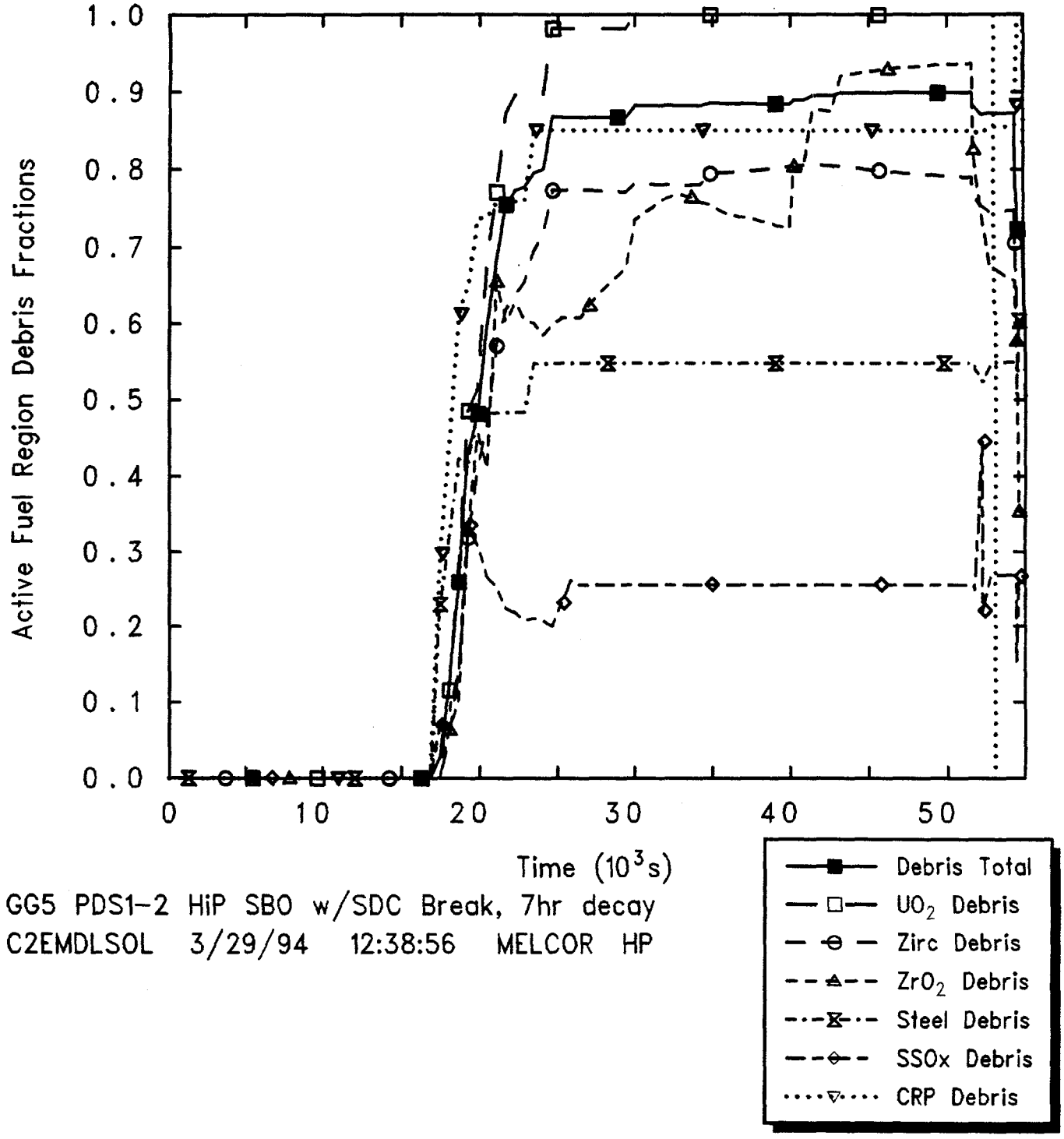

Figure 4.3.2.13. Core Active Fuel Region Degraded Material Fractions for Grand Gulf POS 5 -- Station Blackout with Failure to Isolate SDC, Initiated 7 hr After Shutdown.

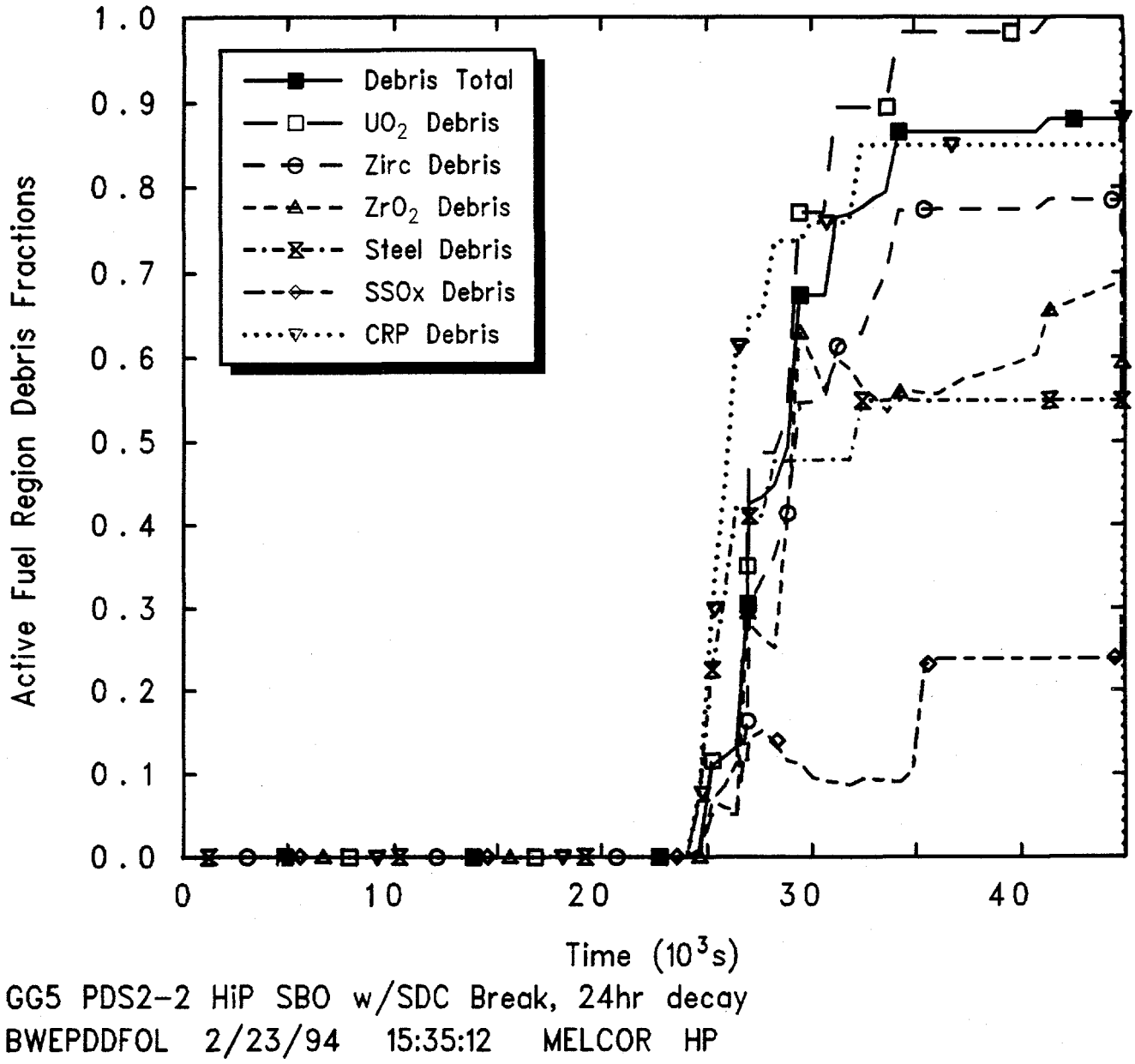

Figure 4.3.2.14. Core Active Fuel Region Degraded Material Fractions for Grand Gulf POS 5 -- Station Blackout with Failure to Isolate SDC, Initiated 24 hr After Shutdown.

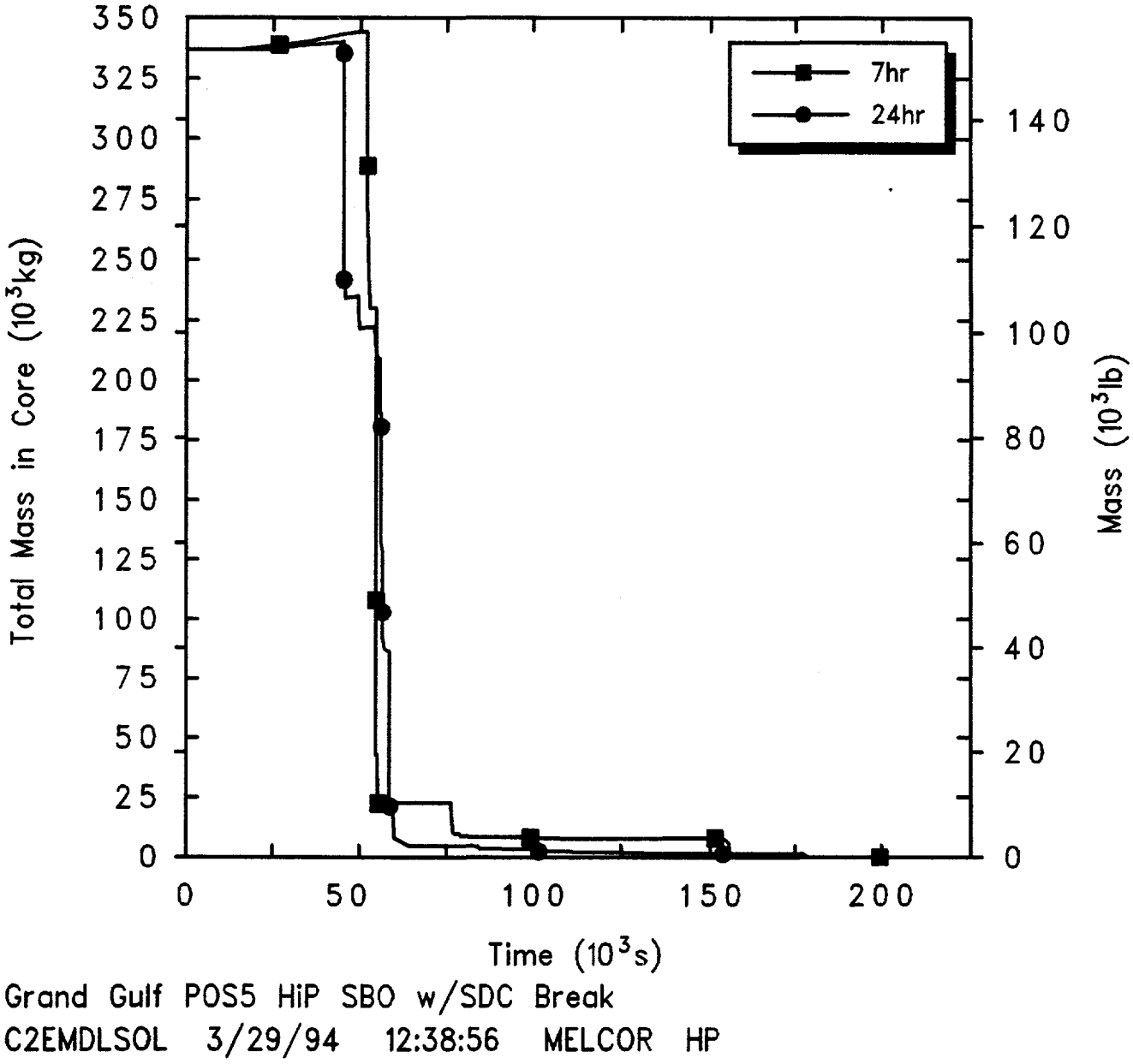

Figure 4.3.2.15. Total Core Material Masses for Grand Gulf POS 5 -- Station Blackout with Failure to Isolate SDC, Initiated at Various Times After Shutdown.

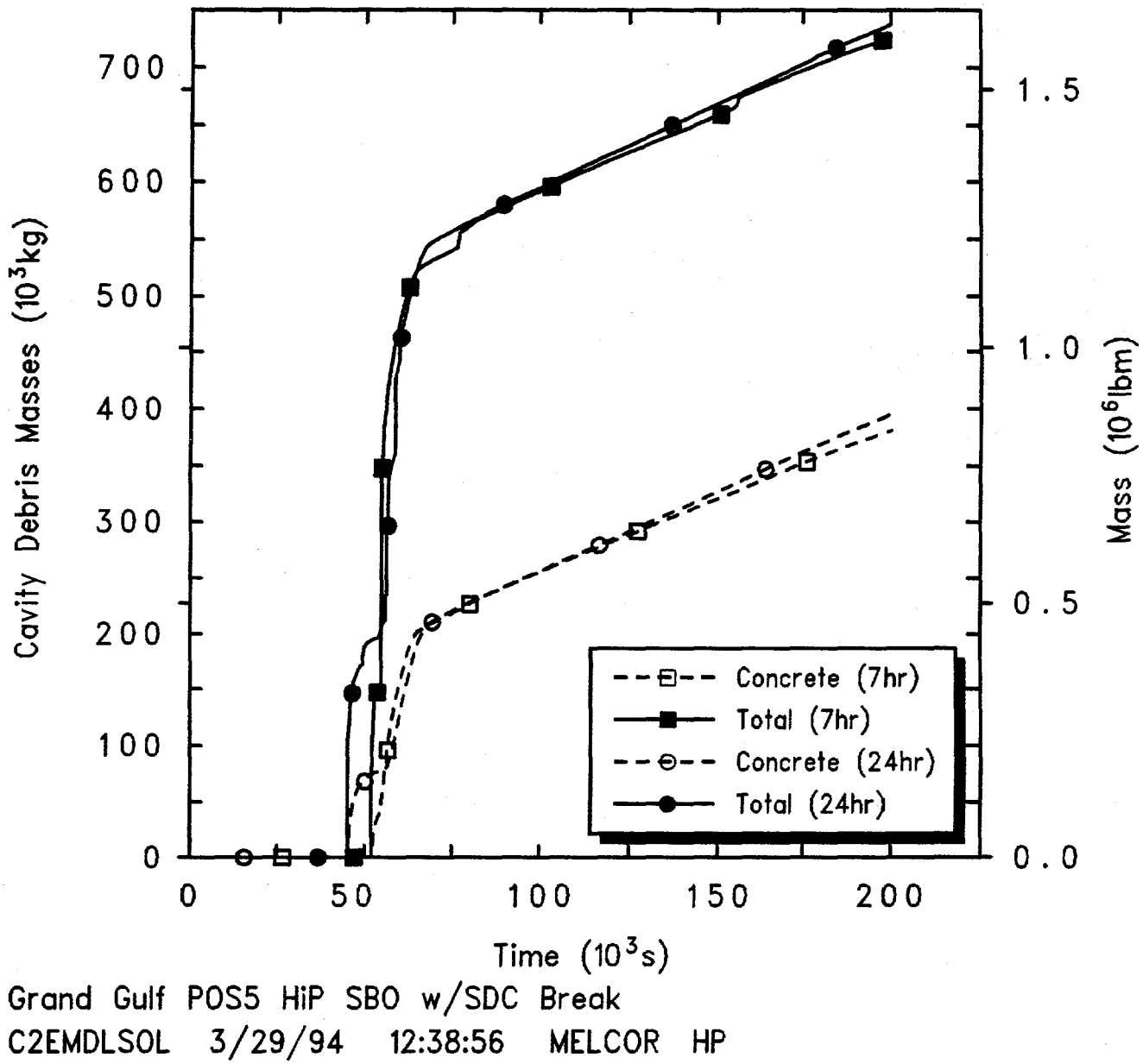

Figure 4.3.2.16. Cavity Total and Concrete Debris Masses for Grand Gulf POS 5 -- Station Blackout with Failure to Isolate SDC, Initiated at Various Times After Shutdown.

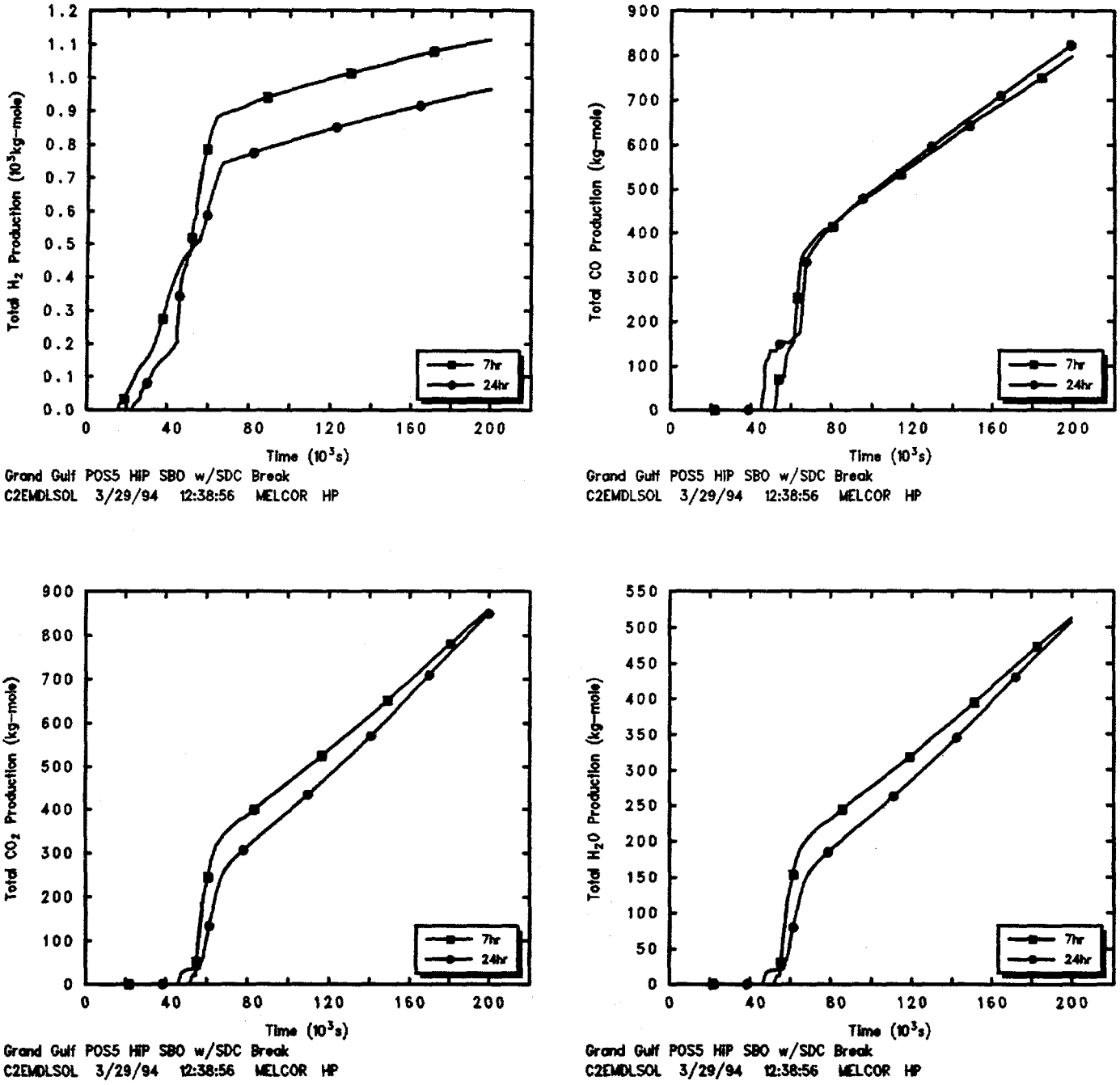

Figure 4.3.2.17. Hydrogen (upper left), Carbon Monoxide (upper right), Carbon Dioxide (lower left) and Steam (lower right) Generation for Grand Gulf POS 5 -- Station Blackout with Failure to Isolate SDC, Initiated at Various Times After Shutdown.

core-concrete interaction resembles the concrete ablation rate: quite rapid soon after debris ejection, later slowing after a CORCON "layer flip" has occurred. On a molar basis, similar amounts are produced of all these gases.

This generation of noncondensables changes the composition of the atmosphere in the containment and in the auxiliary building. The mole fractions in the drywell, containment dome and auxiliary building (first and second floors) are presented in Figures 4.3.2.18 and 4.3.2.19 for this sequence initiated at two different times after shutdown, including vertical dotted lines at auxiliary building failure and at vessel failure for reference. The mole fractions in the cavity resemble the behavior shown for the drywell; the mole fractions in the containment equipment hatch are very similar to those shown for the containment dome; and the mole fractions in the upper floors of the auxiliary building generally resemble the behavior shown for the second floor of the auxiliary building (with the behavior in the first floor different because of the SDC break outlet located there).

The drywell control volume atmosphere consists mostly of steam for relatively short times just before and after auxiliary building failure and vessel failure, and late in the accident, and there is a substantial CO concentration spike a short time after vessel failure. The atmosphere composition in the outer containment volumes remains mostly air (nitrogen and oxygen), with little steam or hydrogen (about 10% each) present. The SDC break vents to the first floor of the auxiliary building, resulting in a very high steam concentration in that volume; higher in the auxiliary building the atmosphere composition closely resembles that in the outer containment (because the containment equipment hatch and both of the containment personnel locks are open). The behavior is qualitatively the same in both cases, just stretched out in time more at the lower decay heat levels compared to higher decay heats.

Figures 4.3.2.20 and 4.3.2.21 illustrate the time-dependent release of radionuclides from the fuel debris both within the vessel and in the cavity, for cases initiated 7 hr and 24 hr after shutdown, respectively. The vertical dotted lines within the plots mark the time of vessel failure, indicating that most of the in-vessel release occurs prior to vessel failure, from the hot debris bed in the active fuel region. Most of the ex-vessel release occurs within a short time period after vessel failure and debris ejection to the cavity, while the core debris is still hot, >2000 K, and consists of a layer of metallic debris above a heavy oxide layer, before enough concrete has been ablated for the debris bed configuration to invert to a light oxide layer above a layer of metallic debris, mixed to a lower average temperature of about 1500 K. Table 4.3.2.2 summarizes the in-vessel, ex-vessel and total amounts of each radionuclide class released, all normalized as mass fractions of the initial inventories of each class. (Note that these amounts generally consider only the release of radioactive forms of these classes, and not additional releases of nonradioactive aerosols from structural materials.)

Unlike the results for the large break LOCA accident simulations described in the previous section, in this station blackout scenario (and the remainder of the Level 2 MELCOR analyses done) the MELCOR model included the formation of CsI from Cs and I_2 released from the fuel, and its subsequent transport, deposition and release. The initial radionuclide inventories are such that all the I_2 released reacts to form CsI while most of the Cs remains unreacted and forms CsOH (the default Cs form).

Almost all (~100%) of the volatile Class 1 (noble gases), Class 2 (CsOH), Class 5 (Te) and Class 16 (CsI) radionuclide species are released from the fuel, primarily in-vessel, as are most (~90-100%) of the Class 3 (Ba) and Class 12 (Sn) inventories. The next major release fraction, dropping rapidly with lower decay heat levels and cooler debris is for uranium. Around 1-10% of the total inventories of Ru and Mo, Ce and La, are released. Finally, a total ≤0.1% of the initial inventory of Class 11 (Cd) is predicted to be released. Note that the CORSOR-M fission product release model option used in these analyses has identically zero release in-vessel of Class 7 (Mo), Class 9 (La) and Class 11 (Cd). These are higher release fractions of Ba, Te, Ru, Ce, La and Sn than seen in MELCOR analyses of the large break LOCA sequences described in the previous subsection, reflecting the very high debris temperatures calculated during in-vessel core degradation (shown in Figures 4.3.2.7 and 4.3.2.8).

Figure 4.3.2.22 gives the total radioactive release to the environment in these two cases. The total releases and time history of the release for this accident initiated at two different decay heat levels are nearly identical. The releases (as mass fractions of the initial inventories) of individual classes to the environment are shown in Figures 4.3.2.23 and 4.3.2.24. With the break in the SDC system and the failure of the auxiliary building early in this scenario, fission products released during in-vessel core heatup and degradation can immediately escape to the environment (although the only significant release fraction is for the noble gases). There is an increased release of all radionuclide classes at vessel failure, as the core debris

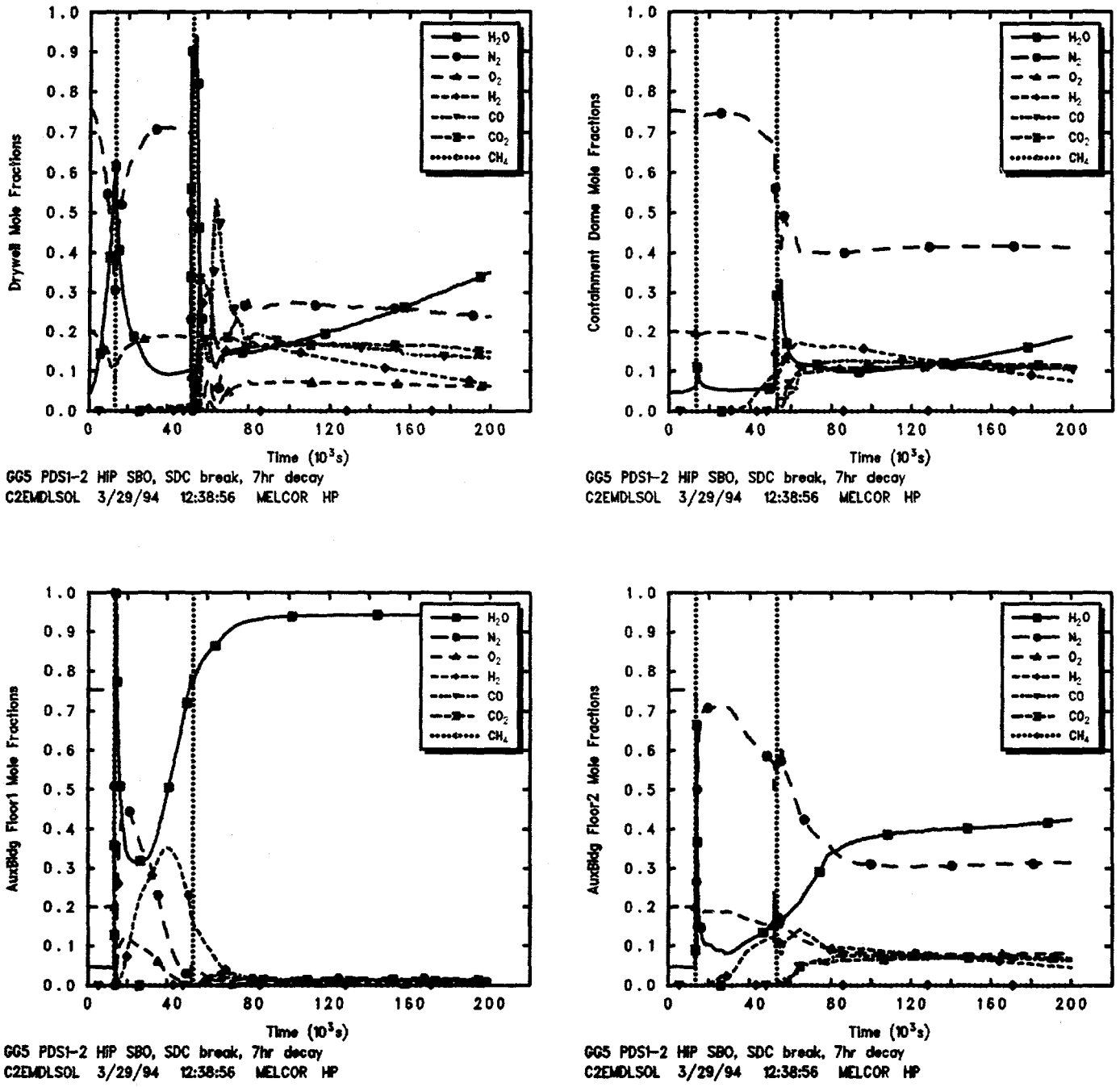

Figure 4.3.2.18. Mole Fractions in Drywell (upper left), Containment Dome (upper right), and Auxiliary Building First Floor (lower left) and Second Floor (lower right) for Grand Gulf POS 5 -- Station Blackout with Failure to Isolate SDC, Initiated 7 hr After Shutdown.

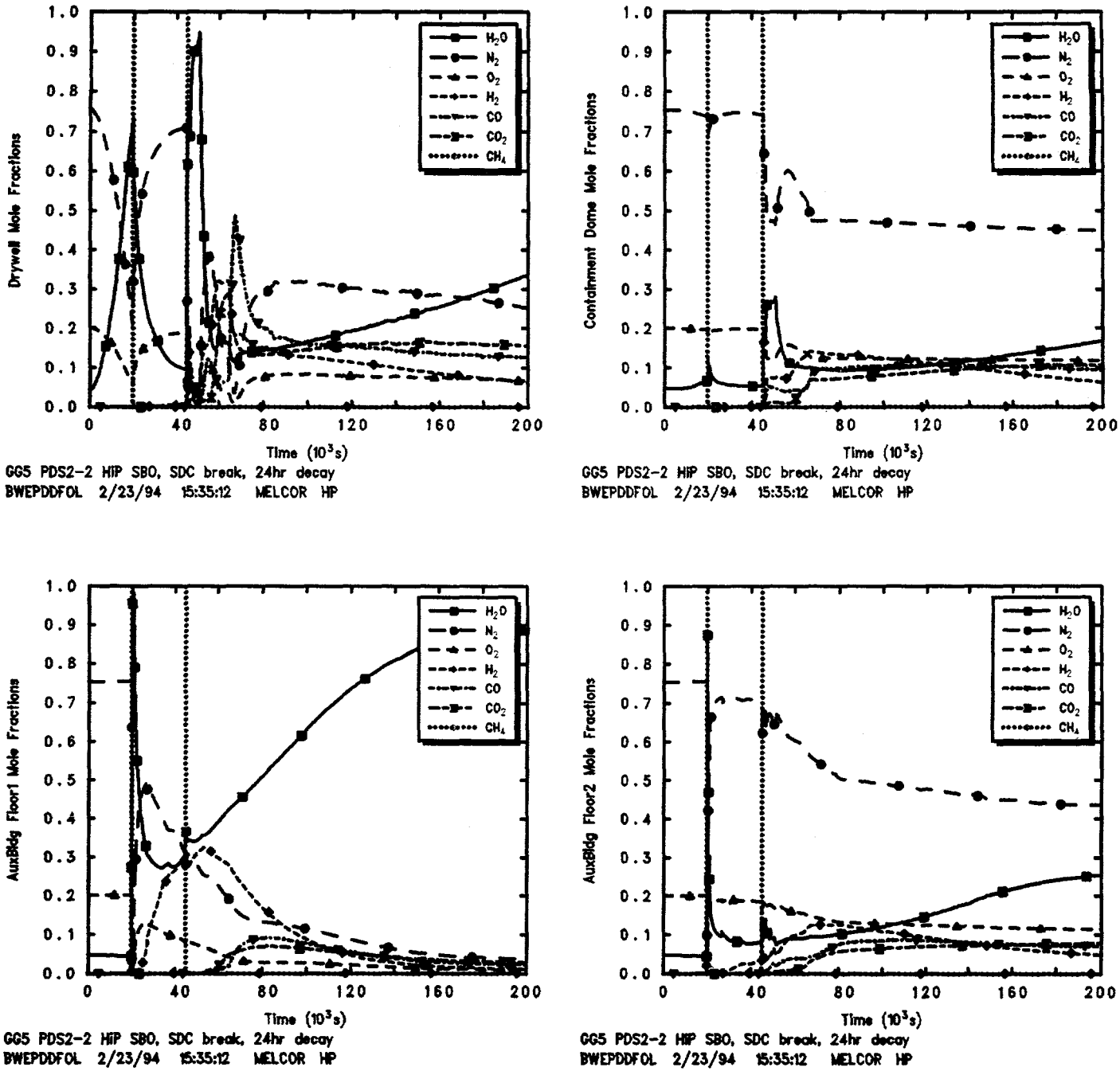

Figure 4.3.2.19. Mole Fractions in Drywell (upper left), Containment Dome (upper right), and Auxiliary Building First Floor (lower left) and Second Floor (lower right) for Grand Gulf POS 5 -- Station Blackout with Failure to Isolate SDC, Initiated 24 hr After Shutdown.

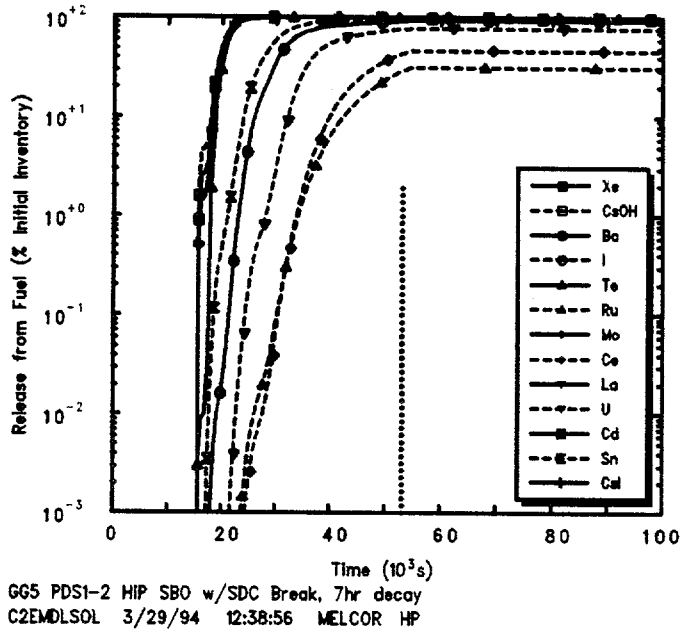

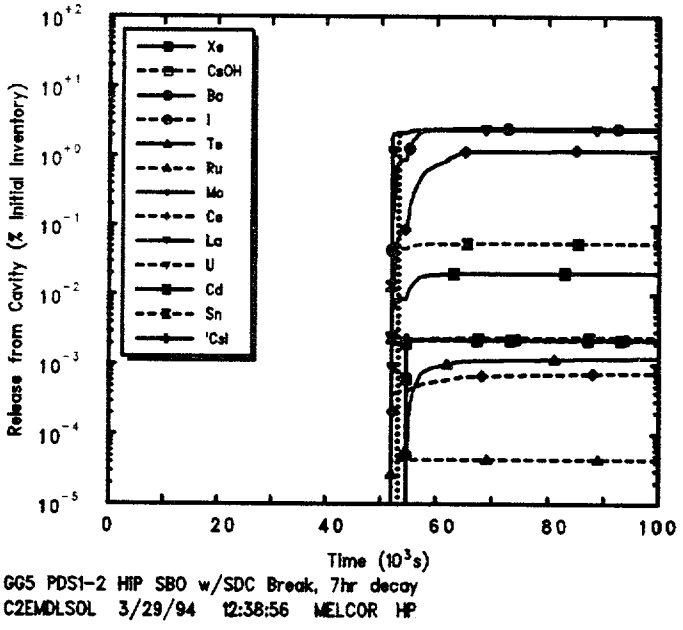

Figure 4.3.2.20. In-Vessel (top) and Ex-Vessel (bottom) Radionuclide Release Mass Fractions for Grand Gulf POS 5 -- Station Blackout with Failure to Isolate SDC, Initiated 7 hr After Shutdown.

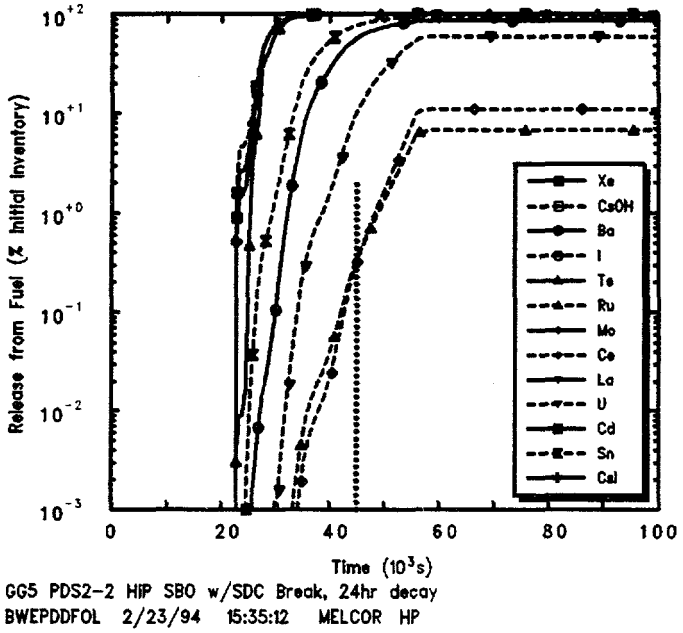

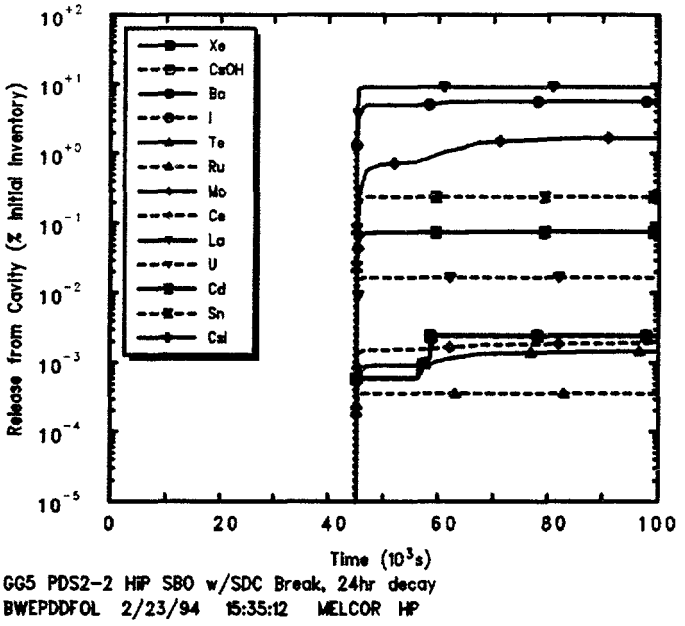

Figure 4.3.2.21. In-Vessel (top) and Ex-Vessel (bottom) Radionuclide Release Mass Fractions for Grand Gulf POS 5 -- Station Blackout with Failure to Isolate SDC, Initiated 24 hr After Shutdown.

Table 4.3.2.2. Final Radionuclide Release Fractions for Grand Gulf POS 5 -- Station Blackout with Failure to Isolate SDC, Initiated at Various Times After Shutdown

Class	Fission Products Released from Fuel (% Initial Inventory-Mass Fraction)					
	7 hr			24 hr		
	In-Vessel	Ex-Vessel	Total	In-Vessel	Ex-Vessel	Total
Xe	99.98	0.0022	99.98	99.99	0.0024	99.99
CsOH	~100	0.002	~100	~100	0.002	~100
Ba	93.16	2.48	95.64	86.01	5.524	91.534
I	~0	~0	~0	~0	~0	~0
Te	99.97	0.0015	99.97	99.99	0.002	99.99
Ru	31.47	0.00004	31.47	6.704	0.0004	6.7
Mo	0	1.2	1.2	0	1.664	1.664
Ce	46.33	0.0009	46.33	10.88	0.0022	10.88
La	0	2.37	2.37	0	8.99	8.99
U	76.64	0.0025	76.64	59.64	0.017	59.66
Cd	0	0.025	0.025	0	0.079	0.079
Sn	98.05	0.056	99.11	96.03	0.25	96.28
CsI	99.99	0.0023	99.99	~100	0.0024	~100

falling into and flashing the lower plenum water pool (either immediately in the lower plenum or subsequently in the cavity) generates a substantial steam spike which is vented out the containment and auxiliary building. There is later a continued low-level release of some radionuclide classes, in particular for the volatiles CsOH, CsI and Te.

These environmental releases do not correspond to immediate release of all radionuclides released from the fuel; there is considerable retention of most radionuclide species within the containment and auxiliary building (as discussed below). The noble gases have the greatest releases (>90%) to the environment by the end of the transient periods simulated, because gaseous forms are not scrubbed, filtered, deposited or otherwise retained. There is some release to the environment of the other volatile species (i.e., CsOH, CsI and Te) also, although these are found mostly in aerosol form (and are generally retained in the auxiliary building); the temperatures are higher enough in this station blackout sequence than in the large break LOCA for the volatiles' vapor form to persist, primarily because the containment was flooded in the large break LOCA scenario and dry in the station blackout scenario.

Tables 4.3.2.3 and 4.3.2.4 summarize the distribution of the initial radionuclide inventory at the end of the two calculations initiated at different times after shutdown; they provide an overview of how much of the radionuclides remain bound up in fuel debris in either the core or the cavity, and of how much of the released radionuclides are retained in the primary system *vs* how much of the released radionuclides are released to, or released in, either the containment or the auxiliary building and the environment, all normalized to the initial inventories of each class. Table 4.3.2.5 presents a slightly different breakdown of the released radionuclide final distribution, giving the fractions of released inventory for each class in control volume atmospheres (including the environment), in pools, or deposited or settled onto heat structures at the end of the calculations. (As in Table 4.3.2.2 these amounts consider only the release of radioactive forms of these classes, and not additional releases of nonradioactive aerosols from structural materials.)

These tables show fission product distributions generally similar to those found for the large break LOCA sequences (discussed in the previous section) for the

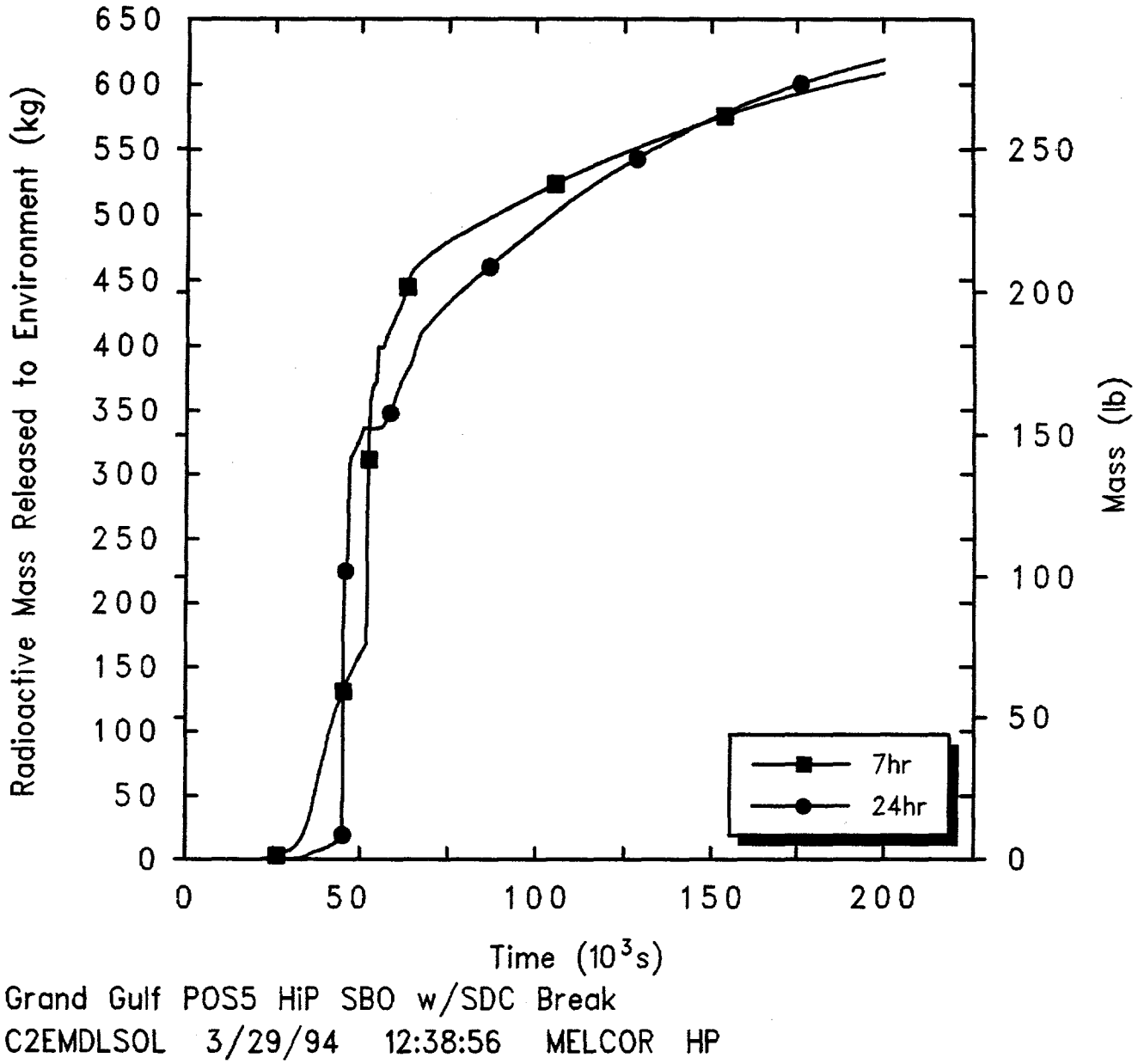

Figure 4.3.2.22. Total Environmental Radionuclide Releases for Grand Gulf POS 5 -- Station Blackout with Failure to Isolate SDC, Initiated at Various Times After Shutdown.

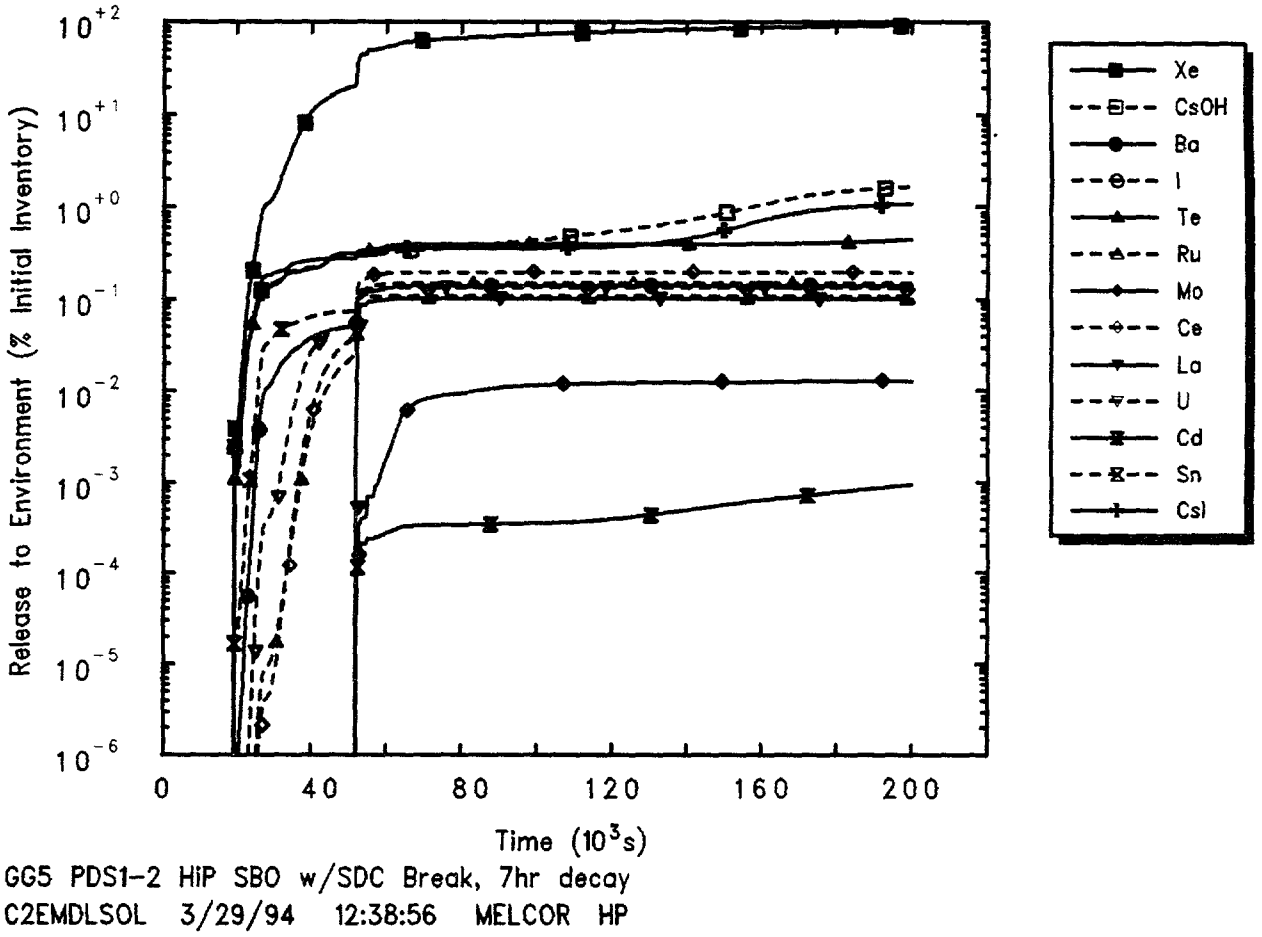

Figure 4.3.2.23. Environmental Radionuclide Release Mass Fractions for Grand Gulf POS 5 -- Station Blackout with Failure to Isolate SDC, Initiated 7 hr After Shutdown.

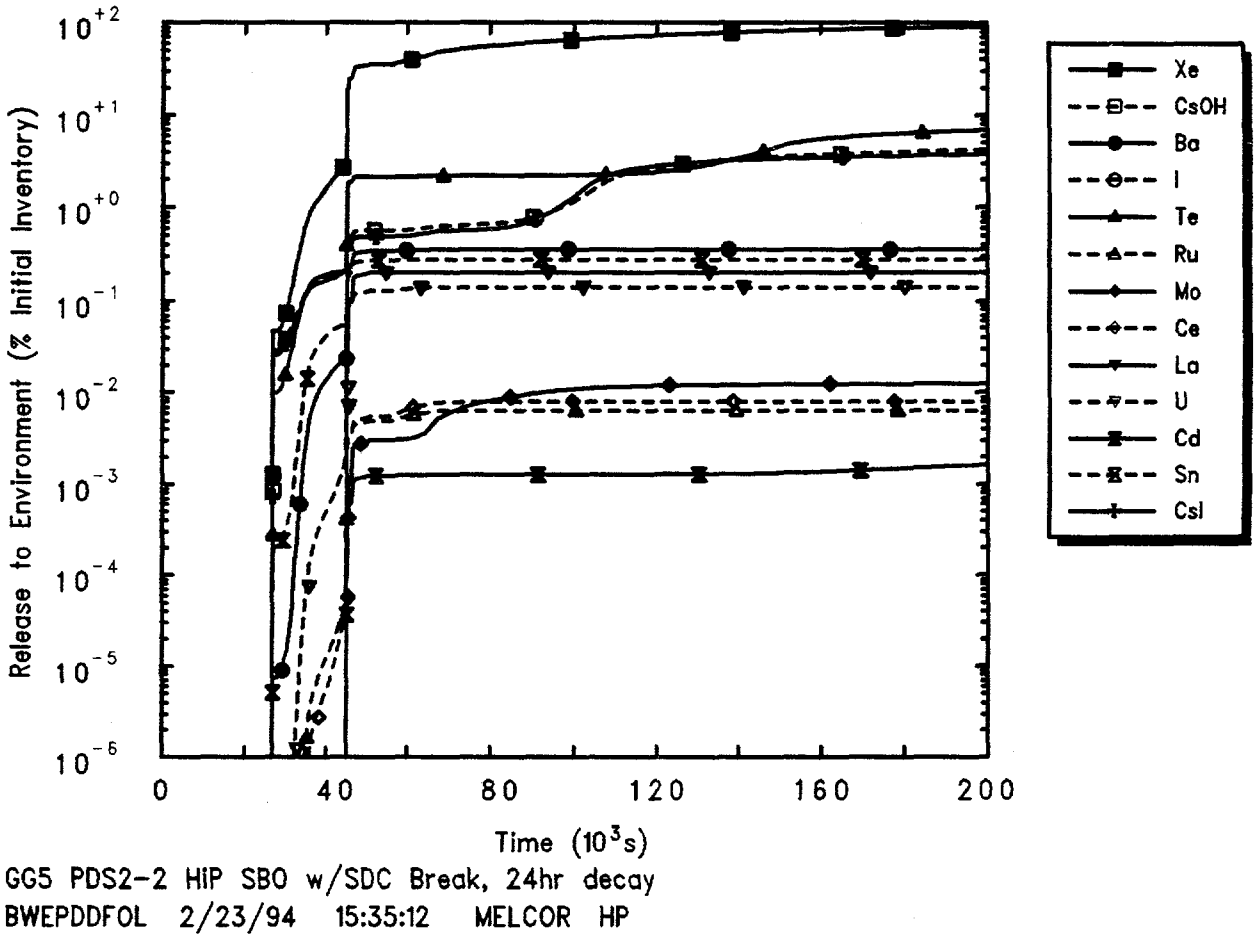

Figure 4.3.2.24. Environmental Radionuclide Release Mass Fractions for Grand Gulf POS 5 -- Station Blackout with Failure to Isolate SDC, Initiated 24 hr After Shutdown.

Table 4.3.2.3. Final Radionuclide Distribution for Grand Gulf POS 5 -- Station Blackout with Failure to Isolate SDC, Initiated at 7 hr After Shutdown

Class	Fission Product Distribution (% Initial Inventory-Mass Fraction)				
	Fuel Debris	Primary System	Containment	Auxiliary Building	Environment
Xe	~0	0.0113	4.36	3.29	92.3
CsOH	~0	1.19	5.43	91.74	1.68
Ba	4.37	49.5	20.52	25.42	0.138
Te	0.289	0.293	5.89	93.39	0.442
Ru	68.5	15.7	4.72	10.95	0.147
Mo	98.8	0.087	0.95	0.147	0.013
Ce	53.7	23.6	6.09	16.44	0.192
La	97.6	0.276	1.79	0.204	0.1
U	29.4	38.2	11.74	20.48	0.12
Cd	~100	0.0023	0.019	0.0027	0.0009
Sn	1.89	50.7	14.9	32.39	0.107
CsI	~0	0.0113	4.81	93.94	1.09

radionuclides with significant (≥80% of initial inventory) release from fuel. In both accident scenarios, most of the noble gases released are in the environment, in the atmosphere. Most of the volatile species (CsOH, CsI and Te) releases occurred in-vessel in both scenarios. However, in this station blackout with the SDC break venting directly to the auxiliary building most of those releases are retained in the auxiliary building, while in the large break LOCA most of those releases are retained in the containment (but primarily in water pools in both cases). About 1-7% of the volatile species are released to the environment in this accident scenario, an order of magnitude more than in the large break LOCA sequence. The two classes of radionuclides forming aerosols which had substantial releases (Ba and Sn, also occurring mostly in-vessel) were predicted to have about half those releases retained in the vessel, primarily deposited on structures, in both accident scenarios; for this station blackout with failure to isolate SDC the other half of the releases is retained about equally in the containment and in the auxiliary building, about equally in water pools and deposited on structure surfaces, while for the large break LOCA the other half of the releases is retained in the containment, mostly in water pools and a small fraction deposited on structure surfaces.

4.3.3 Station Blackout with Firewater Addition Followed by High Pressure Boiloff, Initiated 7 hr After Shutdown

At the initiation of the accident, the reactor vessel is depressurized and the coolant is at the normal level. The vessel water inventory is at 366.5 K (200°F), which corresponds to the maximum temperature allowed by the Grand Gulf technical specifications for operation in POS 5. The reactor pressure vessel head vent is open. At the start of the accident all core cooling and injection is lost and the SRVs are closed. Two hours after the start of the accident two SRVs are opened and firewater is injected into the core bypass region at a flow rate determined by the pump head curve. Twelve hours after the start of the accident the SRVs close due to depletion of the station batteries, and subsequently the SRVs cycle at their pressure relief setpoint. The suppression pool level is 3.86 m (12.67 ft) from the suppression pool floor. The containment is at 305.4 K (90°F) and the suppression pool is at 308.2 K (95°F). The drywell personnel lock is open; the containment equipment hatch and both of the containment personnel locks are open.

This sequence is identical to the Level 1 station blackout sequence with firewater addition followed by a high

Table 4.3.2.4. Final Radionuclide Distribution for Grand Gulf POS 5 -- Station Blackout with Failure to Isolate SDC, Initiated at 24 hr After Shutdown

Class	Fission Product Distribution (% Initial Inventory-Mass Fraction)				
	Fuel Debris	Primary System	Containment	Auxiliary Building	Environment
Xe	~0	0.011	4.45	5.04	90.5
CsOH	~0	0.206	7.42	88.14	4.19
Ba	8.46	41.7	32.3	17.23	0.352
Te	0.003	0.332	8.11	84.62	6.9
Ru	93.3	1.78	4.64	0.28	0.0063
Mo	98.3	0.225	1.29	0.13	0.0124
Ce	89.1	2.8	7.68	0.39	0.008
La	91	1.35	7.04	0.39	0.199
U	45	16.9	34.67	3.22	0.127
Cd	99	0.012	0.062	0.0037	0.0016
Sn	3.72	48.2	20.95	26.81	0.274
CsI	~0	0.151	6.91	89.21	3.77

pressure boiloff discussed in Section 4.2.8 initiated 7 hr after shutdown.

The sequence of events predicted by MELCOR for this accident with different initiation times is given in Table 4.3.3.1.

The pressure response is identical to that presented in Figures 4.2.8.2 and 4.2.8.3 for the vessel and auxiliary building, respectively, in Section 4.2.8 for this sequence initiated 7 hr after shutdown. Initially, the system begins pressurizing as all core cooling is lost; the pressure then begins dropping after two SRVs are opened 2 hr after the start of the accident. Firewater cooling and steaming out the SRVs keep the vessel pressure down until 12 hr, when depletion of the station batteries cause the SRVs to close. Since the SRVs are now closed, the RPV pressurizes until the SRVs begin operating in the relief mode. After some time, the continued inventory loss out the open RPV vent is sufficient to relieve the steaming in the core and the SRVs close. The pressure continues to drop until core heatup and damage begins; there is then a brief repressurization, followed very quickly by a final, sharp depressurization due to vessel failure. The flow out the open RPV vent line and later out the SRVs also pressurizes the containment and the auxiliary building. The auxiliary building fails when the SRVs begin cycling at their safety setpoint. The auxiliary building pressure briefly spikes later when the vessel fails.

The firewater injection rate and the vessel inventory response are also identical to the results discussed for the corresponding Level 1 analysis presented in Section 4.2.8 (shown in Figures 4.2.7.3 and 4.2.8.4, respectively). Firewater injection does not equal and reverse inventory loss for about 5 hr. After the SRVs close at 12 hr, coolant inventory is lost as the SRVs cycle at the safety setpoint until vessel failure, when all the remaining coolant in the vessel drains to the cavity abruptly.

Figure 4.3.3.1 presents the upper plenum, core and lower plenum swollen and collapsed liquid levels for this accident sequence. The upper plenum levels drop for about 5 hr after the SRVs are opened before the firewater addition is sufficient to raise the liquid levels back up briefly. The liquid level in the upper plenum resumes dropping soon after firewater injection is stopped after 12 hr when the SRVs begin cycling in the relief mode. The collapsed level in the core drops below the core midplane before stabilizing and rising again during the 10hr of firewater injection, but the swollen level drops only about a foot into the active fuel region before the firewater addition is sufficient to begin raising the vessel inventory and liquid levels back up. After firewater

Table 4.3.2.5. Final Radionuclide State for Grand Gulf POS 5 -- Station Blackout with Failure to Isolate SDC, Initiated at Various Times After Shutdown

Class	Fission Products Released from Fuel (% Released Inventory-Mass Fraction)					
	Atmosphere	7 hr Pool	Deposited	Atmosphere	24 hr Pool	Deposited
Xe	~100	0	0	~100	0	0
CsOH	2.27	91.1	6.65	5.19	88.2	6.65
Ba	0.145	33.9	66	0.39	31.2	68.4
I	~100	0	0	~100	0	0
Te	0.64	92.2	7.11	8.46	84.8	6.75
Ru	0.47	39.8	59.8	0.0094	25.8	74.1
Mo	1.09	40	58.9	0.77	38	61.3
Ce	0.41	39.7	59.8	0.073	25.4	74.5
La	4.22	40.3	55.5	2.21	35.7	62
U	1.71	34.5	65.3	0.23	27.7	72
Cd	6.3	34.9	58.8	3	34.1	62.9
Sn	0.11	37.7	62.1	0.29	35	64.7
CsI	1.44	93.5	5.06	4.5	89.3	6.15

injection is stopped at 12 hr and the SRVs begin cycling in the relief mode, the vessel liquid level drops smoothly through the upper plenum into the core and continue dropping smoothly partway into the lower plenum, followed by a more gradual loss of the remaining inventory due to boiling and steam outflow. There is very little pool frothing or swelling in any of the vessel volumes in this sequence.

The heatup of the intact fuel and clad is illustrated in Figure 4.3.3.2. The small core uncovery early in the accident progression does not result in significant core heatup before the firewater addition raises the vessel inventory and liquid levels back up After firewater injection ends at 12 hr there is a slow temperature increase, reflecting the rise in saturation temperature as the system pressurizes to the SRV setpoint. Later, after TAF uncovery, core heatup and damage begins. Because the fuel/clad component temperatures in MELCOR are set to zero in a cell when that component fails, this figure shows both the overall heatup rate and the time that the intact fuel/clad component fails through melting of the clad at 2100 K (3320°F).

Figure 4.3.3.3 presents corresponding core debris temperatures in the active fuel region; these are the temperatures of the debris bed formed by the failure of the intact fuel/clad component in MELCOR in a core cell, whose (intact) temperatures were given in Figure 4.3.3.2. The debris bed in the active fuel region reaches peak temperatures ≥3500 K (5840°F), significantly above the UO_2 melt temperature of 3113 K (5144°F), except in the lowermost active fuel level where the debris bed temperature remains below the UO_2 melt temperature. The debris bed temperatures predicted in this station blackout sequence with 10hr of firewater addition are somewhat lower than those predicted in the station blackout sequences with failure to isolate SDC (and no firewater addition) presented in the previous section.

The temperatures of the active fuel region debris bed drop to zero when the core plate fails and the debris relocates to the lower plenum. The predicted temperatures in the debris bed in the lower plenum and core plate are given in Figure 4.3.3.4. Prior to core plate failure there is some cold, refrozen debris both on the core support plate and on the lower core structural material just above the core

Table 4.3.3.1. Sequence of Events Predicted by MELCOR for Station Blackout with Firewater Addition Followed by High Pressure Boiloff, Initiated 7 hr After Shutdown

Event	Time After Shutdown 7 hr
Accident initiation	0
Firewater injection enabled	7,200 s (2 hr)
Core uncovery (TAF) begins	9,787 s (2.72 hr)
Firewater injection stopped	43,200 s (12 hr)
Auxiliary building failed	56,000 s (15.56 hr)
Core heatup begins	56,000 s (15.56 hr)
Clad failure/Gap release	
(Ring 1)	63,097 s (17.53 hr)
(Ring 2)	63,032 s (17.51 hr)
(Ring 3)	63,086 s (17.52 hr)
(Ring 4)	63,427 s (17.62 hr)
(Ring 5)	64,862 s (18.02 hr)
(Ring 6)	79,190 s (22.00 hr)
Core plate failed	
(Ring 1)	90,492 s (25.14 hr)
(Ring 2)	95,165 s (26.43 hr)
(Ring 3)	94,525 s (26.26 hr)
(Ring 4)	94,502 s (26.25 hr)
(Ring 5)	102,598 s (28.50 hr)
(Ring 6)	112,341 s (31.21 hr)
Vessel LH penetration failed	
(Ring 1)	90,582 s (25.16 hr)
(Ring 2)	90,598 s (25.17 hr)
(Ring 3)	90,603 s (25.17 hr)
(Ring 4)	90,653 s (25.18 hr)
(Ring 5)	102,741 s (28.54 hr)
(Ring 6)	112,898 s (31.36 hr)
Commence debris ejection	90,582 s (25.16 hr)
Cavity rupture	199,146 s (55.32 hr)
End of calculation	199,146 s (55.32 hr)

support plate; the cooling and refreezing of this debris is the cause of the continued gradual drop in lower plenum liquid level due to steaming seen in Figure 4.3.3.1. The debris temperature rises gradually to the core support plate failure temperature of 1273 K (1832°F). After core plate failure hot, high-temperature debris begins appearing in the lower plenum as debris falls from the active fuel region into the lower plenum. With the new debris radial relocation model added in MELCOR 1.8.2, the core plate needs to fail in only one ring before debris from cells in the active fuel region in all radial rings can potentially flow sideways and down, fall through the failed plate, and then spread sideways into cells in the lower plenum in all radial rings. (Thus a lower head penetration can now fail in a ring before the core plate in that ring fails.) The lower head penetrations begin failing almost immediately, and the lower plenum debris temperatures begin dropping to zero as debris is ejected from the vessel to the cavity. Some cool, quenched debris remains present in the lower plenum for a

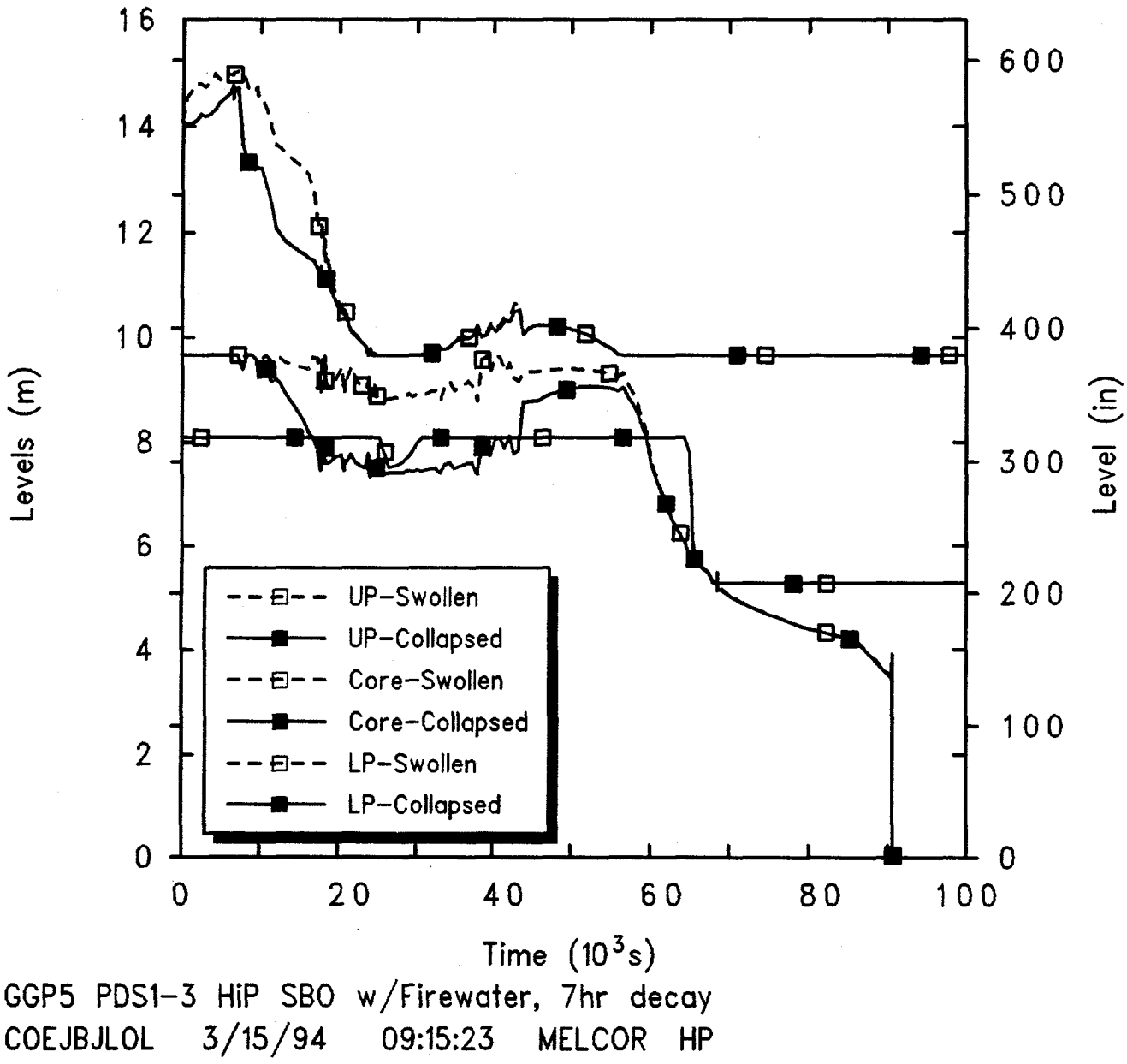

Figure 4.3.3.1. Upper Plenum, Core and Lower Plenum Liquid Levels for Grand Gulf POS 5 -- Station Blackout with Firewater Addition Followed by High Pressure Boiloff, Initiated 7 hr After Shutdown.

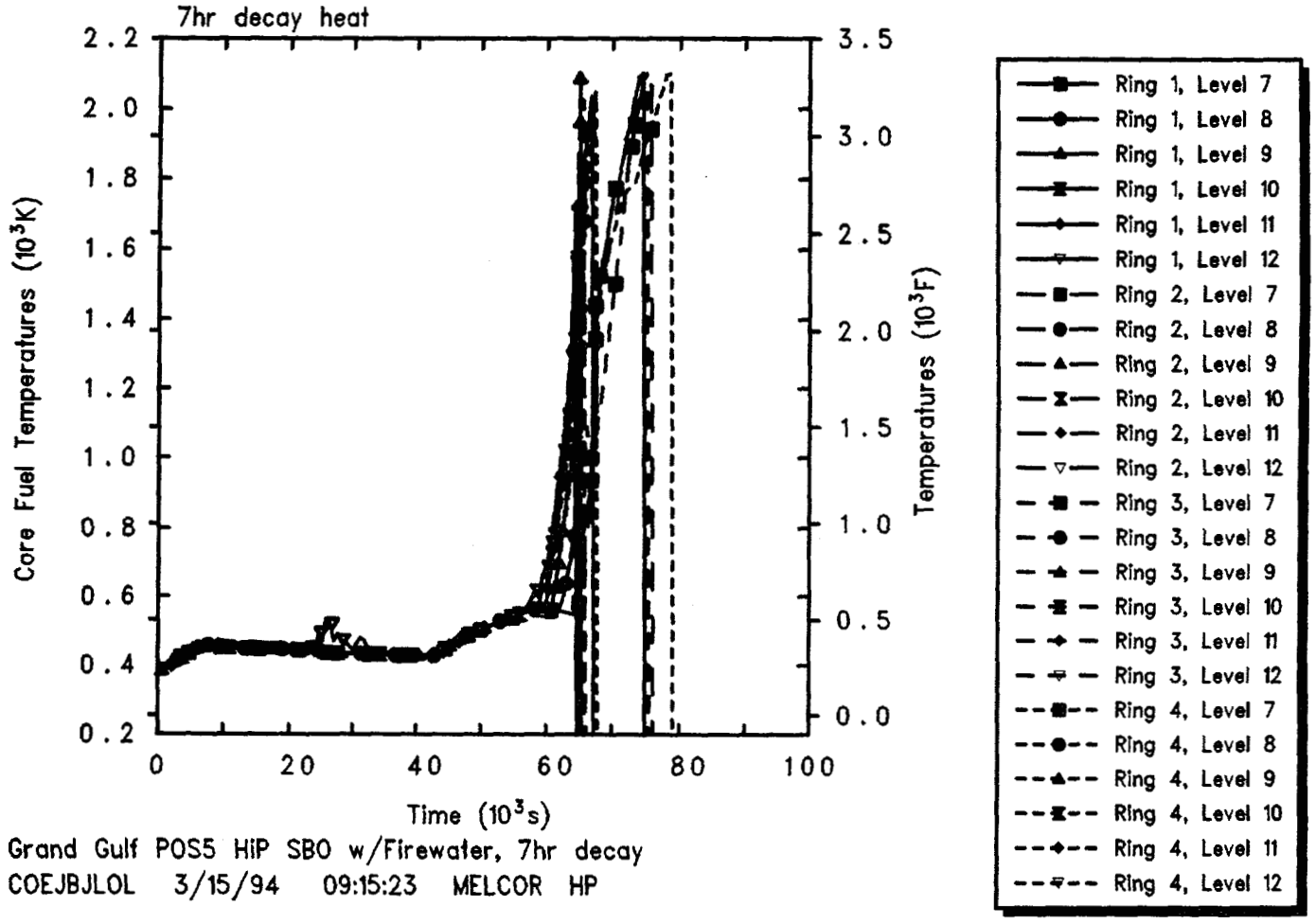

Figure 4.3.3.2. Core Intact Fuel/Clad Temperatures for Grand Gulf POS 5 -- Station Blackout with Firewater Addition Followed by High Pressure Boiloff, Initiated 7 hr After Shutdown.

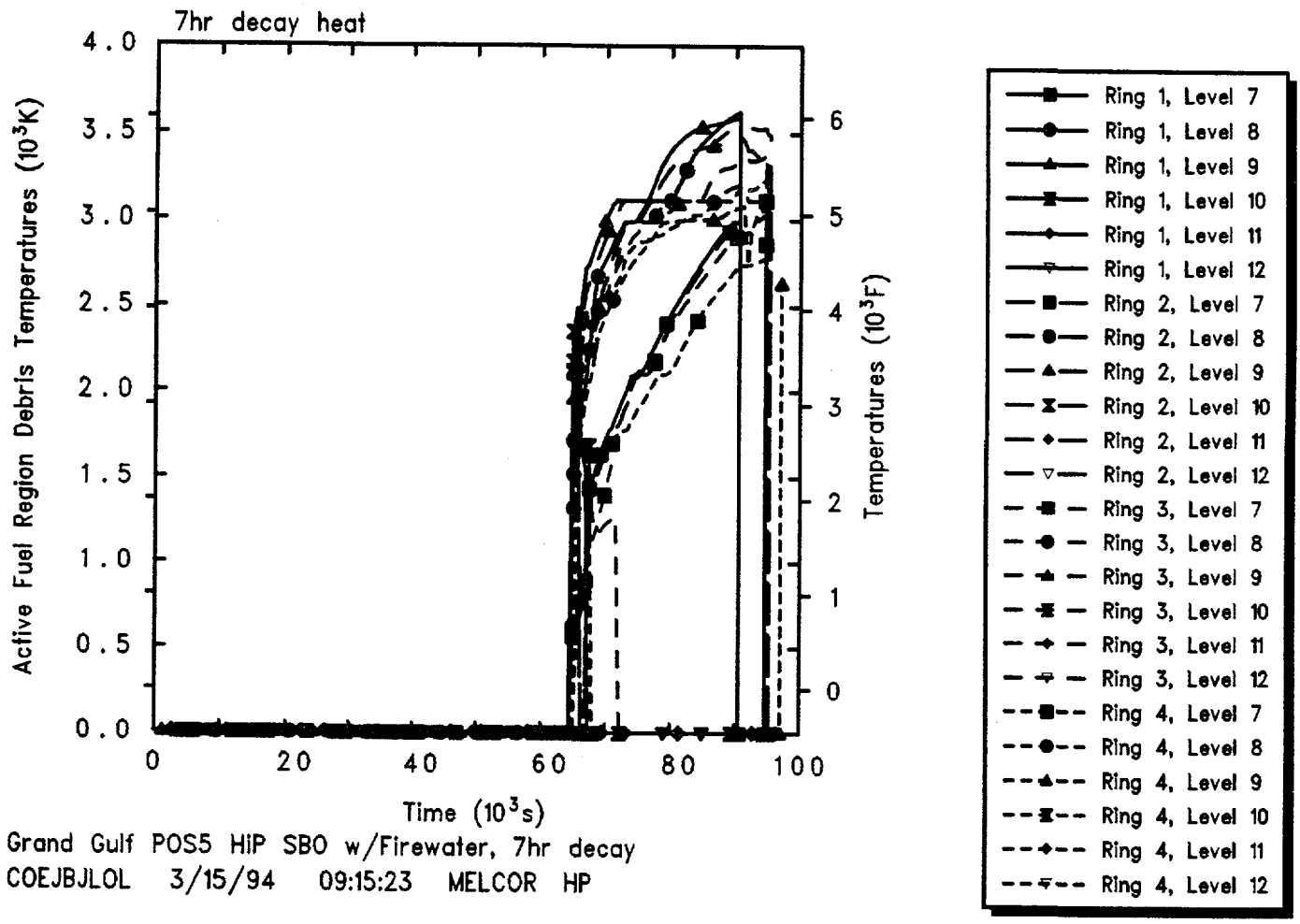

Figure 4.3.3.3. Core Active Fuel Region Debris Bed Temperatures for Grand Gulf POS 5 -- Station Blackout with Firewater Addition Followed by High Pressure Boiloff, Initiated 7 hr After Shutdown.

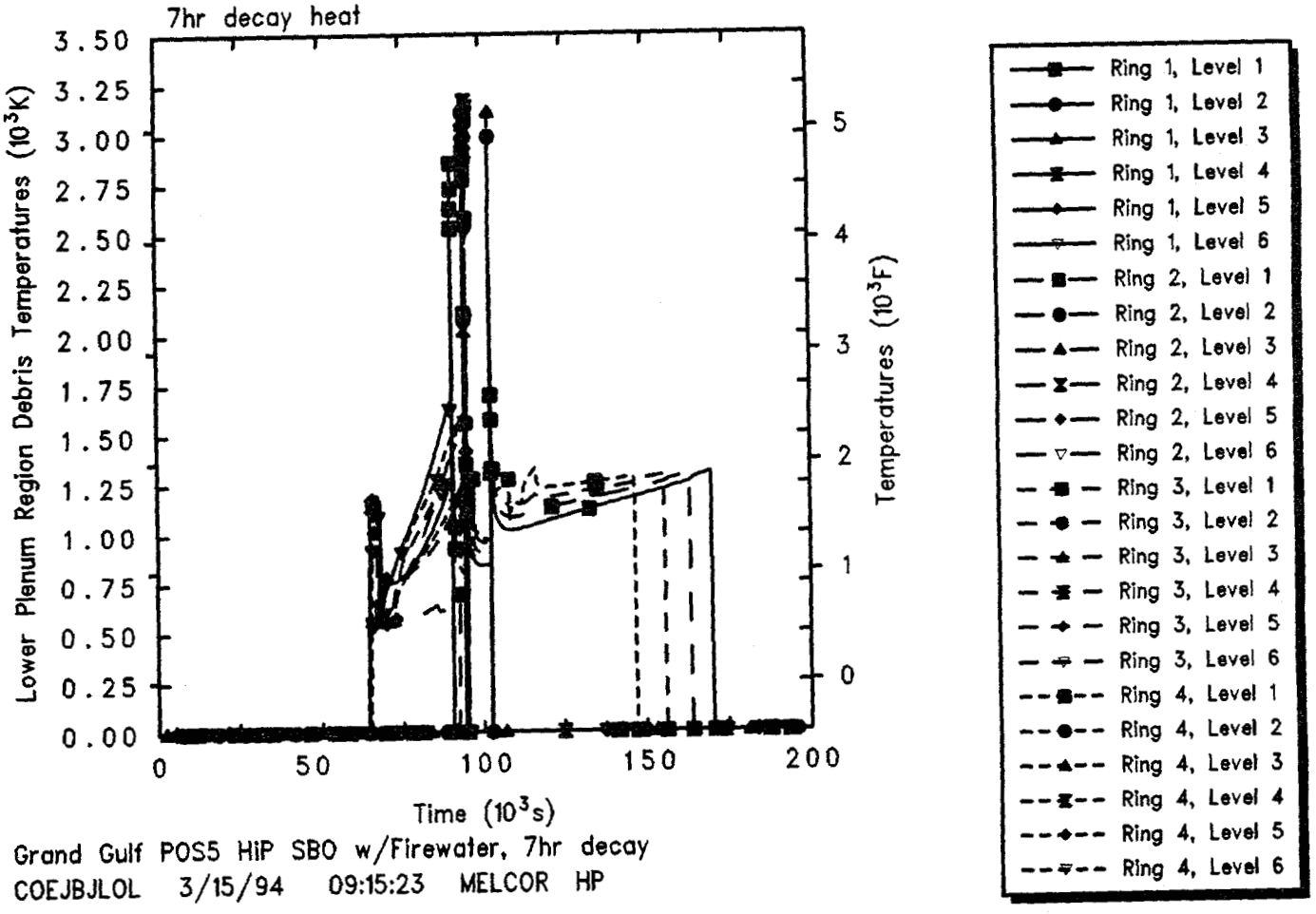

Figure 4.3.3.4. Core Lower Plenum and Core Support Plate Debris Bed Temperatures for Grand Gulf POS 5 -- Station Blackout with Firewater Addition Followed by High Pressure Boiloff, Initiated 7 hr After Shutdown.

significant period of time, however, as indicated by the 1000-1250 K debris temperatures in the lowest level after vessel failure.

Figure 4.3.3.5 illustrates what fraction of each material in the active fuel region has collapsed into a debris rubble bed held up by the core support plate, prior to core plate failure, debris relocation, lower head failure and debris ejection, for this station blackout scenario with firewater. The fractions of each material and the overall fraction of total material in the active fuel region degraded into particulate debris in this sequence are visibly lower than the corresponding fractions predicted for the station *blackout* scenarios without firewater addition and with failure to isolate SDC, due to the relatively lower debris temperatures calculated for this sequence. The debris bed forms later in time, due to the delay in core heatup until after firewater injection is stopped, and remains in the active fuel region for a shorter time than predicted for the station blackout scenarios without firewater addition and with failure to isolate SDC.

Figure 4.3.3.6 shows both the total and the individual masses of core materials (UO_2, zircaloy and ZrO_2, stainless steel and steel oxide, and control rod poison) remaining in the vessel. This includes both material in the active fuel region and in the lower plenum. Debris ejection began very soon after lower head failure. This figure illustrates that most of the core material was lost from the vessel to the cavity quickly, in step-like stages. All of the UO_2 was transferred to the cavity within about 1 hr after the initial vessel lower head penetration failure, as was the unoxidized zircaloy, the associated zirconium oxide and the control rod poison. A small fraction (10-15%) of the structural steel in the lower plenum, and some associated steel oxide, was predicted to remain unmelted and in place, more than in the station blackout scenarios without firewater addition and with failure to isolate SDC.

The debris material lost from the vessel is ejected to the drywell pedestal cavity. Figure 4.3.3.7 presents the amounts of ejected core debris, concrete ablated and the total cavity debris mass (i.e., core debris combined with concrete ablation products). As in the other sequences analyzed, concrete ablation is quite rapid soon after debris ejection while the core debris is hot (>2000 K) and consists of a layer of metallic debris above a heavy oxide layer, and then slows noticably after enough concrete has been ablated for the debris bed configuration to invert to a light oxide layer above a layer of metallic debris, mixed to a lower average temperature of ~1500 K.

The calculated production of steam and noncondensable gases (H_2, CO, CO_2 and H_2O) is depicted in Figure 4.3.3.8. The hydrogen production shown includes both in-vessel production (the initial step increase) and ex-vessel production in the cavity (the later-time increase). The in-vessel hydrogen generation corresponds to the oxidation of about 15% of the zircaloy and about 1% of the steel in the core and lower plenum, prior to vessel failure and debris ejection. As soon as the core debris enters the cavity, core-concrete interaction begins, resulting in the production of carbon dioxide and hydrogen; reduction of these gases by the molten metal in the core debris also gives rise to carbon monoxide and hydrogen. The generation rates and amounts of these gases produced, and the amount of concrete ablated, are generally similar in this station blackout sequence with 10hr of firewater addition followed by a high pressure boiloff to the corresponding rates and amounts calculated in the station blackout scenarios with failure to isolate SDC and no firewater addition, described in the previous section.

The mole fractions in the drywell, containment dome and auxiliary building (first and second floors) are shown in Figure 4.3.3.9, including vertical dotted lines at auxiliary building failure and at vessel failure for reference. The mole fractions in the cavity resemble the behavior shown for the drywell; the mole fractions in the containment equipment hatch are very similar to those shown for the containment dome. and the mole fractions in the upper floors of the auxiliary building generally resemble the behavior shown for the second floor of the auxiliary building (but with more steam higher in the auxiliary building late in time and correspondingly less nitrogen). The inner containment atmosphere consists mostly of steam, building up rapidly after the SRVs are first locked open and later cycle in the relief mode, decreasing somewhat after vessel failure and noncondensable gas generation due to core-concrete interaction, but remaining more than half steam throughout the transient period simulated. The outer containment steam concentration begins rising slowly when the SRVs are locked open and later increases rapidly to almost 50% steam after the SRVs begin cycling in the relief mode. The containment is open to the auxiliary building in the second and fourth floors. The atmosphere in the dead-end first floor of the auxiliary building remains near ambient with small fractions of steam and noncondensables added from the upper floors; higher in the auxiliary building the atmosphere composition closely resembles that in the outer containment (because the containment equipment hatch and both of the containment personnel locks are

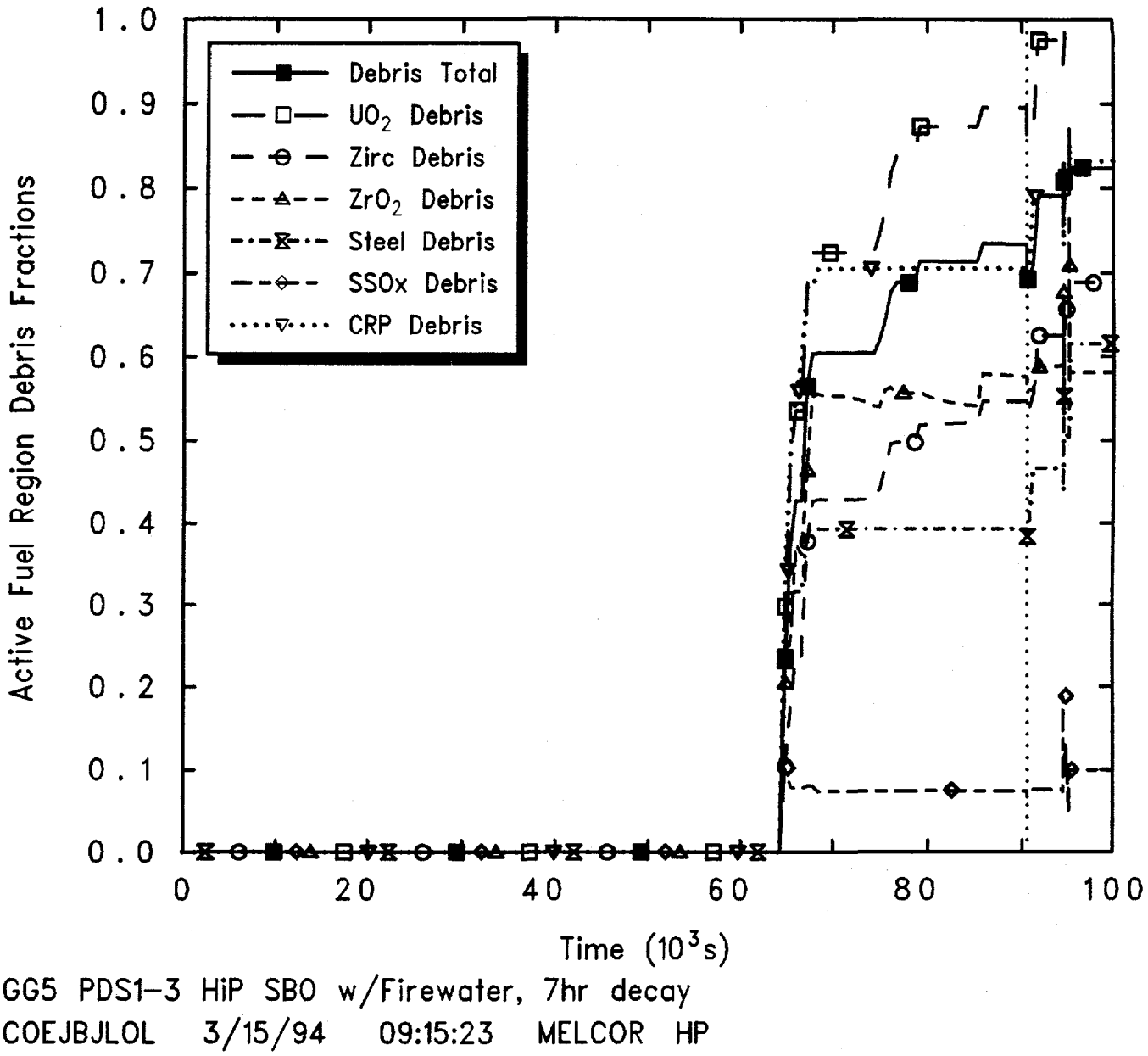

Figure 4.3.3.5. Core Active Fuel Region Degraded Material Fractions for Grand Gulf POS 5 -- Station Blackout with Firewater Addition Followed by High Pressure Boiloff, Initiated 7 hr After Shutdown.

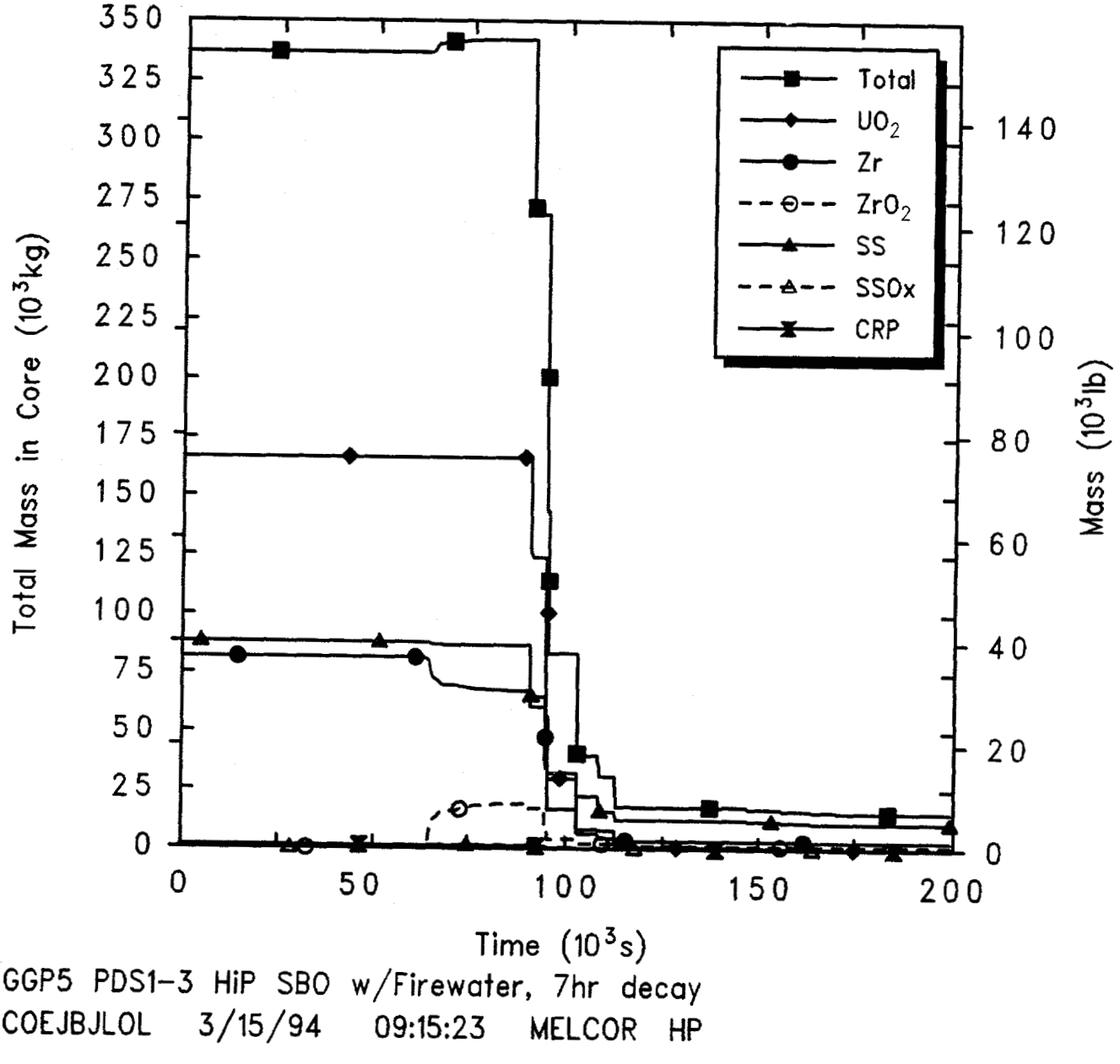

Figure 4.3.3.6. Total and Individual Core Material Masses for Grand Gulf POS 5 -- Station Blackout with Firewater Addition Followed by High Pressure Boiloff, Initiated 7 hr After Shutdown.

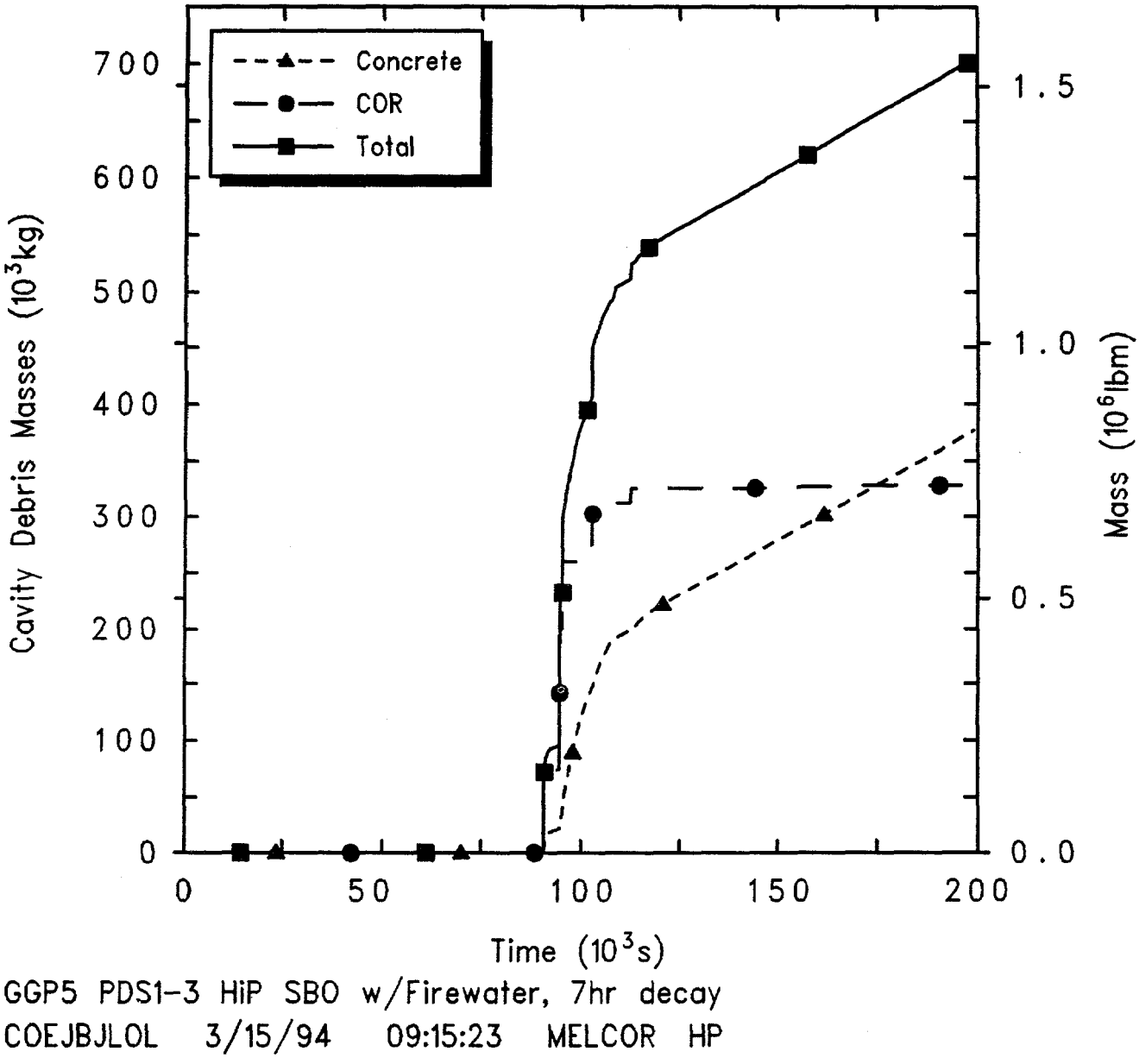

Figure 4.3.3.7. Cavity Total and Core and Concrete Debris Masses for Grand Gulf POS 5 -- Station Blackout with Firewater Addition Followed by High Pressure Boiloff, Initiated 7 hr After Shutdown.

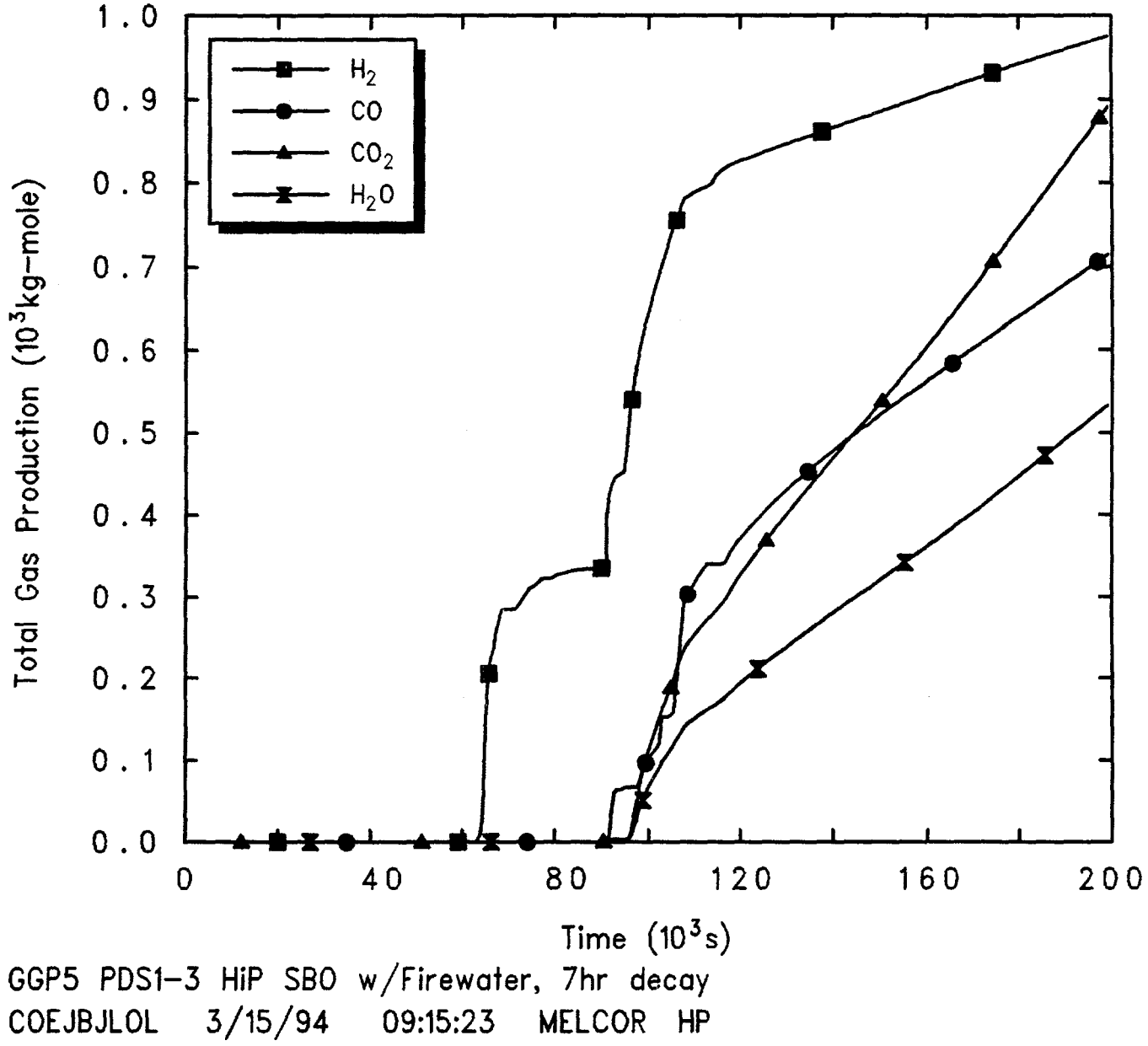

Figure 4.3.3.8. Hydrogen, Carbon Monoxide, Carbon Dioxide and Steam Generation for Grand Gulf POS 5 -- Station Blackout with Firewater Addition Followed by High Pressure Boiloff, Initiated 7 hr After Shutdown.

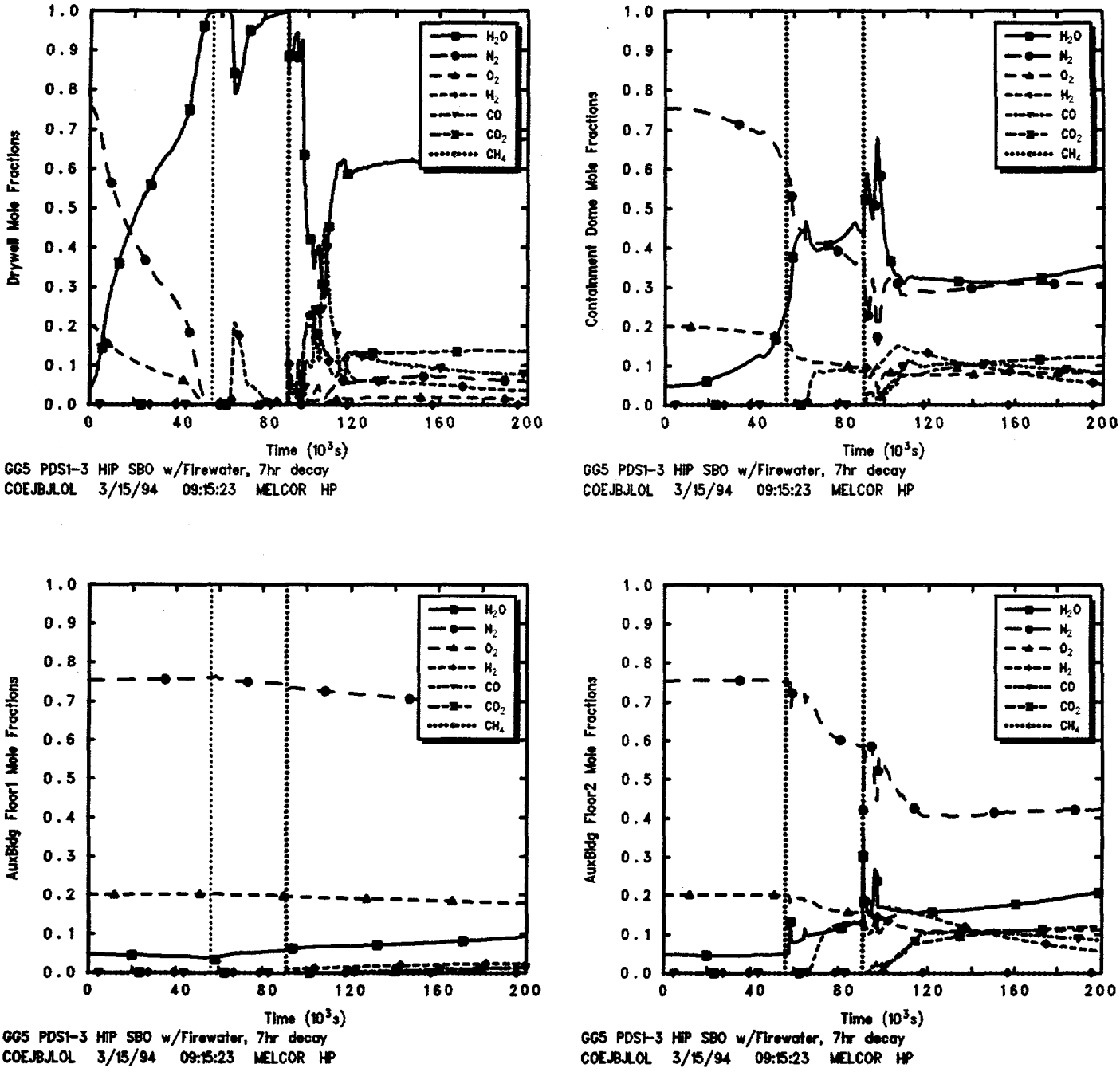

Figure 4.3.3.9. Mole Fractions in Drywell (upper left), Containment Dome (upper right), and Auxiliary Building First Floor (lower left) and Second Floor (lower right) for Grand Gulf POS 5 - Station Blackout with Firewater Addition Followed by High Pressure Boiloff, Initiated 7 hr After Shutdown

open), but with more steam and core-concrete interaction noncondensables higher in the auxiliary building late in time and correspondingly less nitrogen and oxygen.

Figure 4.3.3.10 illustrates the time-dependent release of radionuclides from the fuel debris both within the vessel and in the cavity. The vertical dotted lines within the plots mark the time of vessel failure, indicating that most of the in-vessel release occurs prior to vessel failure, from the hot debris bed in the active fuel region, while most of the ex-vessel release occurs within a short time period after vessel failure and debris ejection to the cavity, while the core debris is still hot, before enough concrete has been ablated for the debris bed configuration to cool and invert; this behavior is seen in most of our MELCOR analyses. Table 4.3.3.2 summarizes the in-vessel, ex-vessel and total amounts of each radionuclide class released, all normalized as mass fractions of the initial inventories of each class. (Note that these amounts generally consider only the release of radioactive forms of these classes, and not additional releases of nonradioactive aerosols from structural materials.)

The release behavior predicted by MELCOR can be grouped into several subdivisions. Almost all (~100%) of the volatile Class 1 (noble gases), Class 2 (CsOH), Class 5 (Te) and Class 16 (CsI) radionuclide species are released, primarily in-vessel, as are most (80-90%) of the Class 3 (Ba) and Class 12 (Sn) inventories. The next major release fraction, dropping rapidly with lower decay heat levels and cooler debris is for uranium. Around 0.1-2% of the total inventories of Ru and Mo, Ce and La, are released. Finally, a total ≤0.01% of the initial inventory of Class 11 (Cd) is predicted to be released. Note that the CORSOR-M fission product release model option used in these analyses has identically zero release in-vessel of Class 7 (Mo), Class 9 (La) and Class 11 (Cd).

Figure 4.3.3.11 gives the total radioactive release to the environment in these two cases. The release fractions of individual classes to the environment are shown in Figure 4.3.3.12. The release to the environment begins before vessel failure in this sequence. Fission products released during the in-vessel core heatup and degradation process are transported to the containment through the cycling SRVs and the open RPV vent line; they then move from the containment to the auxiliary building through the open containment equipment hatch and personnel locks, and can escape to the environment as soon as the auxiliary building fails (at about 56,000 s or 15-16 hr). These environmental releases do not correspond to immediate release of all radionuclides released from the fuel; there is considerable retention of most radionuclide species within the containment and auxiliary building (as discussed below). The noble gases have the greatest releases (>90%) to the environment by the end of the transient period simulated, because gaseous forms are not scrubbed, filtered, deposited or otherwise retained; in addition, there is some release to the environment of the other volatile species (i.e., CsOH, CsI and Te) also, although these are found mostly in aerosol form and are largely retained in the containment. (Note that most of the retention was in the auxiliary building in the station blackout sequences with failure to isolate SDC because that was where the outlet of the SDC break was located; most of the retention is in the containment in this station blackout scenario with firewater addition followed by a high pressure boiloff because in this case the outflow is primarily through the SRVs, the open RPV head vent and the vessel lower head penetration failures, which all go to the containment.)

Table 4.3.3.3 summarizes the distribution of the initial radionuclide inventory, as mass fractions of the initial inventories, at the end of the two calculations initiated at different times after shutdown; they provide an overview of how much of the radionuclides remain bound up in fuel debris in either the core or the cavity, and of how much of the released radionuclides is retained in the primary system *vs* how much of the released radionuclides is released to, or released in, either the containment or the auxiliary building and the environment, all normalized to the initial inventories of each class. Table 4.3.3.4 presents a different breakdown of the released radionuclide final distribution, giving the fractions of released inventory for each class in control volume atmospheres (including the environment), in pools, or deposited or settled onto heat structures at the end of the calculations. (As in Table 4.3.3.2 these amounts consider only the release of radioactive forms of these classes, and not additional releases of nonradioactive aerosols from structural materials.)

These tables show fission product distributions somewhat different than those found for any of the other sequences analyzed, for the radionuclides with significant (≥80% of initial inventory) release from fuel. As in all the accident scenarios analyzed, most of the noble gases released are in the environment, in the atmosphere. Significant fractions of the volatile species (CsOH, CsI and Te) released are retained everywhere, in the primary system (15-35%), containment (40-50%), and auxiliary building (20-25%);

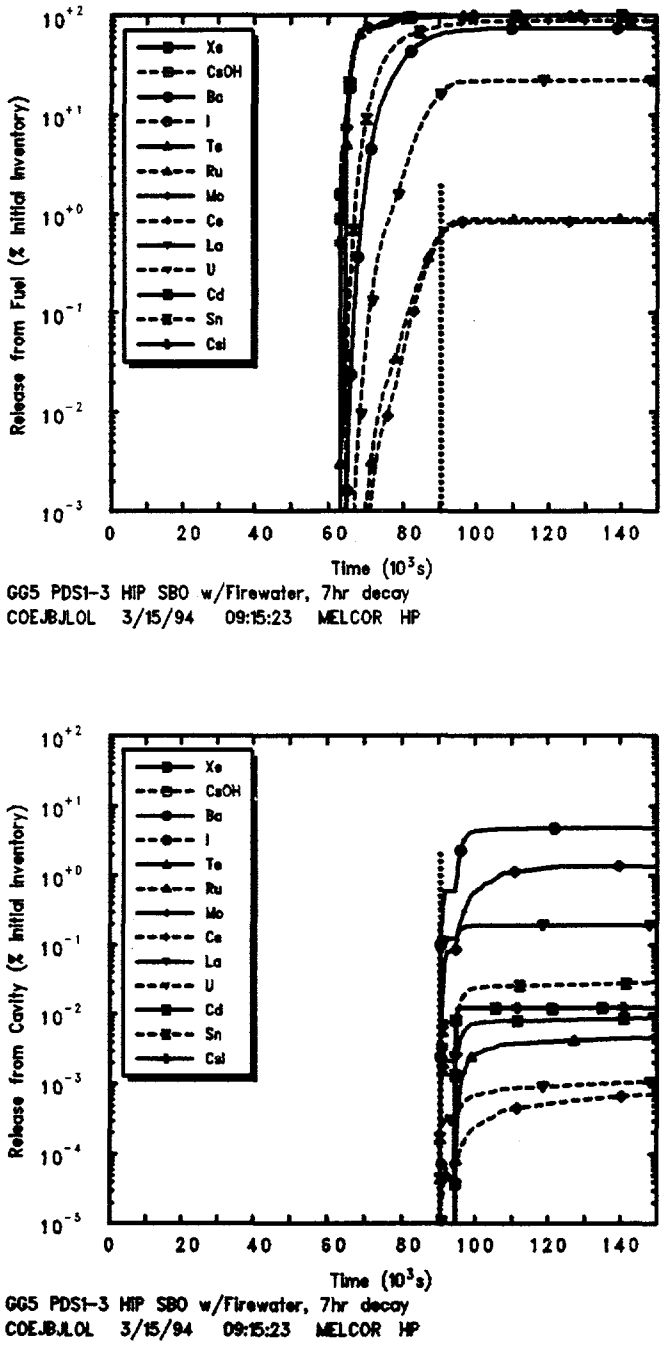

Figure 4.3.3.10. In-Vessel (top) and Ex-Vessel (bottom) Radionuclide Release Mass Fractions for Grand Gulf POS 5 -- Station Blackout with Firewater Addition Followed by High Pressure Boiloff, Initiated 7 hr After Shutdown.

Table 4.3.3.2. Final Radionuclide Release Fractions for Grand Gulf POS 5 -- Station Blackout with Firewater Addition Followed by High Pressure Boiloff, Initiated 7 hr After Shutdown

Class	Fission Products Released from Fuel (% Initial Inventory-Mass Fraction)		
	In-Vessel	Ex-Vessel	Total
Xe	99.99	0.0122	~100
CsOH	~100	0.012	~100
Ba	74.83	4.77	79.6
I	~0	~0	~0
Te	99.98	0.0055	99.99
Ru	0.894	3.0e-06	0.894
Mo	0	1.35	1.35
Ce	0.834	0.0009	0.834
La	0	0.192	0.192
U	22.19	0.00126	22.19
Cd	0	0.014	0.014
Sn	88.85	0.049	88.9
CsI	99.99	0.0124	~100

about 5% of the total initial inventories of these volatiles is released to the environment in this case, an environmental release similar to that for the other station blackout sequence analyzed, with failure to isolate SDC and no firewater addition (discussed in the previous section). The two classes of radionuclides forming aerosols which had substantial in-vessel releases (Ba and Sn) also were predicted to have substantial fractions retained everywhere, slightly more in the primary system (35-45%), about the same in containment (40%), and significantly less in the auxiliary building (2-2.5%).

4.3.4 Low Pressure Boiloff with Flooded Containment, Initiated 7 hr and 24 hr After Shutdown

At the initiation of the accident, the reactor vessel is depressurized. Following the initiating event, two SRVs are opened. For this scenario, the vessel and containment are flooded, i.e., the vessel water level is at the steam lines, 16.46 m or 648 in, and the containment (suppression pool, pedestal cavity and drywell) is flooded up to the lower personnel lock, 9.65 m (31.67 ft) above the suppression pool floor. The vessel water inventory is at 300.5 K (80°F), as is the suppression and containment water; the containment is at 305.4 K (90°F). Since the lower personnel lock is open, the auxiliary building is flooded which results in the loss of all core cooling. The reactor pressure vessel head vent is closed at the beginning of the transient. Since both the drywell and the containment hatches are open, the drywell is open to the containment and the containment is open to the auxiliary building (i.e., "open containment").

This sequence is almost identical to the low-pressure boiloff scenario discussed in Section 4.2.2 except that in those Level 1 analyses the containment was dry while in these Level 2 analyses the containment was assumed to be flooded.

The sequence of events predicted by MELCOR for this accident with different initiation times is given in Table 4.3.4.1.

Figure 4.3.4.1 gives the vessel pressures calculated starting this accident scenario at two different times after shutdown. In both cases, the system begins pressurizing

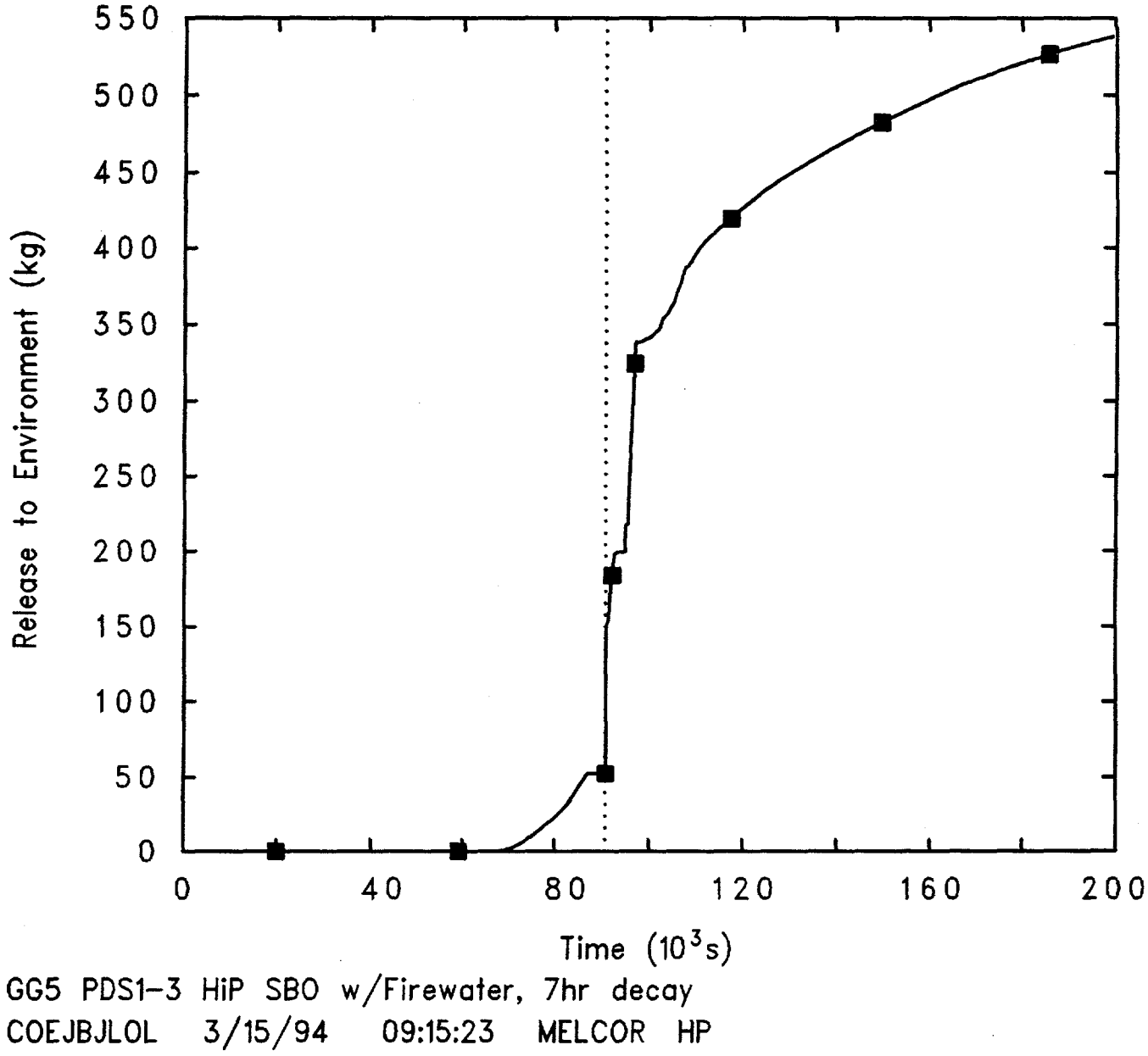

Figure 4.3.3.11. Total Environmental Radionuclide Releases for Grand Gulf POS 5 -- Station Blackout with Firewater Addition Followed by High Pressure Boiloff, Initiated 7 hr After Shutdown.

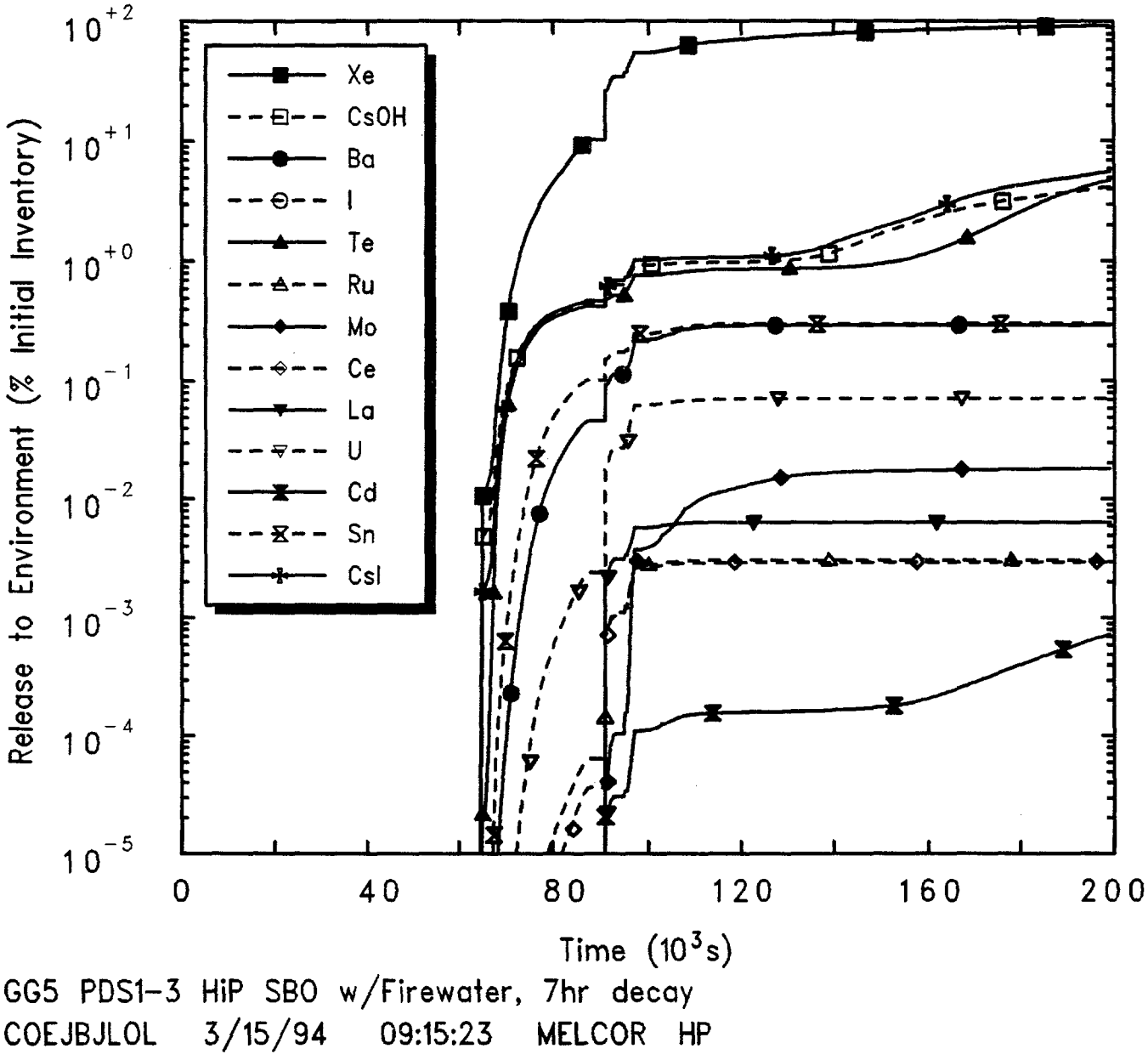

Figure 4.3.3.12. Environmental Radionuclide Release Mass Fractions for Grand Gulf POS 5 -- Station Blackout with Firewater Addition Followed by High Pressure Boiloff, Initiated at 7 hr After Shutdown.

Table 4.3.3.3. Final Radionuclide Distribution for Grand Gulf POS 5 -- Station Blackout with Firewater Addition Followed by High Pressure Boiloff, Initiated at 7 hr After Shutdown

Class	Fission Product Distribution (% Initial Inventory-Mass Fraction)				
	Fuel Debris	Primary System	Containment	Auxiliary Building	Environment
Xe	~0	0.007	2.49	5	92.5
CsOH	~0	33.6	42.6	19.68	4.11
Ba	20.4	33.1	43.9	2.34	0.294
Te	0.009	34.1	42.1	19.08	4.7
Ru	99.1	0.307	0.57	0.0125	0.00305
Mo	98.6	0.095	1.04	0.19	0.018
Ce	99.2	0.282	0.54	0.0121	0.0029
La	99.8	0.02	0.144	0.022	0.0063
U	79.6	7.13	12.95	0.303	0.0654
Cd	~100	0.0095	0.062	0.003	0.0007
Sn	11.1	45	41.02	2.67	0.303
CsI	~0	16.3	53.42	24.72	5.54

as all core cooling is lost but only pressurizes slightly before the steam flow out the two open SRVs is sufficient to remove all the decay heat; the higher the decay heat (i.e., the sooner after shutdown), the higher the early-time pressure peak before the flow out the open SRVs can fully remove the decay heat. The steam flow out the two open SRVs in turn pressurizes the containment and, through the open equipment hatch and personnel locks, pressurizes the auxiliary building, as shown in Figure 4.3.4.2. The longer after shutdown that this accident sequence begins, the lower the decay heat and the longer it takes to fail the auxiliary building.

The coolant inventory in the vessel drops as the decay heat boils water to steam which is lost out the open SRVs, faster for the higher decay heat level than for the lower decay heat, as presented in Figure 4.3.4.3.

Figure 4.3.4.4 presents the upper plenum, core and lower plenum swollen and collapsed liquid levels for this accident sequence initiated at two different times after shutdown. The upper plenum collapsed level initially falls but the two-phase level rises as the primary system pressurizes. There is considerable pool frothing and swelling in both the upper plenum and core volumes and the vessel inventory is boiled away. Both the initial, more rapid level drop in the core and upper plenum and the later, gradual lower plenum uncovery due to continued boiloff is faster for higher decay heat levels than for lower decay heat levels. The lower plenum levels still show substantial amounts of liquid remaining at vessel failure, when that water is either flashed to steam by the falling core debris or drains into the cavity through the failed lower head penetrations.

The heatup of the intact fuel and clad is illustrated in Figures 4.3.4.5 and 4.3.4.6 as calculated for scenarios initiated at 7 hr and 24 hr after shutdown, respectively. Core uncovery and heatup begins sooner and proceeds more rapidly at the higher decay heat level resulting from beginning this accident 7 hr after shutdown than for a lower decay heat in the same accident initiated 24 hr after shutdown, as would be expected. The fuel/clad component temperatures in MELCOR are set to zero in a cell when that component fails, so these figures show both the overall heatup rate and the time that the intact fuel/clad component fails through melting of the clad. The intact fuel/clad component temperatures reach a peak

Table 4.3.3.4. Final Radionuclide State for Grand Gulf POS 5 -- Station Blackout with Firewater Addition Followed by High Pressure Boiloff, Initiated 7 hr After Shutdown

Class	Fission Products Released from Fuel (% Released Inventory-Mass Fraction)		
	Atmosphere	Pool	Deposited
Xe	~100	0	0
CsOH	13.26	42.9	43.9
Ba	0.37	24.8	74.8
I	~100	0	0
Te	17.04	39.6	43.3
Ru	0.34	25.7	74.1
Mo	1.35	46.4	52.3
Ce	0.36	25.7	73.9
La	0.33	49.7	47
U	0.32	25.5	74.2
Cd	15.66	37.8	46.5
Sn	0.35	22.1	77.6
CsI	21.78	48.9	29.3

of ≥2000 K (≥3140°F) since the component generally fails at the zircaloy clad melt temperature, taken as 2098 K (3317°F) in MELCOR.

Figures 4.3.4.7 and 4.3.4.8 present corresponding core debris temperatures in the active fuel region calculated for scenarios initiated at 7 hr and 24 hr after shutdown, respectively; these are the temperatures of the debris bed formed by the failure of the intact fuel/clad component in MELCOR in a core cell, whose (intact) temperatures were given in Figures 4.3.4.5 and 4.3.4.6. The debris bed in the active fuel region reaches peak temperatures ≥3500 K (5840°F), significantly above the UO_2 melt temperature of 3113 K (5144°F), in the middle and upper active fuel regions; in the lower active fuel levels the debris bed temperatures remain below the UO_2 melt temperature. The debris bed temperatures reached in the active fuel region are visibly higher for the accident initiated at a higher decay heat level than at the lower decay heat level.

The temperatures of the active fuel region debris bed drop to zero when the core plate fails and the debris relocates to the lower plenum. The predicted temperatures in the debris bed in the lower plenum and core plate are given in Figures 4.3.4.9 and 4.3.4.10 for scenarios initiated at 7 hr and 24 hr after shutdown, respectively. In both cases, prior to core plate failure there is some cold, refrozen debris both on the core support plate and on the lower core structural material just above the core support plate; the cooling and refreezing of this debris is the cause of the continued gradual drop in lower plenum liquid level due to steaming seen in Figure 4.3.4.4. The debris temperature rises gradually to the core support plate failure temperature of 1273 K (1832°F). After core plate failure hot, high-temperature debris begins appearing in the lower plenum as debris falls from the active fuel region into the lower plenum. With the new debris radial relocation model added in MELCOR 1.8.2, the core plate needs to fail in only one ring before debris from cells in the active fuel region in all radial rings can flow sideways and down, fall through the failed plate, and then spread sideways into cells in the lower plenum in all radial rings. (Thus a lower head penetration can now fail in a ring before the core plate in that ring fails.) The lower head penetrations begin failing almost

Table 4.3.4.1. Sequence of Events Predicted by MELCOR for Low-Pressure Boiloff with Flooded Containment, Initiated 7 hr and 24 hr After Shutdown

Event	Time After Shutdown 7 hr	24 hr
Accident initiation	0	0
Core uncovery (TAF) begins	10,262 s (2.85 hr)	14,339 s (3.98 hr)
Core heatup begins	22,000 s (6.11 hr)	28,500 s (7.92 hr)
Clad failure/Gap release		
(Ring 1)	27,154 s (7.54 hr)	36,361 s (10.10 hr)
(Ring 2)	27,055 s (7.52 hr)	36,260 s (10.07 hr)
(Ring 3)	27,167 s (7.55 hr)	36,383 s (10.11 hr)
(Ring 4)	27,723 s (7.70 hr)	36,963 s (10.27 hr)
(Ring 5)	29,374 s (8.16 hr)	38,565 s (10.71 hr)
(Ring 6)	32,139 s (9.48 hr)	42,863 s (11.91 hr)
Core plate failed		
(Ring 1)	89,990 s (25.00 hr)	112,516 s (31.25 hr)
(Ring 2)	89,164 s (24.77 hr)	111,475 s (30.97 hr)
(Ring 3)	88,949 s (24.71 hr)	112,350 s (31.21 hr)
(Ring 4)	88,000 s (24.44 hr)	112,785 s (31.33 hr)
(Ring 5)	83,548 s (23.21 hr)	110,645 s (30.73 hr)
(Ring 6)	82,308 s (22.86 hr)	109,936 s (30.54 hr)
Vessel LH penetration failed		
(Ring 1)	82,534 s (22.93 hr)	110,098 s (30.58 hr)
(Ring 2)	82,446 s (22.90 hr)	110,065 s (30.57 hr)
(Ring 3)	82,421 s (22.89 hr)	110,047 s (30.57 hr)
(Ring 4)	82,406 s (22.89 hr)	110,034 s (30.57 hr)
(Ring 5)	82,397 s (22.89 hr)	110,025 s (30.56 hr)
(Ring 6)	82,410 s (22.89 hr)	110,302 s (30.64 hr)
Commence debris ejection	82,397 s (22.89 hr)	110,025 s (30.56 hr)
Auxiliary building failed	99,000 s (27.50 hr)	120,000 s (33.33 hr)
Cavity rupture		
End of calculation	400,000 s (111.1 hr)	400,000 s (111.1 hr)

immediately, and the lower plenum debris temperatures begin dropping to zero as debris is ejected from the vessel to the cavity. Some cool, quenched debris can remain present in the lower plenum for a significant period of time, however, as indicated by the 1000-1250 K debris temperatures in the lowest level after vessel failure in the low pressure boiloff scenario initiated 24 hr after shutdown.

Figures 4.3.4.11 and 4.3.4.12 indicate what fraction of each material in the active fuel region has collapsed into a debris rubble bed held up by the core support plate, prior to core plate failure, debris relocation, lower head failure and debris ejection, for this low pressure boiloff with flooded containment initiated at 7 hr and 24 hr after shutdown, respectively. The fractions of each material and the overall fraction of total material in the active fuel

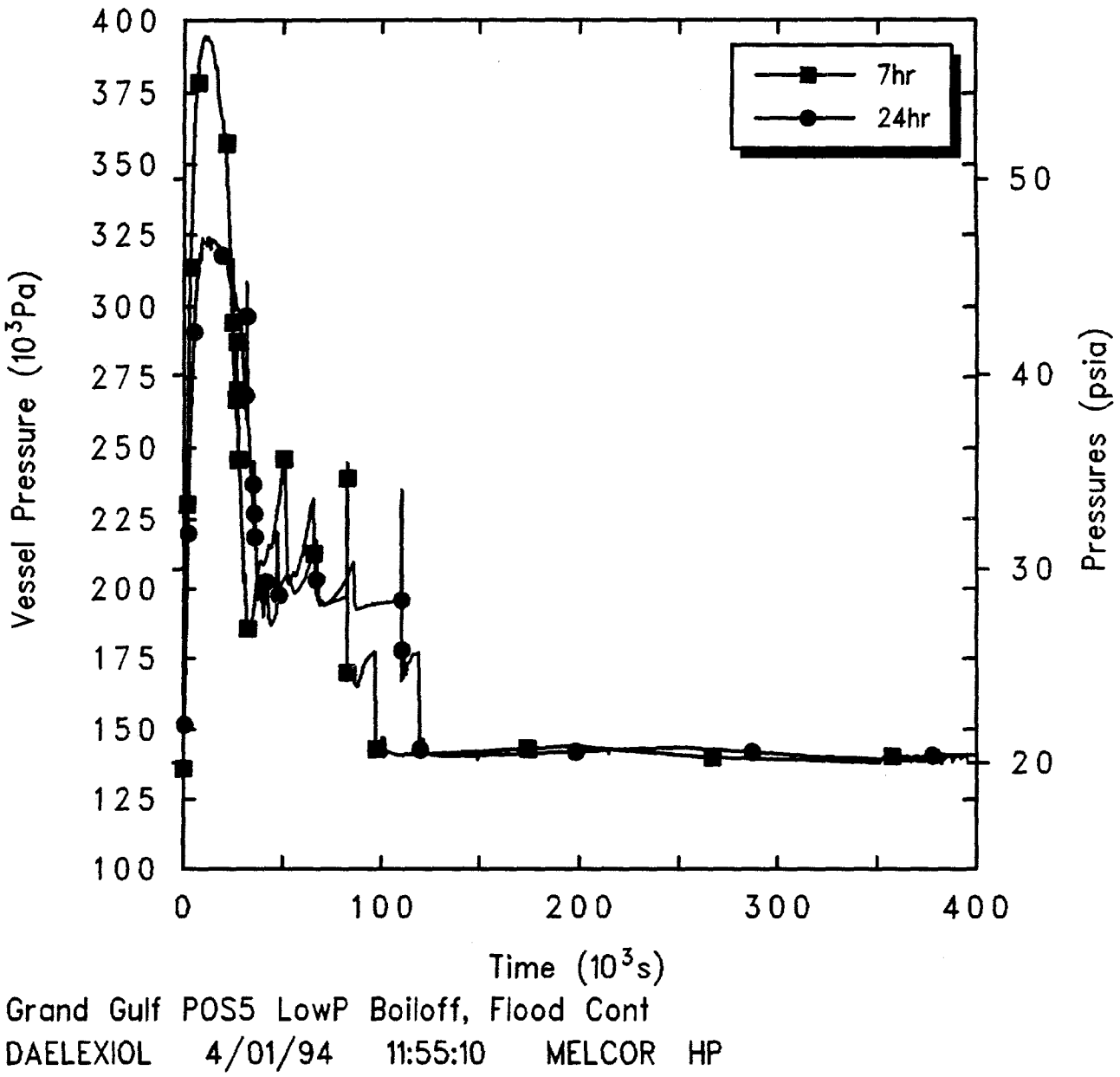

Figure 4.3.4.1. Reactor Vessel Pressures for Grand Gulf POS 5 -- Low Pressure Boiloff with Flooded Containment, Initiated at Various Times After Shutdown.

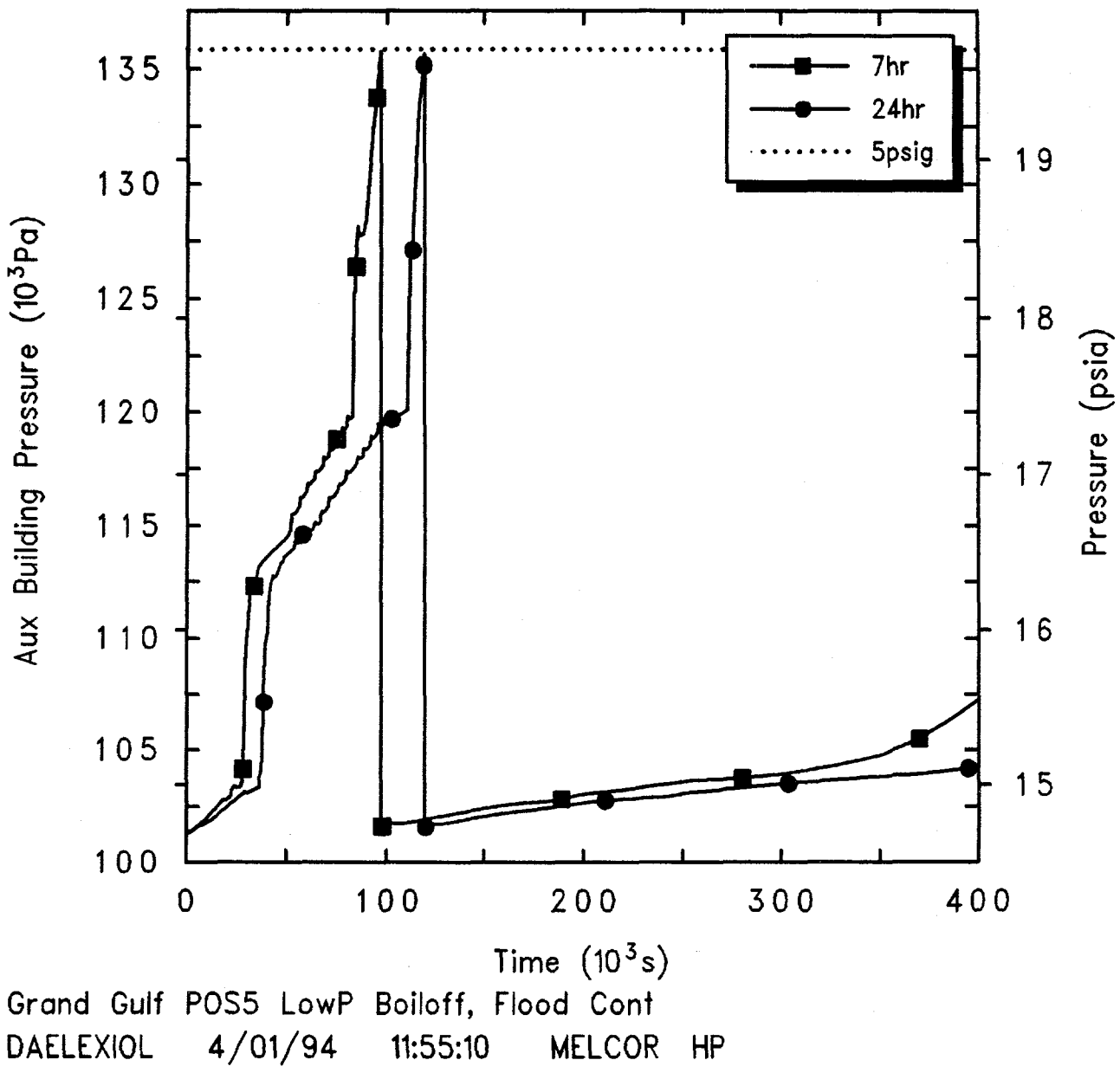

Figure 4.3.4.2. Auxiliary Building Pressures for Grand Gulf POS 5 -- Low Pressure Boiloff with Flooded Containment, Initiated at Various Times After Shutdown.

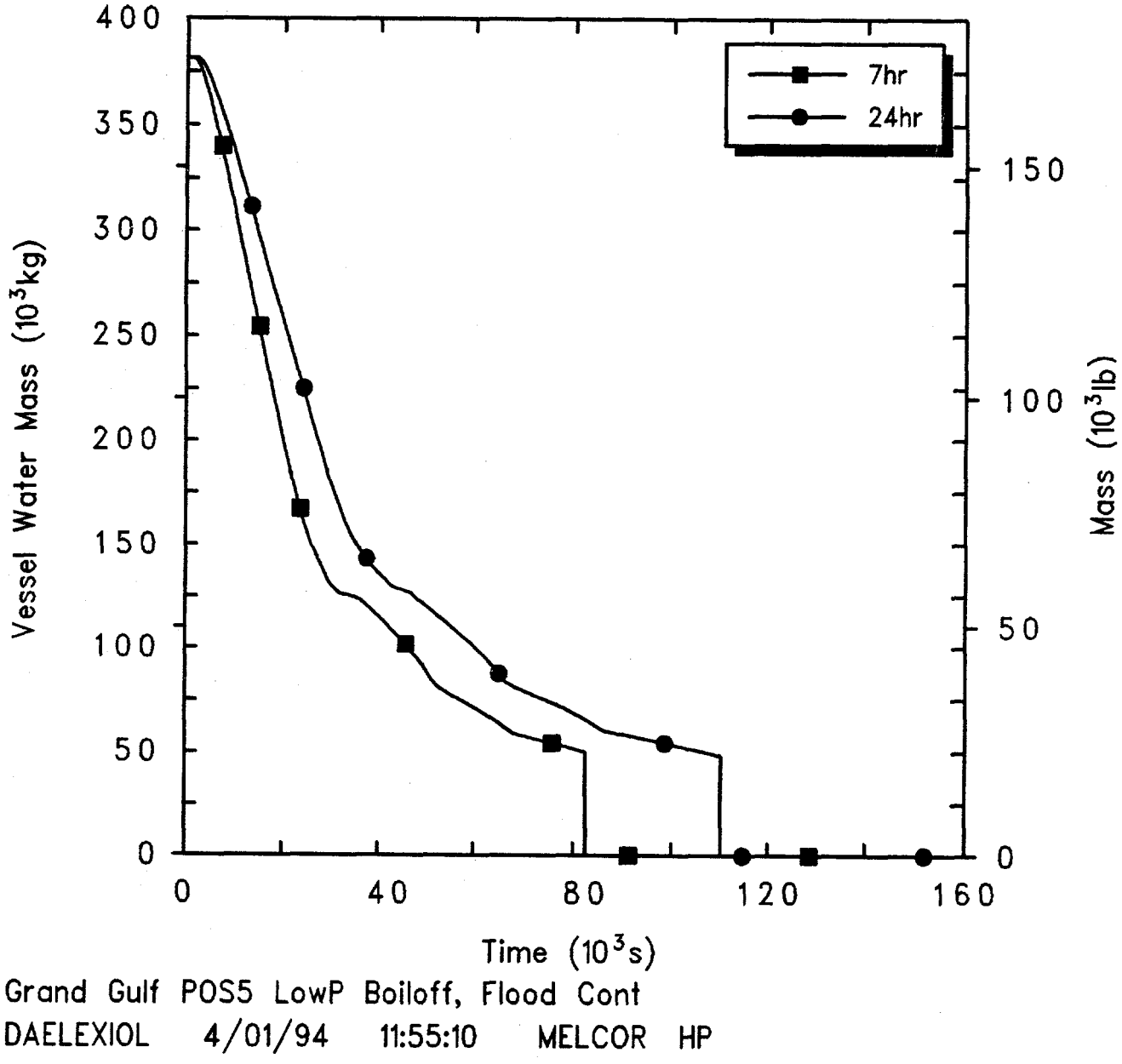

Figure 4.3.4.3. Reactor Vessel Water Masses for Grand Gulf POS 5 -- Low Pressure Boiloff with Flooded Containment, Initiated at Various Times After Shutdown.

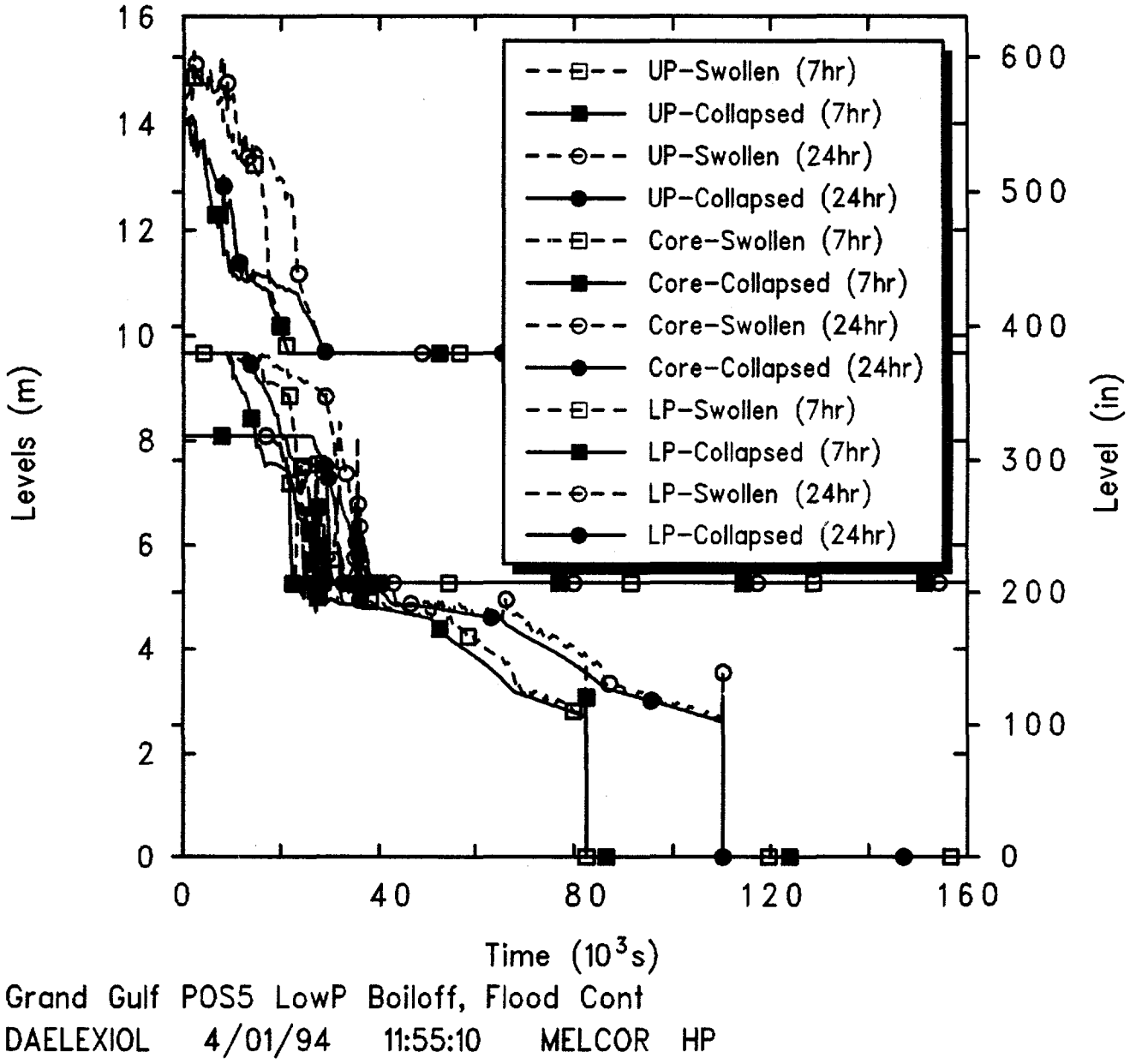

Figure 4.3.4.4. Upper Plenum, Core and Lower Plenum Liquid Levels for Grand Gulf POS 5 -- Low Pressure Boiloff with Flooded Containment, Initiated at Various Times After Shutdown.

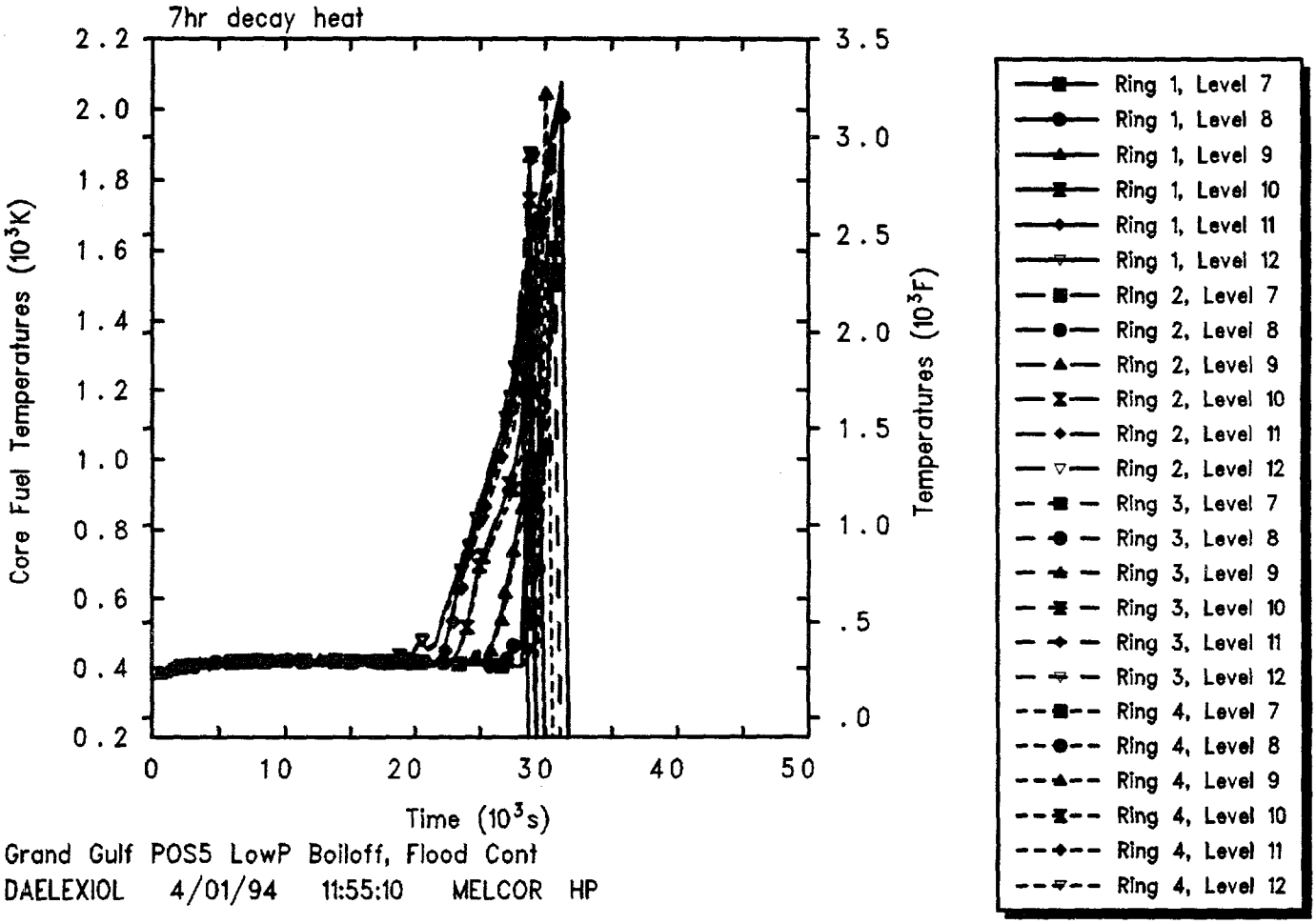

Figure 4.3.4.5. Core Intact Fuel/Clad Temperatures for Grand Gulf POS 5 -- Low Pressure Boiloff with Flooded Containment, Initiated 7 hr After Shutdown.

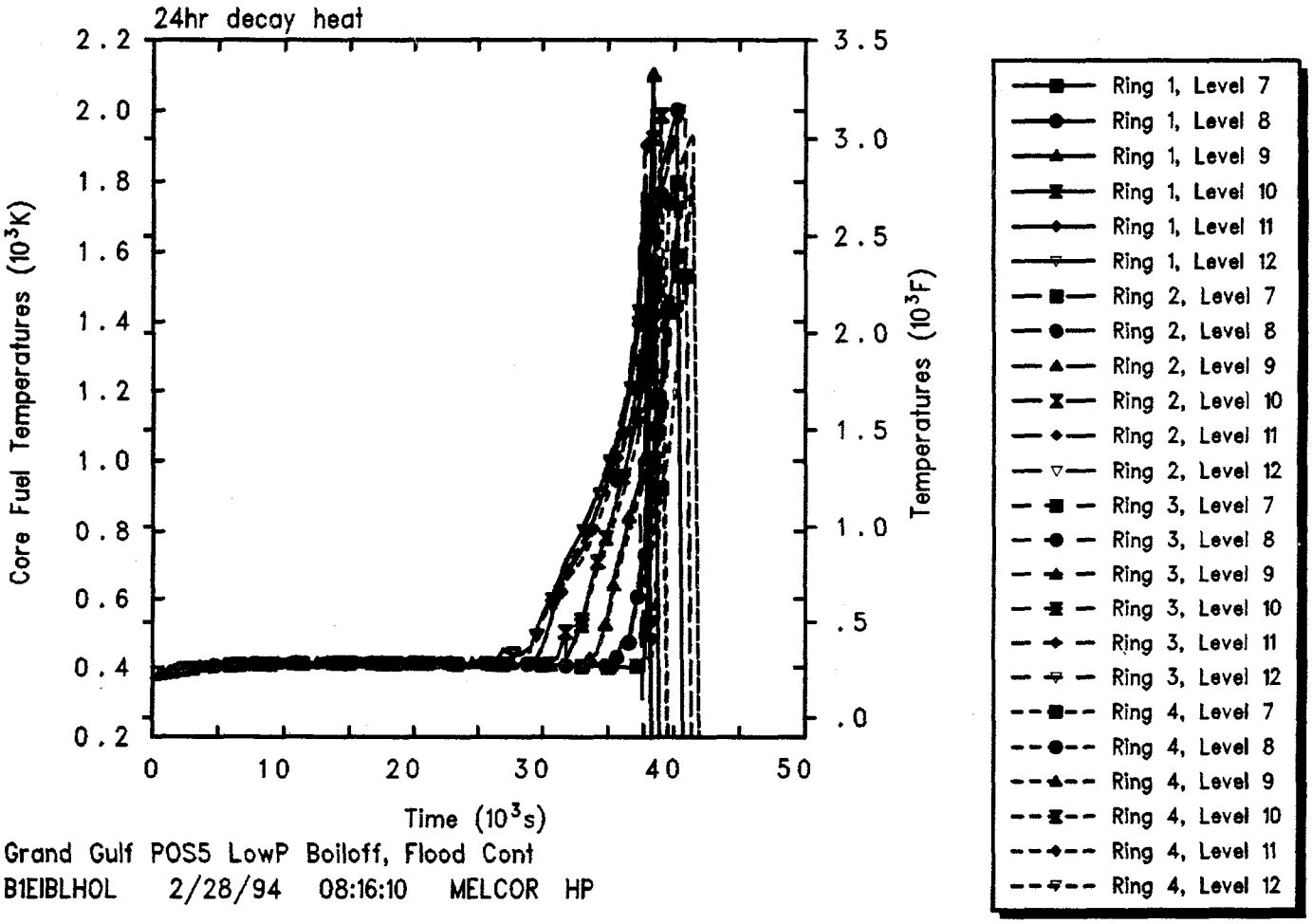

Figure 4.3.4.6. Core Intact Fuel/Clad Temperatures for Grand Gulf POS 5 -- Low Pressure Boiloff with Flooded Containment, Initiated 24 hr After Shutdown.

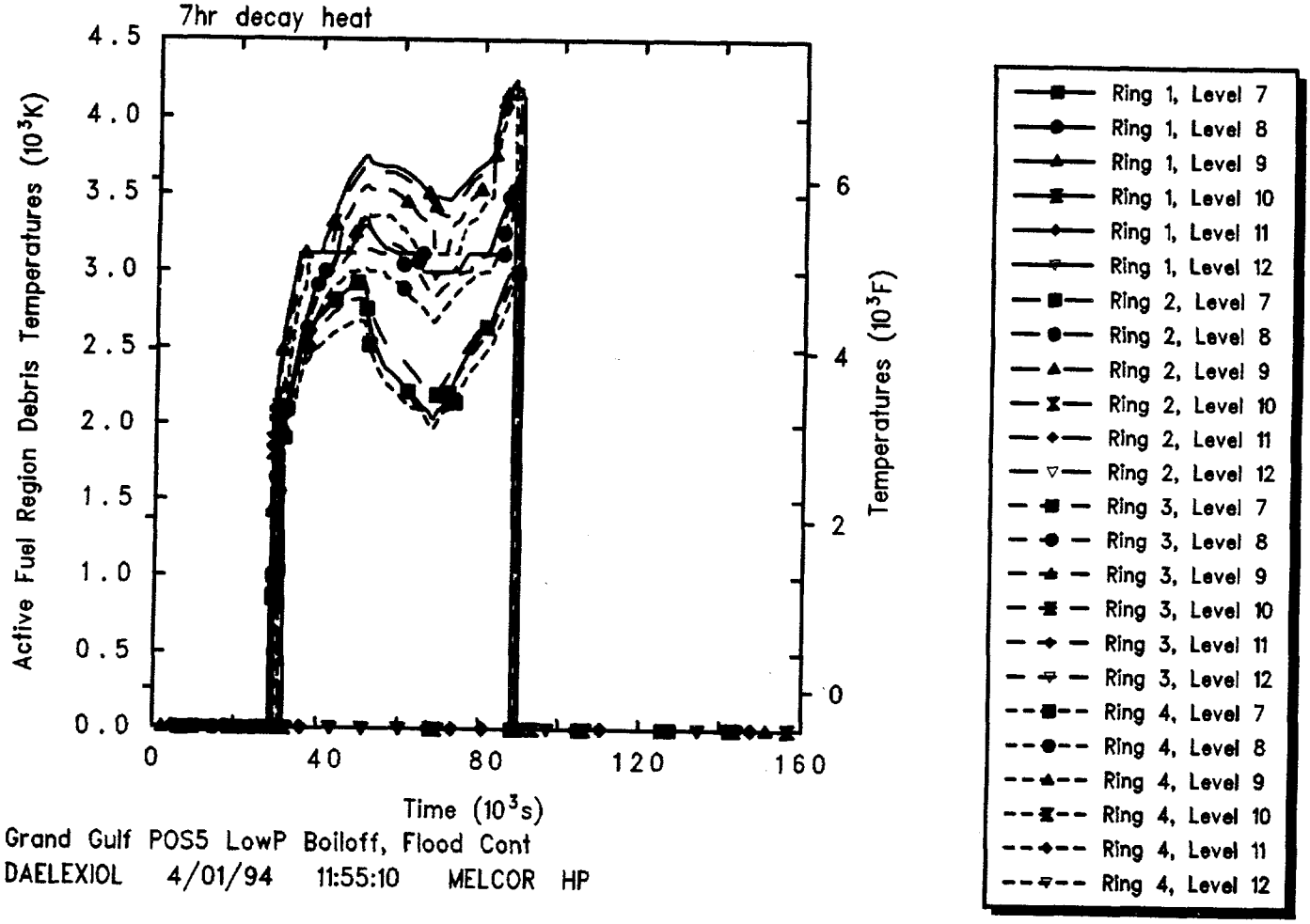

Figure 4.3.4.7. Core Active Fuel Region Debris Bed Temperatures for Grand Gulf POS 5 -- Low Pressure Boiloff with Flooded Containment, Initiated 7 hr After Shutdown.

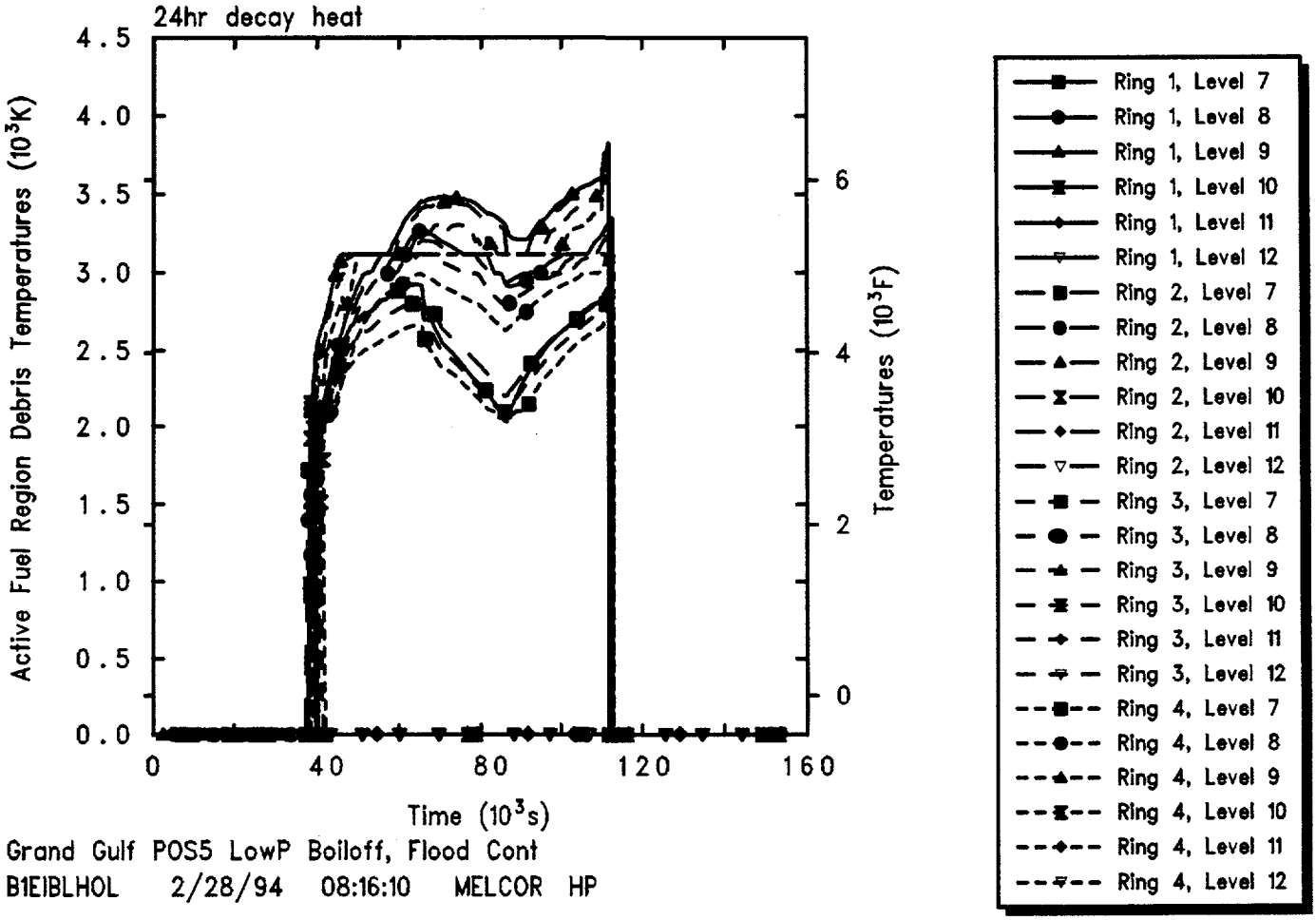

Figure 4.3.4.8. Core Active Fuel Region Debris Bed Temperatures for Grand Gulf POS 5 -- Low Pressure Boiloff with Flooded Containment, Initiated 24 hr After Shutdown.

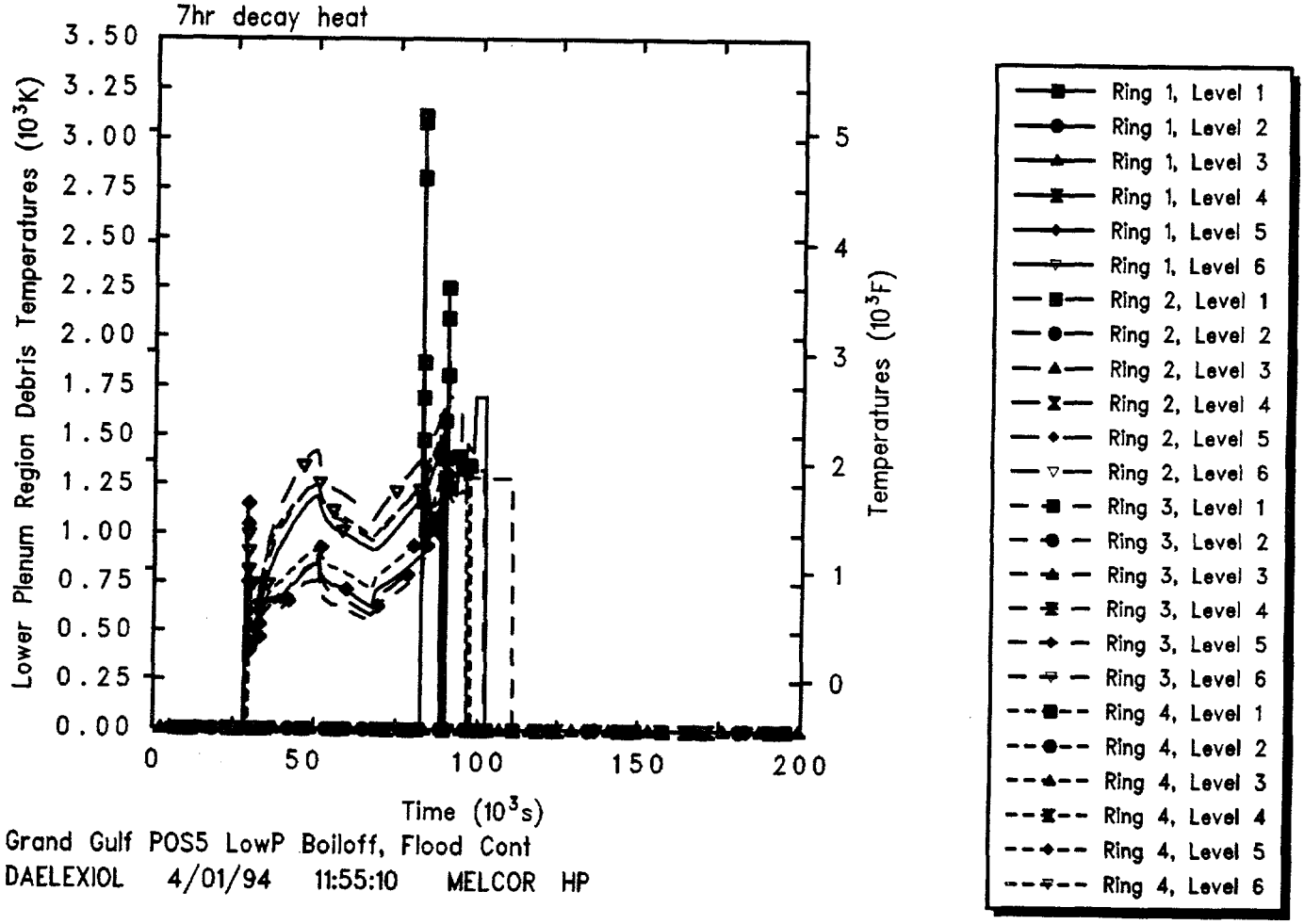

Figure 4.3.4.9. Core Lower Plenum and Core Support Plate Debris Bed Temperatures for Grand Gulf POS 5 -- Low Pressure Boiloff with Flooded Containment, Initiated 7 hr After Shutdown.

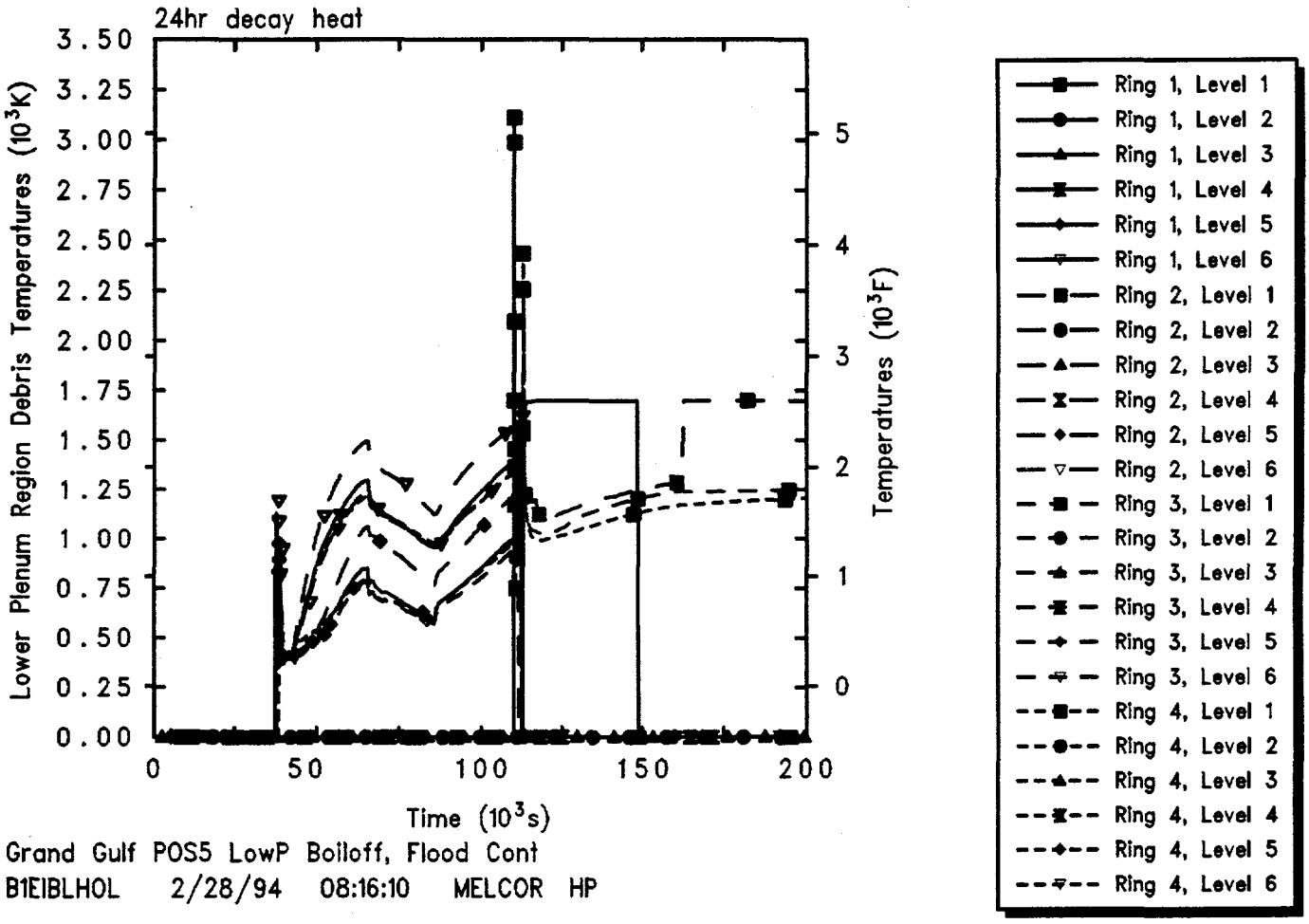

Figure 4.3.4.10. Core Lower Plenum and Core Support Plate Debris Bed Temperatures for Grand Gulf POS 5 -- Low Pressure Boiloff with Flooded Containment, Initiated 24 hr After Shutdown.

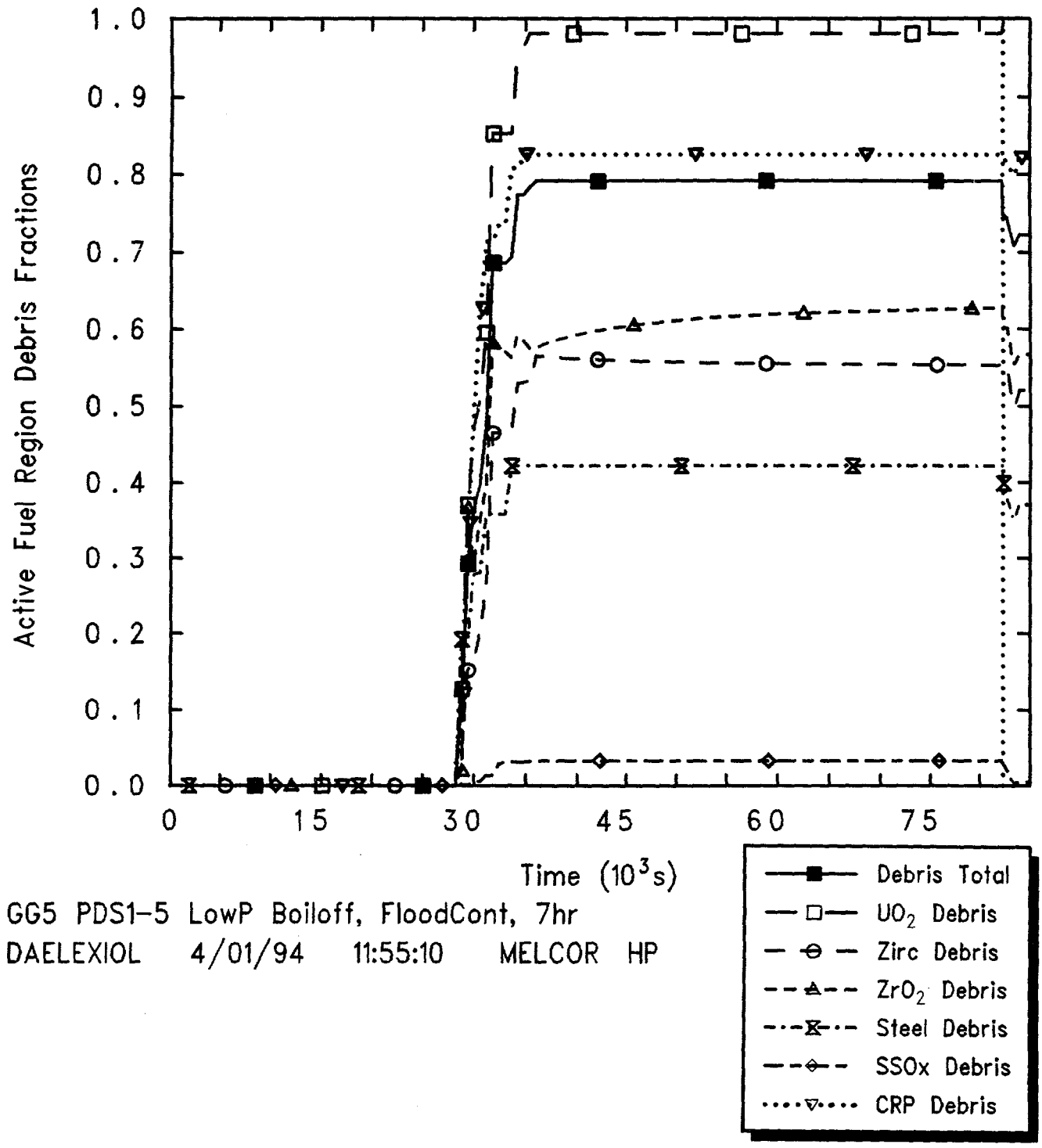

Figure 4.3.4.11. Core Active Fuel Region Degraded Material Fractions for Grand Gulf POS 5 -- Low Pressure Boiloff with Flooded Containment, Initiated 7 hr After Shutdown.

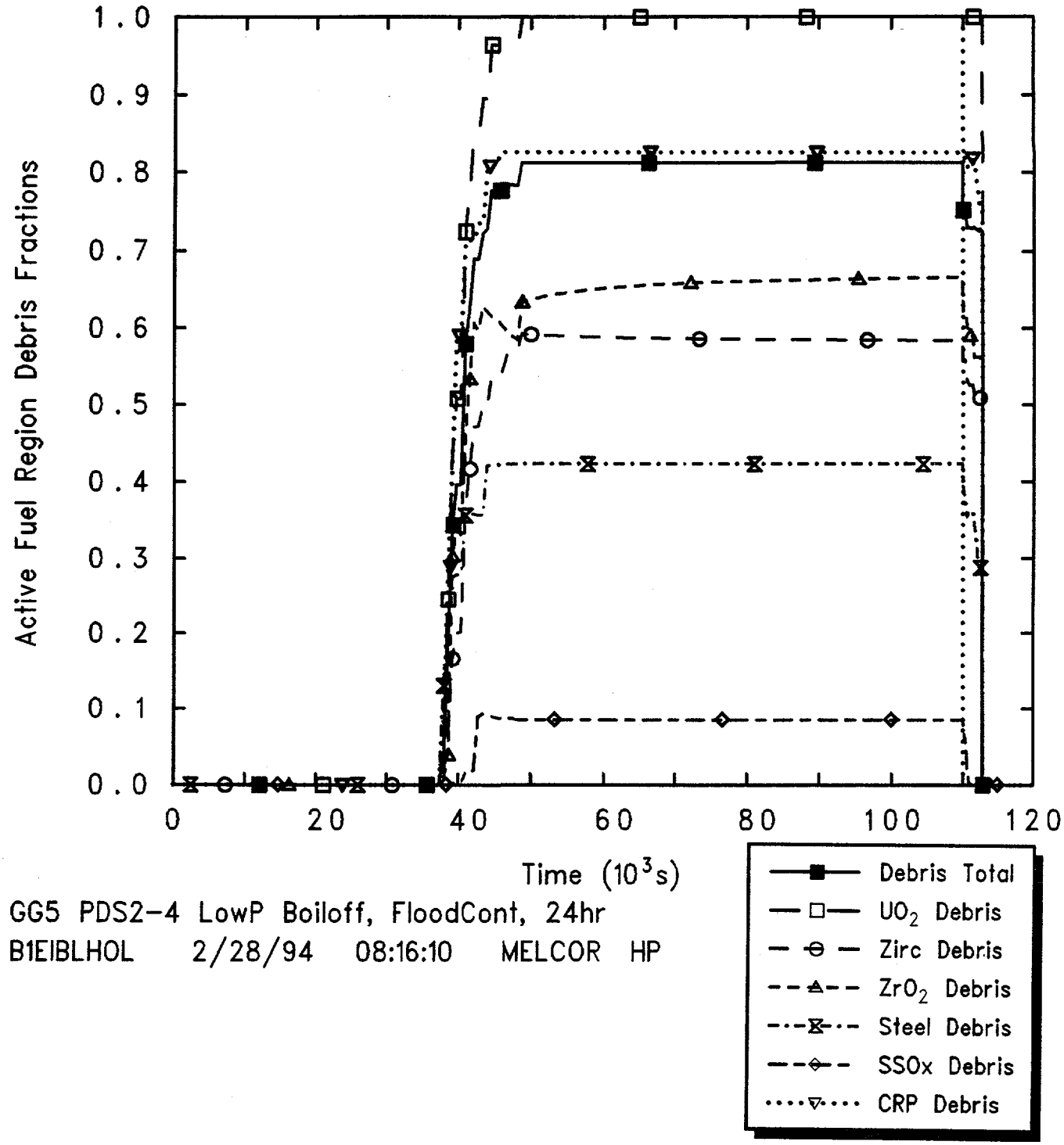

Figure 4.3.4.12. Core Active Fuel Region Degraded Material Fractions for Grand Gulf POS 5 -- Low Pressure Boiloff with Flooded Containment, Initiated 24 hr After Shutdown.

region degraded into particulate debris and are similar in the two calculations. The majority of the debris bed is formed within about 1 hr, and the fractions of material collapsed from the intact geometry to a debris bed then remain very nearly constant for many hours, until vessel failure.

Figure 4.3.4.13 shows the total masses of core materials (UO_2, zircaloy and ZrO_2, stainless steel and steel oxide, and control rod poison) remaining in the vessel. This includes both material in the active fuel region and in the lower plenum. Debris ejection began very soon after lower head failure. This figure illustrates that most of the core material was lost from the vessel to the cavity quickly, in step-like stages. In all cases, all of the UO_2 was transferred to the cavity within ~1 hr after vessel failure, as was the unoxidized zircaloy, the associated zirconium oxide and the control rod poison. A small fraction (15%) of the structural steel in the lower plenum, and some associated steel oxide, was predicted to remain unmelted and in place in the low pressure boiloff scenario initiated 24 hr after shutdown.

Figure 4.3.4.14 presents the amounts of core debris, concrete ablated and the total debris mass (i.e., core debris combined with concrete ablation products) in the cavity. There is a timing shift due to the slower core degradation and later vessel failure at the lower decay heat. Also, since almost all the material in the core active fuel region and lower plenum is ejected in this sequence initiated 7 hr after shutdown while some fraction of the lower plenum structural steel remains unmelted and in place in the same scenario initiated 24 hr after shutdown, the core debris mass in the cavity is slightly greater in the calculation initiated 7 hr after shutdown. However, the mass of concrete ablated and the total cavity debris mass are generally similar for this sequence initiated at two different times after shutdown. As in all our MELCOR analyses, concrete ablation is quite rapid soon after debris ejection (while the core debris is hot, >2000 K, and consists of a layer of metallic debris above a heavy oxide layer), and concrete ablation slows significantly after a short time (after enough concrete has been ablated for the debris bed configuration to invert to a light oxide layer above a layer of metallic debris, mixed to a lower average temperature of ~1500 K).

The calculated production of steam and noncondensable gases (H_2, CO, CO_2 and H_2O) is summarized in Figure 4.3.4.15. The hydrogen production shown includes both in-vessel production (the initial step increase) and ex-vessel production in the cavity (the later-time increase). The in-vessel hydrogen generation corresponds to the oxidation of about 10% of the zircaloy and about 1% of the steel in the core and lower plenum, prior to vessel failure and debris ejection. As soon as the core debris enters the cavity, core-concrete interaction begins, resulting in the production of carbon dioxide and hydrogen; reduction of these gases by the molten metal in the core debris also gives rise to carbon monoxide and hydrogen. The production rate of noncondensables from core-concrete interaction resembles the concrete ablation rate: quite rapid soon after debris ejection, later slowing after a CORCON "layer flip" has occurred. On a molar basis, much less CO_2 and steam are produced than H_2 and CO. More CO_2 and steam are calculated to be produced in this sequence initiated 24 hr after shutdown than initiated 7 hr after shutdown; this is a result of the reduced metal content in the core debris in the case initiated 24 hr after shutdown, due to the retention of some structural steel in the lower plenum.

The resulting mole fractions in the drywell, containment dome and auxiliary building (first and second floors) are presented in Figures 4.3.4.16 and 4.3.4.17 for this sequence initiated at two different times after shutdown, including vertical dotted lines at TAF uncovery and at vessel failure for reference. The mole fractions in the cavity resemble the behavior shown for the drywell; the mole fractions in the containment equipment hatch are very similar to those shown for the containment dome; and the mole fractions in the upper floors of the auxiliary building generally resemble the behavior shown for the second floor of the auxiliary building. The inner containment atmosphere consists mostly of steam, building up from accident initiation since the SRVs are locked open, decreasing somewhat after vessel failure and noncondensable gas generation due to core-concrete interaction, then increasing again throughout the remainder of the transient period simulated. The outer containment steam concentration remains generally low as steam condenses in the flooded containment until after vessel failure, when the core debris fallen into the cavity begins boiling the water flooding the containment in this scenario. The containment is open to the auxiliary building in the second and fourth floors. The atmosphere in the dead-end first floor of the auxiliary building remains near ambient with small fractions of steam and noncondensables from the upper floors; higher in the auxiliary building the atmosphere composition closely resembles that in the outer containment (because the containment equipment hatch and both of the containment personnel locks are open). The behavior is very similar in the calculations for this sequence initiated at two different times after shutdown, just shifted in time.

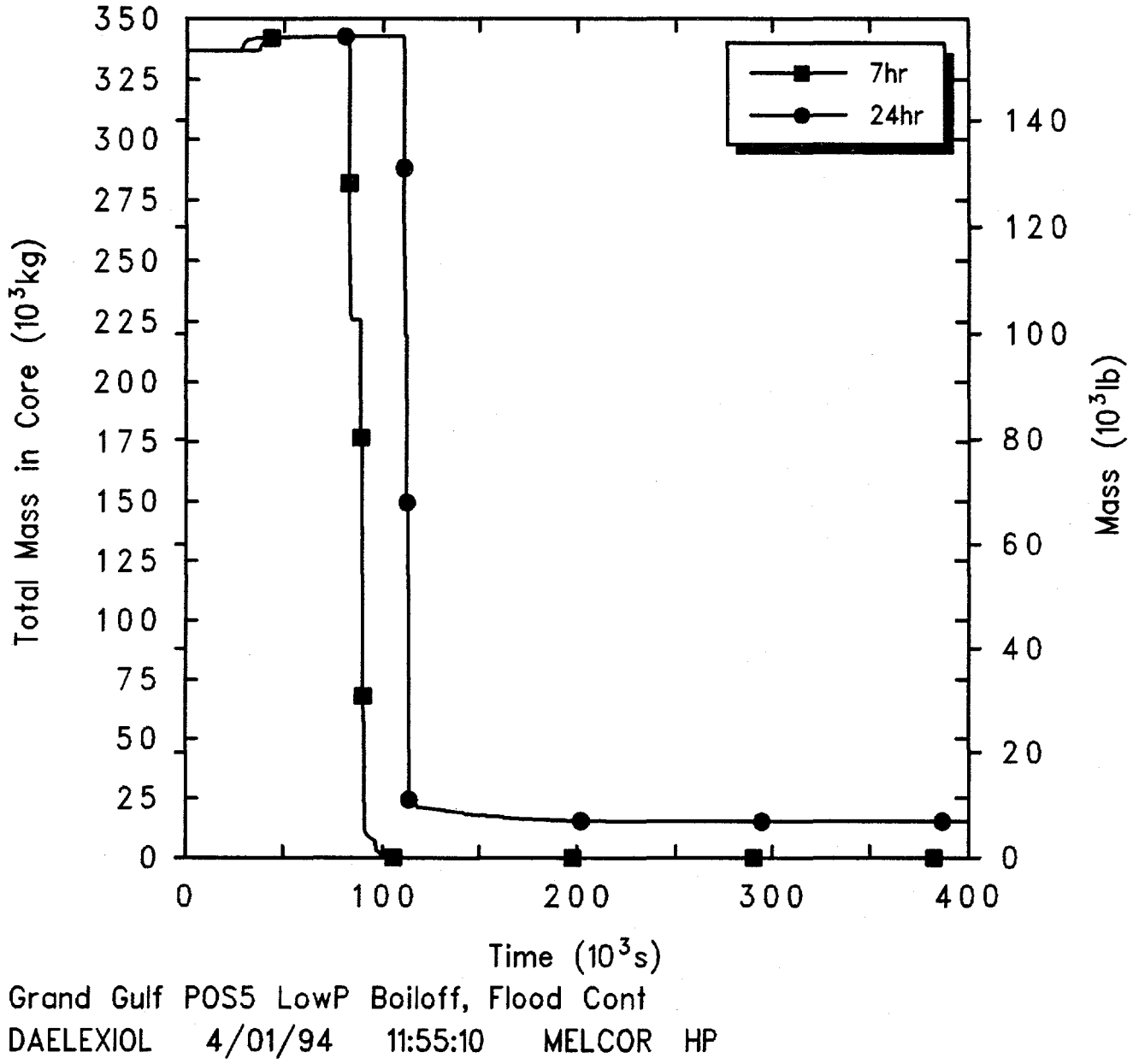

Figure 4.3.4.13. Total Core Material Masses for Grand Gulf POS 5 -- Low Pressure Boiloff with Flooded Containment, Initiated at Various Times After Shutdown.

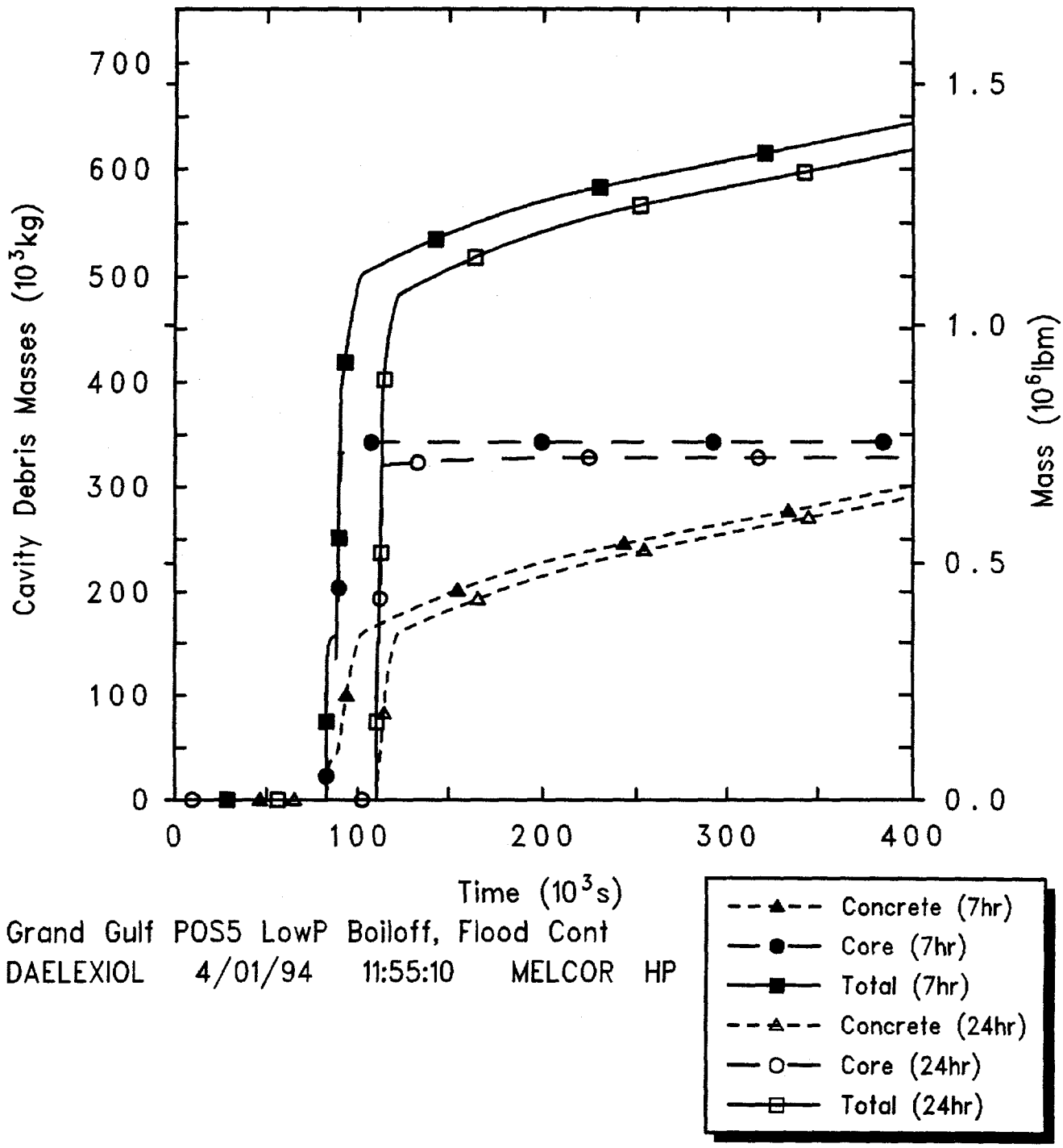

Figure 4.3.4.14. Cavity Total and Concrete Debris Masses for Grand Gulf POS 5 -- Low Pressure Boiloff with Flooded Containment, Initiated at Various Times After Shutdown.

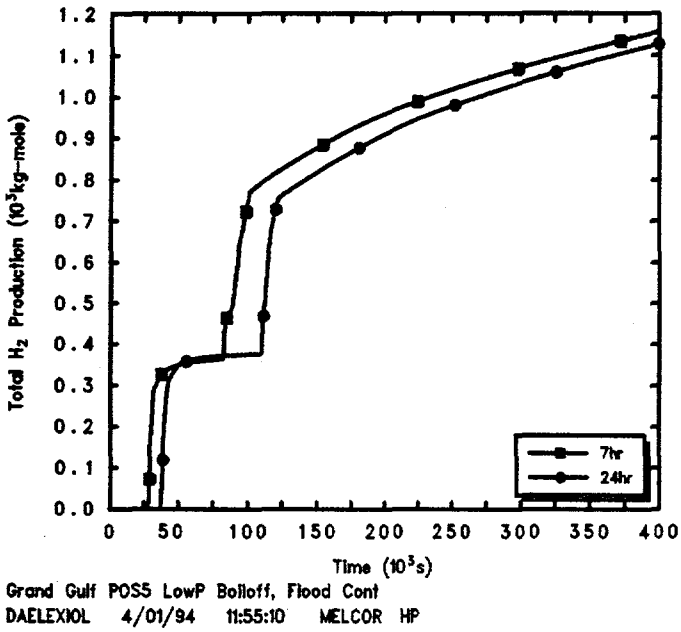

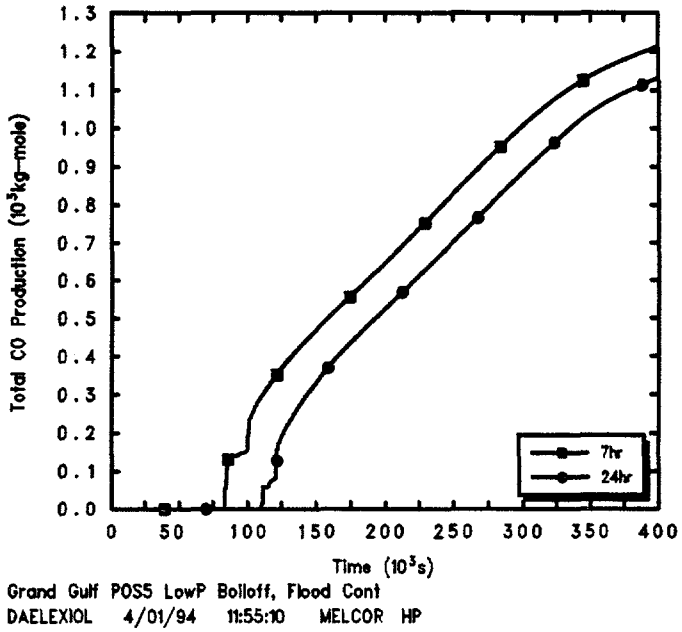

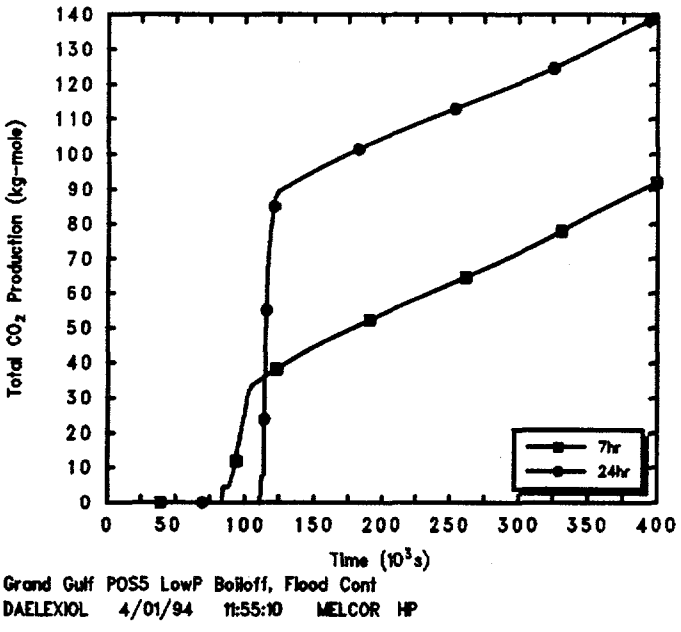

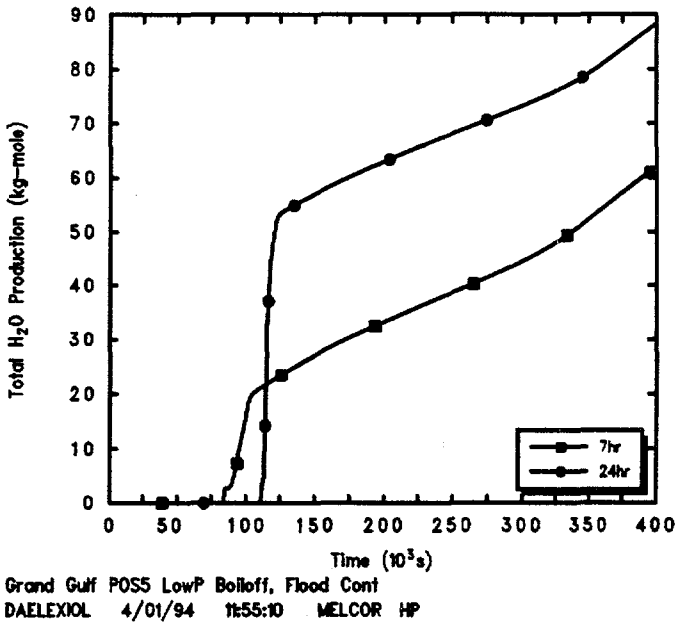

Figure 4.3.4.15. Hydrogen (upper left), Carbon Monoxide (upper right), Carbon Dioxide (lower left) and Steam (lower right) Generation for Grand Gulf POS 5 -- Low Pressure Boiloff with Flooded Containment, Initiated at Various Times After Shutdown.

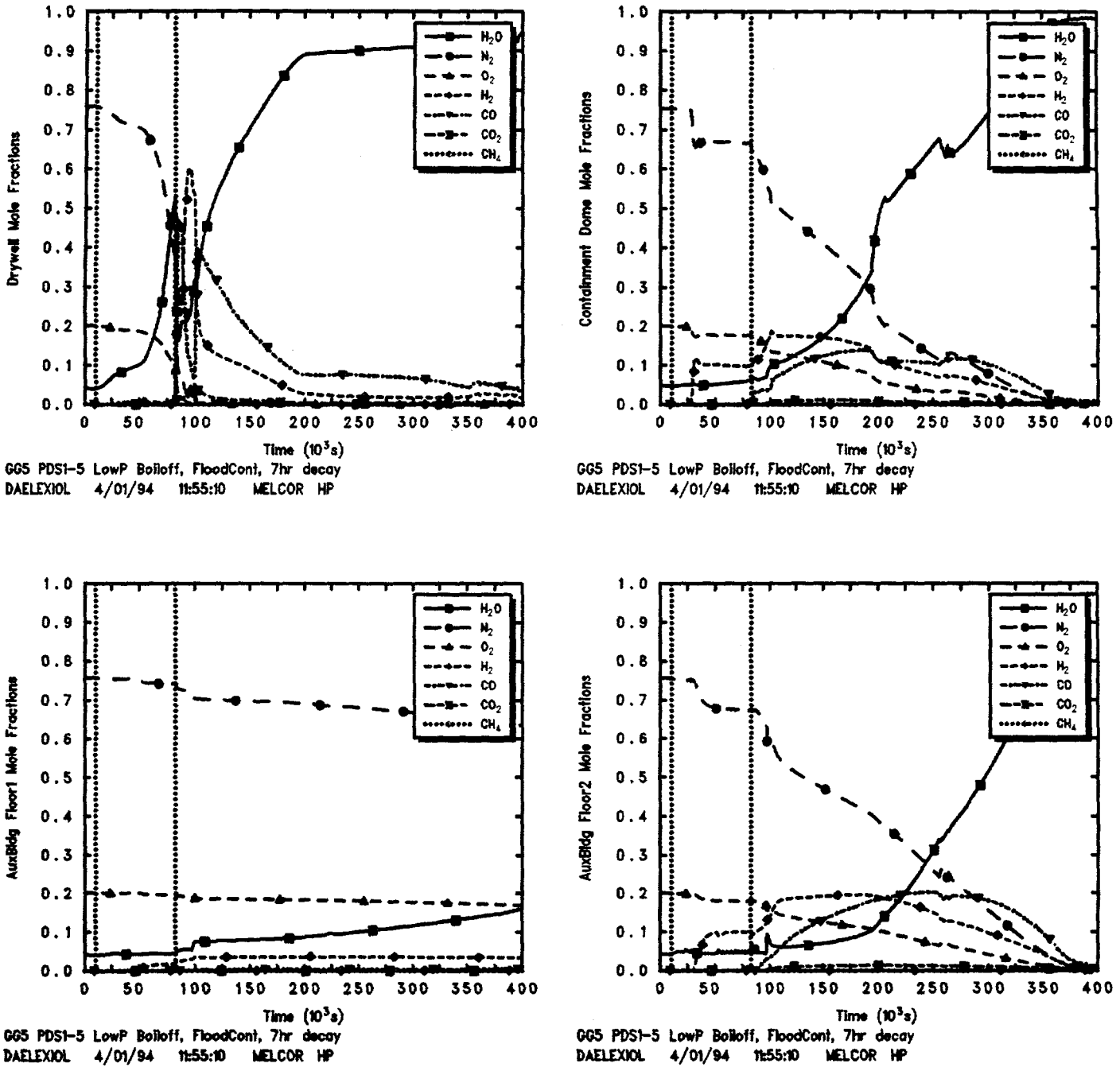

Figure 4.3.4.16. Mole Fractions in Drywell (upper left), Containment Dome (upper right), and Auxiliary Building First Floor (lower left) and Second Floor (lower right) for Grand Gulf POS 5 -- Low Pressure Boiloff with Flooded Containment, Initiated 7 hr After Shutdown.

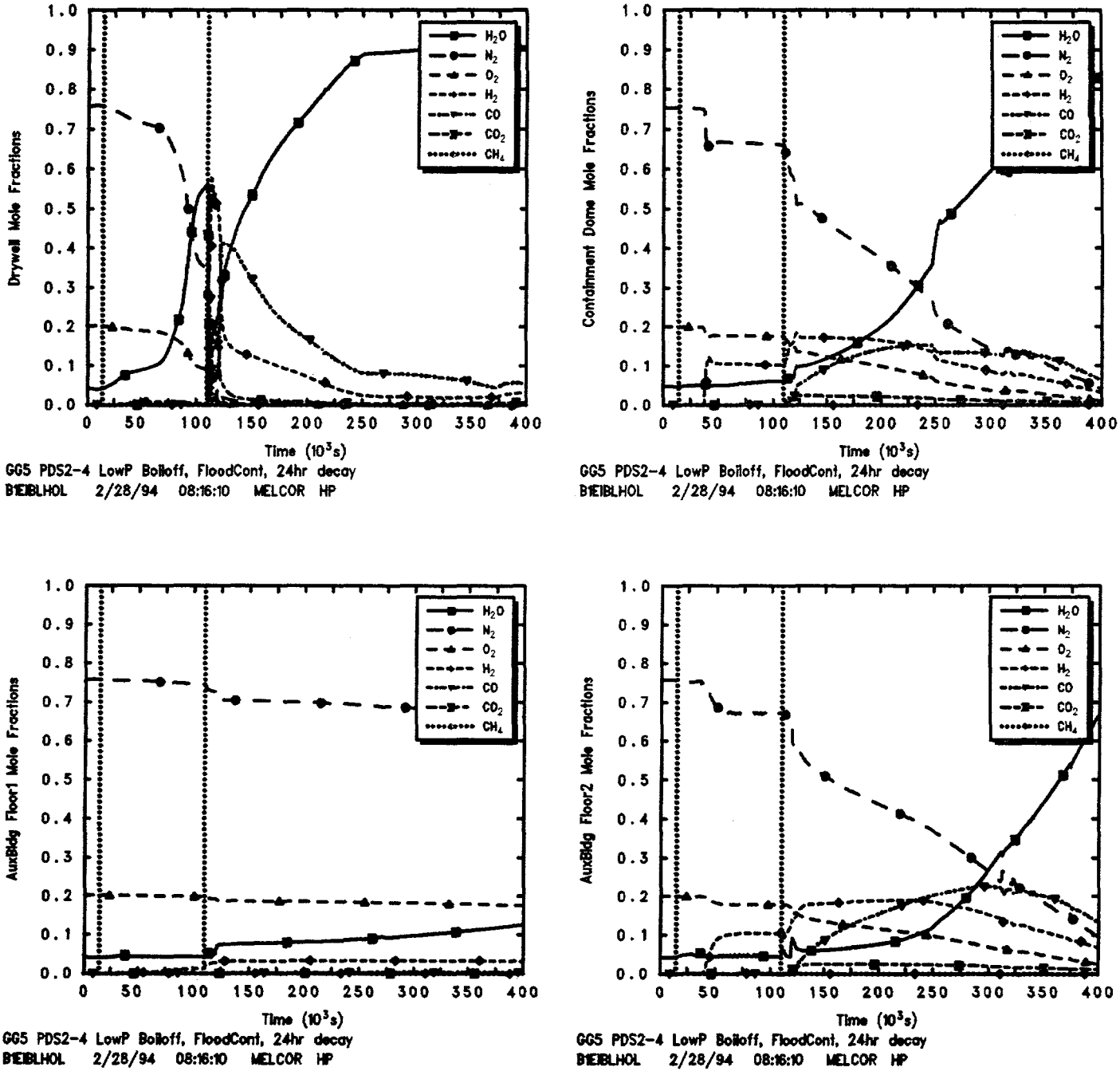

Figure 4.3.4.17. Mole Fractions in Drywell (upper left), Containment Dome (upper right), and Auxiliary Building First Floor (lower left) and Second Floor (lower right) for Grand Gulf POS 5 -- Low Pressure Boiloff with Flooded Containment, Initiated 24 hr After Shutdown.

Figures 4.3.4.18 and 4.3.4.19 illustrate the time-dependent release of radionuclides from the fuel debris both within the vessel and in the cavity, for cases initiated 7 hr and 24 hr after shutdown, respectively. The vertical dotted lines within the plots mark the time of vessel failure, indicating that most of the in-vessel release occurs prior to vessel failure, from the hot debris bed in the active fuel region; most of the ex-vessel release occurs within a short time period after vessel failure and debris ejection to the cavity, while the core debris is still hot, >2000 K, and consists of a layer of metallic debris above a heavy oxide layer, before enough concrete has been ablated for the debris bed configuration to invert to a light oxide layer above a layer of metallic debris, mixed to a lower average temperature of ~1500 K. Table 4.3.4.2 summarizes the in-vessel, ex-vessel and total amounts of each radionuclide class released, all normalized as mass fractions of the initial inventories of each class.

Note that these amounts generally consider only the release of radioactive forms of these classes, and not additional releases of nonradioactive aerosols from structural materials. Also note that the CORSOR-M fission product release model option used in these analyses has identically zero release in-vessel of Class 7 (Mo), Class 9 (La) and Class 11 (Cd). Finally, note that the MELCOR model for this low-pressure boiloff sequence included the formation of CsI from Cs and I_2 released from the fuel, and its subsequent transport, deposition and release. The initial radionuclide inventories are such that all the I_2 released reacts to form CsI while most of the Cs remains unreacted and forms CsOH, which is the default Cs form in MELCOR.

Figure 4.2.4.20 gives the total radioactive release to the environment in these two cases; the releases as mass fractions of individual classes to the environment are shown in Figures 4.3.4.21 and 4.3.4.22]. The releases to the environment begin when the auxiliary building fails. The total releases and time history of the release for this accident initiated at two different decay heat levels are quite similar, except for a timing shift due to the slower core degradation and later vessel and auxiliary building failures at the lower decay heat. These environmental releases do not correspond to immediate release of all radionuclides released from the fuel; there is considerable retention of most radionuclide species within the containment and auxiliary building (as discussed below). Only the noble gases have substantial releases to the environment by the end of the transient periods simulated, because gaseous forms are not scrubbed, filtered, deposited or otherwise retained. There is a total of 484.63 kg of noble gases and halogens released from the fuel; the release to the environment is >90% of this by the end of these low-pressure boiloff simulations. The temperatures are low enough in these shutdown sequences with flooded containments that the other volatile species released from the fuel (i.e., CsOH, CsI and Te) are found mostly in aerosol form and are retained in the primary system, containment and auxiliary building.

Tables 4.3.4.3 and 4.3.4.4 summarize the distribution of the initial radionuclide inventory as mass fractions at the end of the two calculations initiated at different times after shutdown; they provide an overview of how much of the radionuclides remains bound up in fuel debris in either the core or the cavity, and of how much of the released radionuclides is retained in the primary system *vs* how much of the released radionuclides is released to, or released in, either the containment or the auxiliary building and the environment, all normalized to the initial inventories of each class. Table 4.3.4.5 presents a slightly different breakdown of the released radionuclide final distribution, giving the fractions of released inventory for each class in control volume atmospheres (including the environment), in pools, or deposited or settled onto heat structures at the end of the calculations. (As in Table 4.3.4.2 these amounts consider only the release of radioactive forms of these classes, and not additional releases of nonradioactive aerosols from structural materials.)

These tables show fission product distributions generally similar to those found for the large break LOCA sequence with flooded containment (discussed in Section 4.3.1) for the radionuclides with significant (≥80% of initial inventory) release from fuel. In both accident scenarios, most of the noble gases released are in the environment, in the atmosphere. Most of the volatile species (CsOH, CsI and Te) releases occurred in-vessel in both scenarios, but most of those releases are retained in the containment, in water pools. The calculated releases of these volatiles to the environment are much lower for this low pressure boiloff sequence and for the large break LOCA scenario, both of which included flooded containments, than for the other accidents simulated. The two classes of radionuclides forming aerosols which had substantial releases (Ba and Sn, also occurring mostly in-vessel) were predicted to have about half those releases retained in the vessel, primarily deposited on structures, in both accident scenarios; the other half of those aerosol releases are retained in the containment, mostly in water pools and a small fraction deposited on structure surfaces.

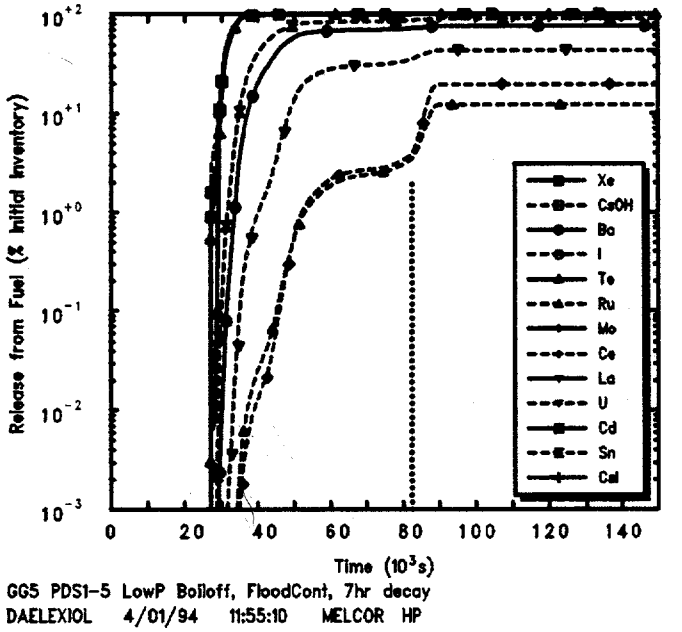

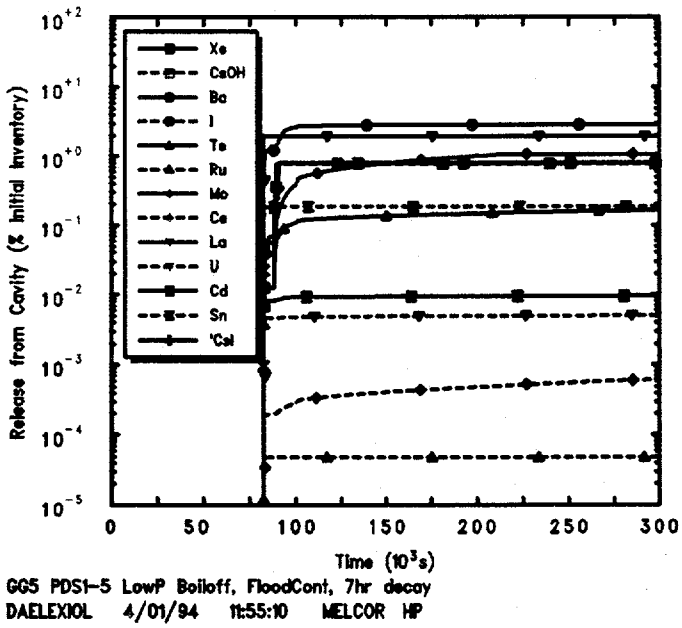

Figure 4.3.4.18. In-Vessel (top) and Ex-Vessel (bottom) Radionuclide Release Mass Fractions for Grand Gulf POS 5 -- Low Pressure Boiloff with Flooded Containment, Initiated 7 hr After Shutdown.

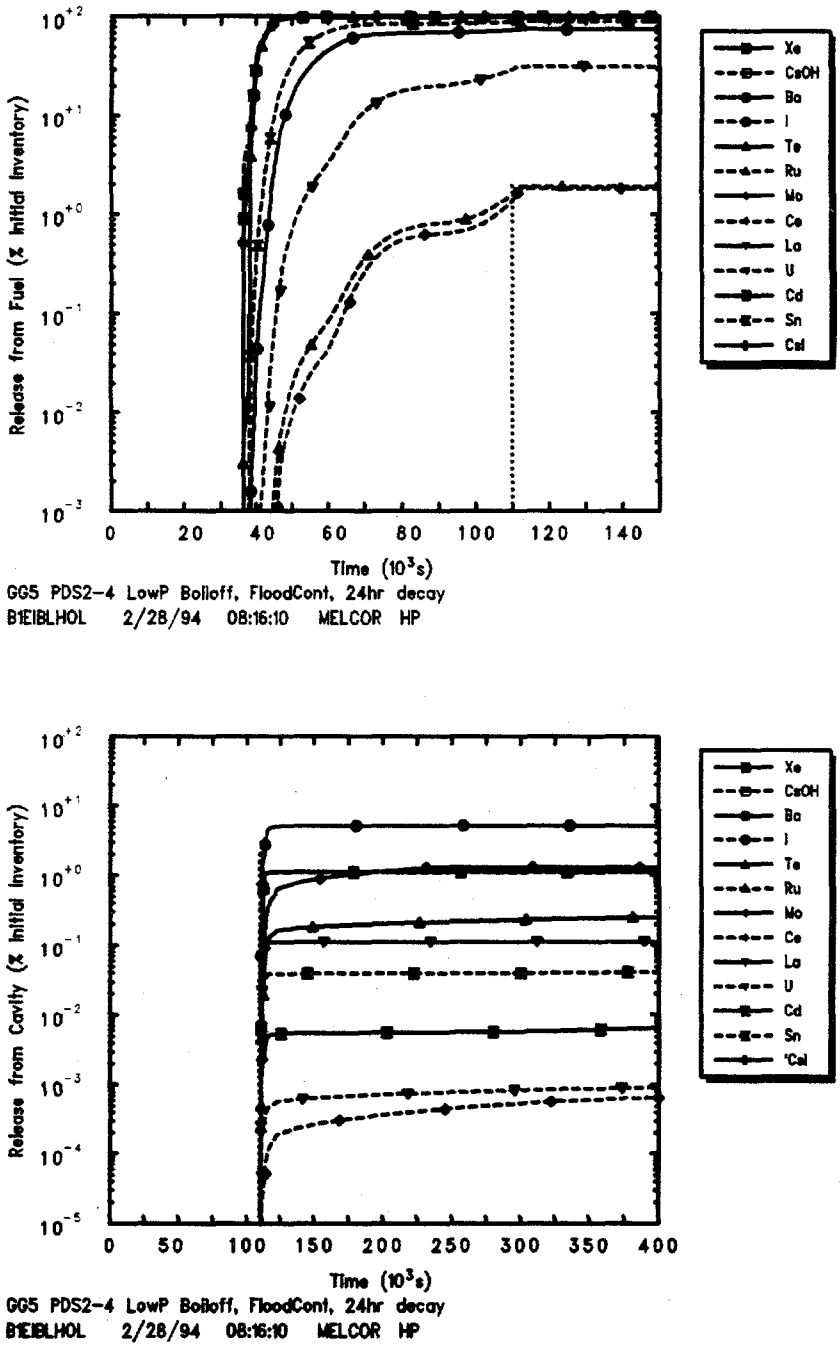

Figure 4.3.4.19. In-Vessel (top) and Ex-Vessel (bottom) Radionuclide Release Mass Fractions for Grand Gulf POS 5 -- Low Pressure Boiloff with Flooded Containment, Initiated 24 hr After Shutdown.

Table 4.3.4.2. Final Radionuclide Release Fractions for Grand Gulf POS 5 -- Low Pressure Boiloff with Flooded Containment, Initiated at Various Times After Shutdown

Class	Fission Products Released from Fuel (% Initial Inventory-Mass Fraction)					
	7 hr			24 hr		
	In-Vessel	Ex-Vessel	Total	In-Vessel	Ex-Vessel	Total
Xe	99.18	0.79	99.97	98.86	1.11	99.97
CsOH	99.16	0.77	99.93	98.85	1.09	99.94
Ba	75.03	2.84	77.87	74.29	5.153	79.44
I	~0	~0	~0	~0	~0	~0
Te	99.09	0.175	99.27	98.77	0.248	99.02
Ru	12.09	0.00005	12.09	1.89	5.0e-07	1.89
Mo	0	1.06	1.06	0	1.288	1.288
Ce	19.42	0.0007	19.42	1.79	0.0006	1.79
La	0	1.93	1.93	0	0.11	0.11
U	43.13	0.005	43.14	31.45	0.0009	31.45
Cd	0	0.01	0.01	0	0.0064	0.0064
Sn	88.86	0.185	89.05	89.68	0.04	89.72
CsI	99.18	0.8	99.98	98.84	1.12	99.96

4.3.5 High Pressure Boiloff with Open RPV Head Vent and Closed Containment, Initiated 24 hr After Shutdown

At the initiation of the accident, the reactor vessel is depressurized, the coolant is at the normal level and the SRVs are closed. Following the initiating event, all core cooling and makeup is lost and cannot be recovered. The operator fails to open the SRVs and steam the core at low pressure, i.e., the SRVs remain closed during the accident and only open to relieve pressure at the safety setpoint. The vessel water inventory is at 366.5 K (200°F), which corresponds to the maximum temperature allowed by the Grand Gulf technical specifications for operation in POS 5. The reactor pressure vessel head vent is open at the beginning of the transient. The suppression pool level is 3.86 m (12.67 ft) above the suppression pool floor. In this scenario the operators successfully close the containment equipment hatch and both personnel locks 5 hr after the initiating event; however, the drywell personnel lock is still open. Containment is assumed to fail at 489 kPa (71 psia), with a 0.0929 m^2 opening above the auxiliary building roof (i.e., "closed containment").

This sequence is almost identical to the high pressure boiloff scenario with open RPV head vent discussed in Section 4.2.4 except that in those Level 1 analyses the containment was open while in these Level 2 analyses the containment was assumed to be closed after 5 hr.

The sequence of events predicted by MELCOR for this accident with different initiation times is given in Table 4.3.5.1.

The vessel pressure response is very similar to that presented in Figures 4.2.5.1 in Section 4.2.5 for this sequence initiated 24 hr after shutdown. The vessel begins pressurizing as all core cooling is lost and continues pressurizing until reaching the SRV setpoint. The SRVs then cycle around the valve setpoints, intermittently opening. However, the system does not remain at the SRV cycling setpoints until vessel failure, but instead remains at the SRV cycling setpoints for only a few valve cycles before dropping due to continual inventory loss out the open RPV vent line. The vessel inventory response is also almost identical to the results discussed for the corresponding Level 1 analysis presented in Section 4.2.5 (shown in Figure 4.2.4.3).

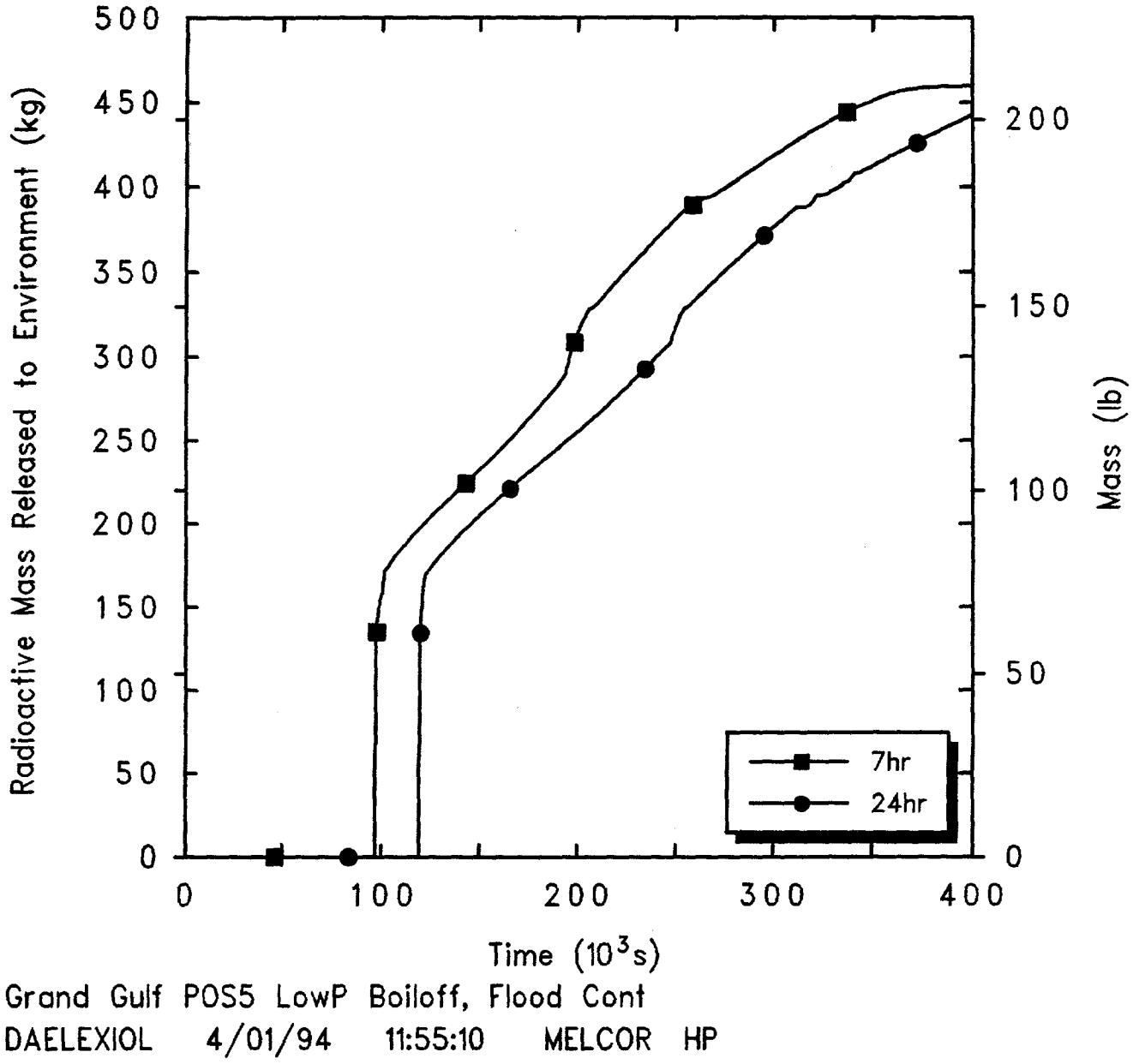

Figure 4.2.4.20. Total Environmental Radionuclide Releases for Grand Gulf POS 5 -- Low Pressure Boiloff with Flooded Containment, Initiated at Various Times After Shutdown.

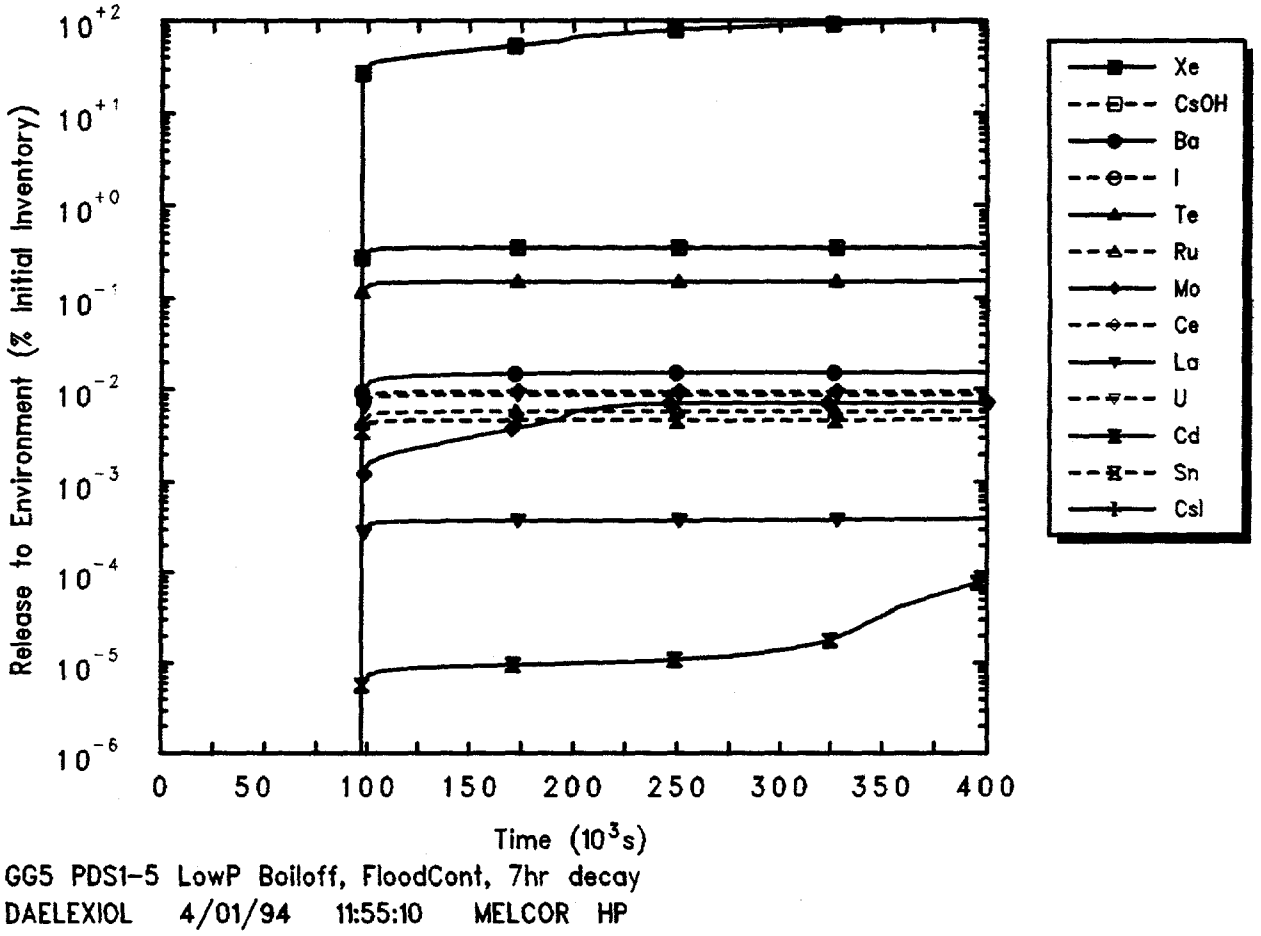

Figure 4.3.4.21. Environmental Radionuclide Release Mass Fractions for Grand Gulf POS 5 -- Low Pressure Boiloff with Flooded Containment, Initiated 7 hr After Shutdown.

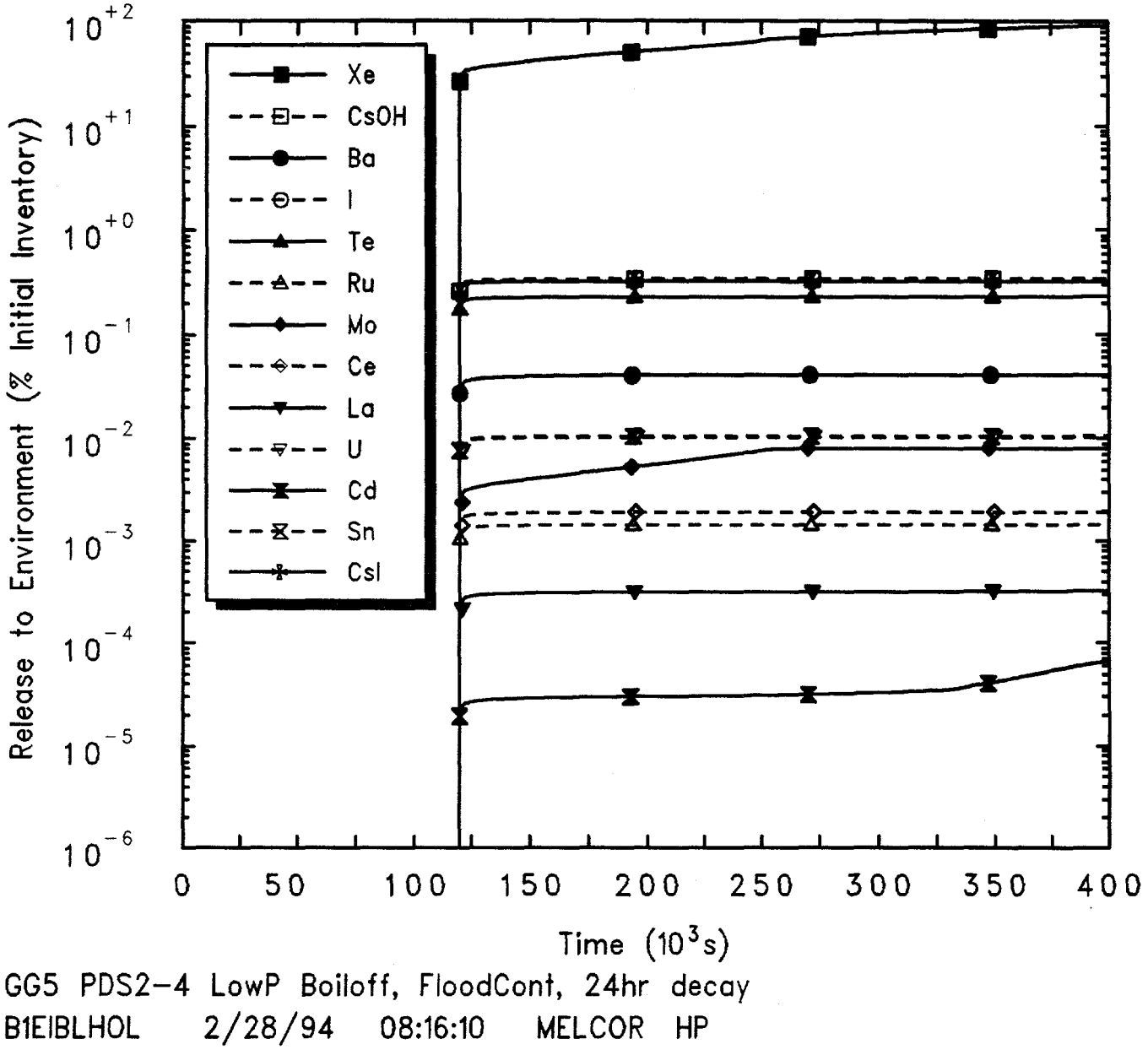

Figure 4.3.4.22. Environmental Radionuclide Release Mass Fractions for Grand Gulf POS 5 -- Low Pressure Boiloff with Flooded Containment, Initiated 24 hr After Shutdown.

Table 4.3.4.3. Final Radionuclide Distribution for Grand Gulf POS 5 -- Station Blackout with Flooded Containment, Initiated at 7 hr After Shutdown

Class	Fission Product Distribution (% Initial Inventory-Mass Fraction)				
	Fuel Debris	Primary System	Containment	Auxiliary Building	Environment
Xe	~0	0.033	0.003	3.59	96.4
CsOH	~0	3.35	85.38	10.9	0.35
Ba	22.1	38.6	36.87	2.33	0.0154
Te	0.72	4.2	85.93	8.92	0.151
Ru	87.8	2.64	9.24	0.201	0.0057
Mo	98.9	0.002	0.99	0.063	0.007
Ce	80.6	3.13	15.98	0.304	0.0095
La	98.1	0.005	1.88	0.037	0.0004
U	60.3	20.2	18.6	0.883	0.0081
Cd	~100	0.00002	0.01	0.0003	0.00008
Sn	11	43.5	42.39	3.06	0.0048
CsI	~0	3.36	85.37	10.95	0.349

The steam flow out both the SRVs and the RPV vent initially pressurizes both the containment and the auxiliary building, as shown in Figure 4.3.5.1. Closing the containment at 5 hr isolates the auxiliary building before it reaches its 5 psig overpressure failure setpoint. The closed containment continues to pressurize due to steam flow out both the SRVs and the RPV vent and later from the failed vessel lower head penetrations. There is a pressure spike in the containment at the time of vessel failure caused by flashing of the remaining lower plenum water by falling core debris. That pressure spike almost reached the containment failure pressure of 489 kPa (71 psia) locally in the cavity but did not challenge the containment global integrity. After that stepped increase in containment pressure at vessel failure, the containment continued to pressurize due to the generation of noncondensable gases from core-concrete interaction, until the containment failure pressure is reached.

Figure 4.3.5.2 presents the upper plenum, core and lower plenum swollen and collapsed liquid levels for this accident sequence. The level initially rises as the vessel pressurizes and then drops as inventory continues to be lost out the RPV vent and the SRV. The vessel liquid level drops smoothly through the upper plenum into the core and continues dropping smoothly partway into the lower plenum, followed by a more gradual loss of the remaining inventory due to boiling and steam outflow. There is very little pool frothing or swelling in any of the vessel volumes in this sequence. The lower plenum liquid level drops quickly to zero when the vessel lower head penetrations fail and any remaining water is dropped into the cavity together with falling core debris.

The heatup of the intact fuel and clad is illustrated in Figure 4.3.5.3. Because the fuel/clad component temperatures in MELCOR are set to zero in a cell when that component fails, this figure shows both the overall heatup rate and the time that the intact fuel/clad component fails through melting of the clad at 2100 K (3320°F). Figure 4.3.5.4 presents corresponding core debris temperatures in the active fuel region; these are the temperatures of the debris bed formed by the failure of the intact fuel/clad component in MELCOR in a core cell, whose (intact) temperatures were given in Figure 4.3.5.3. The debris bed in the active fuel region reaches peak temperatures about equal to the UO_2 melt temperature of 3113 K (5144°F).

The temperatures of the active fuel region debris bed drop to zero when the core plate fails and the debris relocates

Table 4.3.4.4. Final Radionuclide Distribution for Grand Gulf POS 5 -- Low Pressure Boiloff with Flooded Containment, Initiated at 24 hr After Shutdown

Class	Fission Product Distribution (% Initial Inventory-Mass Fraction)				
	Fuel Debris	Primary System	Containment	Auxiliary Building	Environment
Xe	0.0012	0.0214	1.476	6.24	92.3
CsOH	0.0012	3.02	85.9	10.71	0.338
Ba	20.5	41.4	35.39	2.6	0.002
Te	0.934	3.92	85.43	9.54	0.229
Ru	98.1	1.18	0.67	0.043	0.0014
Mo	98.7	0.003	1.44	0.059	0.0079
Ce	98.2	1.04	0.718	0.04	0.0019
La	99.8	0.00008	0.11	0.0025	0.0003
U	71.1	19.4	8.84	0.68	0.0094
Cd	99.9	0.00001	0.006	0.0003	0.00007
Sn	10.3	43.5	42.76	3.41	0.0106
CsI	~0	3.07	85.89	10.62	0.325

to the lower plenum. The predicted temperatures in the debris bed in the lower plenum and core plate are given in Figure 4.3.5.5. Prior to core plate failure there is some cold, refrozen debris both on the core support plate and on the lower core structural material just above the core support plate; the cooling and refreezing of this debris is the cause of the continued gradual drop in lower plenum liquid level due to steaming seen in Figure 4.3.5.2. The debris temperature rises gradually to the core support plate failure temperature of 1273 K (1832°F). After core plate failure hot, high-temperature debris begins appearing in the lower plenum as debris falls from the active fuel region into the lower plenum. With the new debris radial relocation model added in MELCOR 1.8.2, the core plate needs to fail in only one ring before debris from cells in the active fuel region in all radial rings can potentially flow sideways and down, fall through the failed plate, and then spread sideways into cells in the lower plenum in all radial rings. The lower head penetrations begin failing almost immediately, and the lower plenum debris temperatures begin dropping to zero as debris is ejected from the vessel to the cavity. Some cool, quenched debris remains present in the lower plenum for a significant period of time, however, as indicated by the 1000-1250 K debris temperatures in the lowest level after vessel failure.

Figure 4.3.5.6 illustrates what fraction of each material in the active fuel region has collapsed into a debris rubble bed held up by the core support plate, prior to core plate failure, debris relocation, lower head failure and debris ejection, for this high pressure boiloff scenario.

Figure 4.3.5.7 shows both the total and the individual masses of core materials (UO_2, zircaloy and ZrO_2, stainless steel and steel oxide, and control rod poison) remaining in the vessel. This includes both material in the active fuel region and in the lower plenum. Debris ejection began very soon after lower head failure. This figure illustrates that most of the core material was lost from the vessel to the cavity quickly, in step-like stages. In all cases, all of the UO_2 was transferred to the cavity within a short time after the initial vessel lower head penetration failure, as was the unoxidized zircaloy, the associated zirconium oxide and the control rod poison. A substantial fraction (75%) of the structural steel in the lower plenum, and some associated steel oxide, was predicted to remain unmelted and in place, more than in any of the other scenarios analyzed with MELCOR.

The debris material lost from the vessel is ejected to the drywell pedestal cavity. Figure 4.3.5.8 presents the amounts of ejected core debris, concrete ablated and the

Table 4.3.4.5. Final Radionuclide State for Grand Gulf POS 5 -- Low Pressure Boiloff with Flooded Containment, Initiated at Various Times After Shutdown

Class	Fission Products Released from Fuel (% Released Inventory-Mass Fraction)					
	Atmosphere	7 hr Pool	Deposited	Atmosphere	24 hr Pool	Deposited
Xe	~100	0	0	~100	0	0
CsOH	0.35	96.3	3.36	0.34	96.67	3.03
Ba	0.02	50.23	49.75	0.05	47.71	52.25
I	~100	0	0	~100	0	0
Te	0.15	95.6	4.25	0.23	95.79	3.97
Ru	0.06	77.38	22.57	0.075	37.34	62.58
Mo	0.66	95.85	3.47	0.62	96.23	3.14
Ce	0.05	83.02	16.95	0.11	41.35	58.54
La	0.02	98.73	1.23	0.29	98.99	0.71
U	0.02	48.69	51.29	0.033	32.63	67.32
Cd	1.12	97.46	1.43	1.79	95.81	2.07
Sn	0.006	51.03	48.97	0.012	51.46	48.53
CsI	0.35	96.26	3.39	0.33	96.56	3.08

total cavity debris mass (i.e., core debris combined with concrete ablation products). As in the other sequences analyzed, concrete ablation is quite rapid soon after debris ejection while the core debris is hot (>2000 K) and consists of a layer of metallic debris above a heavy oxide layer, and then slows noticably after enough concrete has been ablated for the debris bed configuration to invert to a light oxide layer above a layer of metallic debris, mixed to a lower average temperature of ~1500 K.

The calculated production of steam and noncondensable gases (H_2, CO, CO_2 and H_2O) is depicted in Figure 4.3.5.9. The hydrogen production shown includes both in-vessel production (the initial step increase) and ex-vessel production in the cavity (the later-time increase). The in-vessel hydrogen generation corresponds to the oxidation of about 10-15% of the zircaloy and about 1% of the steel in the core and lower plenum, prior to vessel failure and debris ejection. As soon as the core debris enters the cavity, core-concrete interaction begins, resulting in the production of carbon dioxide and hydrogen; reduction of these gases by the molten metal in the core debris also gives rise to carbon monoxide and hydrogen.

The mole fractions in the drywell, containment dome and equipment hatch, and the second floor of the auxiliary building are shown in Figure 4.3.5.10 including vertical dotted lines at TAF uncovery and at vessel and containment failure for reference. The mole fractions in the cavity resemble the behavior shown for the drywell. The inner containment atmosphere consists mostly of steam, building up rapidly after the SRVs cycle in the relief mode, decreasing somewhat after vessel failure and noncondensable gas generation due to core-concrete interaction, but remaining more than half steam throughout the transient period simulated. The outer containment steam concentration begins rising after the SRVs begin cycling in the relief mode. By the time the containment fails, the outer containment atmosphere consists of nearly early parts of steam, air and the noncondensable gases generated by core-concrete interaction. The atmosphere in the auxiliary building remains near ambient throughout the transient period

Table 4.3.5.1. Sequence of Events Predicted by MELCOR for High Pressure Boiloff with Open RPV Head Vent and Closed Containment, Initiated 24 hr After Shutdown

Event	Time After Shutdown 24 hr
Accident initiation	0
Containment closed	18,000 s (5 hr)
Core uncovery (TAF) begins	42,875 s (11.91 hr)
Core heatup begins	43,500 s (12.08 hr)
Clad failure/Gap release	
(Ring 1)	49,945 s (13.87 hr)
(Ring 2)	49,857 s (13.85 hr)
(Ring 3)	49,931 s (13.87 hr)
(Ring 4)	50,362 s (13.99 hr)
(Ring 5)	51,959 s (14.16 hr)
(Ring 6)	70,680 s (19.63 hr)
Core plate failed	
(Ring 1)	73,667 s (20.46 hr)
(Ring 2)	73,628 s (20.45 hr)
(Ring 3)	76,631 s (21.29 hr)
(Ring 4)	78,988 s (21.94 hr)
(Ring 5)	80,344 s (22.32 hr)
(Ring 6)	85,320 s (23.70 hr)
Vessel LH penetration failed	
(Ring 1)	73,712 s (20.48 hr)
(Ring 2)	73,712 s (20.48 hr)
(Ring 3)	73,712 s (20.48 hr)
(Ring 4)	73,714 s (20.48 hr)
(Ring 5)	73,718 s (20.48 hr)
(Ring 6)	73,720 s (20.48 hr)
Commence debris ejection	73,712 s (20.48 hr)
Containment failed	308,264 s (85.63 hr)
Cavity rupture	343,883 s (95.52 hr)
End of calculation	343,883 s (95.52 hr)

simulated because the containment is closed at 5 hr, before much outflow from the vessel has occurred and after which there is no path from the vessel or the containment and the auxiliary building. Figure 4.3.5.11 illustrates the time-dependent release of radionuclides from the fuel debris both within the vessel and in the cavity. The vertical dotted lines within the plots mark the time of vessel failure, indicating that most of the in-vessel release occurs prior to vessel failure, from the hot debris bed in the active fuel region, while most of the ex-vessel release occurs within a short time period after vessel failure and debris ejection to the cavity, while the core debris is still hot, before enough concrete has been ablated for the debris bed configuration to cool and invert; this behavior is seen in most of our MELCOR analyses. Table 4.3.5.2 summarizes the in-vessel, ex-vessel and total amounts of each radionuclide class released, all normalized to the initial inventories of each class. (Note that these amounts generally consider only the release of radioactive forms of these classes, and not additional

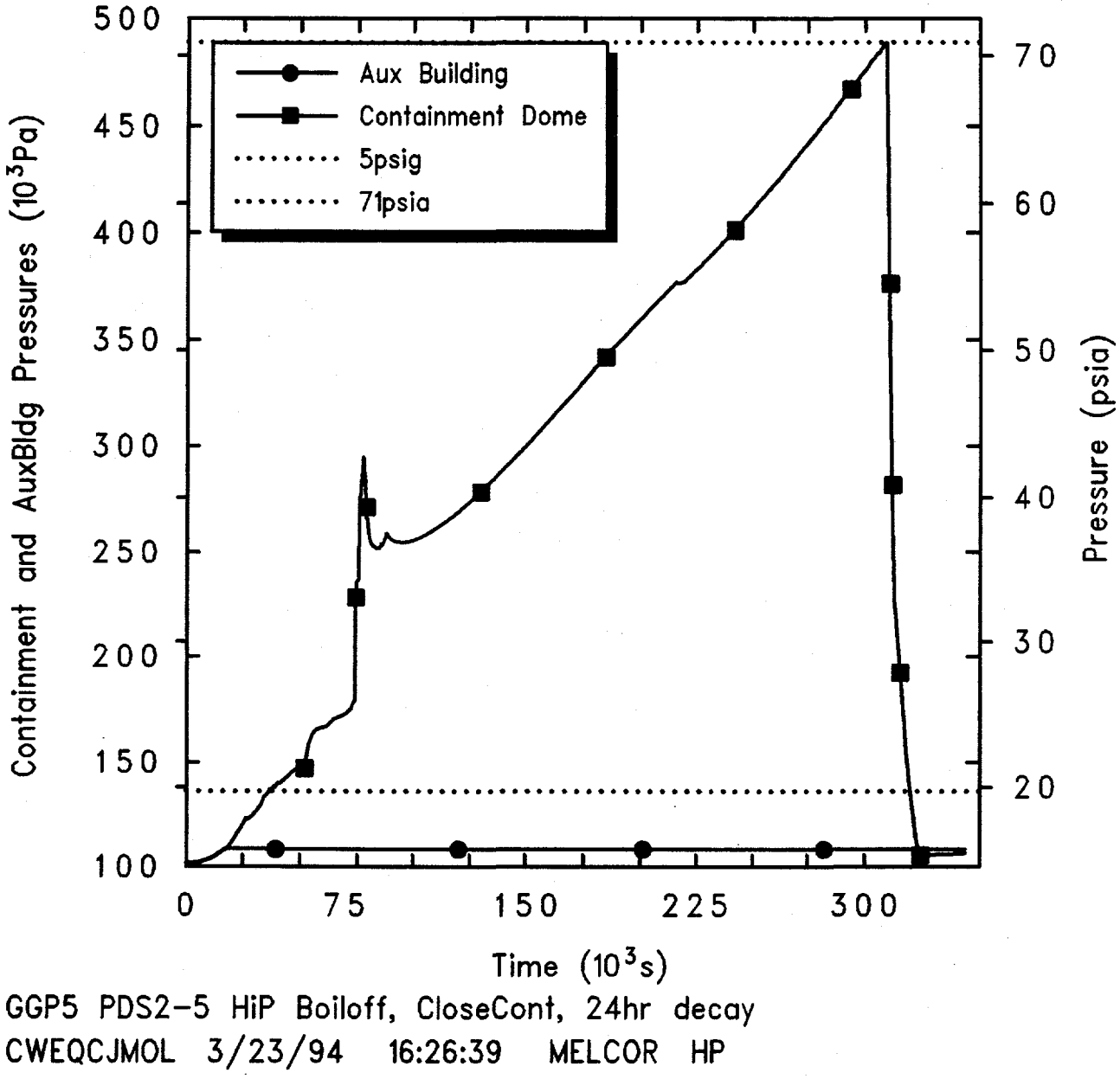

Figure 4.3.5.1. Containment and Auxiliary Building Pressures for Grand Gulf POS 5 -- High Pressure Boiloff with Open RPV Vent and Closed Containment, Initiated 24 hr After Shutdown.

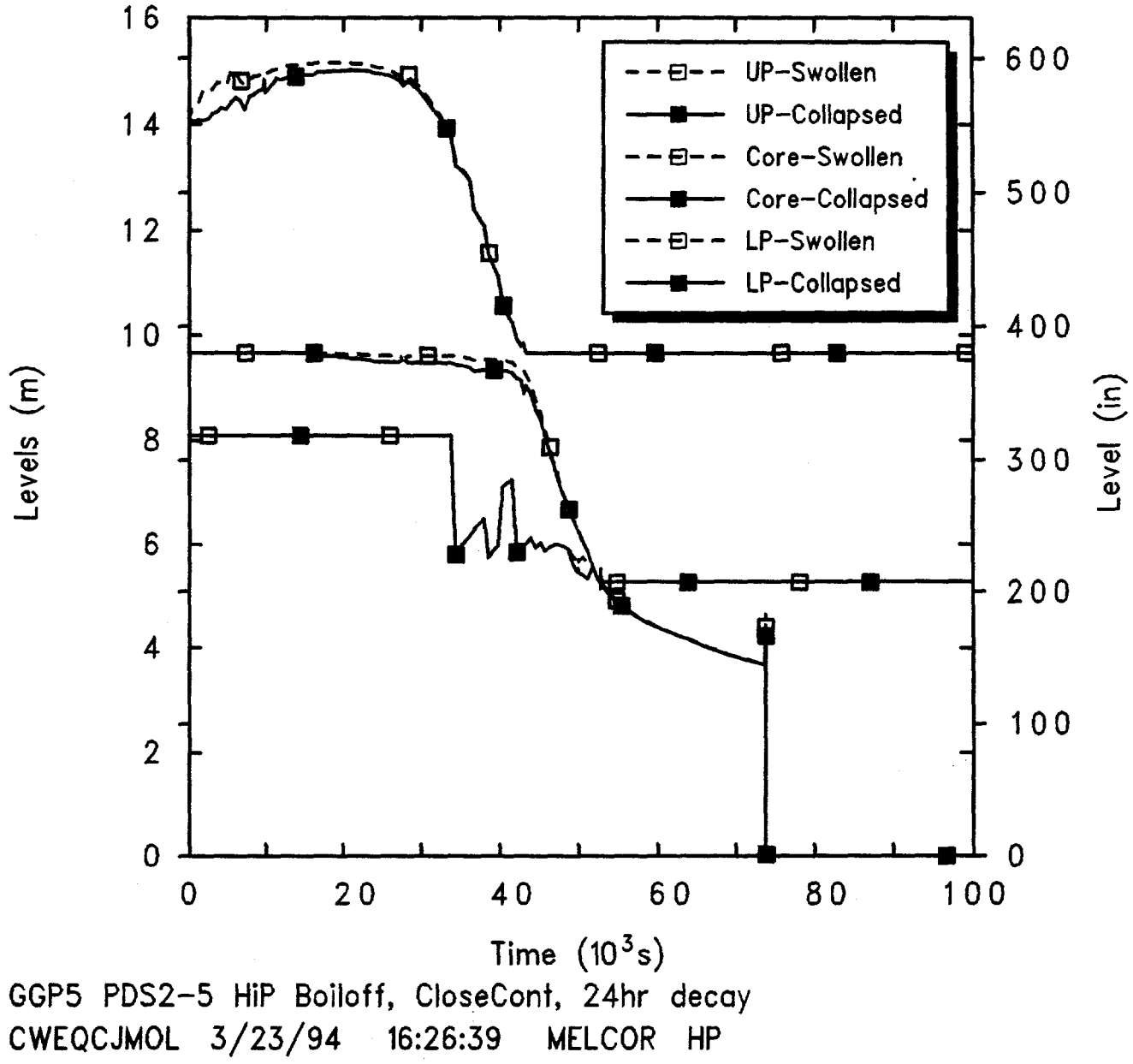

Figure 4.3.5.2. Upper Plenum, Core and Lower Plenum Liquid Levels for Grand Gulf POS 5 -- High Pressure Boiloff with Open RPV Head Vent and Closed Containment, Initiated 24 hr After Shutdown.

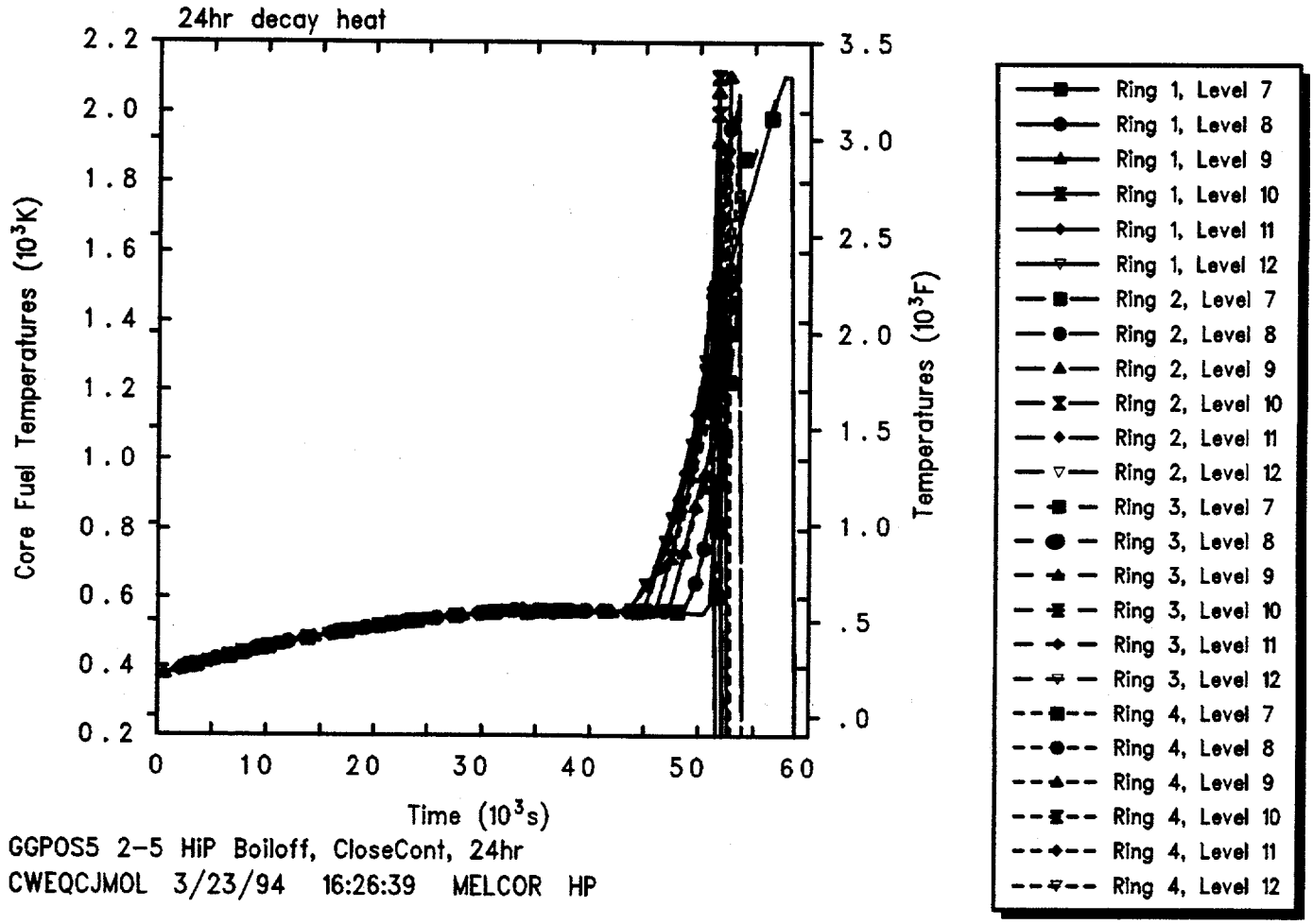

Figure 4.3.5.3. Core Intact Fuel/Clad Temperatures for Grand Gulf POS 5 -- High Pressure Boiloff with Open RPV Head Vent and Closed Containment, Initiated 24 hr After Shutdown.

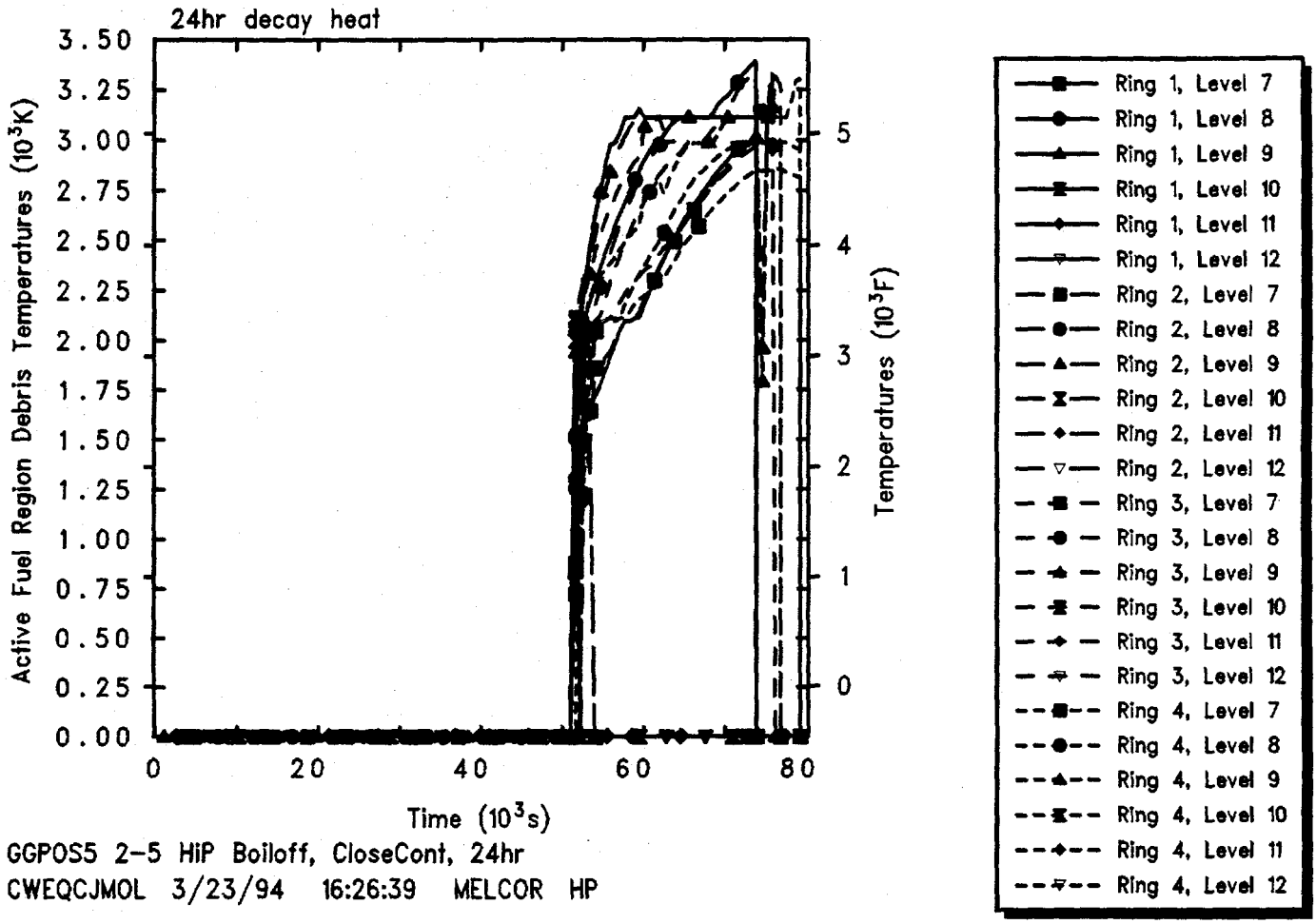

Figure 4.3.5.4. Core Active Fuel Region Debris Bed Temperatures for Grand Gulf POS 5 -- High Pressure Boiloff with Open RPV Head Vent and Closed Containment, Initiated 24 hr After Shutdown.

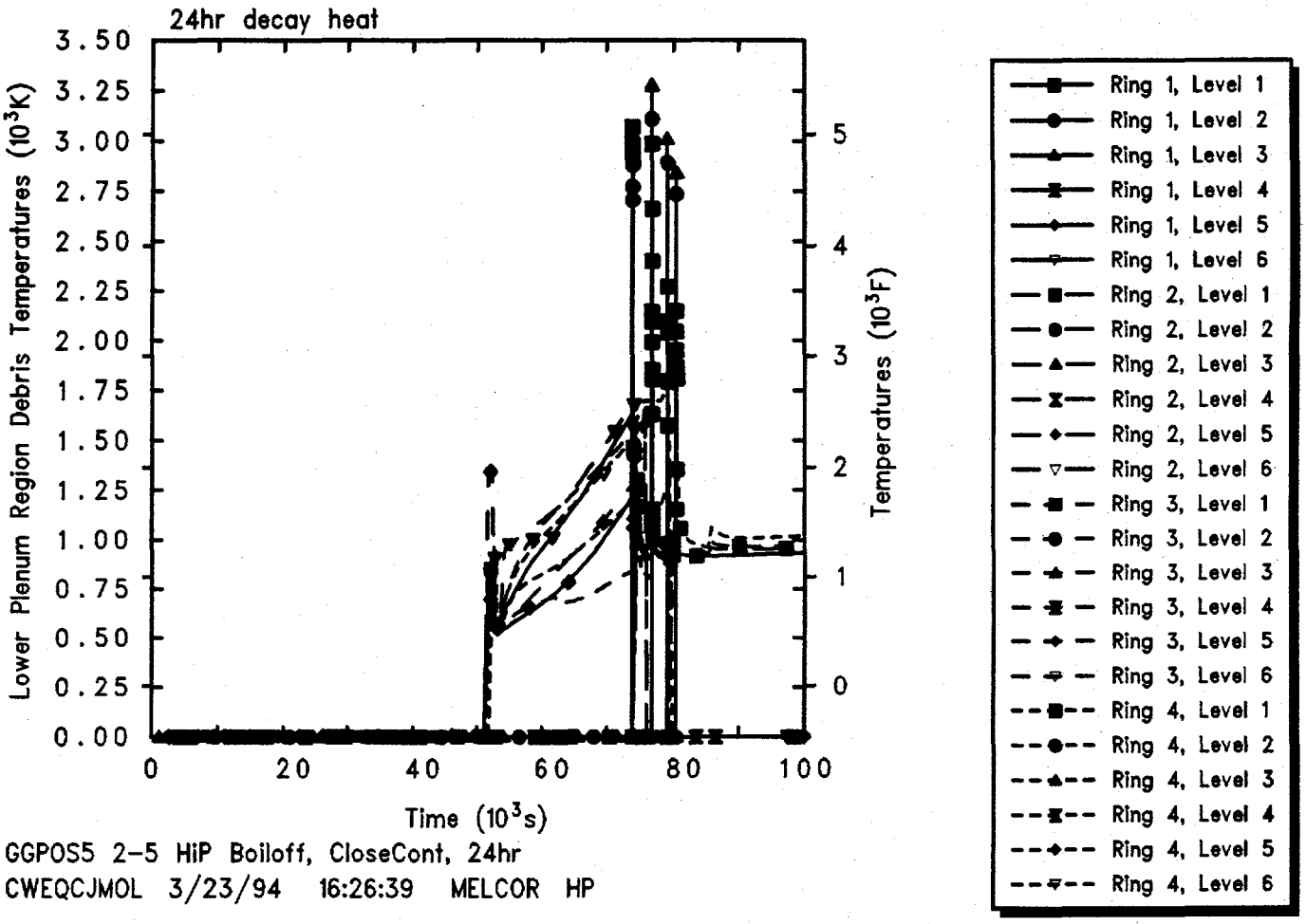

Figure 4.3.5.5. Core Lower Plenum and Core Support Plate Debris Bed Temperatures for Grand Gulf POS 5 -- High Pressure Boiloff with Open RPV Head Vent And Closed Containment, Initiated 24 hr After Shutdown.

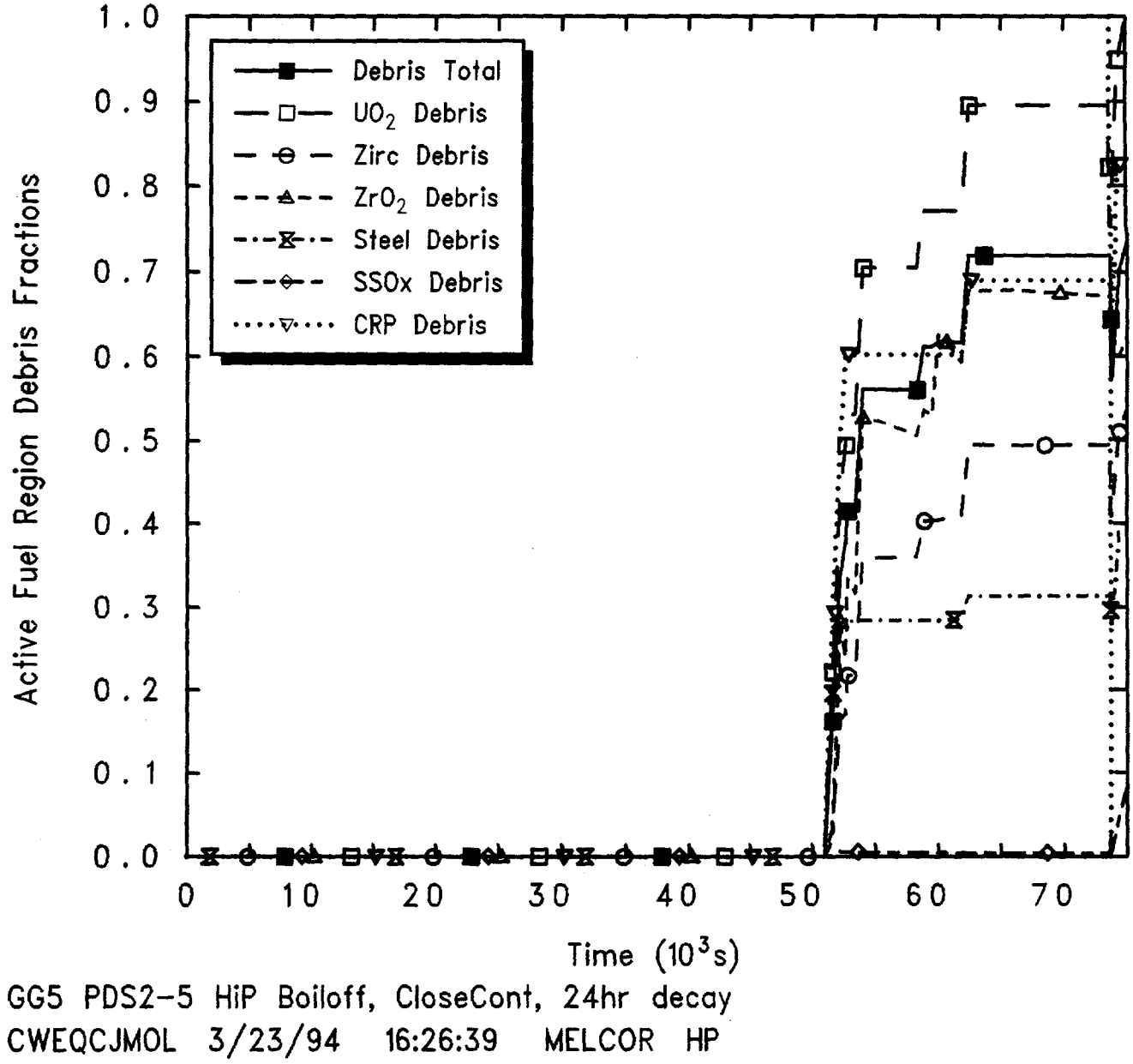

Figure 4.3.5.6. Core Active Fuel Region Degraded Material Fractions for Grand Gulf POS 5 -- High Pressure Boiloff with Open RPV Head Vent and Closed Containment, Initiated 24 hr After Shutdown.

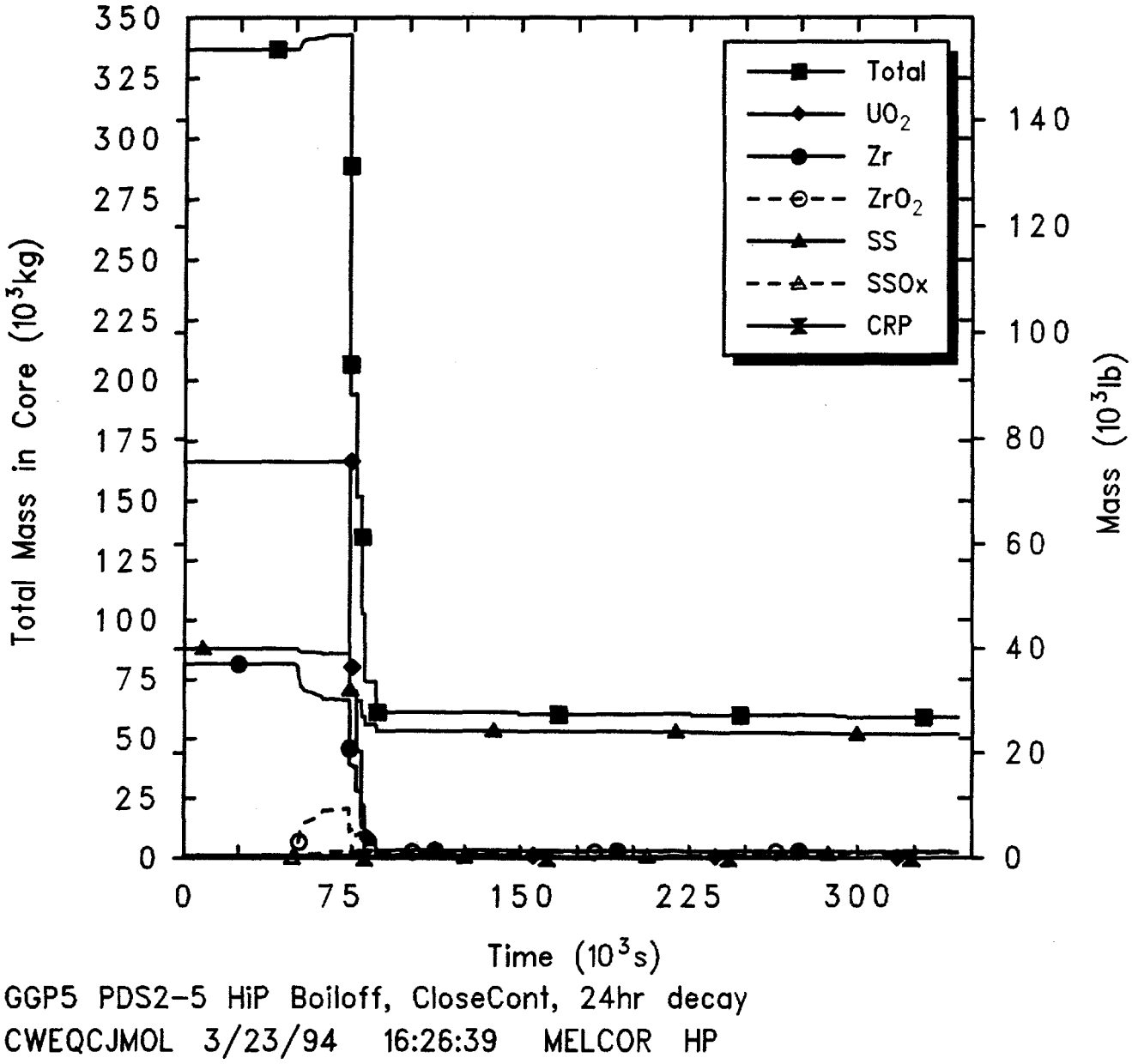

Figure 4.3.5.7. Total and Individual Core Material Masses for Grand Gulf POS 5 -- High Pressure Boiloff with Open RPV Head Vent and Closed Containment, Initiated 24 hr After Shutdown.

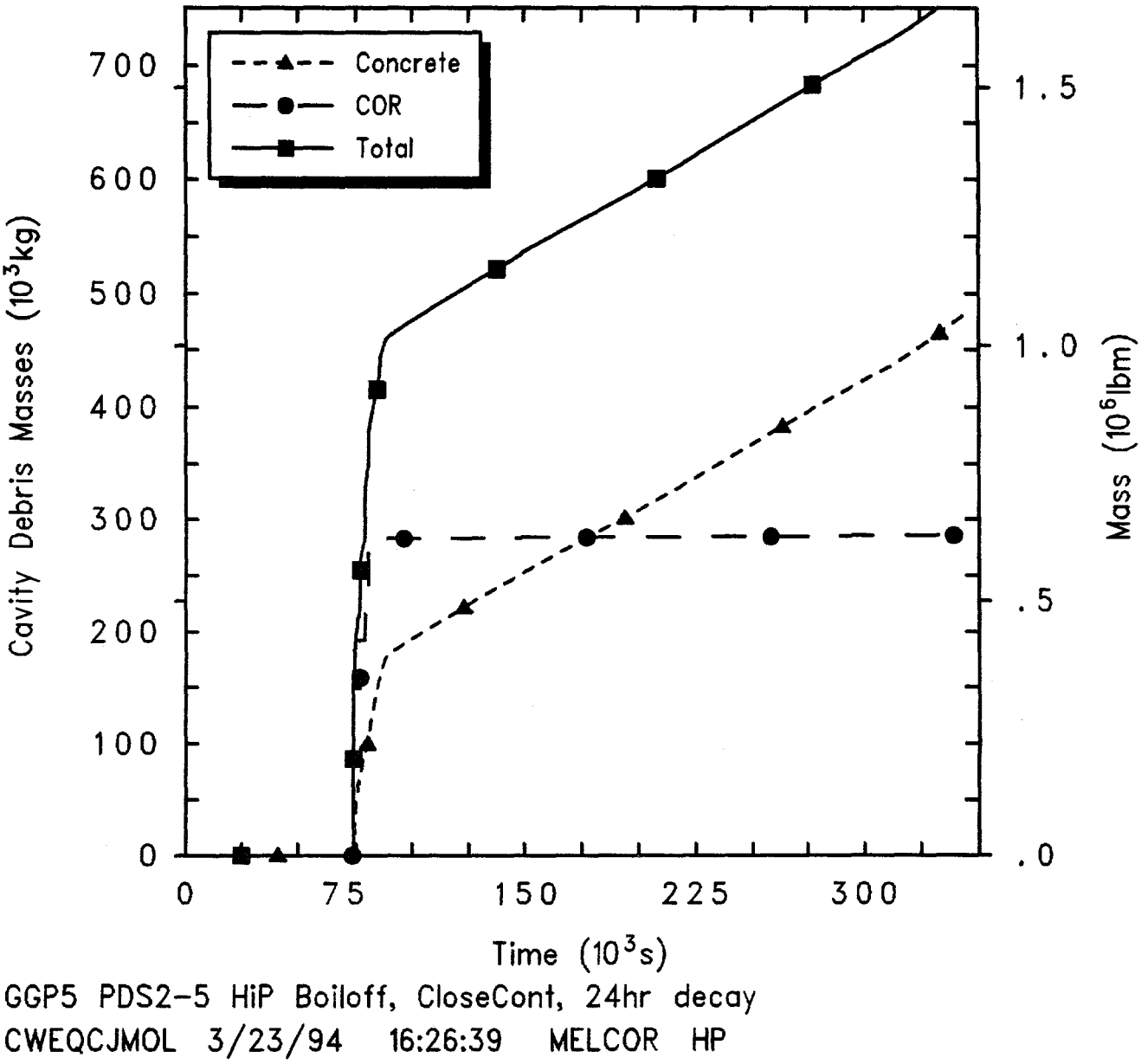

Figure 4.3.5.8. Cavity Total and Core and Concrete Debris Masses for Grand Gulf POS 5 -- High Pressure Boiloff with Open RPV Head Vent and Closed Containment, Initiated 24 hr After Shutdown.

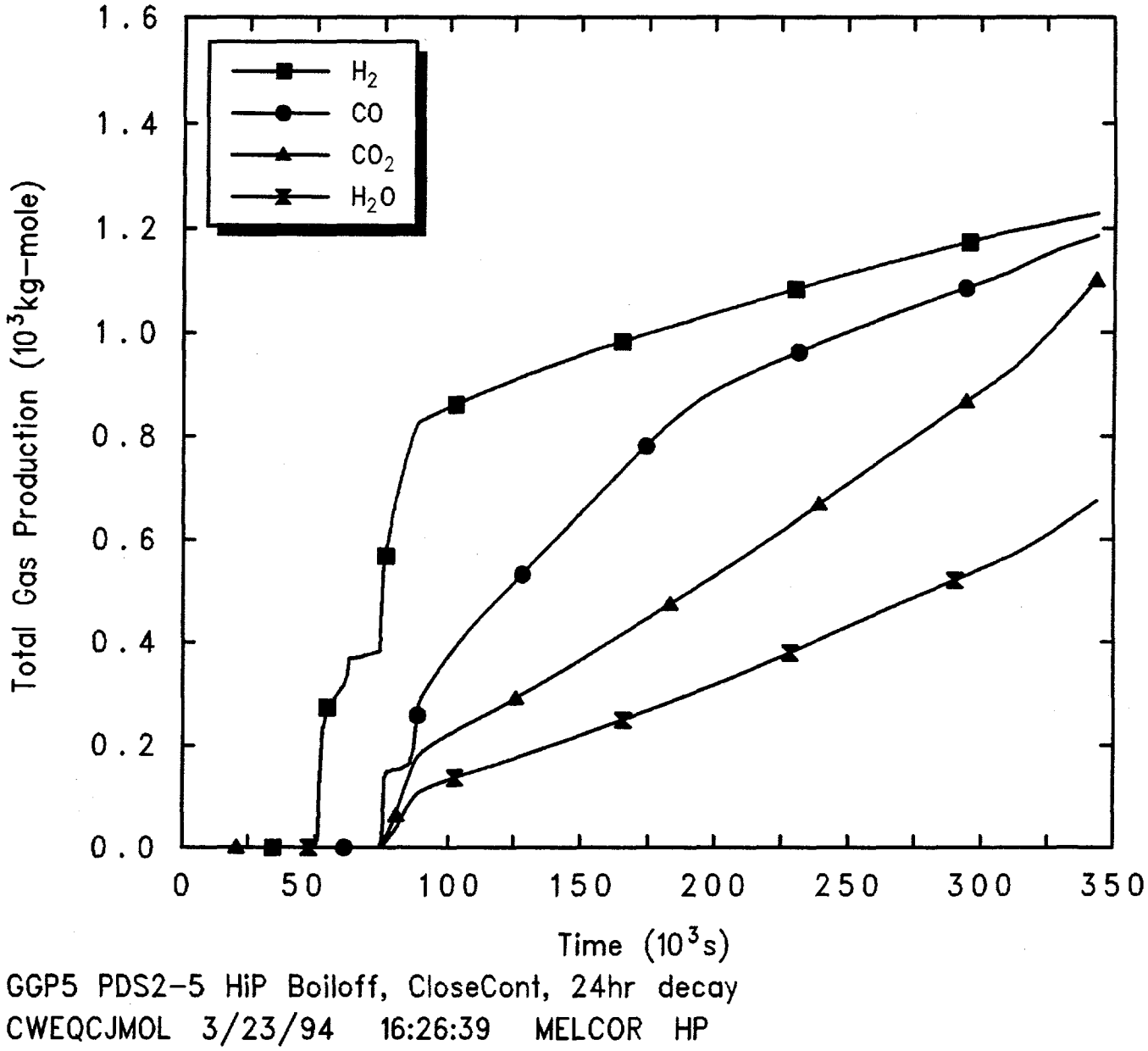

Figure 4.3.5.9. Hydrogen, Carbon Monoxide, Carbon Dioxide and Steam Generation for Grand Gulf POS 5 -- High Pressure Boiloff with Open RPV Head Vent and Closed Containment, Initiated 24 hr After Shutdown.

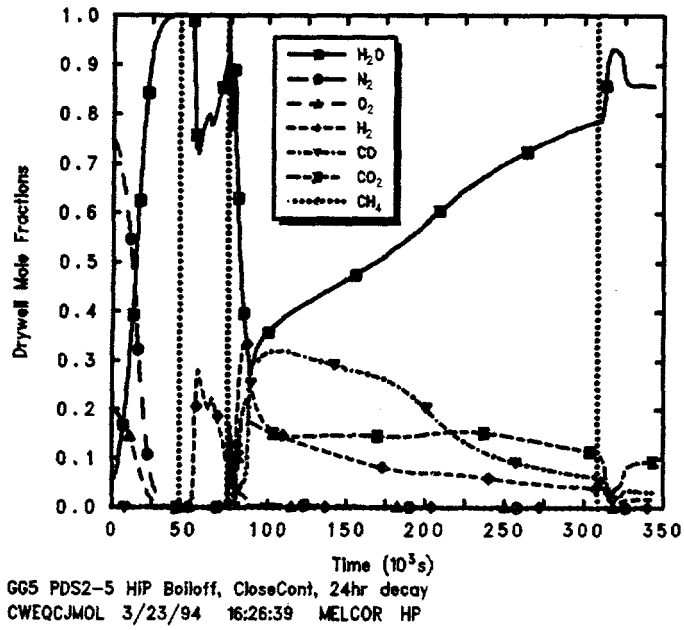

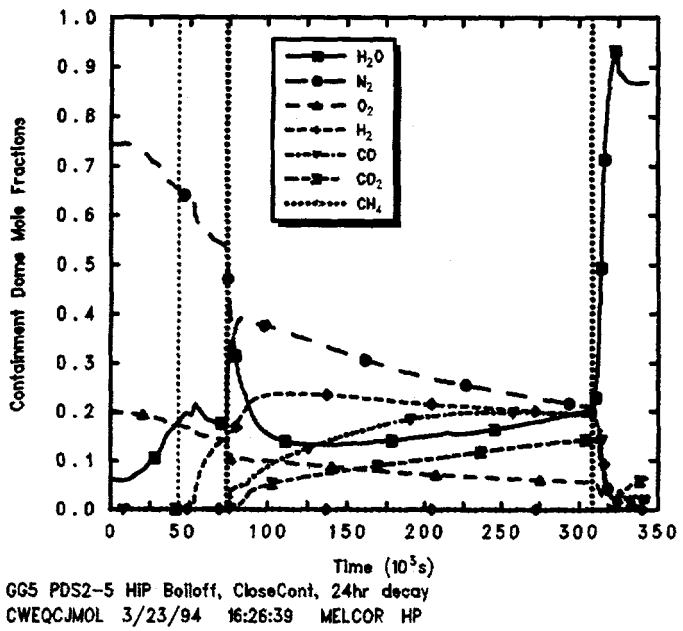

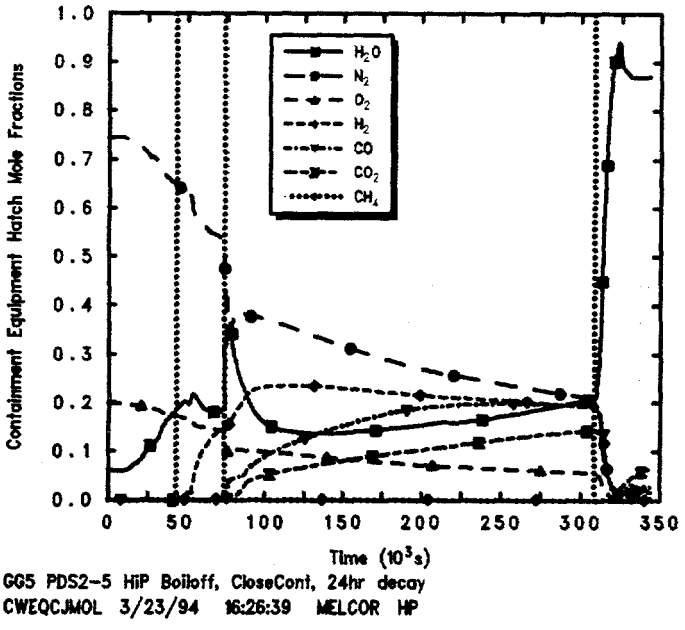

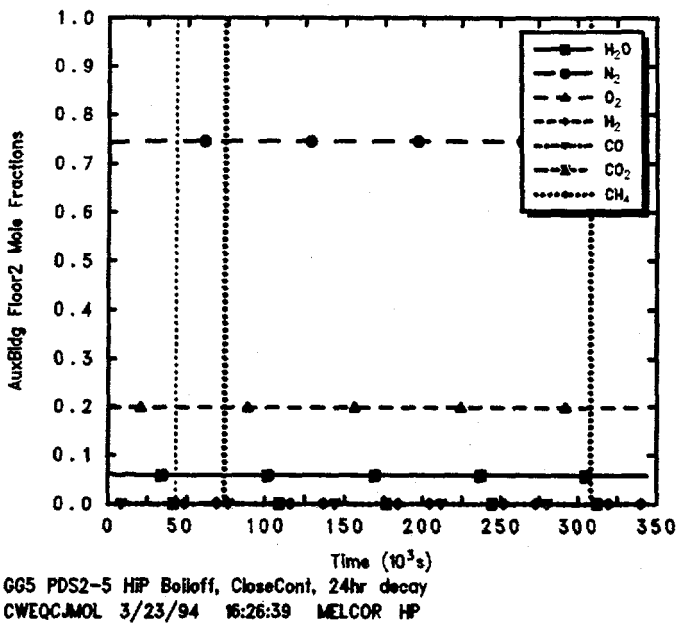

Figure 4.3.5.10. Mole Fractions in Drywell (upper left), Containment Dome (upper right), Containment Equipment Hatch (lower left) and Auxiliary Building (lower right) for Grand Gulf POS 5 -- High Pressure Boiloff with Open RPV Head Vent and Closed Containment, Initiated 24 hr After Shutdown.

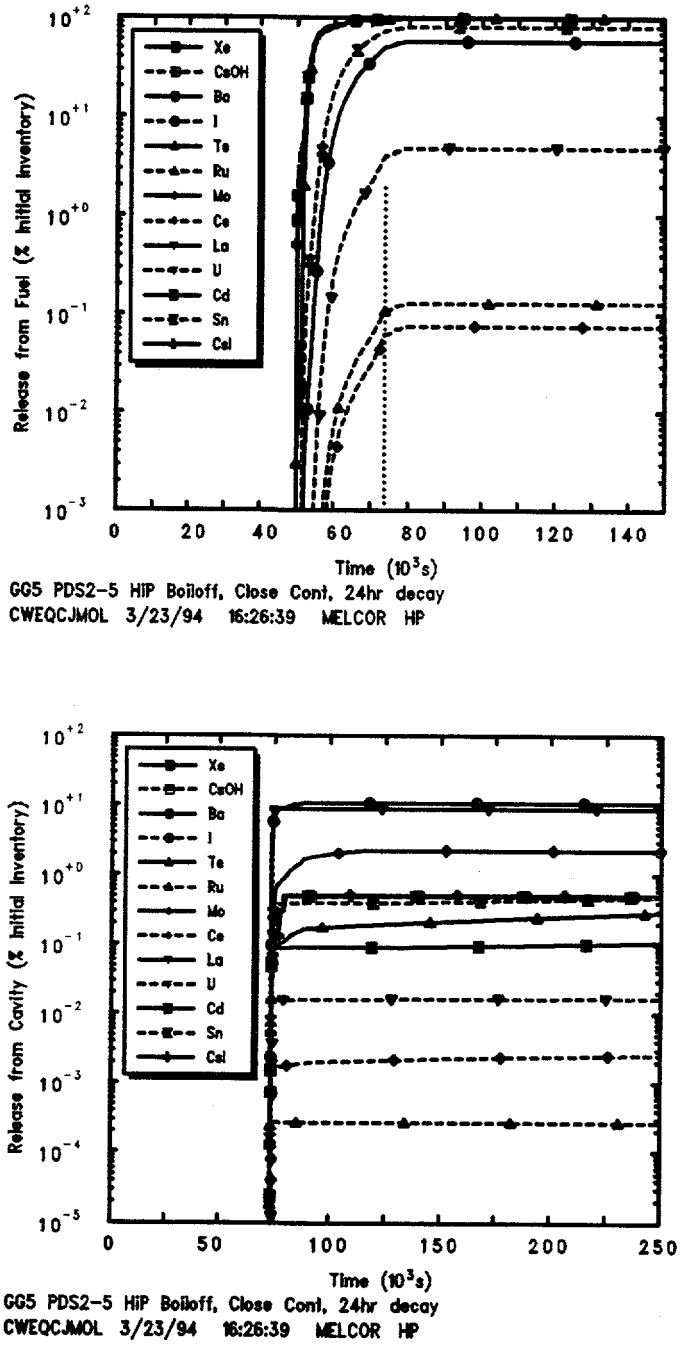

Figure 4.3.5.11. In-Vessel (top) and Ex-Vessel (bottom) Radionuclide Release Mass Fractions for Grand Gulf POS 5 -- High Pressure Boiloff with Open RPV Head Vent and Closed Containment, Initiated 24 hr After Shutdown.

Table 4.3.5.2. Final Radionuclide Release Fractions for Grand Gulf POS 5 -- High Pressure Boiloff with Open RPV Head Vent and Closed Containment, Initiated 24 hr After Shutdown

Class	Fission Products Released from Fuel (% Initial Inventory-Mass Fraction)		
	In-Vessel	Ex-Vessel	Total
Xe	99.46	0.5	99.96
CsOH	99.48	0.49	99.97
Ba	57.14	10.73	67.87
I	~0	~0	~0
Te	99.44	0.44	99.88
Ru	0.129	0.00026	0.129
Mo	0	2.19	2.19
Ce	0.076	0.0027	0.079
La	0	8.76	8.76
U	4.72	0.017	4.74
Cd	0	0.341	0.341
Sn	80.49	1.56	82.05
CsI	99.47	0.5	99.97

releases of nonradioactive aerosols from structural materials.)

The release behavior predicted by MELCOR is somewhat different for this scenario than for the others analyzed. In all cases, almost all (~100%) of the volatile Class 1 (noble gases), Class 2 (CsOH), Class 5 (Te) and Class 16 (CsI) radionuclide species are released, primarily in-vessel, as are most (70-80%) of the Class 3 (Ba) and Class 12 (Sn) inventories. However, for this sequence the next major release fractions predicted, 1-10%, are for Mo, La and uranium. Around 0.1-0.4% of the total inventories of Ru, Ce and Cd, are released. (Recall that the CORSOR-M fission product release model option used in these analyses has identically zero release in-vessel of Mo, La and Cd.)

Figure 4.3.5.12 gives the total radioactive release to the environment, while the release fractions of individual classes to the environment are shown in Figure 4.3.5.13. The release to the environment does not begin at vessel failure in this sequence, but only after containment failure. These environmental releases do not correspond to immediate release of all radionuclides released from the fuel; there is considerable retention of most radionuclide species within the containment (but not within the isolated auxiliary building). Almost all the noble gases (~100%) are released to the environment soon after containment fails; in addition, there is some release to the environment of the other volatile species (i.e., CsOH, CsI and Te) also.

Table 4.3.5.3 summarizes the distribution of the initial radionuclide inventory at the end of the calculation, and provides an overview of how much of the radionuclides remains bound up in fuel debris in either the core or the cavity, and of how much of the released radionuclides is retained in the primary system *vs* how much of the released radionuclides is released to, or released in, either the containment or the auxiliary building and the environment, all normalized to the initial inventories of each class. Table 4.3.5.4 presents a different breakdown of the released radionuclide final distribution, giving the fractions of released inventory for each class in control volume atmospheres (including the environment), in pools, or deposited or settled onto heat structures at the end of the calculations. (As in Table 4.3.5.2 these amounts consider only the release of radioactive forms of

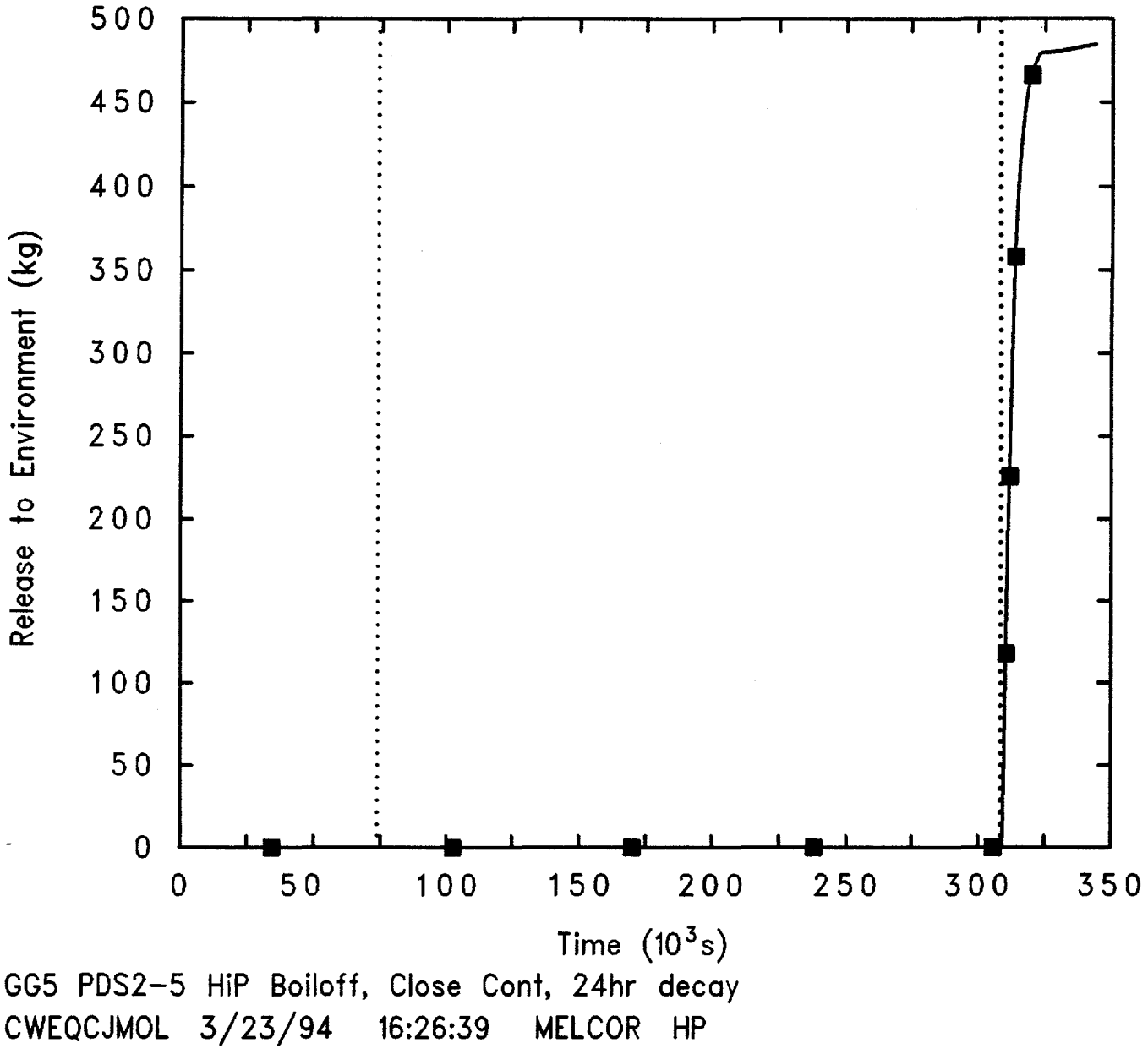

Figure 4.3.5.12. Total Environmental Radionuclide Releases for Grand Gulf POS 5 -- High Pressure Boiloff with Open RPV Head Vent and Closed Containment, Initiated 24 hr After Shutdown.

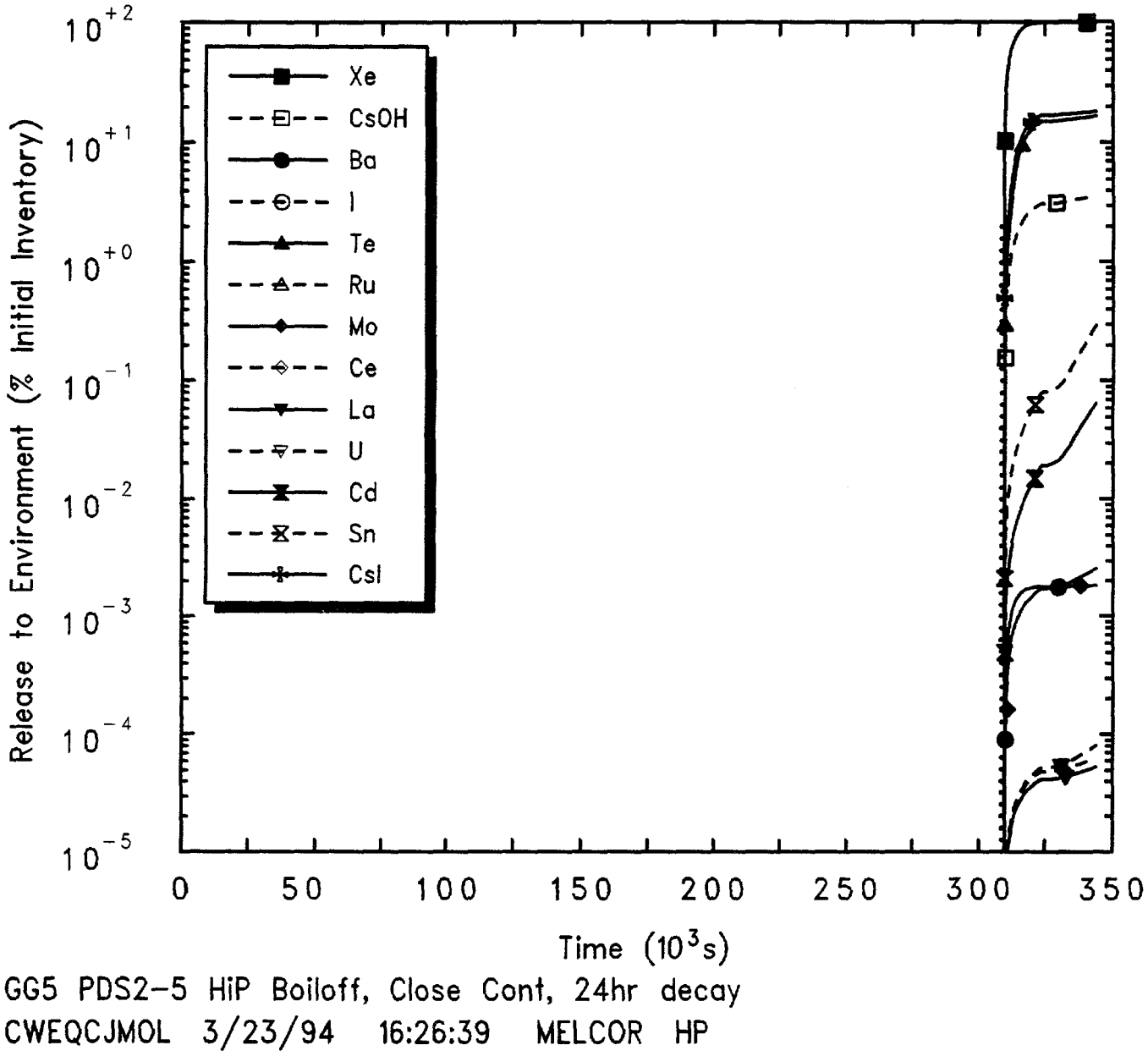

Figure 4.3.5.13. Environmental Radionuclide Release Mass Fractions for Grand Gulf POS 5 -- High Pressure Boiloff with Open RPV Head Vent and Closed Containment, Initiated at 24 hr After Shutdown.

Table 4.3.5.3. Final Radionuclide Distribution for Grand Gulf POS 5 -- High Pressure Boiloff with Open RPV Head Vent and Closed Containment, Initiated 24 hr After Shutdown

Class	Fission Product Distribution (% Initial Inventory-Mass Fraction)				
	Fuel Debris	Primary System	Containment	Auxiliary Building	Environment
Xe	0.04	0.028	0.431	0	99.5
CsOH	0.04	48.8	47.54	0	3.6
Ba	32.14	38.8	34.07	0	0.003
Te	0.12	11.3	64.65	0	16.5
Ru	99.8	0.069	0.06	0	7.0e-07
Mo	97.8	0.217	1.98	0	0.0018
Ce	99.9	0.04	0.038	0	0.00006
La	91.2	0.955	7.8	0	0.00005
U	95.6	2.35	2.02	0	0.00007
Cd	99.6	0.011	0.266	0	0.0643
Sn	17.9	48.4	33.32	0	0.291
CsI	~0	3.49	78.52	0	18

these classes, and not additional releases of nonradioactive aerosols from structural materials.)

These tables show fission product distributions somewhat similar to those found for the large break LOCA sequences (discussed in Section 4.3.1) for the radionuclides with significant (≥80% of initial inventory) release from fuel. In all the accident scenarios simulated, most of the noble gases released are in the environment, in the atmosphere. Most of the volatile species (CsOH, CsI and Te) releases occurred in-vessel in both the large break LOCA and in this high pressure boiloff, with most of those releases retained in the containment. More of the volatiles are released to the environment in this high pressure boiloff with closed containment than in the large break LOCA or station blackout scenarios. This is the only accident sequence analyzed with the calculated environmental release fraction increasing with the volatility (i.e., CsI being the most volatile has the highest environmental release fraction, while CsOH being the least volatile has the lowest environmental release fraction), probably due to the fact that most of the releases to the environment occur with the containment at relatively high pressure compared to ambient. The two classes of radionuclides forming aerosols which had substantial releases (Ba and Sn, also occurring mostly in-vessel) were predicted to have about half those releases retained in the vessel and primarily deposited on structures in both accident scenarios, and the other half retained in the containment mostly in water pools but some deposited on structure surfaces.

4.3.6 Open MSIVs with Closed Containment, Initiated 24 hr After Shutdown

The accident is initiated 24 hr after shutdown. The MSIVs are open; the reactor head vent is closed. The water level in the vessel is at the steam lines, and the water in the vessel is at 366.5 K (200°F), which corresponds to the maximum temperature allowed by the Grand Gulf technical specifications for operation in POS 5. The suppression pool level is at the ECCS suction strainers, 3.05 m (10 ft) from the suppression pool floor. The containment is at 305.4 K (90°F) and the suppression pool is at 308.2 K (95°F). Following the initiating event, the operators close the containment 5 hr after the initiating event, but the drywell personnel lock remains open. Injection is not restored to the core during the accident.

This sequence is virtually identical to the open-MSIV scenario discussed in Section 4.2.1; in those Level 1

Table 4.3.5.4. Final Radionuclide State for Grand Gulf POS 5 -- High Pressure Boiloff with Open RPV Head Vent and Closed Containment, Initiated 24 hr After Shutdown

Class	Fission Products Released from Fuel (% Released Inventory-Mass Fraction)		
	Atmosphere	Pool	Deposited
Xe	~100	0	0
CsOH	4.69	36.9	58.4
Ba	0.006	22	78
I	~100	0	0
Te	24.4	36.6	39
Ru	~0	18.5	81.5
Mo	0.086	36.9	63
Ce	0.11	19.6	80.3
La	0.001	55.7	44.3
U	0.003	18.4	81.6
Cd	49.5	22.4	28
Sn	0.95	16.2	82.8
CsI	22.8	51	26.2

analyses the containment was open while in these Level 2 analyses the containment was assumed to be closed after 5 hr but, because of the open MSIV line providing a path to the auxiliary building, that difference in scenario is not significant.

The sequence of events predicted for this accident with different initiation times is given in Table 4.3.6.1.

Figure 4.3.6.1 gives the vessel, containment and auxiliary building pressures predicted by MELCOR. The pressure responses for the vessel and for the auxiliary building are very similar to that presented in Figures 4.2.1.1 and 4.2.1.2 in Section 4.2.1 for this sequence initiated 24 hr after shutdown. The system begins pressurizing as all core cooling is lost but only pressurizes to ~160kPa before the steam flow out the open MSIVs is sufficient to remove all the decay heat. The steam flow out the MSIVs in turn pressurizes the auxiliary building and, through the open equipment hatch and personnel locks, pressurizes the containment. The auxiliary building fails on a 0.345 kPa (5 psig) overpressure. The closing of the containment at 5 hr allows a pressure differential of ~2 psig to build up between the reactor pressure vessel and the containment, but the open MSIV line keeps the vessel equilibrated and venting to the auxiliary building, which fails soon after 5 hr when the containment is closed.

The vessel inventory response is also almost identical to the results discussed for the corresponding Level 1 analysis presented in Section 4.2.1 (shown in Figure 4.2.1.3). Figure 4.3.6.2 presents the upper plenum, core and lower plenum swollen and collapsed liquid levels for this accident sequence. The level drops as inventory continues to be lost out the open MSIV line. The vessel liquid level drops through the upper plenum into the core and continues dropping smoothly partway into the lower plenum, followed by a more gradual loss of the remaining inventory due to boiling and steam outflow. There is substantial pool frothing and swelling in both the upper plenum and upper core regions during this boiloff. vessel volumes in this sequence. The lower plenum liquid level drops quickly to zero when the vessel lower head penetrations fail and any remaining water is dropped into the cavity together with falling core debris.

Table 4.3.6.1. Sequence of Events Predicted by MELCOR for Open MSIVs with Closed Containment, Initiated 24 hr After Shutdown

Event	Time After Shutdown 24 hr
Accident initiation	0
Core uncovery (TAF) begins	15,714 s (2.72 hr)
Containment closed	18,000 s (5 hr)
Auxiliary building failed	20,000 s (5.56 hr)
Core heatup begins	30,000 s (8.33 hr)
Clad failure/Gap release	
(Ring 1)	35,373 s (17.53 hr)
(Ring 2)	35,290 s (17.51 hr)
(Ring 3)	35,377 s (17.52 hr)
(Ring 4)	35,838 s (17.62 hr)
(Ring 5)	37,452 s (18.02 hr)
(Ring 6)	41,997 s (22.00 hr)
Core plate failed	
(Ring 1)	118,554 s (25.14 hr)
(Ring 2)	113,565 s (26.43 hr)
(Ring 3)	118,141 s (26.26 hr)
(Ring 4)	116,470 s (26.25 hr)
(Ring 5)	118,063 s (28.50 hr)
(Ring 6)	122,243 s (31.21 hr)
Vessel LH penetration failed	
(Ring 1)	113,652 s (25.16 hr)
(Ring 2)	113,666 s (25.124 hr)
(Ring 3)	113,565 s (25.124 hr)
(Ring 4)	113,642 s (25.18 hr)
(Ring 5)	113,647 s (28.54 hr)
(Ring 6)	113,653 s (31.36 hr)
Commence debris ejection	113,565 s (25.16 hr)
Cavity rupture	
End of calculation	250,000 s (55.32 hr)

The heatup of the intact fuel and clad is illustrated in Figure 4.3.6.3. Because the fuel/clad component temperatures in MELCOR are set to zero in a cell when that component fails, this figure shows both the overall heatup rate and the time that the intact fuel/clad component fails through melting of the clad at 2100 K (3320°F). Figure 4.3.6.4 presents corresponding core debris temperatures in the active fuel region; these are the temperatures of the debris bed formed by the failure of the intact fuel/clad component in MELCOR in a core cell, whose (intact) temperatures were given in Figure 4.3.6.3. The debris bed in the active fuel region reaches peak temperatures ≥3500 K (5840°F), significantly above the UO_2 melt temperature of 3113 K (5144°F), except in the lowest active fuel level where the temperature never reaches the UO_2 melt temperature. The temperatures of

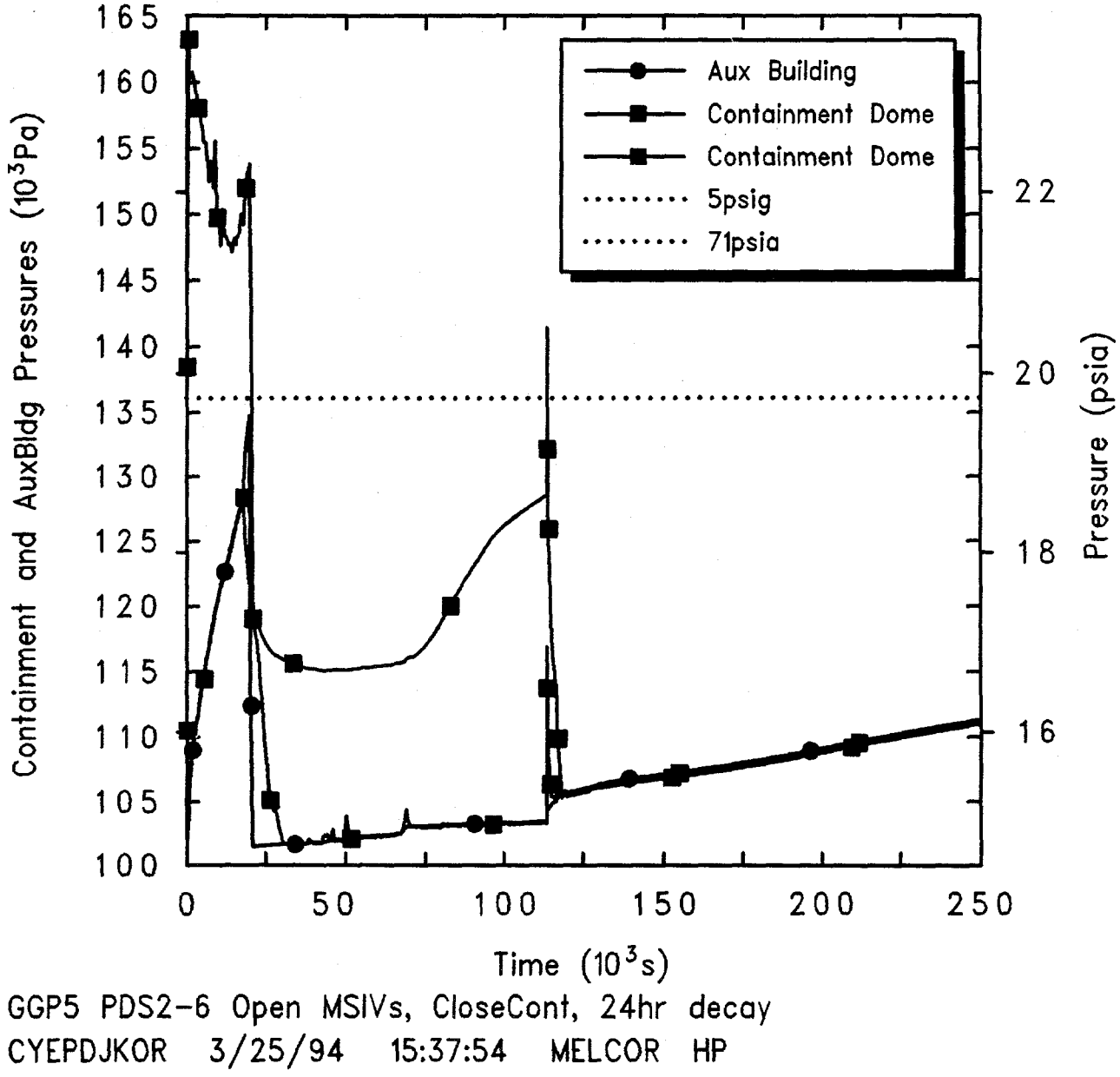

Figure 4.3.6.1. Vessel, Containment and Auxiliary Building Pressures for Grand Gulf POS 5 -- Open MSIVs with Closed Containment, Initiated 24 hr After Shutdown.

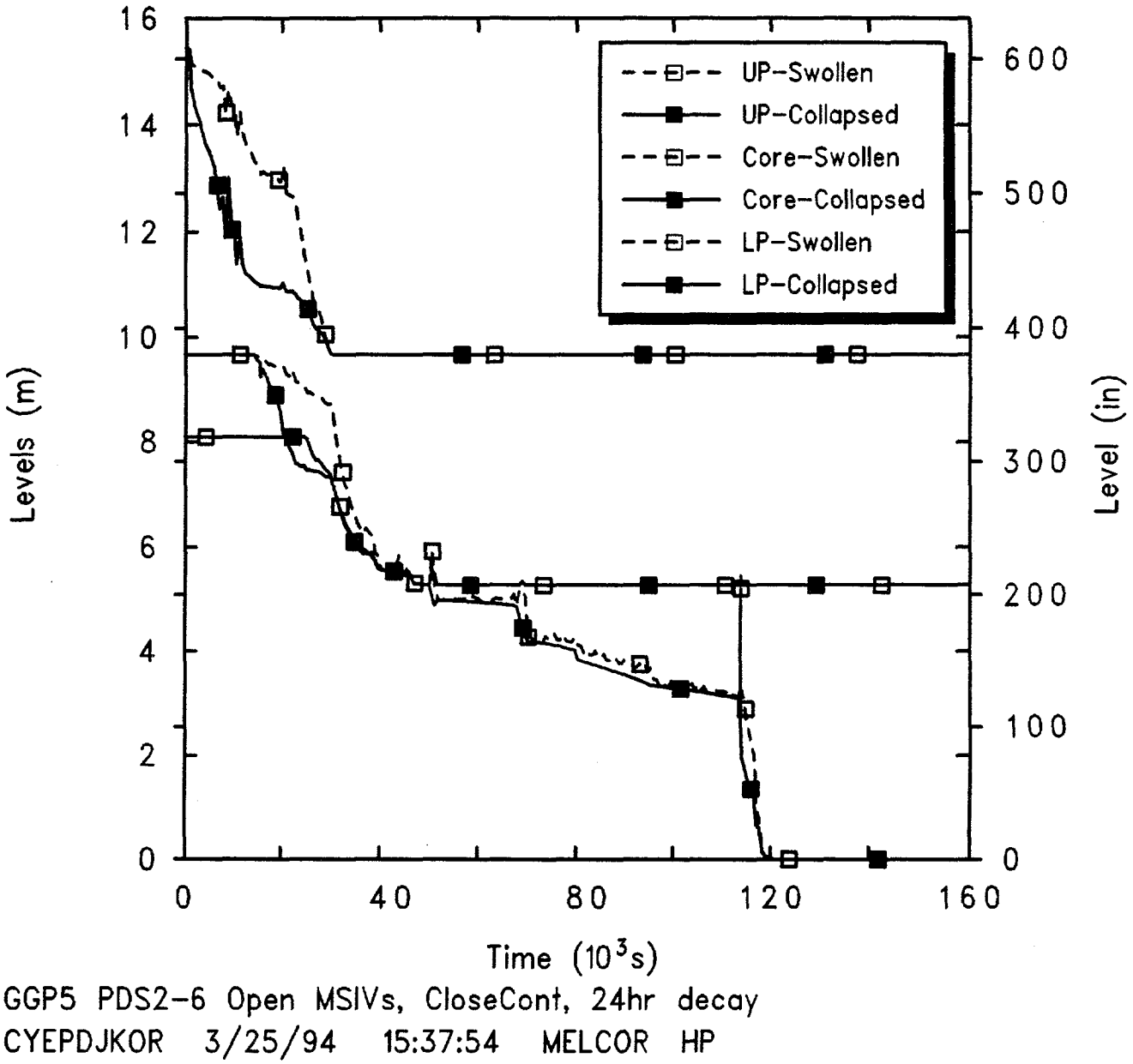

Figure 4.3.6.2. Upper Plenum, Core and Lower Plenum Liquid Levels for Grand Gulf POS 5 -- Open MSIVs with Closed Containment, Initiated 24 hr After Shutdown.

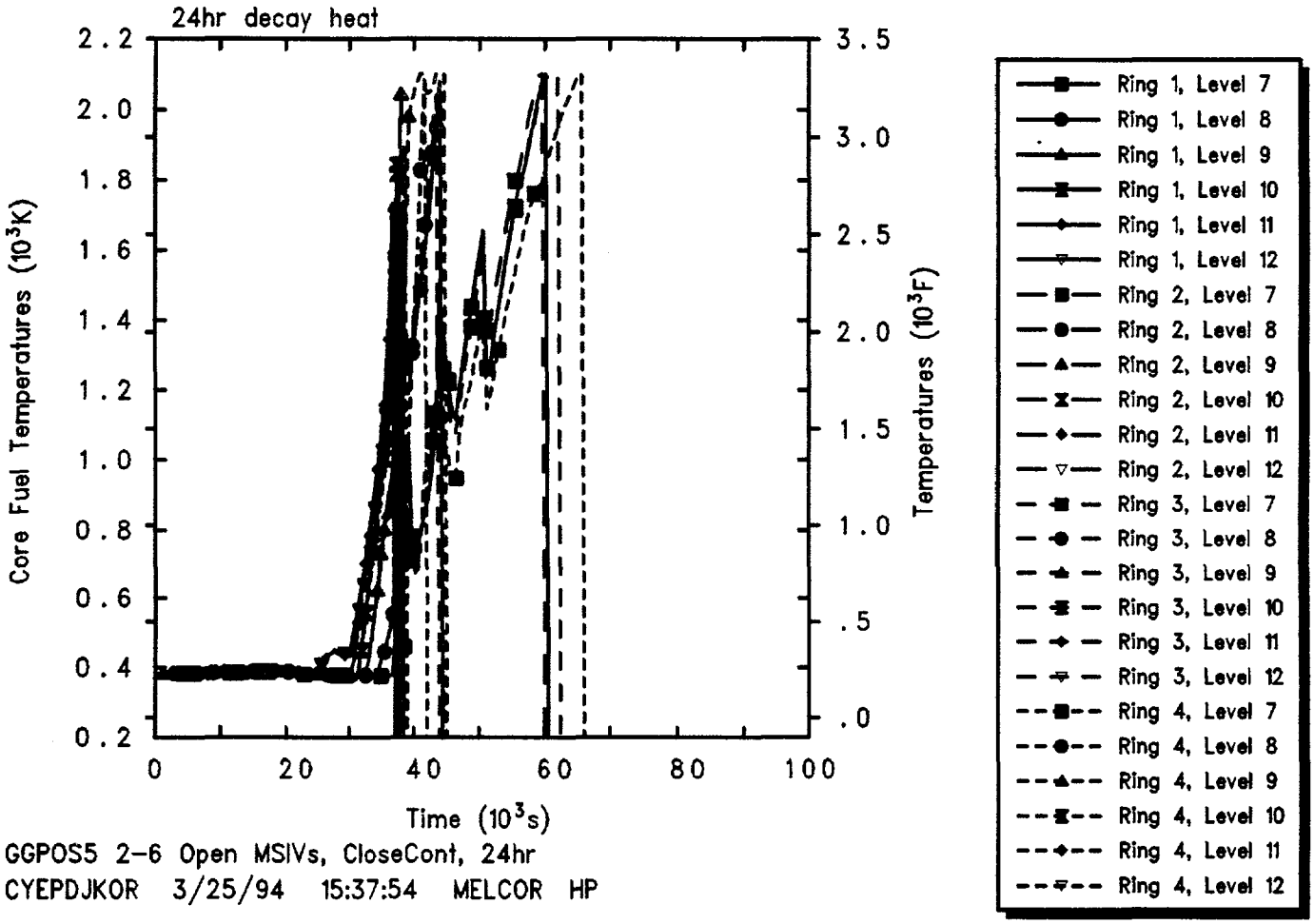

Figure 4.3.6.3. Core Intact Fuel/Clad Temperatures for Grand Gulf POS 5 -- Pressure Open MSIVs with Closed Containment, Initiated 24 hr After Shutdown.

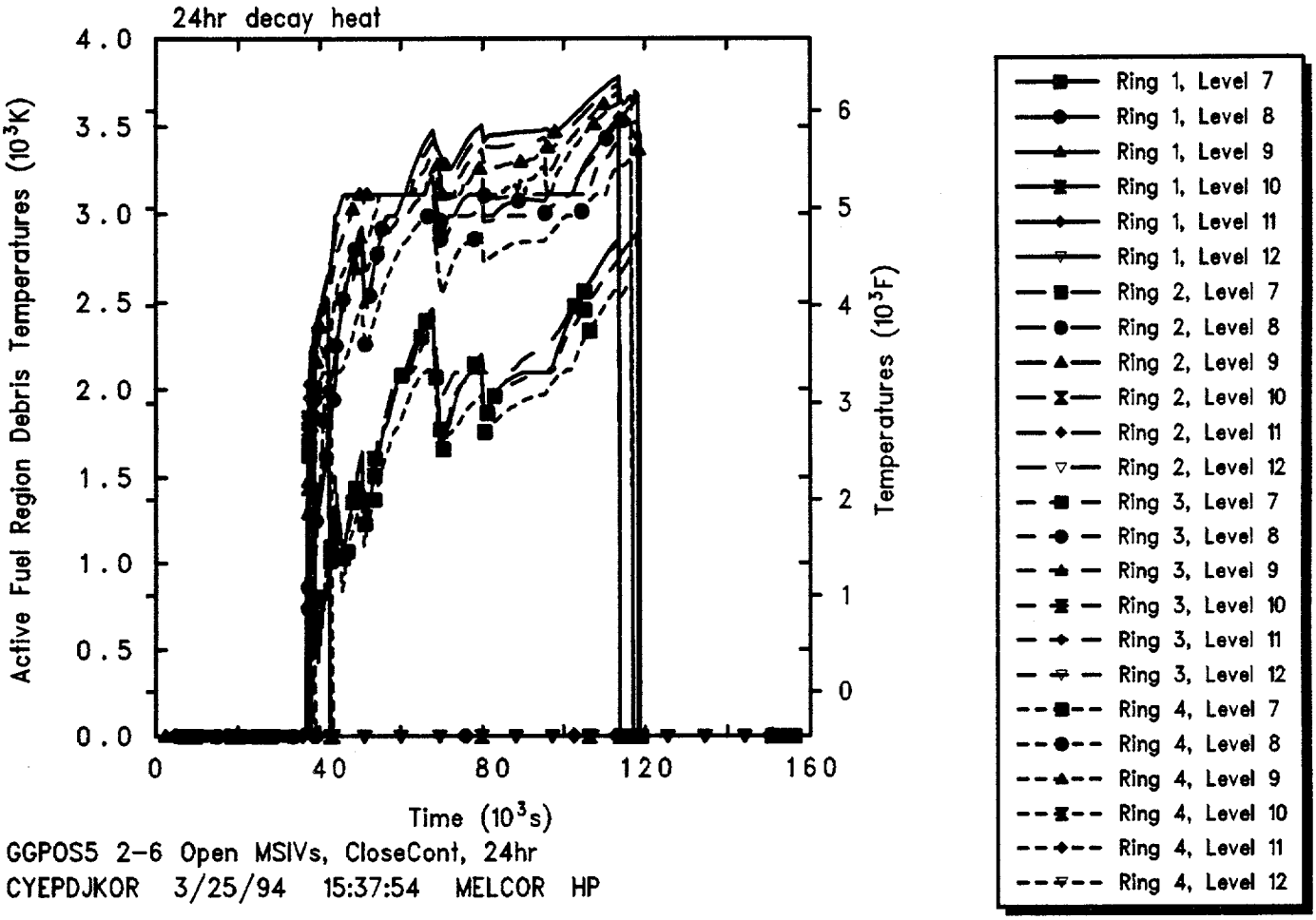

Figure 4.3.6.4. Core Active Fuel Region Debris Bed Temperatures for Grand Gulf POS 5 -- Open MSIVs with Closed Containment, Initiated 24 hr After Shutdown.

the active fuel region debris bed drop to zero when the core plate fails and the debris relocates to the lower plenum.

The predicted temperatures in the debris bed in the lower plenum and core plate are given in Figure 4.3.6.5. Prior to core plate failure there is some cold, refrozen debris both on the core support plate and on the lower core structural material just above the core support plate; the cooling and refreezing of this debris is the cause of the continued gradual drop in lower plenum liquid level due to steaming seen in Figure 4.3.6.2. The lower core debris bed temperatures during this time period are substantially lower than predicted in the other transients analyzed, due to enhanced steam flow and cooling in the core region, and it takes a relatively long time for the debris temperature to rise to the core support plate failure temperature of 1273 K (1832°F). After core plate failure hot, high-temperature debris begins appearing in the lower plenum as debris falls from the active fuel region into the lower plenum. The lower head penetrations begin failing almost immediately, and the lower plenum debris temperatures begin dropping to zero as debris is ejected from the vessel to the cavity.

Figure 4.3.6.6 illustrates what fraction of each material in the active fuel region has collapsed into a debris rubble bed held up by the core support plate, prior to core plate failure, debris relocation, lower head failure and debris ejection, for this high pressure boiloff scenario. The debris bed forms as material (in particular, the zircaloy clad and the UO_2 fuel) reaches melting. The debris bed forms relatively slowly in this scenario, taking 10,000-20,000 s to reach its final configuration. The fraction of material in the debris bed later remains nearly constant as the debris material continues to heat up.

Figure 4.3.6.7 shows both the total and the individual masses of core materials (UO_2, zircaloy and ZrO_2, stainless steel and steel oxide, and control rod poison) remaining in the vessel. This includes both material in the active fuel region and in the lower plenum. Debris ejection began very soon after lower head failure. This figure illustrates that most of the core material was lost from the vessel to the cavity quickly, in step-like stages. In all cases, all of the UO_2 was transferred to the cavity within a short time after the initial vessel lower head penetration failure, as was the unoxidized zircaloy, the associated zirconium oxide and the control rod poison. A substantial fraction (45-50%) of the structural steel in the lower plenum, and some associated steel oxide, was predicted to remain unmelted and in place, more than in any of the other scenarios analyzed with MELCOR except the high pressure boiloff discussed in the previous section.

The debris material lost from the vessel is ejected to the drywell pedestal cavity. Figure 4.3.6.8 presents the amounts of ejected core debris, concrete ablated and the total cavity debris mass (i.e., core debris combined with concrete ablation products). As in the other sequences analyzed, concrete ablation is quite rapid soon after debris ejection while the core debris is hot (>2000 K) and consists of a layer of metallic debris above a heavy oxide layer, and then slows noticably after enough concrete has been ablated for the debris bed configuration to invert to a light oxide layer above a layer of metallic debris, mixed to a lower average temperature of ~1500 K.

The calculated production of steam and noncondensable gases (H_2, CO, CO_2 and H_2O) is depicted in Figure 4.3.6.9. The hydrogen production shown includes both in-vessel production (the initial step increase) and ex-vessel production in the cavity (the later-time increase). The in-vessel hydrogen generation corresponds to the oxidation of about 10-20% of the zircaloy and about 1% of the steel in the core and lower plenum, prior to vessel failure and debris ejection. As soon as the core debris enters the cavity, core-concrete interaction begins, resulting in the production of carbon dioxide and hydrogen; reduction of these gases by the molten metal in the core debris also gives rise to carbon monoxide and hydrogen.

The mole fractions in the containment dome and in the auxiliary building (first, second and fourth floors) are shown in Figure 4.3.6.10 including vertical dotted lines at TAF uncovery and at vessel failure for reference. The mole fractions in the drywell, cavity and containment equipment hatch resemble the behavior shown for the containment dome, while the behavior in the third floor of the auxiliary building resembles the results shown for the second floor. Before vessel failure, the containment atmosphere consists of air with some steam vented out the open MSIV line to the auxiliary building and back into the containment; after vessel failure and debris ejection, the containment atmosphere consists of nearly early parts of steam, air and the noncondensable gases generated by core-concrete interaction. The open MSIV line vents to the third floor of the auxiliary building, causing a high concentration of steam to build up on the second and third floors after the containment is closed and before the vessel fails; after vessel failure, noncondensable gases generated by core-concrete interaction are added to the atmosphere, transported from the cavity into the vessel through the failed lower head, up through the vessel and

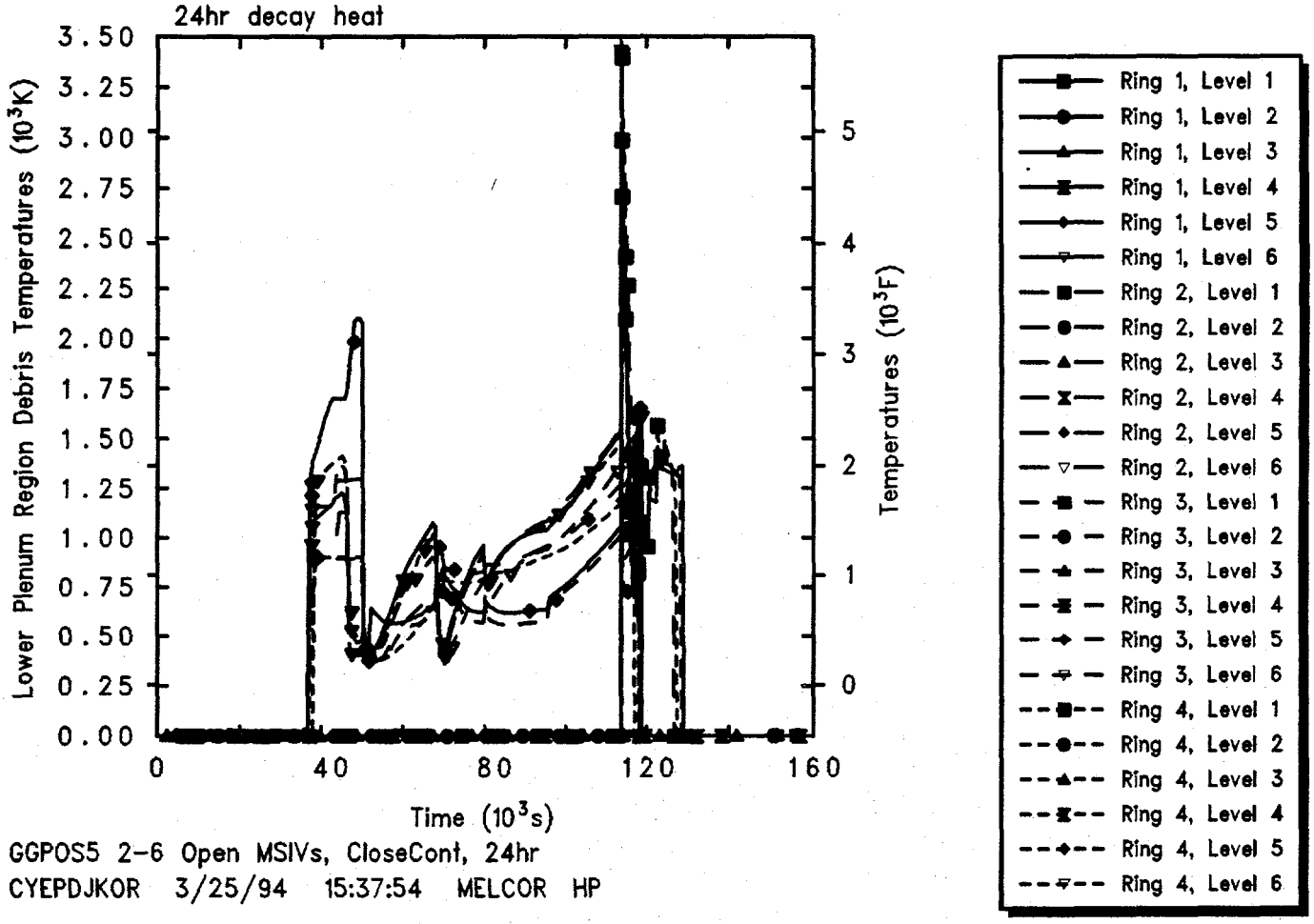

Figure 4.3.6.5. Core Lower Plenum and Core Support Plate Debris Bed Temperatures for Grand Gulf POS 5 -- Open MSIVs and Closed Containment, Initiated 24 hr After Shutdown.

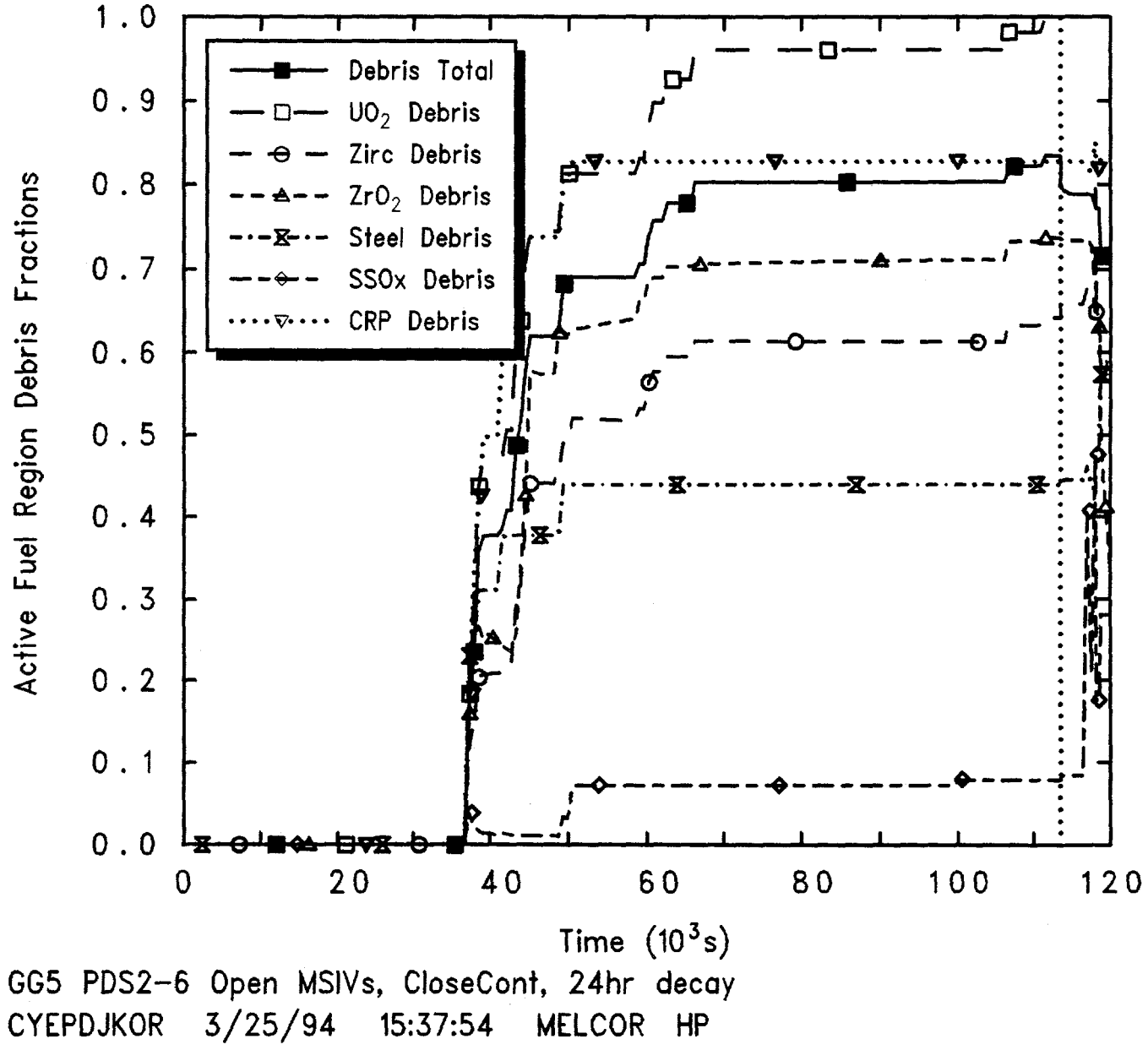

Figure 4.3.6.6. Core Active Fuel Region Degraded Material Fractions for Grand Gulf POS 5 -- Open MSIVs with Closed Containment, Initiated 24 hr After Shutdown.

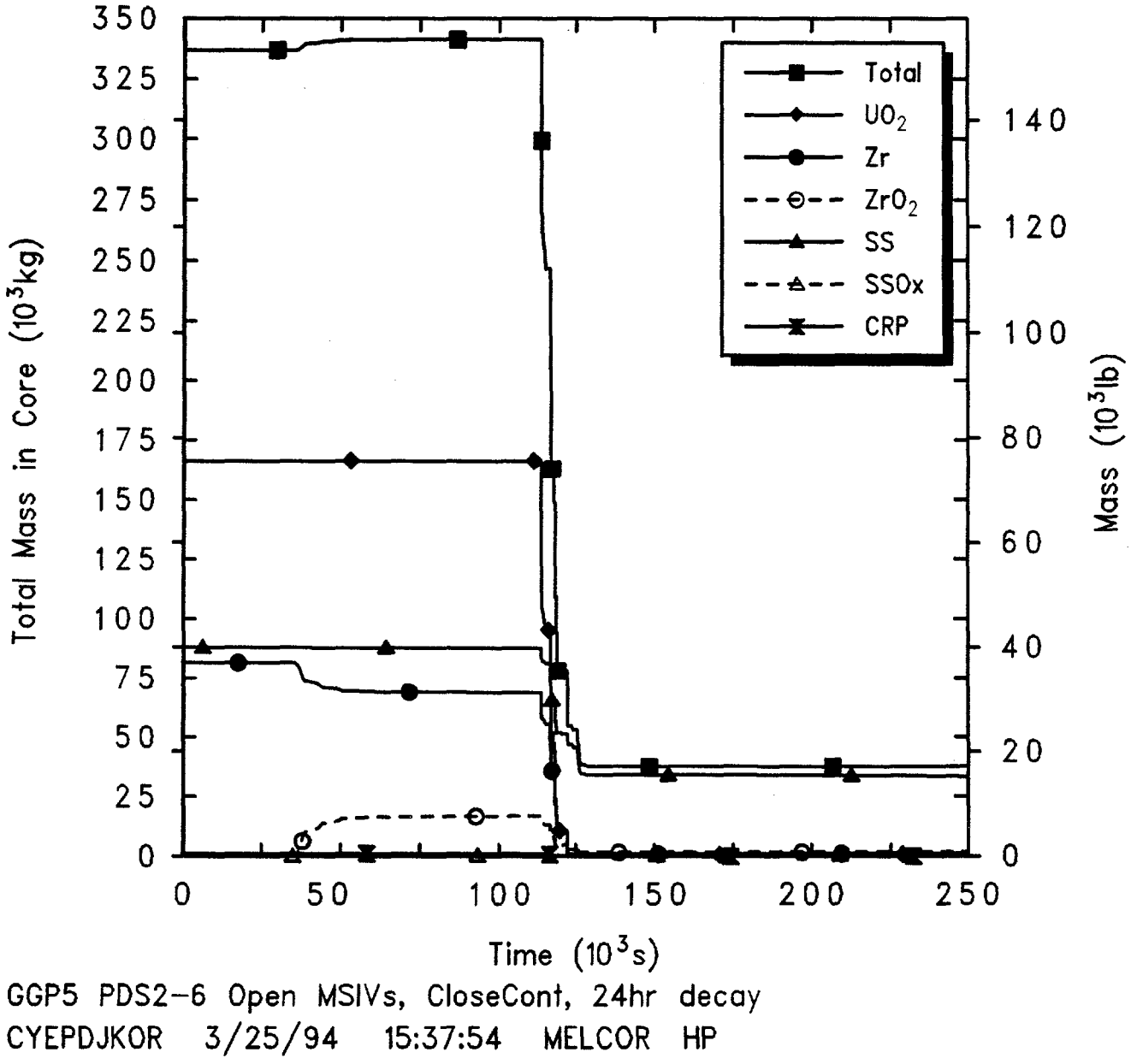

Figure 4.3.6.7. Total and Individual Core Material Masses for Grand Gulf POS 5 -- Open MSIVs with Closed Containment, Initiated 24 hr After Shutdown.

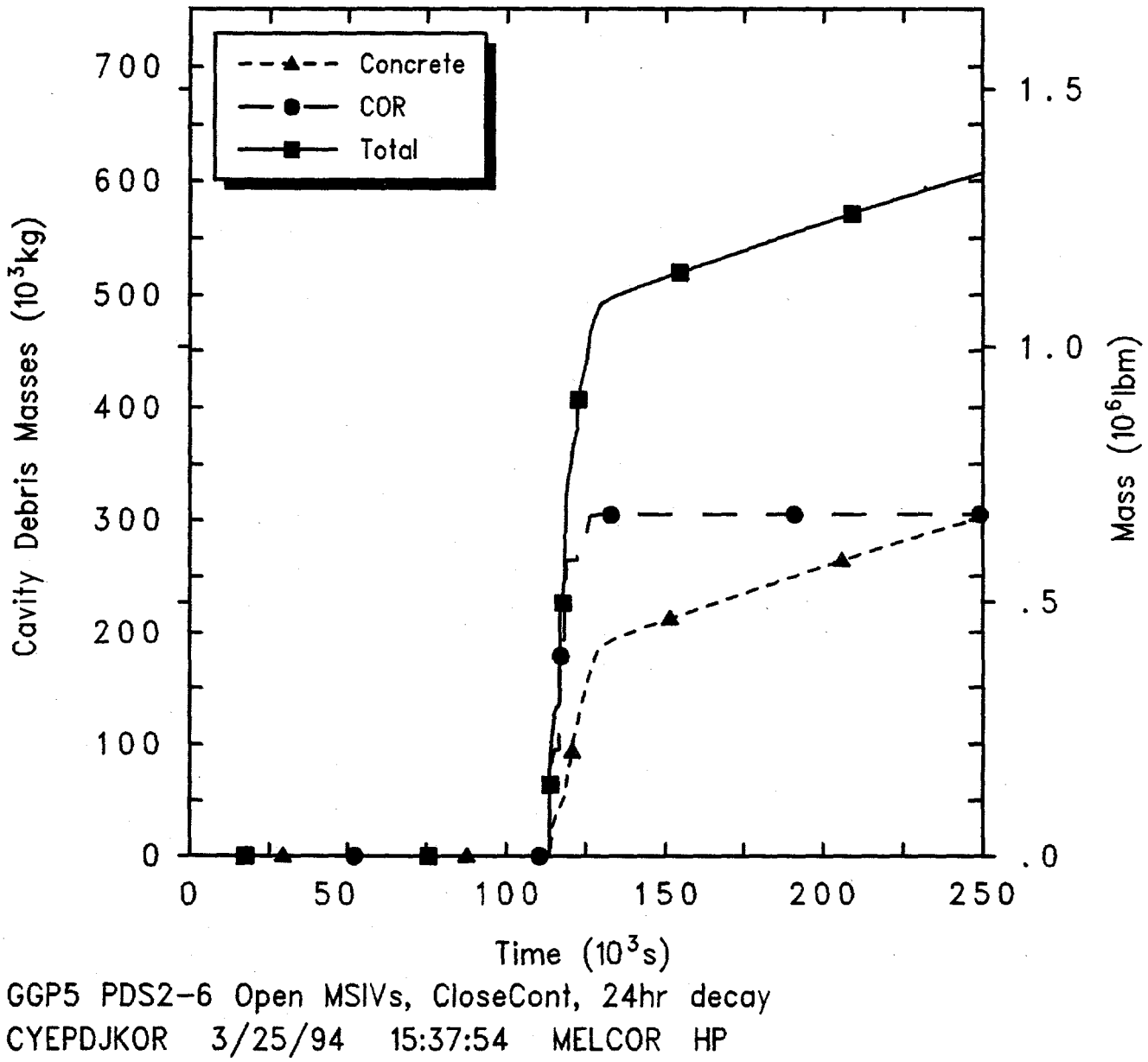

Figure 4.3.6.8. Cavity Total and Core and Concrete Debris Masses for Grand Gulf POS 5 -- Open MSIVs with Closed Containment, Initiated 24 hr After Shutdown.

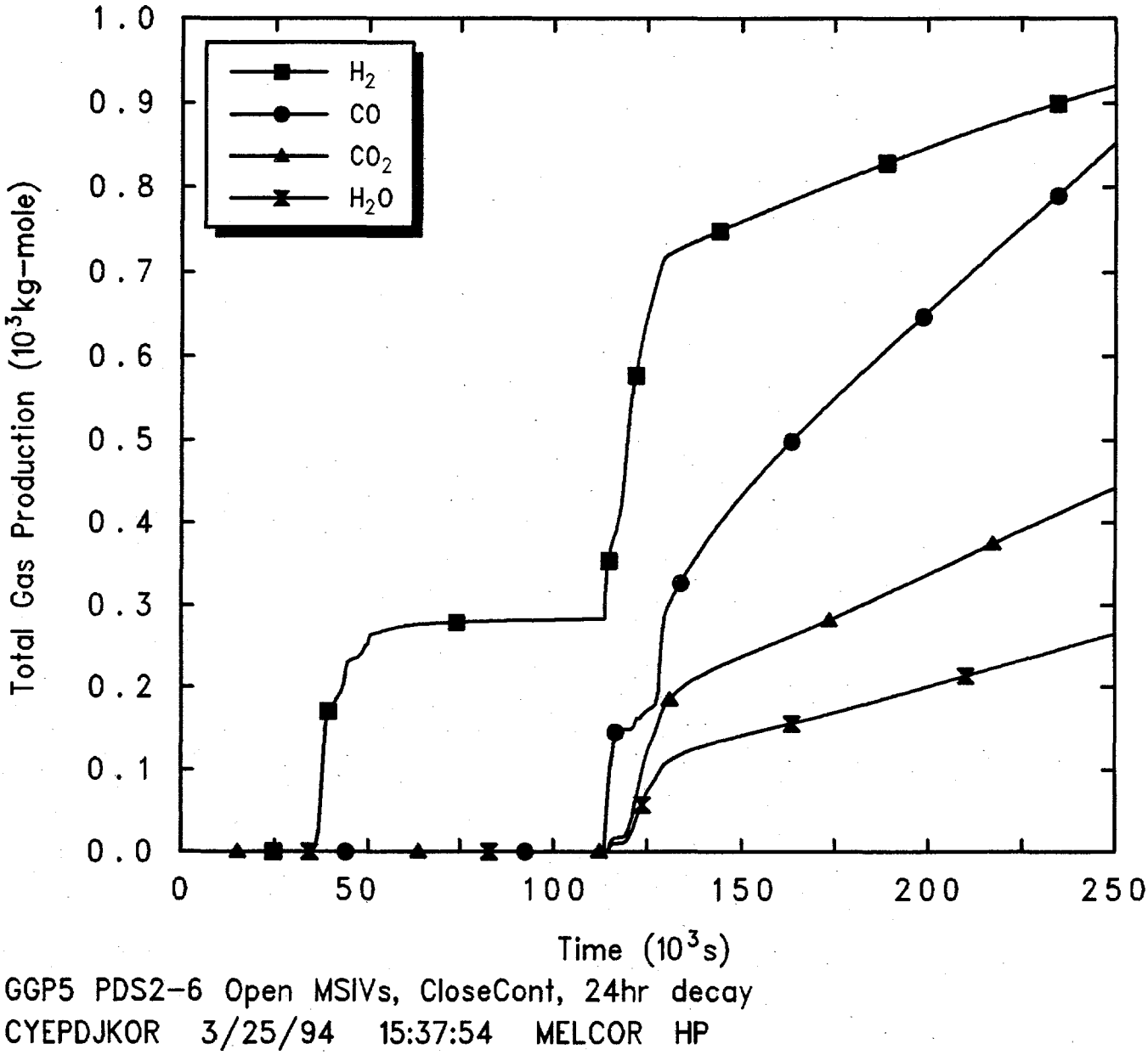

Figure 4.3.6.9. Hydrogen, Carbon Monoxide, Carbon Dioxide and Steam Generation for Grand Gulf POS 5 -- Open MSIVs with Closed Containment, Initiated 24 hr After Shutdown.

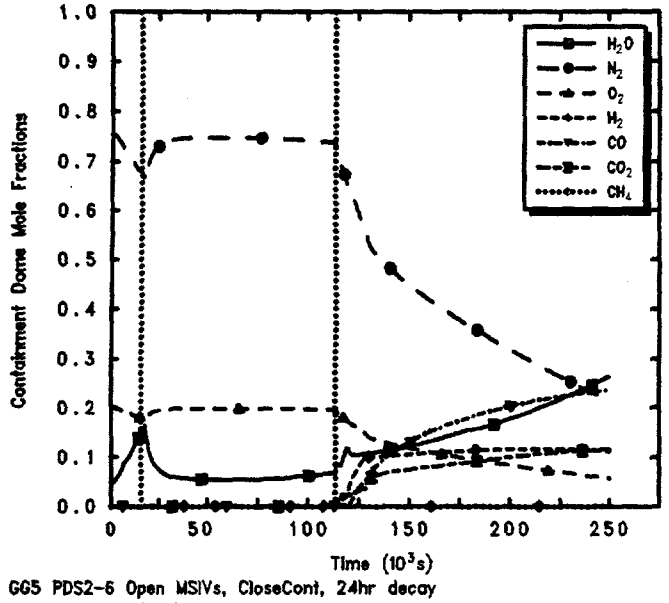

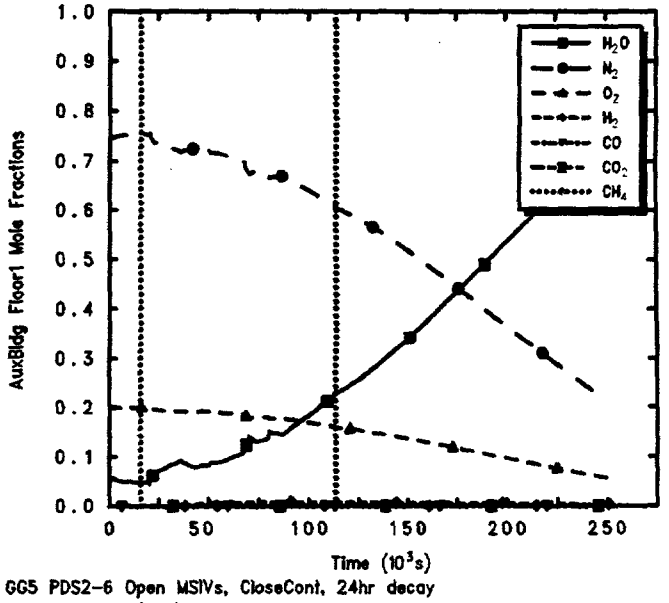

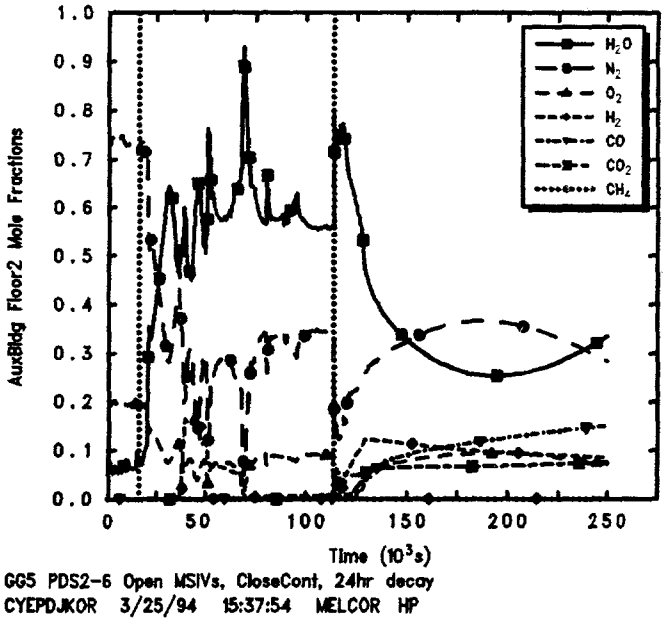

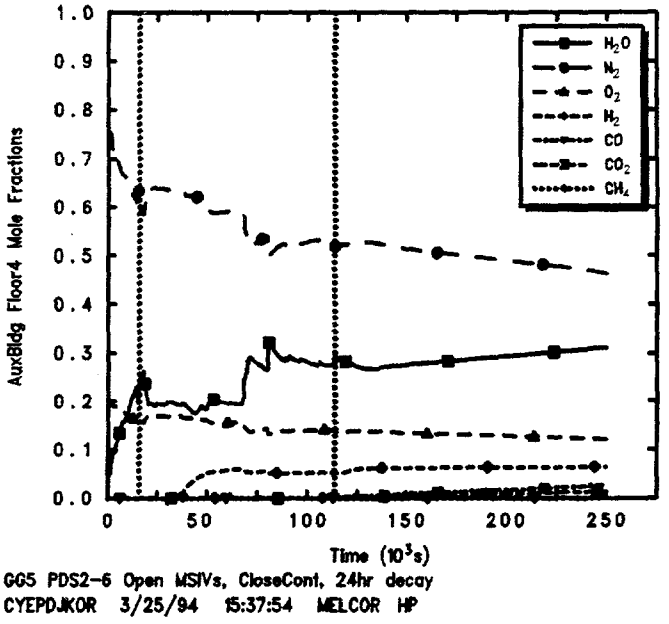

Figure 4.3.6.10. Mole Fractions in Containment Dome (upper left) and Auxiliary Building First (upper right), Second (lower left) and Fourth Floors (lower right) for Grand Gulf POS 5 -- Open MSIVs with Closed Containment, Initiated 24 hr After Shutdown.

out the open MSIV line to the auxiliary building. With the containment equipment hatch and upper personnel lock closed, the fourth floor is a dead-end volume resembling the first floor.

Figure 4.3.6.11 illustrates the time-dependent release of radionuclides from the fuel debris both within the vessel and in the cavity. The vertical dotted lines within the plots mark the time of vessel failure, indicating that most of the in-vessel release occurs prior to vessel failure, from the hot debris bed in the active fuel region, while most of the ex-vessel release occurs within a short time period after vessel failure and debris ejection to the cavity, while the core debris is still hot, before enough concrete has been ablated for the debris bed configuration to cool and invert; this behavior is seen in most of our MELCOR analyses. Table 4.3.6.2 summarizes the in-vessel, ex-vessel and total amounts of each radionuclide class released, all normalized as mass fractions of the initial inventories of each class. (Note that these amounts generally consider only the release of radioactive forms of these classes, and not additional releases of nonradioactive aerosols from structural materials.)

The release behavior predicted by MELCOR is somewhat different for this scenario than for the others analyzed. In all cases, almost all (~100%) of the volatile Class 1 (noble gases), Class 2 (CsOH), Class 5 (Te) and Class 16 (CsI) radionuclide species are released, primarily in-vessel, as are most (80-90%) of the Class 3 (Ba) and Class 12 (Sn) inventories. The next major release fraction is for uranium. Around 2-5% of the total inventories of Ru and Mo, Ce and La, are released. Finally, a total ≤0.05% of the initial inventory of Class 11 (Cd) is predicted to be released. Note that the CORSOR-M fission product release model option used in these analyses has identically zero release in-vessel of Class 7 (Mo), Class 9 (La) and Class 11 (Cd).

Figure 4.3.6.12 gives the total radioactive release to the environment, while the releases as mass fractions of individual classes to the environment are shown in Figure 4.3.6.13. The release to the environment does not begin at vessel failure in this sequence but earlier, after auxiliary building failure. Closing containment is an ineffective measure in this scenario unless the MSIVs are also closed. These environmental releases correspond to rapid escape of most radionuclides released from the fuel. Almost all the noble gases (~100%) are released to the environment soon after the auxiliary building fails. In addition, there is significant release to the environment of the other volatile species (i.e., CsOH, CsI and Te) also, soon after auxiliary building failure, although there is considerable retention of the volatile species within the auxiliary building (but not within the isolated containment).

Table 4.3.6.3 summarizes the distribution of the initial radionuclide inventory at the end of the calculation, and provides an overview of how much of the radionuclides remains bound up in fuel debris in either the core or the cavity, and of how much of the released radionuclides is retained in the primary system *vs* how much of the released radionuclides is released to, or released in, either the containment or the auxiliary building and the environment, all normalized to the initial inventories of each class. Table 4.3.6.4 presents a different breakdown of the released radionuclide final distribution, giving the fractions of released inventory for each class in control volume atmospheres (including the environment), in pools, or deposited or settled onto heat structures at the end of the calculations. (As in Table 4.3.6.2 these amounts consider only the release of radioactive forms of these classes, and not additional releases of nonradioactive aerosols from structural materials.)

These tables show fission product distributions generally similar to those found for the station blackout sequence with failure to isolate SDC (discussed in Section 4.3.2) for the radionuclides with significant (≥80% of initial inventory) release from fuel. Most of the fission product release occurs in-vessel prior to vessel failure in all cases, and both these sequences vent from the vessel directly to the auxiliary building, either through the SDC break or through the open MSIV line, before vessel failure. In all the accident scenarios analyzed, most of the noble gases released are in the environment, in the atmosphere. In both scenarios venting directly to the auxiliary building most of the volatile species (CsOH, CsI and Te) released in-vessel are retained in the auxiliary building; the two classes of radionuclides forming aerosols which had substantial releases (Ba and Sn) were predicted to have about half those releases retained in the vessel, primarily deposited on structures, and the other half of the releases retained in both the containment and in the auxiliary building (with a slightly higher percentage retained in the auxiliary building compared to the containment).

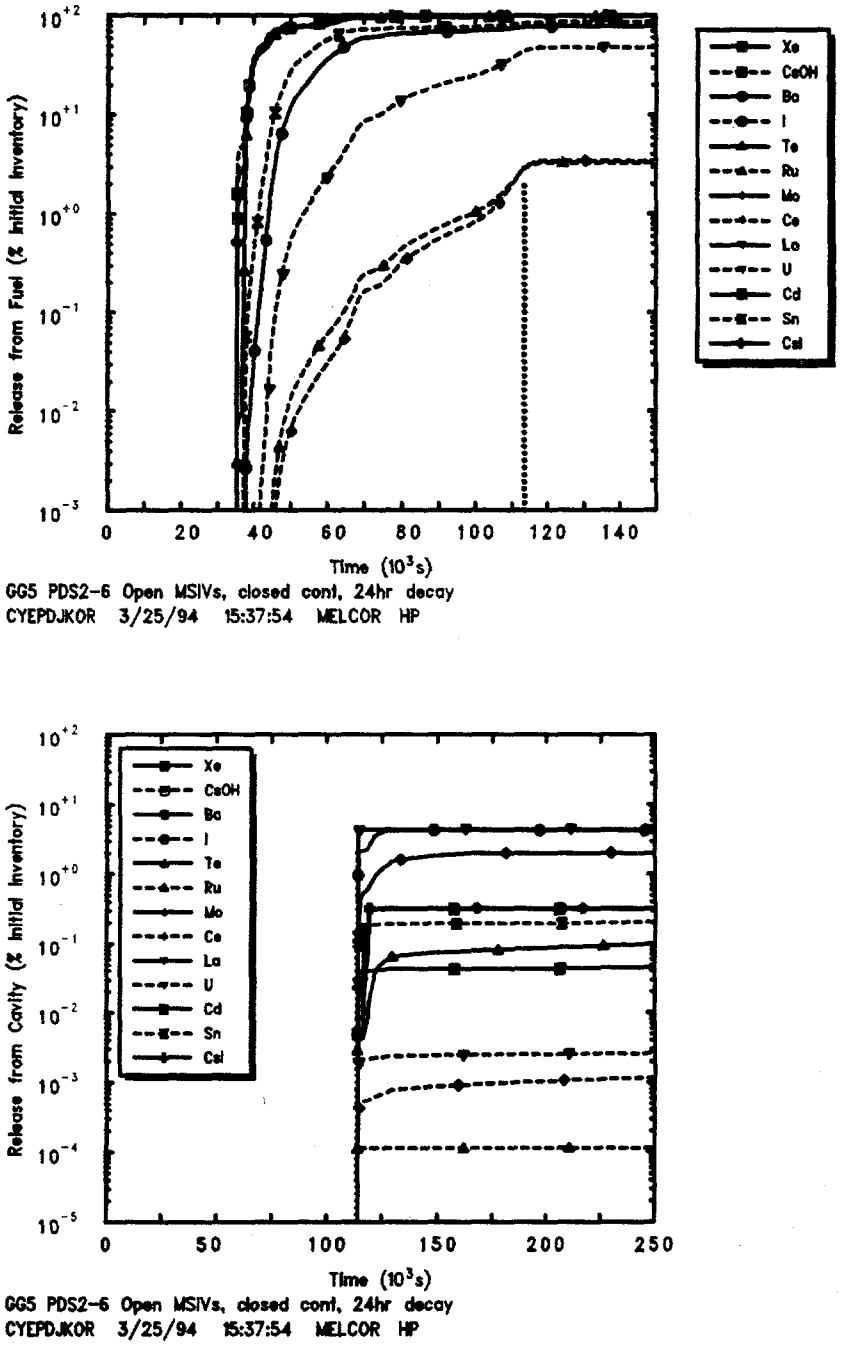

Figure 4.3.6.11. In-Vessel (top) and Ex-Vessel (bottom) Radionuclide Release Mass Fractions for Grand Gulf POS 5 -- Open MSIVs with Closed Containment, Initiated 24 hr After Shutdown.

Table 4.3.6.2. Final Radionuclide Release Fractions for Grand Gulf POS 5 -- Open MSIVs with Closed Containment, Initiated 24 hr After Shutdown

Class	Fission Products Released from Fuel (% Initial Inventory-Mass Fraction)		
	In-Vessel	Ex-Vessel	Total
Xe	99.64	0.32	99.96
CsOH	99.65	0.31	99.96
Ba	78.23	4.33	82.56
I	~0	~0	~0
Te	99.6	0.098	99.61
Ru	3.299	0.00011	3.3
Mo	0	1.98	1.98
Ce	3.444	0.0011	3.45
La	0	4.425	4.43
U	47.6	0.0026	47.6
Cd	0	0.045	0.045
Sn	85.99	0.204	86.2
CsI	99.67	0.32	99.99

4.3.7 Large Break LOCA with Flooded Containment and with Hydrogen Igniters, Initiated 7 hr After Shutdown

The analysis of the large break LOCA scenario with flooded containment initiated 7 hr after shutdown described in Section 4.3.1 was repeated with the hydrogen ignition system assumed functional. Igniters were modelled in every control volume in both the inner and outer containments.

The amounts of hydrogen and carbon monoxide burned in each control volume in the containment are shown in Figures 4.3.7.1 and 4.3.7.2. While combustion occurs throughout the containment, most of the hydrogen and carbon monoxide combustion occurs in the containment dome. In the first portion of the transient only hydrogen is produced, through metal-water reaction in the vessel, so only hydrogen is burned; later, after vessel failure at 92,500 s (25.7 hr), carbon monoxide generated by core-concrete interaction is burned also. Comparison to the total hydrogen and carbon monoxide production given in Figure 4.3.1.20 shows just over 50% of the hydrogen produced and just over 25% of the carbon monoxide generated is burned.

The combustion can be seen to occur in stepped stages. Each such set of burns generates large pressure and temperature excursions in the containment and, through the open equipment hatch, personnel locks and the recirculation pipe break generates large pressure and temperature excursions in the auxiliary building and vessel also. Figure 4.3.7.3 illustrates one impact of hydrogen ignition: the auxiliary building fails much earlier than in the same sequence with no hydrogen combustion, at 38,334 s (10.65 hr) on a sharp pressure spike due to combustion in the containment instead of about 7 hr after vessel failure, at 117,500 s (32.6 hr), due to pressurization by noncondensable gases generated during core concrete interaction in the cavity.

Figures 4.3.7.4 and 4.3.7.5 depict the magnitude of the temperature excursions generated by combustion in the containment dome and auxiliary building, respectively.

The combustion has the general effect of reducing the mole fractions of hydrogen and carbon monoxide present.

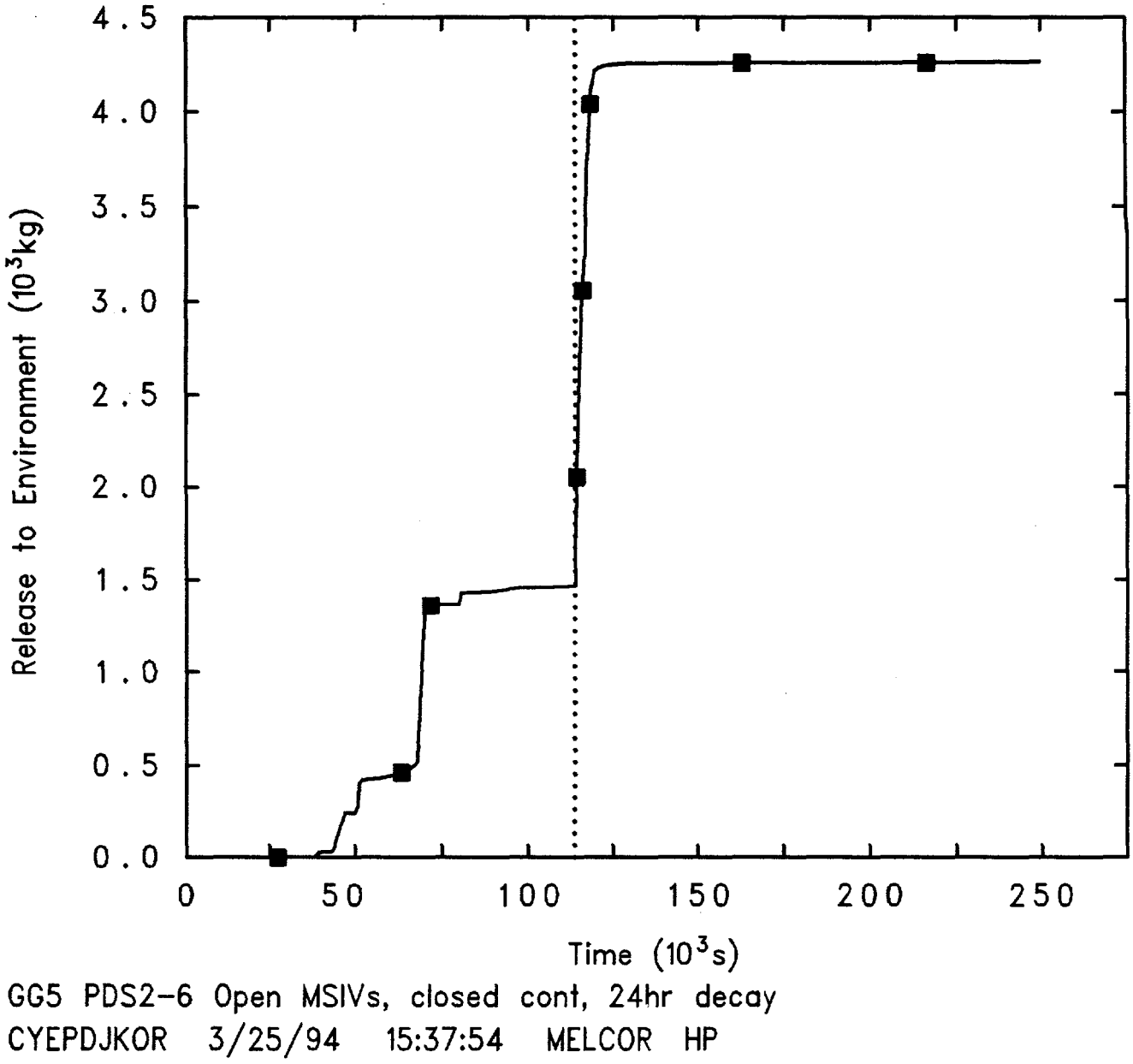

Figure 4.3.6.12. Total Environmental Radionuclide Releases for Grand Gulf POS 5 -- Open MSIVs with Closed Containment, Initiated 24 hr After Shutdown.

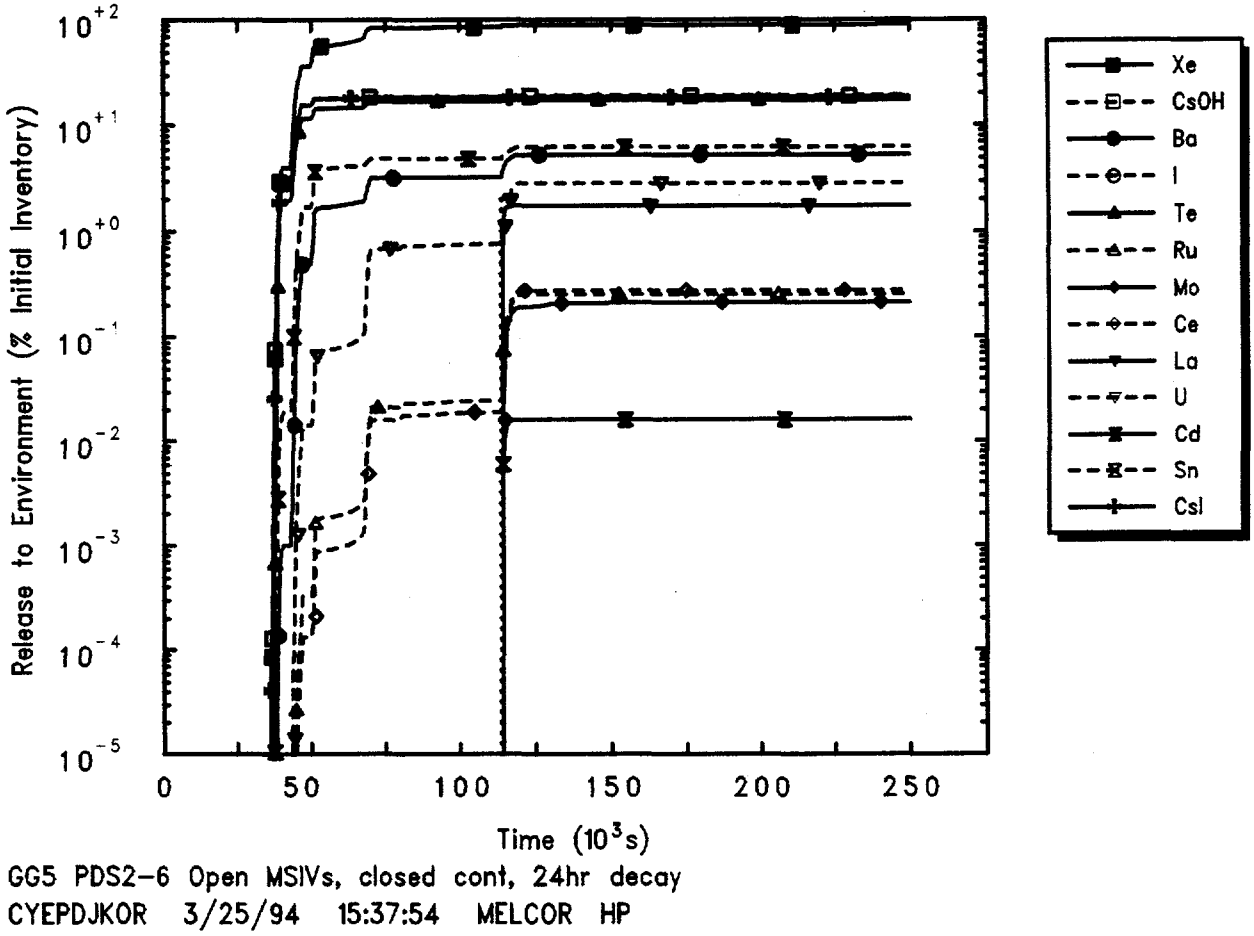

Figure 4.3.6.13. Environmental Radionuclide Release Fractions for Grand Gulf POS 5 -- Open MSIVs with Closed Containment, Initiated 24 hr After Shutdown.

Table 4.3.6.3. Final Radionuclide Distribution for Grand Gulf POS 5 -- Open MSIVs with Closed Containment, Initiated 24 hr After Shutdown

Class	Fission Product Distribution (% Initial Inventory-Mass Fractions)				
	Fuel Debris	Primary System	Containment	Auxiliary Building	Environment
Xe	~0	0.0001	0.03	9.74	90.23
CsOH	~0	2.41	0.54	78.17	18.88
Ba	17.46	34.4	8.12	34.75	5.28
Te	0.237	2.73	0.36	79.21	17.43
Ru	96.7	1.82	0.453	0.775	0.252
Mo	98	0.112	1.14	0.519	0.212
Ce	96.6	1.89	0.532	0.753	0.275
La	95.6	0.292	1.21	1.18	1.74
U	56.1	24.66	4.62	11.96	2.62
Cd	99.9	0.0002	0.036	0.013	0.0016
Sn	13.8	32.8	7.67	40.36	6.19
CsI	~0	2.534	0.43	78.51	18.53

Figures 4.3.7.6 and 4.3.7.7 present the mole fractions in the containment dome and in the second floor of the auxiliary building, respectively, comparing the results obtained with working igniters with the results assuming no hydrogen combustion. The behavior predicted in the containment equipment hatch is almost identical to that shown for the containment dome. The behavior predicted in the top two floors of the auxiliary building is very similar to that shown for the second floor; the first floor is a dead-end volume and remains more near ambient.

Figure 4.3.7.6 shows the combined steam and carbon dioxide mole fraction instead of just the steam mole fraction, because the sum determines whether the volume is inert, and also includes the mole fraction ignition limits. (In the MELCOR calculation, burn occurs in volumes with igniters if $x_{H2} \geq 0.07$ and $x_{CO} \geq 0.129$, $x_{O2} \geq 0.05$, and $x_{H2O} + x_{CO2} \leq 0.55$; the hydrogen and carbon monoxide mole fractions are combined using LeChatelier's formula to determine if the available mixture will burn.)

Table 4.3.6.4. Final Radionuclide State for Grand Gulf POS 5 -- Open SMIVs andClosed Containment, initiated 24 hr After Shutdown

Class	Fission Products Released from Fuel (% Released Inventory-Mass Fraction)		
	Atmosphere	Pool	Deposited
Xe	~100	0	0
CsOH	19	44.34	36.53
Ba	6.39	21.83	71.63
I	~100	0	0
Te	17.45	43.08	39.34
Ru	7.64	9.63	82.67
Mo	10.78	38.15	51.05
Ce	7.99	9.16	82.8
La	39.2	12.9	47.88
U	5.97	11.56	82.4
Cd	37.87	14.47	47.63
Sn	7.18	24.87	67.82
CsI	18.44	44.36	36.8

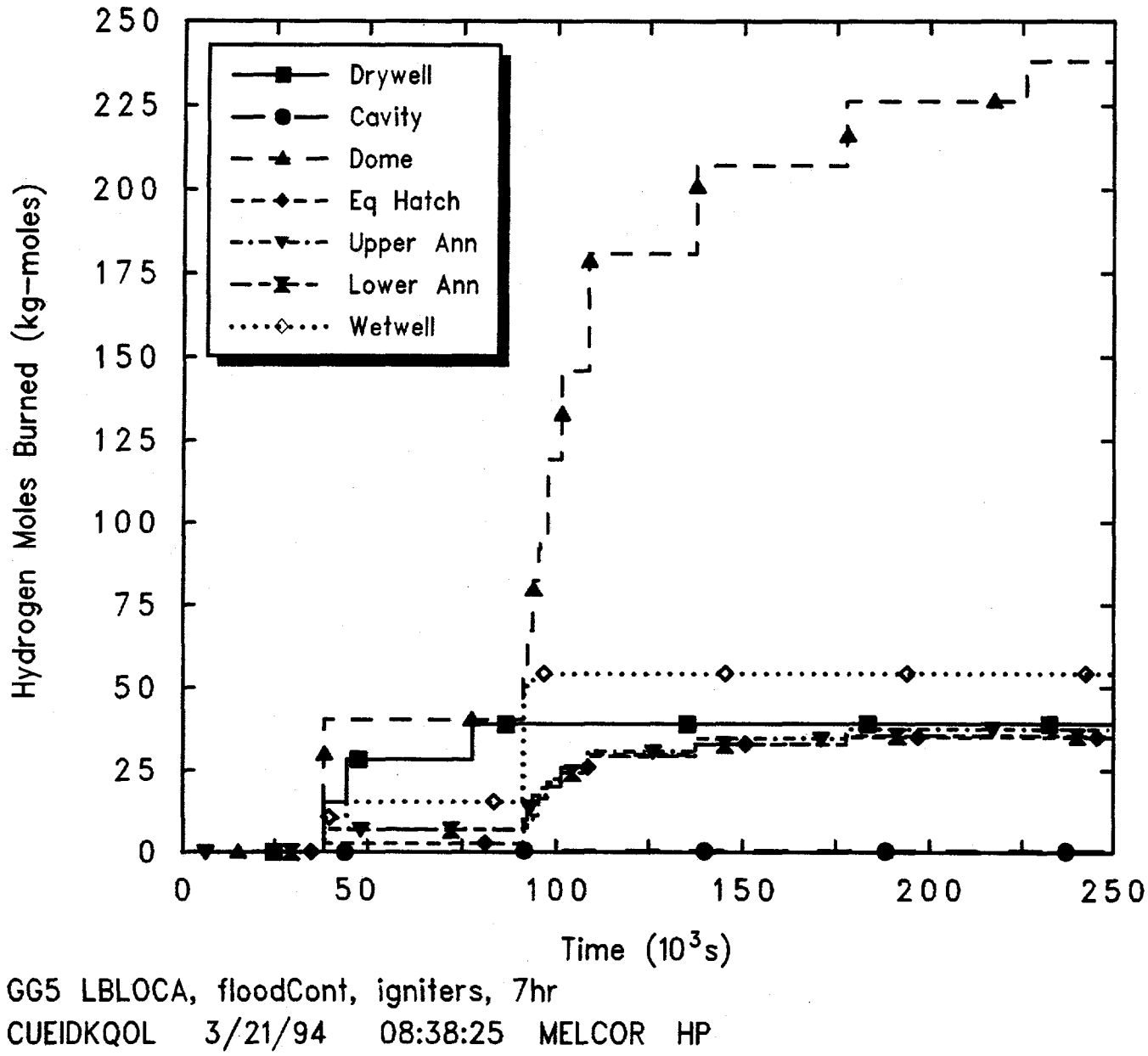

Figure 4.3.7.1. Hydrogen Combustion for Grand Gulf POS 5 -- Large Break LOCA with Flooded Containment, with Hydrogen Ignition; Initiated 7 hr After Shutdown.

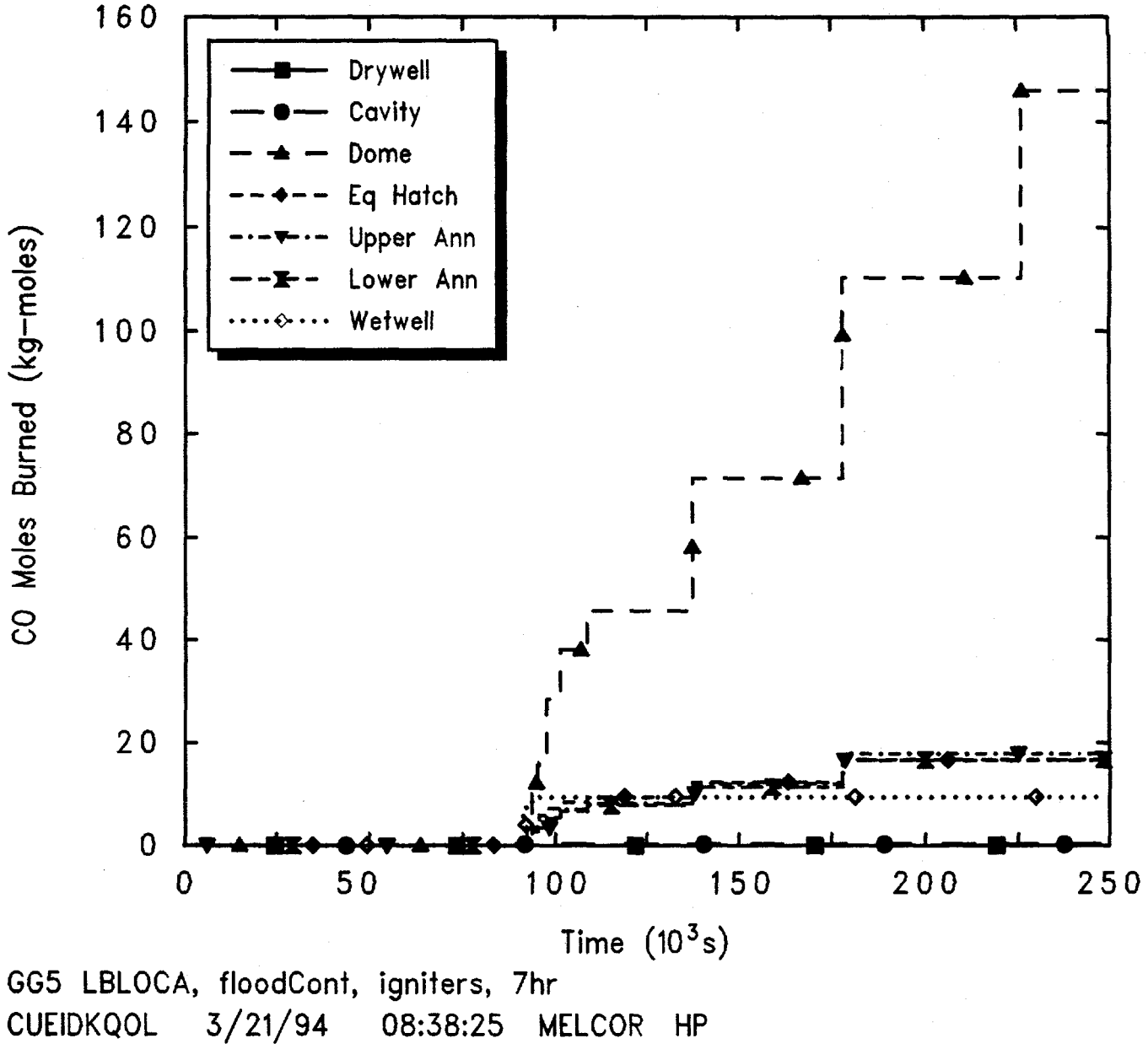

Figure 4.3.7.2. Carbon Monoxide Combustion for Grand Gulf POS 5 -- Large Break LOCA with Flooded Containment, with Hydrogen Ignition, Initiated 7 hr After Shutdown.

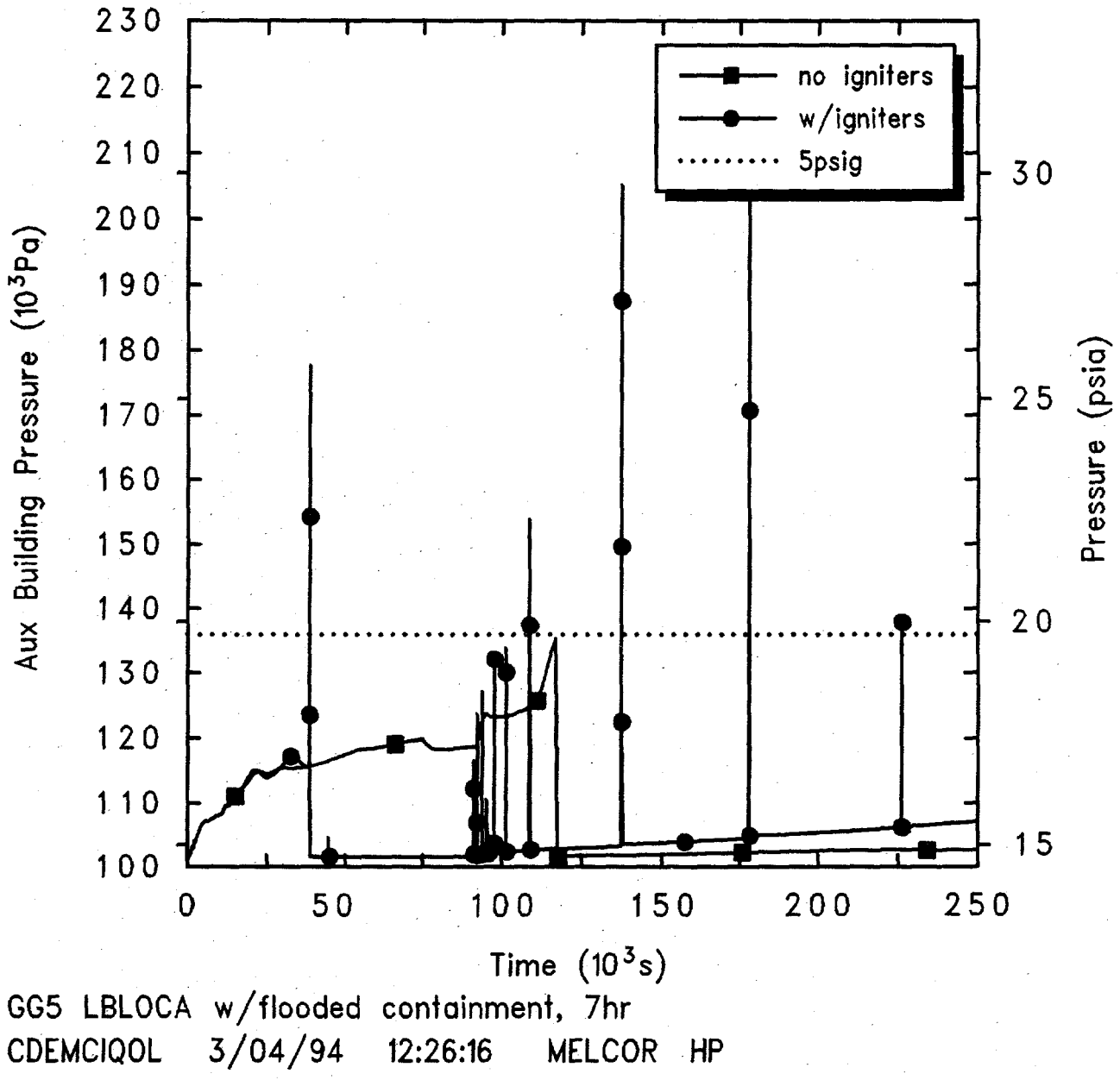

Figure 4.3.7.3. Auxiliary Building Pressures for Grand Gulf POS 5 -- Large Break LOCA with Flooded Containment, with Hydrogen Ignition and without Hydrogen Combustion, Initiated 7 hr After Shutdown.

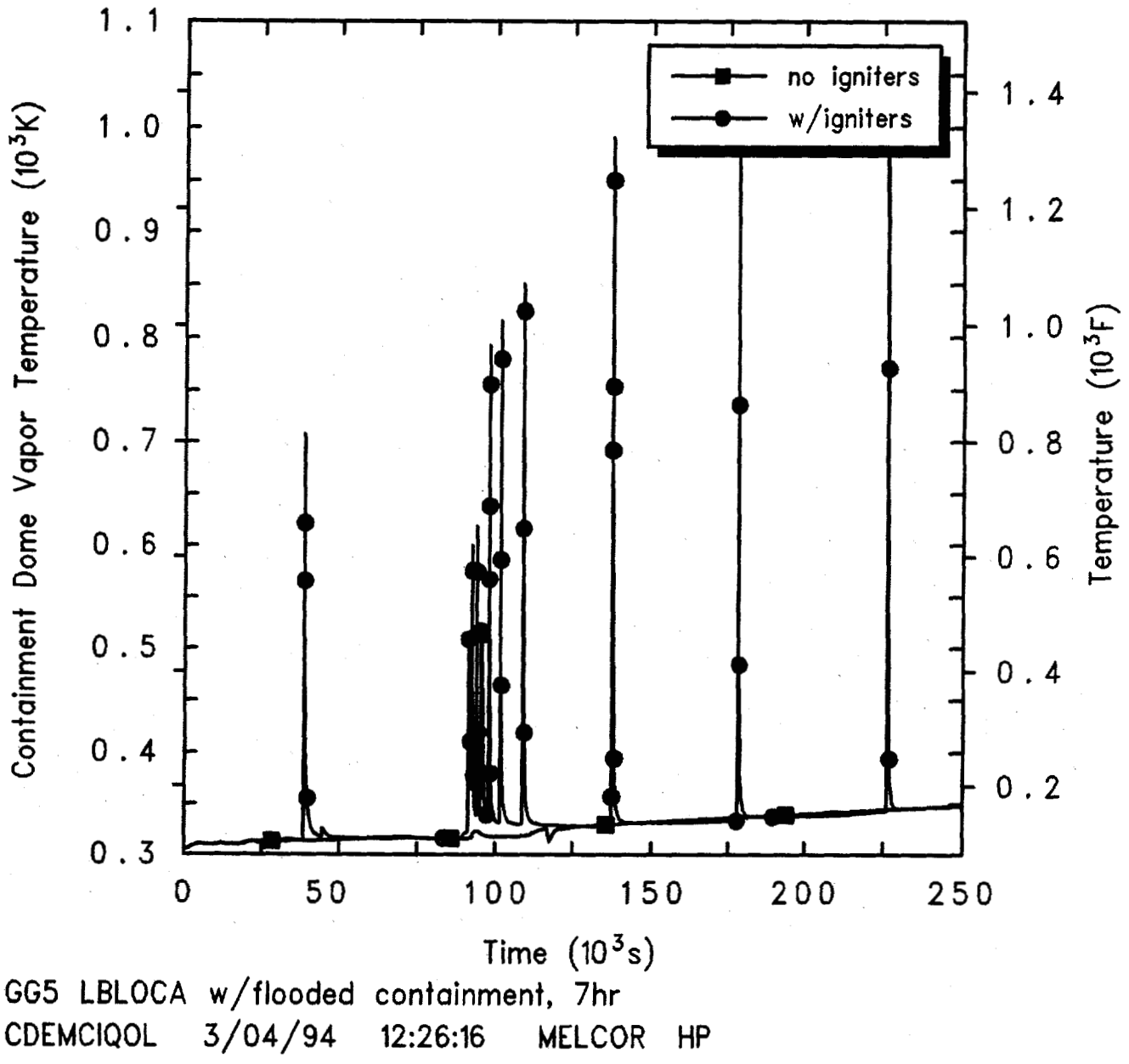

Figure 4.3.7.4. Containment Dome Temperatures for Grand Gulf POS 5 -- Large Break LOCA with Flooded Containment, with Hydrogen Ignition and without Hydrogen Combustion, Initiated 7 hr After Shutdown.

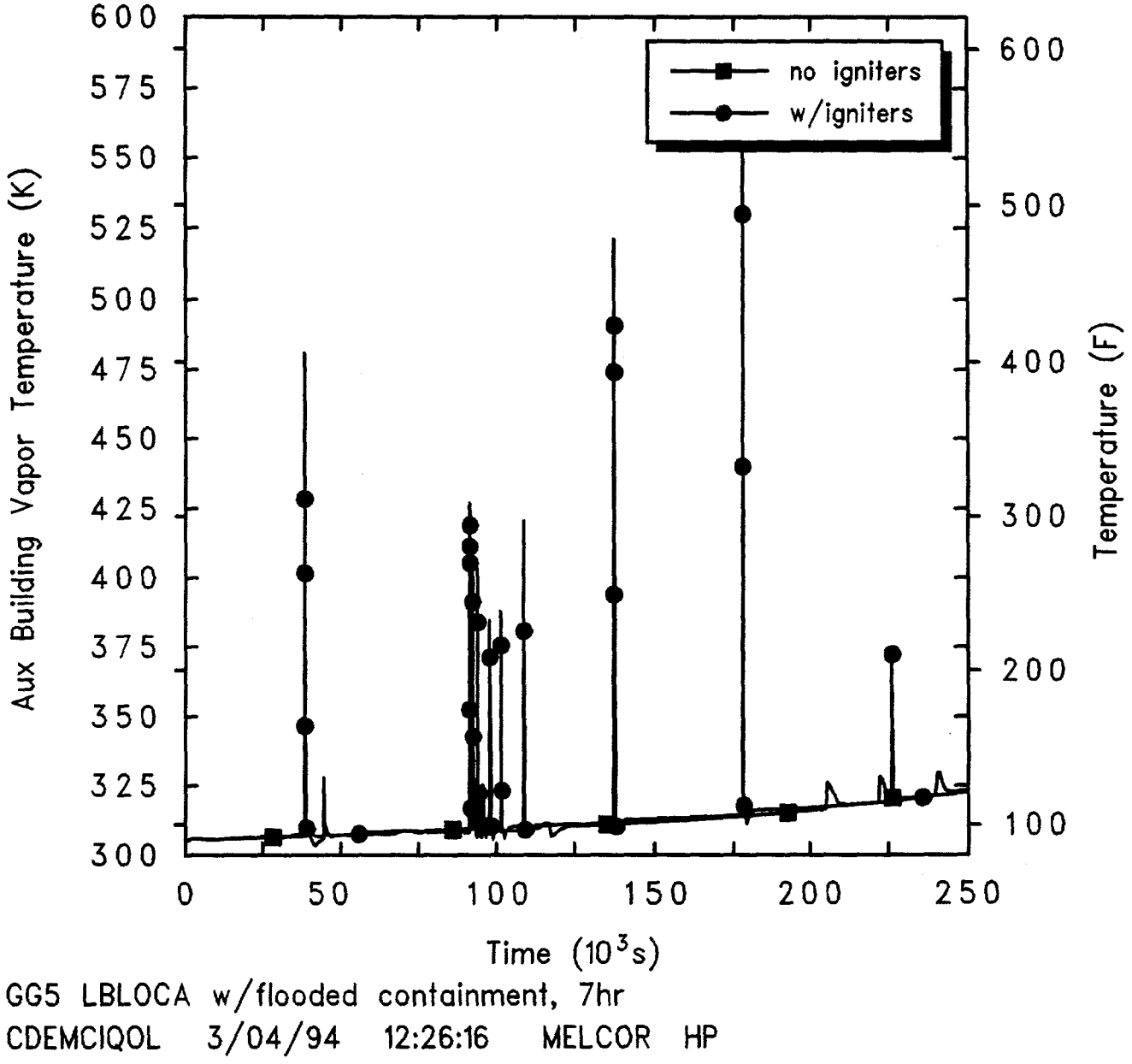

Figure 4.3.7.5. Auxiliary Building Temperatures for Grand Gulf POS 5 -- Large Break LOCA with Flooded Containment, with Hydrogen Ignition and without Hydrogen Combustion, Initiated 7 hr After Shutdown.

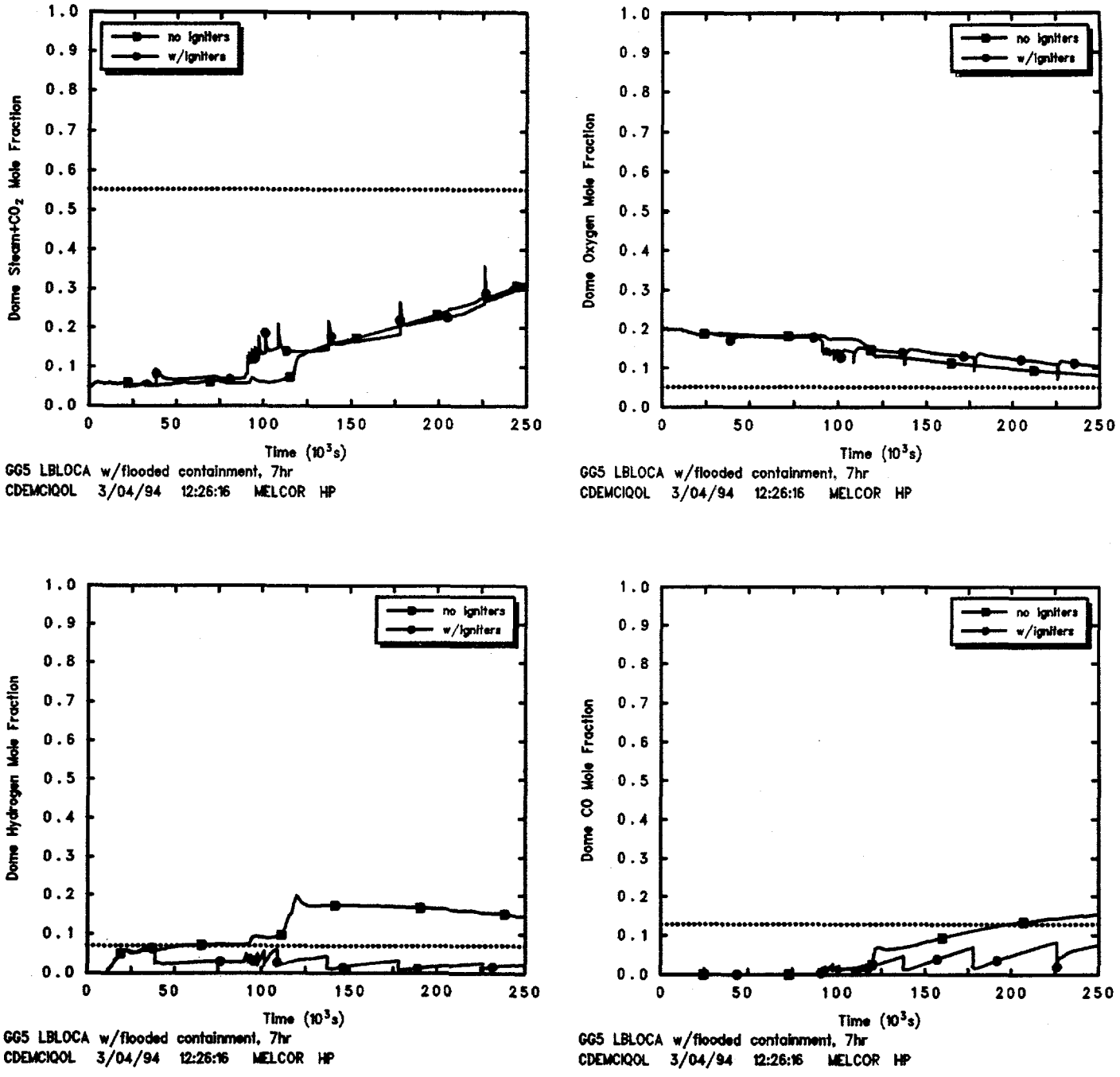

Figure 4.3.7.6. Containment Dome Steam +CO_2 (upper left), Oxygen (upper right), Hydrogen (lower left), and Carbon Monoxide (lower right) Mole Fractions for Grand Gulf POS 5 -- Large Break LOCA with Flooded Containment, with Hydrogen Ignition and without Hydrogen Combustion, Initiated 7 hr After Shutdown

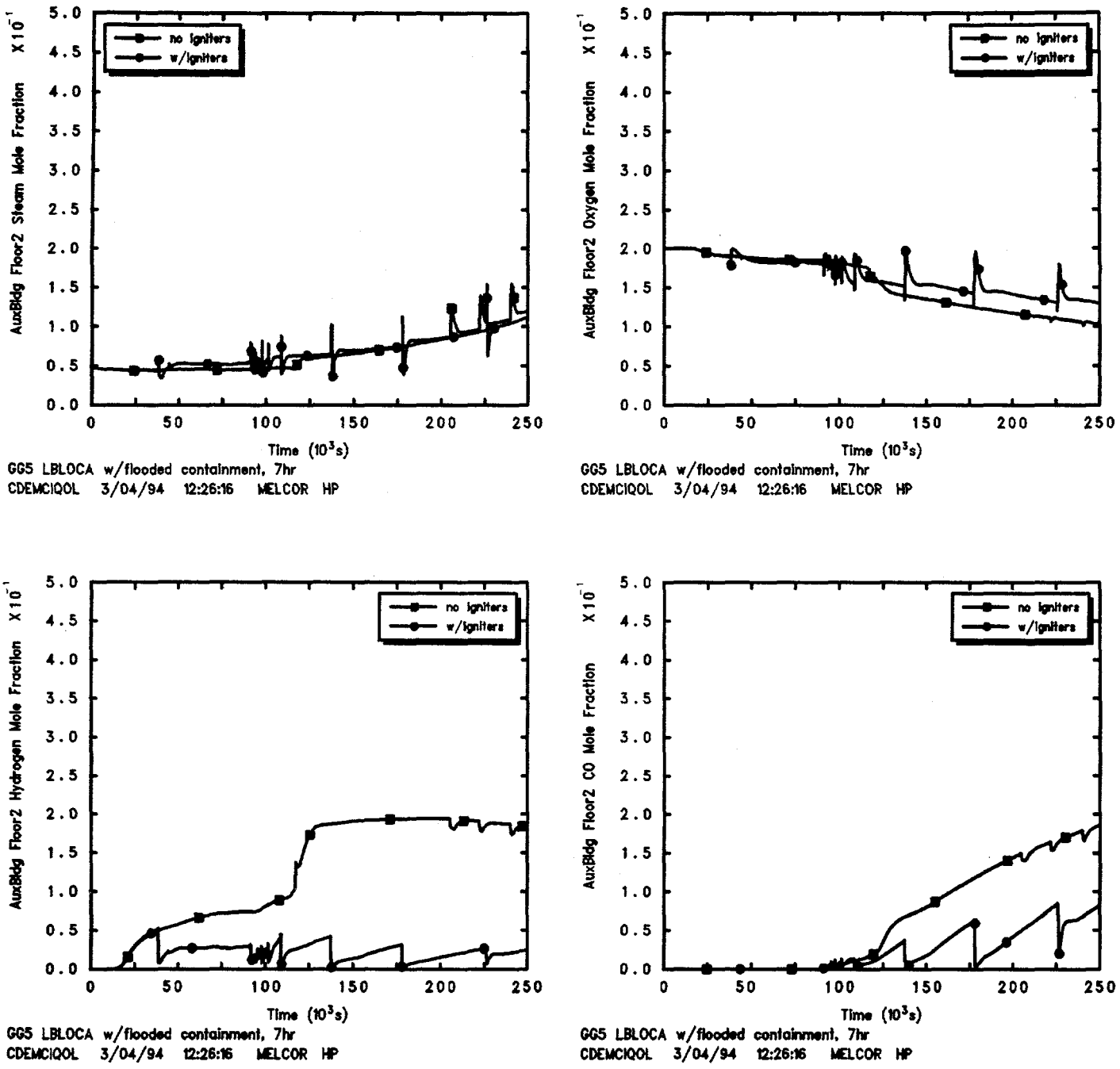

Figure 4.3.7.7. Auxiliary Building Second Floor Steam + CO_2 (upper left), Oxygen (upper right), Hydrogen (lower left), and Carbon Monoxide (lower right) Mole Fractions for Grand Gulf POS 5 -- Large Break LOCA with Flooded Containment, with Hydrogen Ignition and without Hydrogen Combustion, Initiated 7 hr After Shutdown.

5 POS 6 Calculations

5.1 Description of POS 6

The configuration of the plant at the onset of core damage is important because it will determine the framework within which the accident will unfold, i.e., the plant configuration will define the boundary conditions for the analysis. For example, it will define the mitigative features of the plant that will be available during the accident (e.g., containment, suppression pool, containment sprays).

An abridged risk analysis was performed on the early portion of the refueling mode of operation. In the Level 1 coarse screening analysis this mode of operation is referred to as plant operating state 6 (POS 6). During a refueling outage, the plant will enter POS 6 prior to loading fresh fuel (i.e., going down) and then following fuel transfer on the way back up to power conditions (i.e., going up). In the Level 1 analysis, the sequence definitions are based on the going-down phase because (1) more systems are likely to be unavailable (i.e., on the way back up maintenance and repairs may already have been performed on many systems) and (2) the decay heat levels are higher and there is therefore less time to respond to events in the going down phase *vs* the going up phase. Thus, in this POS 6 study, only the going-down phase is analyzed.

POS 6 begins when the vessel head is detached and ends when the upper reactor cavity has been filled with water. During this POS the following tasks are performed:

1. Steam dryers are removed,
2. Vessel water level is lowered to the bottom of the steam lines and the steam lines are plugged,
3. Water level is raised and the steam separators are removed, and
4. Vessel water level is raised to flood the upper reactor cavity.

Prior to this mode of operation, the containment equipment hatch and personnel locks have been opened, the drywell head has been removed and the drywell equipment hatch and personnel locks have been opened. Thus the suppression pool is effectively bypassed both from the vessel and from the drywell (i.e., steam lines are plugged and the drywell is open).

Timing information for the initiation of the accident in POS 6 is based on Grand Gulf refueling outage (RFO) data. Based on this data, the fastest the plant will enter POS 6 from full power is approximately four days after shutdown and the longest the plant has been in POS 6 (in the going-down phase) is approximately 12 days (i.e., 16 days from shutdown). In the Level 1 analysis the time window from the initiating event to core damage was based on the decay heat at four days; this assumption is carried through the Level 2/3 analyses. (Our MELCOR analyses were therefore initiated at 4 days after shutdown, with the exception of a single sensitivity study which assumed the accident sequence to begin 15 days after shutdown.)

All the MELCOR calculations were done assuming that, at the start of the accident, shutdown cooling, suppression pool cooling and containment sprays are all unavailable and remain unavailable during the accident; coolant injection is not provided to the vessel during the accident, and suppression pool makeup is not dumped into the suppression pool. Table 5.1.1 summarizes these and other conditions kept constant in these MELCOR analyses.

The MELCOR POS 6 calculations done included a number of variations on the exact plant configuration assumed, including:

1. The accident is initiated 4 days after reactor shutdown. The hydrogen ignition system is unavailable during the accident. Both of the containment personnel locks are open; the containment equipment hatch is also open. This calculation did not include the auxiliary building model, but vented directly to the environment.
2. The accident is initiated 4 days after reactor shutdown. The hydrogen ignition system is unavailable during the accident. The containment is isolated (i.e., the containment personnel locks and the containment equipment hatch are closed). This calculation did not include the auxiliary building model, but would vent directly to the environment after containment failure would occur.
3. The accident is initiated 4 days after reactor shutdown. The hydrogen ignition system is unavailable during the accident. Both the containment personnel locks are open; the containment equipment hatch is also open.

Table 5.1.1. POS 6 Scenario Assumed in MELCOR Calculations

RPV status		
	Coolant temperature	140°F
	Pressure	Atmospheric
	Water level	Bottom of main steam line
	Vessel head	Off
	Vessel vent	N/A
	SRVs	Steam lines plugged
Containment status		
	Vent	Closed
Drywell status		
	Drywell head	Removed
	Equipment hatch	Open
	Personnel lock	Open
Suppression pool cooling		Unavailable
Containment sprays		Unavailable

The open auxiliary building model (which assumes some of the interior doors are open) is included in this calculation, with failure on a 5 psi overpressure.

4. The accident is initiated 4 days after reactor shutdown. The hydrogen ignition system is unavailable during the accident. Both the containment personnel locks are open; the containment equipment hatch is also open. The closed auxiliary building model (which assumes some of the interior doors are closed) is included in this calculation, with failure on a 5 psi overpressure.

5. The accident is initiated 4 days after reactor shutdown. The hydrogen ignition system is unavailable during the accident. The open auxiliary building model is included in this calculation, with failure on a 5 psi overpressure. The containment equipment hatch is open; however, both of the containment personnel locks are closed.

6. The accident is initiated 4 days after reactor shutdown. The hydrogen ignition system is unavailable during the accident. The closed auxiliary building model is included in this calculation, with failure on a 5 psi overpressure. The containment equipment hatch is open; however, both of the containment personnel locks are closed.

7. The accident is initiated 15 days after reactor shutdown. The hydrogen ignition system is unavailable during the accident. Both of the containment personnel locks are open; the containment equipment hatch is also open. This calculation did not include the auxiliary building model, but vented directly to the environment.

8. The accident is initiated 4 days after reactor shutdown. The hydrogen ignition system is operational during the accident. The containment is isolated (i.e., the containment personnel locks and the containment equipment hatch are closed). This calculation did not include the auxiliary

building model, but was assumed to vent directly to the environment after containment failure would occur.

In addition, a few sensitivity studies were done on various code options and/or parameters. In one calculation, the CORSOR fission product release model was used instead of the (MELCOR default) CORSOR-M fission product release model. Because it was sometimes necessary to back up and reduce the user-specified maximum time step in order to avoid a code abort and complete the analysis, a calculation was done in which that was the only change made, to determine how big an effect reducing the time step would have on the results,

Two calculations were done to address concerns [Powers et al., 1994] raised about the lack of any air oxidation modelling in MELCOR at the time that these POS 6 analyses were being done, and the associated lack of extensive release of ruthenium demonstrated to occur when irradiated reactor fuel is heated in air. (More recent versions of MELCOR include both oxidation of zircaloy by free oxygen, if available, and enhanced ruthenium release models [Kmetyk, 1994a].)

5.2 Reference Analysis

The calculation selected as the POS 6 reference, base case, analysis has the accident initiated 4 days after reactor shutdown. The hydrogen ignition system is unavailable during the accident. Both the containment personnel locks are open; the containment equipment hatch is also open. The closed auxiliary building model (which assumes some of the interior doors are closed) is included in this calculation, with failure on a 5 psi overpressure. The timing of key events as predicted in this reference analysis is presented in Table 5.2.1.

At the start of the accident, the primary system (i.e., reactor vessel), containment and auxiliary building are all assumed to be at atmospheric pressure. The vessel is filled with water at 333 K (140°F) to an elevation of 16.13 m, corresponding to the bottom of the main steam lines. The only assumption in the accident is no intervention, either manual or automatic.

Figure 5.2.1 presents the pressures calculated in various regions of the reactor vessel. A pressure gradient develops immediately, representing simply the head of the liquid water; thus, the lower plenum exhibits the highest pressure, the core and bypass the next highest, and the downcomer and upper plenum pressures nearest atmospheric. The vessel water mass predicted to remain at any given time is given in Figure 5.2.2. As the water inventory is steamed away by the core decay heat, the pressure gradient in the vessel diminishes due to the decreasing pressure head.

The vessel pressure does not drop to atmospheric as the liquid water inventory decreases but instead equilibrates to the containment pressure, shown in Figure 5.2.3. The containment (and the auxiliary building, whose pressure is virtually identical to the containment pressure) pressurizes rapidly as steam generated in the core rises in the vessel and flows out into containment through the removed upper head region. Figure 5.2.4 depicts that steam flow from the vessel out to containment through the removed upper head opening (as well as the breach flow when the vessel first fails at about 25 hr, when Figure 5.2.2 indicates most of the remaining vessel liquid inventory is lost very quickly).

The containment and auxiliary building are kept in pressure equilibrium by three large, open flow paths -- the containment equipment hatch and the upper and lower personnel locks. The flows through these paths are illustrated in Figure 5.2.5. Throughout most of the transient, there is a substantial outflow from containment into the auxiliary building through the equipment hatch and a corresponding inflow into containment from the auxiliary building through the lower personnel lock; the flow through the upper personnel lock is more erratic, switching between periods of inflow and outflow. The auxiliary building reaches its specified 5 psi overpressure failure criterion at just over 20 hr, when the stairwell door to the environment is assumed blown open. After that, the primary system, containment and auxiliary building all remain at essentially atmospheric pressure, equilibrated with the environment. There are no substantive differences in the containment equipment hatch and the upper and lower personnel lock flows after the auxiliary building fails.

The temperatures calculated in the various reactor vessel control volume atmospheres are shown in Figure 5.2.6. The temperature remains low, at saturation, until after the top of the active fuel (TAF) is uncovered at about 13 hr; soon afterward, the temperatures rise rapidly as the core degrades. The temperature oscillations die down after vessel breach at just before 25 hr, but remain elevated throughout the transient. The temperatures calculated in the various containment control volume atmospheres are shown in Figure 5.2.7. The temperatures remain low until after more than 35 hr, when the cavity temperature rapidly rises to ~1500 K, and the drywell and weirwall

Table 5.2.1. Key Event Times for Grand Gulf POS 6 -- Reference Calculation

Event	Time
Level below TAF	13.04 hr
Clad failure/Gap release	
(Ring 1)	18.80 hr
(Ring 2)	18.76 hr
(Ring 3)	18.81 hr
(Ring 4)	19.04 hr
(Ring 5)	19.93 hr
(Ring 6)	23.22 hr
Auxiliary building failure	20 hr
Vessel LH penetration failure	
(Ring 1)	24.52 hr
(Ring 2)	24.74 hr
(Ring 3)	25.49 hr
(Ring 4)	26.50 hr
(Ring 5)	27.87 hr
(Ring 6)	30.22 hr
Cavity rupture	91.41 hr

temperatures also rise. Figure 5.2.8 presents the atmosphere temperatures in the auxiliary building. The elevated temperatures in the drywell/cavity do not propagate through the outer containment and into the auxiliary building; the auxiliary building temperature rise remains limited on all floors.

The reactor vessel water inventory is steamed away by the core decay heat, as indicated by the vessel water mass remaining at any time given in Figure 5.2.2, and also by the primary system control volume liquid levels given in Figure 5.2.9. The top of the active fuel is uncovered at about 13 hr and the core is essentially dry at 20 hr. Most of the lower plenum inventory is lost at vessel breach at 25 hr, after which the last of the water that trapped in the downcomer below the jet pump inlet slowly boils away.

As the reactor vessel water is boiled away, the clad and fuel uncovered begin heating up. The clad temperature histories in the core level just below the active fuel midplane in the six core rings are depicted in Figure 5.2.10, as representative of the overall core response. The clad is assumed to rupture at 1173 K, at times ranging from 19 hr to 23 hr in the various core rings, with consequent release of the gap radionuclides and beginning release of radionuclides from the fuel. Substantial clad oxidation occurs, generating hydrogen. The clad melts and relocates at about 2100 K (the zircaloy melt temperature), as does the still-solid fuel, forming debris continually moving downward. (The drop of clad temperatures to zero, as seen in Figure 5.2.10, indicates the disappearance of intact clad from the location being plotted.) The debris can be supported for a short time on the lower core support plate, but the core support plate also fails eventually, and drops the debris into the lower plenum where it attacks and eventually melts through the lower head. The entire process takes just under 12 hr from core uncovery to lower head failure, and about 6 hr from start of clad heatup and oxidation to lower head failure.

The hydrogen generated in the reactor vessel through oxidation of the zircaloy clad and canister, and steel other structure, is shown in Figure 5.2.11; the 1144 kg of hydrogen produced in the vessel corresponds to oxidation of about 20% of the zircaloy and around 5% of the steel.

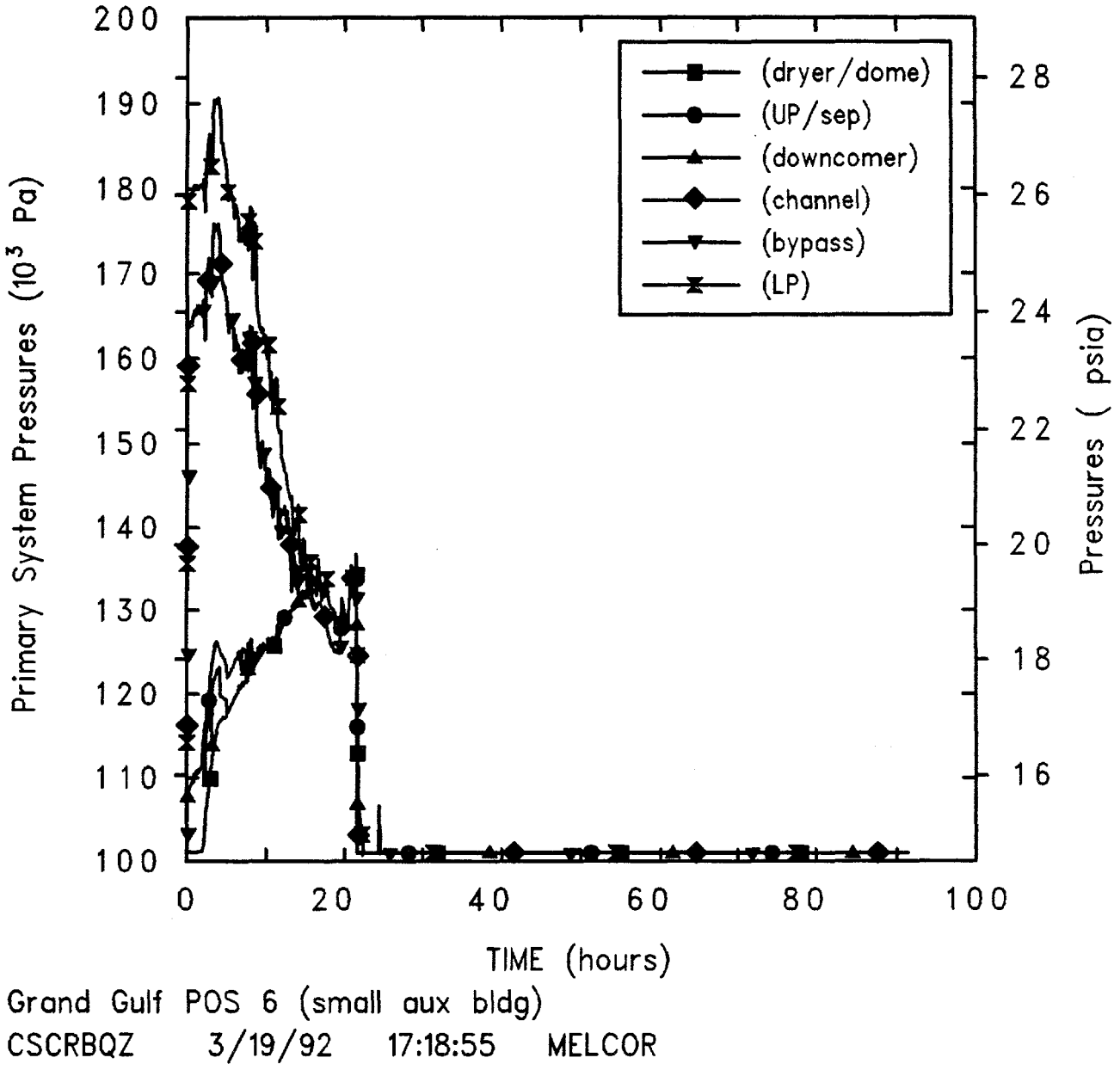

Figure 5.2.1. Reactor Vessel Pressures for Grand Gulf POS 6 -- Reference Calculation.

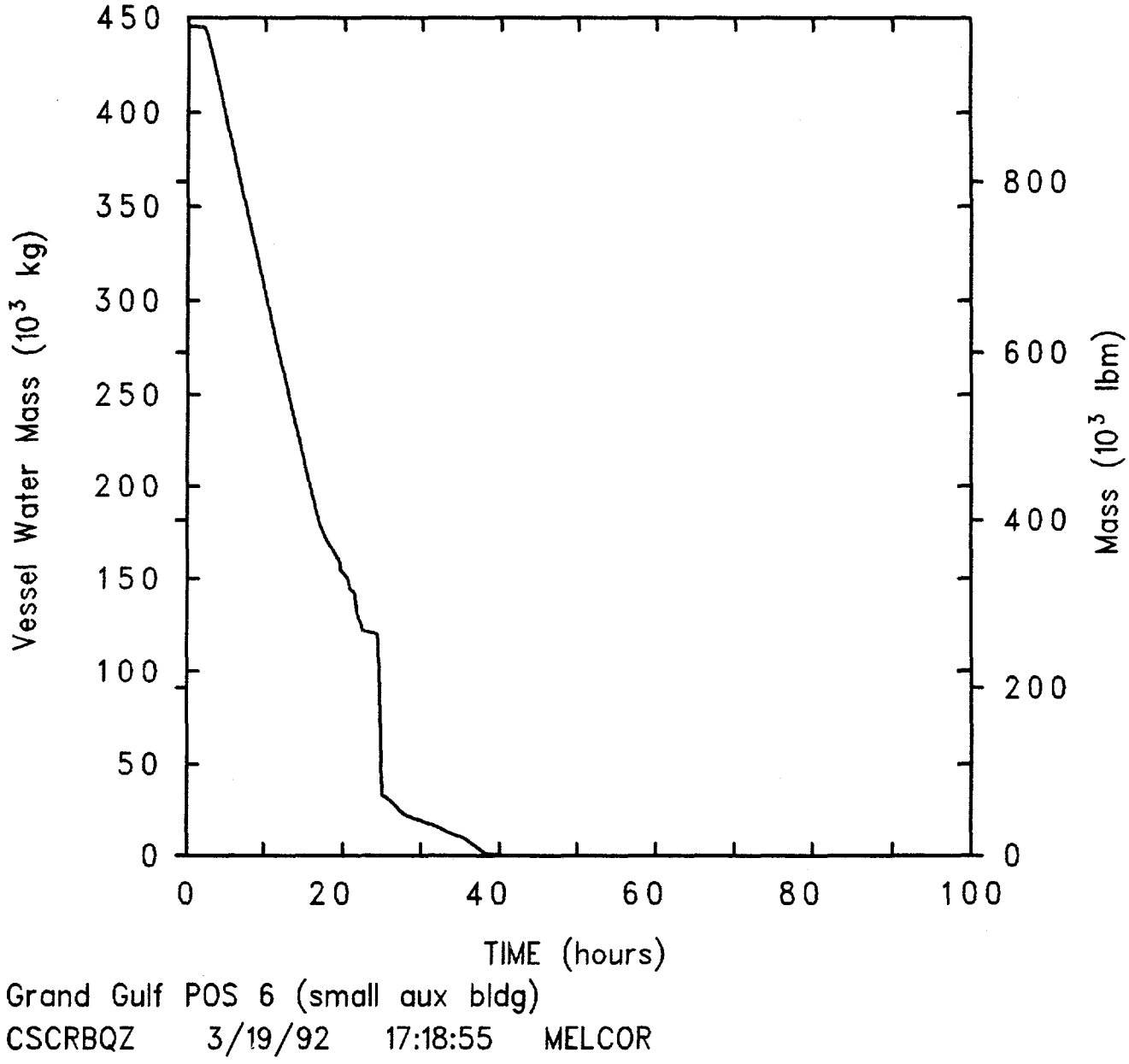

Figure 5.2.2. Reactor Vessel Water Mass for Grand Gulf POS 6 -- Reference Calculation.

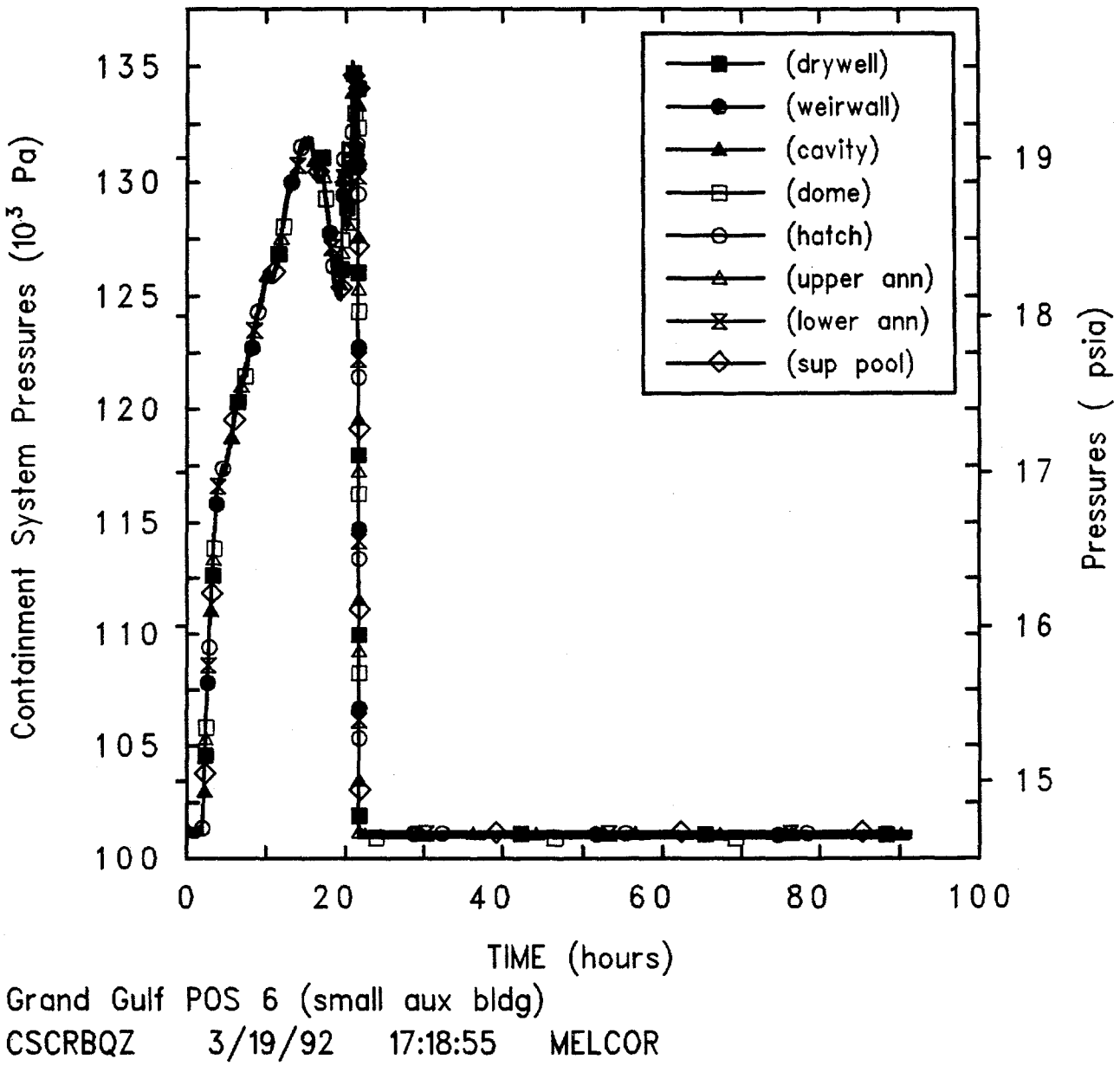

Figure 5.2.3. Containment Pressures for Grand Gulf POS 6 -- Reference Calculation.

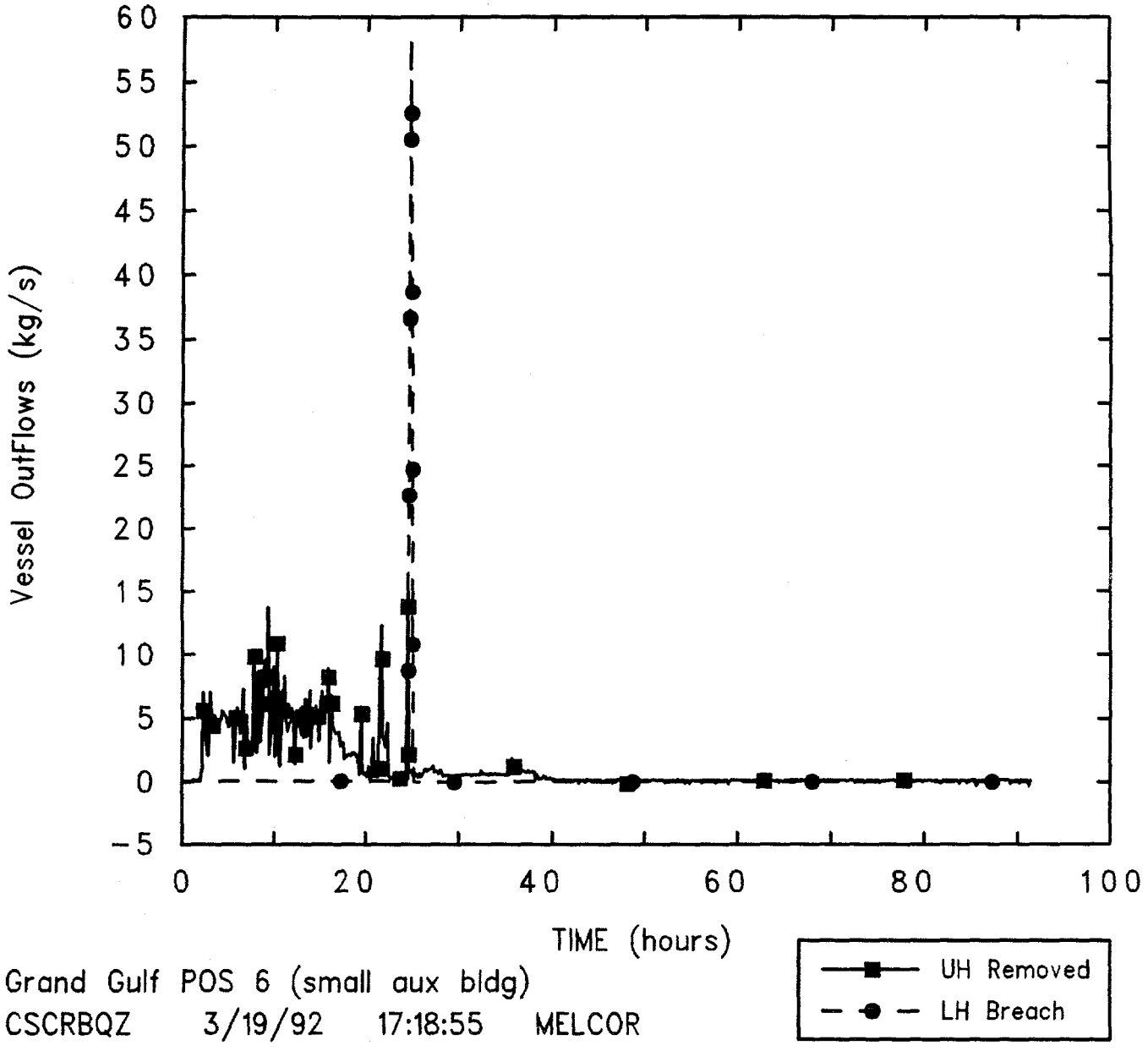

Figure 5.2.4. Reactor Vessel Outflows for Grand Gulf POS 6 -- Reference Calculation.

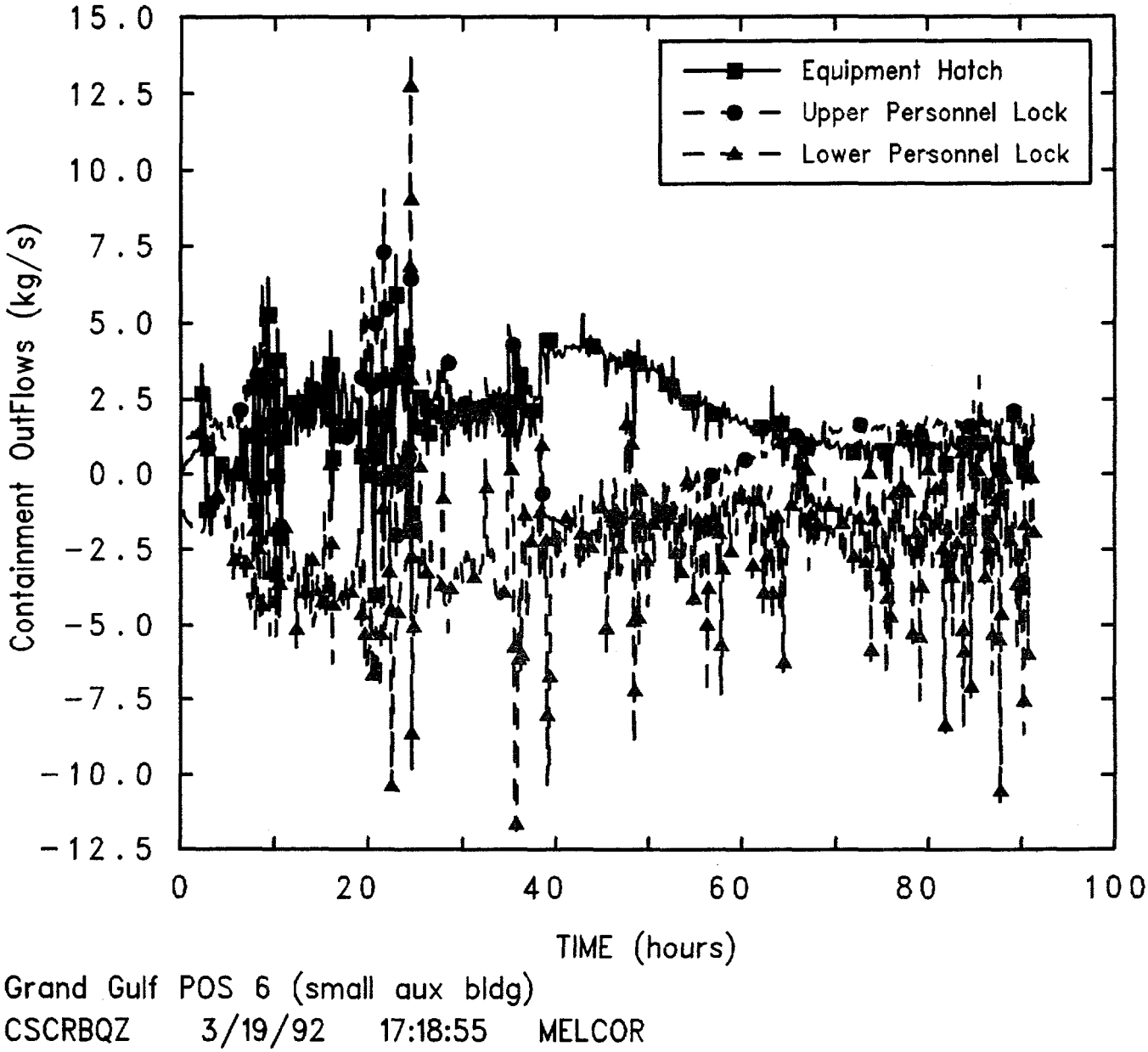

Figure 5.2.5. Containment Outflows for Grand Gulf POS 6 -- Reference Calculation.

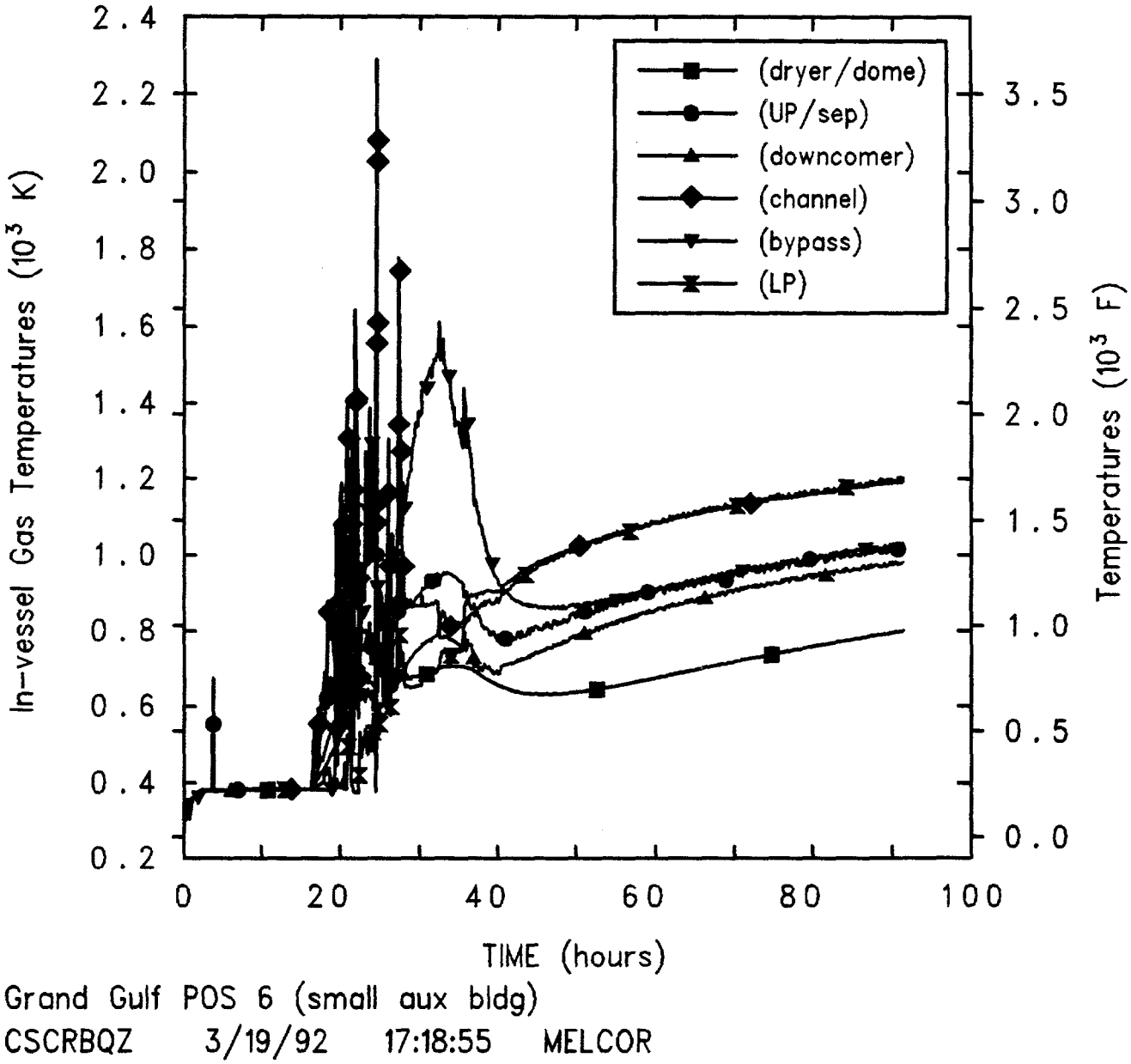

Figure 5.2.6. Reactor Vessel Atmosphere Temperatures for Grand Gulf POS 6 -- Reference Calculation.

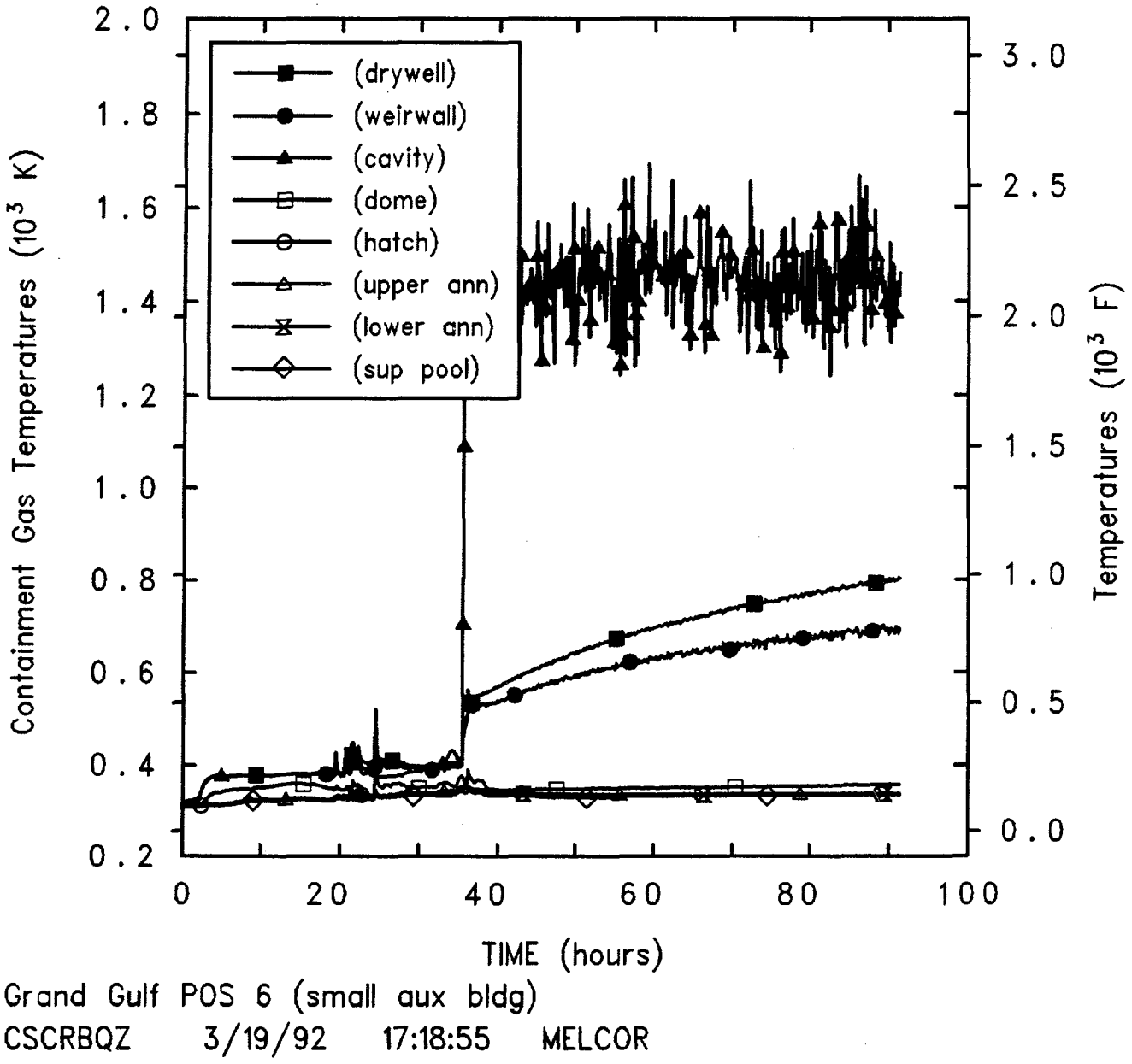

Figure 5.2.7. Containment Atmosphere Temperatures for Grand Gulf POS 6 -- Reference Calculation.

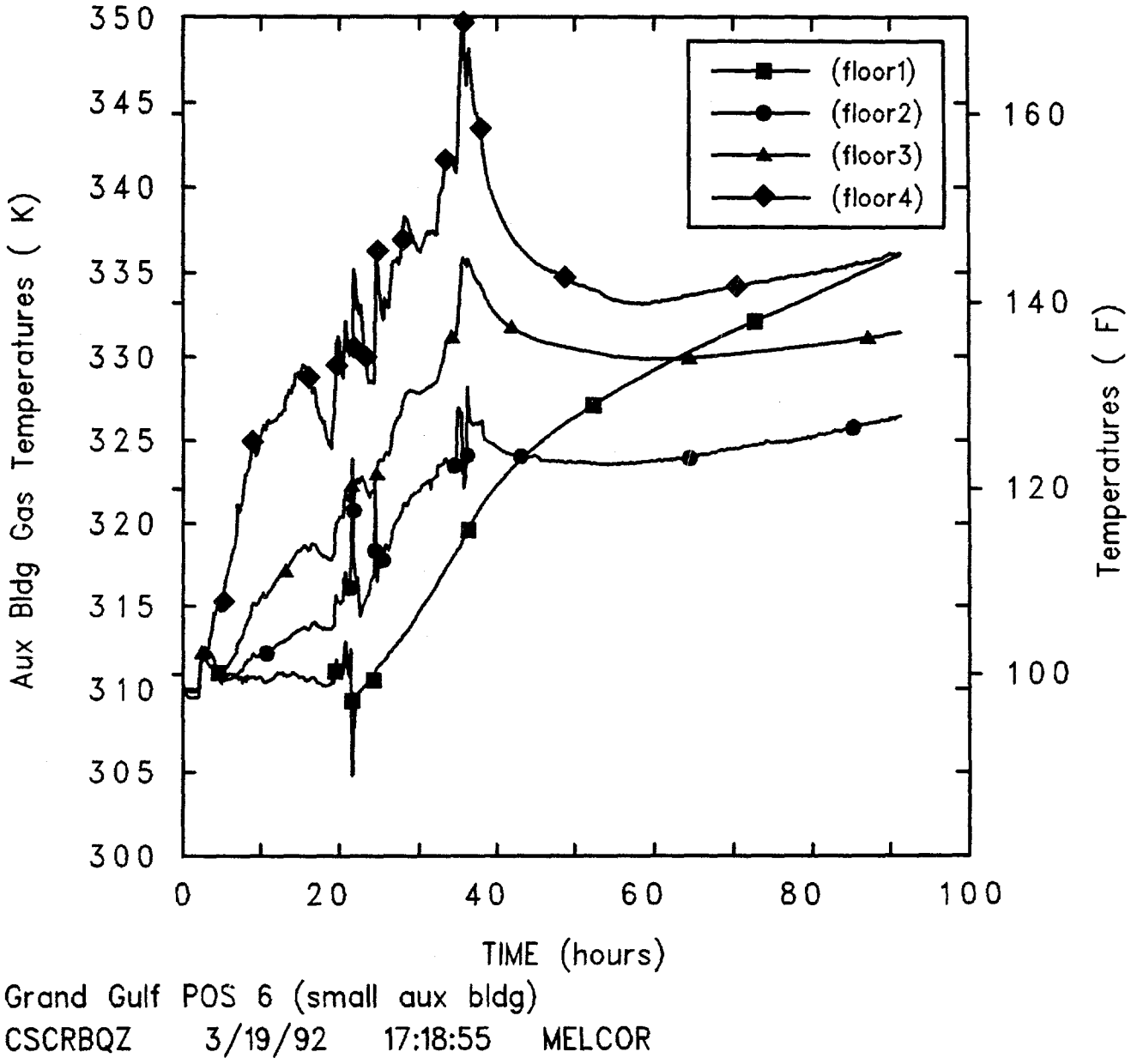

Figure 5.2.8. Auxiliary Building Atmosphere Temperatures for Grand Gulf POS 6 -- Reference Calculation.

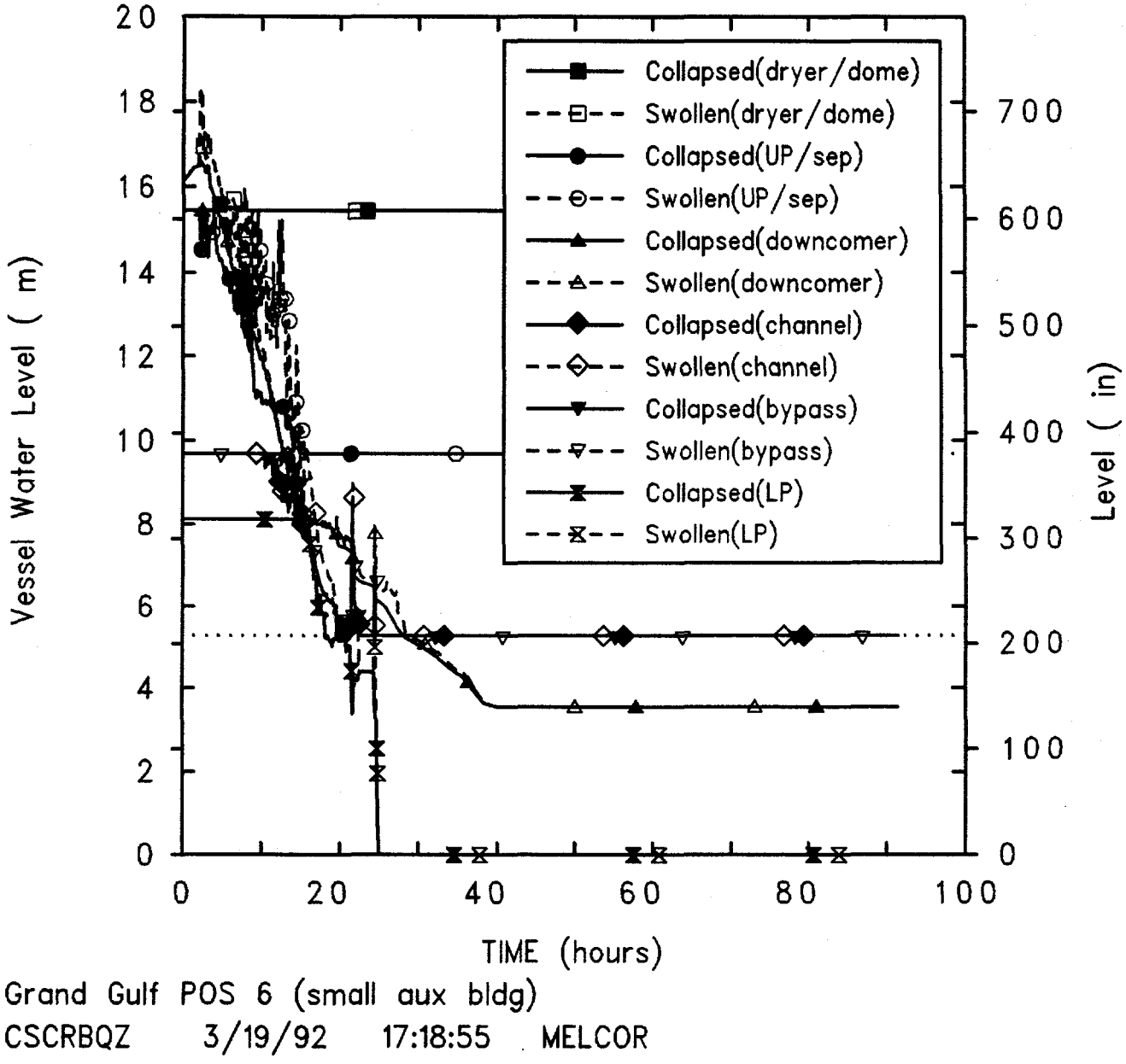

Figure 5.2.9. Reactor Vessel Liquid Levels for Grand Gulf POS 6 -- Reference Calculation.

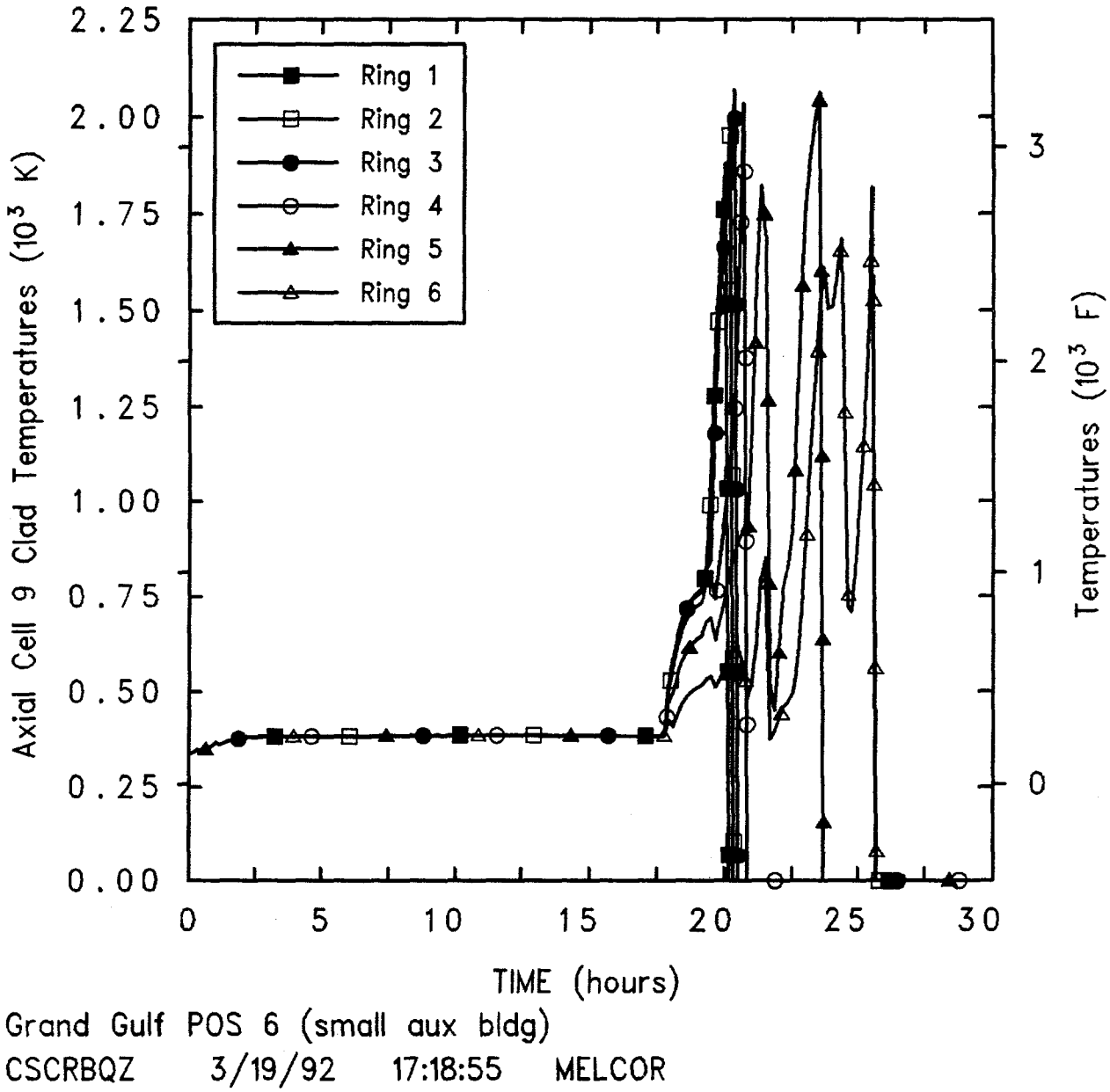

Figure 5.2.10. Level 9 Clad Temperatures for Grand Gulf POS 6 -- Reference Calculation.

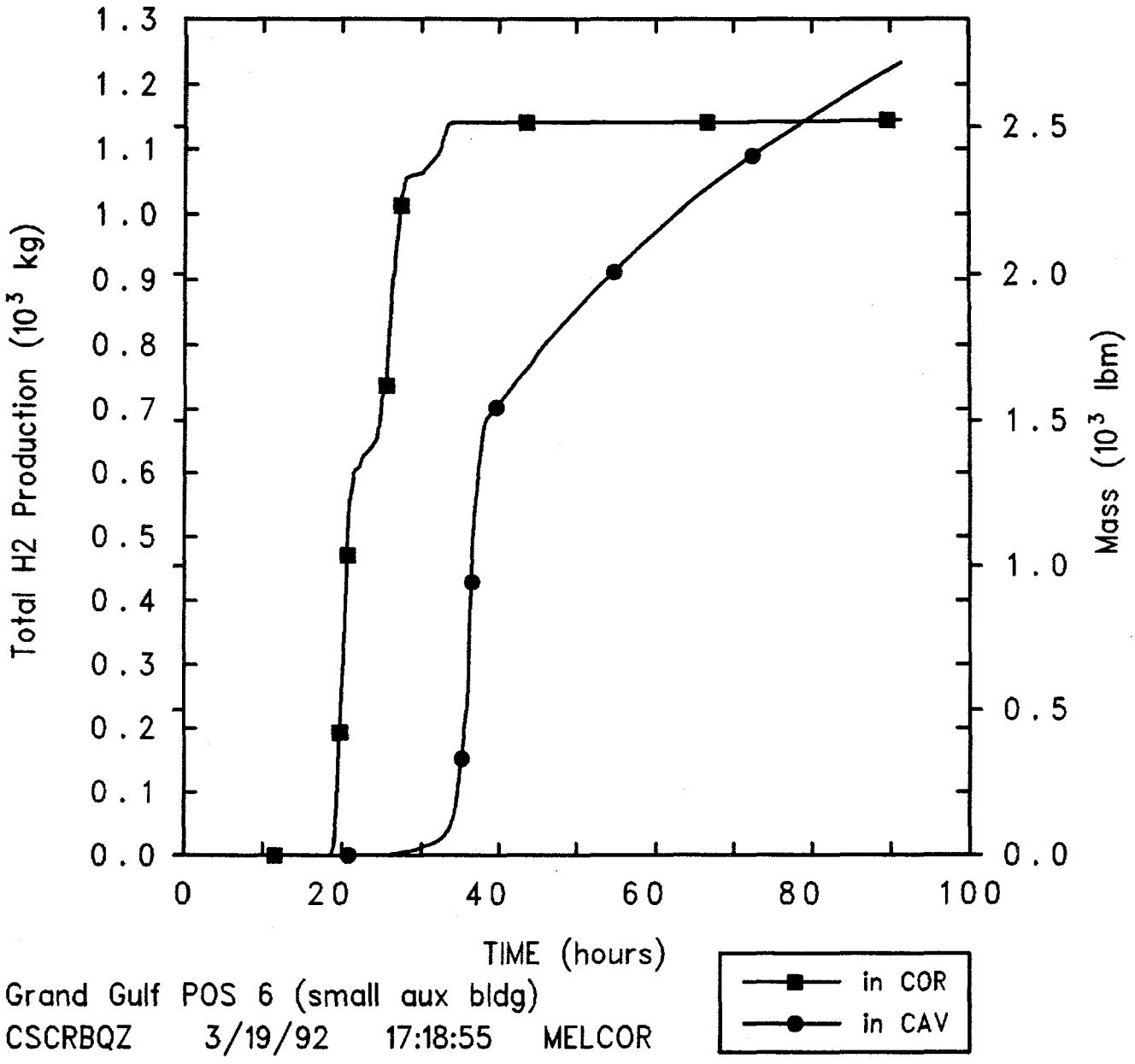

Figure 5.2.11. Total Hydrogen Generation for Grand Gulf POS 6 -- Reference Calculation.

Hydrogen production stops in the vessel as core debris is ejected from the lower plenum in the reactor vessel to the cavity in the inner containment; the core debris in the cavity then continues to generate hydrogen through continued oxidation of zirconium and steel, and through corium-concrete interaction. The amount of hydrogen generated in the cavity by the end of the transient (in this case, by the time the cavity ruptures) is about equal to the amount of hydrogen generated in the vessel earlier in the accident. The hydrogen generated in the cavity in the latter stages of the transient is quite small when compared to the generation rates of other gases, such as CO, CO_2 and water, as illustrated in Figure 5.2.12.

The cavity layer masses and temperatures are given in Figure 5.2.13. Mass first appears in the cavity when the vessel first fails, through a lower head penetration melting, just before 29 hr. Initially, the material consists of mostly heavy oxides and some metals, but changes to a layer of light oxides on top of metals at about 38 hr. The melt temperature drops slightly after this layer inversion, corresponding to the time that elevated cavity atmosphere temperatures in near-equilibrium with the light oxide layer are first seen in Figure 5.2.7.

The MELCOR calculation was stopped when the cavity was ruptured, i.e., when the concrete side and/or bottom walls were completely ablated at at least one point. Figure 5.2.14 shows that, in this calculation, it was the bottom, initially 2 m thick, that was ruptured first (although when the cavity is predicted to rupture in this calculation there is a minimum side wall thickness of only 0.2 m out of an initial side wall thickness of 1.752 m).

The total radionuclide releases predicted by MELCOR (given in terms of fraction of initial inventory) are presented in Table 5.2.2 at two specific times considered of interest: when a lower head penetration first fails (at about 25 hr in this analysis) and at the end of the calculation (i.e., at 91.4 hr when the cavity is predicted to rupture). At the first time, radionuclides have been released within the reactor vessel as the core degrades; at the latter time, most of the additional release has come from core debris in the cavity (although some release continues in the vessel until all the core material is ejected to the cavity). Table 5.2.2 also gives the amounts released to the environment by the end of the calculation.

A large percentage of volatile materials (the noble gases, cesium, iodine and tellurium) is released early and in-vessel, and all or almost all of the initial inventories of these classes are released by the end of the transient considered. Class 3 (the alkaline earths, such as Ba or Sr) and Class 12 (the less volatile main group elements like Sn) show significant releases, with almost half the initial inventories released by the end of the transient. The more refractory trivalents (La) and uranium show about a percent release by the time of cavity rupture, while the most refractory classes (Ru, Mo, Ce and Cd) release only 0.01-0.05% of their initial inventories by the end of the calculation.

Most of the release to the environment is in the form of the noble gases and iodine. This is expected because the volatiles (the noble gases, Cs and I) show the most release from fuel and debris, and most of that released inventory is released to the environment for those classes of volatiles which are assumed to be in the form of fission product vapors (the noble gases and I). This result could change if MELCOR considered iodine chemistry in detail.

The only other significant releases to the environment are for Cs and Te, in percentage terms, and for U, in absolute mass terms. Most of the classes either exhibit little release from fuel and/or debris, or substantial retention in the reactor vessel, containment and auxiliary building.

The releases in Table 5.2.2 give views at two distinct, different times in the transient. Additional information can be obtained by considering the time-dependent releases, in both the vessel and in the cavity, and also by considering the distribution of the radionuclides released.

Figure 5.2.15 presents release and distribution histories for Class 1 (Xe), with both the amounts released and the amounts in any given location at a particular time normalized by the initial mass of the class. (The results for Class 4, iodine and the other halogens, are virtually identical.) As was evident from the values given in Table 5.2.2, most of the noble gas inventory is released early in the in-vessel phase (>90%) with the remainder all released within the cavity. Because it is in the form of a fission product vapor, it is quickly transported through the primary system and containment, to the auxiliary building and out to the environment. By the end of the transient considered, over 90% of the initial inventory of noble gases and 85% of the initial inventory of halogens have been released to the environment.

The release and subsequent distribution histories of the alkali metals (Class 2, characterized by Cs) and the chalcogens (Class 5, represented by Te) are similar to each other, with the results for cesium given in Figure 5.2.16. As with the noble gases and iodine, most of the

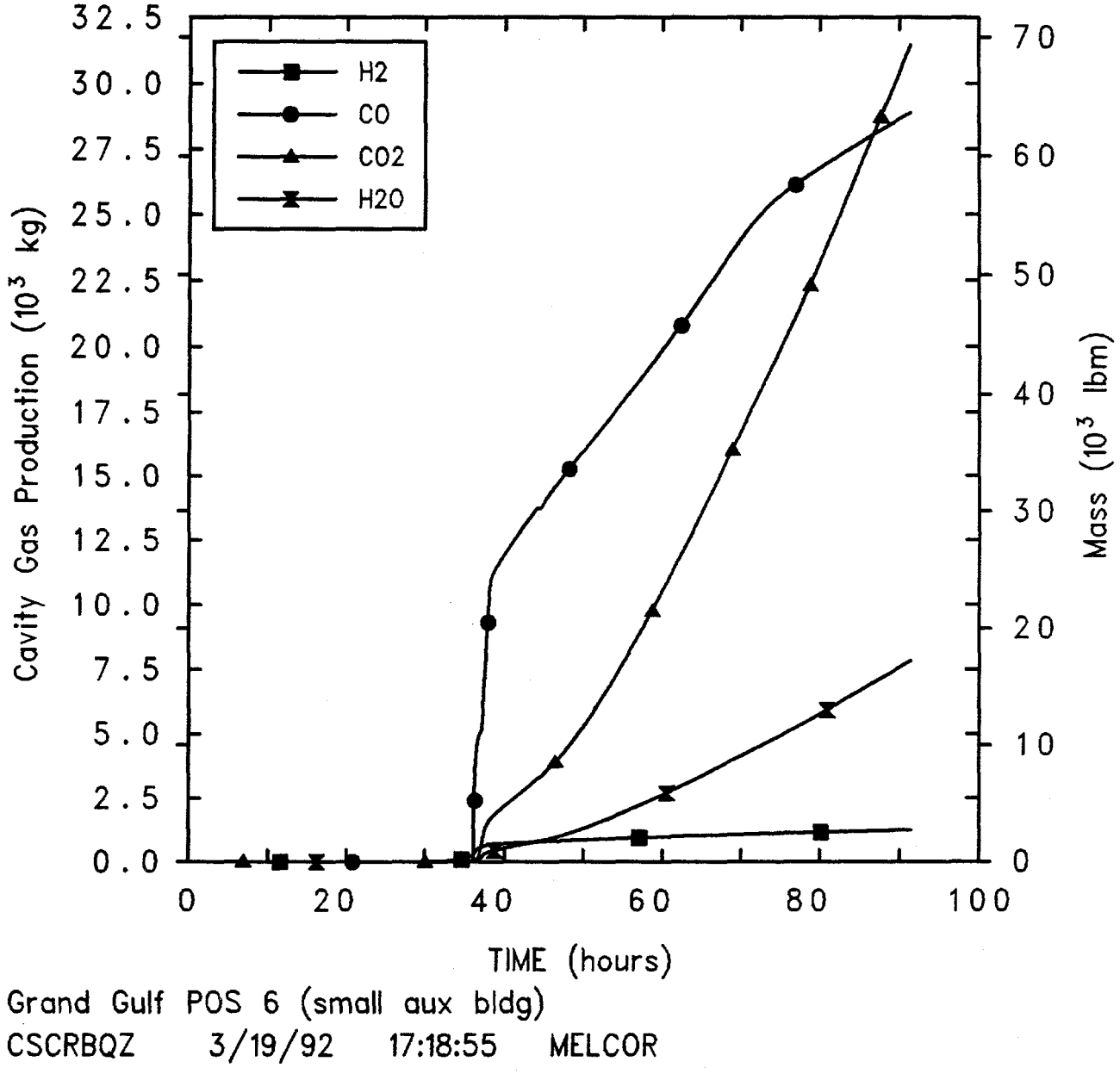

Figure 5.2.12. Cavity Gas Generation for Grand Gulf POS 6 -- Reference Calculation.

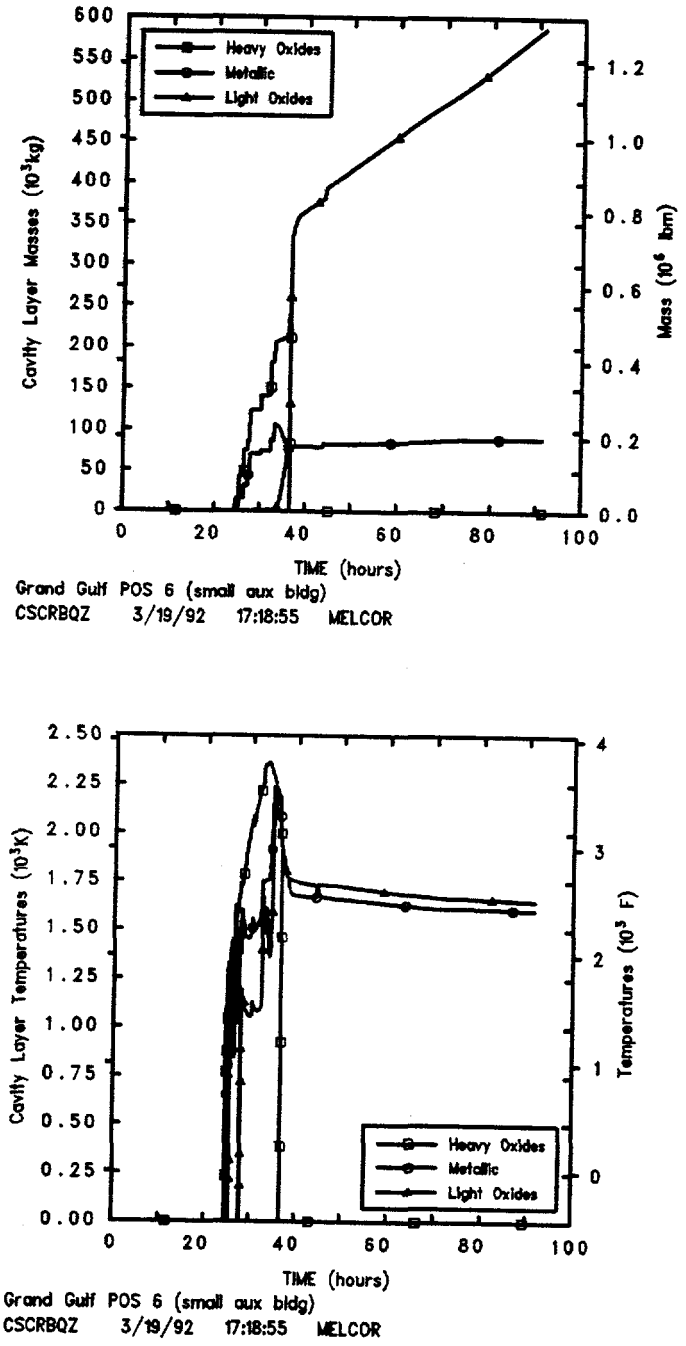

Figure 5.2.13. Cavity Layer Masses (top) and Temperatures (bottom) for Grand Gulf POS 6 -- Reference Calculation.

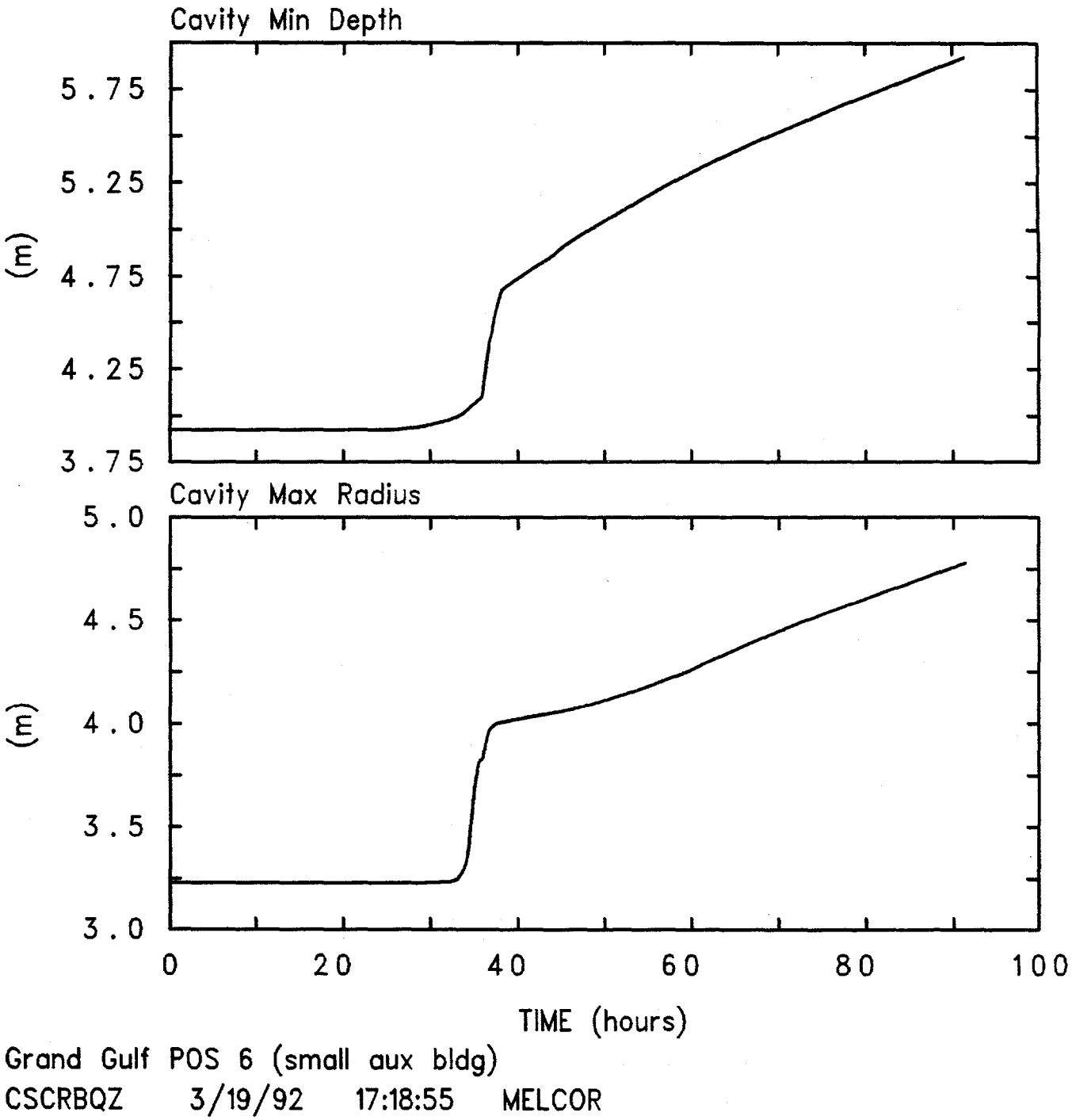

Figure 5.2.14. Cavity Maximum Radius and Minimum Depth for Grand Gulf POS 6 -- Reference Calculation.

Table 5.2.2. Total Fission Product Radioactive Masses Released from Fuel for Grand Gulf POS 6 -- Reference Calculation

Class	% of Initial Inventory Released (Mass Fraction) Before Vessel Failure	Before Cavity Rupture	to Environment
1 (Xe)	76.4	100	93
2 (Cs)	76.9	100	7.35
3 (Ba)	4.22	47.4	0.0615
4 (I)	76.1	93.2	86.8
5 (Te)	62.8	93	5.84
6 (Ru)	0.0023	0.0508	0.00056
7 (Mo)	0	0.0128	0.0102
8 (Ce)	0.00076	0.0264	0.00034
9 (La)	0	0.2809	0.00689
10 (U)	0.1145	2.16	0.0233
11 (Cd)	0	0.0396	0.0018
12 (Sn)	13.53	37.7	0.6603

initial inventories (>90% for Cs and >85% for Te) are released while still in the primary system, and almost all the remaining inventory is released in containment. Very little of the released inventory (less than 10%) finds its way to the environment, and these materials appear to settle into a stable distribution pattern with little transport after about 40 hr; the abrupt shift from the drywell to the sumps at around 35 hr appears to be due to the abrupt rise in drywell temperature (Figure 5.2.7). There is no one predominant location for these classes, with about 30-35% retained in the auxiliary building, and less than 20% each in the primary system, drywell, outer containment and sump pools.

Another set of similar release and distribution behavior is found in the platinoids (Class 6) and the tetravalents (Class 8); the results for both these classes closely resemble the behavior predicted for uranium (Class 10), shown in Figure 5.2.17, even though their release fractions are much lower. Most of the release occurs in-vessel, at the high temperatures characteristic of the degraded core, with little or no release predicted at the slightly lower temperatures predicted in the debris bed in the cavity. Of the material released, about 35% remains in the reactor vessel, with another 20-25% in the sump pools and 15-20% found in the auxiliary building. As with the Cs and Te classes, very little of the released inventory (around 1%) finds its way to the environment (or to the drywell or outer containment, either), and these materials also appear to settle into a stable distribution pattern with little transport after about 40 hr; the abrupt shift from the drywell and outer containment to the sumps at about 35 hr appears to be due to the abrupt rise in drywell temperature (Figure 5.2.7).

The remaining classes (such as Ba and Sn) do not appear to fall into such convenient groupings in terms of their release/distribution behavior. The results for the alkaline earths class (Class 3, characterized by barium) are illustrated in Figure 5.2.18. This is the only class showing about equal amounts released in the vessel and in the cavity. About 25% of the mass released accumulates in the sump pools, where it is relatively immobilized; a second and third quarter of the mass released either remains in the reactor vessel or settles in the auxiliary building. Of the final 25%, most is in the drywell and outer containment, and little (around 2%) is released to the environment.

Figure 5.2.19 gives the corresponding results for Class 12 (Sn). Most of the release occurs at the higher in-vessel temperatures, with very little release at the lower, cavity-debris temperatures. Of the material released, the distribution somewhat resembles that just described for the barium class. The largest fraction (25-30%) is retained in the auxiliary building, with another 20-25%

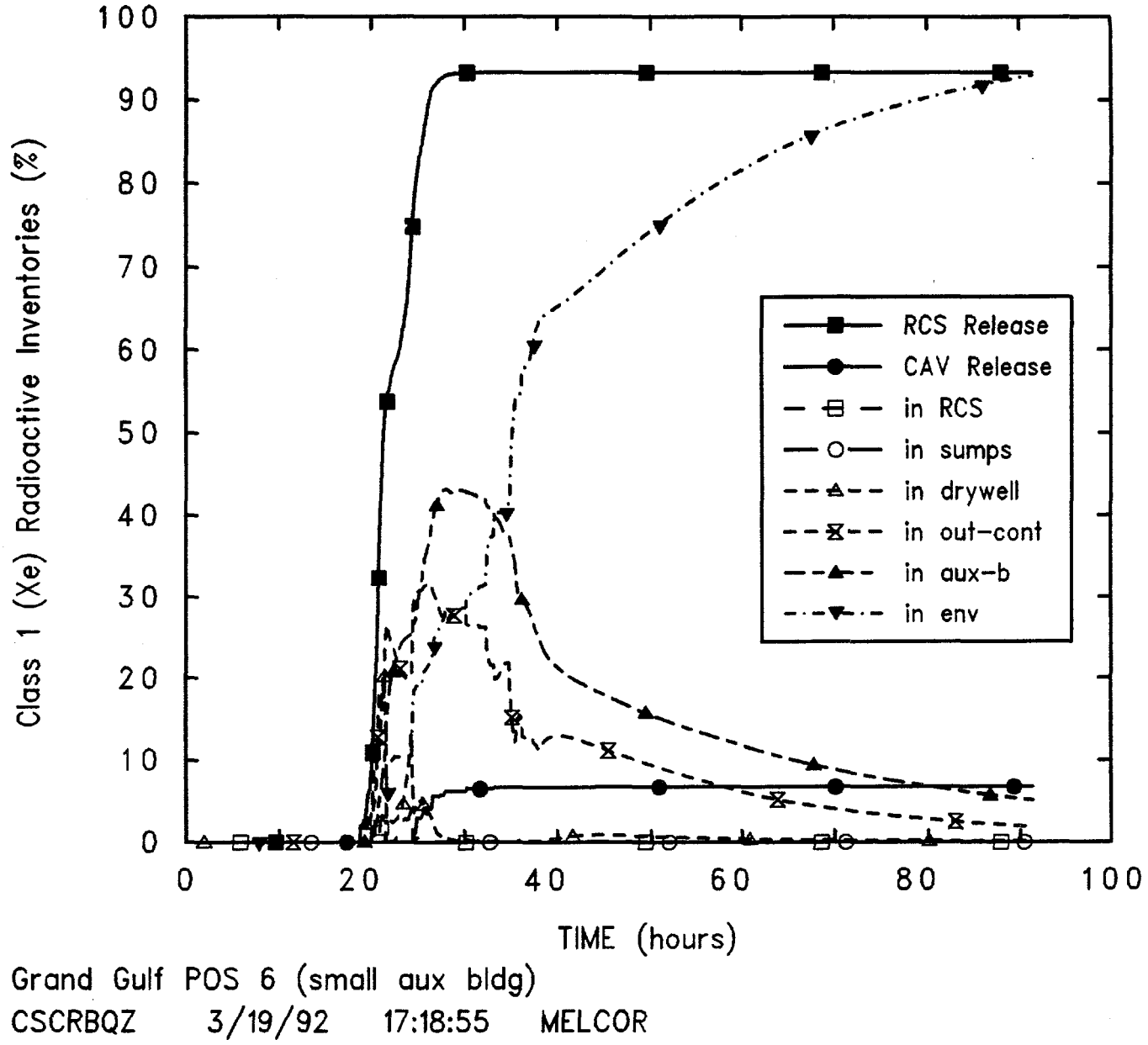

Figure 5.2.15. Class 1 Radioactive Mass Radionuclide Distribution for Grand Gulf POS 6 -- Reference Calculation.

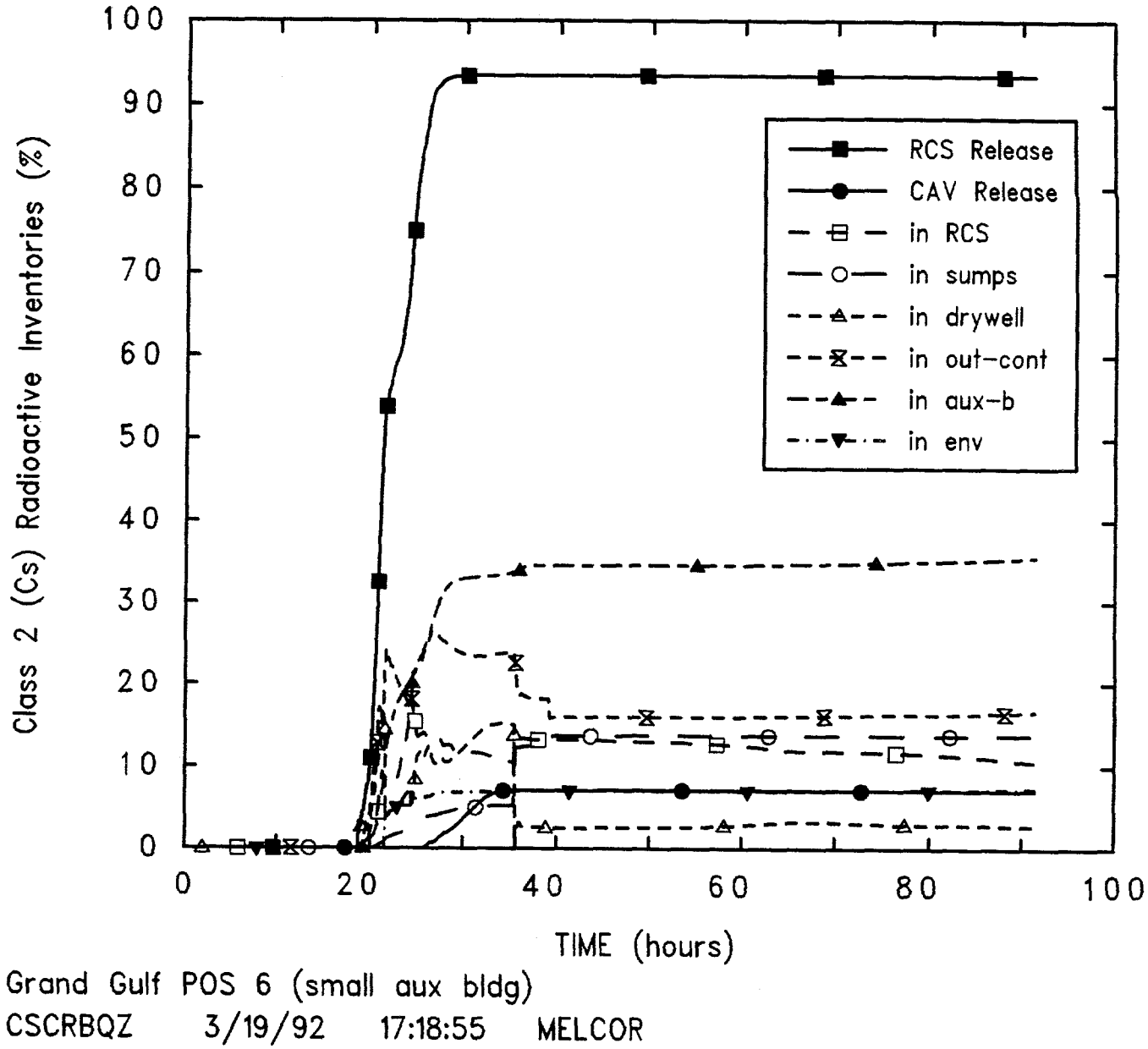

Figure 5.2.16. Class 2 Radioactive Mass Radionuclide Distribution for Grand Gulf POS 6 -- Reference Calculation.

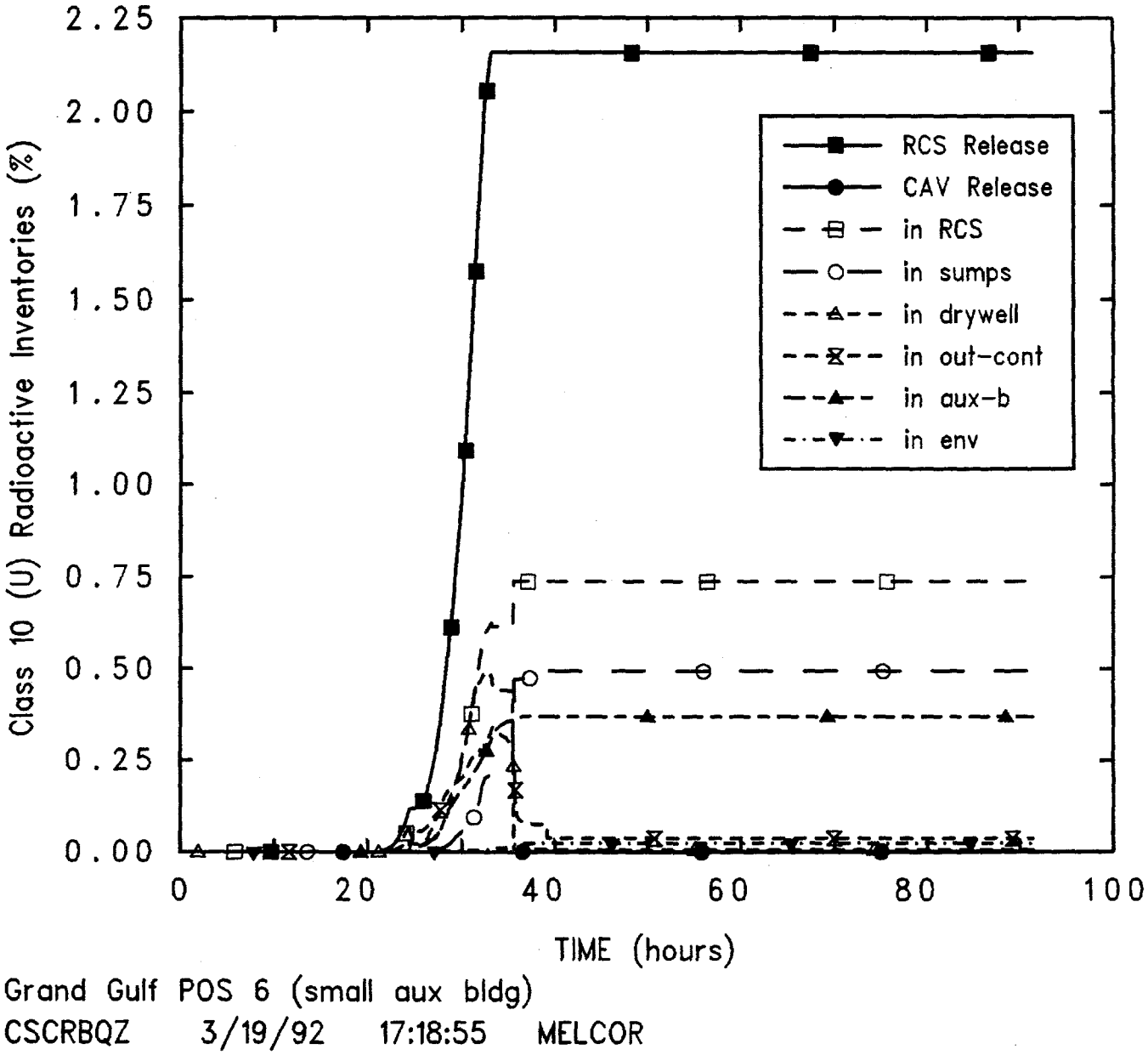

Figure 5.2.17. Class 10 Radioactive Mass Radionuclide Distribution for Grand Gulf POS 6 -- Reference Calculation.

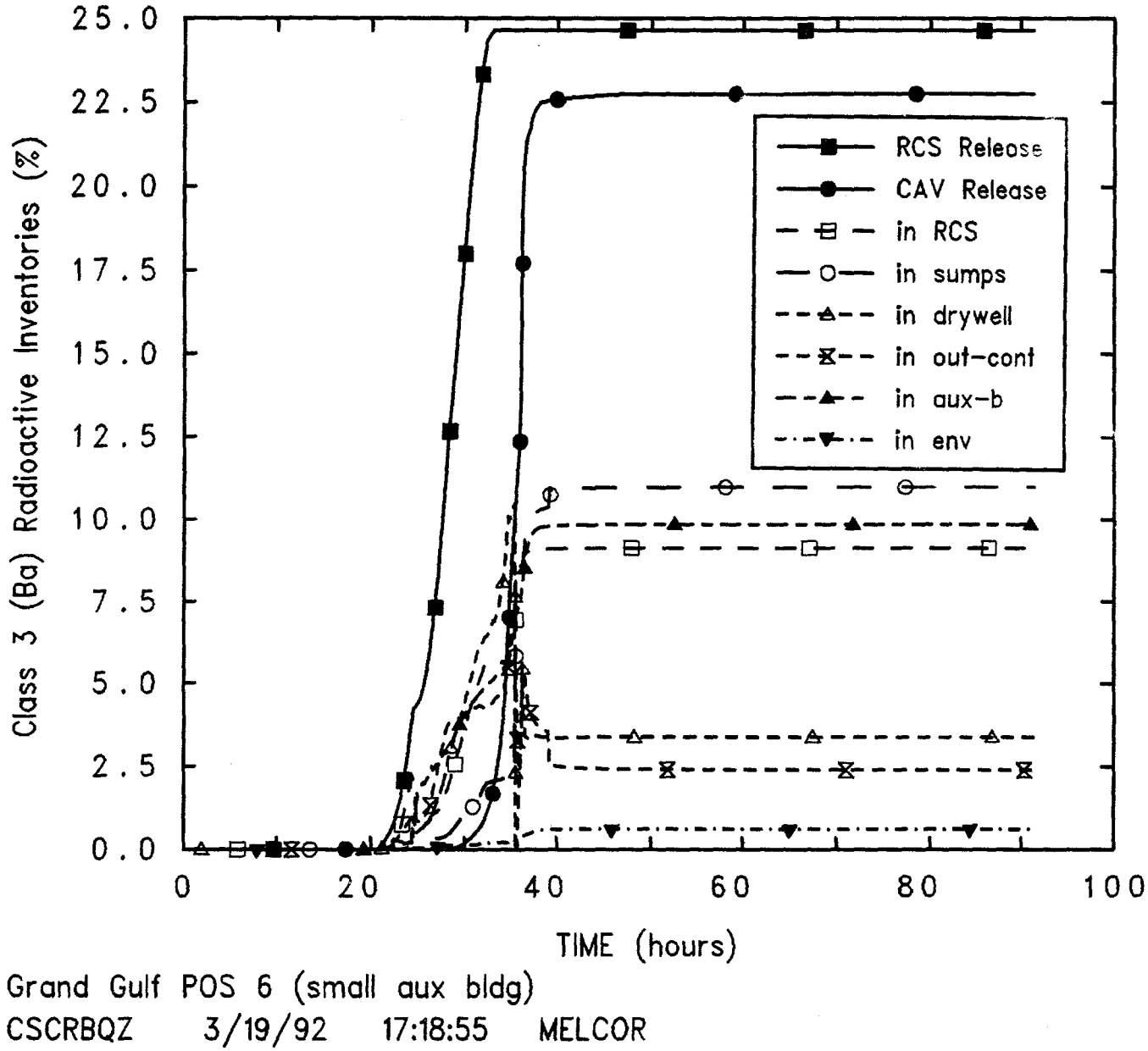

Figure 5.2.18. Class 3 Radioactive Mass Radionuclide Distribution for Grand Gulf POS 6 -- Reference Calculation.

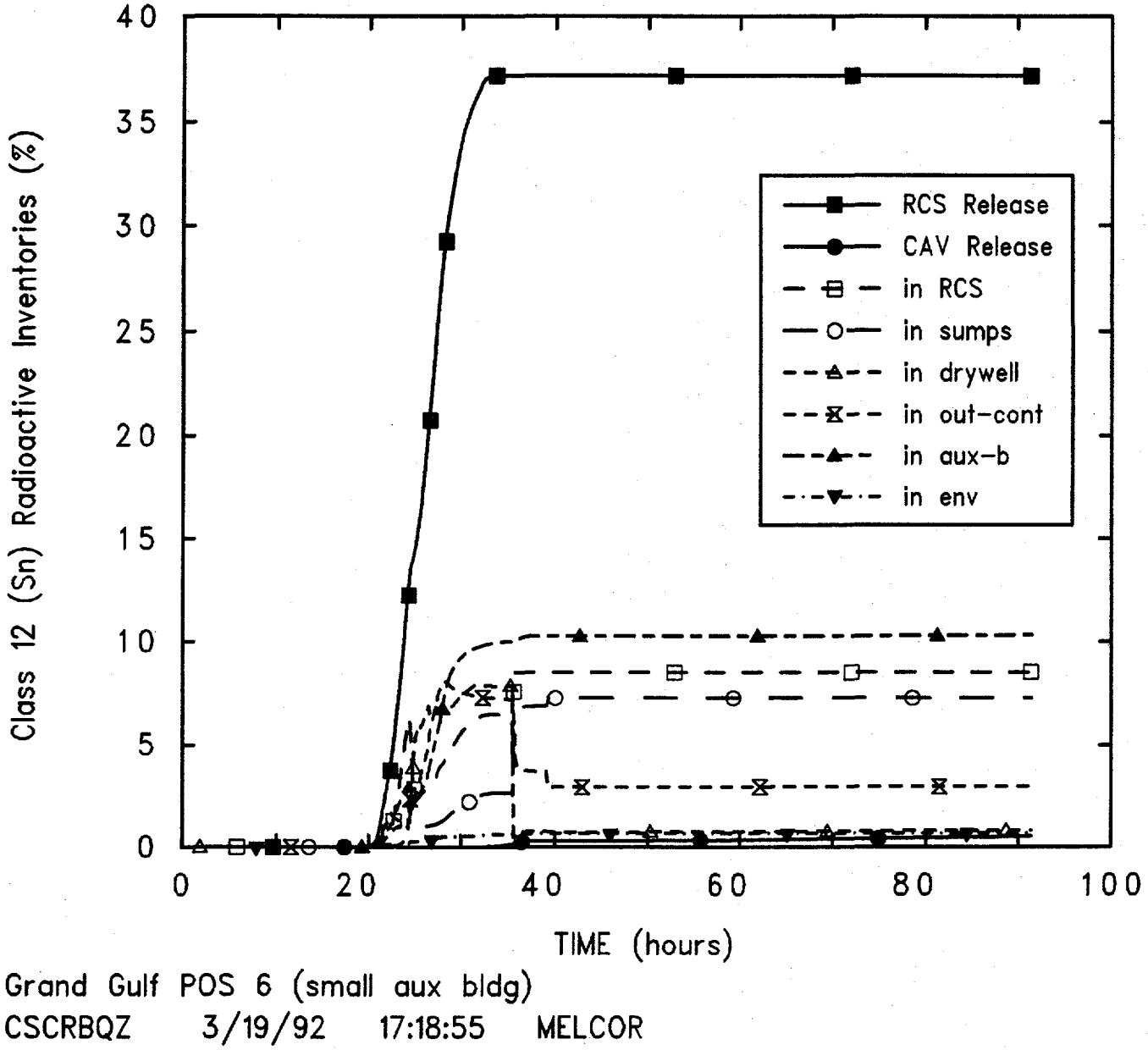

Figure 5.2.19. Class 12 Radioactive Mass Radionuclide Distribution for Grand Gulf POS 6 -- Reference Calculation.

each in the vessel and sump pools. Of the remaining mass released, most is in the outer containment, and little is found in the drywell or released to the environment.

The behavior calculated for the early transition elements such as Mo (Class 7, in Figure 5.2.20), the trivalents represented by La (Class 9, in Figure 5.2.21), and the more volatile main group elements such as Cd (Class 11, in Figure 5.2.22), all share the common trait that the release occurs in the cavity after debris ejection; no release is seen in the primary system. As with all the classes discussed so far, the distribution of the trivalents does not change much after about 40 hr, i.e., after the abrupt rise in drywell temperature (Figure 5.2.7). The distribution of the Class 7 radionuclides also stops changing but later in time, after about 50 hr, because there is still some release of this class occurring between 40 and 50 hr. In contrast, Class 11 shows continued release at a nontrivial, nearly linear rate for the remainder of the transient after the initial step release at about 35 hr. All three of these classes have the largest fractions of their released inventories in the sump pool, auxiliary building, drywell and primary system, with little appearing in the environment (although the amount of Cd in the environment is still increasing at the end of the transient).

5.3 Plant Configuration Studies

The calculations done for POS 6 included variations on the plant configuration, as summarized in Section 5.1. The results of these sensitivity studies are described in this section. These analyses evaluated the effect of including the auxiliary building in the calculations, with various free volumes and deposition surface areas assumed to represent doors being open or closed. The effects of the containment personnel locks being open or closed were investigated also, as was the impact of the drywell head being open or closed. The influence of the time between shutdown and accident initiation was considered, as well as the effect of hydrogen igniters being active.

5.3.1 Auxiliary Building

As discussed in Section 3, a model for the auxiliary building (shown in Figure 3.4), was developed specifically for these analyses, primarily from the limited information in the FSAR [Grand Gulf Nuclear Station]. Because of the uncertainties in the descriptions of the auxiliary building geometry, especially the flow paths, two variations of the auxiliary building model were developed.

In both, the auxiliary building model consisted of the same number of control volumes, flow paths and heat structures, but the volumes and surface areas were changed: the opened (or "big") auxiliary building model represented open interior doors, resulting in larger open volumes and heat structure surface areas for flow-through and potential retention and/or deposition of aerosols before the stairwell door to the environment is blown open; the closed (or "small") auxiliary building model represented closed interior doors while the stairwell door to the environment is blown open. Both auxiliary building models assumed failure on a 5 psi overpressure.

The reference calculation with results described in detail in Section 5.2 used the closed auxiliary building model. To evaluate the impact of the uncertainties in the description of the auxiliary building geometry, calculations were done with the open auxiliary building model as well as with no auxiliary building model (i.e., the containment open directly to the environment).

Table 5.3.1.1 compares the timings of various key events predicted in the calculations with no, opened and closed auxiliary buildings modelled. The start of core uncovery varies by at most about 22 min, while the first gap release varies by at most about 25 min, in the calculations with either auxiliary building *vs* no auxiliary building; the timing difference for these early events is much smaller (1-5 min) for the calculations with the two different auxiliary building models. The auxiliary building modelling affects the calculation both directly through possible outflow and/or backflow, and indirectly by changing the time step used and thus affecting convergence and other numerical sensitivities.

The timing differences shown in Table 5.3.1.1 grow larger at later times, with the first lower head penetration failure occurring 4 hr later in the open auxiliary building analysis (compared to less than 1 hr difference in lower head failure time in the other two calculations); however, this 4 hr difference is to some extent a numerical effect. It was necessary in this particular calculation (as in a few others) to back up and reduce the user-specified maximum time step in order to continue through and past numerical difficulties in modelling the core degradation process in order to be able to complete the analysis. That time-step reduction affected the results calculated to some degree, in addition to any effects of the different auxiliary building

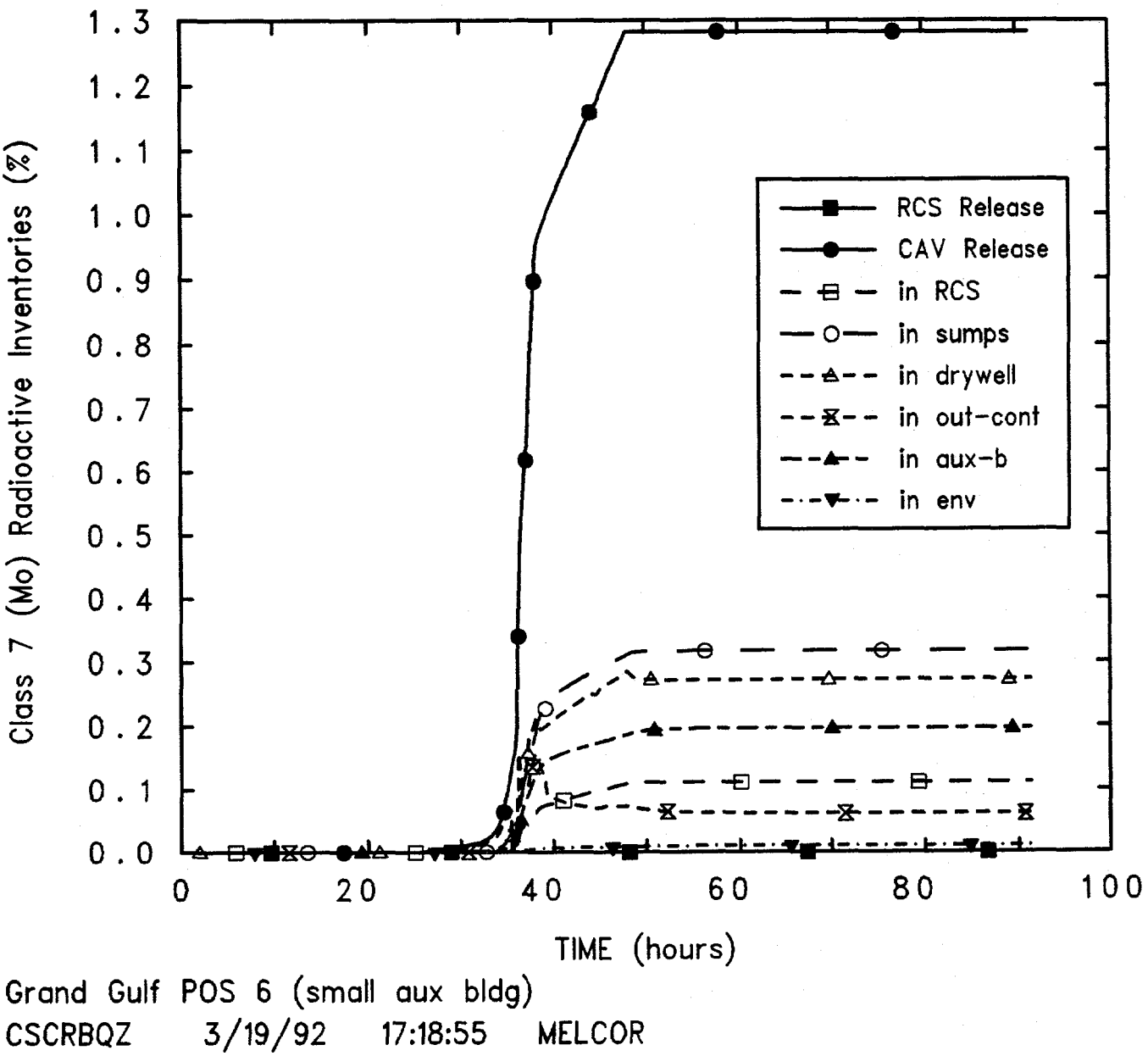

Figure 5.2.20. Class 7 Radioactive Mass Radionuclide Distribution for Grand Gulf POS 6 -- Reference Calculation.

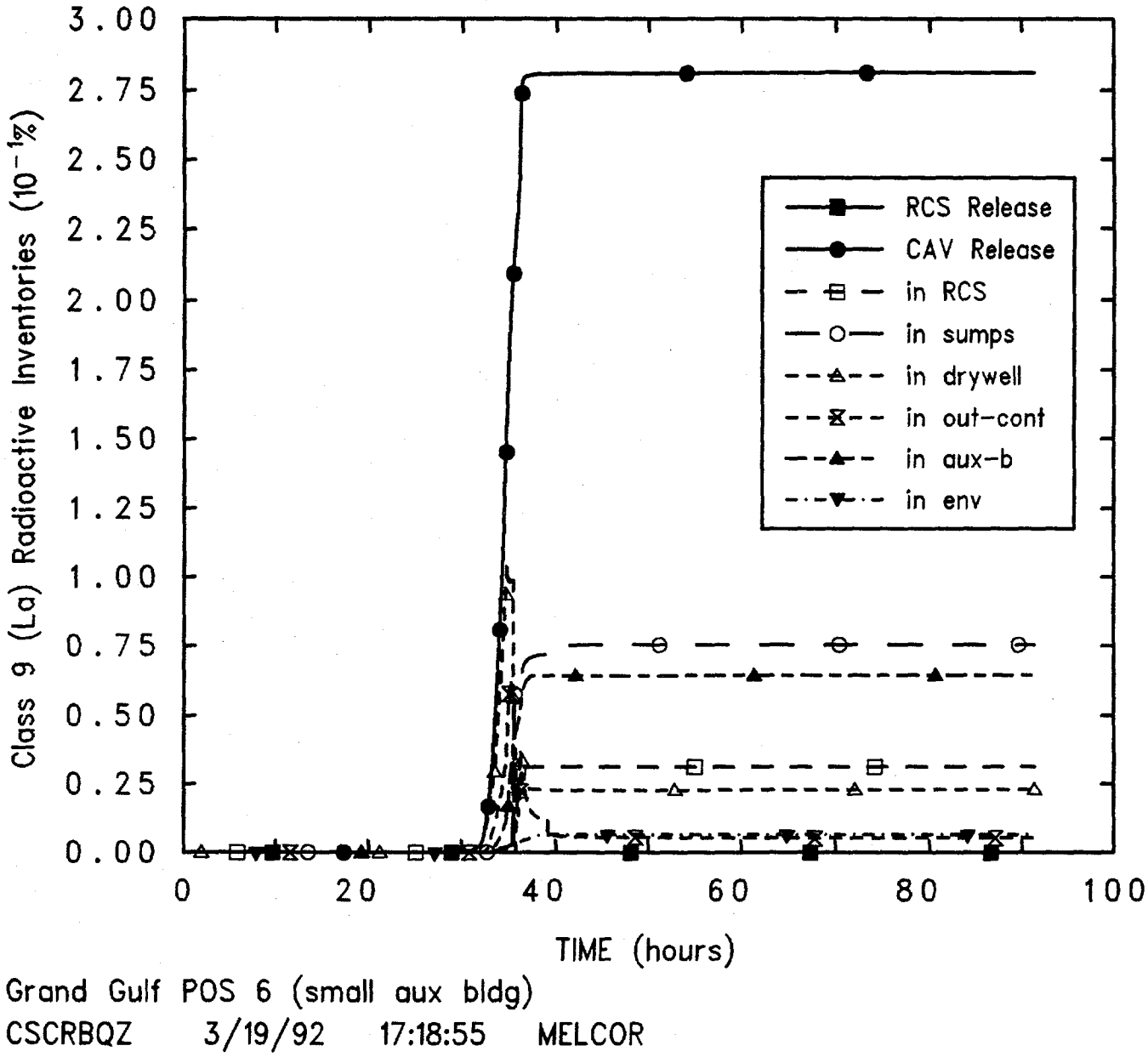

Figure 5.2.21. Class 9 Radioactive Mass Radionuclide Distribution for Grand Gulf POS 6 -- Reference Calculation.

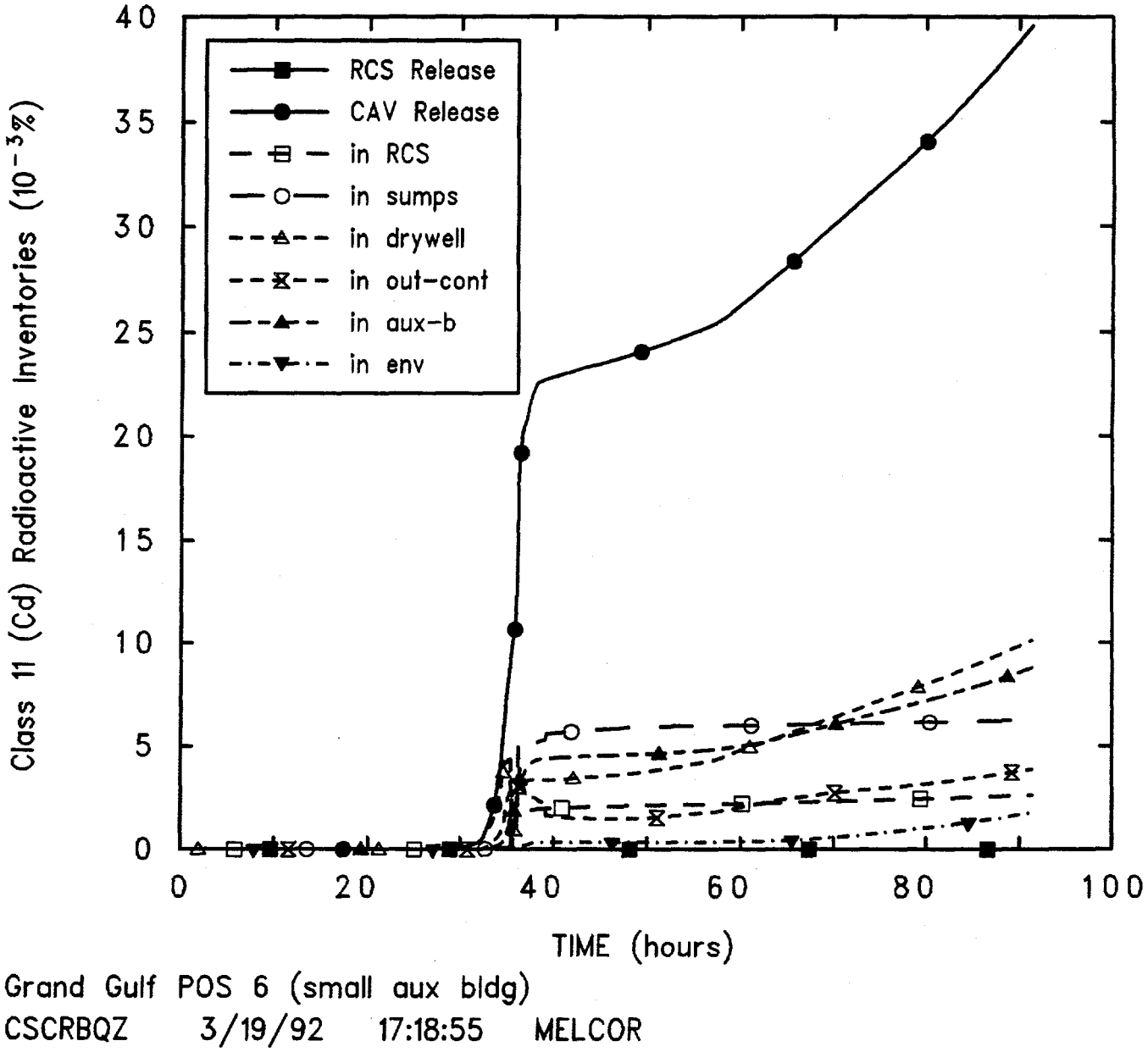

Figure 5.2.22. Class 11 Radioactive Mass Radionuclide Distribution for Grand Gulf POS 6 -- Reference Calculation.

Table 5.3.1.1 Key Event Times for Grand Gulf POS 6 -- Auxiliary Building Model Sensitivity Study

Event	No Aux Bldg	Open Aux Bldg	Closed Aux Bldg
Level below TAF	12.68 hr	12.95 hr	13.04 hr
Clad failure/Gap release			
(Ring 1)	18.37 hr	18.79 hr	18.80 hr
(Ring 2)	18.34 hr	18.75 hr	18.76 hr
(Ring 3)	18.38 hr	18.80 hr	18.81 hr
(Ring 4)	18.61 hr	19.04 hr	19.04 hr
(Ring 5)	20.46 hr	20.93 hr	19.93 hr
(Ring 6)	21.80 hr	21.99 hr	23.22 hr
Auxiliary building failure	--	28.55 hr	21.50 hr
Vessel LH penetration failure			
(Ring 1)	25.45 hr	28.54 hr	24.52 hr
(Ring 2)	25.39 hr	28.83 hr	24.74 hr
(Ring 3)	26.10 hr	29.20 hr	25.49 hr
(Ring 4)	34.49 hr	29.26 hr	26.50 hr
(Ring 5)	30.24 hr	29.71 hr	27.87 hr
(Ring 6)	32.63 hr	32.52 hr	30.22 hr
Cavity Rupture	85.61 hr	73.32 hr	91.41 hr

model (as shown in Section 5.4.2, presenting the results of a calculation in which a time-step cut during the core degradation process was the only change made, to determine how big an effect reducing the time step would have on the results).

The early-time differences found in timing of core uncovery and gap release are due to differences in the pressure response of the primary system and containment in the calculations using different auxiliary building models. Figure 5.3.1.1 presents the lower plenum pressures from these three calculations, as representative of the primary system response. With an auxiliary building modelled, the primary pressures slowly equilibrate to the (rising) containment pressure as water inventory is boiled away, until the auxiliary building fails, after which time the pressures drop rapidly to atmospheric; with no auxiliary building and the containment open directly to the environment, the primary pressures equilibrate directly to atmospheric pressure instead of to rising containment pressures, resulting in lower reactor vessel pressures during the first 20 to 30 hr.

The pressures in the outer containment dome for these three cases are given in Figure 5.3.1.2; the pressures in other containment volumes are virtually identical in each calculation. With no auxiliary building and the containment open directly to the environment, the containment pressure remains constant at atmospheric pressure. With an auxiliary building in the model and assuming a 5 psi overpressure failure criterion, the containment (and auxiliary building) pressures rise as steam is generated in the vessel core as water inventory is boiled away, until the auxiliary building fails (at 21.5 hr with the smaller volume assumed and at 28.5 hr with the larger volume) after which time all the pressures drop rapidly to atmospheric.

The presence or absence of the auxiliary building in the MELCOR model affects the circulation flow found in the reference calculation. A substantial outflow from containment into the auxiliary building develops through the equipment hatch and a corresponding inflow into containment from the auxiliary building goes through the lower personnel lock, as illustrated in Figure 5.3.1.3. With no auxiliary building modelled, the flows go directly

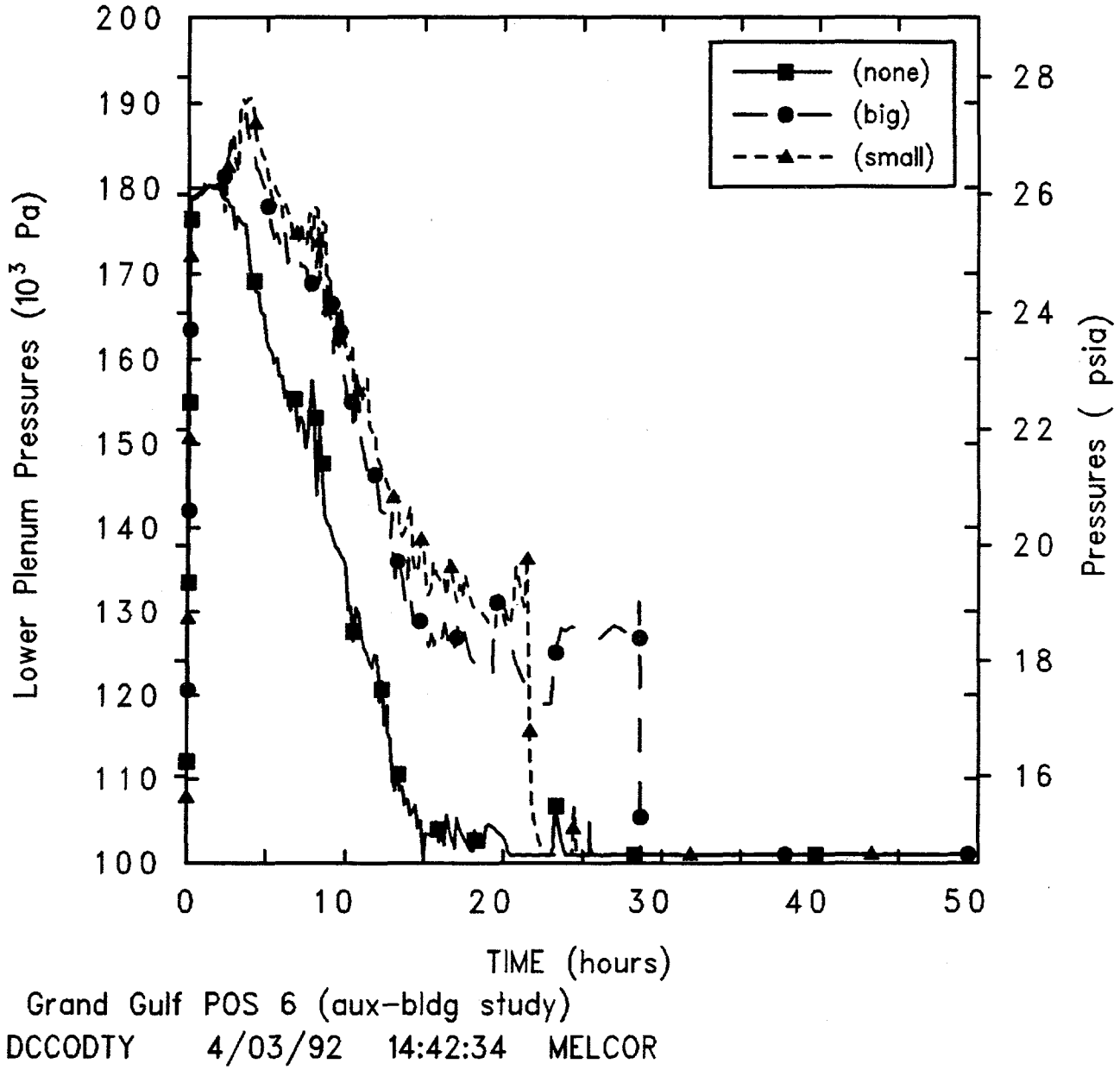

Figure 5.3.1.1. Lower Plenum Pressures for Grand Gulf POS 6 -- Auxiliary Building Model Sensitivity Study.

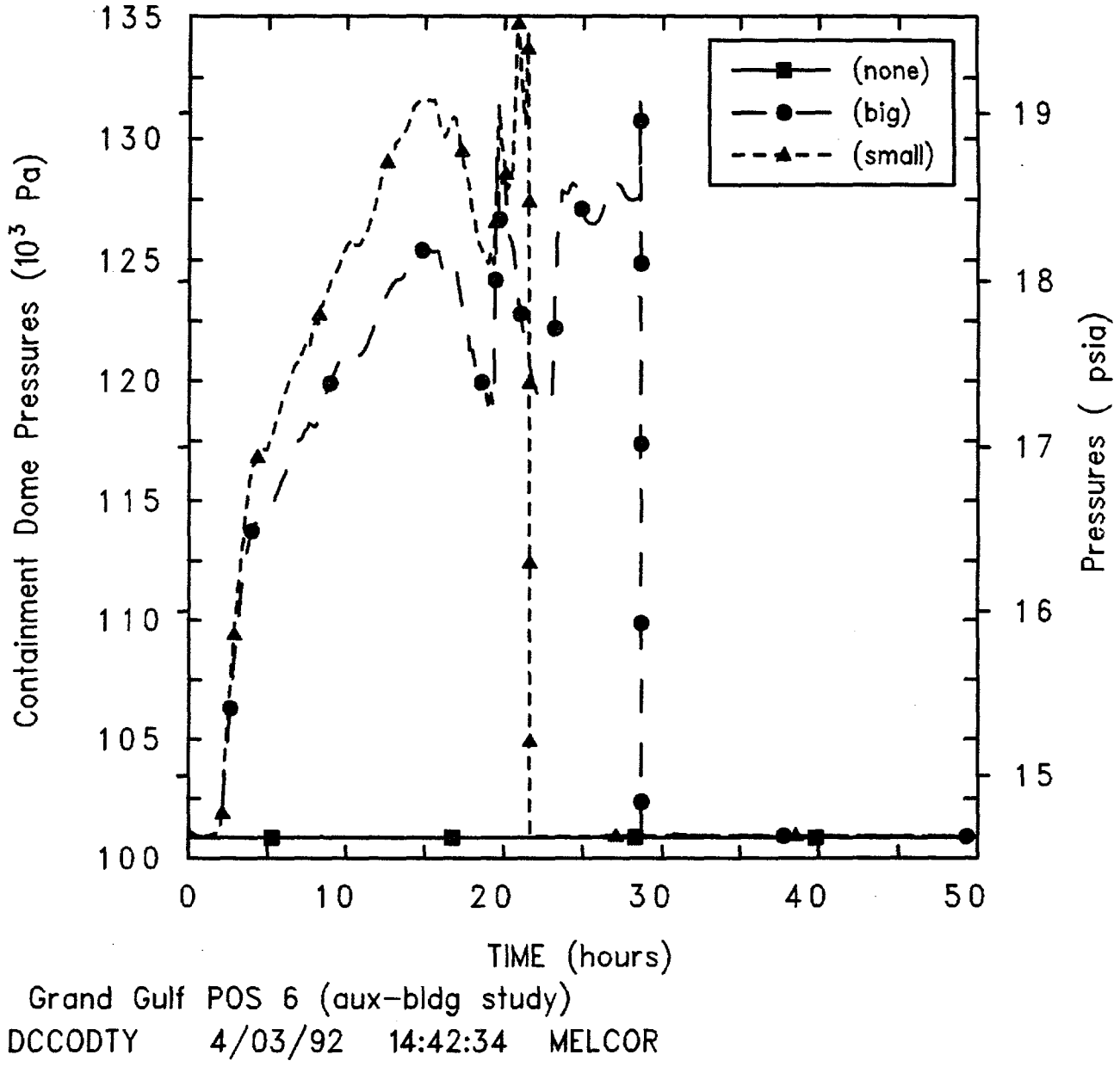

Figure 5.3.1.2. Containment Dome Pressures for Grand Gulf POS 6 -- Auxiliary Building Model Sensitivity Study.

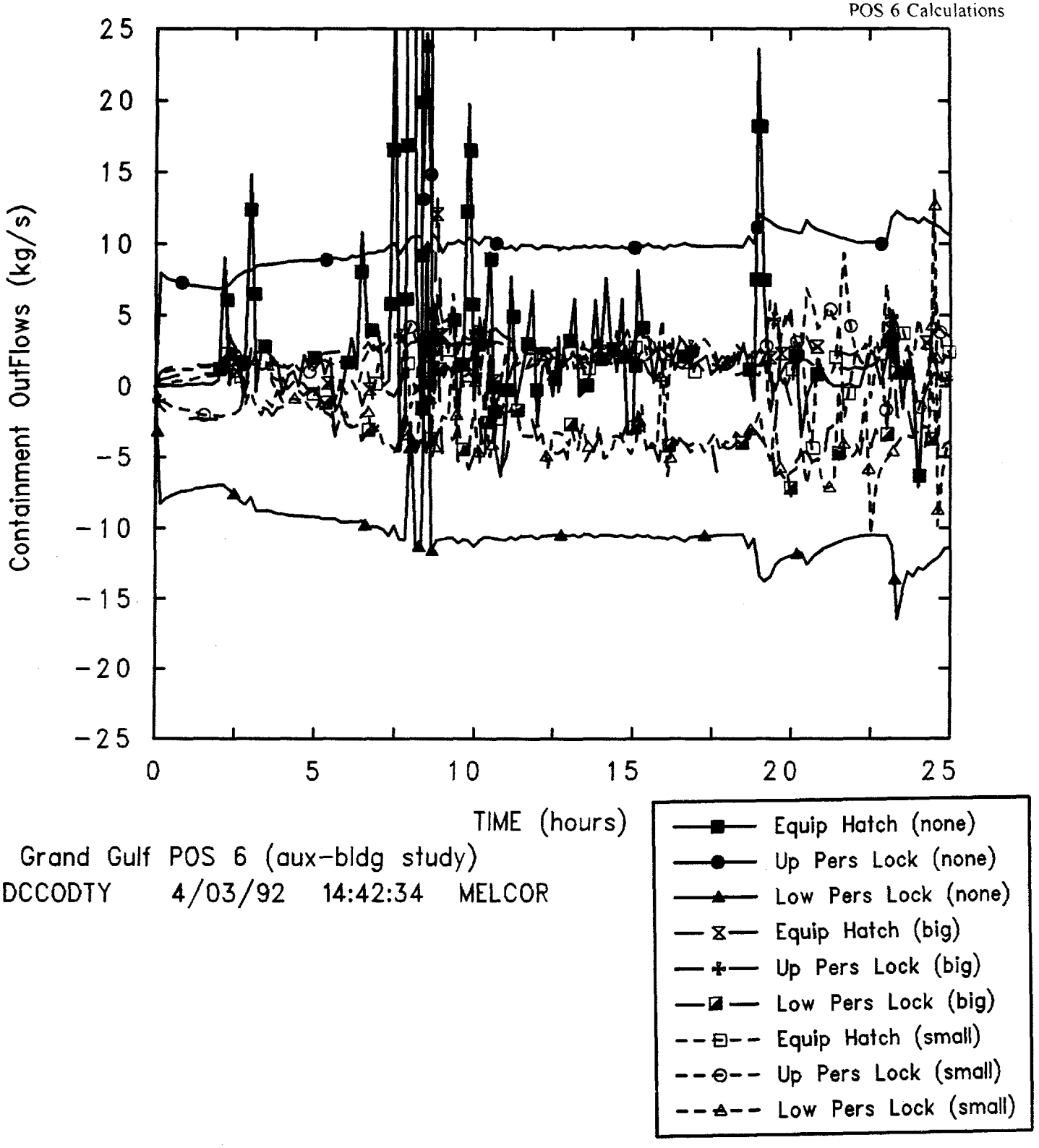

Figure 5.3.1.3. Containment Outflows for Grand Gulf POS 6 -- Auxiliary Building Model Sensitivity Study.

between the containment and the environment, primarily out through the upper personnel lock and back through the lower personnel lock, and are significantly greater in magnitude. Using either model of the auxiliary building model does not significantly affect this circulation flow.

Clad temperature histories in several core cells, in various axial levels and radial rings, are given in Figure 5.3.1.4, as representative of the overall core response in these three calculations. There is no dominant effect of these three different auxiliary building models on the core temperature response -- some cells experience similar heatup and clad/fuel failure behavior, other cells experience faster heatup and earlier clad/fuel failure and yet others later failure.

Table 5.3.1.2 summarizes the radioactive masses released from the fuel and debris for each class, together with the amount released to the environment by the time of cavity rupture, normalized by the initial inventory of each class given in Table 3.1.

The varying amounts released with no or different auxiliary building models primarily reflect the differences in core temperature histories and lower head failure times (e.g., the later vessel failure time in the open auxiliary building analysis is a major factor in the higher fission product release fractions in the vessel prior to breach), and to a lesser degree differences in the cavity response. By the end of the transient, all or most of the volatiles (the noble gases, cesium, iodine and tellurium) are released by the end of the transient considered, in all three calculations. Class 3 (the alkaline earths, such as Ba or Sr) and Class 12 (the less volatile main group elements like Sn) show similar and significant releases, with almost half the initial inventories released by the end of the transient. The more refractory trivalents (La), the transition elements (Mo) and uranium show about a percent release by the time of cavity rupture, while the most refractory classes (Ru, Ce and Cd) release only 0.004-0.05% of their initial inventories by the time of cavity rupture. With an auxiliary building modelled, most of the release to the environment is in the form of the noble gases and iodine; with no auxiliary building modelled, a large fraction of the initial inventories of Ba, Te and Sn are also released to the environment.

Figure 5.3.1.5 presents release and distribution histories for Class 4 (I), with both the amounts released and the amounts in the environment at a particular time normalized by the initial mass of the class. (The results for Class 1, the noble gases, are very similar.) By the end of the transient considered, 100% of the initial inventory of noble gases and over 90% of the initial inventory of halogens have been released to the environment, with or without an auxiliary building modelled; the effect of the auxiliary building is seen primarily as a timing delay and a slower rate of release to the environment.

The release and subsequent distribution histories of the alkali metals (Class 2, Cs) and the chalcogens (Class 5) are similar, with the results for tellurium given in Figure 5.3.1.6. Interestingly, although only about 30-35% of these class masses released are retained in the auxiliary building (if modelled), the release to the environment increases much more (to over 60%) if the auxiliary building is neglected. The behavior predicted for the alkaline earths (Class 3) and the less volatile main group elements (Class 12, Sn) also shows the release to the environment increasing much more (from about 1% to less than 20%) if no auxiliary building is modelled.

The changes in release and distribution of the other classes present much less coherent a pattern for these three different calculations. To a large degree this is because the amounts released are very low, and the behavior extremely sensitive to minor changes in temperature histories and flow patterns predicted. It is not clear whether the differences observed are significant, since for these other classes the releases to environment by the time of cavity rupture are under 1% in all three analyses.

These three calculations all ended on cavity rupture, at various times. The 6 hr difference between the no and closed auxiliary building models probably represents a more reasonable timing difference than the 18 hr difference between the opened and closed model calculations, because of the probable long-term impact of the perturbing time-step effects. Figure 5.3.1.7 shows that these three calculations all predict that the cavity concrete will first be ruptured in depth, with various minimum side wall thicknesses of concrete remaining.

5.3.2 Personnel Locks

POS 6 begins when the vessel head is detached and ends when the upper reactor cavity has been filled with water. The steam dryers are removed, vessel water level is lowered to the bottom of the steam lines and the steam lines are plugged, water level is raised and the steam separators are removed, and vessel water level is raised to flood the upper reactor cavity. Prior to this mode of operation, the containment equipment hatch and personnel

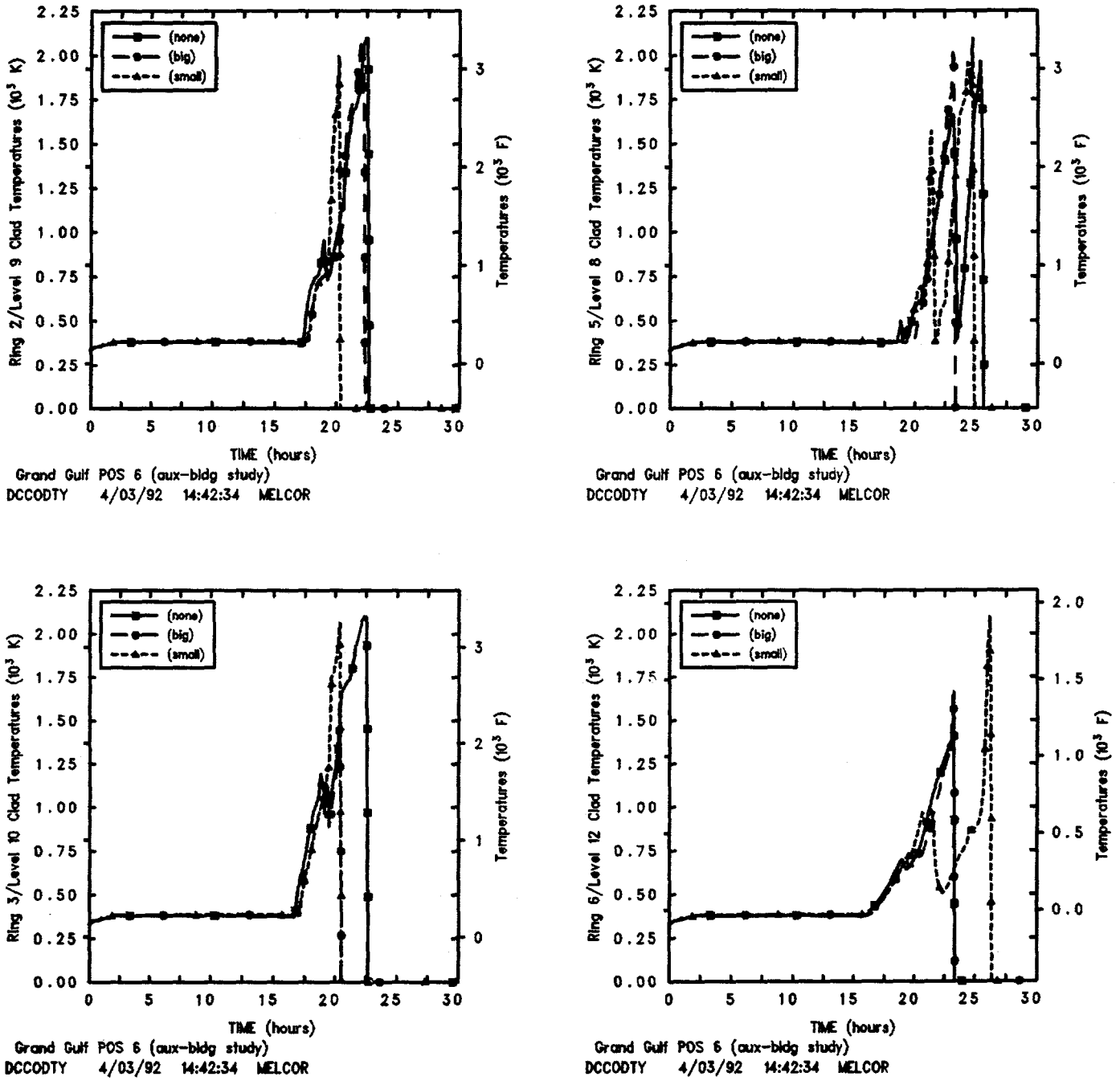

Figure 5.3.1.4. Clad Temperatures for Grand Gulf POS 6 -- Auxiliary Building Model Sensitivity Study.

Table 5.3.1.2 Total Fission Product Radioactive Mass Releases for Grand Gulf POS 6 -- Auxiliary Building Model Sensitivity Study

Class	% of Initial Inventory Released (Mass Fraction) From Fuel			To Environment		
	None	Open	Closed	None	Open	Closed
1 (Xe)	100	100	100	100	84.3	93
2 (Cs)	100	100	100	67.6	2.54	7.35
3 (Ba)	42	44.8	47.4	21.3	1.011	0.0615
4 (I)	95.5	97.3	93.2	95.5	82.5	86.8
5 (Te)	95.2	97.1	93	62.3	2.77	5.84
6 (Ru)	0.007	0.0456	0.05	0.0045	0.00103	0.00056
7 (Mo)	1.61	1.57	0.012	0.642	0.024	0.0102
8 (Ce)	0.0037	0.0237	0.026	0.00215	0.00056	0.00034
9 (La)	0.217	2.94	0.28	0.1024	0.1562	0.00689
10 (U)	1.62	1.99	2.16	0.212	0.0447	0.0233
11 (Cd)	0.0385	0.0555	0.039	0.0189	0.0023	0.0018
12 (Sn)	22.5	55.6	37.7	15.5	1.163	0.6603

locks have been opened, the drywell head has been removed and the drywell equipment hatch and personnel locks have been opened.

A circulation flow was found in the reference calculation (Figure 5.2.5), consisting of a substantial outflow from containment into the auxiliary building through the equipment hatch and a corresponding inflow into containment from the auxiliary building through the lower personnel lock. Some of that strong recirculation flow may be physical, while some may be only numerical; the fraction of each contributing is hard to judge. To investigate the impact of this recirculation flow, calculations were done in which the upper and lower personnel locks were assumed closed and only the containment equipment hatch was available as a flow path.

The timings of various key events for calculations with the closed auxiliary building model with the containment personnel locks either both open (i.e., the reference calculation) or both closed are compared in Table 5.3.2.1. There is very little difference in most of the predicted results. The earliest events, such as core uncovery and first clad failure and gap inventory release, occur at almost the same times. The auxiliary building does reach its 5 psi overpressure failure about 2 hr earlier with no recirculation flow, so all primary system, containment and auxiliary building pressures drop suddenly to ambient earlier. However, there is little change in the first vessel lower head penetration failure times, despite the different auxiliary building failure times.

Although the auxiliary building does reach its 5 psi overpressure failure about 2 hr earlier with no recirculation flow, the auxiliary building pressures in Figure 5.3.2.1 (in the second floor control volume) indicate that a very minor difference in the pressure spikes seen in both calculations after ~19 hr would cause either calculation to fail the auxiliary building on either the 19.5 hr or the 21.5 hr pressure peaks (or at some other time).

The calculations with the closed personnel locks were not run further because of code problems; the results to vessel failure were considered sufficient to evaluate the potential impact of a significant numerical component in the circulation flow predicted.

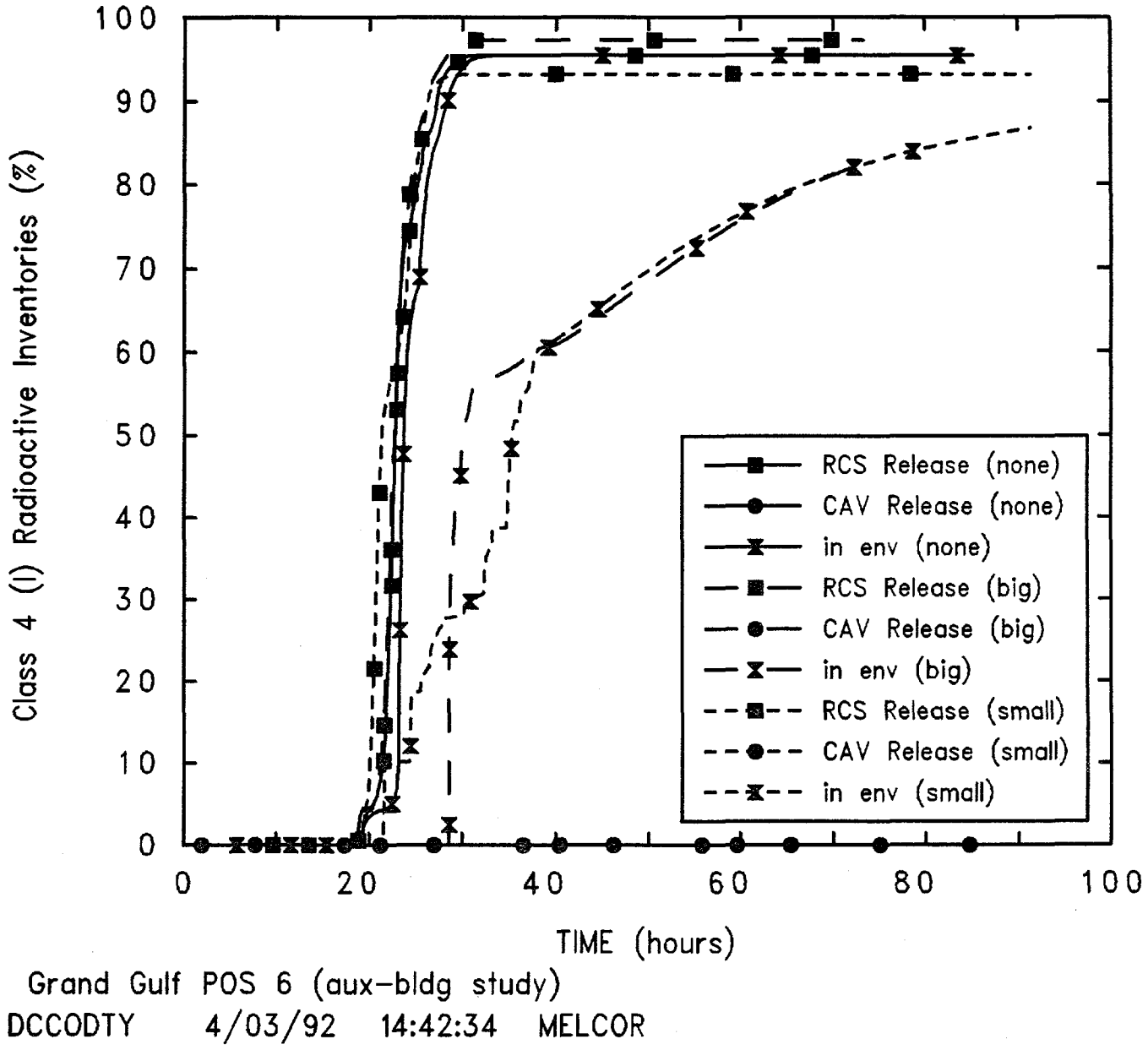

Figure 5.3.1.5. Class 4 Radioactive Mass Radionuclide Distribution for Grand Gulf POS 6 -- Auxiliary Building Model Sensitivity Study.

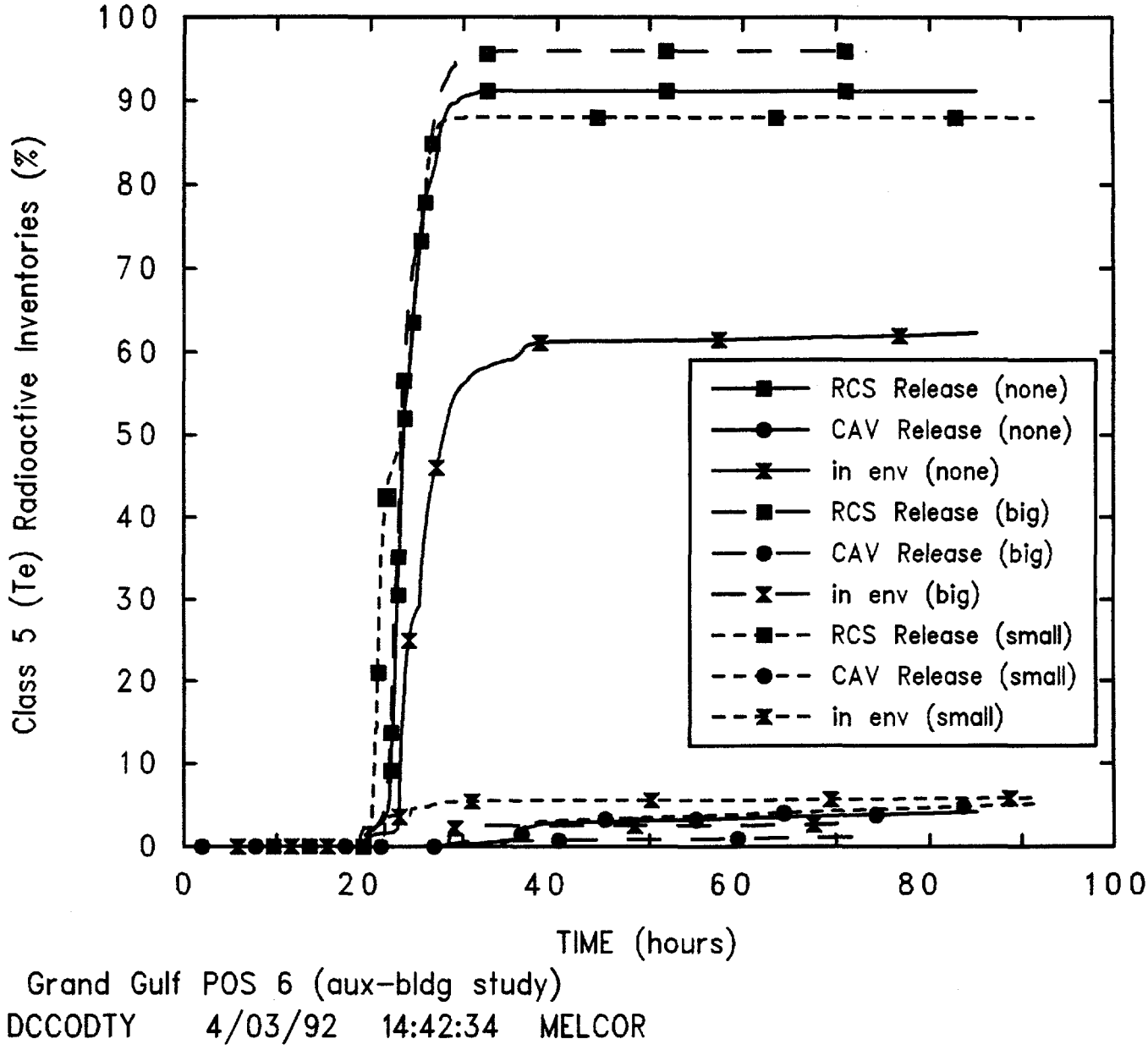

Figure 5.3.1.6. Class 5 Radioactive Mass Radionuclide Distribution for Grand Gulf POS 6 -- Auxiliary Building Model Sensitivity Study.

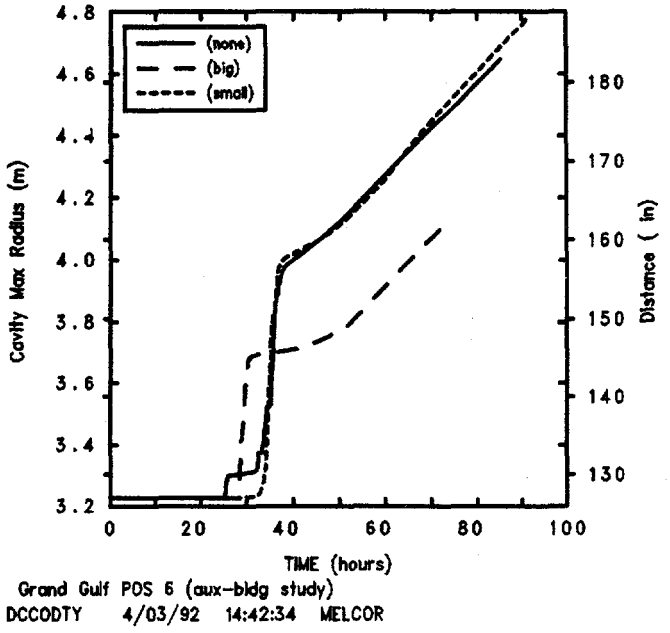

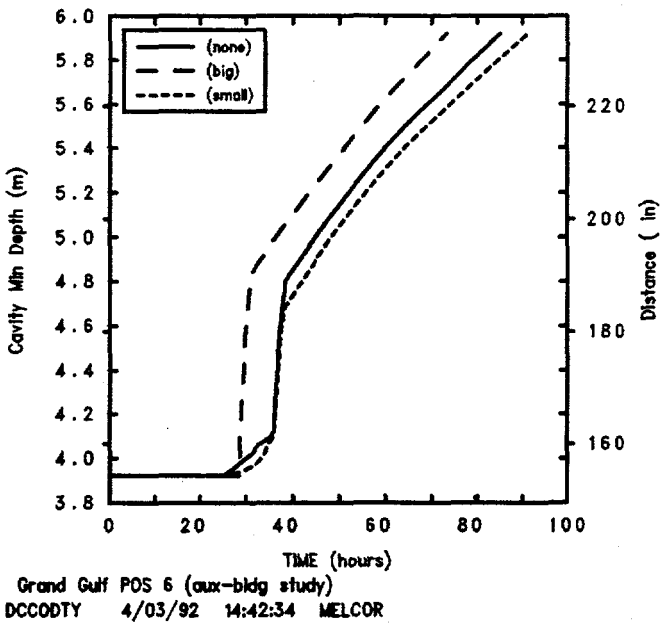

Figure 5.3.1.7. Cavity Maximum Radius and Minimum Depth for Grand Gulf POS 6 -- Auxiliary Building Model Sensitivity Study.

Table 5.3.2.1. Key Event Times for Grand Gulf POS 6 -- Personnel Locks Sensitivity Study

Event	Closed (hr)	Open (hr)
Level below TAF	13.10	13.04
Clad failure/Gap release		
(Ring 1)	18.81	18.80
(Ring 2)	18.77	18.76
(Ring 3)	18.82	18.81
(Ring 4)	19.04	19.04
(Ring 5)	22.00	19.93
(Ring 6)	23.05	23.22
Aux building failure	19.55	21.50
Vessel LH penetration failure	23.89	24.52

5.3.3 Closed Containment

The sensitivity study just discussed studied the effects of open *vs* closed containment personnel locks, with the containment equipment hatch open in both cases. Another calculation was done in which the containment equipment hatch was assumed closed, in addition to closed personnel locks, so that the containment remains isolated until the assumed 71 psi containment failure pressure is reached. (This calculation was done with no auxiliary building model). The timings of various key events predicted assuming either an open or an isolated containment are presented in Table 5.3.3.1. With the containment isolated, most events take place progressively later, with the exception of cavity rupture terminating the analysis earlier.

Some primary system component and the outer containment dome pressures calculated assuming either an open or an isolated containment are given in Figures 5.3.3.1 and 5.3.3.2, respectively. With the containment open, the containment pressure remains atmospheric and the primary pressure quickly equilibrates to atmospheric as the vessel water inventory is boiled away by the core decay heat. With an isolated containment, the steam generated in the core pressurizes the containment, with the primary system and containment equilibrating at about 175 kPa when the vessel water has fully uncovered the core; afterwards, the reactor vessel, drywell and outer containment pressures are virtually identical. There is a wide pressure spike beginning when the vessel first fails and rising rapidly until all the condensate water drained into the cavity has been evaporated by the hot debris falling from the vessel; the pressure then drops as most of the steam condenses onto walls and pool surfaces, followed by a gradual pressurization later in the transient as the hot cavity atmosphere diffuses through and heats the rest of the containment. The containment failure pressure has not been reached by the time cavity rupture is predicted to occur.

The total amount of hydrogen produced by the time the cavity is breached is quite similar regardless of whether the containment is open or isolated, as demonstrated in Figure 5.3.3.3. With the containment open, 1001 kg of hydrogen is calculated to be produced in the vessel before the core debris falls into the cavity and 1280 kg of hydrogen is generated in the cavity before the cavity is ruptured, for a total of 2281 kg; in the sensitivity study analysis with the containment isolated, more hydrogen is produced through oxidation in the vessel before all the core debris falls into the cavity (1207 kg) but less hydrogen (1098 kg) is generated attacking concrete in the cavity by the time the cavity is ruptured, for a total of 2305 kg, or a 1% difference.

Figure 5.3.3.4 illustrates the clad temperature histories in a core level below the top of the active fuel region in the six core rings, predicted assuming either an open or a closed containment. The heatup rate appears slightly

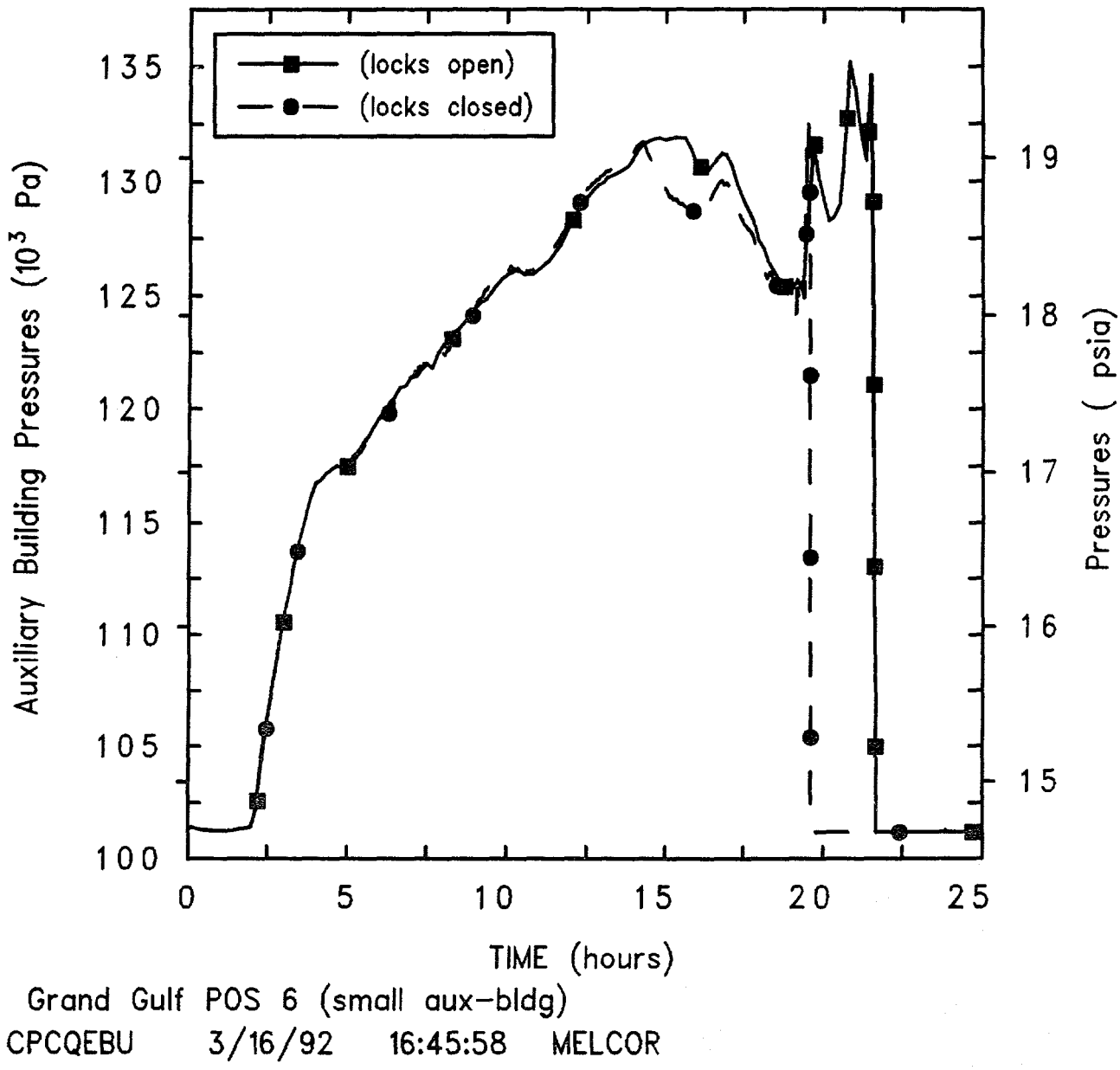

Figure 5.3.2.1. Auxiliary Building Pressures for Grand Gulf POS 6 -- Personnel Locks Sensitivity Study.

Table 5.3.3.1. Key Event Times for Grand Gulf POS 6 -- Containment Isolation Sensitivity Study

Event	Containment Open (hr)	Containment Isolated (hr)
Level below TAF	12.68	13.57
Clad failure/Gap release		
(Ring 1)	18.37	19.40
(Ring 2)	18.34	19.37
(Ring 3)	18.38	19.42
(Ring 4)	18.61	19.68
(Ring 5)	20.46	20.45
(Ring 6)	21.80	21.36
Vessel LH penetration failure		
(Ring 1)	25.45	28.95
(Ring 2)	25.39	28.96
(Ring 3)	26.10	28.56
(Ring 4)	34.49	28.88
(Ring 5)	30.24	29.75
(Ring 6)	32.63	62.22
Cavity Rupture	85.61	78.83

slower in the isolated-containment case than in the open-containment analysis, probably due to the higher system pressures calculated in the closed-containment scenario and resulting in the later lower head penetration failure times.

Table 5.3.3.2 compares the total radioactive masses of radionuclides released in this pair of MELCOR calculations, by the time when a lower head penetration first fails and at the end of the calculation (i.e., when the cavity is predicted to rupture), normalized to the initial masses of each class. The later vessel breach time calculated with the containment isolated (28.5 *vs* 25.4 hr) results in significantly higher release fractions of all of the radionuclide classes (with nonzero releases) by the time of vessel breach. The most volatile classes (Xe, Cs, I and Te) all yield almost 100% release by the end of the transient in both analyses. For all of the less volatile classes, a larger fraction of the initial inventories is released by the time of cavity rupture. For several of the more refractory elements (e.g., Ru and Ce) the amounts released by the end of the transient differ simply by the different amounts released prior to vessel breach; for the others (those with less than 1% release), the increase is not as great because the response is more nonlinear. Of the species with no in-vessel release, a difference is seen only in the trivalents (La), but not for the early transition elements such as Mo and the more volatile main group elements such as Cd. (Because the calculation with the containment isolated did not reach the containment failure pressure prior to transient termination on cavity rupture, there is no release to the environment in this sensitivity study.)

Both calculations ended on cavity rupture, at slightly different times, ~6-7 hr different. Figure 5.3.3.5 shows that both calculations predict that the cavity concrete will first be ruptured in depth.

5.3.4. Initiation Time

Timing information for the initiation of the accident in POS 6 is based on Grand Gulf refueling outage (RFO) data. Based on this data, the fastest the plant will enter POS 6 from full power is approximately four days after shutdown and the longest the plant has been in POS 6 (in the going-down phase) is approximately 12 days (i.e.,

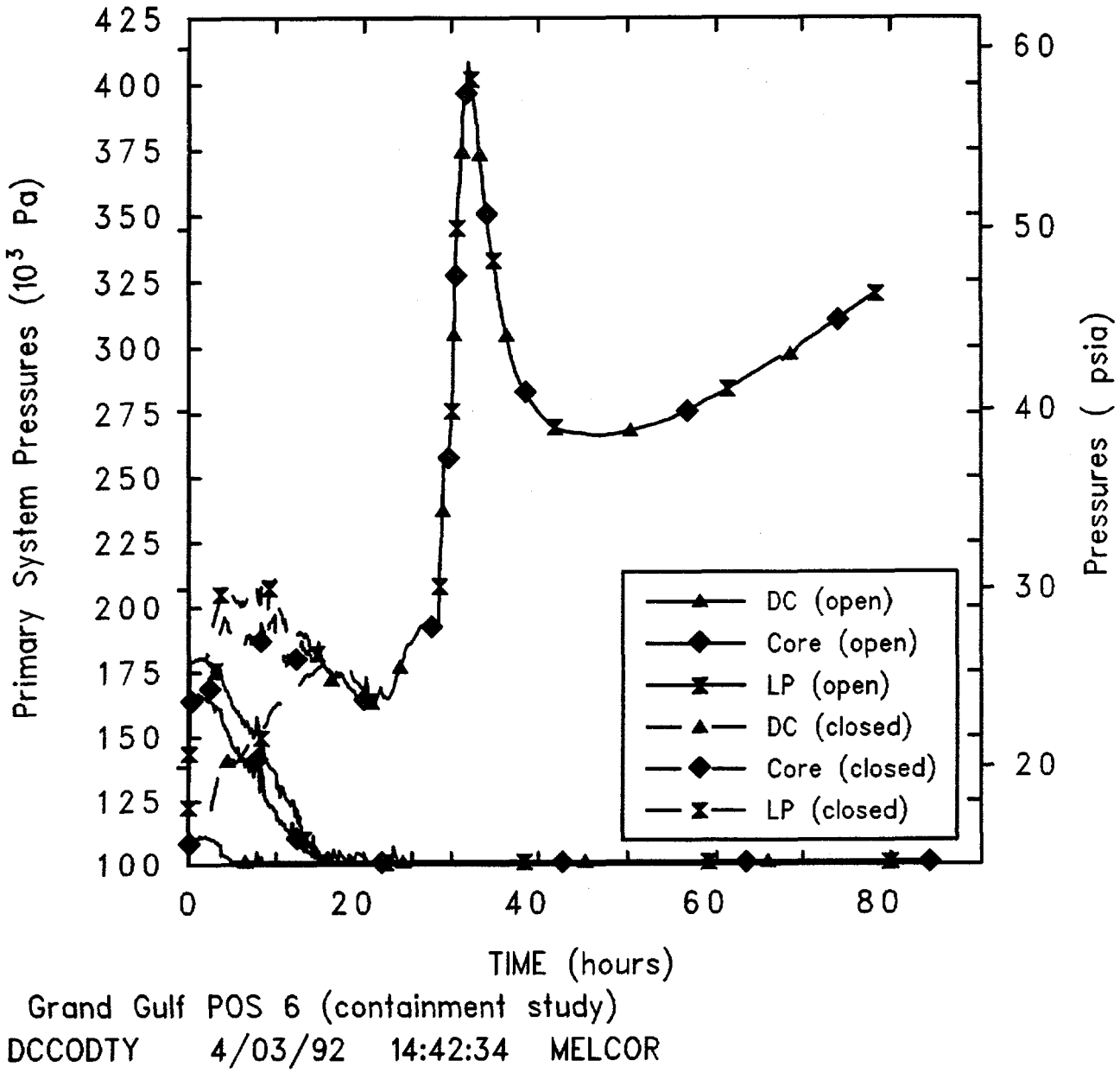

Figure 5.3.3.1. Primary System Pressures for Grand Gulf POS 6 -- Containment Isolation Sensitivity Study.

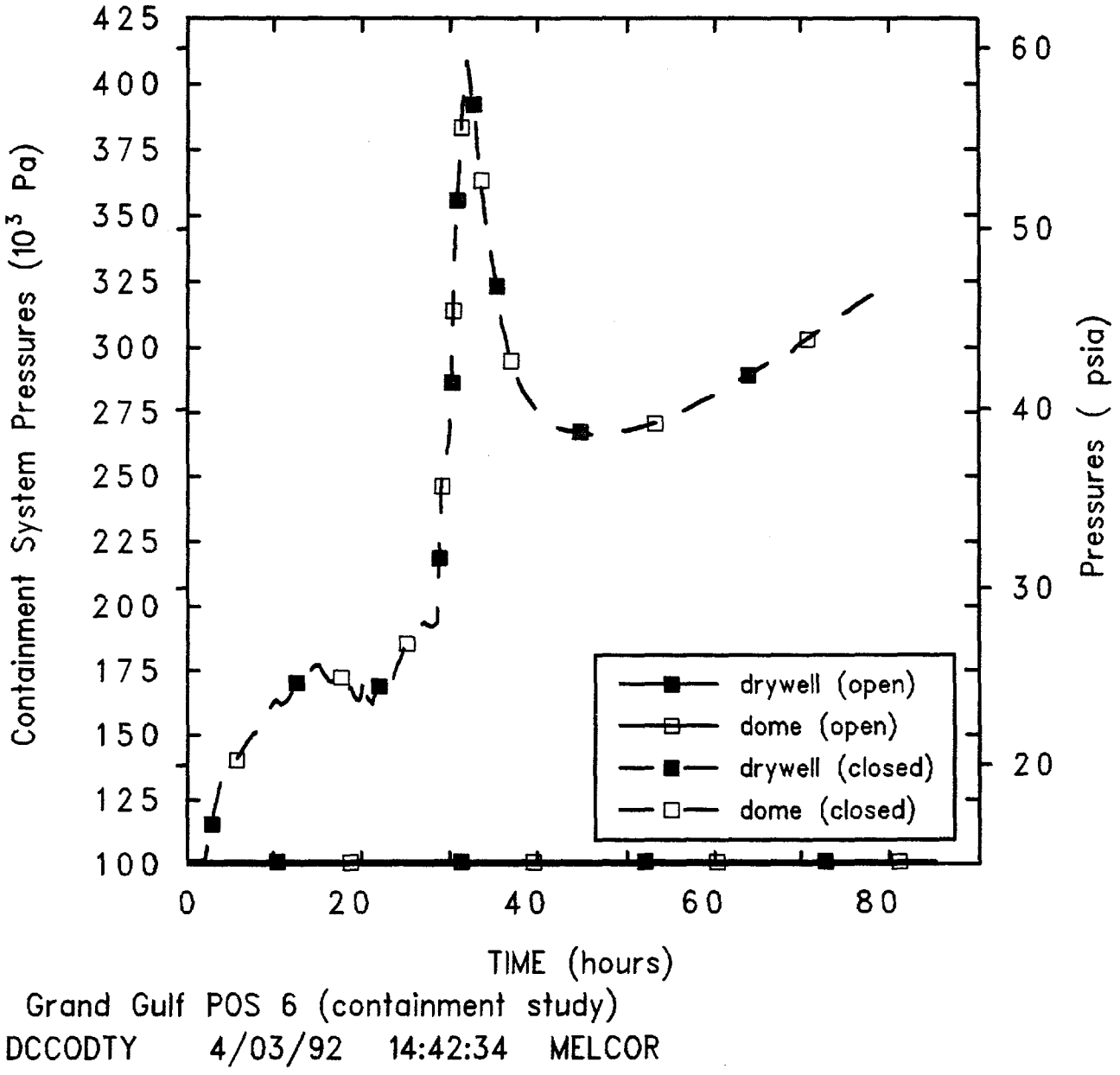

Figure 5.3.3.2. Containment Dome Pressures for Grand Gulf POS 6 -- Containment Isolation Sensitivity Study.

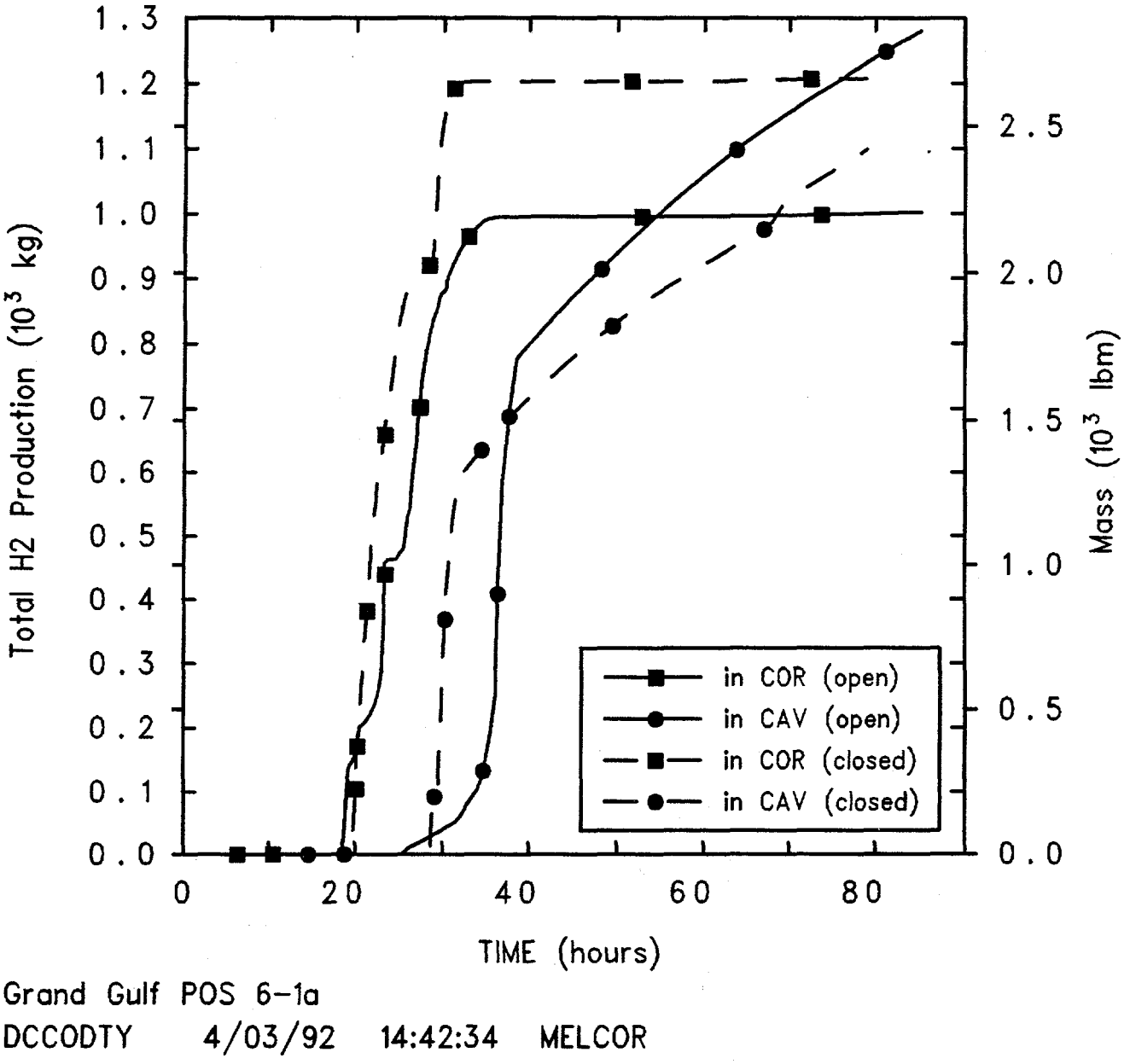

Figure 5.3.3.3. Hydrogen Generation for Grand Gulf POS 6 -- Containment Isolation Sensitivity Study.

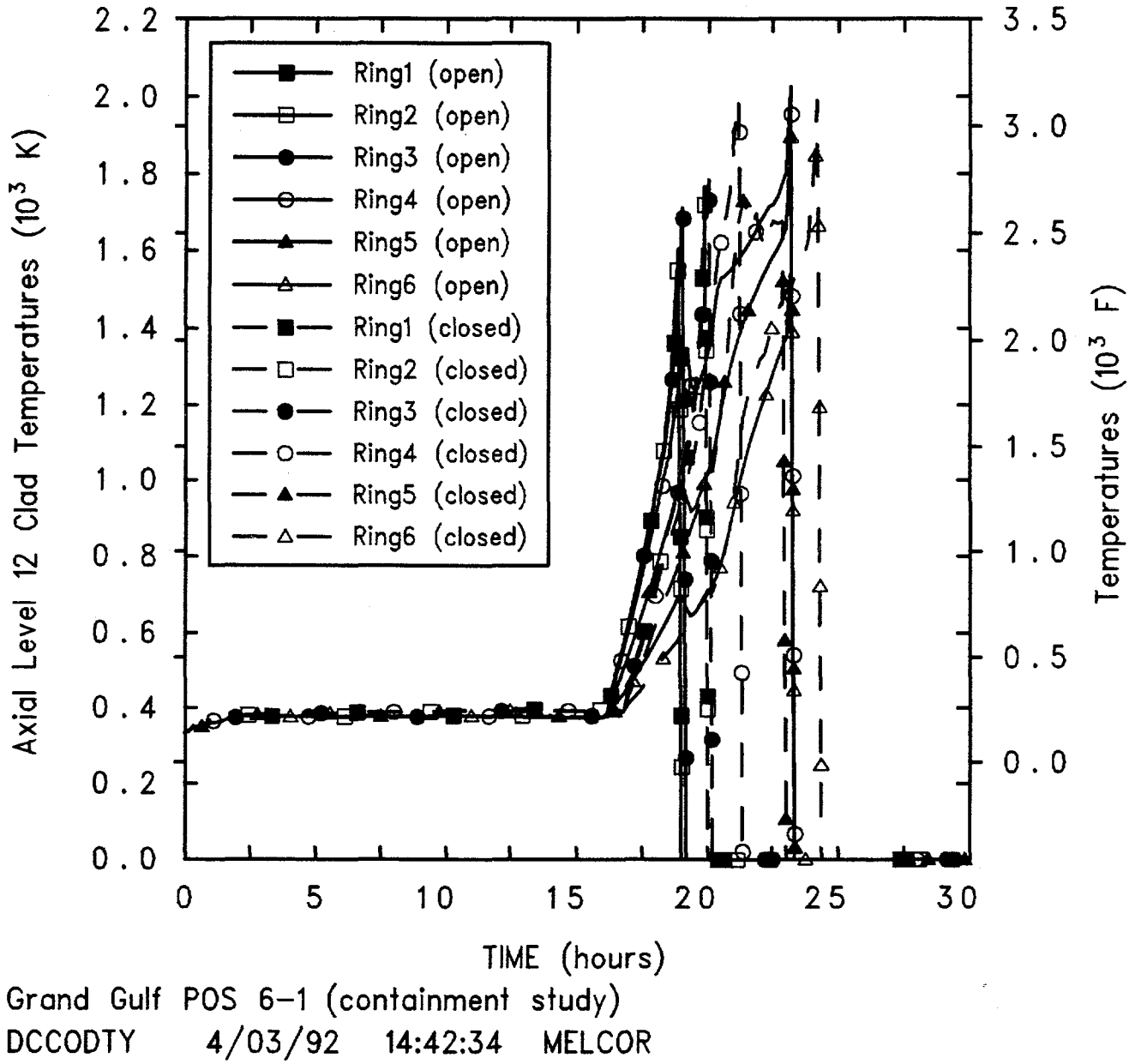

Figure 5.3.3.4. Level 12 Clad Temperatures for Grand Gulf POS 6 -- Containment Isolation Sensitivity Study.

Table 5.3.3.2. Total Fission Product Radioactive Masses Released from Fuel for Grand Gulf POS 6 -- Containment Isolation Sensitivity Study

Class	% of Initial Inventory Released (Mass Fraction) Before Vessel Breach		Before Cavity Rupture	
	Open	Isolated	Open	Isolated
1 (Xe)	81.3	95.6	100	100
2 (Cs)	81.7	95.7	100	100
3 (Ba)	2.38	42.6	42	59.5
4 (I)	81	95.5	95.5	97.1
5 (Te)	72.5	93.5	95.2	97
6 (Ru)	0.00002	0.0757	0.007	0.0847
7 (Mo)	0	0	1.61	1.61
8 (Ce)	3.0e-06	0.0376	0.0037	0.0436
9 (La)	0	0	0.217	1.201
10 (U)	0.00156	3.26	1.62	3.62
11 (Cd)	0	0	0.0385	0.0361
12 (Sn)	2.866	61.9	22.5	64.7

16 days from shutdown). In the Level 1 analysis the time window from the initiating event to core damage was based on the decay heat at four days; this assumption is carried through the Level 2/3 analyses. Our MELCOR analyses were therefore initiated at 4 days after shutdown, with the exception of a single sensitivity study which assumed the accident sequence to begin 15 days after shutdown. This initiation-time sensitivity study was run with the containment personnel locks and equipment hatch open and venting directly to the environment (i.e., with no auxiliary building modelled).

The decay heat assuming the accident to begin 15 days after shutdown is about 70% of the decay heat level driving an accident beginning 4 days after shutdown, as shown in Figure 5.3.4.1. The main effect of the later accident initiation assumed is to delay the timing of all events, as illustrated by comparing the decay power in the primary system (also in Figure 5.3.4.1). The delay in timing is also clearly seen in the vessel water masses in Figure 5.3.4.2, and in the clad temperature histories just below the active fuel midplane presented in Figure 5.3.4.3, and is quantified by comparing the timings of various key events as done in Table 5.3.4.1.

Figure 5.3.4.4 shows that the total amount of hydrogen produced by the time the cavity is breached is quite similar regardless of whether the accident was initiated 4 or 15 days after shutdown. In the calculation begun 4 days after shutdown, 1001 kg of hydrogen is produced in the vessel before the core debris falls into the cavity and 1280 kg of hydrogen is generated in the cavity before the cavity is ruptured, for a total of 2281 kg; in the sensitivity study analysis initiated 15 days after shutdown, more hydrogen is produced through oxidation in the vessel before the core debris falls into the cavity (1318 kg) but less hydrogen (1035 kg) is generated attacking concrete in the cavity before the cavity is ruptured, for a total of 2353 kg, or a 3% difference.

Table 5.3.4.2 compares the total radioactive masses of radionuclides released in this pair of MELCOR calculations, by the time when a lower head penetration first fails and at the end of the calculation (i.e., when the cavity is predicted to rupture), normalized to the initial masses of each class. Before vessel breach, the longer time period that core temperatures are elevated for an accident started 15 days after shutdown cause significantly higher releases; at the time of cavity rupture, the final

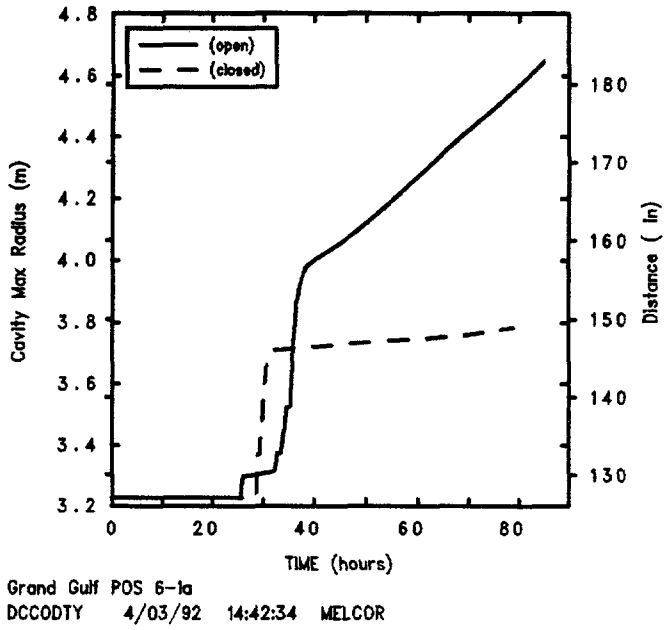

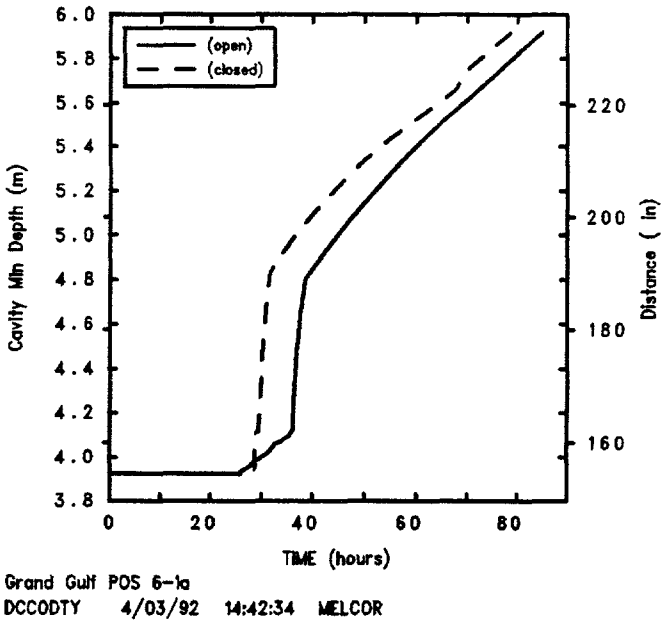

Figure 5.3.3.5. Cavity Maximum Radius and Minimum Depth for Grand Gulf POS 6 -- Containment Isolation Sensitivity Study.

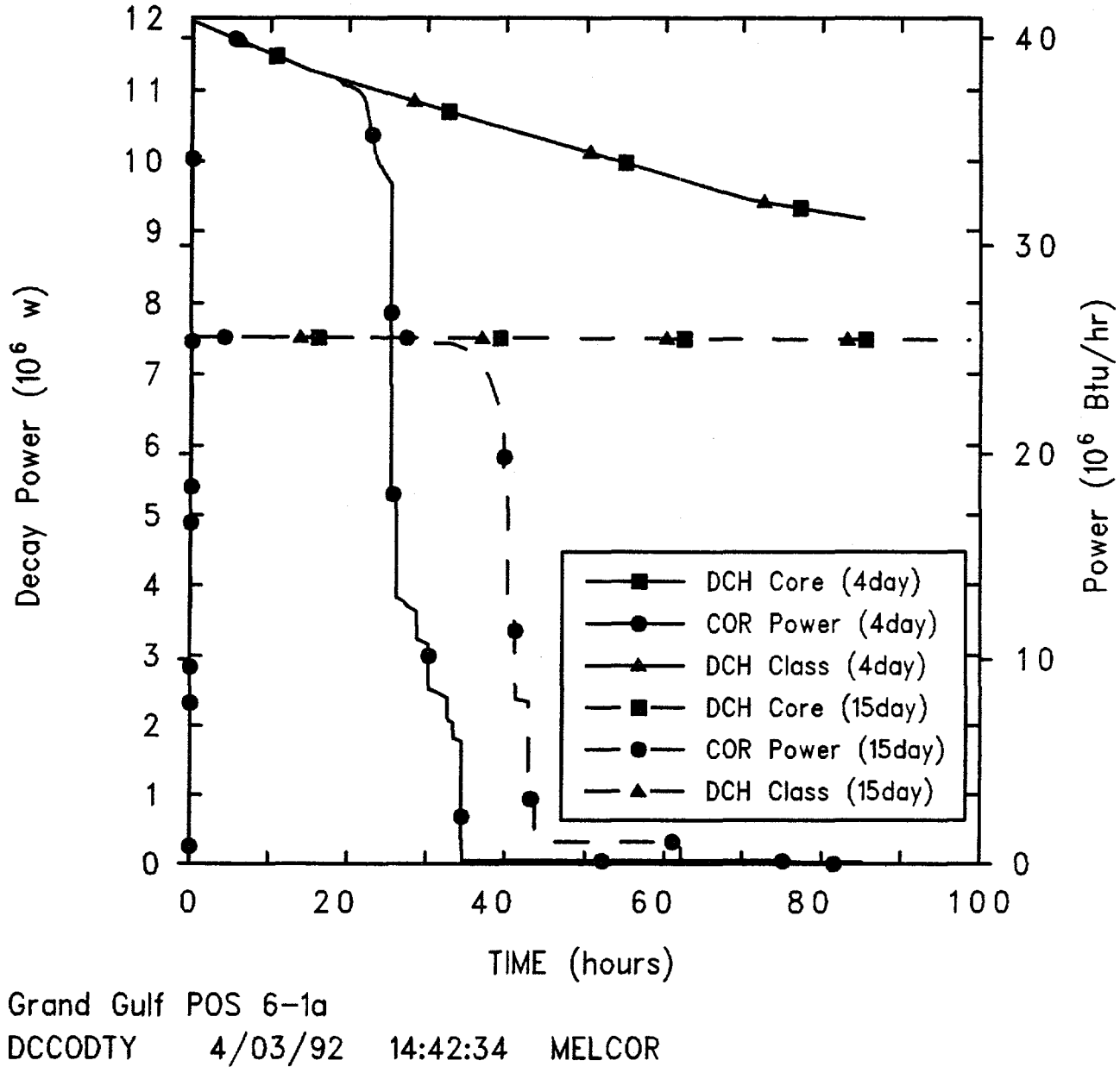

Figure 5.3.4.1. Decay Heat (Total and In-Vessel) for Grand Gulf POS 6 -- Accident Initiation Time Sensitivity Study.

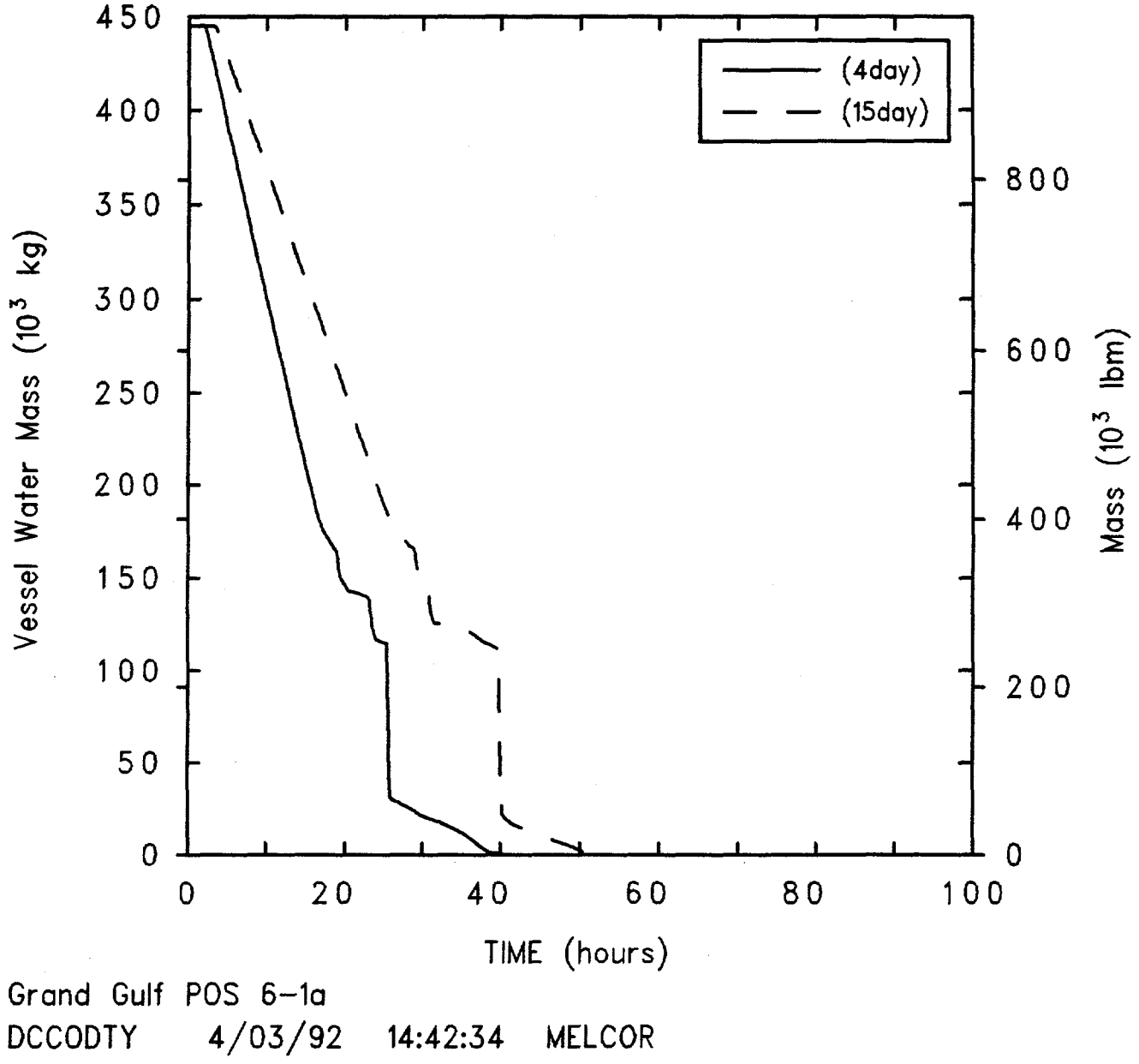

Figure 5.3.4.2. Vessel Water Masses for Grand Gulf POS 6 -- Accident Initiation Time Sensitivity Study.

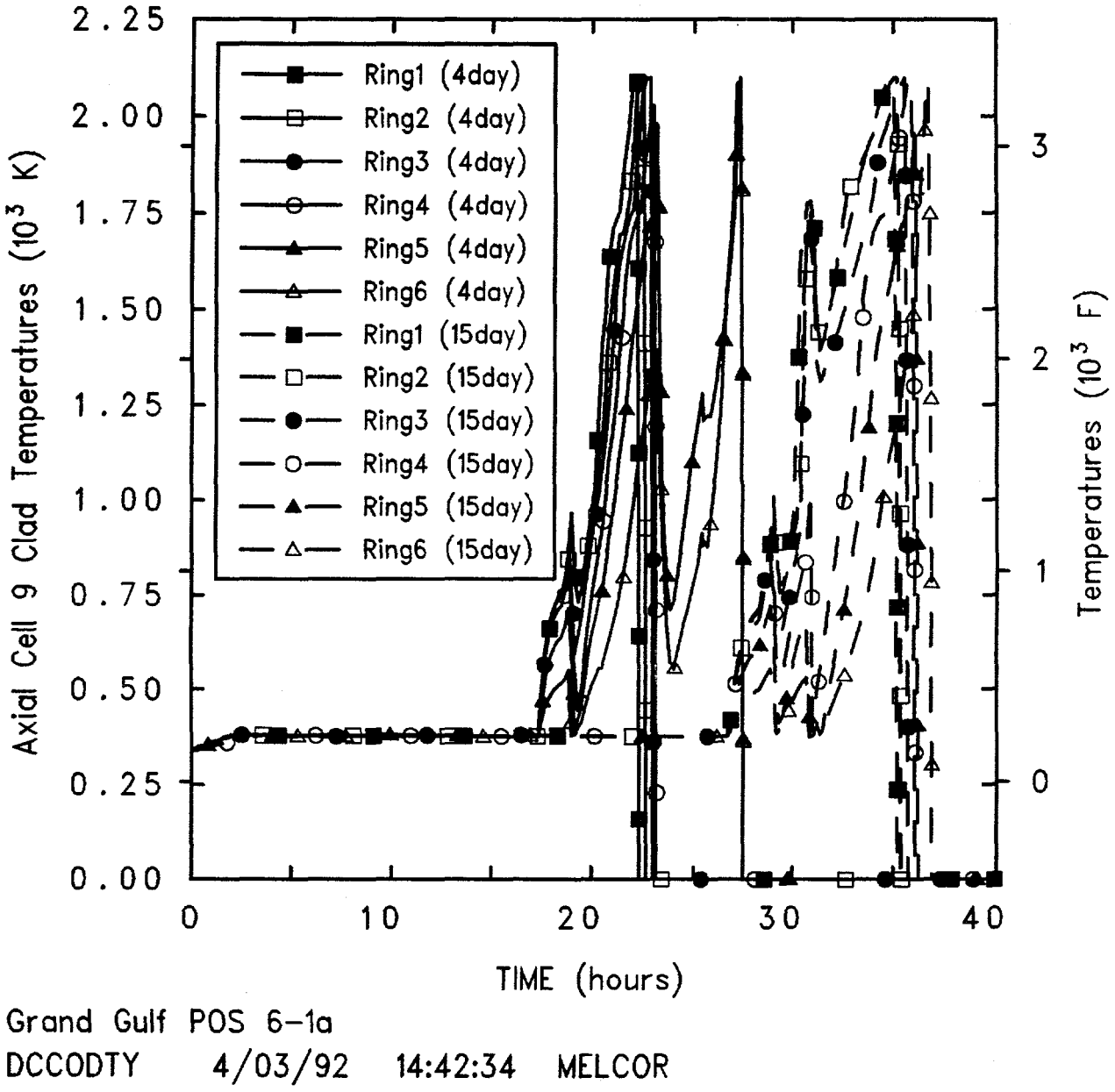

Figure 5.3.4.3. Level 9 Clad Temperatures for Grand Gulf POS 6 -- Accident Initiation Time Sensitivity Study.

Table 5.3.4.1. Key Event Times for Grand Gulf POS 6 -- Accident Initiation Time Sensitivity Study

Event	Time after shutdown 4 days	15 days
Level below TAF	12.68 hr	19.71 hr
Clad failure/Gap release		
(Ring 1)	18.37 hr	28.35 hr
(Ring 2)	18.34 hr	28.31 hr
(Ring 3)	18.38 hr	28.37 hr
(Ring 4)	18.61 hr	28.62 hr
(Ring 5)	20.46 hr	30.28 hr
(Ring 6)	21.80 hr	34.57 hr
Vessel LH penetration failure		
(Ring 1)	25.45 hr	39.79 hr
(Ring 2)	25.39 hr	40.29 hr
(Ring 3)	26.10 hr	41.22 hr
(Ring 4)	34.49 hr	42.95 hr
(Ring 5)	30.24 hr	43.74 hr
(Ring 6)	32.63 hr	45.68 hr
Cavity rupture	85.61 hr	98.65 hr

releases to environment are some lower and some higher for accidents started 4 days *vs* 15 days after shutdown, but are generally similar for these two accident scenario calculations.

5.3.5 Igniters

In most of our POS 6 calculations, the hydrogen igniters were assumed to be inactive. A calculation was done, assuming an isolated containment (and no auxiliary building model), in which the igniters were used. The isolated-containment case was chosen to evaluate the effect of the igniters on the calculated pressure rise.

Figure 5.3.5.1 compares the pressures in the outer containment dome, with and without the igniters active. Instead of a large and broad pressure peak around the time of vessel breach, a series of sharp pressure spikes indicating hydrogen burns are calculated prior to vessel breach. The magnitude of the burn-generated pressure spikes is not much less than the peak pressure predicted in the absence of igniters. After vessel breach there is no indication of hydrogen burns even with active igniters (because the containment is then steam-inert), and the pressure rises more rapidly, nearing the containment failure pressure at the end of the transient.

The gas temperatures in the containment are presented in Figure 5.3.5.2, in the drywell, cavity and in the outer containment dome, for the calculations with and without active igniters. Temperature spikes indicating hydrogen burns are seen during the 20 to 30 hr period with active igniters. After vessel breach, the calculation with no igniters has a very hot cavity, a cold outer containment dome and an intermediate temperature in the drywell, for a very pronounced temperature gradient; the calculation with hydrogen burns earlier shows very little temperature gradient among the containment control volumes, with all temperatures remaining relatively low.

Table 5.3.5.1 compares the timings of various key events predicted in these closed-containment calculations with and without active igniters. Before the first hydrogen burn (just before 19 hr), the timing of events is identical. Afterwards, there are a few minor differences in first gap release in a few of the rings, and the failure of the lower head penetrations in most of the rings varies by only about 30 min. And, even with the large differences in

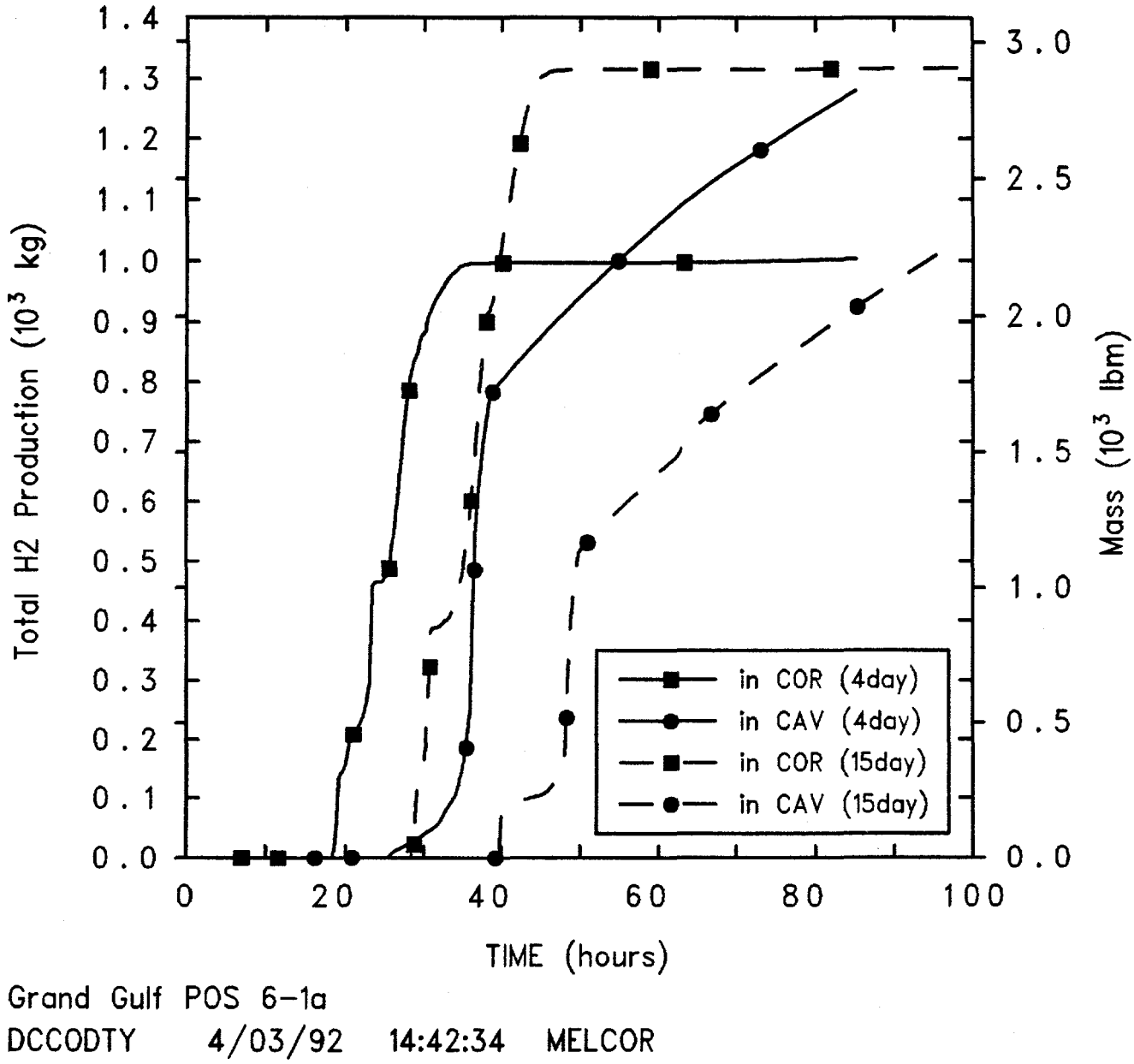

Figure 5.3.4.4. Hydrogen Generation for Grand Gulf POS 6 -- Accident Initiation Time Sensitivity Study.

Table 5.3.4.2. Total Fission Product Radioactive Masses Released from Fuel for Grand Gulf POS 6 -- Accident Initiation Time Sensitivity Study

Class	% of Initial Inventory Released (Mass Fraction) Before Vessel Breach		Before Cavity Rupture	
	4 days	15 days	4 days	15 days
1 (Xe)	76.9	93.8	100	100
2 (Cs)	76.9	93.9	100	100
3 (Ba)	4.22	21.6	47.4	41.6
4 (I)	76.1	93.7	93.2	95.2
5 (Te)	62.8	91.6	93	95.9
6 (Ru)	0.0023	0.0326	0.0508	0.0403
7 (Mo)	0	0	0.0128	1.5
8 (Ce)	0.00076	0.0154	0.0264	0.0198
9 (La)	0	0	0.2809	0.7518
10 (U)	0.1145	1.43	2.16	1.77
11 (Cd)	0	0	0.0396	0.0334
12 (Sn)	13.53	36.15	37.7	44.4

later-time containment pressure and temperature histories, the end times for these two calculations, when the cavity is predicted to rupture, differ only by about 1 hour.

Table 5.3.5.2 compares the total radioactive masses of radionuclides released in this pair of MELCOR calculations, by the time when a lower head penetration first fails and at the end of the calculation (i.e., when the cavity is predicted to rupture), normalized to the initial masses of each class. In this study, despite the later vessel breach time calculated with active igniters (29 *vs* 28.5 hr), slightly lower release fractions of all of the radionuclide classes (with nonzero releases) are predicted by the time of vessel breach. The most volatile classes (Xe, Cs, I and Te) all have almost 100% release by the end of the transient in both analyses. For all of the less volatile classes, except Mo, a smaller fraction of the initial inventories also is released by the time of cavity rupture in the calculation with igniters active, as much as 50% less than in the no-igniter analysis. (Because these calculations did not reach the containment failure pressure prior to transient termination on cavity rupture, there is no release to the environment in this sensitivity study.)

5.4 Code Option Studies

In addition to the plant-configuration sensitivity studies discussed in the previous section, a few sensitivity studies were done on various code options and/or parameters. In one calculation, the CORSOR fission product release model was used instead of the (MELCOR default) CORSOR-M fission product release model. In another sensitivity study, because it was sometimes necessary to back up and reduce the user-specified maximum time step in order to complete the analysis, a calculation was done in which that was the only change made, to determine how big an effect reducing the time step would have on the results. Two calculations were done to address concerns [Powers et al., 1994] raised about the lack of air oxidation modelling in MELCOR at that time, and the associated lack of the extensive release of ruthenium

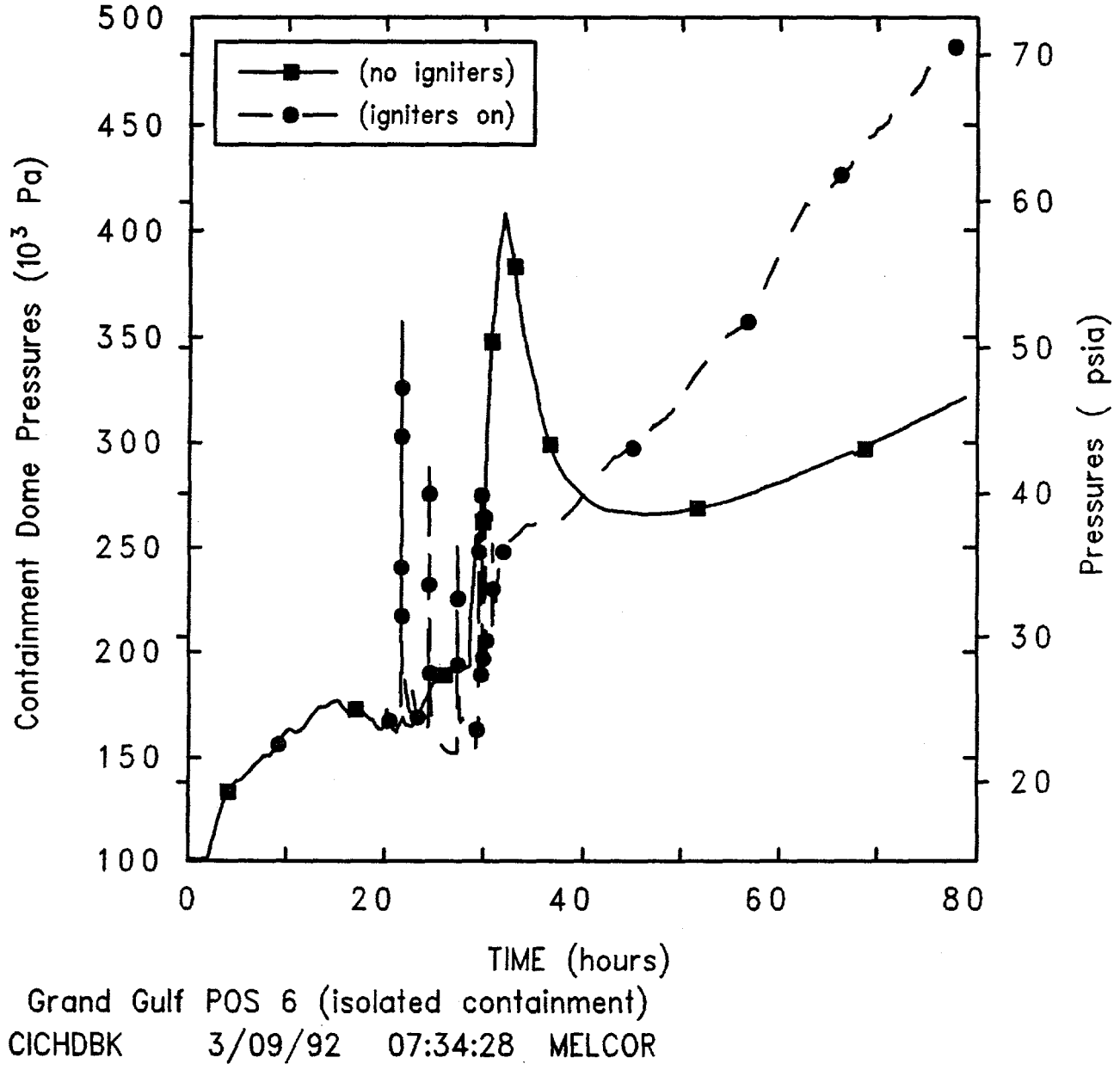

Figure 5.3.5.1. Containment Dome Pressures for Grand Gulf POS 6 -- Igniter Sensitivity Study.

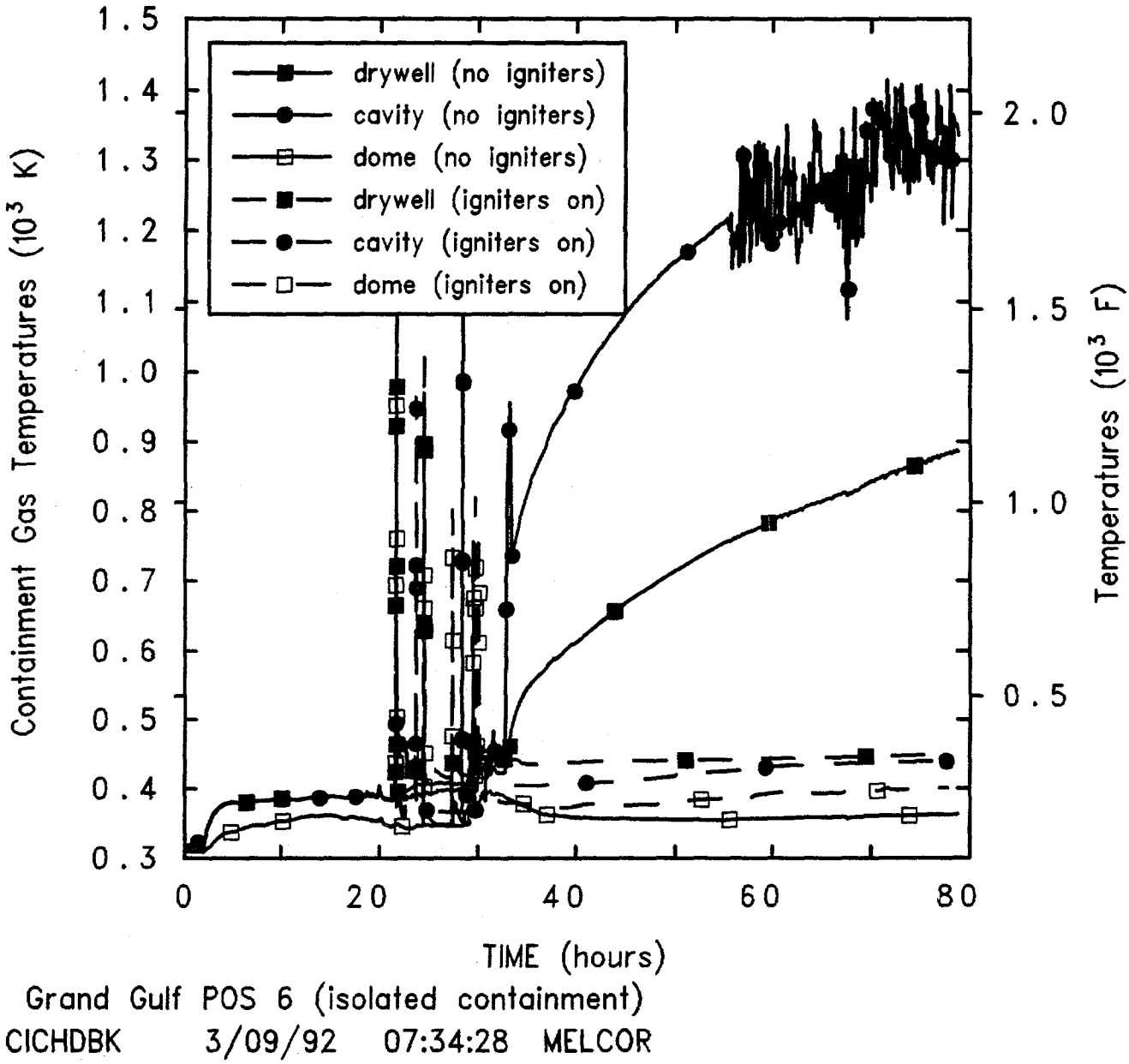

Figure 5.3.5.2. Drywell and Cavity Temperatures for Grand Gulf POS 6 -- Igniter Sensitivity Study.

Table 5.3.5.1. Key Event Times for Grand Gulf POS 6 -- Igniter Sensitivity Study

Event	Igniters Inactive (hr)	Igniters Active (hr)
Level below TAF	13.57	13.57
Clad failure/Gap release		
(Ring 1)	19.40	19.40
(Ring 2)	19.37	19.36
(Ring 3)	19.42	19.42
(Ring 4)	19.68	19.65
(Ring 5)	20.45	20.45
(Ring 6)	21.36	21.36
Vessel LH penetration failure		
(Ring 1)	28.95 hr	29.54 hr
(Ring 2)	28.96 hr	29.49 hr
(Ring 3)	28.56 hr	29.09 hr
(Ring 4)	28.88 hr	29.13 hr
(Ring 5)	29.75 hr	30.37 hr
(Ring 6)	62.22 hr	--
Cavity rupture	78.83 hr	77.77 hr

demonstrated to occur when irradiated reactor fuel is heated in air.

5.4.1 Source Term

The POS 6 analysis has been run with a different release model option enabled in MELCOR, as a sensitivity study on fission product source term. The options available include the CORSOR and CORSOR-M models. (The new CORSOR-Booth model was not available in the code version used for these POS 6 analyses.) This source-term sensitivity study was run with the containment personnel locks and equipment hatch open and venting directly to the environment (i.e., with no auxiliary building modelled).

The CORSOR model is a simple correlational relationship based on data from early experiments [Nuclear Regulatory Commission, 1981b]. Release of volatiles is assumed to be limited by diffusion, and all volatiles share the same release parameters, obtained by averaging experimental results; release of nonvolatiles is assumed to be limited by vaporization, and vapor pressures are scaled for consistency with experimental observations. The fractional release coefficients in CORSOR are simple exponentials, with constants selected for each species in specific temperature ranges based upon fitting experimental data. The fractional release coefficients used in CORSOR-M (the MELCOR default) utilize an Arrhenius-type equation with constants representing empirical fits to experimental data.

Table 5.4.1.1 compares the radioactive masses of radionuclides calculated to be released using the CORSOR and CORSOR-M model options, when a lower head penetration first fails and at the end of the calculation (i.e., when the cavity is predicted to rupture), and the amounts that have been released to the environment, all normalized to the initial masses of each class (given in Table 3.1).

In both calculations, most of the noble gases (Xe), alkali metals (Cs) and halogens (I) have been released by the time of first lower head penetration failure, and most or all of these three classes have been released by the end of the transient, with half or more released to the environment. The CORSOR correlations predict more release of the alkaline earths (Ba), the platinoids (Ru), the tetravalents (Ce) and the less volatile main group elements

Table 5.3.5.2. Total Fission ProductRadioactive Masses Released from Fuel for Grand Gulf POS 6 -- Igniter Sensitivity Study

Class	% of Initial Inventory Released (Mass Fraction)			
	Before Vessel Breach		Before Cavity Rupture	
	Inactive	Active	Inactive	Active
1 (Xe)	95.6	94.3	100	99.5
2 (Cs)	95.7	94.4	100	99.8
3 (Ba)	42.6	37.5	59.5	58.2
4 (I)	95.5	94.2	97.1	95.6
5 (Te)	93.5	92	97	96.5
6 (Ru)	0.0757	0.0597	0.0847	0.0667
7 (Mo)	0	0	1.61	2.11
8 (Ce)	0.0376	0.0295	0.0436	0.034
9 (La)	0	0	1.2	0.95
10 (U)	3.26	2.58	3.62	2.87
11 (Cd)	0	0	0.0361	0.0624
12 (Sn)	61.9	59	64.7	61.8

(Sn); the CORSOR correlations also predict non-zero releases of the early transition elements (Mo), the trivalents (La) and the more volatile main group elements (Cd) prior to vessel breach. The CORSOR-M relations give a higher release for the chalcogens (Te), as well as for the volatiles (i.e., the noble gases, alkali metals and halogens). The total releases up to the time of cavity rupture (the end of the calculations) and the releases to the environment follow the qualitative trends seen comparing the in-vessel releases prior to lower head breach. (These trends are the same as seen in several recent MELCOR assessment calculations [Kmetyk, 1992a, Kmetyk, 1992b]). However, the releases to the environment calculated for the two release options are not simply equal fractions of the amounts released from the fuel and debris; the fission product transport is apparently dependent to some extent on the amounts and relative amounts of the fission products present.

5.4.2 Time Step

Several of the grand Gulf POS 6 MELCOR calculations aborted with various error messages at assorted times during the core degradation process. In all cases, it was possible to back up, reduce the user-specified maximum time step to below that used by the code just prior to developing problems, and complete the analysis. There has been a lot of discussion in the past few years [Boyack et al., 1992] on numeric effects seen in various MELCOR calculations, producing either differences in results for the same input on different machines or differences in results when the time step used is varied. To determine how big an effect reducing the time step would have on the results, a calculation was done in which that was the only change made.

In most of our calculations, the maximum allowed time step was set through user input to be 99 s, so that the code used its internal logic to select a time step. In this sensitivity study, the time step was reduced to 0.5 s from 70,000 s (19.444 hr) to 100,000 s (27.778 hr).

The change in time step affects some of the event timings, as illustrated in Table 5.4.2.1. There is, of course, no difference in the timing of events before the time step reduction. The changes in timing of key events after the time step reduction are generally small.

There are no major differences observable in primary and containment systems pressure histories, or core inventory boiloff. Figure 5.4.2.1 compares clad temperature histories in a core level above the active fuel midplane in the six core rings as representative of the overall core

Table 5.4.1.1. Total Fission Product Radioactive Masses Released from Fuel for Grand Gulf POS 6 -- CORSOR Option Sensitivity Study

Class	% of Initial Inventory Released (Mass Fraction)					
	Before Vessel Breach		Before Cavity Rupture		To Environment	
	CORSOR	CORSOR-M	CORSOR	CORSOR-M	CORSOR	CORSOR-M
1 (Xe)	76.9	81.3	100	100	100	100
2 (Cs)	76.9	81.7	100	100	52.6	67.6
3 (Ba)	17.6	2.38	52.7	42	22	21.3
4 (I)	76.5	81	91.2	95.5	91.2	95.5
5 (Te)	17.1	72.5	60.1	95.2	29.3	62.3
6 (Ru)	0.743	0.00002	1.366	0.007	0.574	0.0045
7 (Mo)	10.03	0	16.7	1.61	6.7	0.642
8 (Ce)	0.0168	0.000003	0.0305	0.0037	0.0128	0.00215
9 (La)	0.077	0	0.6844	0.217	0.325	0.00056
10 (U)	0.077	0.00156	0.176	1.62	0.078	0.1562
11 (Cd)	38.2	0	57	0.0385	22.6	0.0023
12 (Sn)	38.2	2.866	57.7	22.5	23	15.5

response. Small offsets are visible in the temperatures predicted with the reduced time step, resulting in the slightly later lower head penetration failure times.

The total amount of hydrogen produced by the time the cavity is breached is greater in the calculation with the temporarily-reduced time step (2450 kg, ~7.4% high compared to 2281 kg). Figure 5.4.2.2 indicates that the major difference is in significantly more hydrogen generated during in-vessel core degradation (1299 kg *vs* 1001 kg of hydrogen produced in the vessel in the base case); less is generated later in the cavity (~1151 kg compared to 1280 kg in the base case) before the cavity is ruptured.

Table 5.4.2.2 compares the total radioactive masses of radionuclides released in this pair of MELCOR calculations, by the time when a lower head penetration first fails and at the end of the calculation (i.e., when the cavity is predicted to rupture), together with the release to the environment by the end of the transient, normalized to the initial masses of each class. The increased in-vessel hydrogen generation in the calculation with the time-step reduction is associated with increased release of all radionuclide classes prior to vessel breach. (The same trend, increased release fractions with reductions in time step, were found in MELCOR assessment analyses of the ACRR ST-1/ST-2 source term experiments [Kmetyk, 1992a]). These increased releases early in the transient do not significantly change the total amounts of most classes released by the end of the calculations, but larger amounts of the trivalents (La) and both the more and less volatile main group elements (Cd and Sn) are released by the time of cavity rupture; however, less uranium is released by the time of cavity rupture, even though more uranium is released in-vessel during the (relatively brief) reduced time dtep period. The amounts released to the environment also vary somewhat for most of the classes, but not proportionally to the differences in either early-time or end-time releases. These variations are not very significant because the differences in amounts released to the environment are smallest for those classes with the greatest release from the fuel; the differences increase as the fractional amounts released to the environment decrease and only the release to the environment of the trivalents (La) and the more volatile main group elements (Cd) differ by more than an order of magnitude.

The calculation with the time-step reduction at the time of vessel breach predicts cavity rupture about 3 hr earlier; the comparison of cavity maximum radii and minimum altitudes in Figure 5.4.2.3 demonstrates that the axial ablation is very similar in both cases, but that there is

Table 5.4.2.1. Key Event Times for Grand Gulf POS 6 -- Time Step Sensitivity Study

Event	Base Δt (hr)	Reduced Δt (hr)
Level below TAF	12.68	12.68 hr
Clad failure/Gap release		
(Ring 1)	18.37	18.37
(Ring 2)	18.34	18.34
(Ring 3)	18.38	18.38
(Ring 4)	18.61	18.57
(Ring 5)	20.46	20.85
(Ring 6)	21.80	21.69
Vessel LH penetration failure		
(Ring 1)	25.45	26.00
(Ring 2)	25.39	26.01
(Ring 3)	26.10	26.15
(Ring 4)	34.49	31.05
(Ring 5)	30.24	33.13
(Ring 6)	32.63	33.69
Cavity rupture	85.61	82.22

much less radial ablation during the time the time step is cut, resulting in a constant offset in maximum radii throughout the remainder of the transient, even after the time step is increased back to its original value.

5.4.3 Air Oxidation

Two sensitivity-study calculations were done to address concerns [Powers et al., 1994] raised about the lack of air oxidation modelling in MELCOR 1.8.1, and the associated lack of extensive release of ruthenium demonstrated to occur when irradiated reactor fuel is heated in air. In both, the effect of oxidation with free oxygen in addition to the oxygen in steam was included in the code; in one calculation a constant release rate coefficient was used for Class 6 (Ru), while the other used a variable coefficient dependent on the partial pressure of oxygen in the core. These air-oxidation sensitivity studies were run with the containment personnel locks and equipment hatch open and venting directly to the environment (i.e., with no auxiliary building modelled).

The POS 6 calculations done all indicate that the lack of an air-oxidation model in MELCOR, and the associated lack of extensive release of ruthenium, is not an issue because no oxygen is predicted to be drawn into the core until late in the transient, after the core material has fallen into the cavity; this is visible in both the oxygen mole fractions in the core and the oxygen mass flow rates in the core inlet and outlet junctions, shown for the reference calculation in Figures 5.4.3.1 and 5.4.3.2, respectively.

To investigate the impact of air oxidation and enhanced ruthenium release, we had to artificially introduce air directly into the core control volume. A total of 28,608 kg of O_2 (the amount that would be required to oxidize the clad in the core), at a uniform rate starting when the core liquid level drops below the top of the active fuel until a lower head penetration first fails (i.e., from 13.04 hr to 18.76 hr). The free oxygen sourced into the core control volume during the core heatup period in these sensitivity study analyses is visible in both the oxygen mole fractions in the core and the oxygen mass flow rates in the core inlet and outlet junctions, in Figures 5.4.3.3 and 5.4.3.4, respectively.

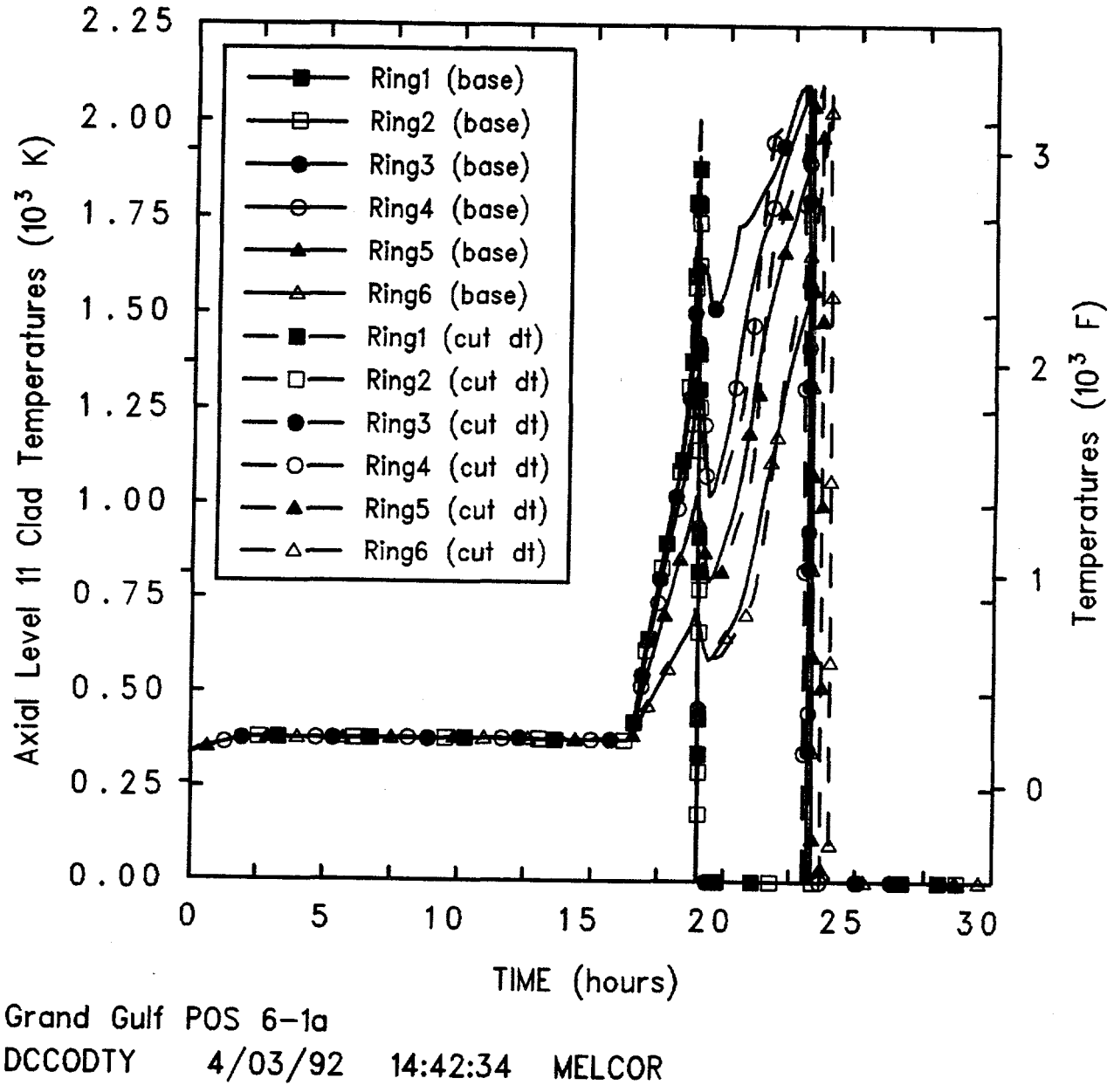

Figure 5.4.2.1. Level 10 Clad Temperatures for Grand Gulf POS 6 -- Time Step Sensitivity Study.

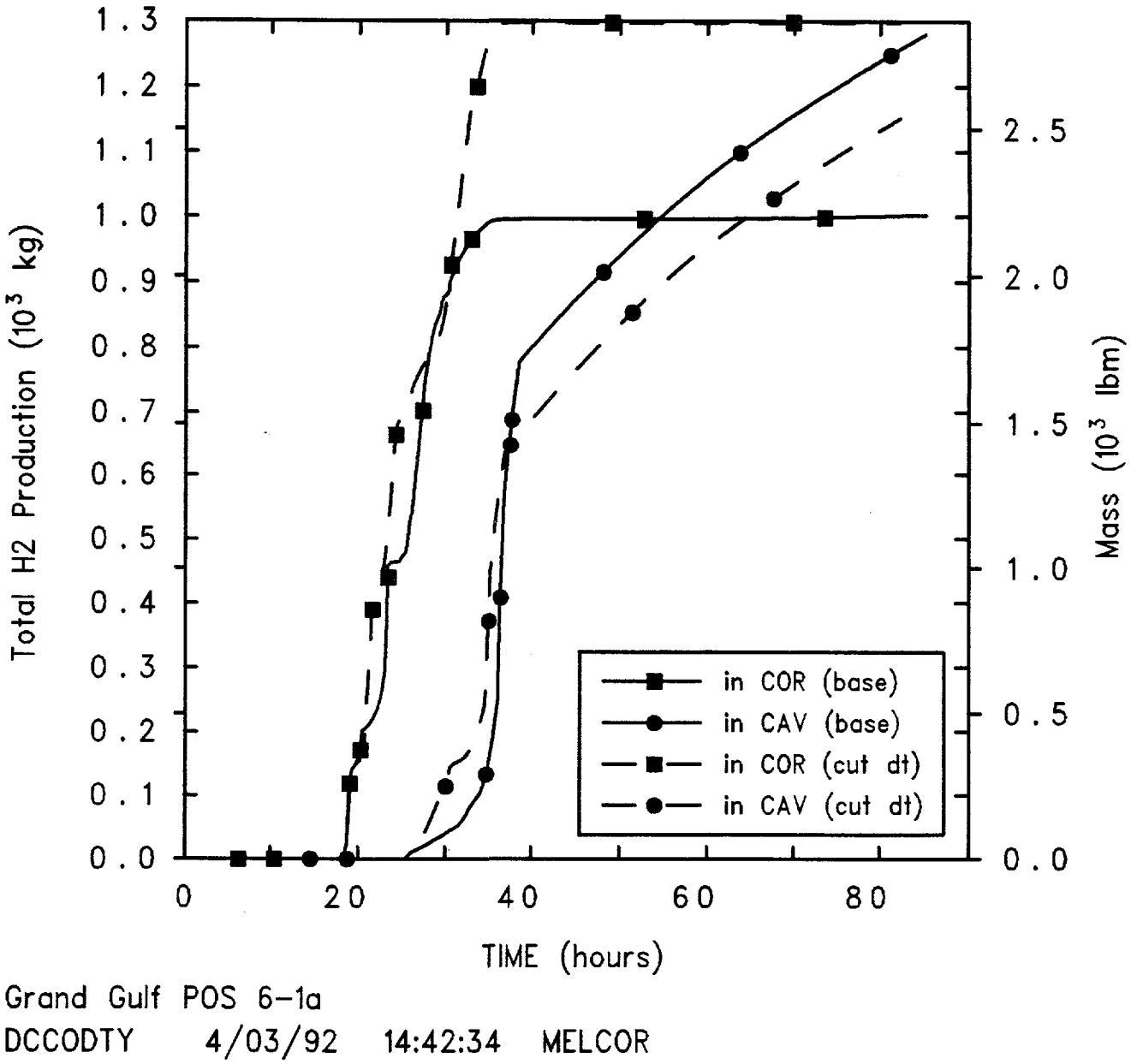

Figure 5.4.2.2. Hydrogen Generation for Grand Gulf POS 6 -- Time Step Sensitivity Study.

Table 5.4.2.2. Total Fission Product Radioactive Masses Released from Fuel for Grand Gulf POS 6 -- Time Step Sensitivity Study

Class	% of Initial Inventory Released (Mass Fraction)					
	Before Vessel Breach		Before Cavity Rupture		To Environment	
	Base Δt	Cut Δt	Base Δt	Cut Δt	Base Δt	Cut Δt
1 (Xe)	81.3	92.8	100	100	100	100
2 (Cs)	81.7	92.9	100	100	67.6	52
3 (Ba)	2.38	6.85	42	41.9	21.3	20.3
4 (I)	81	92.7	95.5	95.7	95.5	95.7
5 (Te)	72.5	80.2	95.2	95.3	62.3	58.2
6 (Ru)	0.00002	0.0048	0.007	0.0068	0.0045	0.003
7 (Mo)	0	0	1.61	1.76	0.642	0.739
8 (Ce)	3.0e-06	0.0019	0.0037	0.0035	0.00215	0.00156
9 (La)	0	0	0.217	0.4974	0.00056	0.26
10 (U)	0.00156	0.226	1.62	0.332	0.156	0.151
11 (Cd)	0	0	0.0385	0.0757	0.0023	0.039
12 (Sn)	2.866	20.8	22.5	34.8	15.5	17.4

Table 5.4.3.1 compares the timings of various key events predicted in the two air-oxidation calculations with a corresponding base case analysis. There is no difference in timing on any events before the extra oxygen is first sourced in. The gap release and the failure of the lower head penetrations in the various rings are predicted to occur somewhat earlier, because of the slightly accelerated core heatup due to more clad oxidation.

There are no major differences observable in primary and containment systems pressure histories, or core inventory boiloff. Clad temperature histories in the core level just below the active fuel midplane in one of the six core rings are presented in Figure 5.4.3.5, as representative of the overall core response. The two air-oxidation sensitivity study calculations both show more rapid clad heatup due to the increased degree of (exothermic) clad oxidation, resulting in earlier melt, relocation and lower head failure.

The masses of zircaloy and zirconium oxide, stainless steel and steel oxide, steam and oxygen consumed and hydrogen generated by the end of these transient calculations are presented for these air-oxidation sensitivity studies in Table 5.4.3.2. With the free oxygen source, 10-20% more zircaloy and 100% more steel is oxidized in-vessel. Because 30-60% less steam is consumed, 30-60% less hydrogen in generated in-vessel; with 10-20% less hydrogen generated in the cavity, the total amount of hydrogen generated is 20-40% less in the two air oxidation sensitivity studies. (Most of the oxygen sourced into the core control volume therefore escapes out through the upper head and vessel breach, to the containment and then the environment, without being consumed in oxidation processes.)

Figure 5.4.3.6 shows the hydrogen generation rates, both in-vessel and in the cavity. The lower amounts of hydrogen produced in the air oxidation sensitivity studies are seen to be primarily a result of sharp differences during the time period the free oxygen is being added, not gradual divergences throughout the remainder of the transient.

Table 5.4.3.3 compares the radioactive masses of radionuclides released in this set of MELCOR calculations, when a lower head penetration first fails and at the end of the calculation (i.e., when the cavity is predicted to rupture), normalized to the initial masses of each class (given in Table 3.1). The primary difference is the (as expected) ~100% release of ruthenium in-vessel in the two air-oxidation sensitivity study analyses, both using a constant release rate coefficient and using a variable coefficient dependent on the partial pressure of oxygen in the core. But there are other differences. More of the more refractory classes (Ba, Ce, U and Sn) are released

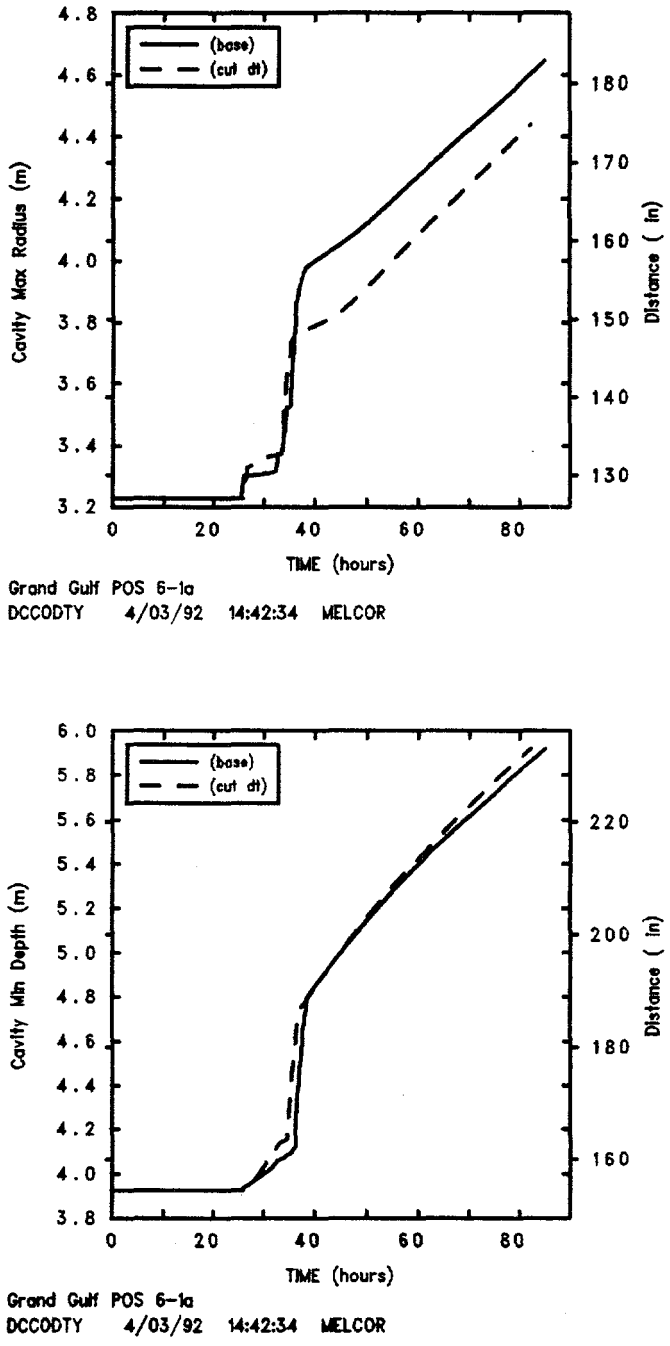

Figure 5.4.2.3. Cavity Maximum Radius and Minimum Depth for Grand Gulf POS 6 -- Time Step Sensitivity Study.

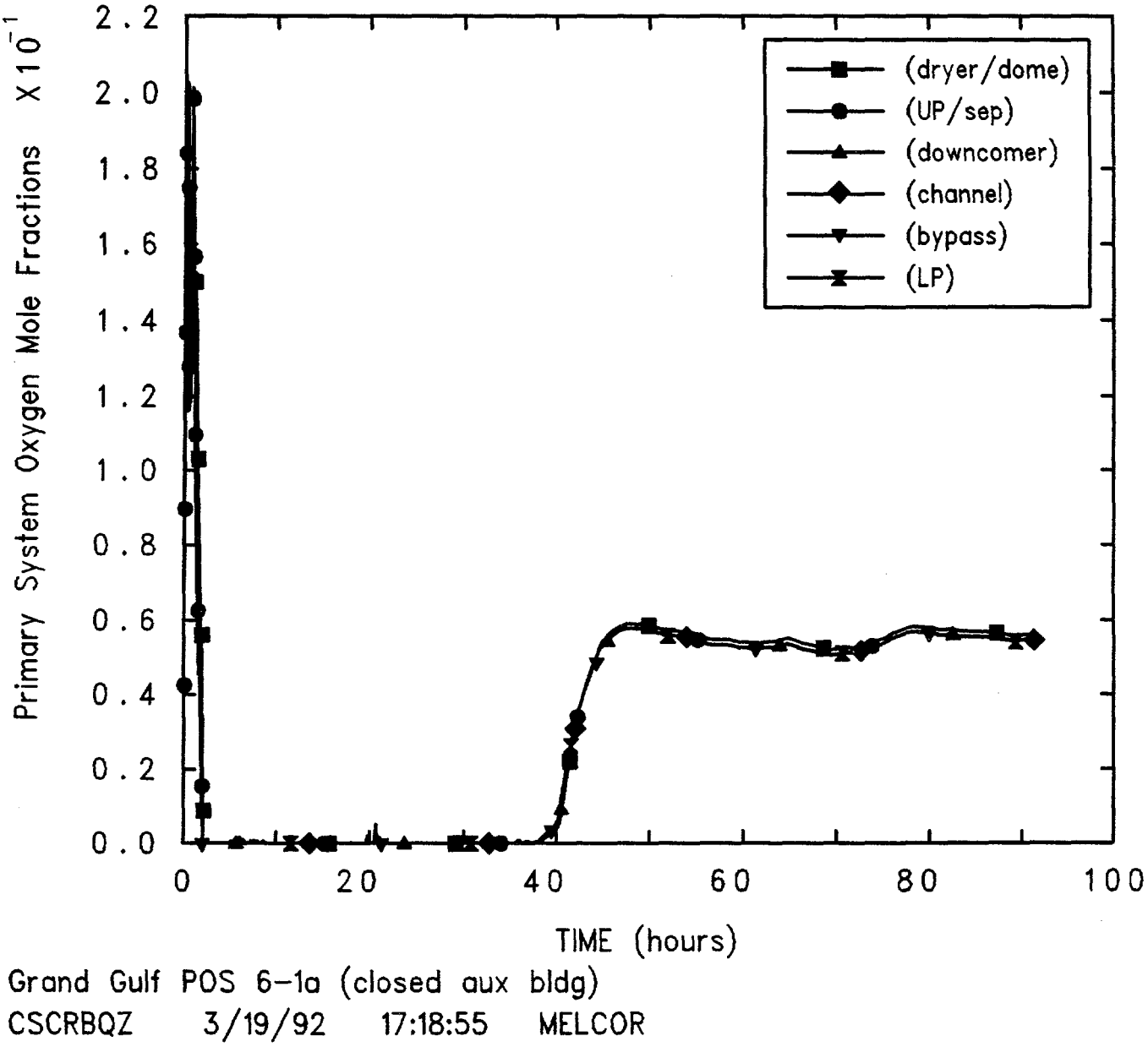

Figure 5.4.3.1. Primary Oxygen Mole Fractions for Grand Gulf POS 6 -- Reference Calculation.

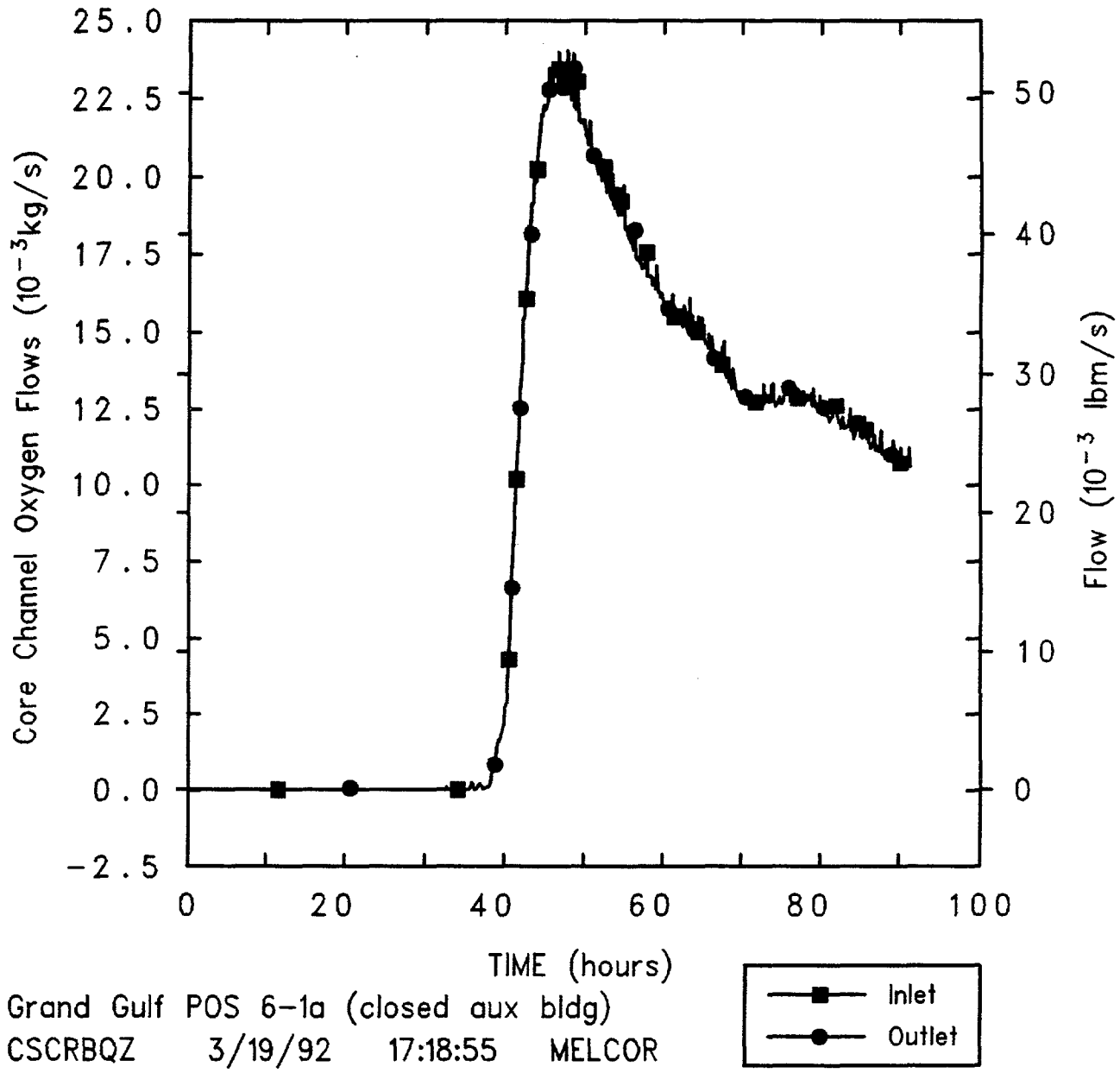

Figure 5.4.3.2. Core Oxygen Inlet and Outlet Mass Flows for Grand Gulf POS 6 -- Reference Calculation.

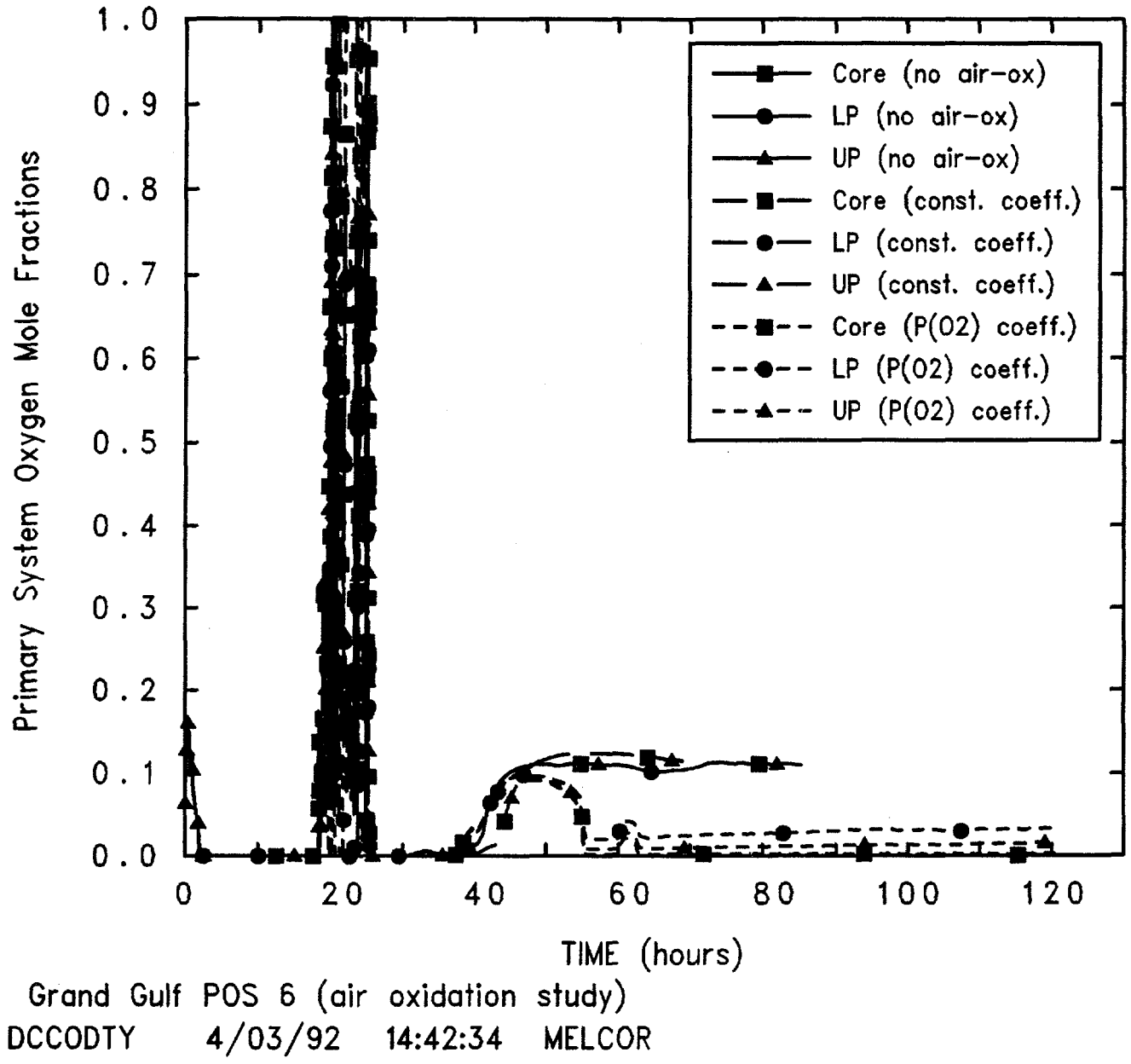

Figure 5.4.3.3. Primary Oxygen Mole Fractions for Grand Gulf POS 6 -- Air Oxidation Sensitivity Study.

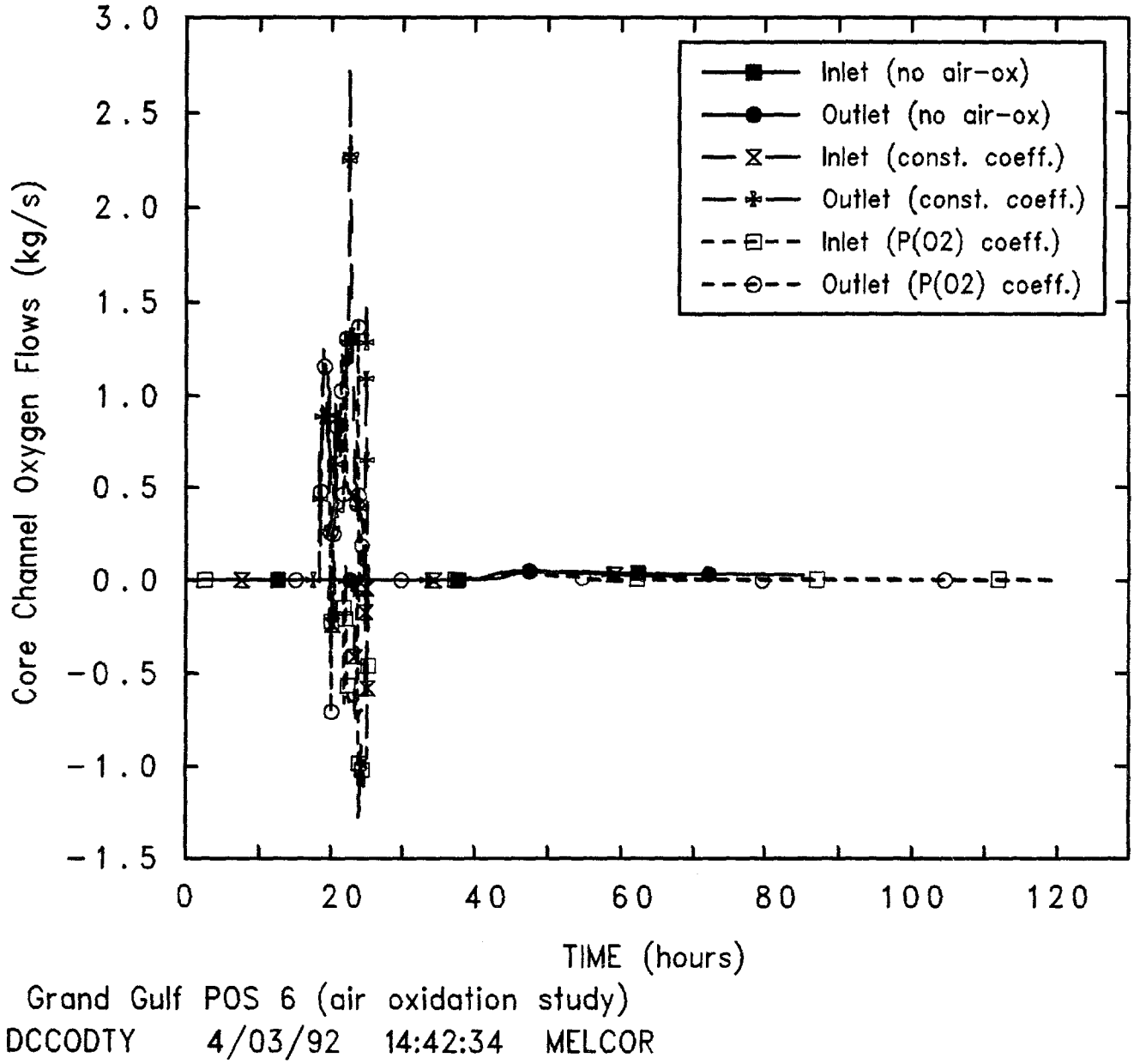

Figure 5.4.3.4. Core Oxygen Inlet and Outlet Mass Flows for Grand Gulf POS 6 -- Air Oxidation Sensitivity Study.

Table 5.4.3.1. Key Event Times for Grand Gulf POS 6 -- Air Oxidation Sensitivity Study

Event	No Air-Ox (hr)	Constant Coeff. (hr)	$P(O_2)$ Coeff. (hr)
Level below TAF	12.68	12.68	12.68
Clad failure/Gap release			
(Ring 1)	18.37	18.34	18.34
(Ring 2)	18.34	18.34	18.34
(Ring 3)	18.38	18.34	18.34
(Ring 4)	18.61	19.28	19.24
(Ring 5)	20.46	20.04	19.96
(Ring 6)	21.80	20.51	20.02
Vessel LH penetration failure			
(Ring 1)	25.45	24.81	25.78
(Ring 2)	25.39	24.81	26.00
(Ring 3)	26.10	25.15	24.61
(Ring 4)	34.49	24.83	23.63
(Ring 5)	30.24	24.85	24.21
(Ring 6)	32.63	--	54.88
Cavity rupture	85.61	68.79	120.44

prior to vessel breach in the two air-oxidation sensitivity study calculations; unexpectedly, while more of the more volatile classes (Xe, Cs, I and Te) are released using a constant Ru release rate coefficient, slightly less are released using a variable Ru release coefficient dependent on the partial pressure of oxygen in the core than predicted with no air oxidation at all.

The comparison of releases by the time of cavity rupture is more confused. The three classes with identically-zero in-vessel releases all show the greatest release fraction for the air-oxidation sensitivity study using a constant release coefficient for Class 6; the other more refractory classes (Ba, Ce, U and Sn) show higher release in the calculation with a variable Ru release coefficient dependent on the partial pressure of oxygen; the volatiles (Xe, Cs, I and Te) all show 90-100% releases with no clear pattern of variation.

The total radioactive masses released from the fuel and debris for each class, and the amount released to the environment by the time of cavity rupture (given in terms of the initial inventory) are summarized in Table 5.4.3.4. Almost all of the ruthenium is released from the fuel in these two air-oxidation sensitivity study analyses, and over half of that is released to the environment (in the absence of any additional retention in the auxiliary building, not included in these calculations).

Both air-oxidation calculations ended on cavity rupture, at very different times. Figure 5.4.3.7 shows that the calculations with no air-oxidation and with air oxidation and a constant Ru release coefficient predict that the cavity concrete will first be ruptured in depth, with the calculation using a variable coefficient dependent on the partial pressure of oxygen predicts that the cavity concrete will first be ruptured radially, but with less than 3.5 cm depth remaining axially at that time.

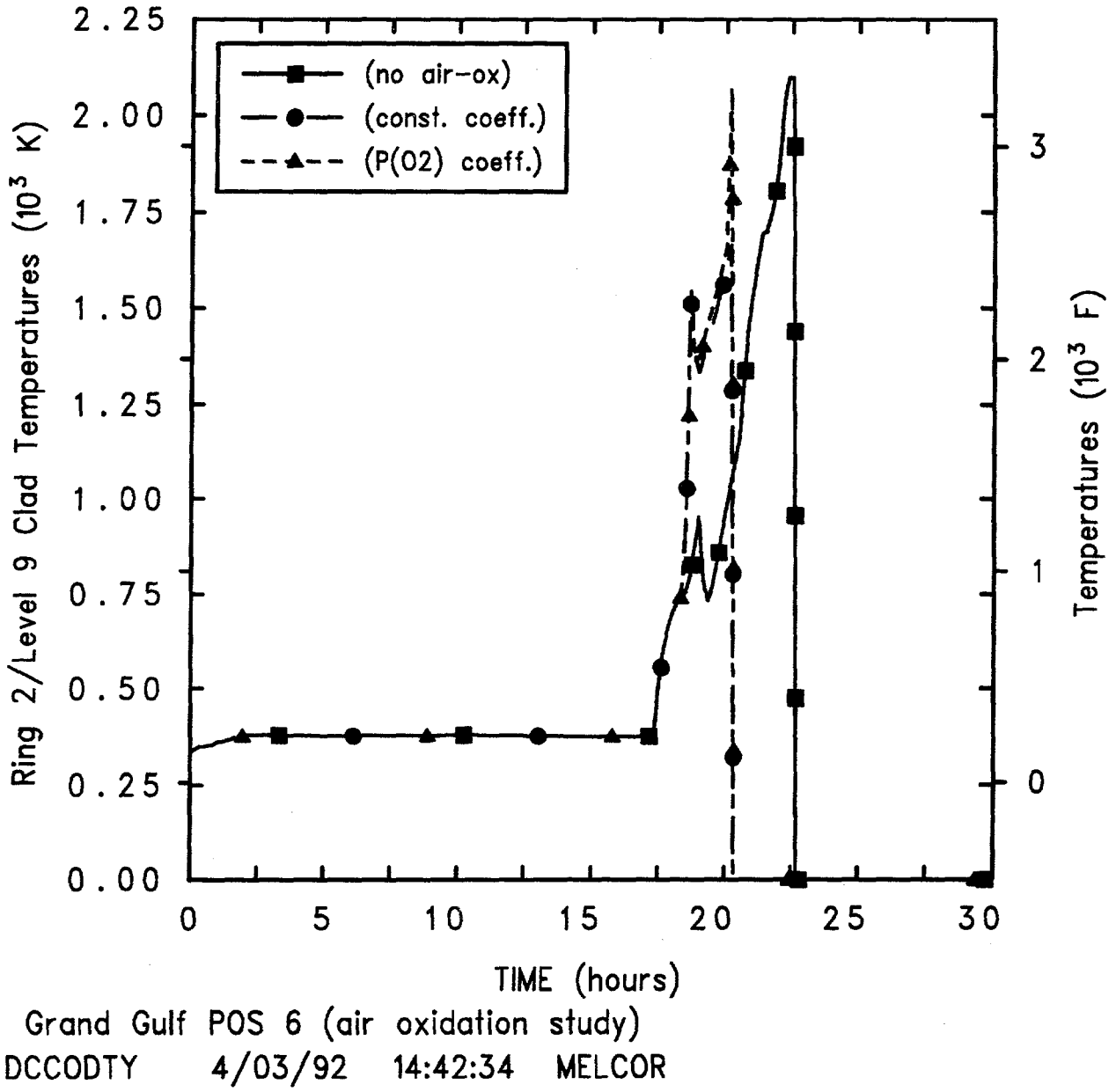

Figure 5.4.3.5. Level 9 Clad Temperatures for Grand Gulf POS 6 -- Air Oxidation Sensitivity Study.

Table 5.4.3.2. Oxidation Masses for Grand Gulf POS 6 -- Air Oxidation Sensitivity Study

Material	Total Masses at End of Transient (kg)		
	No Air-Ox	Constant Coeff.	$P(O_2)$ Coeff.
In COR Package			
Zircaloy	12356	24551	6848
Zirconium oxide	7211	7890	8784
Stainless steel	35299	35875	33650
Steel oxide	1809	1688	3658
Steam consumed	8750	3078	5738
Oxygen consumed	--	4862	6291
In CAV Package			
Metal layer	83959	7746	87965
(Light) oxide layer	591150	413250	618710
Hydrogen			
Produced in vessel	1001	344	642
Produced in cavity	1280	1019	1159
Total produced	2281	1363	1801

Table 5.4.3.3. Fission Product Radioactive Masses for Grand Gulf POS 6 -- Air Oxidation Sensitivity Study

Class	% of Initial Inventory Released					
	Before Vessel Breach			Before Cavity Rupture		
	No Air-Ox	Constant Coeff.	$P(O_2)$ Coeff.	No Air-Ox	Constant Coeff.	$P(O_2)$ Coeff.
1 (Xe)	81.3	93.2	79.5	100	97.7	100
2 (Cs)	81.7	93.3	79.9	100	97.9	100
3 (Ba)	2.38	8.65	22.1	42	42.7	47.1
4 (I)	81	93.1	79.2	95.5	93.4	89
5 (Te)	72.5	92.6	76.3	95.2	95.8	92.8
6 (Ru)	0.00002	99.9	100	0.007	100	100
7 (Mo)	0	0	0	1.61	3.23	1.405
8 (Ce)	3.0e-06	0.0074	0.1186	0.0037	0.0082	0.1276
9 (La)	0	0	0	0.217	0.666	0.3588
10 (U)	0.00156	0.52	4.59	1.62	0.522	5.1
11 (Cd)	0	0	0	0.0385	0.0808	0.0763
12 (Sn)	2.866	19.3	28	22.5	20.7	34.8

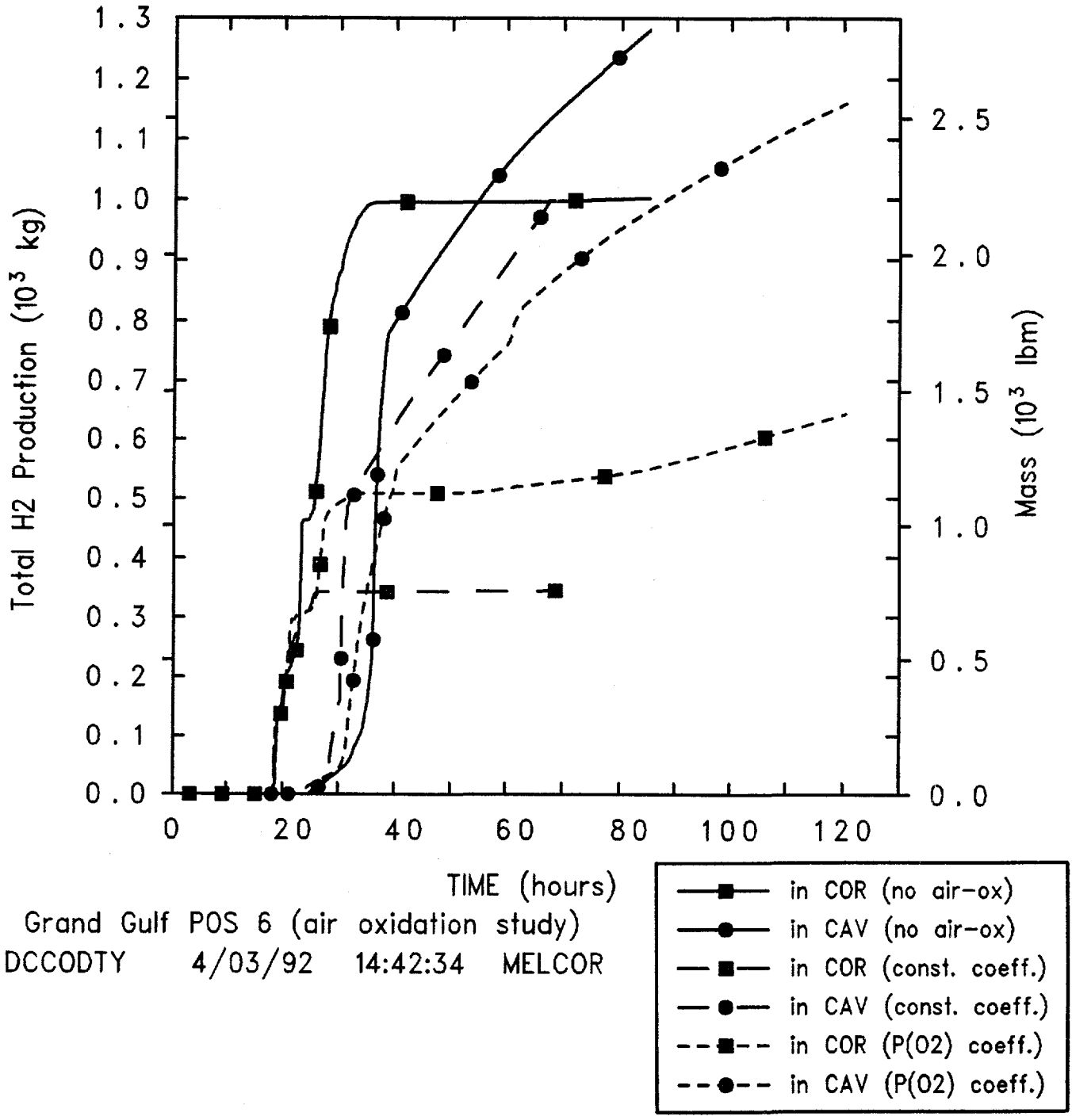

Figure 5.4.3.6. Hydrogen Generation for Grand Gulf POS 6 -- Air Oxidation Sensitivity Study.

Table 5.4.3.4. Total Fission Product Radioactive Mass Released from Fuel for Grand Gulf POS 6 -- Air Oxidation Sensitivity Study

Class	% of Initial Inventory					
	Released Before Cav-Rupture			Released to Environment		
	No Air-Ox	Constant Coeff.	$P(O_2)$ Coeff.	No Air-Ox	Constant Coeff.	$P(O_2)$ Coeff.
1 (Xe)	100	97.7	100	100	97.5	100
2 (Cs)	100	97.9	100	67.6	62.6	60.7
3 (Ba)	42	42.7	47.1	21.3	21.8	16.9
4 (I)	95.5	93.4	89	95.5	93.4	88.9
5 (Te)	95.2	95.8	92.8	62.3	60.6	47
6 (Ru)	0.007	100	100	0.0045	62.2	54.6
7 (Mo)	1.61	3.23	1.405	0.642	1.26	0.487
8 (Ce)	0.0037	0.0082	0.1276	0.00215	0.00467	0.0259
9 (La)	0.217	0.666	0.3588	0.1024	0.365	0.168
10 (U)	1.62	0.522	5.1	0.212	0.305	1.2
11 (Cd)	0.0385	0.0808	0.0763	0.0189	0.0388	0.04
12 (Sn)	22.5	20.7	34.8	15.5	12.5	14.3

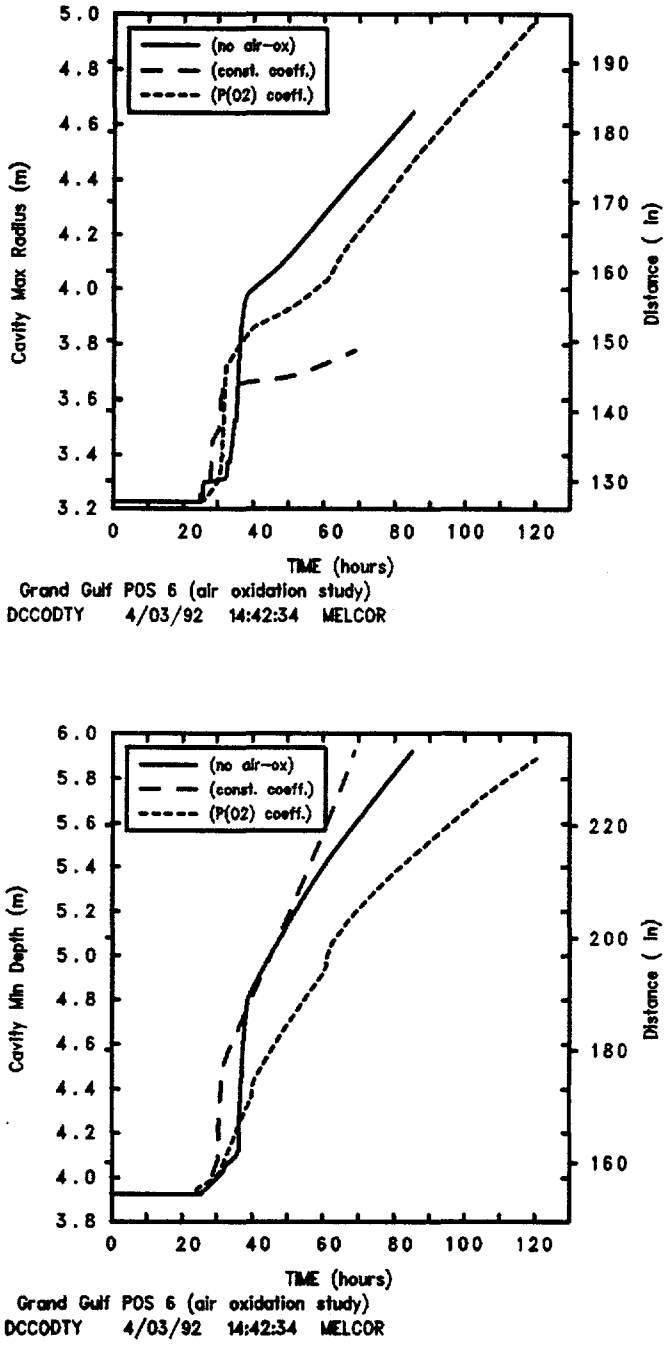

Figure 5.4.3.7. Cavity Maximum Radius and Minimum Depth for Grand Gulf POS 6 -- Air Oxidation Sensitivity Study.

6 References

[Boyack,1992] B. E. Boyack, V. K. Dhir, J. A. Gieseke, T. J. Haste, M. A. Kenton, M. Khatib-Rahbar, M. T. Leonard, R. Viskanta, "MELCOR Peer Review", LA-12240, Los Alamos National Laboratory, March 1992.

[Carbajo, 1993] J. J. Carbajo, "Severe Accident Source Term Characterization for a Low Pressure, Short-term Station Blackout Sequence in a BWR-4", NUREG/CR-5942, ORNL/TM-12229, Oak Ridge National Laboratory, September 1993.

[Cole et al., 1984] R. K. Cole, Jr., D. P. Kelly, M. A. Ellis, "CORCON-Mod2: A Computer Program for Analysis of Molten-Core Concrete Interactions", NUREG/CR-3920, SAND84-1246, Sandia National Laboratory, August 1984.

[Dingman, 1986] S. E. Dingman, "HECTR Version 1.5 User's Manual", NUREG/CR-4507, SAND86-0101, Sandia National Laboratories, April 1986.

[Dingman et al., 1991] S. E. Dingman, C. J. Shaffer, A. C. Payne, Jr., M. K. Carmel, "MELCOR Analysis for Accident Progression Issues", NUREG/CR-5331, SAND89-0072, Sandia National Laboratories, January 1991.

[Fauske & Associates, 1990] Fauske and Associates. "MAAP 3.0B Users Manual", Electric Power Research Institute, March 1990.

[Gelbard, 1982] F. Gelbard, "MAEROS User Manual", NUREG/CR-1391, SAND80-0822, Sandia National Laboratories, December 1982.

[Grand Gulf, UFSAR] System Energy Resources, Inc., "Grand Gulf Updated Final Safety Analysis Report", 1992.

[Harper, 1994] F. T. Harper, "Evaluation of Severe Accident Risks: Quantification of Major Input Parameters: Determination of Parameter Values Not Quantified Using Formal Expert Elicitation", NUREG/CR-4551, Volume 2, Revision 1, Part 6, Sandia National Laboratories, 1994.*

[Kmetyk, 1992a] L. N. Kmetyk, "MELCOR 1.8.1 Assessment: ACRR Source Term Experiments ST-1/ST-2", SAND91-2833, Sandia National Laboratories, April 1992.

[Kmetyk, 1992b] L. N. Kmetyk, "MELCOR 1.8.1 Assessment: LOFT Integral Test LP-FP-2", SAND92-1373, Sandia National Laboratories, December 1992.

[Kmetyk, 1994a] L. N. Kmetyk, "Air Ingression Calculations for Selected Plant Transients Using MELCOR", SAND93-3808, Sandia National Laboratories, January 1994.

[Kmetyk, 1994b] L. N. Kmetyk, "MELCOR 1.8.2 Assessment: Surry PWR TMLB' (with a DCH Study)", SAND93-1899, Sandia National Laboratories, February 1994.

[Kmetyk, 1994c] L. N. Kmetyk, "Survey of MELCOR Assessment and Selected Applications", SAND92-1273, Sandia National Laboratories, April 1994.*

[Kmetyk & Smith, 1994] L. N. Kmetyk, L. N. Smith, "Summary of MELCOR 1.8.2 Calculations for Three LOCA Sequences (AG, S2D, and S3D) at the Surry Plant", NUREG/CR-6107, SAND93-2042, Sandia National Laboratories, March 1994.

* Copies are available for inspection or copying for a fee in the NRC Public Document Room.

References

[Kuhlman et al., 1986] M. R. Kuhlman, V. Kogan, P. M. Schumacher, "TRAP-MELT2 Code: Development and Improvement of Transport Modeling", NUREG/CR-4667, BMI-2141, Battelle Columbus, July 1986.

[NUREG/CR-6144] T. L. Chu et al., "Evaluation of Potential Severe Accidents During Low Power and Shutdown Operations at Surry, Unit 1", NUREG/CR-6144, BNL-NUREG-52399, (multiple volumes), Brookhaven National Laboratories, 1994.

[Owczarski et al, 1985] P. C. Owczarski, R. I. Schreck, A. K. Postma, "Technical Bases and User's Manual for the Prototype of a Suppression Pool Aerosol Removal Code (SPARC)", NUREG/CR-3317, PNL-4742, Pacific Northwest Laboratory, May 1985.

[Payne, 1992] A. C. Payne, Jr. "Analysis of the LaSalle Unit 2 Nuclear Power Plant: Risk Methods Integration and Evaluation Program (RMIEP); Volume 1: Summary", NUREG/CR-4832, SAND92-0537, Sandia National Laboratories, March 1992.

[Powers et al., 1986] D. A. Powers, J. E. Brockmann, A. W. Shiver, "VANESA: A Mechanistic Model of Radionuclide Release and Aerosol Generation during Core Debris Interactions with Concrete", NUREG/CR-4308, SAND85-1370, Sandia National Laboratories, July 1986.

[Powers et al., 1994] D. A. Powers, L. N. Kmetyk, R. C. Schmidt, "A Review of the Technical Issues of Air Ingression During Severe Reactor Accidents", NUREG/CR-6218, SAND94-0731, Sandia National Laboratories, September 1994.

[Ramamurthi & Kuhlman, 1990] M. Ramamurthi, M. R. Kuhlman, "Final Report on Refinement of CORSOR -- An Empirical In-Vessel Fission Product Release Model", Battelle Memorial Institute, October 31, 1990.

[Shaffer, memo, 1991] C. J. Shaffer, "Grand Gulf Low Power/Shutdown MELCOR Calculations", memo from C. J. Shaffer to T. D. Brown, May 17, 1991 (included as Appendix).

[Shaffer et al., 1992] C. J. Shaffer, L. A. Miller, A. C. Payne, Jr. "Integrated Risk Assessment for the LaSalle Unit 2 Nuclear Power Plant: Phenomenology and Risk Uncertainty Evaluation Program (PRUEP); Volume 3: MELCOR Code Calculations", NUREG/CR-5305, SAND90-2765, Sandia National Laboratories, October 1992.

[Summers et al., 1991] R. M. Summers et al. "MELCOR 1.8.0: A Computer Code for Severe Nuclear Reactor Accident Source Term and Risk Assessment Analyses", NUREG/CR-5531, SAND90-0364, Sandia National Laboratories, January 1991.

[Nuclear Regulatory Commission, 1975] U. S. Nuclear Regulatory Commission, "Reactor Safety Study -- An Assessment of Accident Risks in U. S. Commercial Nuclear Power Plants", WASH-1400, October 1975.

[Nuclear Regulatory Commission, 1981] U. S. Nuclear Regulatory Commission, "Technical Basis for Estimating Fission Product Behavior During LWR Accidents", NUREG-0772, June 1981.

[Nuclear Regulatory Commission, 1994] U. S. Nuclear Regulatory Commission, "Technical Specifications, Grand Gulf Nuclear Station Unit No. 1", Docket No. 50-416, Appendix "A" to License No. NPF-29, NUREG-0934, October, 1984.

[Nuclear Regulatory Commission, 1989] U. S. Nuclear Regulatory Commission, "Severe Accident Risks: An Assessment for Five U. S. Nuclear Power Plants", NUREG-1150, June 1989.

Appendix Additional Level 1 Supporting Calculations

Copy of Memo to T. D. Brown, SNL,
from C. J. Shaffer, SEA*

***Science and Engineering Associates, Inc.**

Sandia National Laboratories

Albuquerque, New Mexico 87185

date: **May 17, 1991**

to: **T. D. Brown, Org.6413**

from: **C. J. Shaffer, Org. 6418**

subject: **Grand Gulf Low Power/Shutdown MELCOR Calculations**

INTRODUCTION

Severe accident calculations with MELCOR were run to support the Grand Gulf Low Power/Shutdown PRA. The Grand Gulf Nuclear Station located in southwestern Mississippi is a BWR-6 boiling water reactor with an 800 fuel assembly core contained inside a Mark III containment. The calculations all assume that the reactor vessel upper head was removed when the accidents were initiated four days after the reactor tripped (PRA plant state 6).

Three calculations were done. First, a low decay power boiloff without any ECCS and all piping intact, then two LOCA accidents with a recirculation loop double-ended pipe rupture. The first LOCA calculation assumed only one Low Pressure Coolant Injection (LPCI) pump was operated and the other LOCA calculation assumed two pumps were available. The LPCI pumped water from the containment suppression pool into the core bypass region. The broken recirculation pipe allowed all the reactor vessel water above the jet pump throats to drain from the vessel which left the reactor core about 2/3 covered with water and allowed the upper 1/3 of the core to heat and possibly become damaged. The LPCI may or may not over fill the core bypass allowing water to flow into the core channels.

BRIEF MELCOR DESCRIPTION

MELCOR [1] is a fully integrated, relatively fast-running code that was developed at SNL to model the progression of severe accidents in light water reactor nuclear power plants. Characteristics of severe accident progression that can be treated with MELCOR include the thermal-hydraulic response in the reactor coolant system, reactor cavity, and containment; core heatup and degradation; core-concrete attack; combustible gas generation, transport, and combustion; plant-structure thermal response; radionuclide release and transport; and the impact of engineered safety features on thermal-hydraulic and radionuclide behavior. MELCOR has been designed to facilitate sensitivity and uncertainty analyses through the use of sensitivity coefficients. Many parameters in the correlations are coded as sensitivity coefficients changeable through user input.

MELCOR has a structured, modular architecture that accesses only those modules called 'packages' required for a particular calculation and that facilitates the incorporation of additional or alternative phenomenological models. MELCOR has an input preprocessor called MELGEN which generates the initial restart and a plot processor called MELPLT. Separate input is required for each; MELGEN, MELCOR, and MELPLT.

Five major MELCOR packages were employed to model the thermal/hydraulic behavior for these calculations. The Control Volume Hydrodynamics Package (CVH) models the behavior of water and non-condensible gases in a control volume. The Flow Path Package (FP) models the movement of water and non-condensible gases between the control volumes. The Control Volume Thermodynamics package (CVT) handles thermodynamic calculations for the control volumes and together with the CVH and FP packages advance the thermal/hydraulic state in the control volumes from one time level to the next. The Heat Structures package (HS) calculates one-dimensional heat conduction within an intact solid structure and energy transfer across its boundary surfaces into control volumes. The core package (COR) treats the processes associated with chemical and mechanical degradation of the core and associated structures brought about as the core heats and degrades.

MELCOR MODEL DESCRIPTION

The following describes the MELCOR model development for the Grand Gulf low power/shutdown study. Previous Grand Gulf calculations [2] used a modified LaSalle core and reactor cooling system. These models, particularly the core model, have been improved to ensure that these calculations represent Grand Gulf. These models still contain LaSalle specific data [3] but the parameters of importance have been converted to or verified as Grand Gulf data to the extent possible given the limited available plant data. For instance, the core model has the proper fuel assembly and control rod masses, the primary system volumes are in reasonable agreement with the volumes stated in the FSAR [4] but certain flow loss coefficients which were critical to determining whether or not the bypass water overflowed the top of the core into the fuel assemblies were not known specifically for Grand Gulf.

Core Input Model

Core input was developed specifically for the Grand Gulf 800 assembly core as previous Grand Gulf calculations used a modified version of the LaSalle input.

Decay Power The time dependent decay power is calculated using the normalized time dependent power distribution developed for the LaSalle plant (this is the same power curve used in the previous Grand Gulf calculations). The operating power level was 3833 Mw when the reactor was tripped and these low decay power calculations begin 4 days after the reactor was tripped. The initial power level at 4 days is .309% of operating power (11.86 Mw).

The core decay power distribution was developed from FSAR EOC data. The radial power factors are listed in FSAR Figure 4.3-21 for each fuel assembly. These power factors were used to determine the power factors for the six ring core model illustrated in Figure 1. Since the power distribution dips at the core center, the inner portion of the core was subdivided to focus on the region with the highest power density (second ring). It is important to remember that some fuel assemblies have higher power factors than their associated ring averages (the highest is 1.232). The number of assemblies in each ring, the volume fractions, the outer radii, the power fractions, and power factors are listed in Table 1.

The axial power factor distribution shown in FSAR Figure 4.3-22 was used to develop the axial power factors for MELCOR. The resulting axial power factors are listed in Tables 2a and 2b for a course and fine axial nodalization and these power factors were adjusted to include the non-fueled portions of the core. For the course axial nodalization, the entire active fuel region of the core was subdivided into 6 cells of equal height (25 inches) but in the fine nodalization, the upper half of the active fuel region was further subdivided into cells with a height of 6.25 inches. The core water level for the LOCA accidents involving a recirculation line break remained above the jet pump throats which is about 2/3 the way up the active fuel.

The core nodalization is shown in Figures 2 and 3 for the course and fine nodalization schemes, respectively. In the cell numbering system, each cell has a 3 digit identifying number. The first digit is the ring number, with the rings numbered from the core center outward, and the second and third digits indicate the axial level, beginning with level 1 at the bottom of the lower plenum. Level 5 represents the core plate, and levels 13 and 22 represent the top cells for the course and fine nodalization schemes, respectively. For example, cell 212 (course nodalization) is top cell containing fuel located in the second ring. The top cells did not contain fuel.

Component Masses The 800 assembly Grand Gulf core contains a total of 179,760 lbm of Zr. There is 98.7 lbm in each assembly canister and 126 lbm in the fuel rods. In addition, the FSAR lists the total fuel mass as 458 lbm/assembly for a total UO_2 mass of 366,400 lbm. The total fuel assembly and control masses are given as 699 and 218 lbm, respectively. There are 193 control rods in the core.

The Grand Gulf fuel rods appear to be identical to the LaSalle rods and both have an 8 by 8 matrix. Grand Gulf, however, has a thicker canister than LaSalle, in addition to 36 more fuel assemblies and 8 more control rods than LaSalle.

The fuel assembly and control rod masses are listed in Table 3. LaSalle data was used for the top guide, core plate, fuel supports, control rod tubes and housings masses. These masses were subdivided into radial and axial cells corresponding to the cells for the power distribution. The subdivided masses are reasonably accurate for the active fueled core region and the correct total masses were maintained. The mass

distribution outside of the fueled region (i.e., the handles, the lower tie plate, the fuel support pieces, control rod velocity limiters, etc.) were estimated from the available data and schematic drawings.

Other Input Other core model input were computed in a similar manner as were the masses. These include the component surface areas, the flow areas, cross sectional areas, and the equivalent diameters. Inputs for the vessel lower head and penetrations still reflect the LaSalle data. However, because the Grand Gulf calculations do not include core meltdown, the results will not be particularly sensitive to this input and, therefore, it is felt that the LaSalle numbers are adequate.

Hydrodynamic Models

Vessel Control Volumes The reactor vessel control volumes were adapted from the LaSalle input model with modifications. The available Grand Gulf data included a few basic dimensions and volumes from the FSAR and plant drawings. FSAR Figure 5.1-2 lists six primary system volumes which total to 21745 ft^3. The LaSalle model, which was developed from RETRAN input, totals 21444 ft^3 (with the volume of the steam lines deleted). These two totals differ by 1.4% and it is likely that the primary system designs are very similar. There are however differences when comparing the LaSalle model and the Grand Gulf data. The Grand Gulf core shroud has a larger diameter than LaSalle to accommodate the larger core. Grand Gulf has 24 jet pumps compared to 20 for LaSalle and have different jet pump designs.

Since the LaSalle input was derived from a more detailed RETRAN input model, the LaSalle model is a good framework for developing an adequate Grand Gulf primary system model for these low power calculations. The LaSalle input was adapted and modified to include the larger Grand Gulf core shroud and the Grand Gulf jet pump designs. A few other numbers such as elevations were changed to coincide with data from the plant drawings.

The volumes and elevations for the Grand Gulf models are listed in Table 4. The basic model consists of 6 volumes with a total volume of 22182 ft^3. This volume includes the steam line volume of 1454 ft^3 and excludes the recirculation loop volume of 1020 ft^3 and agrees closely with the Grand Gulf FSAR data. However, the MELCOR volume nodalization is not the same as the FSAR nodalization. The core volume nodalization (channels and bypass) go from the core plate to the top of the fuel assembly canisters. The volume within the jet pumps is contained in the lower plenum control volume.

A more sophisticated core volume model which has 6 control volumes representing the fuel assembly channels and 1 volume for the bypass region was developed for the LOCA calculations. The core channels were subdivided according to the core model ring volume fractions.

The recirculation loop piping was not modeled for these calculations. In the boiloff calculation, it was assumed that circulation within the recirculation piping would not significantly effect the boiloff results. In the LOCA calculations, the recirculation loop double-ended rupture

resulted in the draining of the downcomer so that a loop model was not needed.

Vessel Flow Paths The primary system was modeled with eight internal flow paths and three external flow paths. The entrance and exit elevations, the forward and reverse loss coefficients, and the flow area for each path are listed in Table 5. The internal flow paths include the core channel and bypass inlets and exits, steam separators and separator returns, dryer drains, and the jet pump diffusers. The external flow paths include a path to simulate the vessel with its upper head removed, the recirculation pump suction lines, and the recirculation inlet nozzles.

Again the LaSalle input was used as a framework for the Grand Gulf models. The flow paths which are critical to these low power calculations were the jet pump diffusers and the core plate. Significant errors in the input of the other flow paths should not significantly impact the results of these calculations, therefore the LaSalle input was adopted for these paths.

Input data was developed specifically for the Grand Gulf jet pumps. The jet pump diffusers consist of three sections; the throat section, the diffuser section, and the extension section. Diameters and elevations were obtained or estimated from the FSAR and drawings. The jet pump flow path data which are listed in Table 6 were developed for the throat flow area. Most of this data are more than adequate for these calculations. The one parameter which has an uncertainty potentially important to the conclusions from these calculations is the throat exit loss coefficient judged at 1. This coefficient dominates the total reverse loss coefficient for the water flow through the jet pumps during the LOCA calculations which was in the reverse direction. This uncertainty is discussed further in the uncertainty section.

The most sensitivity parameter for the LOCA calculations was the reverse core plate loss coefficient for water flow from the core bypass to the lower plenum. This determined the water head in the bypass and whether or not the water overflowed the bypass into the fuel assemblies. Due to the lack of applicable Grand Gulf data, the core loss coefficients developed for LaSalle were used. The uncertainty of this parameter on the final conclusions was investigated and is discussed in the uncertainty section.

The LaSalle core loss coefficients were developed from the RETRAN input and since this input was developed by engineers with access to GE proprietary information, the LaSalle coefficients were the best available for these calculations. The RETRAN coefficients used in developing the LaSalle coefficients included the coefficients for forward and reverse flow through the fuel assemblies. The bypass loss coefficients were then calculated to establish the ratio of channel to bypass flow at 10 [4] for steady state operation (reverse flow assumed the same ratio as the forward flow). The MELCOR core flows were all based on the channel or bypass flow areas in an unrestricted portion of the core. The RETRAN coefficients were then modified by the ratio of squared areas (MELCOR/RETRAN) to get coefficients applicable to MELCOR and since the RETRAN nodalization was much more detailed, coefficients were summed for the more course MELCOR

nodalization. The channel inlet included the lower tie plate (which has an inlet orifice) and half of the seven grid spacers. The channel exits included the upper tie plate and the other half of the spacers. The channel loss coefficients are dominated by the lower tie plate orifice. The resulting coefficients are listed in Table 7 and despite their uncertainty, they should be adequate for these calculations.

Flow paths were included to simulate the recirculation pump suction lines, and the recirculation inlet nozzles during a double-ended break LOCA in a recirculation loop. The suction line flow path modeled two 24 inch OD lines of 10 m length which were always fully open. The inlet nozzles modeled twelve 10 inch OD lines and the header and pumps and were initially open but closed when the water level dropped below the nozzle entrance. A flow path with an area equal to reactor vessel cross sectional area was included to simulate the vessel with its upper head removed.

Emergency Core Cooling Systems During the low pressure LOCA calculations, ECCS was supplied to the core bypass control volume simulating LPCI. The FSAR (Table 5.4-2d) gives the flow rate per pump at 7620 gpm. These calculations involved either 1 or 2 pumps and the 2 pump flow was just double the 1 pump flow. The temperature of the injected water was 90 F which was the estimated suppression pool temperature. ECCS was not applicable to the boiloff calculation.

Vessel Heat Structures The reactor vessel heat structures in the LaSalle model were inserted unchanged into the Grand Gulf model. These heat structures were relatively unimportant to the objective of determining whether or not fuel damage would occur during these low decay power calculations.

Containment The containment was not modeled for these calculations. A large control volume was included to provide a dump for steam and water flows leaving the reactor vessel and to maintain a constant system pressure initialized at one atmosphere.

CALCULATION DESCRIPTIONS AND RESULTS

Boiloff Calculation

A simple boiloff calculation was run for Grand Gulf. This particular calculation used just one volume to model the core channels and the six ring course axial node core model. The upper head was removed, all piping remained intact, but all sources of cooling water to the core failed. The calculation was initialized at 4 days after the reactor was tripped with the water level just below the steam lines at an elevation of 635 inches and the vessel water temperatures were all initialized at 333.15 K (140 F). The initial water mass was 444,910 kg.

The boil-off results are illustrated by Table 8 which lists the timing of events during the calculation and in Figures 4 through 6 showing the

subcooled pool temperatures, the vessel water levels, and the second ring cladding temperatures during the fuel heating.

The first portion of the calculation involved heating the subcooled pools until boiling occurred. Natural circulation, with the heated core water rising and the colder downcomer water falling, tended to equilibrate the water temperatures. The first boiling occurred at 2.0 hours in the dome volume due to its lower pressure and saturation temperature. Before boiling occurred, 340 kg of water were evaporated from the pool surface. This initial boiling was at a relatively slow rate until the upper plenum volume saturated at 2.1 hours and then the boiling rate increased to the rate sustained throughout most of the boiloff.

The time for boiling to occur calculated with the level I analysis [5] was 1.8 hours. There were two significant differences between the two calculations. First, the level I calculation used a decay power that was about 22% greater than that used in the MELCOR calculation (the two decay power correlations came from different sources). Second, the level I calculation assumed that the initial water level was at the flange, whereas, in the MELCOR calculation, it was set to just below the steam lines. Thus, the level I calculation was initialized with about 13% more water than was done in the MELCOR calculation. When 1.8 hours is multiplied by 1.22 and divided by 1.13, the result is 1.94 hours which is in excellent agreement with the MELCOR result.

The first voiding within the core occurred at 10.5 hours. The initial voiding was small and unstable as steam was formed and then replaced by water from above. The collapsed water level, as measured in the downcomer volume, reached the top of the core and the top of the active fuel at 12.6 and 13.1 hours, respectively.

The level I calculation predicted that the time to boil the water to the top of the fuel was 13.8 hours. The major difference between the level I hand boiloff calculation and the MELCOR calculation was that the level I calculation boiled away 26% more water to reach the top of active fuel than did MELCOR. This was primarily due to the water level being initialized at the flange.

Convective cooling of the core continued after exposure. The downcomer water level reached the jet pump throats at 16 hours, after which the core water levels dropped faster because the water flow from the downcomer through the jet pumps ceased. A water pool continued to exist in the upper plenum until 16.1 hours, held in place by steam flows exiting the core.

The first fuel heating began in cell 212 (top fuel in second ring) at about 16.5 hours as the convective cooling decreased. The cladding oxidation began at about 18.8 hours as indicated when 0.0001 kg of hydrogen had been produced. About 2 minutes later, the hydrogen production had reached 1 kg. Cladding was modeled to fail and release radioactive fission products from the fuel when it reached 1173 K. The cladding failure criteria of 1173 K (900 C) was adapted from the CORSOR

code [6]. The first core cell cladding to reach this temperature was cell 211 (upper second ring) at 18.9 hours. Once oxidation began, the heating and damage to the core fuel progressed rapidly.

In conclusion, the more complex MELCOR calculation verified the hand calculation results for core uncovery and in addition provided an estimate of when initial fuel damage occurred. While the collapsed water reached the top of the active fuel at about 13.1 hours, the fuel did not begin to heat until about 16.5 hours with the onset of oxidation occurring at 18.8 hours.

Recirculation Pipe LOCA with One LPCI Pump

A low decay power shutdown LOCA was run involving the double-ended rupture of a pump suction pipe in a recirculation loop with ECCS provided by only one LPCI pump. The LPCI pumps water from the containment suppression pool into the core bypass region. The broken recirculation pipe allowed all the reactor vessel water above the jet pump throat to drain from the vessel leaving the upper 1/3 core exposed, without significant cooling, and subject to damage.

This calculation was run with 6 control volumes representing the core channels, i.e., one for each core ring. The upper head was removed, the recirculation loop flow paths simulating a LOCA were active, and the six ring fine node core model was used. The calculation was initialized at 4 days after the reactor was tripped with the water level initialized at the normal water level (569.7 inch), the vessel water temperatures at 333.15 K (140 F), and the LPCI water temperature at 305.37 K (90 F). The LPCI flow rate to the core bypass was 7620 gpm.

The reactor vessel water quickly (less than 3 minutes) drained from the vessel until the downcomer level dropped below the jet pump throats. The water levels, which are shown in Figure 7, then remained relatively stable for the remainder of the calculation. The average channel and the bypass levels remained about .1 m and .7 m, respectively, above the top of the jet pump throats. The core channel water levels did vary slightly from channel to channel due to their variation in water density but the maximum difference was not more than a few centimeters. After the initial transient was complete, none of the LPCI water over flowed the core from the bypass into the core channel. After the initial phase of the transient, the downcomer water level remained below the jet pumps and so had no effect on the core water levels.

Basically, the LPCI water entered the core bypass, flowed downward to the lower plenum, upwards through the jet pump diffusers into the downcomer and then out of the vessel. Only a small amount of water entered the core channels to replace water lost to steaming within the channels. The steaming rates were quite small (less than .04 kg/sec for the total core) and were due to pool surface evaporation which was enhanced by radiative heat transfer from the exposed core.

The 2/3 of the core under water was cooled by heat transfer to the pool within the fuel assemblies. This pool remained subcooled due to heat transfer through the channel boxes to the bypass pool. Thus, the only steam generated within the fuel assemblies was from pool surface evaporation. The core water temperatures are shown in Figure 8 along with the atmospheric saturation temperature and the LPCI injection temperature. The channel pools remained subcooled by about 17, 16, 17, 21, 33, and 48 K for core rings 1 through 6, respectively. The injected water was heated by about 5.5 K before flowing out of the vessel.

A code error affecting the pool temperatures as seen in Figure 8 became apparent at the onset of hydrogen generation at about 9000 seconds. The cooling of these pools at this time was unrealistic and the cause of the problem is unknown at this time. However, since the objective of the calculation was to determine whether or not fuel damage could occur and this error cooled the convective fluid and fuel damage was predicted anyway, this problem should not affect any of the study conclusions.

The core heating is shown in the next five figures. Figure 9 shows the cladding temperatures of ring 2 which had the highest power density and therefore the highest temperatures of all the rings. The cladding temperature for the cells at axial level 20 for each ring are shown in Figure 10. The cell component temperatures for cells 220, 218, and 214 are shown in Figures 11, 12, and 13, respectively.

The upper most core cells which did not have any fuel and therefore did not have any decay power heated only by convection heat transfer from the rising hot gases within the channels. The localized channel fluid temperatures (DTDZ model) closely followed the cladding temperatures as the gases rose within the core. The cladding temperature of cell 222 reached as high as 496 K.

The highest cladding temperature in the calculation was for cell 220 near the top of the core. Its final temperature was 1217 K. The cladding of this cell was predicted to reach 1173 K and fail at 9570 seconds (2.66 hours) which would have released the first cladding gap fission products at this time. There was sharp increase in this temperature at about 9000 seconds due to the energy released from cladding oxidation.

Cell 219, 220, and 221 in ring 2 continue to increase throughout the calculation and would continue to increase further, perhaps melting, if the calculation was continued. These cells were above the core water levels in both the core channels and the bypass. The component temperatures for cell 220 in Figure 11 show that all components heat together with even the control rod approaching structural failure (at roughly 1273 K).

Cells 215 through 218 were uncovered inside the fuel assemblies but the outside of the canisters were cooled by the cold bypass water. The component temperatures for cell 218 in Figure 12 illustrate the heat transfer associated with these cells. The exposed fuel rods temperatures peaked at about 722 and 717 K for the fuel and cladding. At these

temperatures, the heat transfer from the fuel rods to the colder canister became sufficient to prevent the rods from heating further. The cooling of these rods after the onset of oxidation was associated with increased convection heat transfer coefficients due to the addition of hydrogen to the control volumes. This increased the heat transfer rates to the colder canisters. The canister and control rods for cell 218 were cooled by the bypass water pool.

Cell 214 was partially covered by water within the fuel assemblies. Cells 206 through 214 were all kept cooled. The component temperatures for cell 214 in Figure 13 show that the fuel rods peaked at about 362 K and the canisters at about 334 K. The heat generated within the fuel rods was transferred to the water within the fuel assemblies and then conducted through the canisters to the colder bypass water. The heat transfer through the canisters was sufficient to keep the water within the assemblies subcooled. These cells cooled after the onset of cladding oxidation because the pool temperatures were decreasing unrealistically due to the unknown code error discussed above.

Cladding oxidation is illustrated by the production of hydrogen as shown in Figure 14. The oxidation began at about 9010 seconds (2.50 hours). The convection heat transfer coefficient for a section of the core shroud is shown in Figure 15 along with bypass hydrogen mole fraction.

Recirculation Pipe LOCA with Two LPCI Pumps

A low decay power shutdown LOCA was run involving the double-ended rupture of a pump suction pipe in a recirculation loop with ECCS provided by two LPCI pumps. The LPCI pumps water from the containment suppression pool into the core bypass region. The broken recirculation pipe allowed all the reactor vessel water above the jet pump throat to drain from the vessel leaving the upper 1/3 core exposed, without significant cooling, and subject to damage. The initialization of this calculation was identical to the one pump calculation except that the LPCI flow rate to the core bypass was 15240 gpm.

The water levels for the two pump calculation are shown in Figure 16. The bypass volume completely filled and over flowed into core channel with the average channel level remaining about .24 m above the top of the jet pump throats. After the initial transient was complete, about 24% of the LPCI water over flowed the core from the bypass into the core channel. The downcomer water level remained below the jet pumps and so had no effect on the core water levels. The water that over flowed the core into the channels flowed downwards through the fuel assemblies and into the lower plenum. Core channel evaporation was very minor.

The 2/3 of the core under water was cooled by heat transfer to the pool within the fuel assemblies. This pool remained subcooled due to the bypass over flow and to heat transfer through the channel boxes to the bypass pool. The channel pools remained subcooled by about 57, 57, 57, 58, 61, and 64 K for core rings 1 through 6, respectively. The injected

water was heated by only 1.0 K within the bypass and by about 3.0 K before flowing out of the vessel.

The core heating is shown in the next four figures. Figure 17 shows the cladding temperatures of ring 2 which had the highest power density and therefore the highest temperatures of all the rings. The cladding temperature for the cells at axial level 17 for each ring are shown in Figure 18. The cell component temperatures for cells 217, and 214 are shown in Figures 19, and 20, respectively.

The highest temperatures in this calculation were 691 and 685 K for the fuel and cladding of cell 217 as shown in Figure 19. Since the bypass over flowed the core in this calculation, all of the fuel assembly canisters were cooled which limited the fuel rod heating even for the uncovered cells.

Cell 214 was covered by water within the fuel assemblies. Cells 206 through 215 were all kept cooled. The component temperatures for cell 214 in Figure 20 show that the fuel rods peaked at about 319 K and the canisters at about 311 K. These cells were cooled by both the water over flowing the top of the core and by conduction through the canisters to the colder bypass water.

The temperatures of this calculation were over predicted because MELCOR lacks the fuel rod film model needed for calculating the heat transfer to the water running down the fuel rods from the bypass core over flow. Therefore, the actual fuel rod cooling would have been much greater than calculated. However, the temperatures predicted in this calculation did not even approach either the cladding failure temperature or the temperature needed to initiate oxidation. No hydrogen was produced and fuel damage was not predicted.

UNCERTAINTY DISCUSSION

Flow Loss Coefficients

The reverse bypass inlet and the reverse jet pump loss coefficients were major uncertainties in determining whether or not the core bypass water level over flowed the top of the core into the fuel assemblies. Core damage will generally be prevented if water over flows the top of the core into the fuel assemblies. The coefficients used in these calculations represent a reasonably good estimate considering the lack of data required to compute accurate numbers but uncertainty still exists. Therefore, a parameter study was performed to determine the sensitivity of the bypass water level to these coefficients.

The bypass water level is shown in Figure 21 as a function of the reverse bypass inlet coefficients at three different jet pump coefficients and at LPCI flow rates corresponding to 1 and 2 operating pumps. The bypass inlet coefficient ranges from zero to a number sufficient to cause the bypass to over flow the core. The jet pump coefficient values are 0, 1, and 5 for the unknown throat exit number plus 0.0531 calculated for flow

into and through the diffuser. Also marked in the figure are levels for the jet pump throat exit, the top of the active fuel, and the top of the fuel assembly canisters. The bypass water level for the base case coefficients used in these calculations was .7 m above the jet pumps.

The bypass inlet coefficient would need to be more than a factor of two higher to force the flow from just one pump over the top of the core and it would have to be reduced by 40% or more to prevent the flow from two pumps from going over the top. The FSAR shows nine different paths for water to flow from the lower plenum to the core bypass. If one attempts to estimate the flow area of the lower tie plate holes and leakage between parts and treat this area as an orifice in a channel with the bypass flow area, a range of coefficients can be calculated which includes the base case coefficient. While it is not possible to prove with the limited available Grand Gulf data, it unlikely that one operating LPCI pump will prevent fuel damage and it is very likely that two pumps will.

Fuel Bundle Center Peaking

MELCOR calculates cell average temperatures which is appropriate to calculating the heating of a fully uncovered core. But for conditions encountered during these calculations where the dominate heat transfer was to a cooled canister, center bundle temperature peaking is a concern.

When a core cell was uncovered within the fuel assembly but the bypass was water filled, the heat transfer from the fuel rods to the canister has a radiative heat transfer component. The center bundle fuel rods are shielded from the canister by the outer rods and their temperatures would be higher than the outer rods. The input fuel-to-canister radiative exchange factor could also be considered an uncertainty factor. The question is how much higher is the peak temperatures than the bundle average temperature.

When a core cell was completely covered by water both inside and outside the canister, the fuel rods were cooled by a subcooled pool. Water near the inner rods would have been hotter than the pool average and possibly boiling could have occurred locally where it was not predicted by the volume average temperature. This would have enhanced the convective cooling of the upper exposed fuel.

Decay Power

The normalized time dependent decay power distribution used in these calculations was developed for the LaSalle plant and is another uncertainty in the results. Using a higher powered decay heat curve or initiating the calculation earlier would increase the predicted temperatures.

Some fuel assemblies had higher power factors than their associated ring averages (the highest was 1.232). Therefore, some fuel assemblies will heat to higher temperatures than predicted in these calculations.

Further, certain fuel rods within a particular fuel assembly have higher power densities than the assembly averages.

Nodalization

Higher temperatures may have been predicted with finer nodalization. For instance, finer control volume nodalization within the exposed core would have created cells with higher power densities resulting in higher temperature predictions. Finer control volume nodalization within the subcooled pool would have predicted portions of the pool with less subcooling and localized boiling would then have been more probable.

CONCLUSIONS

The more complex MELCOR boiloff calculation verified the results of the level I hand calculation for the time of core uncovery and in addition provided an estimate of the onset of fuel damage. While the collapsed water level reached the top of the active fuel at about 13.1 hours, the fuel did not begin to heat until about 16.5 hours with the onset of oxidation at 18.8 hours.

The MELCOR low decay power LOCA (recirculation loop pipe break) calculations predicted severe fuel damage with cladding oxidation beginning at about 2.5 hours if only one LPCI pump operated and no fuel damage if two pumps operated. Although uncertainties exist in these calculations, core damage will generally be prevented if water over flows the top of the core into the fuel assemblies. The loss coefficient sensitivity study generally showed that it is unlikely that one operating LPCI pump will over flow the top of the core but that it is likely that two pumps will.

REFERENCES

1. R. M. Summers, et. al., MELCOR 1.8.0: A Computer Code for Severe Nuclear Reactor Accident Source Term and Risk Assessment Analysis, NUREG/CR-5531, SAND90-0364, Sandia National Laboratories, January, 1991.

2. S. E. Dingman, et. al., MELCOR Analyses for Accident Progression Issues, NUREG/CR-5331, SAND89-0072, Sandia National Laboratories, January, 1991.

3. C. J. Shaffer, et. al., Integrated Risk Assessment for the LaSalle Unit 2 Nuclear Power Plant: Phenomenology and Risk Uncertainty Evaluation Program (PRUEP), Volume 3: MELCOR Code Calculations, NUREG/CR-5305/3 of 3, SAND90-2765, RX, Sandia National Laboratories, DRAFT, December, 1990.

4. Updated Final Safety Analysis Report, Grand Gulf Nuclear Station.

5. John Darby, Thermodynamic Calculations for Grand Gulf, Work Sheet SEA C90-492-001-A:2, February 15, 1991.

6. M. R. Kuhlman, et. al., CORSOR User's Manual, NUREG/CR-4173, BMI-2122, Battelle Columbus Laboratories, March, 1985.

Table 1: Six Ring Core Model Data

Ring Number	Number of Assemblies	Outer Radius (ft)	Volume Fraction	Power Fraction	Power Factor
1	112	3.	.140	.1608	1.149
2	204	5.	.255	.2996	1.175
3	132	6.	.165	.1908	1.156
4	168	7.	.210	.2194	1.045
5	100	7.5	.125	.0923	.738
6	84	8.	.105	.0371	.353

Table 2a: Course Axial Power Distribution Model

Cell Number	Cell Height (m)	Volume Fraction	Power Fraction	Power Factor
13	.3591	.08170	0.	0.
12	.6350	.14446	.1069	.7400
11	.6350	.14446	.1648	1.1409
10	.6350	.14446	.1828	1.2655
9	.6350	.14446	.1936	1.3403
8	.6350	.14446	.2000	1.3846
7	.6350	.14446	.1519	1.0516
6	.2268	.05160	0.	0.

Table 2b: Fine Axial Power Distribution Model

Cell Number	Cell Height (m)	Volume Fraction	Power Fraction	Power Factor
22	.3591	.08169	0.	0.
21	.15875	.03611	.0152	.4209
20	.15875	.03611	.0244	.6757
19	.15875	.03611	.0316	.8751
18	.15875	.03611	.0357	.9886
17	.15875	.03611	.0385	1.0662
16	.15875	.03611	.0401	1.1105
15	.15875	.03611	.0425	1.1770
14	.15875	.03611	.0437	1.2102
13	.15875	.03611	.0445	1.2323
12	.15875	.03611	.0453	1.2545
11	.15875	.03611	.0461	1.2767
10	.15875	.03611	.0469	1.2988
9	.6350	.14446	.1936	1.3402
8	.6350	.14446	.2000	1.3845
7	.6350	.14446	.1519	1.0515
6	.2268	.05161	0.	0.

Table 3: Fuel Assembly and Control Rod Masses

Material	Fuel Assembly Each	Fuel Assembly Total	Control Rod Each	Control Rod Total
UO_2	458.0	366400	0	0
Zr	224.7	179760	0	0
Steel	16.3	13040	203.7	39314
B_4C	0	0	14.3	2760
Total	699.0	559200	218.0	42074

Table 4: Reactor Vessel Control Volumes

Volume Description	Volume (ft^3)	Volume (m^3)	Elevation Lower (m)	Elevation Upper (m)
Lower Plenum	3814.6	108.03	0.	8.0936
Downcomer	6935.6	196.42	3.5462	15.4304
Core - Channels	1304.7	36.95	5.2672	9.6630
Core - Bypass	1086.8	30.78	5.2672	9.6630
Upper Plenum & Separators	2280.4	64.58	9.6630	15.4304
Dryers & Steam Dome	6759.9	191.44	15.4304	22.2493
Total	22182.0	628.20		

Table 5: Reactor Vessel Flow Paths

Description	Elevations From (m)	Elevations To (m)	Loss Coefficients Forward	Loss Coefficients Reverse	Flow Area (m^2)
Core Channel Inlet	5.267	5.267	21.81	29.64	7.861
Core Bypass Inlet	5.267	5.267	1338.	1637.	5.528
Core Channel Outlet	9.663	9.663	9.13	9.37	7.861
Core Bypass Outlet	9.663	9.663	446.	546.	5.528
Separators	15.43	15.43	9.1	2.8	3.318
Dome to Downcomer	15.43	15.43	1.	1.	13.9
Separator Drains	13.1	13.1	3.	3.	3.2
Jet Pump Diffusers	8.064	3.459	.178	1.0531	.4981[a]
Upper Head	19.4	19.4	1.	1.	31.9
Recir Pump Suction	4.377	-5.7	2.	2.	.4576[b]
Recir Inlet Nozzle	8.750	-5.7	350.	350.	.4995[c]

a - throat area
b - two 24 inch nominal O.D. pipes
c - twelve 10 inch nominal O.D. pipes

Table 6: Jet Pump Flow Data

Parameter	Unit	Throat Segment	Diffuser Segment	Extension Segment	Totals
Individual Area [a]	m^2	.0208	.0564[b]	.110	
Total Area	m^2	.498	1.35	2.63	
Lower Elevation[c]	m	6.18	4.23	3.49	
Length	m	1.86	1.95	.740	4.54
Hydraulic Diameter	m	.163	.268	.373	
Surface Roughness	m	7.6E-7	7.6E-7	7.6E-7	
Loss Coefficients[d]					
Forward		.05[e]	.092[f]	.036[g]	.178
Reverse		.018[h]	.035[i]	1.[j]	1.053

a - 24 Individual Pumps
b - based on average diameter
c - top throat elevation estimated at 8.03 m
d - Ref. Crane and adjusted to throat area (i.e., d_1^4/d_2^4)
e - rounded protruding entrance
f - expansion (Crane, page A-26, formula 3)
g - pipe exit to reservoir (nominal 1.)
h - right angle entrance flush with wall (nominal .5)
i - contraction (Crane, page A-26, formula 1)
j - exit into empty reservoir with an obstruction (judgement)

Table 7: Core Loss Coefficients

	Forward	Reverse
Channel Inlet	21.8	29.6
Channel Outlet	9.1	9.4
Bypass Inlet	1340	1640
Bypass Outlet	450	550

Table 8: Boil-Off Calculation Event Times

Event	Event Times Seconds	Minutes	Hours
On-Set of Boiling	7050	119	2.0
Rapid Boiling	7510	125	2.1
Core Cavitation	37920	632	10.5
Core Uncovery (Collapsed)	45392	757	12.6
TAF Uncovery (Collapsed)	47014	784	13.1
Jet Pump Throat Uncovered	57600	960	16.0
Upper Plenum Water Exhausted	57800	963	16.1
On-Set of Fuel Heating	59410	990	16.5
On-Set of Oxidation	67730	1129	18.8
1 kg of Hydrogen	67872	1131	18.9
First Fission Product Release	68034	1134	18.9

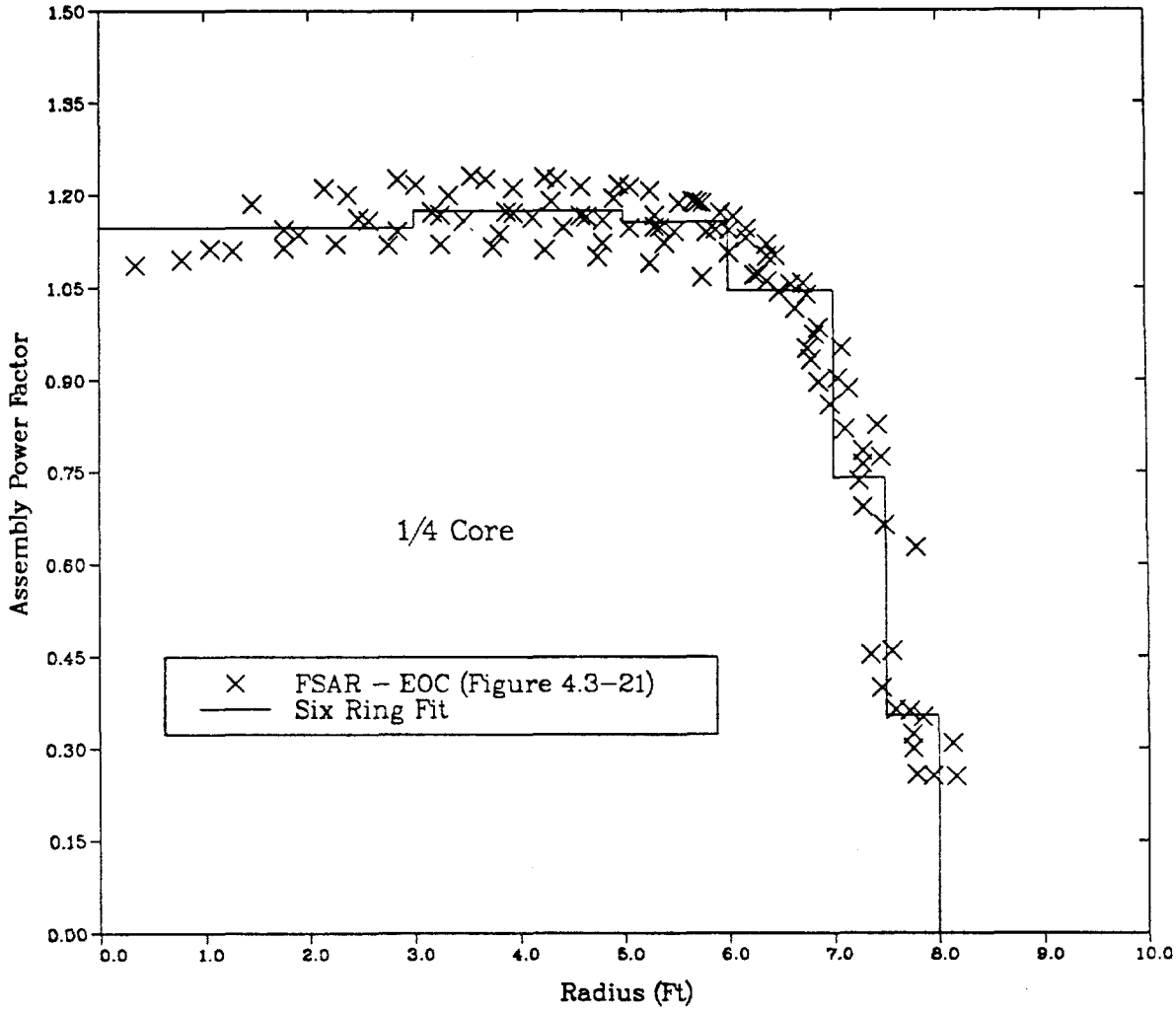

Figure 1: Grand Gulf Radial Power Factors

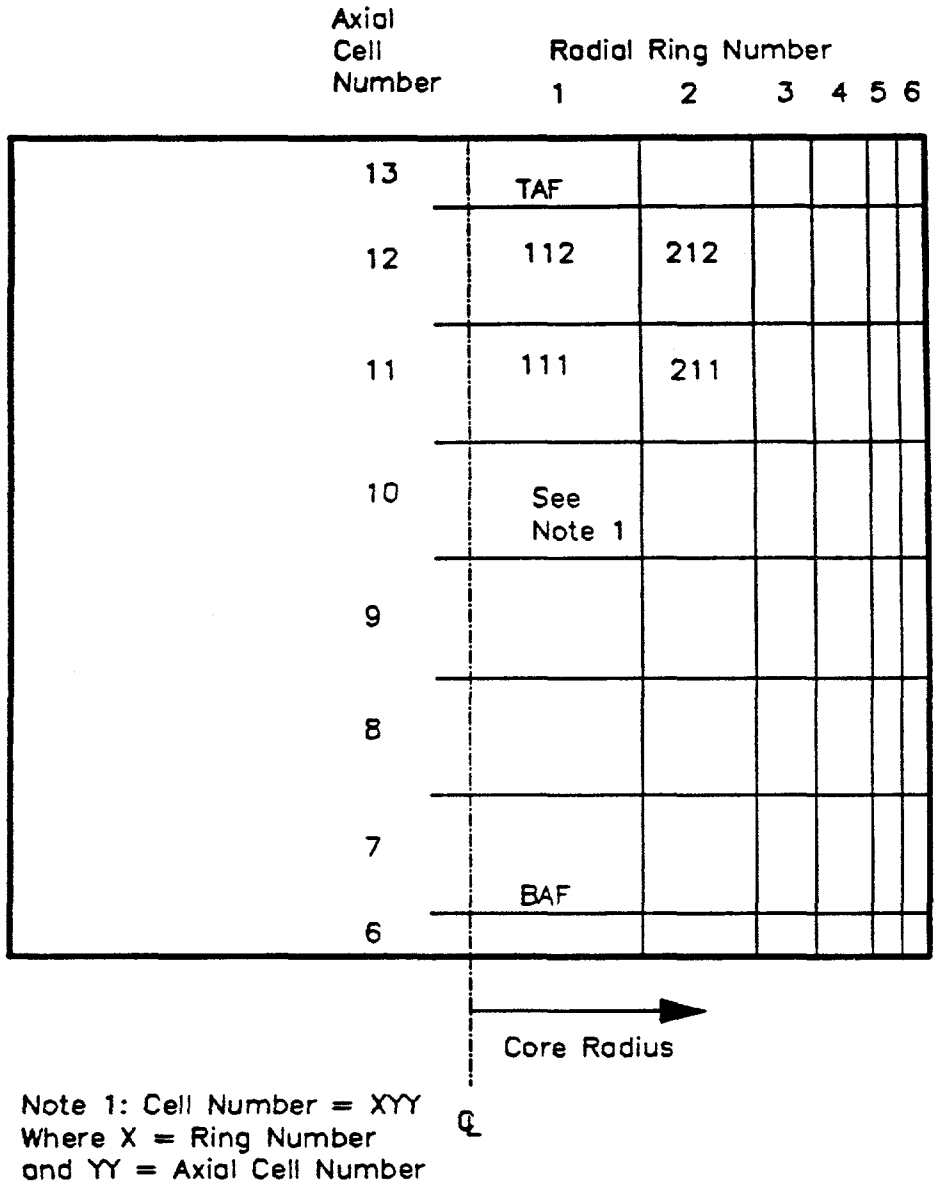

Figure 2

Six Ring Course Node Core Model

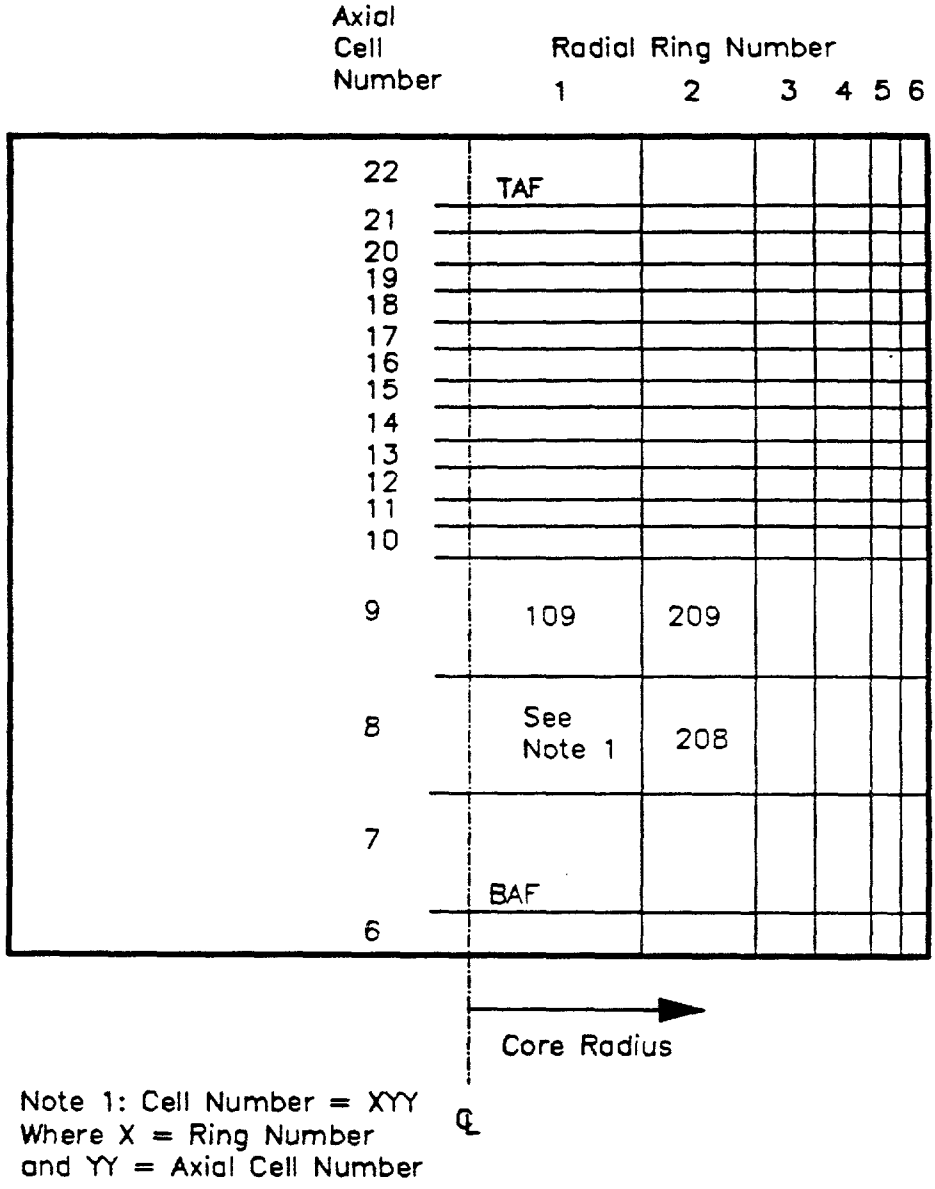

Figure 3

Six Ring Fine Node Core Model

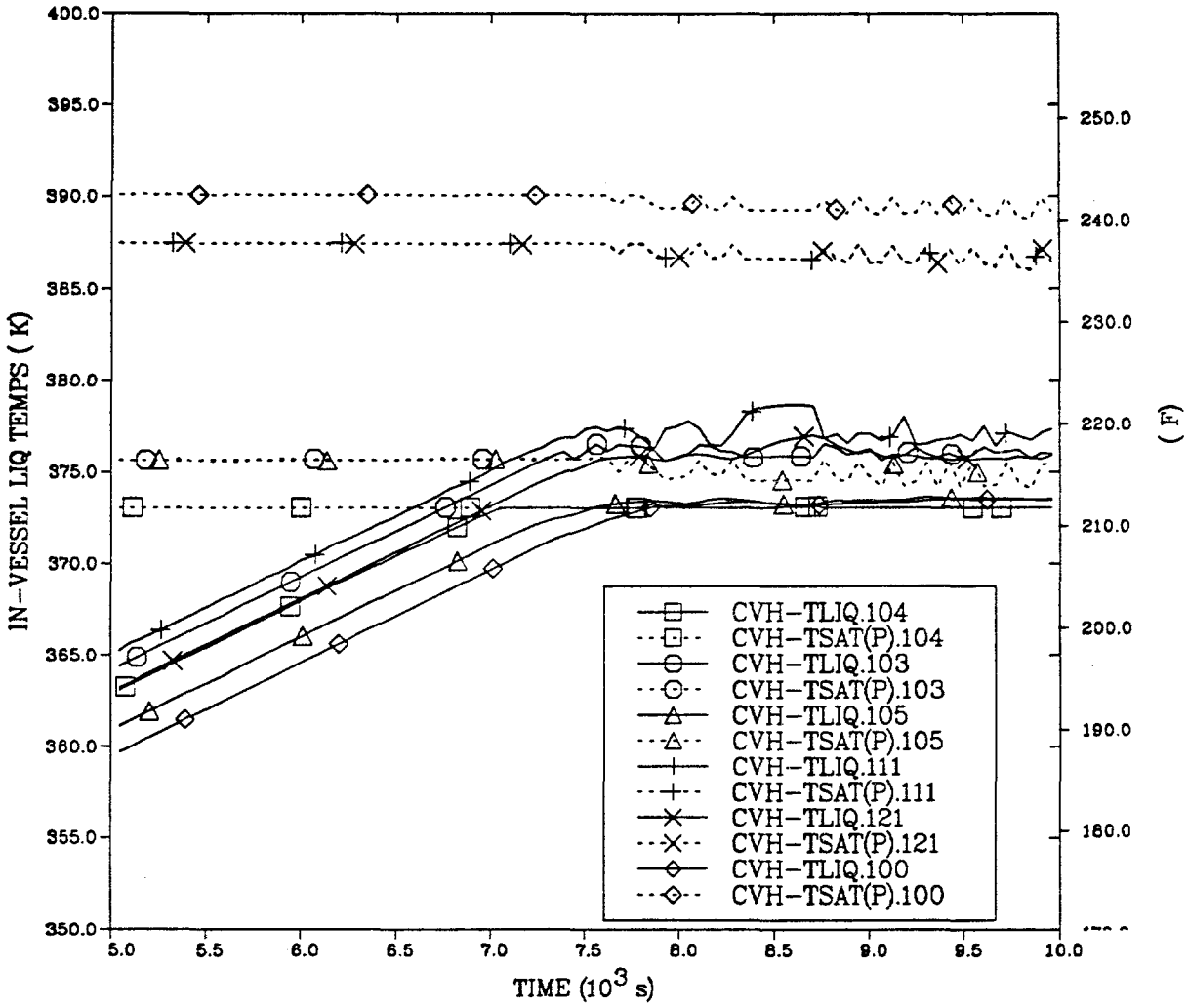

Figure 4: Pool and Saturation Temperatures

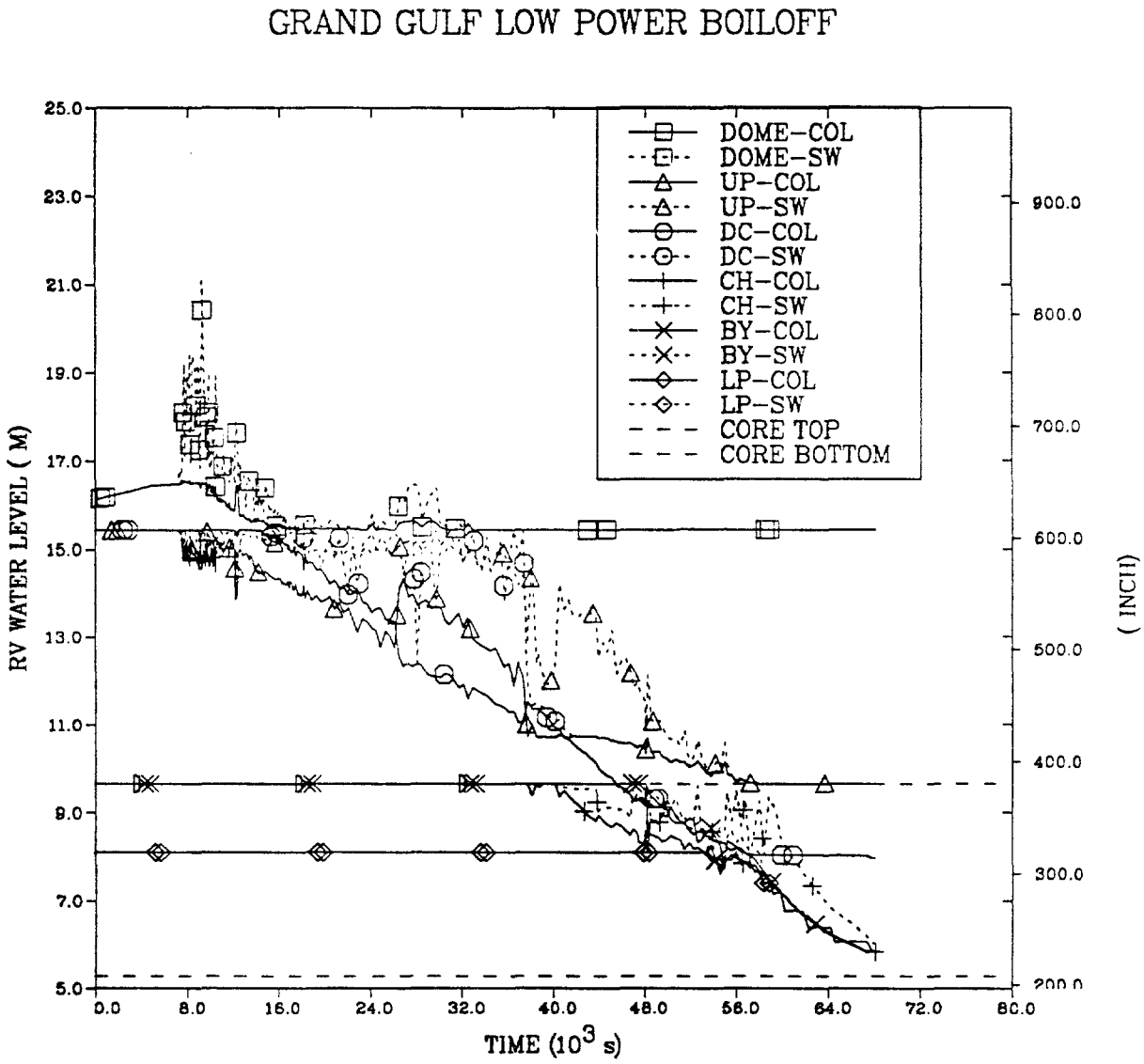

Figure 5: Collapsed and Swollen Water Levels

GRAND GULF LOW POWER BOILOFF

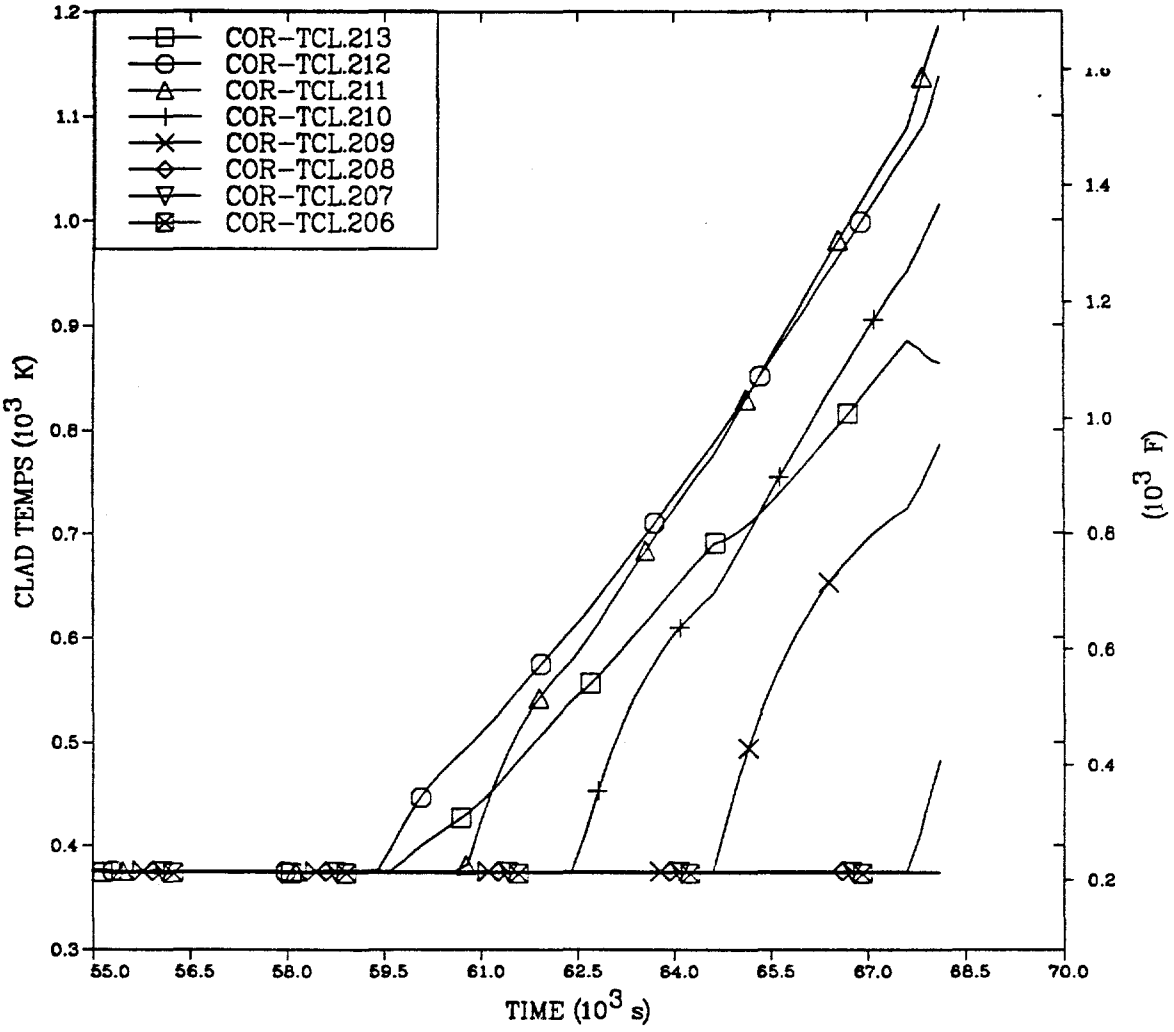

Figure 6: Second Ring Cladding Temperatures

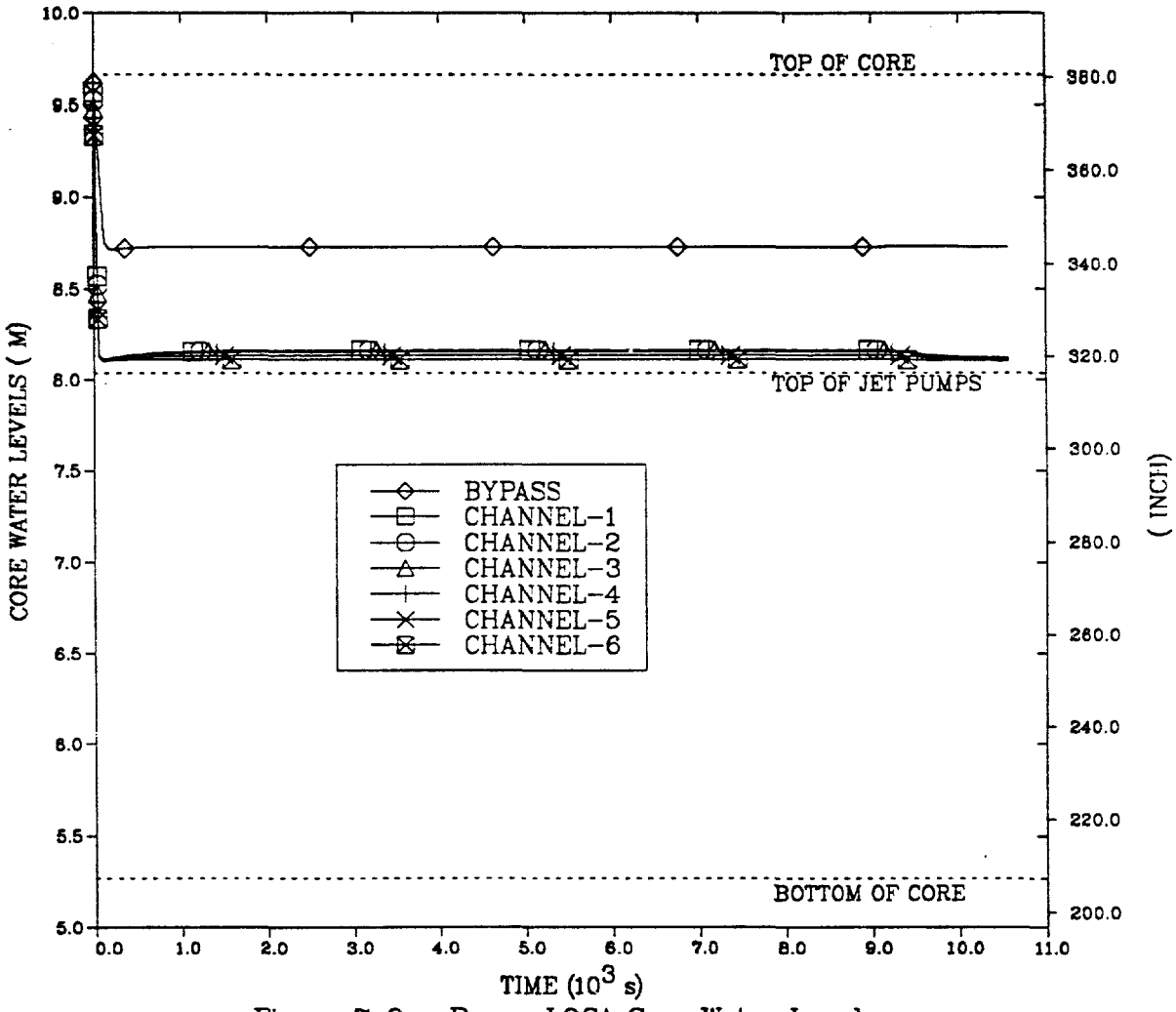

Figure 7: One Pump LOCA Core Water Levels

GRAND GULF LOW POWER LOCA ACCIDENT

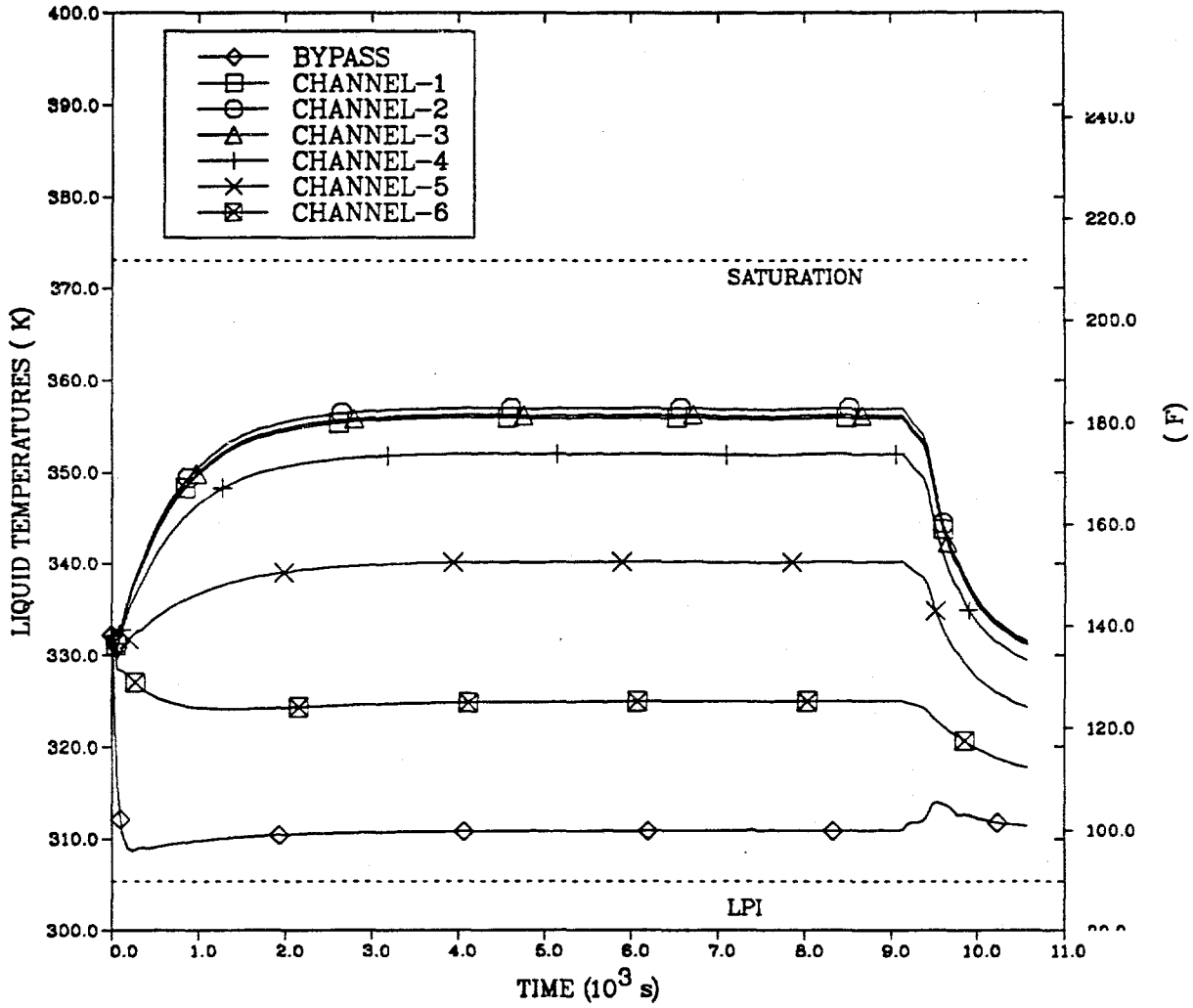

Figure 8: One Pump LOCA Water Temperatures

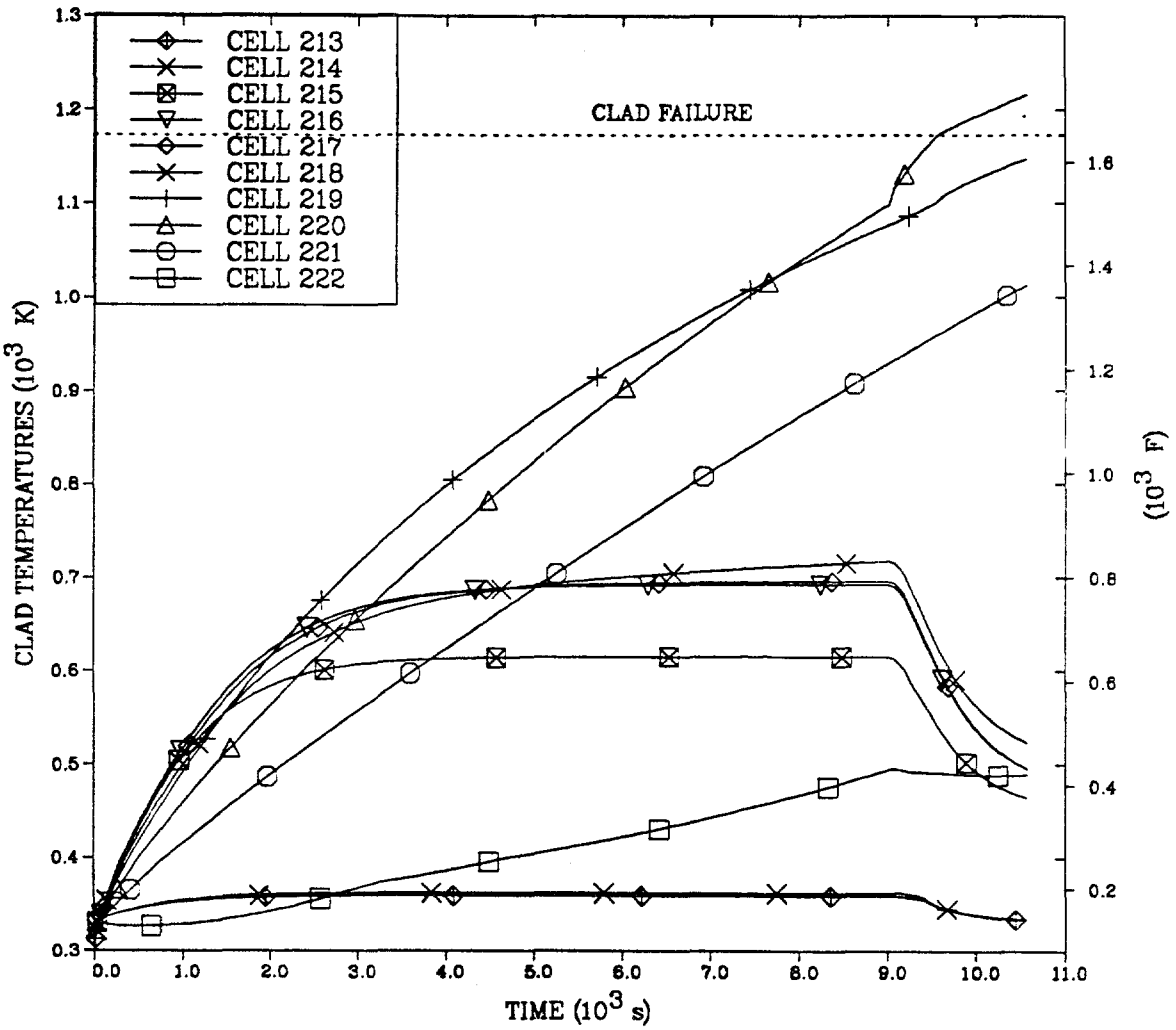

Figure 9: Second Ring Clad Temperatures

GRAND GULF LOW POWER LOCA ACCIDENT

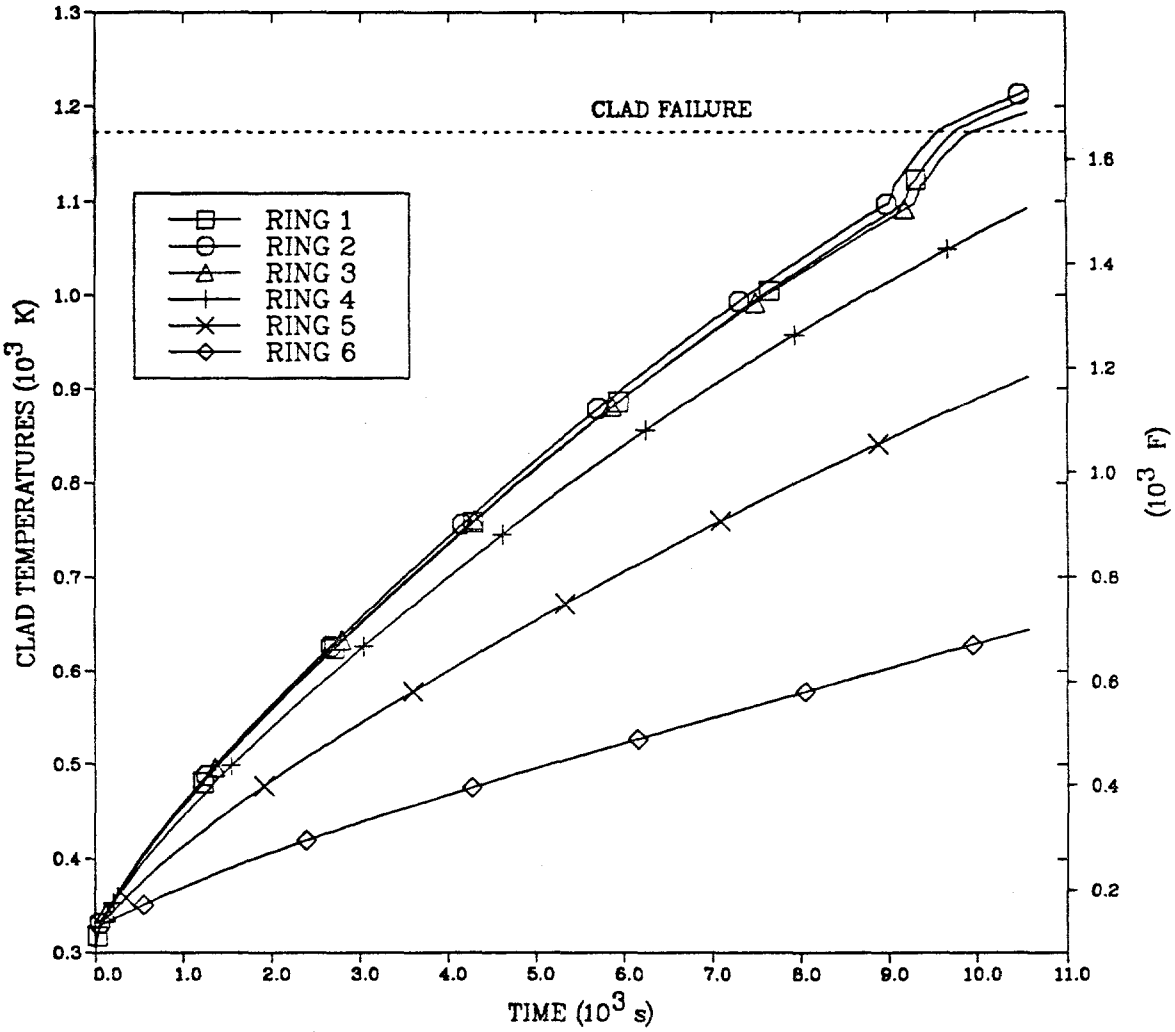

Figure 10: Axial Level 20 Clad Temperatures

GRAND GULF LOW POWER LOCA ACCIDENT

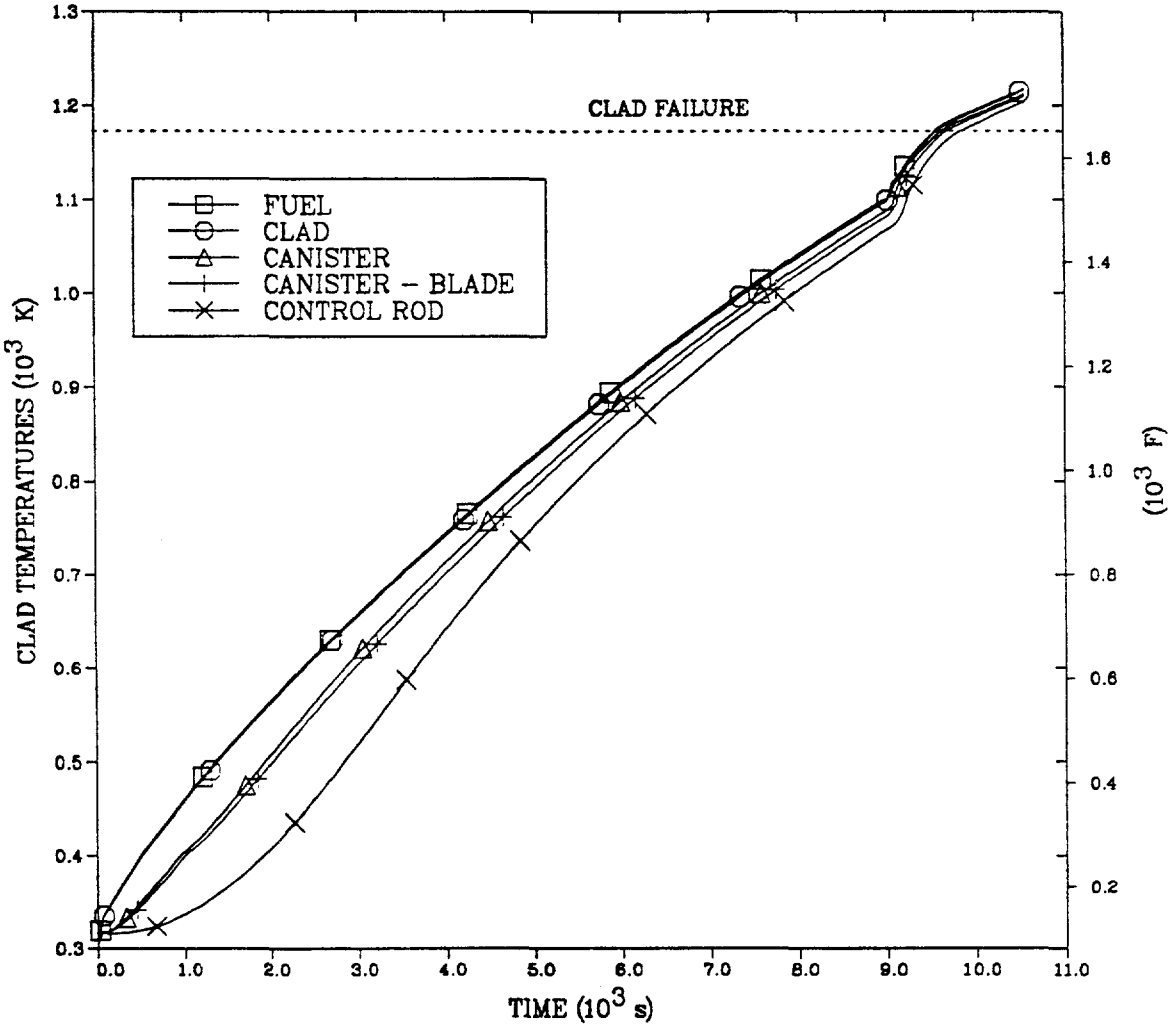

Figure 11: Cell 220 Temperatures

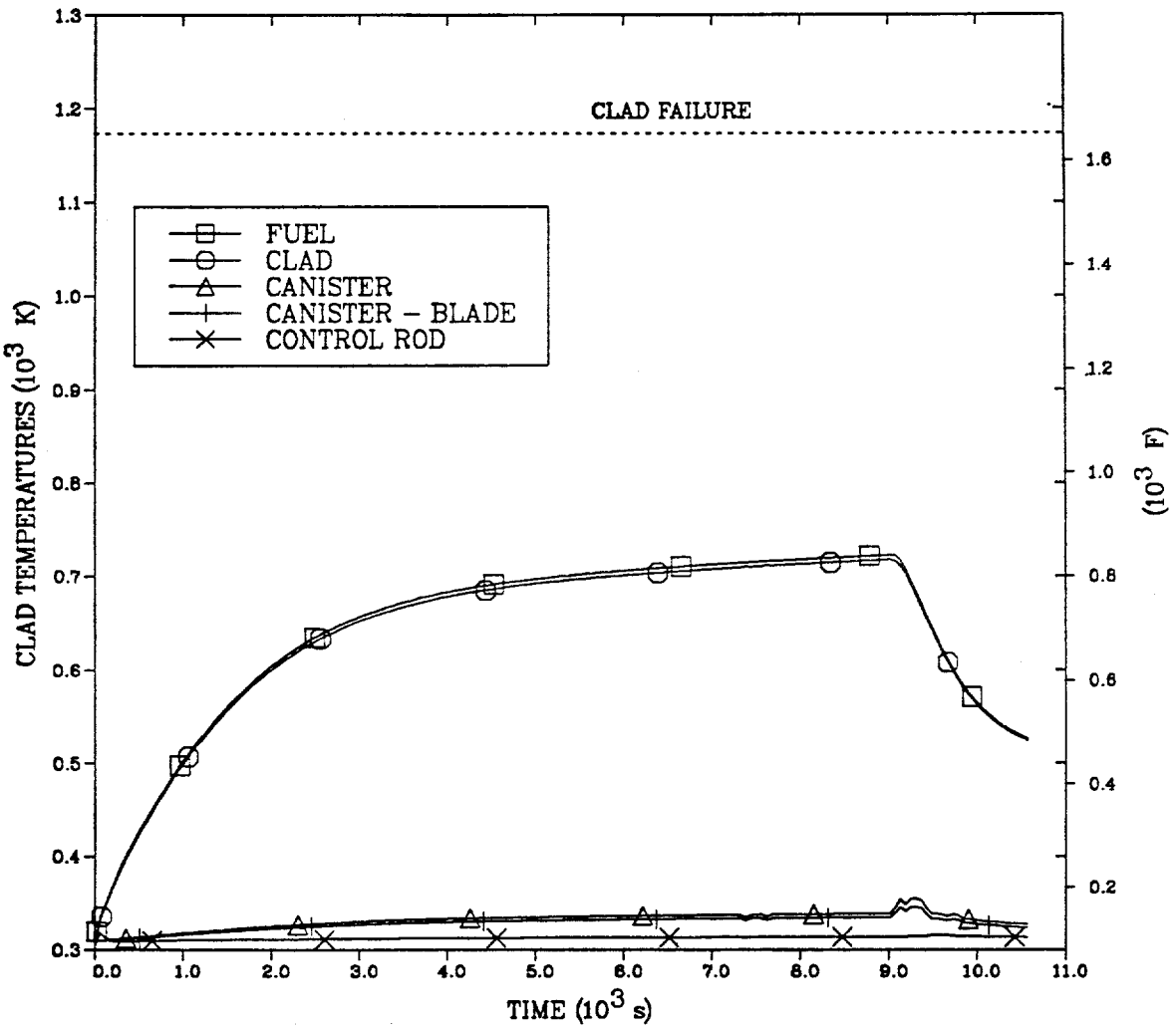

Figure 12: Cell 218 Temperatures

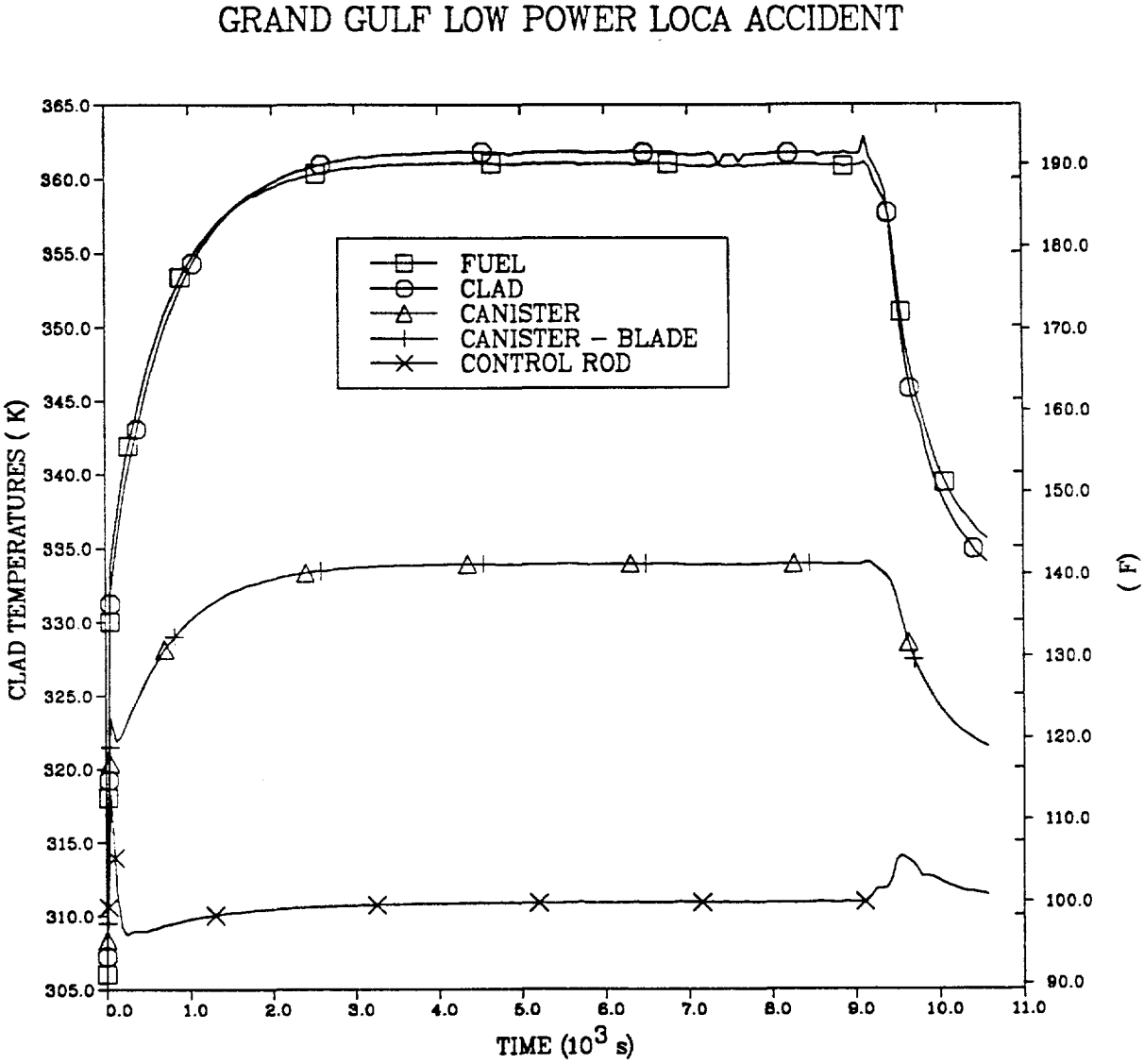

Figure 13: Cell 214 Temperatures

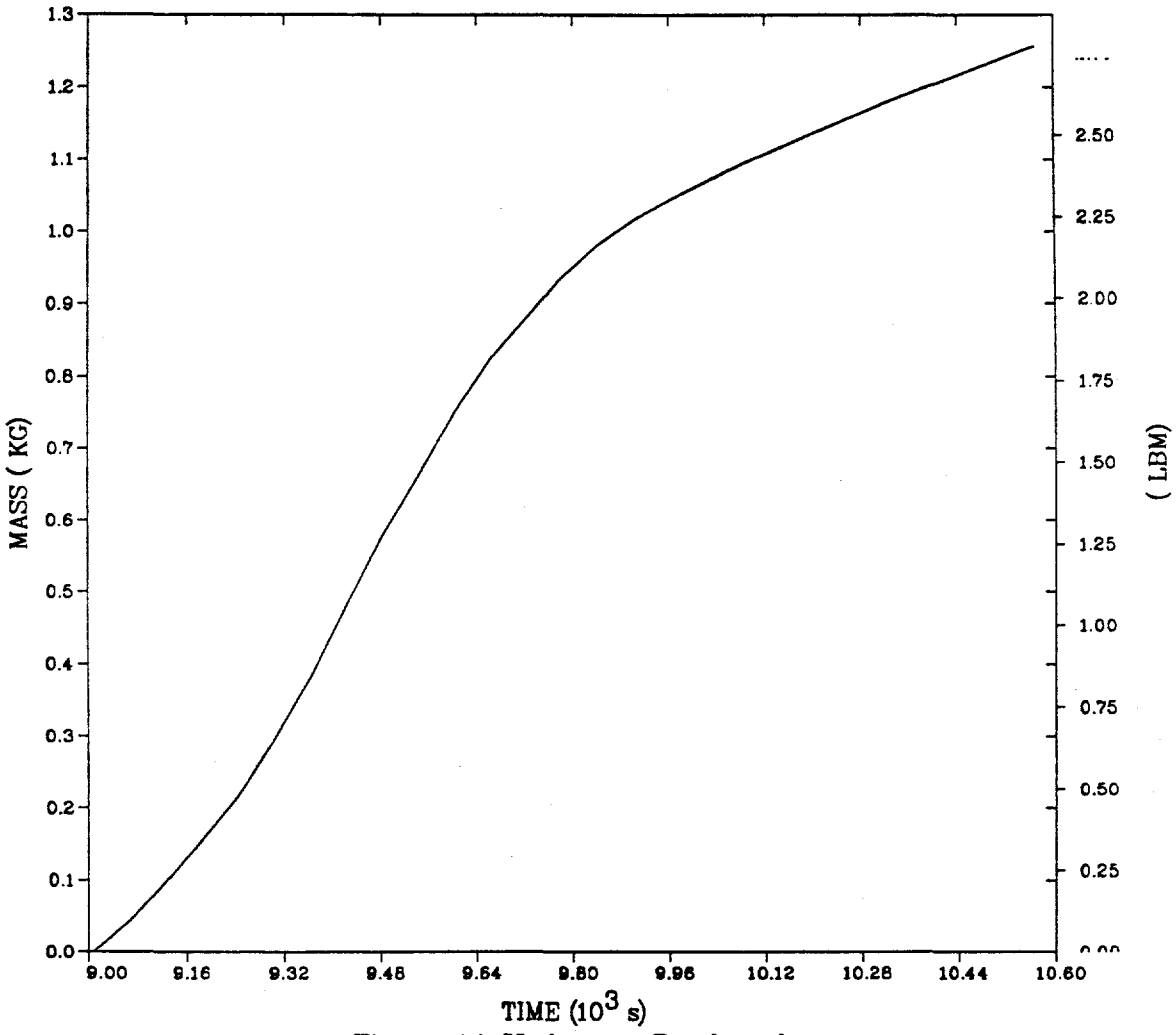

Figure 14: Hydrogen Produced

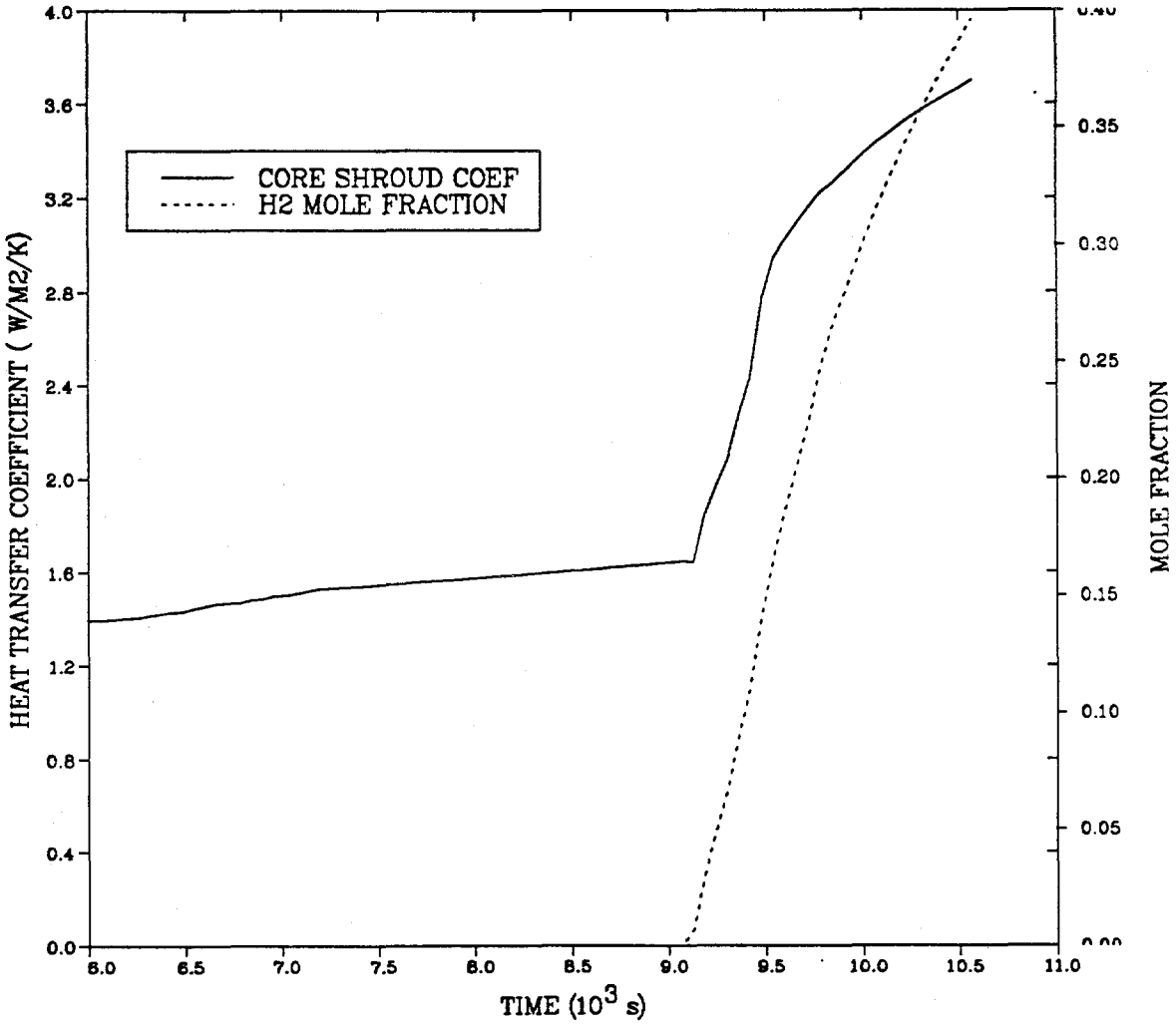

Figure 15: Hydrogen Effect on Convection Heat Transfer

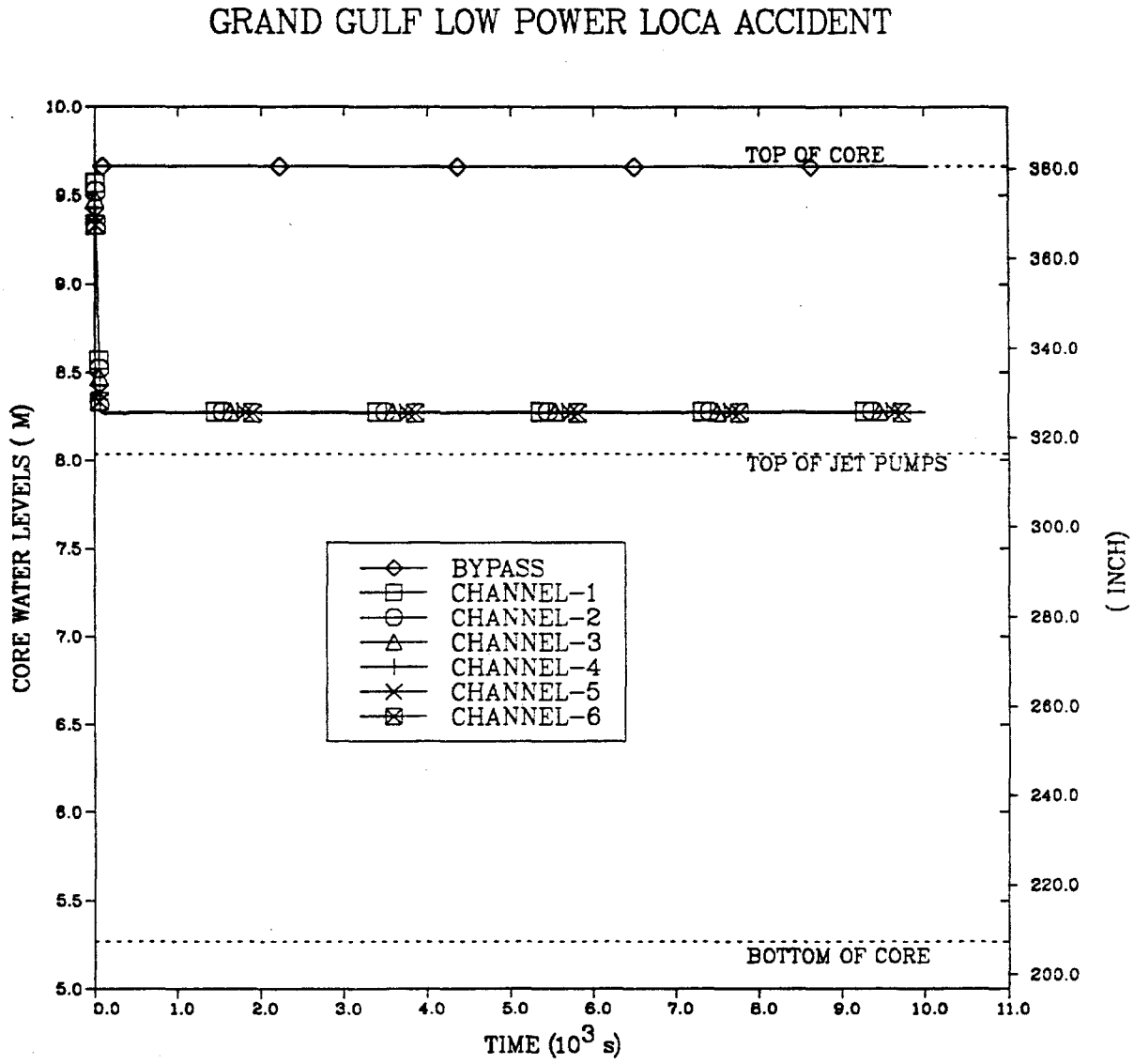

Figure 16: Two Pump LOCA Core Water Levels

GRAND GULF LOW POWER LOCA ACCIDENT

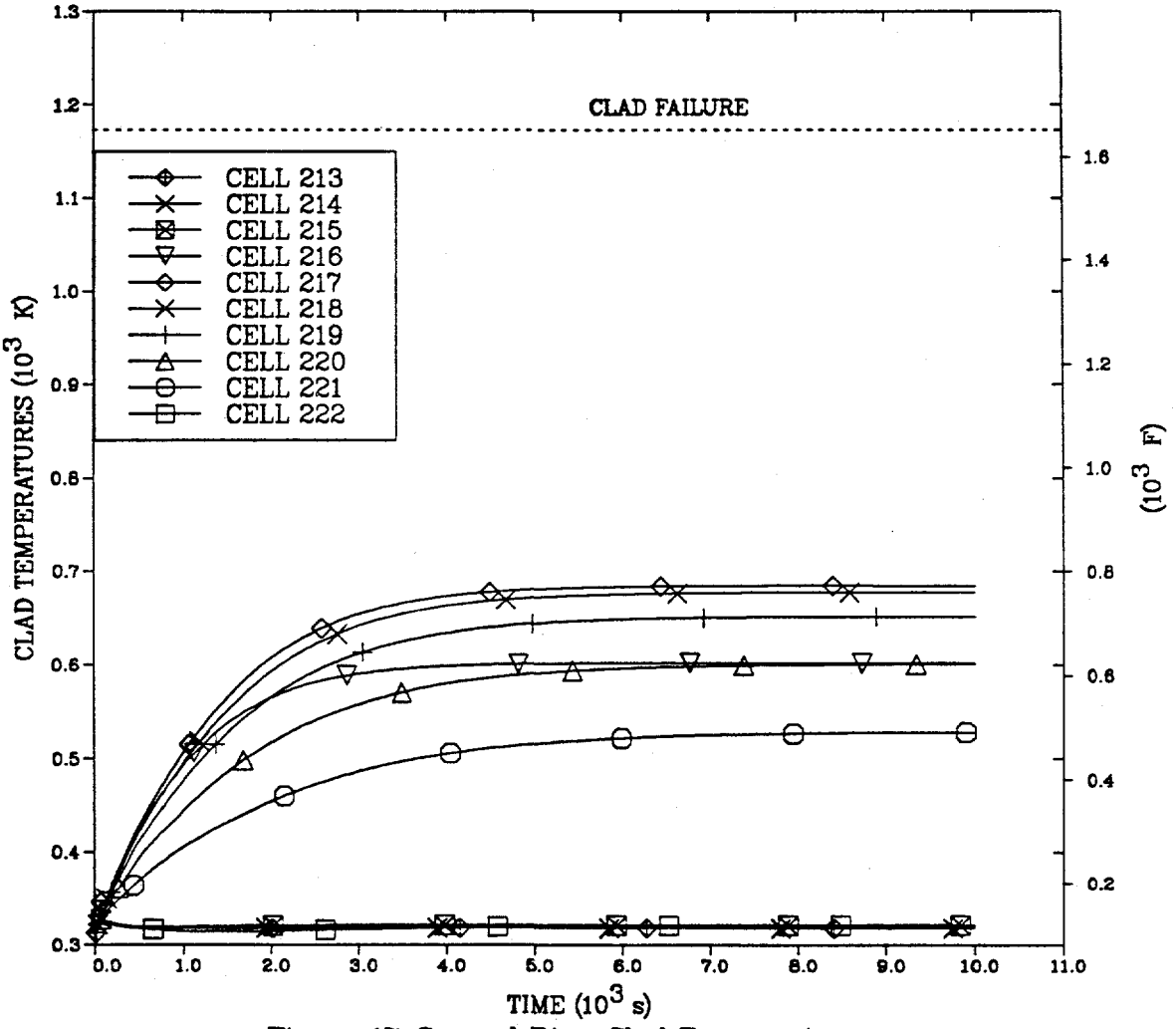

Figure 17: Second Ring Clad Temperatures

GRAND GULF LOW POWER LOCA ACCIDENT

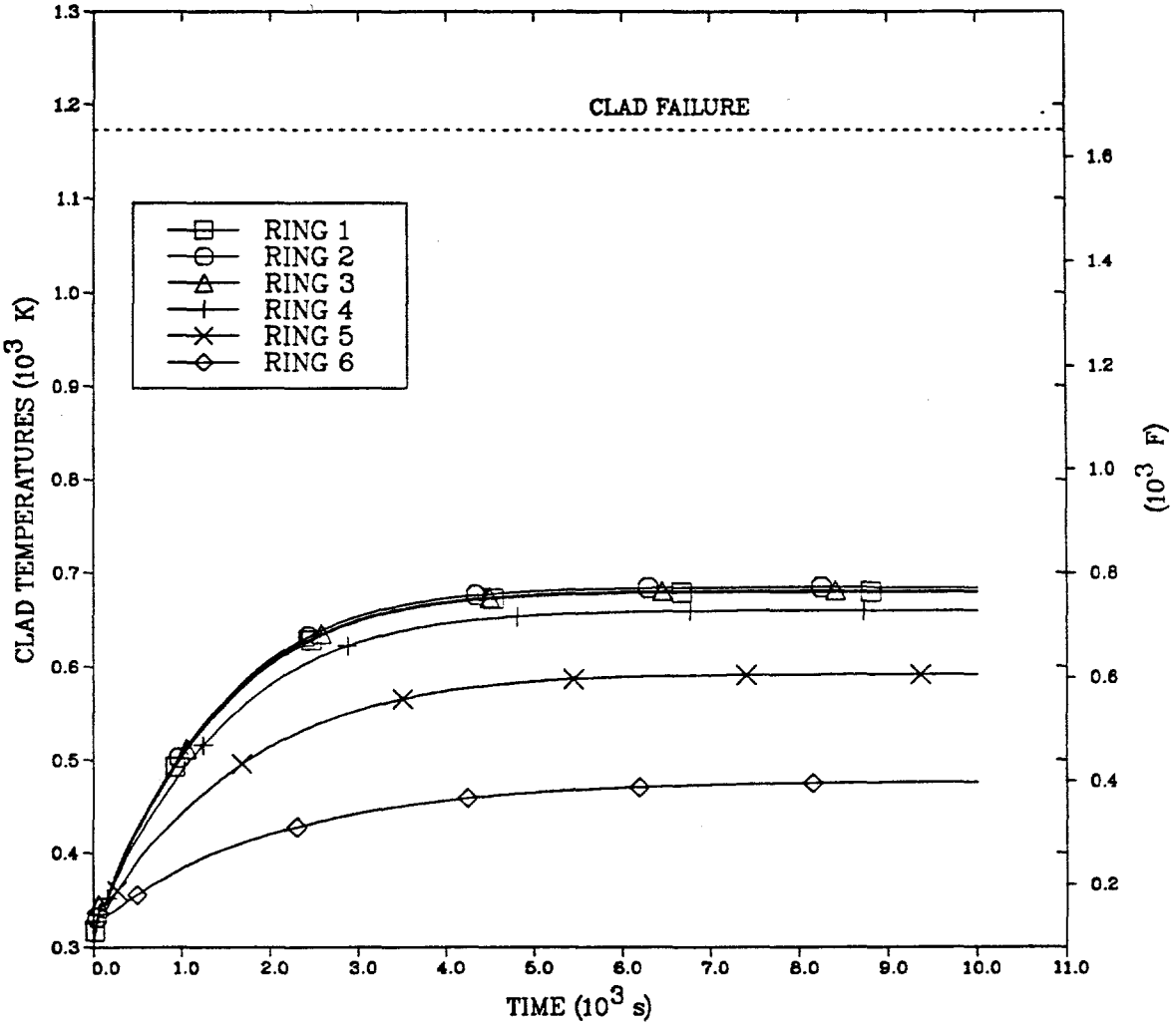

Figure 18: Axial Level 17 Clad Temperatures

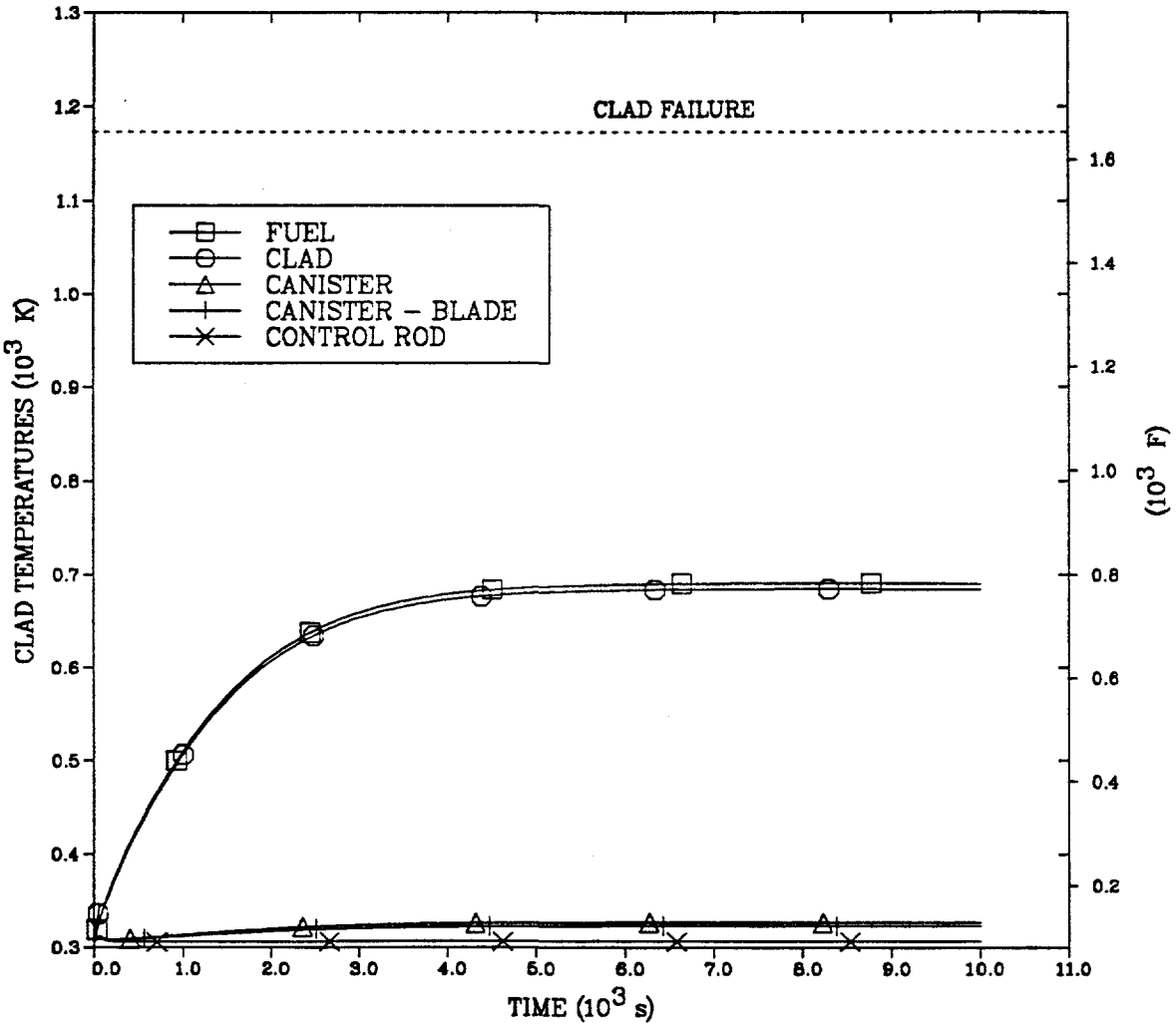

Figure 19: Cell 217 Temperatures

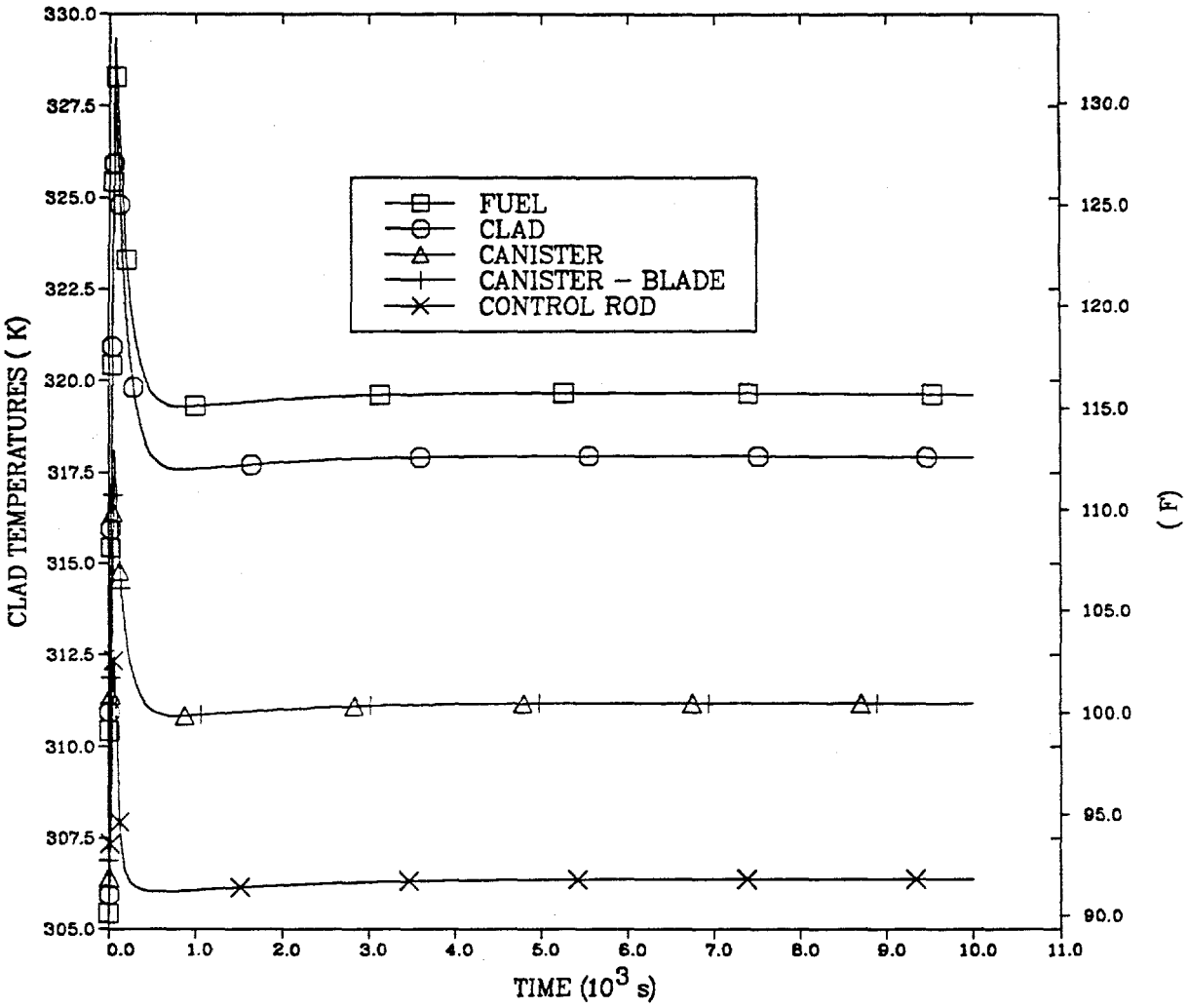

Figure 20: Cell 214 Temperatures

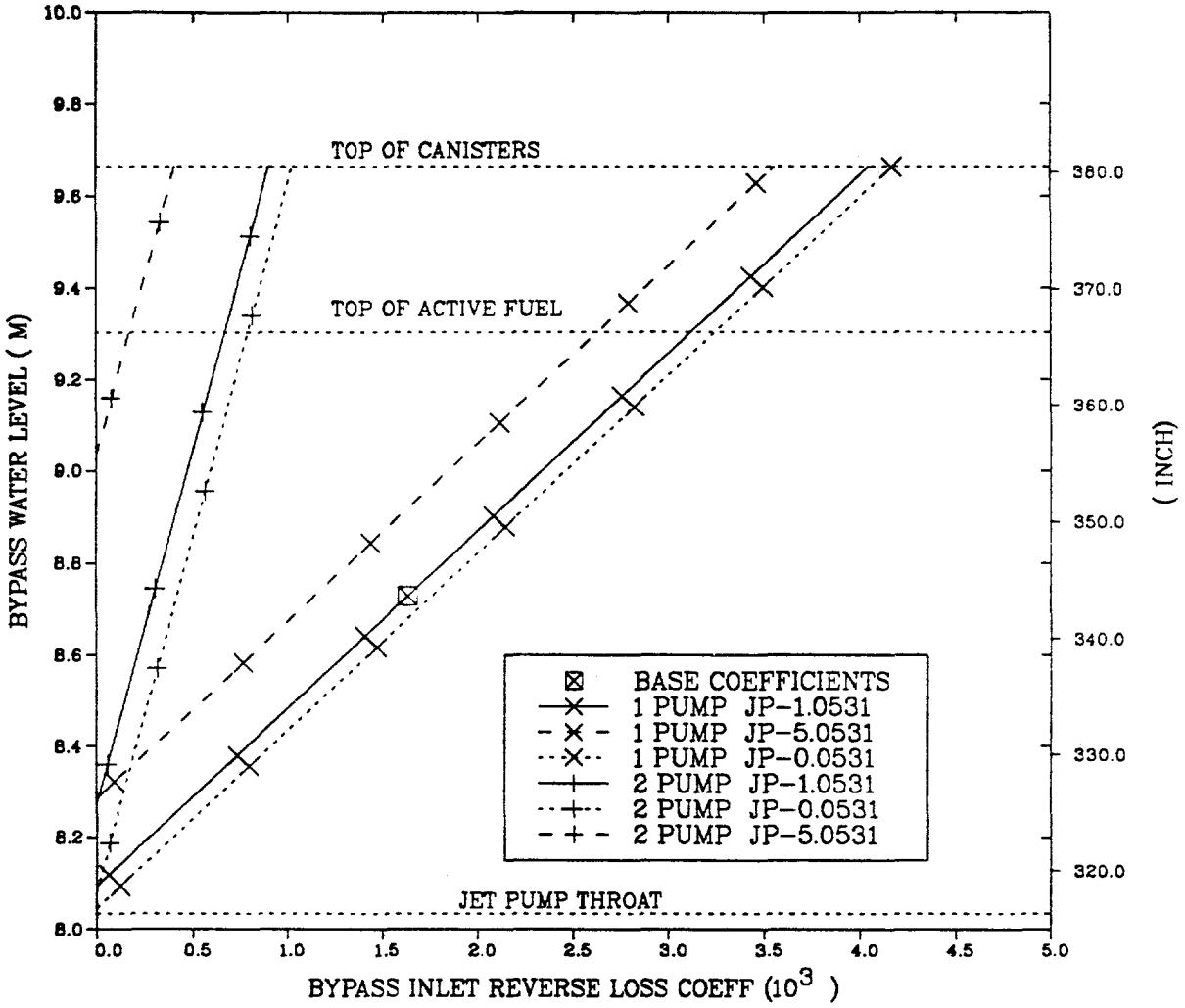

Figure 21: Height Sensitivity to Loss Coefficient

Distribution

Kiyoharu Abe
Dept. of Reactor Safety Research
Nuclear Safety Research Center
Tokai Research Establishment
JAERI
Tokai-mura, Naga-gun
Ibaraki-ken,
JAPAN

Sarbes Acharya
Department of Energy
NS-1/FORS
Washington, DC 20585

Dr. Ulvi Adalioglu
Cekmece Nukleer Arastraima ve
Egitim Merekezi
P.K. 1
Havaalani/ISTANBUL
TURKEY

Dr. Eng. Kiyoto Aizawa
Senior Engineer
Reactor Eng. Dev. Department
PNC
9-13, Chome, Akasaka
Minato-K, Tokyo
JAPAN

Harry Alter
Manager Applied Tech
Nuclear Systems Tech
NE-46
US DOE
Washington, DC 20585

R.M. Andrews
Nuclear Installations Insp.
St. Peters House
Balliol Raod, Bootle
Merseyside L20 31Z
UNITED KINGDOM

George Apostolakis
UCLA
Boelter Hall, Room 5532
Los Angeles, CA 90024-1597

Director of Reactor Engineering
Argonne National Laboratory
9700 S Cass Ave
Bldg 208
Argonne, IL 60439

Ephraim Asculai
Division of Nuclear Safety
Wagramestrasse, 5
P.O. Box 100
A-1400 Wien
AUSTRIA

Vladimar Asmolov
Head, Nuclear Safety Department
I. V. Kurchatov Institute
of Atomic Enegry
Moscow, 123181
RUSSIA

J. de Assuncao
Cabinete de Proteccao è
Seguranca Nuclear
Ministerio da Indusstria
Ave. de Republica 45-6
1000 Lisbon
PORTUGAL

H.P. Balfanz, Head
Institute of Probabilistic
Safety Analysis
TUV Nord
Grosse Bahnstrasse 31
D-22525 Hamburg 54
GERMANY

Pat Baranowsky
USNRC-AEOD/TPAB
MS: T-4A9

Robert A. Bari, Deputy Chairman
Dept of Nuclear Energy
Bldg 197C
Brookhaven National Laboratory
Upton, NY 11973

Librarian
Technical Information Section
Battelle Pacific Northwest Lab
P. O. Box 999
Richland, WA 99352

Dr. John Baum
Dept of Nuclear Energy
Radiological Sciences Div
Bldg 703 M
Brookhaven National Laboratory
Upton, NY 11973

Eric Beckjord
USNRC-RES/DO
MS: T-10F12

Robert Bernero
USNRC-NMSS/DO
MS: T-8A23

Andrea Besi
Institute for Systems Engineering
and Informatics
CEC Joint Research Centre
CP N 1
1-21020 Ispra (Varese)
ITALY

John Bickel
Idaho National Engineering Lab.
EG&G MS: 3850
P.O. Box 1625
Idaho Falls, ID 83415

Vicki Bier
Dept. of Industrial Engineering
University of Wisconsin-Madison
1513 University Avenue, Room 389
Wisconsin, WI 53706

Scott Bigelow
S-CUBED
2501 Yale SE, Suite 300
Albuquerque, NM 87106

Prof. Dr. Dr.-Ing. E. H. Adolf
Birkhofer
Gesellschaft für Anlagen und
Reaktorsicherheit (GRS) mbH
Forschungsgelände
D-8046 Garching
Federal Republic of Germany

David Black
American Electric Power
1 Riverside Plaza
Columbus, OH 43215

Harold Blackman
Idaho National Engineering Lab.
EG&G MS: 3850
P.O. Box 1625
Idaho Falls, ID 83415-3850

Dennis Bley
Buttonwood Consulting
17291 Buttonwood St.
Fountain Valley, CA 92708

Roger Blond
Booz-Allen & Hamilton
4330 East West Highway
Bethesda, MD 20814

Dr. Mario Bonaca
Manager, Reactor Engineering
Northeast Utilities
P.O. Box 270
Hartford, Conn. 06141

Robert B. Borsum
Nuclear Power Division
B & W Nuclear Tech
1700 Rockville Pike
Suite 525
Rockville, MD 20852

Stephen Boult
Electrowatt Engineering Services
(UK) Ltd.
Grandford House
16 Carfax, Horsham
West. Sussex RH12 IUP
ENGLAND

Gary Boyd
Safety & Reliability Optimization
Services
9724 Kingston Pike, Suite 102
Knoxville, TN 37922

Brookhaven National Laboratory (2)
Attn: Lev Neymotin
Arthur Tingle
Building 130
Upton, NY 11973

David M. Brown
Paul C. Rizzo Associates, Inc.
300 Oxford Drive
Monroeville, PA 15146-2347

Tom D. Brown
Sandia National Laboratories
Dept. 6413
P.O. Box 5800
Albuquerque, NM 87185

Robert J. Budnitz
Future Resources Associates, Inc.
2039 Shattuck Avenue, Suite 402
Berkeley, CA 94704

Gary Burdick
USNRC-RES/SAIB
MS: T-10F13

Arthur Buslik
USNRC-RES/PRAB
MS: T-9F31

Edward Butcher
USNRC-NRR/SPSB
MS: O-10E4

Technical Library
B&W Nuclear Service Co
P. O. Box 10935
Lynchburg, VA 24506

Stefaan Caeymaex
Safety & Systems Section
Nuclear Generation Dept.
TRACTEBEL
Avenue Ariane 7
B-1200 Bruxelles
BELGIUM

Leonard Callan, Administrator
U.S. Nuclear Regulatory Commission
Harris Tower and Pavilion
611 Ryan Plaza Drive, Suite 400
Arlington, TX 76011-8064

J. Calvo
Division of PSA & Human Factors
Consejo de Seguridad Nuclear
Calle Justo Dorado, 11
28040 Madrid
SPAIN

John Forbes Campbel
HM Superintending Inspector
Health & Safety Executive
St. Peter's House
Balliol Road
Bootle L20 31Z
UNITED KINGDOM

Leonel Canelas
New University of Lisbon
Quinta de Torre
2825 Monte de Caparica
PORTUGAL

Harold Careway
General Electric Co., M/C 754
175 Curtner Ave.
San Jose, CA 95129

Jose E. De Carlos
CSN International Coordinator
Consejo de Seguridad Nuclear
Calle Justo Dorado 11
28040 Madrid
SPAIN

Annick Carnino
International Atomic Energy Agency
Wagramerstrasse 5, P.O. Box 100
A-1400 Vienna
AUSTRIA

S. Chakraborty
Swiss Federal Nuclear Safety
Inspectorate
Hauptabteilung für die Sicherheit
der Kernanlagen
CH-5232 Villigen-HSK
SWITZERLAND

Erulappa Chelliah
USNRC-RES/PRAB
MS: T-9F31

Mike Cheok
NUS
910 Clopper Road
Gaithersburg, MD 20878

Nilesh Chokshi
USNRC-RES/SSEB
MS: T-10L1

T. L. Chu
Brookhaven National Laboratory
Department of Nuclear Energy
Bldg. 130
Upton, NY 11973

Peter Cooper
SRD/AEA Technology
Wigshaw Lane
Culcheth
Cheshire WA3 4NE
England

Susan E. Cooper
Science Applications Int'l. Corp.
11251 Roger Bacon Drive
Reston, VA 22090

Michael Corradini
University of Wisconsin
1500 Johnson Drive
Madison, WI 53706

E. R. Corran
ANSTO Reasearch Establishment
Lucas Heights Reserch Labs.
Private Mail Bag 1
Manai, NSW 2234
AUSTRALIA

Massimo Cozzone
A.N.P.A.
Via V. Brancati, 48
I-00144 Rome
ITALY

George Crane
1570 E. Hobble Creek Dr.
Springville, Utah 84663

Mark Cunningham
USNRC-RES/PRAB
MS: T-9F31

S. Daggupaty
Environment Canada
4905 Dufferin Street
Downsview
Ontario, M3H ST4
CANADA

Louise Dahlerup
Inspectorate of Nuclear Inst.
Danish Civil Defense &
Emergency Planning Agency
16, Datavej
DK-3460 Birkerod
DENMARK

John Darby
SEA, Inc.
6100 Uptown Blvd. NE
Albuquerque, NM 87110

Gerald Davidson
Fauske and Associates, Inc.
16 W 070 West 83rd Street
Burr Ridge, IL 60521

Peter Davis
PRD Consulting
P.O. Box 2046
Sheridan, WY 82801

P. De Gelder
Secretary, BELGIAN NUCLEAR
SOCIETY (BNS)
A V Nuclear
Avenue du Roi 157
B-1060 Brussels
BELGIUM

Lennart Devell
Studsvik Nuclear
Studsvik Energiteknik AB
S-611 82 Nykoping
SWEDEN

J. Devooght
Service de la Metrologie Nucl
University Libre de Bruxelles
Faculte des Sciees Appliqu.
50 Avenue F-D Roosevelt
Bruxelles 5
BELGIUM

G. Diederick
Commonwealth Edison Co.
LaSalle County Station
RR1, Box 220
2601 North 21st Rd.
Marsielles, IL 61341

Chuck Dobbe
Idaho National Engineering Lab.
EG&G MS: 3840
P.O. Box 1625
Idaho Falls, ID 83415

Mary Drouin
USNRC-RES\SAIB
MS: T-10F13

Duke Power Co. (2)
Attn: Duncan Brewer
Steve Deskevich
422 South Church Street
Charlotte, NC 28242

Bill Eakin
Northeast Utilities
Box 270
Hartford, CT 06141

Stewart D. Ebneter
USNRC
101 Marietta St., Suite 2900
Atlanta, GA 30323-0199

Adel A. El-Bassioni
USNRC-NRR/PRAB
MS: O-10E4

ENEA/DISP (2)
Attn: Alvaro Valeri
Alfredo Bottino
Via Vitaliano Brancati, 48
00144 Roma EUR
ITALY

Walter P. Engel
PRAG MGR Analysis & Reg Matter
NE-60
CRYCITY
US DOE
Washington, DC 20585

John Flack
USNRC-RES/SAIB
MS: T-10F13

Karl Fleming
Pickard, Lowe & Garrick
2260 University Drive
Newport Beach, CA 92660

Terry Foppe
Safety Analysis Engineering
Rocky Flats Plant
Energy Systems Group
Rockwell International Corp
P.O. Box 464
Golden, CO 80401

R H. Gauger
Manager-Reliability Engr
A/E Div
Holmes & Narver Inc.
R Roanne Circle
Irvine, CA 92714

Robert Gobel
Clark University
Center for Technology, Environment
and Development
950 Main St.
Worcester, MA 01610-1477

Paul Govaerts
Studiecentrum voor Kernenergie
(SCK/CEN)
Boeretang, 200
B-2400 Mol
BELGIUM

Mr. Gubler
International Atomic Energy Agency
NENS/SAD BO842
Wagramerstrasse 5, P.O. Box 100
A-1140 Vienna
AUSTRIA

Paul M. Haas, President
Concord Associates, Inc.
725 Pellissippi Parkway
Suite 101, Box 6
Knoxville, TN 37933

Dr. U. Hauptmanns
Gesellschaft Für Anlagen und
Reaktorsicherheit (GRS) mgH
Schwertnergasse 1
D-5000 Köln 1
GERMANY

Sharif Heger
UNM Chemical and Nuclear
Engineering Department
Farris Engineering, Room 209
Albuquerque, NM 87131

Jon C. Helton
Dept. of Mathematics
Arizona State University
Tempa, AZ 85287

Dr. P. M. Herttrich
Gesellschaft für Anlagen und
Reaktorsicherheit (GRS) mbH
Schwertnergasse 1
5000 Köln 1
GERMANY

Dr. D.J. Higson
Radiological Safety Bureau
Australian Nuclear Science &
Technology Organisation
P.O. Box 153
Roseberry, NSW 2018
AUSTRALIA

Dr. Mitsumasa Hirano
Deputy General Manager
Institute of Nuclear Safety
NUPEC
3-6-2, Toranomon, Minato-ku
Tokyo 108
JAPAN

Dr. S. Hirschberg
Paul Scherrer Institute
Vurenlingen and Villigen
CH-5232 Villigen PSI
SWITZERLAND

Steven Hodge
Oak Ridge National Laboratories
P. O. Box Y
Oak Ridge, TN 37831

Gary Holahan
USNRC-AEOD/OSP
MS: T-4A9

N.J. Holloway
A72.1
Atomic Weapons Establishment
Ademaston
Reading RG7 4PR
UNITED KINGDOM

Griff Holmes
Westinghouse Electric Co.
Energy Center East
Bldg. 371
P.O. Box 355
Pittsburgh, PA 15230

William Hopkins
Bechtel Power Corporation
15740 Shady Grove Road
Gaithersburg, MD 20877

Dean Houston
USNRC-ACRS
MS: P-315

Der-Yu Hsia
Institute of Nuclear Energy Research
Lung-Tan 325
TAIWAN

Alejandro Huerta-Bahena
National Commission on Nuclear
Safety and Safeguards (CNSNS)
Insurgentes Sur N. 1776
C. P. 04230 Mexico, D. F.
MEXICO

Peter Humphreys
US Atomic Energy Authority
Wigshaw Lane, Culcheth
Warrington, Cheshire
UNITED KINGDOM, WA3 4NE

W. Huntington
Commonwealth Edison Co.
LaSalle County Station
RR1, Box 220
2601 North 21st Rd.
Marsielles, IL 61341

J.S. Hyslop
USNRC-RES/PRAB
MS: T-9F31

Idaho National Engineering Lab. (2)
Attn: Doug Brownson
Darrel Knudson
EG&G MS: 3840
P.O. Box 1625
Idaho Falls, ID 83415

Idaho National Engineering Lab. (2)
Attn: Art Rood
Mike Abbott
EG&G MS: 2110
P.O. Box 1625
Idaho Falls, ID 83415

Hanspeter Isaak
Abteilung Strahlenschutz
Hauptabteilung für die Sicherheit
der Kernanlagen (HSK)
CH-5303 Wurenlingen
SWITZERLAND

Brian Ives
UNC Nuclear Industries
P. O. Box 490
Richland, WA 99352

Kamiar Jamili
DP-62/FTN
Department of Energy
Washington, D.C. 20585

Robert Jones
USNRC-NRR/DSSA
MS: O-8E1

Edward Jordan
USNRC-AEOD/DO
MS: T-4D18

Dr. H. Kalfsbeek
DG/XII/D/1
Commission of the European Communities
Rue de la Loi, 200
B-1049 Brussels
BELGIUM

Yoshio Kano
General Mngr. & Sr. Engineer
Systems Analysis Section
O-arai Engineer. Centr, PNC
Higashi-Ibaraki-gun
Ibaraki-Ken, 133-13
JAPAN

William Kastenberg
UCLA
Boelter Hall, Room 5532
Los Angeles, CA 90024

Barry Kaufer
OECD/NEA
"Le Seine St. Germain" 12
Boulevard des Iles
92130 Issy-les-Moulineaux
FRANCE

Paul Kayser
Division de la Radioprotection
Avenue des Archiducs, 1
L-1135 Luxembourg-Belair
LUXEMBOURG

Ken Keith
TVA
W 20 D 201
400 West Surmnit Hill
Knoxville, TN 37092

G. Neale Kelly
Commission of the European Communities
Joint Research Centre
Rue de la Loi 200
B-1049 Brussels
BELGIUM

Knolls Atomic Power Laboratory (2)
Attn: Ken McDonough
Dominic Sciaudone
Box 1072
Schenectady, NY 12301

Dr. K. Koberlein
Gesellschaft für Reaktorsicherheit mbH
Forschungsgelände
D-8046 Garching
GERMANY

Alan Kolaczkowski
Science Applications International Corporation
2109 Air Park Rd. S. E.
Albuquerque, NM 87106

Jim Kolanowski
Commonwealth Edison Co.
35 1st National West
Chicago, IL 60690

John G. Kollas
Institute of Nuclear Technology and Radiation Protection
N.R.C.P.S. "Demokritos"
P.O. Box 60228
GR-153 10 Aghia Paraskevi
Attiki
GREECE

S. Kondo
Department of Nuclear Engineering
Facility of Engineering
University of Tokyo
3-1, Hongo 7, Bunkyo-ku
Tokyo
JAPAN

D. Lamy
CEN/SCK
Dept. Scientific Irradiation Experiment & Study BR2
Boeretang, 200
B-2400 Mol
BELGIUM

Dr. J.M. Lanore
CEA/IPSN/DAS
Centre d'Etudes Nucléaires de Fontenay-aux-Roses
B.P. n° 6
92265 Fontenay-aux-Roses CEDEX
FRANCE

Jose A. Lantaron
Consejo de Seguridad Nuclear
Sub. Analisis y Evaluaciones
Calle Justo Dorado, 11
28040 Madrid
SPAIN

Josette Larchier-Boulanger
Electricte de France
Direction des Etudes Et Recherches
30, Rue de Conde
75006 Paris
FRANCE

H. Larsen
Head of Department
Riso National Laboratory
P.O. Box 49
DK-4000 Roskilde
DENMARK

Lawrence Livermore Nat'l Lab. (4)
Attn: George Greenly
Marvin Dickerson
Rolf Lange
Sandra Brereton
Livermore, CA 94550

Shengdar Lee
Yankee Atomic Electric Company
580 Main St.
Boston, MA 17407

B.T.F. Liwaang
Dept. of Plant Safety Assessment
Swedish Nuclear Power Inspec.
P.O. Box 27106
S-10252 Stockholm
SWEDEN

Peter Lohnberg
Expresswork International, Inc.
1740 Technology Drive
San Jose, CA 95110

Steven M. Long
USNRC-NRR/SPSB
MS: O-10E4

D. Eugenio Gil Lopez
Consejo de Seguridad Nuclear
Calle Justo Dorado, 11
28040 Madrid
SPAIN

Los Alamos National Laboratory (2)
Attn: Kent Sasser
N-6, K-557
Los Alamos, NM 87545

Christiana H. Lui
USNRC-RES/PRAB
MS: T-9F31

John Luke
Florida Power & Light
P.O. Box 14000
Juno Beach, FL 33408

Daniel Manesse
ISPN
Boite Postale n° 6
92265 Fontenay-aux-Roses CEDEX
FRANCE

Fred Mann
Westinghouse Hanford Co.
WIA-53
P.O. Box 1970
Richland, WA 99352

Nadia Soido Falcao Martins
Comissao Nacional de Energia Nuclear
R General Severianao 90 S/408-1
Rio de Janeiro
BRAZIL

Harry F. Martz
Analysis and Assessment Division
Los Alamos National Laboratory
Los Alamos, NM 87545

Herbert Massin
Commonwealth Edison Co.
35 1st National West
Chicago, IL 60690

Hideo Matsuzuru
Tokai Research Establishment
Tokai-mur
Maka-gun
Ibaraki-ken, 319-11
JAPAN

Jim Mayberry
Ebasco Services
60 Chubb Ave.
Lyndhurst, NJ 07071

Andrew S. McClymont
IT-Delian Corporation
1340 Saratoga-Sunnyvale Rd.
Suite 206
San Jose, CA 95129

Michael McKay
Los Alamos National Laboratory
A-1, MS F600 Services
P.O. Box 1663
Los Alamos, NM87545

Zen Mendoza
SAIC
5150 El Camino Real
Suite C3 1
Los Altos, CA 94022

Dr. J. Mertens
Division of Risk Analysis &
Reactor Technology
Institute of Safety Research
Research Centre Julich (KFA)
D-52425 Julich
GERMANY

Jim Meyer
Scientech
11821 Parklawn Dr.
Suite 100
Rockville, MD 20852

Joe Minarick
Science Applications Int'l Corp.
301 Laboratory Road
P.O. Box 2501
Oak Ridge, TN 37830

Jose I. Calvo Molins, Head
Division of P.S.A. and Human Factors
Consejo de Seguridad Nuclear
Calle Justo Dorado, 11
28040 Madrid
SPAIN

Ken Muramatsu
Risk Analysis Laboratory
Japan Atomic Energy Research Institute
Tokai-mura, Naka-gun
Ibaraki-ken, 319-11, Tokyo
JAPAN

Joseph A. Murphy
Division of Safety Issue Resolution
U.S. Nuclear Regulatory Commission
MS: T-10E50
Washington, DC 20555

Kenneth G. Murphy, Jr.
US Department of Energy
19901 Germantown Rd.
Germantown, MD 20545

Shankaran Nair
Central Electricity
Generating Board
Berkeley Nuclear Laboratories
Berkeley
Gloucestrshire CL13 9PB
UNITED KINGDOM

Ray Ng
NEI
1776 Eye St. N
Suite 300
Washington, DC 20006-2496

G. Niederauer
Los Alamos National Laboratory
P. O. Box 1663
MSK 575
Los Alamos, NM 87545

Oak Ridge National Laboratory (2)
Attn: Steve Fisher
Sherrel Greene
MS-8057
P.O. Box 2009
Oak Ridge, TN 37831

Ken O'Brien
University of Wisconsin
Nuclear Engineering Dept.
153 Engineering Research Blvd.
Madison, WI 53706

Theresa Oh
INEL Tech Library
EG&G MS: 2300
P. O. Box 1625
Idaho Falls, ID 83415-2300

Robert Ostmeyer
U.S. Department of Energy
Rocky Flats Area Office
P. O. Box 928
Golden, CO 80402

Robert Palla
USNRC-NRR/SPSB
MS: O-10E4

Gareth Parry
NUS Corporation
910 Clopper Rd.
Gaithersburg, MD 20878

Vern Peterson
Building T886B
EG&G Rocky Flats
P.O. Box 464
Golden, CO 80402

G. Petrangeli
ENEA Nuclear Energy ALT Disp
Via V. Brancati, 48
00144 Rome
ITALY

Ing. Jose Antonio Becerra Perez
Comision Nacional De Seguridad
Nuclear Y Salvaguardias
Insurgentes Sur 1806
01030 Mexico, D. F.
MEXICO

William T. Pratt
Brookhaven National Laboratory
Building 130
Upton, NY 11973

Urho Pulkkinen
Technical Research Centre of
Finland
Laboratory of Electrical &
Automation Engineeering
Otakaari 7B, 02150 Espoo 15
FINLAND

Blake Putney
Science Applications
International Corporation
5150 El Camino Real, Suite C31
Los Altos, CA 94022

Dr. V. M. Raina
Project Manager-Risk Assessment
Ontario Hydro H11 G1
700 University Ave.
Toronto, Ontario M5G 1X6
CANADA

William Raisin
NEI
1726 M. St. NW
Suite 904
Washington, DC 20036

Ann Ramey-Smith
USNRC-RES/PRAB
MS: T-9F31

Dale Rasmuson
USNRC-AEOD/TPAB
MS: T-4A9

John Ridgely
USNRC-RES/SAIB
MS: T-10F13

Richard Robinson (2)
USNRC-RES/PRAB
MS: T-9F31

M. Roch
Manager of Design, Nuclear
Department
TRACTEBEL
Avenue Ariane 7
B-1200 Bruxelles
BELGIUM

A.E. Rogers
General Electric Co
175 Curtner Ave
MC-489
San Jose, CA 95125

Judy Rollstin
GRAM Inc
8500 Menual Blvd. NE
Albuquerque, NM 87112

Marc Rothschild
Halliburton NUS
1303 S. Central Ave.
Suite 202
Kent, WA 98032

Christopher Ryder
USNRC-RES/PRAB
MS: T-9F31

Takashi Sato, Deputy Manager
Nuclear Safety Engineering Section
Reactor Design Engineering Dept.
Nuclear Energy Group, Toshiba Corp.
Isogo Engineering Center
8, Shinsugita-cho, Isogo-ku,
Yokohama 235, JAPAN

Martin Sattison
Idaho National Engineering Lab.
P. O. Box 1625
Idaho Falls, ID 83415

Dr. U. Schmocker
Hauptabteilung für die
Sicherheit der Kernanlagen
CH-5232 Villigen HSK
SWITZERLAND

A. J. Seebregts
ECN Nuclear Energy
Westerduinweg, 3
Postbus 1
NL-1755 Petten ZG
THE NETHERLANDS

Dr. S. Serra
Ente Naxionale per I'Energia
Electtrica (ENEL)
via G.B. Martini 3
I-00198 Rome
ITALY

H. Shapiro
Licensing & Risk Branch
Atomic Energy of Canada Ltd.
Sheridan Park Research Comm.
Mississauga, Ontario L5K 1B2
CANADA

Nathan O. Siu
Center for Reliability and Risk Assessment
Idaho National Engineering Lab.
EG&G MS: 3850
P.O. Box 1625
Idaho Falls, ID 83415-3855

E. Soederman
ES-Konsult AB
Energy and Safety
P.O. Box 3096
S-16103 Bromma
SWEDEN

Desmond Stack
Los Alamos National Laboratory
Group Q-6, Mail Stop K556
Los Alamos, NM 87545

Jao Van de Steen
KEMA Laboratories
Utrechtseweg, 310
Postbus 9035
NL 800 ET Arnhem
THE NETHERLANDS

Eli Stern
Israel AEC Licensing Div.
P.O. Box 7061
Tel-Aviv 61070
ISRAEL

Dr. Egil Stokke
Advisory Group
OECD Halden Reactor Project
P.O. Box 173
N-1751 Halden
NORWAY

Stone & Webster Engineering Corp
Technical Information Center
A. Hosford
245 Summer Street
245/01
Boston, MA 02210

Dennis Strenge
Pacific Northwest Laboratory
RTO/ 125
P.O. Box 999
Richland, WA 99352

Technadyne Engineer. Consultants (3)
Attn: David Chanin
Jeffery Foster
Walt Murfin
Suite A225
8500 Menual Blvd. N
Albuquerque, NM 87112

Ashok Thadani
USNRC-NRR/ADT
MS: O-12G18

T. G. Theofanous
University of California, S. B.
Department of Chemical and Nuclear Engineering
Santa Barbara, CA 93106

Catherine Thompson
USNRC-RES/SAIB
MS: T-10F13

Soren Thykier-Nielsen
Riso National Laboratory
Postbox 49
DK4000 Roskile
DENMARK

R. Toossi
Physical Research, Inc.
25500 Hawthorn Blvd.
Torrance, CA 90505

Ennio Traine
ENEL
Via Vialiano, 48
00144 Rome
ITALY

Ulf Tveten
Environmental Physics Section
Institutt for Energiteknikk
Postboks 40
N-2007 Kjeller
NORWAY

US Department of Energy
Energy Library
Room G 034/GTN
AD-622.1
Washington, DC 20585

US Department of Energy
NS-50 (GTN)
NS-10.1
S-161
Washington, DC 20585

U.S. Environmental
Protection Agency (2)
Attn: Allen Richardson
Joe Logsdon
Office of Radiation Programs
Environmental Analysis Division
Washington, DC 20460

Harold VanderMolen
USNRC-RES/PRAB
MS: T-9F31

Dr. A. Valeri
A.N.P.A.
Via Vitaliano Brancati, 48
I-00144 Rome
ITALY

Magiel F. Versteeg
Ministry of Social Affairs
and Employment
P.O. Box 90804
2509 LV Den Haag
THE NETHERLANDS

Martin Virgilio
USNRC-NRR/DSSA
MS: O-8E2

R. Virolainen, (Chairman PWG5)
Systems Integ. Off. (STUK)
P.O. Box 268
Kumpulanite 7
SF-60101 Helsinki
FINLAND

Seppo Vuori
Technical Research Centre of Finland
Nuclear Engineering Laboratory
Lonnrotinkatu 37
P.O. Box 169
Sf-00181 Helsinki 18
FINLAND

Dr. Ian B. Wall
81 Irving Avenue
Atherton, CA 94027

Edward Warman
Stone & Webster Engineering Corp.
P.O. Box 2325
Boston, MA 02107

J.E. Werner
Reactor Research & Techn Division
US DOE Idaho Operations
MS: 1219
850 Energy Drive
Idaho Falls, ID 83401-1563

Dr. Wolfgang Werner
Safety Assessment Consulting GmbH
Veilchenweg 8
D 83254 Breitbrunn
GERMANY

Westinghouse Electric Corp
Technical Library
P. O. Box 355
East 209
Pittsburgh, PA 15230

Westinghouse Electric Corp
NTD
Central File Nuclear Safety
P. O. Box 355
408 1-A
Pittsburgh, PA 15230

Westinghouse Electric Company (3)
Attn: John Lacovin
Burt Morris
Griff Holmes
Energy Center East, Bldg. 371
P.O. Box 355
Pittsburgh, PA 15230

Westinghouse Savannah River Co. (2)
Attn: Kevin O'Kula
Jackie East
Safety Technology Section
1991 S. Centennial Ave., Bldg. 1
Aiken, SC 29803

Keith Woodard
PLG, Inc.
7315 Wisconsin Ave.
Suite 620 East
Bethesda, MD 20814-3209

John Wreathall
John Wreathall & Co.
4157 MacDuff Way
Dubin, OH 43017

M. K. Yeung
University of Hong Kong
Mechanical Engineering Dept.
Polfulam
HONG KONG

Bob Youngblood
Brookhaven National Laboratory
Department of Nuclear Energy
Bldg. 130
Upton, NY 11973

Carlo Zaffiro
A.N.P.A.
Directorate for Nuclear
Via Vitaliano Brancate, 48
I-00144 Rome
ITALY

Dr. X. Zikidis
Greek Atomic Energy Comm.
N.R.C.P.S. "Demokritos"
GR-153 10 Agia Paraskevi
Attiki
GREECE

INTERNAL DISTRIBUTION

MS0405	D. D. Carlson, 6411
MS0747	A. L. Camp, 6412
MS0747	V. J. Dandini, 6412
MS0747	S. L. Daniel, 6412
MS0747	S. E. Dingman, 6412
MS0747	J. A. Forrester, 6412
MS0747	K. M. Hays, 6412
MS0747	H. K. Schriner, 6412
MS0747	D. B. Mitchell, 6412
MS0747	B. D. Staple, 6412
MS0747	J. A. Lambright, 6412
MS0747	D. W. Whitehead, 6412
MS0747	G. D. Wyss, 6412
MS0748	F. T. Harper, 6413
MS0748	T. D. Brown, 6413 (10)
MS0737	M. P. Bohn, 6449
MS0742	J. E. Kelly, 6414
MS0745	L. N. Kmetyk, 6418
MS0736	N. R. Ortiz, 6400
MS1175	L. A. Miller, 6513
MS9018	Central Technical Files, 8523-2
MS0899	Technical Library, 13414 (5)
MS0619	Technical Publications, 12613

NRC FORM 335 (2-89) NRCM 1102, 3201, 3202

U.S. NUCLEAR REGULATORY COMMISSION

BIBLIOGRAPHIC DATA SHEET

(See instructions on the reverse)

1. REPORT NUMBER (Assigned by NRC, Add Vol., Supp., Rev., and Addendum Numbers, if any.)
NUREG/CR-6143
SAND93-2440
Vol. 6, Part 2

2. TITLE AND SUBTITLE
Evaluation of Potential Severe Accidents During Low Power and Shutdown Operations at Grand Gulf, Unit 1

Evaluation of Severe Accident Risks for Plant Operational State 5 During a Refueling Outage

Supporting MELCOR Calculations

3. DATE REPORT PUBLISHED
MONTH: March
YEAR: 1995

4. FIN OR GRANT NUMBER
L1679

5. AUTHOR(S)
L. N. Kmetyk, T. D. Brown

6. TYPE OF REPORT
Technical

7. PERIOD COVERED *(Inclusive Dates)*

8. PERFORMING ORGANIZATION – NAME AND ADDRESS *(If NRC, provide Division, Office or Region, U.S. Nuclear Regulatory Commission, and mailing address; if contractor, provide name and mailing address.)*
Sandia National Laboratories
Albuquerque, NM 87185

9. SPONSORING ORGANIZATION – NAME AND ADDRESS *(If NRC, type "Same as above"; if contractor, provide NRC Division, Office or Region, U.S. Nuclear Regulatory Commission, and mailing address.)*
Division of Systems Technology
Office of Nuclear Regulatory Research
U.S. Nuclear Regulatory Commission
Washington, DC 20555-0001

10. SUPPLEMENTARY NOTES

11. ABSTRACT *(200 words or less)*

The document contains the deterministic code calculations performed with the MELCOR Code that were used to support the development and quantification of the PRA models used in the analysis of internally initiated events for Grand Gulf, Unit 1, as it operates in the Low Power and Shutdown Plant Operational State 5 during a refueling outage. The background for the work documented in this report is summarized including how deterministic codes are used in PRAs, why the MELCOR code is used, what the capabilities and features of MELCOR are and how the code has been used by others in the past. Brief descriptions of the Grand Gulf plant and its configuration during LP&S operation and of the MELCOR input model developed for the Grand Gulf plant in its LP&S configuration are given. The results of MELCOR analyses of various accident sequences for the plant operating state (POS) 5 configuration during refueling (approximately Cold Shutdown as defined by Grand Gulf Technical Specifications) are presented for accidents initiated at several different times after scram and shutdown including shortened thermal hydraulic and core damage calculations done in support of the Level 1 analysis and full plant analyses including containment response and source terms supporting the Level 2 analysis.

12. KEY WORDS/DESCRIPTORS *(List words or phrases that will assist researchers in locating the report.)*
Probabilistic Risk Assessment, Low Power and Shutdown Operations, Boiling Water Reactor, MELCOR, Plant Calculations, Severe Accidents

13. AVAILABILITY STATEMENT
Unlimited

14. SECURITY CLASSIFICATION
(This Page)
Unclassified
(This Report)
Unclassified

15. NUMBER OF PAGES

16. PRICE